Biodiversity and palaeoecological significance of Tertiary fossil floras from King George Island, West Antarctica

Richard John Hunt

Submitted in accordance with the requirements for the degree of Doctor of Philosophy

The University of Leeds
School of Earth Sciences

November 2001

The candidate confirms that the work submitted is his own and that appropriate credit has been given where reference has been made to the work of others.

Abstract

Palaeogene volcanics with plant-bearing sediment intercalations crop out extensively on King George Island in the South Shetland Islands, West Antarctica. The plant fossil assemblages are the most complete Palaeogene terrestrial foliar record in Antarctica. Compositional variations in the flora have previously been used to construct climate change models for the Tertiary.

King George Island is part of the late Triassic to Recent, Andean – West Antarctic subducting margin. Eastwards subduction oceanic crust beneath the Antarctic Peninsula resulted in mountain building and crustal melting at depth that in turn led to large stratovolcanoes and active pyroclastic volcanism (Leat *et al.*, 1995). Consequently the flora is preserved in a range of primary and reworked volcaniclastic sediments, that were deposited in lacustrine and ephemeral lacustrine basins developed on the volcanic surface.

The King George Island flora consists of impressions and carbonised compressions of leaves of angiosperms, gymnosperms, and ferns, in addition to new records of an angiosperm infloresence, fruits and coniferous cones. The flora comprises vegetation elements with a disjunct modern Southern Hemisphere distribution, such as Cunoniaceae, Nothofagaceae, Proteaceae, Sterculiaceae, Lauraceae and Myrtaceae. Close affinities are suggested with the cool to warm temperate forests of southern South America. Morphotype analyses based on leaf venation architecture have been used to group the flora into 85 morphotypes based on 428 specimens. The morphotypes have been used in foliar physiognomic and nearest living relative palaeoclimate analyses, which suggest warm microthermal climates for the Middle Eocene in West Antarctica.

The Dragon Glacier and Mt. Wawel floras from Point Hennequin are currently regarded as impoverished Upper Oligocene, post-glacial floras. However, $^{40}Ar/^{39}Ar$ dating of the encapsulating lavas indicates that they are Middle Eocene in age (44 - 49 Ma) and field collections have yielded a diverse range of plant fossils from the localities.

In composition, tectonic setting and climatic regime, the closest modern analogue for the King George Island flora is the Valdivian rainforests of Chile. The composition of these forests is controlled by disturbance, largely of volcanic origin. As such, local variations in vegetation composition previously attributed to climatic change during the Palaeogene could be explained in terms of disturbance related succession.

ACKNOWLEDGEMENTS

So many people have helped me and supported me during the past four years that it is hard to know where to begin. Jane Francis and David Cantrill are thanked for setting up this project, for their supervision, for their encouragement and for their patience. A NERC-British Antarctic Survey CASE research studentship is acknowledged. The Trans-Antarctic Association and the Organising Committees of the 8th ISAES, NAPC and Palaeogene Climate and Biota meetings are thanked for travel and subsistence funding. I am indebted to Ash Morton, the BAS logistics team and the 1999 crew of the HMS Endurance for field support, and company, in Antarctica. John Smellie has given a lot valuable time for discussion about KGI, access to field notes and slides. Thanks also to Alistair Crame, Christine Phillips, Mike Tabecki (for thin sections) Janet Thomson, Mike Thomson and Rob Willan, who have given advice and assistance at BAS.

Phil Guise taught me the dying art of Leeds geochronology and helped me put the world to rights in excellent conversations over the mass-spec. Martin Timmermann and Bob Cliff helped me to learn some of the intricacies of geochronological petrology and Gary and Rod kept me company during those endless hours of mineral separation. Lawrence helped to see me through the murky waters of a seddy chapter and paper, not to mention a few pints along the way.

Richard Barnes, Kristoph Birkenmajer, Tania Dutra, Dave Ferguson, Dave Greenwood, Bob Hill, Greg Jordan, Liz Kennedy, Steve McGloughlin, Scott Wing, Jack Wolfe and Eva Zastawniak have provided me with reprints and also advice on morphotype identifications. Thanks to Bob Spicer for running the CLAMP analysis and to Torsten Utescher for the coexistence analysis. The Sheffield Group is thanked for the use of the inflorescence microscope. Guy Harrington is acknowledged for processing palyno-samples. The Royal Botanic Gardens, Kew are thanked for permission to work at the Herbarium and the Herbarium staff are thanked for assistance and useful discussions. Drs M. Gardiner and S. Knees at the RBG, Edinburgh are also thanked for information, discussion and a virtual tour of the Valdvian rainforests. Chris Page gave some excellent insights into the modern South American forests.

Life would not have been half as fun at Leeds if not for my office companions Zahir (the dude - mf), Alison, Chris, Dave M and more recently Jo and Dave B (Davrovski Vudge to his Tovareshi). James Cleverley helped to spur me on, drink too much and listened to me grumble incessantly about the pressure of work. Likewise Anne-Marie (Bruce), Helena, Kate, Mike Steve, Sidney, my football compadres and all my friends outside of the University who haven't seen much of me for the last year (in particular Batty for always looking after me in Cambs).

Nicky, Julie, Julie F, Shirley, Tara and Katrina never did bake me a cake but were always great to gossip with. Thanks to Phil and Bob in the prep room for various things; Fashion tips, career advice, microscopes, general sarcasm and derision (I still don't know anything about the dragon fly). Thanks to Dave H (for ethanol), Neil C (for sections) and Phil down in the workshops (I still have your varnish and a small chisel - oops!). Thanks to Mark F for putting up with my endless need for slide scanning and conversation down in the seddy lab. The University of Leeds media service did a wonderful job taking photos of a large number of fossiliferous rocks.

Without the encouragement and enthusiasm of Imogen Poole, I might not have completed this project. She has been a friend, co-author and unofficial third supervisor for the past four years and has shown me the best side of research. Thanks also to Pim who has inadvertently given advice with my writing and encouragement with my research. My family has supported me ever since I went to University and given me lots of encouragement (and teasing – Briony and Ed) over the years to get this far. Brian, Margaret, Doris and Liza have been very encouraging.

Ros has awed me in being constant source of strength, confidence, love, laughter and hope over the last four years and has helped me through the best and worst parts of this project. Her support has been unstinting and has helped me to achieve a dream I have held for years.

Table of Contents

Volume 1

List of Figures

Chapter 11

List of Tables

Chapter 9

Chapter 10

Chapter 11

Chapter 1 Introduction and Synopsis

1.1 Introduction

The Antarctic continent is one of the most extreme environments on Earth, sheltering only a few of the hardiest plants. Lying predominantly south of latitude 70° S (Figure 1.1a) Antarctica experiences 24-hour daylight in summer, up to 4 months of winter darkness and has a mean annual temperature of - 20° C. Receiving less than 5 cm of precipitation annually, much of the continent is classified as desert (British Antarctic Survey (BAS) website, 2001). Within 5° latitude of the South Pole, temperatures frequently drop to - 70° C (min. recorded – 89° C).

On mountain flanks in continental East Antarctica vegetation generally constitutes less than 1 % of ground cover (Stonehouse, 1989). The flora comprises a few species of moss growing alongside algae, lichen, bacteria and fungi. *Deschampsia antarctica* Desvaux, a grass forming low mats, and *Colobanthus quitensis* (Kunth) Bartling (Caryophyllaceae) are the only angiosperms present in Antarctica (Longton, 1985). The peninsula region, forming a large part of West Antarctica (Figure 1.1), extends from ~ 80° S to nearly 60° S (only 950 km from Cape Horn) and has a comparatively mild maritime climate, which supports larger and relatively more diverse plant communities (Longton, 1985).

The discovery of fossilised Antarctic wood by James Eights in 1833 and of leaves, fruits, seeds and pollen by other expeditions in the 19th and 20th centuries demonstrated that the present day Antarctic vegetation and climate are atypical (Zinsmeister, 1988). Studies of the marine oxygen isotope record (Miller *et al.*, 1987; Flower, 1999; Zachos *et al.*, 2001) reveal a transition from a uniformly warm 'greenhouse' world, to a more heterogeneous 'icehouse' world during the Late Eocene-earliest Oligocene (Figure 1.2). During this icehouse period, first East and then West Antarctica underwent a series of glaciations (Barron *et al.*, 1991; Birkenmajer, 1997; Barker *et al.*, 1999) that eventually led to extinction of the terrestrial flora (Francis and Hill, 1996). The nature of this environmental change on land is poorly understood (Francis, 1999). Studies of the Tertiary Antarctic fossil floras are of fundamental importance because modern relationships between climate, the environment and plant populations can be extrapolated to the floras to obtain palaeoclimatic and palaeoenvironmental data for this period.

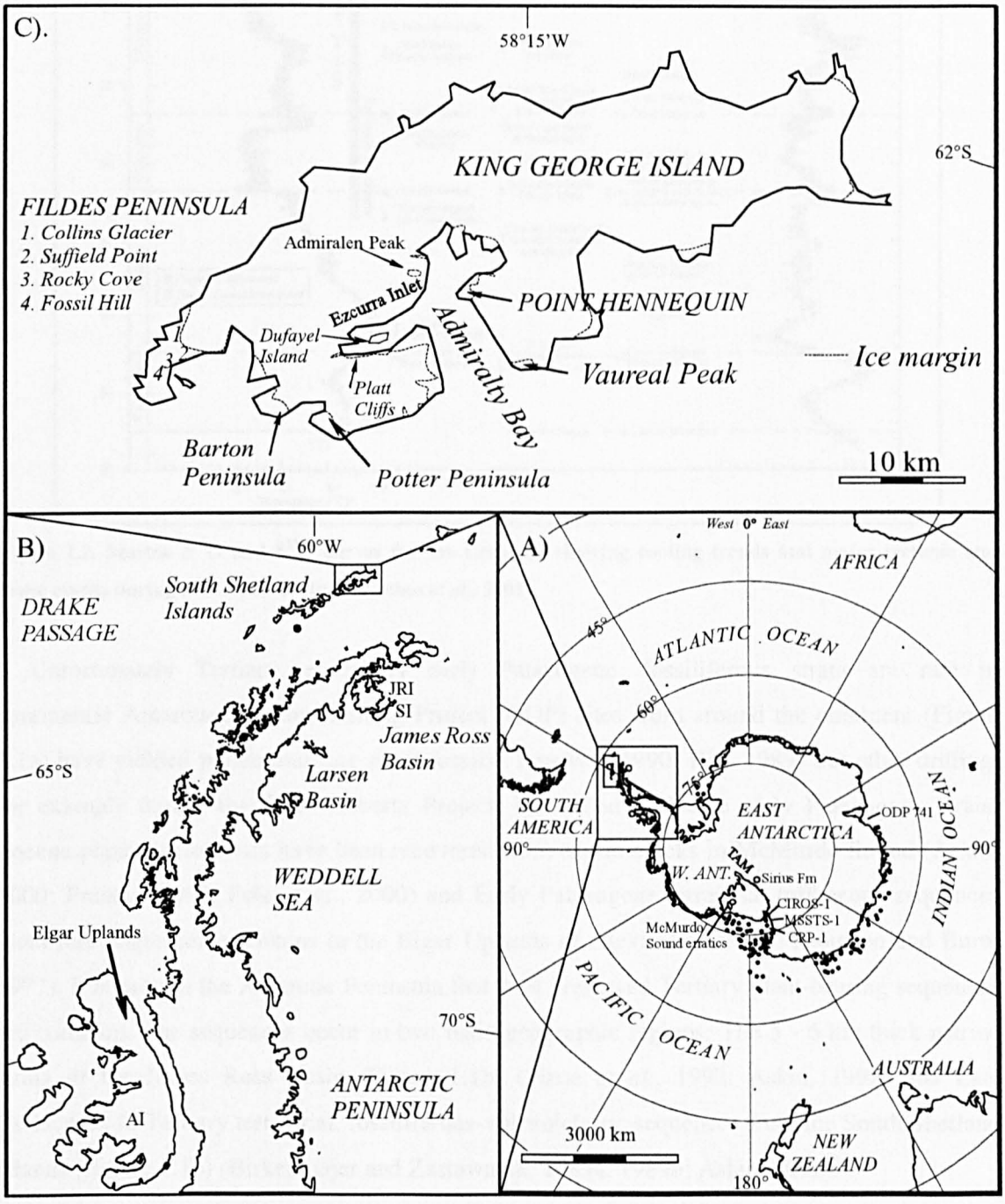

Figure 1.1. Locality maps of Antarctica map showing terrestrial flora localities. A) Antarctica W. Ant - West Antarctica, TAM - Trans-Antarctic Mountains, CIROS-1, ODP etc - drillcores, CRP - Cape Roberts Project. Black circles indicate drillcores (data fromTruswell, 1990; Cape Roberts Science Team, 1998).B) Antarctic Peninsula. AI - Alexander Island, JRI - James Ross Island, SI - Seymour Island. C). Location map of Tertiary British Antarctic Survey collections on King George Island.

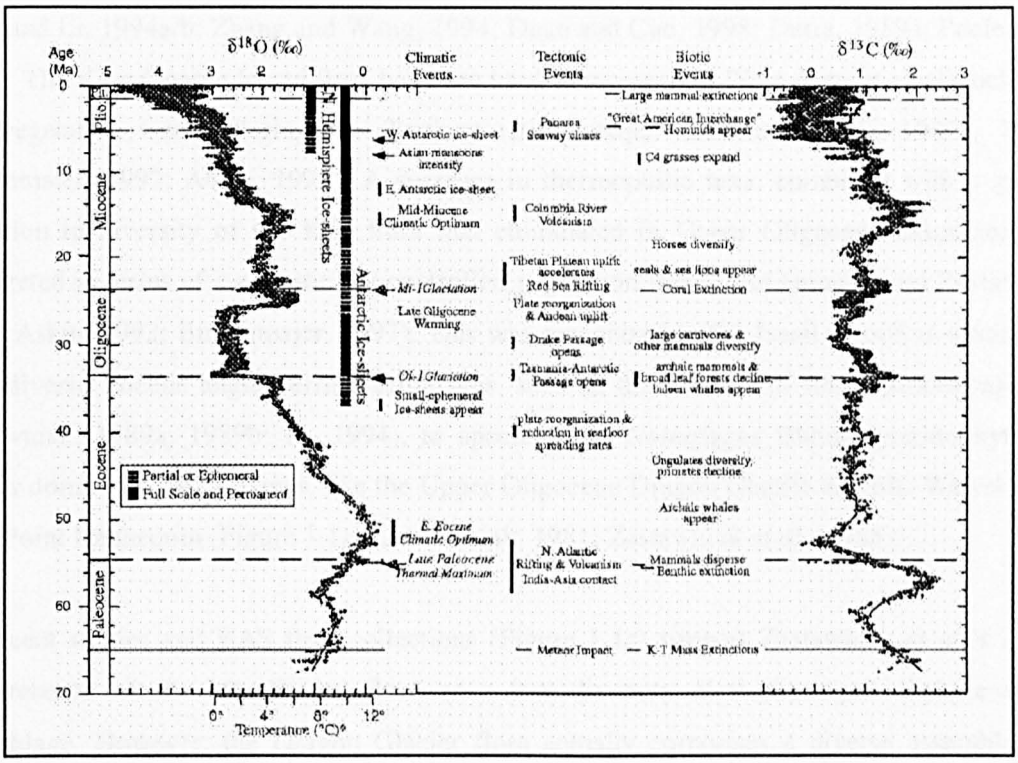

Figure 1.2. Marine $\delta^{18}O$ and $\delta^{13}C$ curves for the Cenozoic showing cooling trends and major tectonic and biotic events during the Cenozoic (from Zachos *et al.*, 2001).

Unfortunately Tertiary, especially early Palaeogene, fossiliferous strata are rare in continental Antarctica. Ocean Drilling Project (ODP) sites from around the continent (Figure 1.1a) have yielded pollen and rare plant fossils (Truswell, 1990; Hill, 1989) but other drilling, for example during the Cape Roberts Project, has failed to locate early Palaeogene strata. Eocene plant macrofossils have been recovered from exotic blocks in McMurdo Sound (Askin, 2000; Francis, 2000; Pole *et al.*, 2000) and Early Palaeogene terrestrial tuffaceous sequences yield rare angiosperm remains in the Elgar Uplands of Alexander Island (Thomson and Burn, 1977). It is only in the Antarctic Peninsula that well preserved Tertiary plant-bearing sequences are common. The sequences occur in two main geographic regions: The 5 - 6 km thick marine strata of the James Ross Basin (Figure 1.1b) (Pirrie *et al.*, 1992; Askin, 1992) and Late Cretaceous to Tertiary terrestrial, fossiliferous-volcaniclastic sequences from the South Shetland Islands (Figure 1.1b) (Birkenmajer and Zastawniak, 1989a, 1989b; Askin, 1992).

To date the most complete Tertiary terrestrial plant record in Antarctica occurs in a nearly 3 km thick sequence of volcanic and volcaniclastic deposits (Birkenmajer *et al.*, 1986b) on King George Island (KGI) within the South Shetlands Islands (Figure 1.1b) (Barton, 1964a,1964b; Orlando, 1963, 1964; Lucas and Lacey, 1981; Stuchlik, 1981; Birkenmajer and Zastawniak, 1986, 1989a, 1989b; Cao, 1992, 1994; Cortegmiglia *et al.*, 1981; Zastawniak, 1981; Del Valle *et al.*, 1984; Torres, 1984; Torres *et al.*, 1984; Czajkowski and Rösler, 1986; Lyra, 1986; Troncoso, 1986; Palma-Heldt, 1987; Rohn *et al.*, 1987; Tokarski *et al.*, 1987; Li and Song, 1988; Torres and Lemoigne, 1988; Li and Shen, 1989; Torres and Meon, 1990; Li, 1992; 1994;

Zhou and Li, 1994a/b; Zhang and Wang, 1994; Duan and Cao, 1998; Dutra, 1989a; Poole *et al.*, 2001). The King George Island flora has been used to reconstruct West Antarctic palaeoclimatic and vegetation trends during the Tertiary (Birkenmajer and Zastawniak, 1989a, 1989b; Birkenmajer, 1997; Askin, 1992). A decrease in thermophilic taxa, combined with a gradual reduction in diversity of the KGI flora that culminated in Upper Oligocene extinction, was interpreted in terms of a climatically-controlled vegetation trend (Birkenmajer and Zastawniak, 1989; Askin, 1992; Birkenmajer, 1997). This was recognised in the fossil record as a transition from diverse Eocene angiosperm assemblages, such as the Fossil Hill flora (Birkenmajer and Zastawniak, 1989a, 1989b; Li, 1994), to species poor *Nothofagus* Blume, pteridophyte and conifer dominated assemblages, like the Upper Oligocene Dragon Glacier and Mt. Wawel floras from Point Hennequin (Figure 1.1c) (Zastawniak, 1981; Zastawniak *et al.*, 1985).

Recent studies and BAS field collections (Figure 1.1c) support Zastawniak *et al.*'s (1985) interpretation of the Mt. Wawel flora as a low diversity *Nothofagus*-pteridophyte-conifer assemblage. However, the Dragon Glacier flora actually comprises a diverse assemblage of angiosperm morphotypes with pteridophyte and conifer components (Hunt and Poole, submitted). In addition, new palaeoenvironmental models proposed for floras from King George Island suggest that changes in the diversity of plant assemblages may instead be interpreted in terms of a dynamic plant community in various states of succession (Poole *et al.*, 2001).

These opposing models of a climatic or disturbance control on vegetational composition are not necessarily mutually exclusive. Undisturbed vegetation should reflect a true palaeoclimatic signal and even disturbed, low diversity vegetation must comprise plants that grow in the climatic range specific to the locality in consideration. Quantitative and qualitative palaeoclimate data can therefore be obtained from the King George Island floras, provided that the palaeoecological setting of the floras is understood.

Dingle and Lavelle (1998a, 1998b) defined two major glacial intervals in West Antarctica: The Polonez (~30 Ma) and Melville (~23 Ma) glaciations with the single intervening Wawel Interglacial. Their interglacial interpretation was based largely on the absence of coeval glacial deposits and the presence of the supposed low diversity Upper Oligocene Dragon Glacier and Wawel floras from Point Hennequin (Figure 1.1c) (Zastawniak, 1981; Zastawniak *et al.*, 1985) but previous K-Ar age data and $^{40}Ar/^{39}Ar$ dating undertaken during this study suggests an Eocene age for the sequence (Smellie *et al.*, 1984), rather than the Upper Oligocene age proposed by Birkenmajer *et al.* (1983).

In summary, previous models of climate and vegetation history need to be revised in light of new plant collections and dynamic vegetation models. Moreover, a large body of data has been

produced since the publication of the review papers of Birkenmajer and Zastawniak (1989a, 1989b) and Askin (1992) that needs collating (e.g. Cao, 1994; Li, 1994; Duan and Cao, 1998) and none of these studies include the large but essentially unpublished British Antarctic Survey plant collections. Additionally, the K-Ar dating of certain sequences and floras needs to be re-examined and these models do not take into account the strontium isotope stratigraphy of Dingle and Lavelle (1998a, 1998b) and its implications for climatic trends. In the broader context, improved constraint of the Tertiary high latitude floras provides new information for Tertiary palaeoclimatic reconstructions globally.

1.2 Synopsis

In light of the discussion above, the aim of the research presented in this thesis was to provide answers to some or all of the following points:

- What age are the main plant-bearing sequences on King George Island, for example the Dragon Glacier flora, and how does this affect climate and vegetation models?
- What is the taxonomic composition of the King George Island flora and how does this compare with contemporaneous South Hemisphere floras?
- What sedimentary and taphonomic palaeoenvironments are present on King George Island and how does this affect vegetation models?
- What palaeoclimatic data may be derived from the King George Island flora?
- Is climate or disturbance the main control on vegetational composition and diversity and can this be distinguished in the fossil record of King George Island?

In **Chapter 2** these questions are considered in a review of the geological background of the Tertiary King George Island flora. K-Ar and $^{40}Ar/^{39}Ar$ geochronological data is presented in **Chapter 3** and the new ages of the fossil floras are assessed in terms of data quality and their impact on stratigraphic and climatic models. **Chapter 4** summarises sedimentary data that is the basis for palaeoenvironmental reconstructions. Taphonomic data and presence-absence data from Chapters 6 – 9 is presented in **Chapter 5.** The implications for climate and vegetation models are considered. In **Chapters 6 - 9** the plant fossil assemblages are grouped into morphotypes and their taxonomic affinities are discussed with reference to modern and fossil plant records. Palaeoclimatic analyses based on these morphotype groupings are presented in **Chapter 10** and results from different methods e.g. Nearest Living Relative, leaf margin analysis and CLAMP analyses are compared. **Chapter 11** discusses the data from previous chapters, comparing the KGI flora with contemporaneous plant fossil assemblages to provide an overall reconstruction for King George Island and, where appropriate, the Antarctic Peninsula, Antarctica and the Southern Hemisphere during the Cenozoic. Finally, **Chapter 12** summaries the main conclusions of the thesis.

Chapter 2 Geological and palaeoenvironmental background

2.1 Introduction

Chapter two introduces the materials and their localities described in this thesis. The Tertiary climate and vegetation history of Antarctica is discussed, in order to define the palaeoenvironmental and palaeoclimatic context of the King George Island floras. Previous palaeoenvironmental research on King George Island is reviewed in terms of the geological and palaeogeographical setting of KGI with respect to the Antarctic Peninsula. As part of the South Shetland Islands magmatic arc, KGI has a long history of active volcanism, resulting from subduction on the western margin of the Antarctic continent. The strata of KGI are therefore dominated by volcanic and volcaniclastic deposits.

2.2 Materials

Field collections, mapping and logging were undertaken at Point Hennequin (62°7'S 58°24'W) and Fildes Peninsula (62°12'S 58° 53'W) during the 1999 summer field season and a total of 36 plant bearing localities were studied (Figure 2.1, Figure 2.2, Table 2.1, Appendix I). Normal collection strategies were limited by the scattered nature of the moraine blocks and the general lack of *in-situ* plant material. Fossil material was collected on the basis of preservation and on the range of material preserved. The collections are therefore considered to represent the best possible range of diversity of material, although collection bias cannot be ruled out. The majority of sites yielded only fragmentary leaf or silicified wood remains but the Fossil Hill and Collins Glacier sequences on Fildes Peninsula and the Dragon Glacier moraines at Point Hennequin yielded abundant impression and carbonised leaf fossils and silicified wood (Appendix Table I.1). Leaf material was supplemented by collections from previous BAS expeditions (Table 2.2). Geochronological samples were taken from Fossil Hill and geochronological samples previously collected by JL Smellie (BAS) from Vaureal Peak and Point Hennequin were also used in this study [All material is deposited at the British Antarctic Survey, Cambridge].

Sample numbers follow the BAS reference system. The prefix 'P.' indicates the South Shetland Islands, followed by a station number and sample number, for example 'P.3001.1' is specimen one

from field site P.3001. Additional numbering indicates a rock slab with multiple specimens 'P.3001.1.1, P.3001.1.2'. Lettering indicates part and counterpart(s) e.g. 'P.3001.1a, P.3001.1b'. Old collections include previous station prefixes such as G for localities in Admiralty Bay (Figure 2.1). ? indicates a specimen from a known area without a suffix e.g. G.53. Brackets indicate an original figure number made by Barton (1965) , e.g. G.53(27) is figured specimen 27 from locality G.53. U and L as suffixes indicate Upper and Lower parts of the horizon e.g. P.3031.4U/4L.

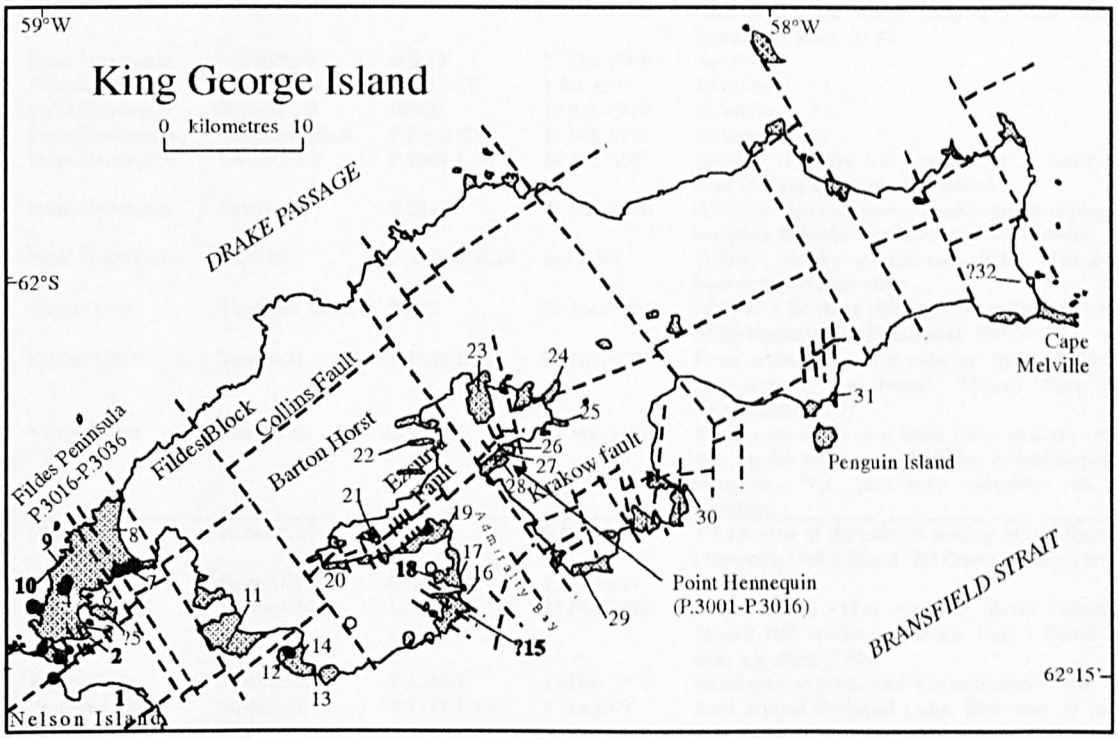

Figure 2.1. Locality map of King George Island, showing Tertiary plant-bearing localities. Bold numbering indicates Cretaceous localities. Grey, stippled areas indicate areas of outcrop. Black circles indicate volcanic centres, unfilled circles are inferred centres. Locality names are defined in Table 2.1. Structural data according to Birkenmajer (1983).

Locality	Name	Locality	Name	Locality	Name
1	Rip Point	11	Barton Peninsula	22	Admiralen Peak
2	Half Three Point	12-14	Potter Peninsula	23	Keller Peninsula
3	Great Wall Base	15	Paradise Cove	24	Precious Peaks
4	Fossil Hill	16	Block Point	25	Ullman Ridge
5	Ardley Island	17	Sphinx Hill	26-28	Point Hennequin
6	Rocky Cove	18	Zamek	29	Vaureal Peak
7	Suffield Point/Profound Lake	19	Petrified Forest Creek	30	Lions Rump
8	Collins Glacier	20	Platt Cliffs/Cytadela	31	Three Sisters Point
9	Skua Bay	21	Dufayel Island	32	Cape Melville
10	Winkel Point				

Table 2.1. Locality names and numbers referred to in Figure 2.1.

	Area	Collector	Locality	Date	Additional Information
Warzawa Block	Platt Cliffs	Bibby JS	G.47.1-16	30 Jan 1958	Equivalent to the Cytadela flora (Birkenmajer and Zastawniak, 1989a)
	Platt Cliffs	Bibby JS	G.50.1-22	30 Jan 1958	Composition of flora, preservation style and sediment differs from other Platt Cliffs material
	Platt Cliffs	Hobbs GJ	G.309.1-19	14 Jan 1959	Same as G.319, from third waterfall of the largest melt stream descending cliffs. Equivalent to Cytadela flora (Birkenmajer and Zastawniak, 1989a)
	Platt Cliffs	Hobbs GJ	G.319.1-20	17 Jan 1959	Same as G.309, western end of Platt Cliffs
	Point Hennequin	H-Smith, G	G.9.3	1 Jan 1949	North and north-north west of Mt. Wawel, from the coast to 0.5 km inland. Dragon Glacier flora of Zastawniak *et al.* (1985)
	Point Hennequin	H-Smith, G	G.9.13	27 Dec 1948	As above
	Point Hennequin	H-Smith, G	G.9.17-21	1 Jan 1949	As above
	Point Hennequin	H-Smith, G	G.9.25	19 Feb 1949	As above
	Point Hennequin	Thomson MRA	P.236.1-25	12 Feb 1975	As above
	Point Hennequin	Davies RES	P.1404.1-30	14 Jan 1976	Locality as above but separate unit – Smok Hill flora of Hunt and Poole (submitted)
	Point Hennequin	Smellie JS	P.2810	22 Mar 1996	As G.9.3. Also includes complete geochronological sampling from the sequence used in this study.
	Point Hennequin	Hunt RJ	P.3001-P.3016	Jan 1999	H-Smith locality, summit area of Mt. Wawel and base of Mt. Wawel cliffs
	Potter Cove	Thomson MRA	P.232	25 Jan 1975	NNE of 3 Brothers Hill (e.g. Potter Peninsula flora of Birkenmajer and Zastawniak, 1989a)
	Sphinx Hill*	Smellie JL	P.1249.1-16	3 Mar 1976	From moraine on SW side of Sphinx Hill (not discussed in this study). ?Zamek flora (e.g. Zastawniak, 1994)
	Vaureal Peak	Smellie JS	P.2799	07 Mar 1996	South side of Vaureal Peak three quarters of the way up the main scree. Includes geochronological sampling. Not previously described in the literature.
Fildes Block	Fossil Hill	Barton CM	G.439.5	6 Jan 1960	1.5 km west of the isthmus joining Ardley Island to Peninsula. Unit 4 Fossil Hill flora e.g. Shen (1994)
	Fossil Hill	Barton CM	G.458.1-9	7 Feb 1960	As above
	Fossil Hill	Barton CM	G.473.1-2	24 Feb 1960	Large stream ~1km south of above collection. ?Fossil Hill southern sections. Unit 2 Fossil Hill flora e.g. Shen (1994)
	Rocky Cove	Smellie JL	P.1130.1	14 Dec 1975	Sediments on south west side of Suffield Point
	Profound Lake*	Smellie JL	P.1174.1-13	4 Jan 1976	Area around Profound Lake, 2km west of above P.1130
	Fossil Hill	Davies RES	P.933.2	9 Dec 1975	Area west of Ardley Island tombolo. Lithology equivalent to P.3034 and P.3036. Unit 2 Fossil Hill flora of e.g. Shen (1994)
	Fossil Hill	Davies RES	P.935.1-29	10 Dec 1975	As above
	Norma Cove area	Davies RES	P.207	14 Jan 1975	Moraine to NNE of Suffield Point
	Rocky Cove	Thomson MRA	P.212	15 Jan 1975	Rocky Cove same locality as P.3029 and P.3035 and collections by Shen (1994)
	Fildes Peninsula	Hunt RJ	P.3017-P.3036	Feb-Mar 1999	Fossil Hill (including geochronological samples), Collins Glacier and Rocky Cove.
Barton Horst	Admiralen Peak*	Hobbs GJ	G.328.1	28 Jan 1959	Sediments beneath a thick lava flow
	Admiralen Peak*	Hobbs GJ	G.329.1-13	28 Jan 1959	See above
	Admiralen Peak*	Hobbs GJ	G.330.1-34	29 Jan 1959	See above
	Barton Peninsula	Armstrong D	P.2145	21 Feb 1993	South west coast of Barton Peninsula (D. Armstrong, unpublished notes). Cliff section above beach, ~ 600 m east of 'Chinstrap Point'. Same locality as collections by Tokarski *et al.* (1987) and Del Valle (1984).
	Dufayel Island	Bibby JS	G.53.1-32	31 Jan 1958	East end of Dufayel Island, same location as Birkenmajer and Zastawniak (1986)
	Dufayel Island	Hobbs GJ	G.312.1-16	15 Jan 1959	See above

Table 2.2. Locality data for the British Antarctic Survey collection of King George Island floras and geochronological samples. Structural divisions according to Birkenmajer (1982). *Flora not discussed in this study.

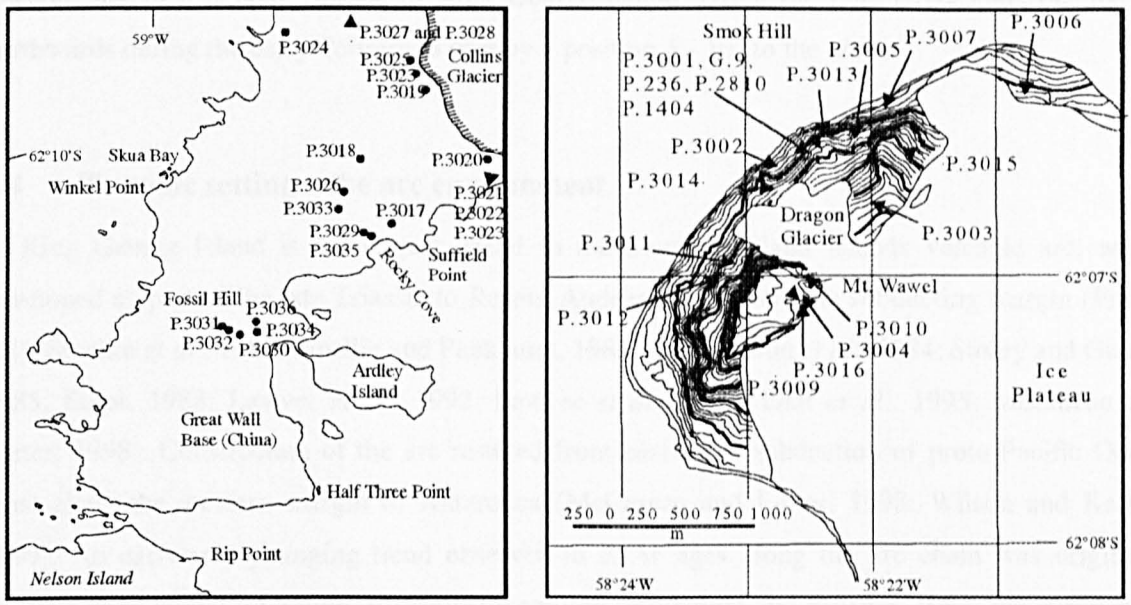

Figure 2.2. Locality maps showing location of material collected during this study, A) Fildes Peninsula and B) Point Hennequin (also includes data from previous BAS collections).

Sedimentary thin sections were studied using transmitted light microscopy. Thin section and field descriptions follow standard sedimentary (Pettijohn, 1975) and volcaniclastic terminology (Fisher and Schmincke, 1984; Cas and Wright, 1987). The term volcaniclastic is used to refer to any clastic sediment with a volcanic component that has been transported and deposited by any mechanism in any environment (Fisher, 1966). Tuffaceous refers to sediment that has both pyroclastic and reworked elements.

2.3 Palaeogeography

East and West Antarctica attained their present day positions with respect to each other by the Late Cretaceous (~ 110 Ma) and, in terms of absolute geography, have experienced little change since that time (Figure 2.3) (Lawver *et al.*, 1992). Wise *et al.* (1991) suggest that a significant shallow water seaway separated East and West Antarctica in the Early Tertiary. The Antarctic Peninsula itself consisted of several landmasses (Lawver *et al.*, 1992) and as such is likely to have experienced a milder maritime climate rather than the continental climate of East Antarctica.

King George Island situated at a latitude of 62° S is approximately coincident with its Tertiary position (Figure 2.3) (Lawver *et al.*, 1992). Tasmania and south eastern Australia during the Palaeocene (60 Ma), and Tasmania in the Eocene and Early Oligocene, occupied approximately the same latitude as KGI. By the Late Oligocene both Tasmania and Australia had moved to more mid latitude positions and continued to migrate northwards (Lawver *et al.*, 1992). Southern New

Zealand shared a similar latitude to King George Island during the Late Cretaceous but moved northwards during the early Tertiary to occupy a position 5 - 10° to the north.

2.4 Tectonic setting – the arc environment

King George Island is the largest island in the South Shetland Islands volcanic arc, which developed as part of the late Triassic to Recent Andean-West Antarctic subducting margin (Figure 2.4) (Smellie *et al.*, 1980; Smellie and Pankhurst, 1983; Farquharson *et al.*, 1984; Storey and Garret, 1985; Elliot, 1988; Lawver *et al.*, 1992; Lawver *et al.*, 1995; Leat *et al.*, 1995; McCarron and Larter, 1998). Construction of the arc resulted from eastwards subduction of proto-Pacific Ocean crust along the western margin of Antarctica (McCarron and Larter, 1998; Wilson and Kelley, 1999). An eastwards younging trend observed in K-Ar ages along the arc chain was originally interpreted as lateral migration of magmatic activity (Pankhurst and Smellie, 1983) but subsequent $^{40}Ar/^{39}Ar$ dating of dike complexes on Livingston Island reveals five distinct phases of magmatic activity in the mid-Late Cretaceous (~108-74Ma), the Early Eocene at ~52Ma, at 51-45Ma, in the Middle-Late Eocene (44-36Ma) and finally during the Oligocene (31-29Ma) (Willan and Kelley, 1999).

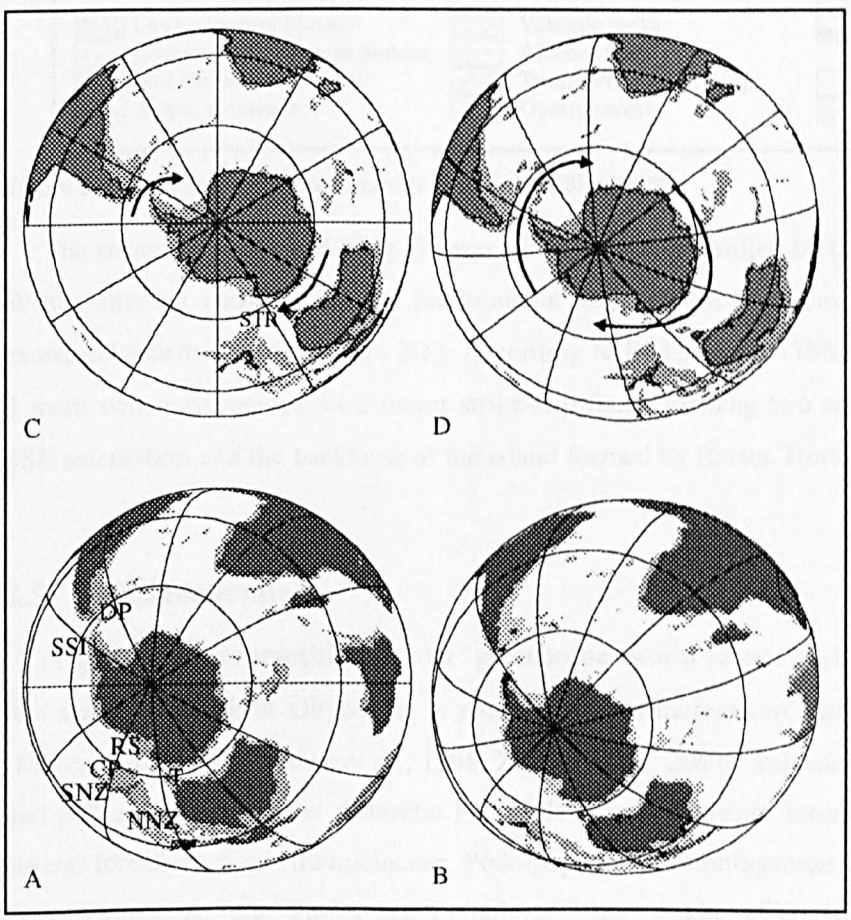

Figure 2.3. Palaeogeographic maps of the Southern Hemisphere for the Palaeocene to Miocene. A, Palaeocene 60 Ma. B, Eocene 50 Ma. C, Oligocene 33.5 Ma, showing limited ocean circulation around Antarctica. D, Miocene 20 Ma, showing fully developed Circum-Antarctic deep water circulation. (Reconstructions produced by Roy Livermore (BAS) with modifications by D Cantrill (BAS). DP – Drake Passage, NNZ/SNZ, – north/south New Zealand, STR – South Tasman Rise, T – Tasmania.

An east-west transect of the Antarctic Peninsula (Figure 2.4) shows the fore-arc position of the South Shetland Islands during the Tertiary (Elliot, 1998). Much of the magmatic arc, that formed the spine of the Antarctic Peninsula, is absent due to uplift and erosion (Elliot, 1998). Uplift of the arc also resulted in back arc subsidence and the accumulation of 5-6 km thickness of marine sediments in the James Ross and Larsen Basins (Pirrie *et al.*, 1992). The marine sediments preserve an abundant palaeoflora that records extensive forest coverage on the nearby Antarctic Peninsula (Hayes, 1999). On King George Island, arc volcanism is expressed by a basaltic to andesitic volcanic sequence up to 3500 m thick (Birkenmajer *et al.*, 1991). The lavas are interbedded with tuffs and rare dacites and have a low-K, transitional calc-alkaline to island arc tholeiite chemistry (Pankhurst and Smellie, 1983; Smellie *et al.*, 1984; Birkenmajer *et al.*, 1991).

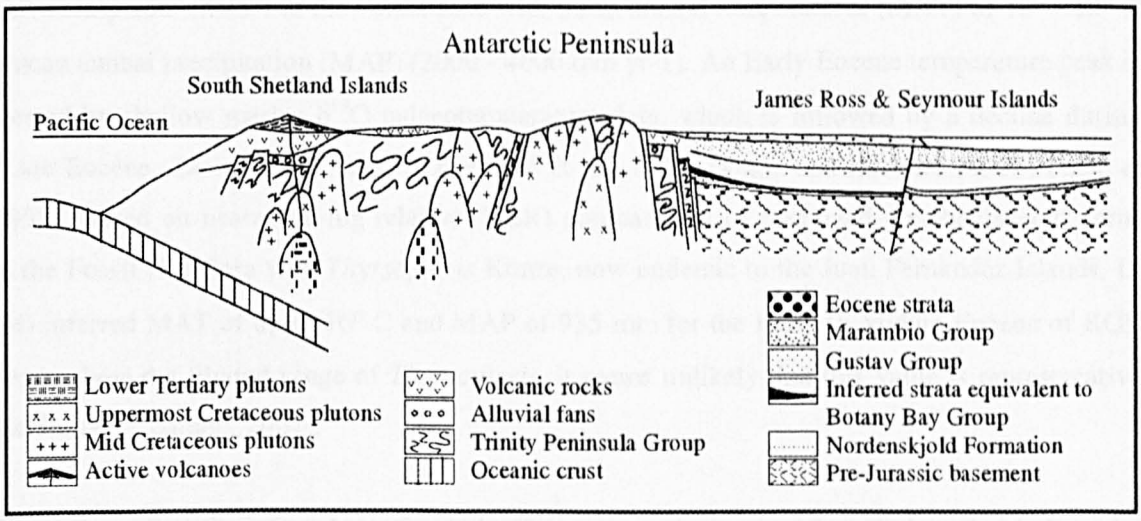

Figure 2.4. Cross section of the Antarctic Peninsula (Elliot, 1998).

The structural history of King George Island is also controlled by the tectonics of the subducting West Antarctic margin with the predominant deformation style comprising brittle strike slip or extensional deformation (Figure 2.1). According to Birkenmajer (1983) KGI may be separated into 3 main structural regions with major strike-slip faults forming two sets in ENE-WSW and NNW-SSE orientation and the backbone of the island formed by Barton Horst.

2.5 Palaeoclimate

A global climate transition from a 'greenhouse' world to an 'ice-house' world, initiating in the late Eocene to earliest Oligocene, is recorded by an increase in marine $\delta^{18}O$ values (Figure 1.2) (Miller *et al.*, 1987; Wilson *et al.*, 1998; Zachos *et al.*, 2001). Palaeocene to ?Oligocene leaf, wood and pollen floras from the Antarctic Peninsula record elements associated with modern temperate austral forests such as Araucariaceae, Podocarpaceae, Nothofagaceae, Cunoniaceae, Lauraceae and some Proteaceae (e.g. Torres and Lemoigne, 1988; Askin, 1992; Li, 1992, 1994; Zhou and Li,

1994*a*, Markgraf *et al.*, 1996). Warm temperate alongside relatively tropical taxa such as Gunneraceae, Monimiaceae and Sterculiaceae, are also recognised in these floral assemblages (Orlando, 1964; Askin, 1992; Dettmann, 1989). The composition of the vegetation suggests warm to cool, moist climates and an absence of freezing conditions is indicated by frost sensitive taxa (Askin, 1992; Askin and Spicer, 1995).

A cooling event is apparent in the Late Cretaceous to mid-Palaeocene on Seymour Island, with mean annual temperatures of 8-15° C and frostless climates (Askin, 1992; Dingle and Lavelle, 1998b). Foliar evidence from the Dufayel Island flora on King George Island (Birkenmajer and Zastawniak, 1986) and from Seymour Island (Dusén, 1908; Case, 1988) supports a prevailing cool to warm temperate climate in the Palaeocene with mean annual temperatures (MAT) of 10° - 12° C and mean annual precipitation (MAP) (2000 - 4000 mm yr-1). An Early Eocene temperature peak is suggested by shallow marine $\delta^{18}O$ palaeotemperature data, which is followed by a decline during the Late Eocene (Zachos et al., 1993; Ditchfield et al., 1994; Dingle and Lavelle, 1998b; Pirrie et al.,1998). Based on nearest living relative (NLR) comparisons of fossilized gleicheniaceous ferns from the Fossil Hill flora with *Thyrsopteris* Kunze, now endemic to the Juan Fernandez Islands, Li (1994) inferred MAT of up to 16° C and MAP of 935 mm for the Early to Middle Eocene of KGI, however given the limited range of *Thyrsopteris*, it seems unlikely that this value is representative (R Askin, pers., comm., 2002).

Climate cooling is inferred in the Late Eocene on the basis of declining floral diversity (Birkenmajer and Zastawniak, 1989a, 1989b; Askin, 1997; Birkenmajer, 1997) and decreasing marine palaeotemperatures recorded by an increase in $\delta^{18}O$ values from molluscan faunas (Ditchfield *et al.*, 1994; Dingle and Lavelle, 1998b; Zachos *et al.*, 2001). On KGI earliest Oligocene low diversity *Nothofagus* fern-bush communities, similar to those on the modern Gough and Kerguelen islands, suggest MAT of c. 11° - 15° C and MAP 1220 – 3225 mm (Birkenmajer and Zastawniak, 1989a), although these MAT values seem high when compared with Eocene estimates.

Birkenmajer (1987; 1988; 1990; 1997) recognised four glacial intervals in the strata of King George Island: Krakow (Eocene, 52 - 50 Ma), possible alpine glaciation; and Polonez (Oligocene, 32 - 30 Ma); Legru (Oligocene, 30 - 26 Ma) and Melville (Miocene, 22 - 20 Ma), which he interpreted as West Antarctic-wide phenomena. Dingle *et al.* (1997) and Dingle and Lavelle (1998a, b) redated the sequences using strontium isotope stratigraphy and found evidence for only two major glacial phases, the Polonez (~30 Ma) and Melville (~23 Ma), with a single intervening Wawel Interglacial. The Wawel Interglacial was based on the absence of coeval glacial deposits and

the presence of the supposed low diversity Upper Oligocene Dragon Glacier and Wawel floras from Point Hennequin (Figure 2.1) (Birkenmajer, 1981; Birkenmajer *et al.*, 1983; Zastawniak, 1981; Zastawniak *et al.*, 1985). The similarity of this *Nothofagus*-podocarp assemblage to modern Patagonian-Magellanian forests led Birkenmajer and Zastawniak (1989a) to infer cool temperate climates with mean annual temperatures of 5 - 8° C and mean annual precipitation 600 - 4300 mm for the flora. The age of the sequence is debated and may however be Eocene and thus pre-glacial (Smellie *et al.*, 1984).

No floras have been reported for the Miocene-Pliocene post-Wawel Interglacial period in the Antarctic Peninsula (Birkenmajer, 1997; Dingle and Lavelle, 1998b). In East Antarctica the same trends of decreasing diversity from the Eocene into the Oligocene are recorded by palynological data from the Eocene McMurdo Sound erratics (Askin, 2000) to the Oligocene – Quaternary CIROS-1 drill core and the Cape Roberts drill cores (Cape Roberts Science Team, 1998; Raine, 1998; Terra Antartica Initial Report on CRP-2/2A, 1999) and supports interpretations of gradual cooling towards the Eocene-Oligocene boundary (Zachos *et al.*, 2001). The Eocene-Oligocene transition began at ~34.5 Ma marked by pronounced ocean cooling (Wilson *et al.*, 1998). Development of a major East Antarctic ice-sheet at ~28.5 Ma (Zachos *et al.*, 2001) is interpreted by Wilson *et al.*, (1998) as the result of circumpolar current initiation and thermal isolation of Antarctica or as a result of Transantarctic Mountain uplift. However, Lawver and Gahagan (1998) considered that although the opening of both the Austral-Antarctic and South America-Antarctic gateways led to a drop in seawater $\delta^{18}O$ values, and cooler ocean temperatures, closure of equatorial gateways had a greater impact on climate.

Terrestrial East Antarctic data are sparse from the Oligocene onwards, and there has been much dispute about the *in-situ* nature of the sediments (Hill and Truswell, 1993). Sparse pollen and spore assemblages from the lower Miocene section of CRP-1 have been interpreted as a possible shrub phase *Nothofagus*-podocarp-Proteaceae vegetation, with July mean temperatures 7° C, based on NLR comparisons (Raine, 1998). The ?Pliocene Sirius flora is the youngest terrestrial macroflora in the Transantarctic Mountains and is interpreted as tundra-like vegetation, with dwarf trees that developed a prostrate habit (Francis and Hill, 1996). Mean annual temperatures are considered to be on the order of -12° C (Francis and Hill, 1996), with warmer summer temperatures of >5° C to account for the growth and reproductive effort observed in *N. beardmorensis* (Hill *et al.*, 1996). Winter temperatures are not thought to have dropped below –22° C, since no extant *Nothofagus* sp., can survive below this temperature. based on NLR comparisons with modern the alpine *Nothofagus gunnii* (Francis and Hill, 1996; Hill *et al.*, 1996).

KGI - families	Present in VRF?	Reference to palaeobotanical literature
Sphenophytes		
Equisetum	present	Barton 1964; Dutra 1989*a*; R Hunt (work in progress)
Pteridophytes		
Adiantaceae	present	Cao 1992
Aspleniaceae	present	Troncoso 1986; Li & Shen 1989
Blechnaceae	present	Troncoso 1986; Birkenmajer & Zastawniak 1989
Cyatheaceae	present	Lyra 1986; Torres & Meon 1990; Cao 1992; Li 1992; Zhou & Li 1994*b*, Duan & Cao 1998
Dennstaedtiaceae	present	Stuchlik 1981
Dicksoniaceae	present	Troncoso 1986; Li & Shen 1989; Cao 1992; Li 1992; Zhou & Li 1994*b*
Gleicheniaceae	present	Stuchlik 1981; Li & Shen 1989; Cao 1992, 1994; Li 1994; Zhou & Li 1994*b*; Duan & Cao 1998
Hymenophyllaceae	present	Stuchlik 1981
Lophosoriaeceae	present	Torres & Meon 1993; R Hunt (work in progress)
Osmundaceae	present	Li & Shen 1989; Li 1992; Cao 1992, 1994; Zastawniak 1994; Zhou & Li 1994*b*
Polypodiaceae	present	Stuchlik 1981; Cao 1992, 1994; Duan & Cao 1998; Hunt & Page (work in progress)
Salviniaceae	present	Stuchlik 1981
Schizeaceae	present	Stuchlik 1981
Lycophytes		
Selaginellaceae	present	Cao 1992
Cycadophytes		
Zamiaceae	absent	Li 1994; Zhou & Li 1994*a*
Coniferophytes		
Araucariaceae	present	Barton 1964; Lucas & Lacey 1981; Davies 1982; Torres 1985; Troncoso 1986; Palma-Heldt 1987; Torres & Lemoigne 1988; Torres & Meon 1990; Hee & Soon 1991; Cao 1992, 1994; *Zastawniak 1994*; Zhou & Li 1994*a*
Cupressaceae	present	Orlando 1963, 1964; Torres *et al.* 1984; Torres 1985; Czajkowski & Rosler 1986; Li & Shen 1989; Li 1992; Zhou & Li 1994*a*;
Podocarpaceae (including *Phyllocladus*)	present	Zastawniak 1981; Zastawniak *et al.* 1985; Torres 1985; Lyra 1986; Troncoso 1986; Palma-Heldt 1987; Torres & Lemoigne 1988; Torres & Meon 1990; Li & Shen 1989; Li 1992; Zhang & Wang 1994; Cao 1992, 1994; *Zastawniak 1994*; Zhou & Li 1994*a*; Duan & Cao 1998,
Angiosperms		
?Araliaceae	present	Li 1992, 1994
?Caesalpinaceae	absent	Troncoso 1986; *Birkenmajer & Zastawniak* 1986
?Hydrangeaceae	present	Czajkowski & Rosler 1986
?Malvaceae	present	Dutra & Batten 2000
?Poaceae	present	Stuchlik 1981; Birkenmajer & Zastawniak 1986; Troncoso 1986; Palma-Heldt 1987
Anacardiaceae	present	*Zastawniak 1981*; Czajkowski & Rosler 1986; Li & Shen 1989; Li 1992, 1994
Chusquea	present	Stuchlik 1981
Cochlospermaceae	absent	Zastawniak *et al.* 1985; *Birkenmajer & Zastawniak 1986*
Cunoniaceae (inc. Eucryphiaceae)	present	Torres 1985; Czajkowski & Rosler 1986; Li & Shen 1989; Zhang & Wang 1994 but see Poole *et al.* 2000
Dilleniaceae	absent	Orlando 1964; *Birkenmajer & Zastawniak 1986*; Zastawniak 1994
Gunneraceae	present	Torres & Meon 1990
Icacinaceae	present	Troncoso 1986
Lauraceae	present	Orlando 1964; Del Valle *et al.* 1984; *Birkenmajer & Zastawniak 1986*; Troncoso 1986
Loranthaceae	present	Cao 1992
Melastomataceae	absent	Li & Shen 1989; Li 1992, 1994
Monimiaceae	present	Orlando 1964; Del Valle *et al.* 1984; Troncoso 1986; Birkenmajer & Zastawniak 1989
Myricaceae	present	*Czajkowski & Rosler 1986*; Rohn *et al.*, 1987; Troncoso 1986; *Dutra 1989a*
Myrtaceae	present	Orlando 1964; Czajkowski & Rosler 1986; Palma-Heldt 1987; Cao 1992; Li 1994; Zastwaniak 1994
Nothofagaceae	present	Barton 1964; Zastawniak 1981; Del Valle *et al.* 1984; Torres 1984, 1985; Zastawniak *et al.* 1985; Czajkowski & Rosler 1986; Lyra 1986; Troncoso 1986; *Tokarski et al. 1987*; Torres & Lemoigne 1988; Dutra 1989*a* 1989*b*; Li & Shen 1989; Cao 1992, 1994; Li 1992, 1994; Zastawniak 1994; Zhang & Wang 1994; Duan & Cao 1998; Dutra & Batten 2000
Proteaceae	present	Orlando 1964; Czajkowski & Rosler 1986; *Troncoso 1986*; Dutra 1989*b*; Li & Shen 1989; Torres & Meon 1990; Cao 1992; Li 1992, 1994;
Rhamnaceae	present	Stuchlik, 1981; Zastawniak *et al.* 1985; Dutra 1989*a*, *1989b*
Sapindaceae	absent	*Zastawniak 1981*; Troncoso 1986; Dutra 1989*a*
Sterculiaceae	present	Orlando 1964; Del Valle *et al.* 1984; Czajkowski & Rosler 1986; Birkenmajer & Zastawniak 1986; Li & Shen 1989; Shen 1994
?Verbenaceae	present	Birkenmajer & Zastawniak 1986

Table 2.3. Summary of plant families present in the King George Island palaeoflora (Poole *et al.*, 2001). The degree of similarity with the modern Valdivian rain forests is marked by simple presence or absence data. Italicised names indicate uncertainty in the identifications expressed by the authors.

2.6 Tertiary vegetation history of the Antarctic Peninsula

Leaves, wood and pollen are preserved in abundance in the Late Cretaceous to Tertiary fossiliferous strata of the Antarctic Peninsula (Table 2.3) and are accompanied by an increasingly well defined macrofauna (Covacevich and Lamperein, 1972; Covacevich and Rich, 1982; Case *et al.*, 1988; Case, 1989; Li and Zhen, 1994; Vizcaino *et al.*, 1997). Early research by Dusén (1908) and Gothan (1908) highlighted the diversity of material preserved in the Antarctic Peninsula but the 'picture matching' techniques applied to studies of leaf fossils during this period (e.g. Dilcher, 1973, 1974) mean that many of the taxonomic comparisons are doubtful.

2.6.1 Palaeocene floras

On King George Island the Dufayel Island and Barton Peninsula floras are of probable Palaeocene age and comprise dicotyledonous leaves, including *Nothofagus* sp. (Del Valle *et al.*, 1984; Tokarski *et al.*, 1987; Birkenmajer and Zastawniak, 1986). Birkenmajer and Zastawniak (1986) described a diverse assemblage of dicots from Dufayel Island, including possible Cochlospermaceae, Dilleniaceae, Leguminosae, Sapindaceae, Sterculiaceae and Verbenaceae. Other leaf types included myrtaceous and laurophyllous specimens, possible fern fragments and a fragmentary monocot. The composition of the assemblage was considered to be similar to that of the extant Valdivian rainforests of southern Chile (Birkenmajer and Zastawniak, 1986). Fluvial sediments of the Barton Peninsula flora locality also comprise *Nothofagus* sp. but other angiosperms are present. These were described (although not illustrated) by Del Valle *et al.* (1984) as *Ocotea menendezi* Hunicken, *Nectandra prolifica* Berry, *Laurelia guinazui* Berry, *Sterculia washburni* Berry and *Nothofagus* cf. *densinervosa* Dusén. Tokarski *et al.* (1987) described lobed leaves of *Sterculia* L./*Cochlospermum* Kunth type from the same site, in addition to indeterminable angiosperms. Fragments of wood with araucariaceous affinity are also present (Hee and Soon-Keun, 1991).

Similar leaf assemblages were described by Dusén (1908) and Case (1988) from the Upper Palaeocene Cross Valley Formation on Seymour Island, which include diverse ferns and angiosperms in addition to some coniferous taxa. According to Dusén (1908) the flora comprises cool temperate taxa such as Cunoniaceae, *Nothofagus*, Proteaceae (*Lomatia* Brown and *Knightia* Solander ex. Brown) and Winteraceae, combined with more subtropical taxa including Monimiaceae and Melastomataceae. These identifications are supported by recent studies of wood floras from the James Ross Basin, which have identified abundant Nothofagaceae, with Monimiaceae and Cunoniaceae as well as Illiciaceae, Atherospermataceae, Lauraceae (*Sassafras* Nees & Eberm.) (e.g. Francis, 1991; Poole and Francis, 1999; Poole *et al.*, 2000b; Poole and

Cantrill, 2001; Poole and Gottwald, 2001; Poole *et al.*, 2000c; Poole, in press). Cranwell (1959) and Case (1988) both suggested that the vegetation comprised a diverse *Nothofagus* flora with subsidiary angiosperms, podocarps and *Araucaria* Juss. In addition, angiosperm pollen includes the Cruciferae, Myrtaceae, Proteaceae (aff. *Lomatia*) Loranthaceae, Winteraceae (confirmed from the wood flora; Poole and Francis, 2000) and probable Cunoniaceae (cf. *Weinmannia* L.; present in the wood flora; Poole *et al.*, 2000a) or Elaeocarpaceae (Cranwell, 1959).

Palynological analyses of the Lower Palaeocene section of the Lopez de Bertodano Formation on Seymour Island have yielded common cryptogam spores, gymnosperms *Phyllocladidites mawsonii* Cookson ex Couper, podocarps, cycadalean or *Ginkgo* L. pollen, *Araucaria* and *Ephedra* L. (Askin, 1989). Angiosperms are represented by Liliaceae, Aquifoliaceae, Casuarinaceae, Ericales, Gunneraceae, Myrtaceae, Bombacaceae, Nothofagaceae, Loranthaceae, Proteaceae, ?Pedaliaceae.

In the southern portion of the Antarctic Peninsula, on Alexander Island an Early Tertiary flora comprising Nothofagus sp. and other indeterminable pinnately veined dicot leaves is present in the Elgar Uplands (Thomson and Burn, 1977). The size of these leaves > 10 cm may indicate a warm temperate climate (Askin, 1992). Jefferson (1980) also found poorly preserved leaves and pollen of probable *Nothofagus* on nearby Adelaide Island.

2.6.2 Eocene floras

On Fildes Peninsula the Early to Middle Eocene Fossil Hill flora reflects a diverse mixed angiosperm vegetation, including *Sterculia*-type leaves and the form genera *Monimiophyllum antarcticum* Dusén and *Dicotylophyllum duseni* Zastawniak (Czajkowski and Rosler, 1986; Troncoso, 1986; Birkenmajer and Zastawniak, 1989b; Cao, 1992; Li, 1994; Zhou and Li, 1994a/b). According to Li (1992, 1994) there are a total of 20 angiosperm morphotypes present in the flora, including *Lomatia mirabilis* (Dusén) Li (Proteaceae), *Rhoophyllum nordenskjoeldi* Dusén (Anacardiaceae), *Myrtiphyllum* Dusén (Myrtaceae), *Pentaneurum dusenii* (Zastawniak) Li (Melastomataceae) (see also Li and Song, 1988; Li and Shen, 1989). The ?Caesalpinaceae, Dilleniaceae, Icacinaceae, Gunneraceae, Monimiaceae, Myricaceae, Sapindaceae are also thought to be present in the flora in addition to the fossil genera *Caldcluvia mirabilis* Dusén and *Hydrangeiphyllum affine* Dusén (Czajkowski and Rosler, 1986; Troncoso, 1986; Rohn *et al.*, 1987; Cao, 1992). The flora has been interpreted as *Nothofagus* poor (Birkenmajer and Zastawniak, 1989a, 1989b), although more recent studies suggest that *N.* sp. are present throughout the entire sequence (Li, 1994; Shen, 1994). Cao (1992) considered the flora to be a Podocarpaceae-Araucariaceae-*Nothofagus* assemblage based on palynological data. The dominant gymnosperms in

terms of numbers are Podocarpaceae (including *Acmopyle* Pilger, *Phyllocladus* Mirbel, *Dacrydium* Sol. ex Forst and *Podocarpus* L'Hérit ex Pers.) but there are also leaves of *Araucaria* Sect. *Eutacta* and cupressoid leaves with affinities to the *Austrocedrus* Florin & Boutelje/*Libocedrus* Endlicher/*Papuacedrus* Li group (Troncoso, 1986; Torres and Meon, 1990; Cao, 1992; Zhou and Li, 1994b; Hill and Brodribb, 1999). Fern genera are represented by the Cyatheaceae, Dicksoniaceae, Gleicheniaceae, Lophosoriaceae, Osmundaceae (Torres and Meon, 1993; Zhou and Li, 1994a).

Orlando (1963, 1964) described a diverse and compositionally similar flora from Ardley Island but other geological descriptions locate the flora at Fossil Hill (Schauer and Fourcade, 1964). The Ardley Island plant beds have never been relocated and it is suggested that the plant locality was mislocated in his original study and should be included with the Fossil Hill flora (T Dutra, pers. comm., 2001).

The Rocky Cove flora (Cao, 1992; Shen, 1994) and the Collins Glacier flora (Zhang and Wang, 1994; Poole *et al.*, 2001) are contemporary Middle Eocene floras that are considered to post-date the Fossil Hill sequence (Smellie *et al.*, 1984; Shen, 1994, 1999). Palynomorph assemblages from Rocky Cove comprise fern and fungal spores (38 %), Podocarpaceae and Araucariaceae (30 %) and *Nothofagus*, Proteaceae and other angiosperms (32 %) (Cao, 1992). Cao (1992) considered the flora to be similar to Eocene palynofloras of South America, Australia and New Zealand. Shen (1994) found *Nothofagoxylon antarcticus* Torres and fragments of some fossil leaves in the Rocky Cove sediments but did not describe any of the collected material. Studies of the Collins Glacier flora, undertaken during the course of this study but not included in this thesis have yielded wood of *Cupressinoxylon* Goeppert, *Podocarpoxylon fildesense* Zhang and Wang, *Caldcluvioxylon* Torres (Zhang and Wang, 1994), two species of *Nothofagoxylon* Gothan and two previously undescribed morphotypes with greatest similarity to modern woods of *Luma* A. Gray (Myrtaceae) and *Eucryphia* Cav. (Cunoniaceae) (Poole *et al.* 2001).

An inferred Early Eocene flora from Block Point in Admiralty Bay was found to contain leaves referred to the Sapindaceae, Myricaceae, Rhamnaceae and five types of *Nothofagus* (Dutra, 1989a). Jagmin (1987) also described *Nothofagoxylon* from this area. Early Tertiary wood of probable Araucariaceae and Podocarpaceae were reported from Keller Peninsula (Lucas and Lacey, 1981). Barton (1961, 1964a/b) described an angiosperm-free Araucariaceae flora of Eocene age (43 ± 4.8 Ma; Birkenmajer *et al.*, 1986) comprising leafy shoots and bark from Admiralen Peak. A single fragmentary angiosperm leaf was found in the flora during the present study, suggesting that the composition of the flora may be taphonomically controlled. Barton (1964b) referred the leaves to

the fossil genus *Araucarites ruei* Sew., from the Kerguelen Islands and to the modern *Araucaria rulei* Muell., a tree that grows at higher altitudes in the New Hebrides. The Middle Eocene Petrified Forest Creek flora is represented by a spore-pollen assemblage that is dominated by ferns (c. 55 - 18 %) and *Nothofagus* (three types; c. 36 - 70 %) with rare Ephedraceae, Gramineae and Rhamnaceae pollen (Stuchlik, 1981). In addition the wood flora comprises *Phyllocladoxylon antarcticum* Gothan, *Araucarioxylon* Kraus sp., and two species of *Nothofagoxylon* (Torres and Lemoigne, 1988), although these have now been synonymised (I Poole, pers. comm., 2001). Cortemiglia *et al.* (1981) suggested that some of the wood fossils from the locality had an intermediate *Fagus* L.-*Nothofagus* character. Birkenmajer and Zastawniak (1989a) mentioned a diverse Middle Eocene moraine and *in-situ* flora from Potter Peninsula, however this flora has yet to be described.

The Cytadela flora (equivalent to the Platt Cliffs G.47/G.309 flora of Bibby and Hobbs; Table 2.2) is considered to be 'Eocene-Oligocene boundary' in age (Birkenmajer and Zastawniak, 1989a). Ferns, including *Blechnum* L. sp., *Nothofagus*-type leaves and other pinnate veined dicots were recorded with ?Podocarpaceae remains (Birkenmajer and Zastawniak, 1989a).

The La Meseta Formation on Seymour Island has a diverse leaf macrofossil assemblage, which has yet to be elaborated. According to Askin (1992) the Eocene palynoflora is enriched in *Nothofagus*, which differs from earlier floras on Seymour Island that were conifer dominated. Askin (1988a; 1997) found evidence for levels of diversity similar to those found in the Palaeocene leaf and wood floras, including Podocarpaceae, Araucariaceae, Nothofagaceae, Proteaceae, Gunneraceae, Myrtaceae, Epacridaceae/Ericaceae, Casuarinaceae, Liliaceae, ?Arecaceae, Restionaceae, Aquifoliaceae, Cunoniaceae/Elaeocarpaceae, Trimeniaceae, Droseraceae, Euphorbiaceae, Olacaceae, Sapindaceae and cryptogam spores. A drop both in diversity and in the proportion of warmth-loving taxa in the assemblages in the Late Eocene is consistent with climate cooling models (Askin, 1997). Further decreases in diversity and composition in the uppermost part of the section may represent increased earliest Oligocene cooling. The leaf flora is also described as a *Nothofagus* dominated-araucarian-podocarp vegetation with several species of ferns (Case, 1988; Doktor *et al.*, 1996).

Coeval strata on Cockburn Island yield low diversity palynomorph assemblages with a typical *Nothofagus*-conifer-Proteaceae composition (Askin *et al.*, 1991). The presence of the frost sensitive taxon *Beaupreadites elegansiformis* Cookson was used to infer mild, equable climates, in an cool temperate southern beech forest assemblage (Askin *et al.*, 1991).

2.6.3 Oligocene floras

Oligocene floras are rare on King George Island. On Fildes Peninsula Torres (1984, 1985, 1990) and Torres *et al.* (1984) have described ?Miocene *Nothofagoxylon*, *Cupressinoxylon*, *Araucarioxylon* and *Podocarpoxylon* from Suffield Point (Shen, 1994). However the age of the Suffield Point sediments is controversial. According to Smellie *et al.* (1984) the whole peninsula comprises Palaeocene – Eocene strata, and the composition of the flora resembles other Eocene assemblages (e.g. Poole *et al.*, 2001). Further dating is required to place this flora in context.

Plant remains derived from supposed Upper Oligocene exotic moraine blocks and *in-situ* deposits at Point Hennequin have been described as low diversity *Nothofagus*-podocarp (± pteridophyte) assemblages (Zastawniak, 1981; Zastawniak *et al.*, 1985). *Cochlospermum* and ?*Rhamnaceae* also occur in the assemblage but *Nothofagus* is dominant in terms of numbers and species (Zastawniak *et al.*, 1985). Lower in the sequence, pollen assemblages comprise abundant fern spores (45 %), Podocarpaceae (including *Phyllocladus*) (42 %) and a surprisingly low proportion of *Nothofagus* (< 5 %) given its abundance in the leaf flora (Duan and Cao, 1998). No younger floras are known from King George Island, except for possible driftwood found in the Miocene Cape Melville Formation (Birkenmajer and Zastawniak, 1989a).

2.7 Tertiary vegetation history of East Antarctica

No Palaeocene floras have yet been reported from East Antarctica, the first record of Tertiary plants being the McMurdo Sound erratics, which are considered to range from Middle Eocene to possible Oligocene age (Askin, 2000; Francis, 2000, Pole *et al.*, 2000). The wood record from the erratics comprises *Araucarioxylon*, *Phyllocladoxylon* and *Nothofagoxylon* (Francis, 2000), while Pole *et al.* (2000) found leaves of *Araucaria*, at least two species of *Nothofagus*, three types of non-*Nothofagus* dicot leaves as well as 2 types of *Nothofagus* fruits. One of the *Nothofagus*-type leaves has plicate vernation, indicative of deciduousness. The pollen record is more diverse with > 49 taxa and only a minor component of reworked palynomorphs, but a trend of decreasing diversity is apparent in younger samples (Askin, 2000). The palynoflora yielded common *Nothofagus*, Liliaceae, Gunneraceae, Sterculiaceae, Myrtaceae, Loranthaceae, Pedaliaceae, podocarps, cycad/*Ginkgo*, cryptogam spores (ferns and lycopods) fungal spores, hyphae and microthyriaceous fruiting bodies (Askin, 2000). Records of recycled palynomorphs from the Ross Sea region with supposed Late Cretaceous to Tertiary ranges also include Sapindaceae (Cupanieae tribe), Ericaceae/Epacridaceae, Casuarinaceae, Euphorbiaceae, Restionaceae and Spargianaceae/ Typhaceae (Truswell, 1983). The overall diversity of the palynoflora is lower than that of contemporary records from the Antarctic Peninsula although this may reflect taphonomic processes,

lithology or the small sample size (Askin, 2000). The assemblage essentially reflects a *Nothofagus*-podocarp-Proteaceae vegetation with other angiosperms and cryptogams, that grew in temperate climates (Askin, 2000). In the ?early Oligocene and post–Eocene a massive drop in diversity is apparent in the assemblage that is consistent with climate deterioration, Proteaceae diversity is also reduced (Askin, 2000). The youngest floras are suggestive of a tundra vegetation with at least one *Nothofagus* sp., one podocarpaceous conifer and a few other angiosperms and cryptogams, some of which still survive in subantarctic and southern alpine floras today.

The CIROS-1 core has sampled both Upper Eocene and Oligocene strata (Wilson *et al.*, 1998). Mildenhall (1989) found abundant *Nothofagus* pollen, Podocarpaceae, cryptogam spores and other angiosperm pollen in the core, including clumped material indicating a local provenance, which he used to suggested that temperate *Nothofagus*-podocarp-Proteaceae forests existed in the Ross Sea region until at least the late Oligocene. A single *Nothofagus* leaf from the Oligocene section of the CIROS-1 drillhole, similar to the extant Tasmanian deciduous, alpine species *N. gunnii* supports this hypothesis (Hill, 1989; 1991).

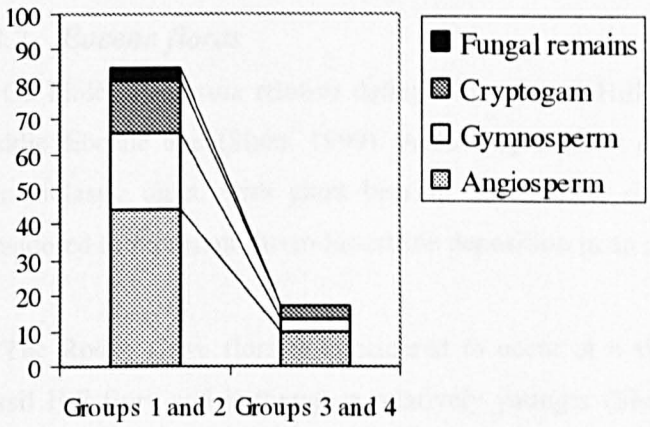

Figure 2.5. Total palynomorph species abundance in the McMurdo Sound erratics showing decrease in vegetational diversity due to climate cooling and glaciation (data from Askin, 2000). Groups 1 and 2 are Middle to Upper Eocene. Groups 3 and 4 are ?Oligocene and post-Eocene. Y-axis scale is in percent.

Drill cores retrieved during the Cape Roberts project have yielded relatively abundant Miocene palynomorph assemblages comprising *Nothofagus*-podocarp-angiosperm taxa with cryptogams (Cape Roberts Science Team, 1998; Terra Antartica Initial Report on CRP-2/2A, 1999) but overall diversity is reduced compared with the Eocene section of CIROS-1 and the McMurdo Sound erratics. Raine (1998) suggested a low diversity, persistent angiosperm-moss-liverwort assemblage, possibly reflecting a contemporaneous herb-moss tundra, growing in a climate similar to that of the Antarctic Convergence islands today, based on spore-pollen assemblages from the lower Miocene section of CRP-1. At lower stratigraphic levels a possible shrub phase *Nothofagus*-podocarp-Proteaceae assemblages, with July mean temperatures 7°C at lower levels in the core (Raine, 1998).

2.8 Geology of the plant-bearing beds on King George Island

2.8.1 Palaeocene floras

The Dufayel Island flora has been K-Ar dated between 51.9-56.8 Ma (Birkenmajer *et al.*, 1983). The flora occurs in a tuffaceous interval in a sequence comprising conglomerates and agglomerates at the base that is capped by basaltic to andesitic lavas (Figure 2.1) (Birkenmajer, 1980; Birkenmajer and Zastawniak, 1986). The material described in this study was collected as scree blocks fallen from the base and middle section of this sequence (Bibby, 1961) and is considered to originate from the same green tuffaceous beds as those described by Birkenmajer (1980) and Birkenmajer and Zastawniak (1986).

The plant-bearing sediments on Barton Peninsula (locality 11; Figure 2.1) are considered to be of Palaeocene age based on K-Ar dating of underlying volcanics (Tokarski *et al.*, 1987). The sequence comprises a cliff section comprising outcrops of layered tuff with channelised conglomerates and sandstones, which support a fluvial origin for the deposits (Del Valle *et al.*, 1984; Tokarski *et al.*, 1987).

2.8.2 Eocene floras

On Fildes Peninsula relative dating of the Fossil Hill flora supports an early Middle Eocene to Middle Eocene age (Shen, 1999). According to Xue *et al.* (1996) the sequence comprises six volcaniclastic units, with plant bearing horizons at six separate intervals, which Shen (1994) considered to represent fluvio-lacustrine deposition in an intermontane basin.

The Rocky Cove flora is considered to occur at a slightly higher stratigraphic level than the Fossil Hill flora and is therefore relatively younger (Shen, 1999). The sequence comprises 35 m thickness of tuffs, coarse volcaniclastics and interbedded lavas. Shen (1994) and Poole *et al.* (2001) considered that the Collins Glacier plant beds were contemporaneous with the Rocky Cove sequence but Shen (1999) preferred a Palaeocene age based on lithological data. In this study the original interpretation of Shen (1994) is maintained which is also supported by petrographic studies of Smellie *et al.* (1984) who considered the tuffaceous sequences to be lithologically the same. Neither Smellie *et al.* (1984) nor Shen (1994, 1999) suggested a depositional environment for the sediments.

The tuffaceous sediments of the Potter Peninsula flora have been assigned an Eocene age (Birkenmajer and Zastawniak, 1989a) but no further sedimentological data has been published. The BAS collections comprise two separate floras, both using the station number P.232; The Potter

Peninsula impression flora, preserved in a purple tuffaceous sandstone; and the Potter Peninsula compression flora, preserved in a green tuffaceous sandstone.

2.8.3 Oligocene floras

The Platt Cliffs flora originates from the same locality as the Cytadela flora (Barton, 1961; Birkenmajer and Zastawniak, 1989a). In the British Antarctic Survey collections the material is divided into two distinct subfloras: material of G.50 and material of G.47, G.309, G.319. The latter material comprising carbonised angiosperm, fern and conifer material, matches the description of the Cytadela flora (Birkenmajer and Zastawniak, 1989a) and this name is adopted throughout the rest of this thesis. The G.50 flora is here named the Platt Cliffs flora and retains this name throughout. The undifferentiated tuffaceous sediments in which the plants are preserved are considered to be Upper Eocene to Lower Oligocene in age (Birkenmajer and Zastawniak, 1989a).

At Suffield Point and Profound Lake extremely fine grained tuffaceous sediments, which yield rare plant remains have been considered to be ?Oligocene-Miocene in age (Shen, 1994), however K-Ar dating by Smellie *et al.* (1984) suggests that the entire Fildes Peninsula sequence is not younger than Eocene. In addition, the wood floras described from this locality (Torres, 1984, 1985, 1990; Torres *et al.*, 1985) are similar to Eocene assemblages (Poole *et al.*, 2001), therefore it seems likely that the assemblage may have been incorrectly dated and that a Middle Eocene age seems more appropriate.

At Point Hennequin, the Dragon Glacier moraine flora and the *in-situ* Mt. Wawel flora originate from the ?Upper Oligocene Mt. Wawel Formation (Birkenmajer, 1981; Zastawniak, 1981; Birkenmajer *et al.*, 1983; Zastawniak *et al.*, 1985). The volcaniclastic sediments are interpreted as ephemeral lacustrine on the basis of mudcracking, rootlet horizons and well developed planar laminations (Birkenmajer, 1981). A newly described flora from this area is termed the Smok Hill flora (Hunt and Poole, submitted). The Mt. Wawel flora is considered to post-date both the Dragon Glacier flora (Zastawniak *et al.*, 1985) and the Smok Hill flora (Hunt and Poole, submitted) but the relative age of the latter two floras is uncertain. The dating of the floras is contentious, since Smellie *et al.* (1984) derived an entirely Eocene age for the flora based on K-Ar dating. Birkenmajer *et al.* (1983) used a single K-Ar date from the middle of the sequence to propose the 24 ± 0.5 Ma age and to support the lithostratigraphic division of the sequence into the basal Eocene Vieville Glacier Formation and overlying Upper Oligocene Mt. Wawel Formation.

Chapter 3 Geochronology and stratigraphy

3.1 Introduction

This chapter discusses the results of $^{40}Ar/^{39}Ar$ and K-Ar dating from Point Hennequin, Fildes Peninsula and Vaureal Peak. The aim of this geochronological study was to constrain the age of three plant-bearing sequences: the Mt. Wawel Formation at Point Hennequin; Unit Four of the Great Wall Bay Member of the Fossil Hill Formation (Shen, 1994, 1999; Xue *et al.*, 1996) and the Vaureal Peak lavas and Cape Vaureal Formation from Vaureal Peak. All other floras discussed in this study retain the ages previously assigned to them. Possible causes of dating inaccuracy are considered and previous stratigraphic schemes are modified using the new data. This information is then discussed in terms of its impact on palaeoenvironmental models.

3.2 Materials and methods

Geochronological samples from Fossil Hill were collected during this study and all other samples were collected by JL Smellie (BAS) on previous King George Island field seasons. Basic-intermediate lava samples were dated from Point Hennequin and Vaureal Peak and two samples from a plagioclase-rich tuff horizon were dated from Fossil Hill (Appendix Table II.2). The age data from the Point Hennequin and Vaureal Peak lavas are ages of crystallisation, which equate to an age of extrusion. Dating of the Fossil Hill tuff samples should yield an age of eruption of the pyroclastic material. Both types of data are maximum ages for the samples dated.

Emplacement of Eocene plutons in the South Shetland Islands may have led to potassium (K) metasomatism and argon (Ar) loss, which could in turn affect the reliability of K-Ar age data (Birkenmajer, 1990; Soliani and Bonhomme, 1994; Willan and Kelley, 1999). Unlike the K-Ar method, $^{40}Ar/^{39}Ar$ step heating reveals the internal distribution of argon in a sample because argon is extracted by heating the sample at progressively higher temperature steps and each extracted gas fraction is analysed to obtain $^{40}Ar/^{39}Ar$ ratios from which an age is calculated. This can be visually assessed using a step-age spectrum, which provides a visual record of the internal consistency of age data (Appendix Figure II.1). In combination with thin section data this information may be used to evaluate the degree of alteration or isotopic resetting of the sample during its history and therefore the reliability of the age data. K-Ar dating is still useful in areas that are unaffected by alteration, and has the benefit of being cheaper and faster to analyse. For very fresh samples in thin section K-Ar dates were also obtained. Derivations of the K-Ar and $^{40}Ar/^{39}Ar$ methodologies, thin section descriptions,

summaries of previous geochronological data and new $^{40}Ar/^{39}Ar$ data are presented in Appendix II. Isotopic notation used in this study is summarised in Table 3.1. The geomagnetic timescale of Cande and Kent (1992, 1995) is used throughout, unless otherwise specified.

^{40}Ar, ^{39}Ar, ^{38}Ar, ^{37}Ar, ^{36}Ar	Isotopes of argon
$^{40}Ar^*$	Radiogenic argon
$^{40}Ar/^{36}Ar = 295.5$	Atmospheric composition of non-radiogenic argon in terrestrial rocks
^{40}K	Radiogenic isotope of potassium
K_{total}	Total amount of potassium from all sources present in nature
$^{40}Ar_E$	Excess or extraneous argon
Rb-Sr	Rubidium-strontium dating method
$^{40}Ar/^{39}Ar$ method	$^{40}Argon$-$^{39}Argon$ dating method
K-Ar	Potassium argon dating method
WR	Whole rock - dating using the whole of a crushed specimen for dating
Plagioclase separate	Uses only plagioclase for dating
Å	Angstrom
T_0	Time of initial formation
λ_E, λ_B	Partial decay constants for the decay branch ^{40}K-^{40}Ar
λ	Constant for the decay branch ^{40}K-^{40}Ar
J-value	Dimensionless irradiation parameter
$1\sigma/2\sigma$	1/2 sigma error – one/two standard deviation(s)
MSWD	Mean square of weighted deviates. Measure of the degree of departure of a point from a best fit line
XRF	X-ray fluorescence spectroscopy

Table 3.1. Isotopic notation used in this study.

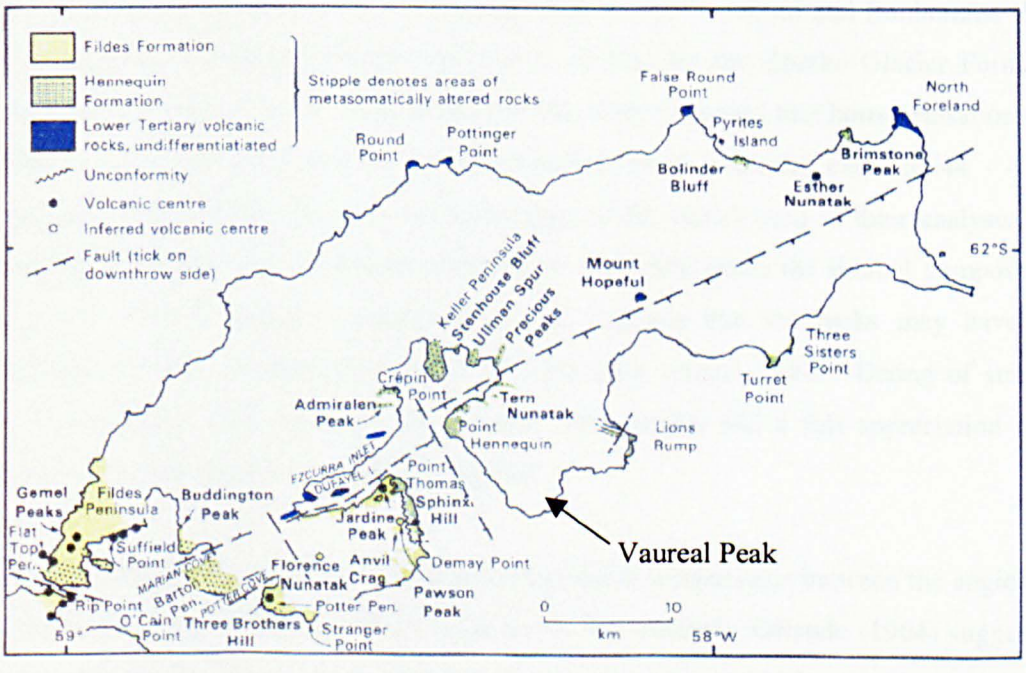

Figure 3.1. Stratigraphy of King George Island according to Smellie *et al.* (1984), also highlighting areas of exposure.

3.3 Stratigraphy

King George Island stratigraphy is based on the petrographic relations of lava sequences since sedimentary horizons are thin and often discontinuous (Barton, 1959, 1961, 1964b, 1965;

Hawkes, 1961; Birkenmajer, 1980, 1981, 1987; Smellie *et al.*, 1984; Fensterseifer *et al.*, 1988; Li and Liu, 1989; Shen, 1994, 1999). The stratigraphy of KGI is complex due to the difficulty of correlating the geographically-isolated outcrops that are separated by large icesheets. A broad division can be made between Late Cretaceous to ?Oligocene terrestrial volcanic and volcaniclastic sequences in the west and central portions of KGI, and with the Late Tertiary–Quaternary, predominantly glacio-marine sequences, on the south east coast (Figure 3.1) (Birkenmajer, 1980, 1994; Smellie et al., 1984; Birkenmajer et al., 1986, 1988).

Early geological studies of KGI subdivided the strata as Jurassic and Cenozoic, based on petrological similarities with Andean intrusive rocks in Graham Land, Antarctic Peninsula (Ferguson, 1921; Tyrell, 1921, 1945; Hawkes, 1961; Barton, 1965). Subsequent geochronological studies have found no evidence for Jurassic rocks. Instead, the strata yield Late Cretaceous to Miocene K-Ar ages (Appendix II) (Grikurov and Polyakov, 1968; Birkenmajer, 1989, 1990; Birkenmajer *et al.*, 1983, 1986, 1989; Dupre, 1982; Watts, 1982; Pankhurst and Smellie, 1983; Smellie et al. 1984; Kawashita and Soliani, 1988; Soliani *et al.*, 1988; Jwa and Kim, 1992; Soliani and Bonhomme, 1993, Wang and Shen, 1994; Hu *et al.*, 1997), with the oldest strata on southern Fildes Peninsula dated as Cretaceous (109 ± 10 Ma; Valencio *et al.*, 1979). However, nearly half of the age data available for the South Shetland Islands may be unreliable, because high level emplacement of plutons during the Eocene may have led to Ar-loss and K-metasomatism (Pankhurst and Smellie, 1983; Birkenmajer *et al.*, 1990; Soliani and Bonhomme, 1994; Willan and Kelley, 1999). Soliani and Bonhomme (1988) used Rb-Sr dating to obtain a Palaeocene age (c. 60 Ma) for the Znosko Glacier Formation, Admiralty Bay, otherwise K-Ar dated at 40 - 50 Ma. They proposed that homogenisation of K-Ar ratios in the northern portion of the bay resulted from a thermal event at 44 - 41 Ma (Birkenmajer *et al.*, 1990). However the high range of Rb values used in their analyses, with approximately 35 orders of magnitude variation, is untenable given the limited compositional range of the basaltic-andesite samples dated and suggests that the rocks may have been contaminated by older continental material (B Cliff pers. comm., 2001). Dating of strata on King George Island must therefore be regarded with caution and a full appreciation of the freshness of geochronological samples is required.

Alternative dating strategies have used palaeobotanical comparisons between the angiosperm leaf floras from King George Island and elsewhere. For example, Orlando (1964) suggested a Miocene age for the 'Ardley Island' flora based on comparisons with floras with contemporary floras in South America (see also Del Valle, 1984), and Duan and Cao (1998) used pollen sequences to support an Oligocene age for the Point Hennequin strata. However, evidence of stepwise plant migrations (Dettmann, 1989) across the fragmenting Gondwanan continent

implies that any flora found on KGI during the Late Cretaceous and Tertiary periods may be diachronous to some degree, and therefore difficult to relate to an absolute time scale.

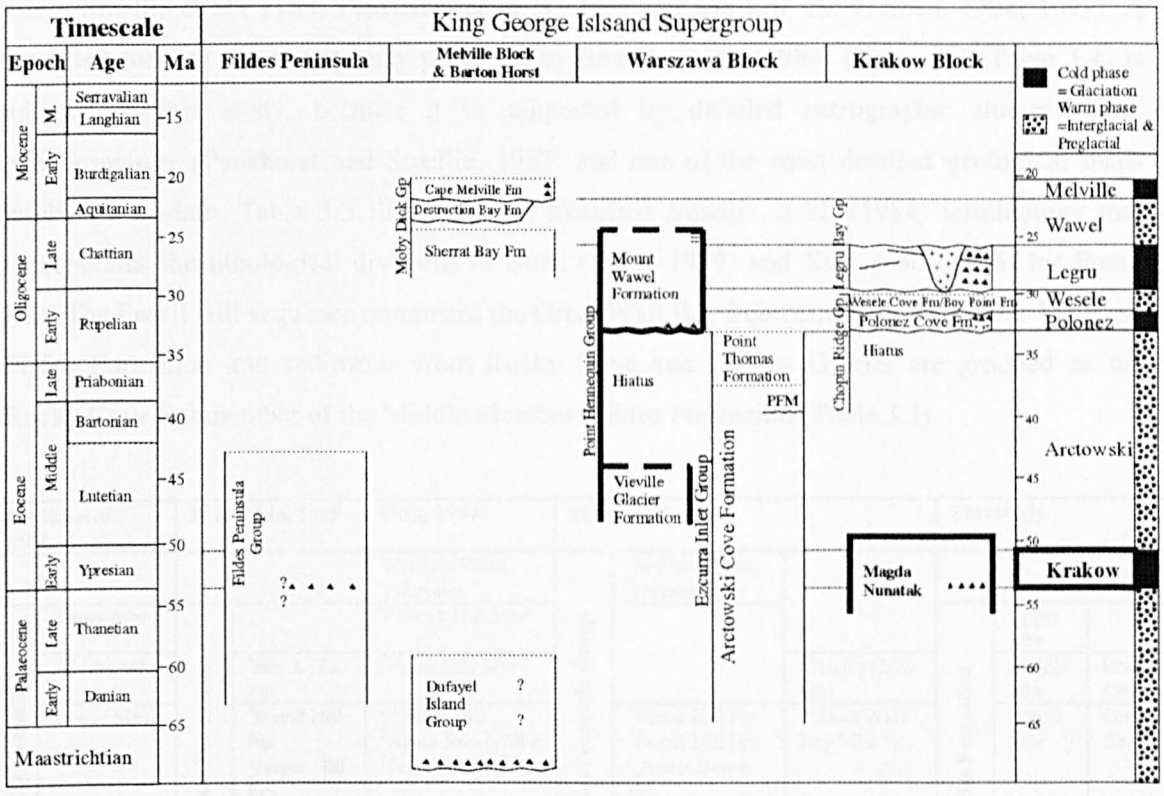

Figure 3.2. Stratigraphic division of King George Island Stratigraphic division of King George Island according to Birkenmajer (1980, 1987, 1989, 1990).

Unit	Location	Type area	Major lithological characteristics	Age
Hennequin Fm	KGI, mainly east of Admiralty Bay	Point Hennequin	Fine grained and glassy hypersthene-augite-andesites and dacites	Eocene – Oligocene
Fildes Fm	Mainly KGI, west of Admiralty bay; also Stansbury Peninsula and other outcrops on eastern Nelson Island	Fildes Peninsula	Weathered olivine basalts and basaltic andesites; rare pyroxene-andesites and dacites	Palaeocene - Eocene

Table 3.2. Two-fold lithological division for King George Island proposed by Smellie *et al.* (1984).

Detailed stratigraphic schemes have been proposed for Admiralty Bay and the south east coastal areas by Birkenmajer (1980, 1981, 1987, 1989, 1990) (Figure 3.2), which treat each geographically isolated area as a separate formation. Smellie *et al.* (1984) argued against this subdivision based on evidence of synchronous volcanism in different areas of King George Island, instead proposing a broad two-fold lithological division of the strata into the Fildes and Hennequin formations (Table 3.2). However, although Smellie *et al.*'s (1984) scheme is a more strict interpretation of KGI stratigraphy, Birkenmajer's (1980, 1981, 1987, 1989, 1990) scheme is more widely used and provides more detailed maps and subdivision of the strata, and is adopted in this study. The exception is Fildes Peninsula, where Smellie *et al.* (1984) have produced the most detailed study of the entire area to date. Future stratigraphic studies are needed to resolve the conflicting schemes.

3.3.1 *Fildes Peninsula – the Fossil Hill flora*

Numerous stratigraphies have been proposed for Fildes Peninsula (Table 3.3) (Hawkes, 1961; Smellie et al., 1984; Fensterseifer et al., 1988; Li and Liu, 1989; Shen, 1994, 1999). A modified form of the stratigraphy proposed by Smellie et al. (1984) (Table 3.3; Table 3.4) is adopted in this study, because it is supported by detailed petrographic studies, K-Ar geochronology (Pankhurst and Smellie, 1983) and one of the most detailed geological maps published to date. Table 3.3 illustrates the modified Smellie et al. (1984) terminology that incorporates the lithological divisions of Shen (1994; 1999) and Xue et al. (1996) for Fossil Hill. The Fossil Hill sequence comprises the Great Wall Bay Submember of the Lower Member, Fildes Formation and sediments from Rocky Cove and Collins Glacier are grouped as the Rocky Cove Submember of the Middle Member, Fildes Formation (Table 3.3).

Smellie *et al.*, 1984		Li and Liu, 1989		Shen, 1994	Shen, 1999			This study		
				[5]Suffield Point Volcanics	Fildes Peninsula Group	[6]Suffield Point Volcanics				
Fildes Formation	Upper Mbr	Fildes Formation		[7][4]Block Hill Mbr				Fildes Formation	Upper Mbr	
	Middle Mbr		[4]Block Hill Fm	[3]Fossil Hill Mbr			[3b]Rocky Cove Mbr		Middle Mbr	Rocky Cove Sbr
	Lower Mbr		[3]Fossil Hill Fm [2]Jasper Hill Fm [1]Agate Beach Fm	[7][4]Block Hill [2]Agate Beach Mbr [1]Jasper Hill Mbr		[5]Block Hill Fm [3]Fossil Hill Fm [2] Agate Beach Fm [1]Jasper Hill Fm	[3a]Great Wall Bay Mbr		Lower Mbr	Great Wall Bay Sbr

Table 3.3. Stratigraphic divisions of the Fildes Peninsula strata compared to the terminology of Smellie *et al.* (1984). Numbering indicates internal order of each stratigraphic scheme and highlights variations in interpretations. Fm – formation, Mbr – member, Sbr – submember.

Member	Description	Field Relations
Upper Member	Fine-grained aphyric and micro-porphyritic andesite and dacite lavas	Top of sequence not exposed; conformably overlies the middle member
Middle Member	Mainly volcaniclastic rocks (locally plant bearing) with a few basalt and basaltic andesite lavas	Base of sequence not exposed; down-faulted against the lower member
Lower Member	Coarsely porphyritic basalt and basaltic-andesite lavas interbedded with laterally impersistent volcaniclastic rocks (some with plant fossils)	Neither base nor top of sequence exposed

Table 3.4. Lithostratigraphic division of the Fildes Formation (Smellie *et al.*, 1984).

Covacevich and Lamperein, (1970) in their study of the Fossil Hill bird ichnite fauna, recognised the sequence as an easterly dipping group of tuffaceous sediments, unconformably overlying the basaltic and andesitic volcanics that constitute much of the peninsula. The upper boundary of the sequence is an erosional unconformity and in consequence there are no strata available to give a minimum age constraint for the sequence. Recent studies favour a latest Palaeocene to Middle Eocene age (Figure 3.3) based on K-Ar geochronology of the underlying lavas to give a maximum age.

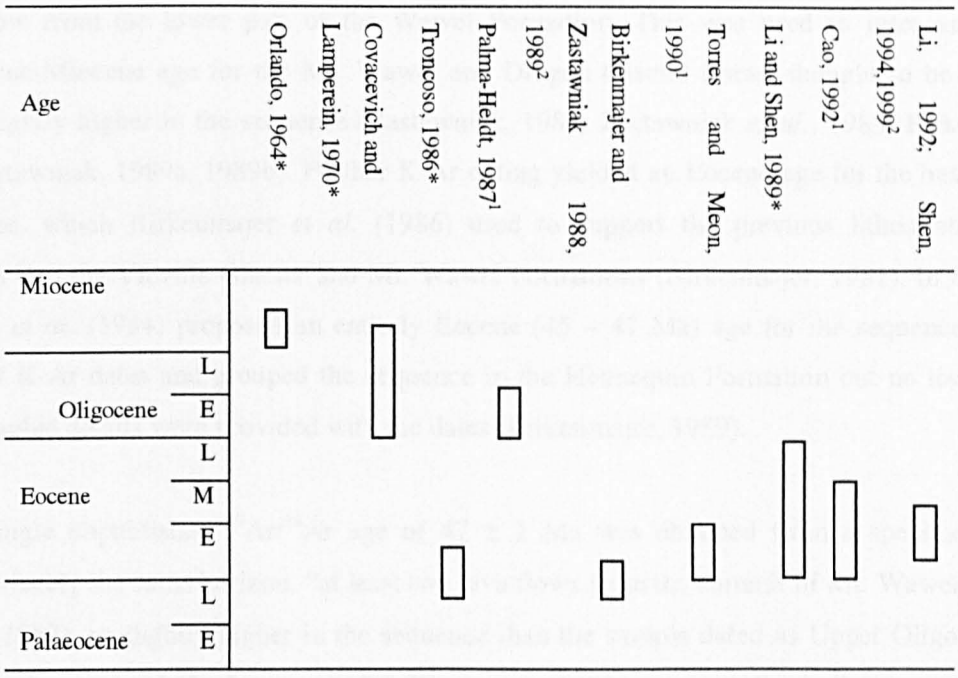

Figure 3.3. Summary of previous age ranges suggested for the Fossil Hill flora based on *comparisons of the leaf flora with supposed contemporary South American fossil localities, [1]comparative pollen studies, [2]relative K-Ar geochronology.

Xue *et al.* (1996) divided the Great Wall Bay Submember sediments at Fossil Hill into six units. In this study a 1.5 m thick tuffaceous bed from Unit Four of Xue *et al.* (1996) (Figure 3.4) was selected for $^{40}Ar/^{39}Ar$ dating in order to obtain a maximum age (age of eruption) for the pyroclastic sediments.

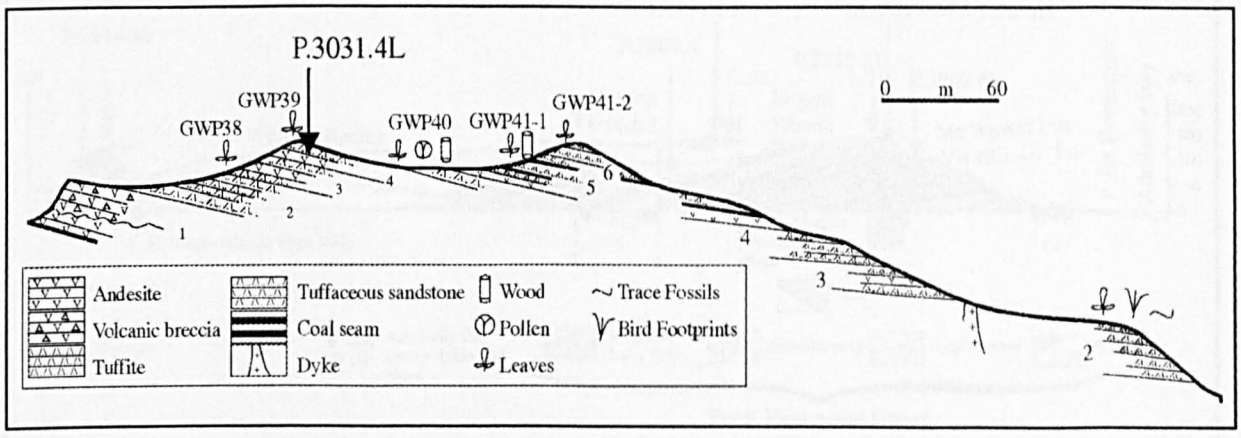

Figure 3.4. Cross section of the Fossil Hill sediments (Shen, 1994) of the Great Wall Bay Submember (Table 3.3), showing position of geochronological sampling.

3.3.2 Point Hennequin – the Smok Hill, Dragon Glacier and Mt. Wawel floras

Birkenmajer (1981) subdivided the andesite, trachyandesite, agglomerate and plant bearing tuffaceous sediment horizons at Point Hennequin into the lower Vieville Glacier Formation and upper Mt. Wawel Formation (Figure 3.5), but despite providing detailed lithostratigraphic descriptions for the sequence, no justification is given for the formational divisions. Birkenmajer *et al.* (1983) obtained an Upper Oligocene age (24 ± 0.5 Ma) for a single andesite

lava flow from the lower part of the Wawel Formation. This was used to infer an Upper Oligocene-Miocene age for the Mt. Wawel and Dragon Glacier floras, thought to be derived from slightly higher in the sequence (Zastawniak, 1981; Zastawniak *et al.*, 1985; Birkenmajer and Zastawniak, 1989a, 1989b). Further K-Ar dating yielded an Eocene age for the base of the sequence, which Birkenmajer *et al.* (1986) used to support the previous lithostratigraphic division into the Vieville Glacier and Mt. Wawel Formations (Birkenmajer, 1981). In contrast, Smellie *et al.* (1984) proposed an entirely Eocene (45 – 47 Ma) age for the sequence on the basis of K-Ar dates and grouped the sequence in the Hennequin Formation but no locality or stratigraphic details were provided with the dates (Birkenmajer, 1989).

A single unpublished $^{40}Ar/^{39}Ar$ age of 47 ± 2 Ma was obtained from a specimen from approximately the same horizon, "at least two lava flows from the summit of Mt. Wawel" (p 42, Dupre, 1982), or slightly higher in the sequence than the sample dated as Upper Oligocene by Birkenmajer *et al.* (1983). It supports Smellie *et al.*'s (1984) argument for an Eocene age for the Point Hennequin strata. Birkenmajer's (1981) interpretation of the western summit of Mt. Wawel as a volcanic neck, on the basis of cross-cutting relations, has yet to be confirmed by other studies, which instead indicate a simple dipping sequence of lavas interbedded with epiclastic and pyroclastic material at a distance from the volcanic centre. These inconsistencies in stratigraphic interpretations are the basis for redating the Point Hennequin sequence using $^{40}Ar/^{39}Ar$ geochronology.

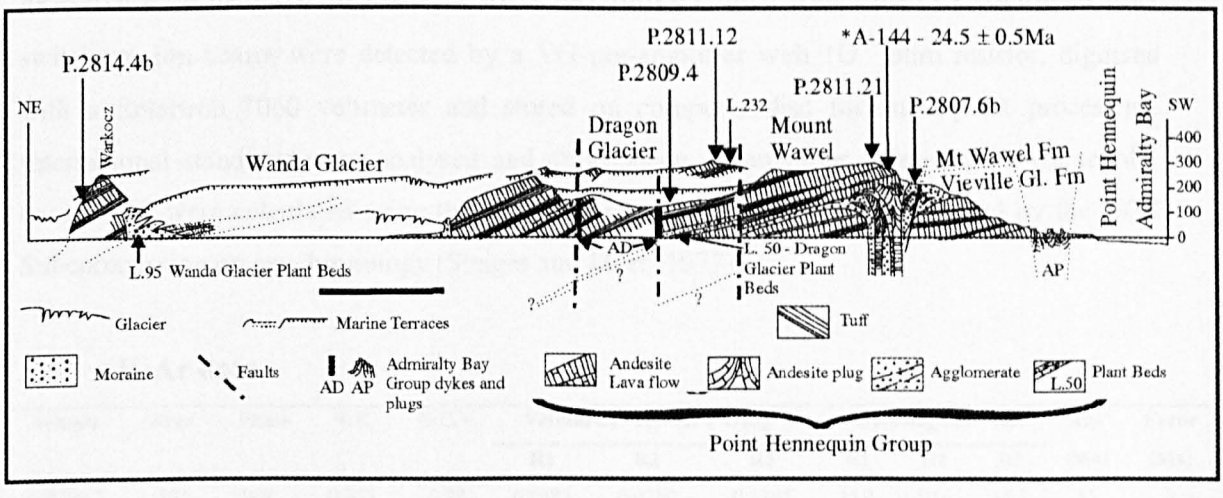

Figure 3.5. Cross section of the Point Hennequin sequence (Zastawniak *et al.*, 1985), with position of geochronological samples used in this study. *Birkenmajer *et al.* (1983). Black horizontal scale bar = 500m.

3.3.3 Vaureal Peak – the Vaureal Peak flora

The Vaureal Peak flora is a newly described flora from sediments on the eastern side of Vaureal Peak (Figure 2.1 and Figure 3.1). Both the plants and the geochronological samples were collected by JL Smellie (BAS). The stratigraphy is poorly described and is currently undergoing revision (Smellie and Hunt, work in progress). A single sample from lavas overlying the sedimentary beds was dated using both K-Ar and $^{40}Ar/^{39}Ar$ dating to obtain a

minimum age for the flora, and is here termed the Vaureal Peak lava. Two additional samples of material from underlying volcanics, termed the Cape Vaureal Formation, were also dated to constrain the age of the underlying volcanic strata and provide a maximum age for the flora.

3.4 K-Ar methodology

Whole rock samples (P.2788.6, P.2799.1, P.2811.12) were prepared using the following standard procedure: Sample material was crushed, sieved, washed and dried. In the case of plagioclase separates (P.3031.4L and P.3031.4U) the 170 μm - 250 μm mesh fraction was taken for plagioclase concentration by Frantz magnetic separator and, after surface leaching in 20% acetic acid followed by 7 % HF, was finally purified by hand-picking under a binocular microscope. Samples were washed with deionised water between steps. Aliquots of the separates were taken for both potassium and argon determinations. Three separate dissolutions of the samples were used for the potassium determinations and the mean value taken. The potassium concentrations were measured using a Ciba-Corning 480 flame photometer incorporating a Lithium internal standard. International and laboratory standards are analysed on a routine basis. Argon was extracted in a glass vacuum line using an ^{38}Ar tracer from an aliquoting system. Special attention was given to the purity of the gas sample before it was analysed. A two-stage clean-up procedure was used, stage one incorporating a Ti sponge furnace and liquid Nitrogen trap. The gas was then transferred to a second stage Ti/Zr sponge furnace by absorption on activated charcoal at liquid Nitrogen temperature. Argon isotopes were measured on a modified AEI MS 10 mass spectrometer fitted with computer controlled peak switching. Ion beams were detected by a VG pre-amplifier with 10^{11} ohm resistor, digitised with a Solartron 7060 voltmeter and stored on computer disc for subsequent processing. International standards were analysed and atmospheric argon ratios determined on a regular basis. Ages were calculated using the decay constants and branching ratio agreed by the UGS Subcommission on geochronology (Steiger and Jäger, 1977).

3.5 K-Ar data

Sample	Area	Phase	%K	%C.V.	Volume of $^{40}Ar^{*}$ ($x10^{-5}cm3g^{-1}$)			% Radiogenic ^{40}Ar			Age	Error
					R1	R2	R3	R1	R2	R3	(Ma)	(Ma)
P.2799.1	VP	WR	0.203	0.28	0.0283	0.0280	0.1382	11.4	10.6	16.9	35	2
P.2811.12	PH	WR	1.199	0.30	0.1396	0.0167	0.0170	16.3	6.5	6	29.6	1.7
P.3031.4L	FH	Plag	0.149	6.2							29	2
P.3031.4U	FH	Plag	Abandoned - Negligible volumes of $^{40}Ar^{*}$.									

Table 3.5. K-Ar data for the Point Hennequin and Vaureal Peak areas. * Reading not used in calculation. PH - Point Hennequin, VP - Vaureal Peak. WR - whole rock, Plag – plagioclase separates. %C.V – coefficient of variation of %potassium. R1-R3 – replicate sample number. Radiogenic argon values are low for most samples suggesting argon loss. P.3031.4L/P.3031.4U – samples from Lower and Upper portion of the same bed.

3.6 $^{40}Ar/^{39}Ar$ methodology

Samples for step heating $^{40}Ar/^{39}Ar$ geochronology were crushed and sieved for the 165-250 μm and 250-500 μm fractions, avoiding veining and weathered surfaces. Both fractions were passed through a Frantz magnetic separator to concentrate plagioclase feldspar, washed in 1M HNO_3 for 10 minutes to remove carbonates, decanted then washed in 7 % HF for a further 10 minutes to remove fines, rinsed in deionised water and then dried. The samples, weighing approximately 60 mg, were then hand picked under a binocular microscope to remove altered and inclusion rich grains. The $^{40}Ar/^{39}Ar$ analysis was carried out at the University of Leeds and followed the method described by Rex et al. (1993) with the following variations: Samples (P.2788.6, P.2789.1, P.2792.4, P.2799.1a-d, P.2809.4, P.2811.12WR, P.2811.21, P.2814.4b) were irradiated at the Risø Reactor, Roskilde Laboratory, Denmark, interference correction factors were (40/39)K = 0.048, (36/39)Ca = 0.38 and (37/39)Ca = 1492. Samples P.2799.1a-d, P.2807.6b, P.2811.12(30-60), P.2811.12(60-90), P.3031.4L were irradiated at the McMasters Reactor, Ontario, Canada, interference correction factors were (36/39)Ca = 0.32, (37/39)Ca = 1515 and (40/39)K = 0.02. The University of Leeds internal standard is Tinto biotite (Rex et al., 1986) with assigned age of 409.2Ma and biotite LP-6 (Engels et al. 1971). Isotopic analyses were performed with a modified MS10 mass spectrometer, measured atmospheric $^{40}Ar/^{36}Ar$ was 287.8 ± 0.2 and sensitivity 1.12 x $10^{-7}cm^3V^{-1}$. Gas volumes are corrected to STP. For all summary data tables of $^{40}Ar/^{39}Ar$ analyses, see Appendix II.

The $^{40}Ar/^{39}Ar$ ratio, age and errors for each gas fraction were calculated using the methodology of Dalrymple and Lamphere (1971). Errors in these ratios were evaluated by numerical differentiation of the equation used to determine the isotope ratios and quadratically propagating the errors in the measured ratios. J-value uncertainty is included in the errors quoted on the total gas ages but the individual step ages have analytical errors only. All errors are quoted at the 1σ level unless otherwise stated. Ages are calculated using the constants recommended by Steiger and Jäger (1977). Data for isotope correlation plots is reduced using in-house software 'Isoplot/Ex' developed by Ludwig (1998). Chlorine-Calcium isotope data are plotted for samples for Risø reactor samples but samples irradiated at McMasters were shielded, inhibiting the formation of Cl-isotopes.

3.7 $^{40}Ar/^{39}Ar$ step heating results

3.7.1 Fossil Hill (Figure 3.6c-e)

$^{40}Ar/^{39}Ar$ analyses of sample P.3031.4L yielded a weighted age of 40 ± 3 Ma based on a bipartite age spectrum with three initial low temperature steps comprising ~ 59.1 % of the ^{39}Ar (Figure 3.6c-e). Scattered high temperature steps correlate with variations in the Ca/K ratios (Figure 3.6c). This could represent incorporation of excess argon into the sample but, given the

distinct separation between the high and low temperature steps, it might also represent gas release from two different plagioclase phases (McDougall and Harrison, 1999). For example, a higher temperature altered plagioclase phase and a low temperature unaltered plagioclase. Since the sample is tuffaceous, this could also be the result of mixing older host rocks into the erupted tuff.

The $^{40}Ar/^{39}Ar$ age falls within the range of relative data suggested for the flora/Fossil Hill strata. Comprising nearly 60 % of the ^{39}Ar the age fits one of the criteria for a plateau age (Ludwig, 1998). It is therefore tempting to suggest that this is a 'true' age of crystallisation/eruption of the tuffaceous material. However, given that this is the age of a single sample and that the spectra is rather disturbed, further dating is required to determine the validity of this age data.

K-Ar dating of sample P.3031.4L yielded a mean age of 29 ± 2 Ma (Oligocene) (Table 3.6), which conflicts with relative dating for the sequence (Figure 3.3) (Birkenmajer and Zastawniak, 1989a; Li and Shen, 1989; Torres and Meon, 1990; Cao, 1992; Shen, 1994; 1999). However, the radiogenic argon content of the sample was low (Table 3.5), suggesting ^{40}Ar loss, which would account for a younger than expected age. Groundmass alteration was observed in thin sections of this sample (Appendix Table II.2), suggesting that groundmass plagioclase might not have quantitatively retained radiogenic argon, which supports a model of argon loss.

3.7.2 Point Hennequin (Figure 3.6a-b, Figure 3.7a-f; Figure 3.8a-f)

P.2807.6b produced a slightly curved age spectrum, with lower aged steps at both low and high temperatures (Figure 3.6a). The variation correlates with the minor variations in the Ca/K ratio at low and high temperatures The plateau age based on 100 % of the ^{39}Ar is 42 ± 1.2 Ma, and agrees with the isotope correlation plot age of 42.5 ± 2.6 Ma (Figure 3.6b). A weighted average age (at 2σ) = 44.0 ± 5.5 Ma, based on 62.3 % of the gas released is obtained from the low error, high gas volume central steps on the age spectrum, which is more consistent with other age data from the same sequence.

P.2811.21 yielded a plateau age of 49.6 ± 2.4 Ma, based on 6 disturbed steps constituting 70.9 % of the ^{39}Ar released (Figure 3.7a). The plateau age is coincident with the total gas age of 48.3 ± 2.8 Ma and the Model 1 isotope correlation age 48.1 ± 5.7 Ma (MSWD = 1.2) (Figure 3.7b). Decreasing Ca/K ratios at higher temperatures are correlated with two old high temperature steps (steps 8 and 9) suggesting incorporation of older excess Ar. However, the contemporaneous sample P.2809.4, the down section equivalent of P.2811.21, yields a weighted average age of 49.8 ± 5.7 Ma and a plateau age of 50.2 ± 1.4 Ma, both of which are within error of P.2811.21 suggesting that the ages are geologically robust.

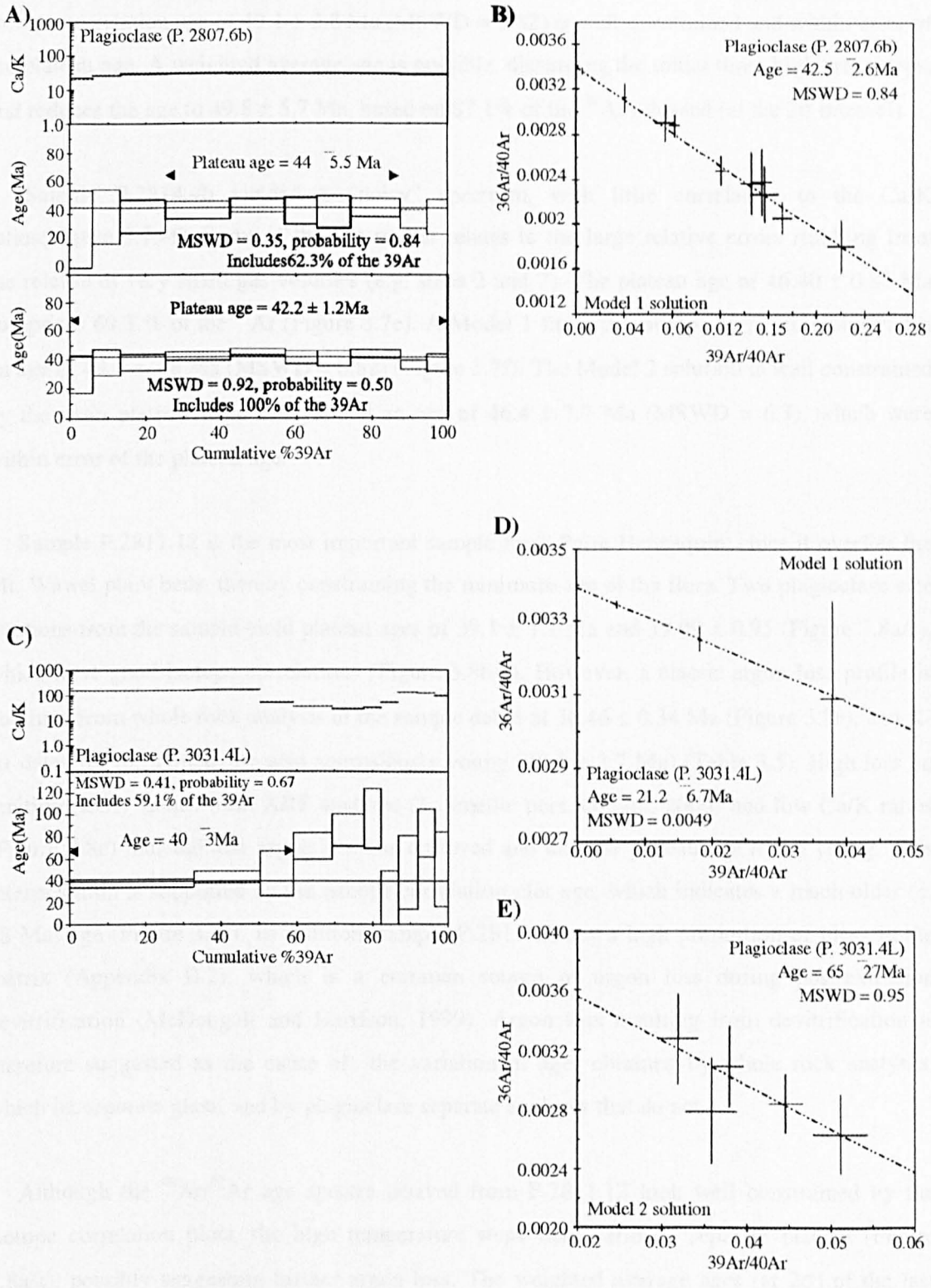

Figure 3.6. $^{40}Ar/^{39}Ar$ stepheating spectra Ca/K and Cl/K profiles (where available) and isotope correlation plots for lavas from A-B. Point Hennequin (P. 2807.6b) and C-E. Fossil Hill (P. 3031.4L). Arrows indicate steps used to calculate plateau age by isoplot.

P.2809.4 gave a plateau age of 50.2 ± 1.4 Ma, with some disturbance in the low temperature steps that correlated with the Ca/K ratios, indicating minor alteration (Figure 3.7c-d). The isotope correlation age of 49.1 ± 2.8 Ma (MSWD = 0.82) is well-constrained and within error of the plateau age. A weighted average age is possible, discarding the initial three high error steps, and reduces the age to 49.8 ± 5.7 Ma, based on 87.1% of the ^{39}Ar released (at the 2σ interval).

Sample P.2814.4b yielded a "noisy" spectrum, with little correlation to the Ca/K ratios(Figure 3.7e-f). Some of the age scatter relates to the large relative errors resulting from the release of very small gas volumes (e.g. steps 2 and 7). The plateau age of 46.40 ± 0.83 Ma comprises 69.3 % of the ^{39}Ar (Figure 3.7e). A Model 1 fit on the isotope correlation plot yields an age of 49.1 ± 2.8 Ma (MSWD = 0.82) (Figure 3.7f). The Model 2 solution is well constrained by the main plateau steps and yielded an age of 46.4 ± 7.7 Ma (MSWD = 6.3), which were within error of the plateau age.

Sample P.2811.12 is the most important sample from Point Hennequin, since it overlies the Mt. Wawel plant beds, thereby constraining the minimum age of the flora. Two plagioclase size fractions from the sample yield plateau ages of 39.1 ± 1.1 Ma and 39.99 ± 0.95 (Figure 3.8a/c), which have good isotope correlations (Figure 3.8b/d). However, a classic argon loss profile is obtained from whole rock analysis of the sample dated at 30.46 ± 0.34 Ma (Figure 3.8e), and K-Ar dates for the sample are also anomalously young (29.6 ± 1.7 Ma) (Table 3.5). High loss on ignition (LOI) values from XRF analyses (J. Smellie pers. comm., 2000) and low Ca/K ratios (Figure 3.8e) indicate that argon loss has occurred and that the plateau age is too young. This interpretation is supported by the isotope correlation plot age, which indicates a much older (c. 38 Ma) age (Figure 3.8f). In addition, sample P.2811.12 has a high proportion of glass in the matrix (Appendix II.2), which is a common source of argon loss during post-extrusion devitrification (McDougall and Harrison, 1999). Argon loss resulting from devitrification is therefore suggested as the cause of the variation in ages obtained by whole rock analyses, which incorporate glass, and by plagioclase separate analyses that do not.

Although the $^{40}Ar/^{39}Ar$ age spectra derived from P.2811.12 look well constrained by the isotope correlation plots, the high temperature steps may define a separate plateau (Figure 3.8a/c), possibly suggesting further argon loss. The weighted average ages (at 2σ) of the last four steps (31.4 % of ^{39}Ar) are 46 ± 11 Ma (P. 2811.12, 30-60) and 47 ± 9 Ma (P.2811.12, 60-90). This is more consistent with the ages obtained from the underlying lava samples (excepting P.2807.6b) and supports the field relations, which show no evidence for a major hiatus within the sequence at Point Hennequin. The weighted average age is therefore accepted as the age of crystallisation for this sample.

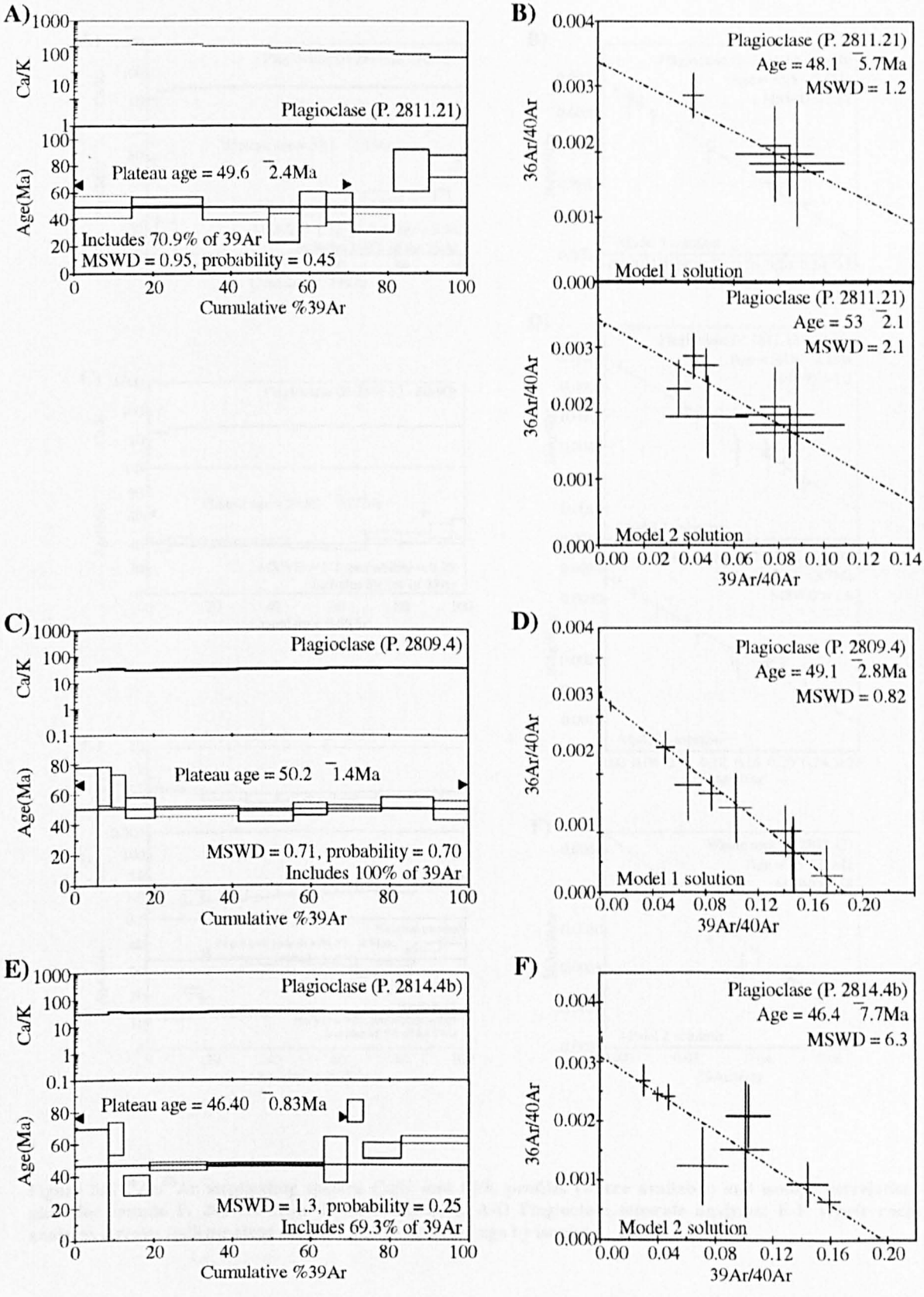

Figure 3.7. $^{40}Ar/^{39}Ar$ stepheating spectra Ca/K and Cl/K profiles (where available) and isotope correlation plots for lavas from Point Hennequin, A-B. P.2811.21, C-D. P.2809.4, E-F, P.2814.4b. Arrows indicate steps used to calculate plateau age by isoplot.

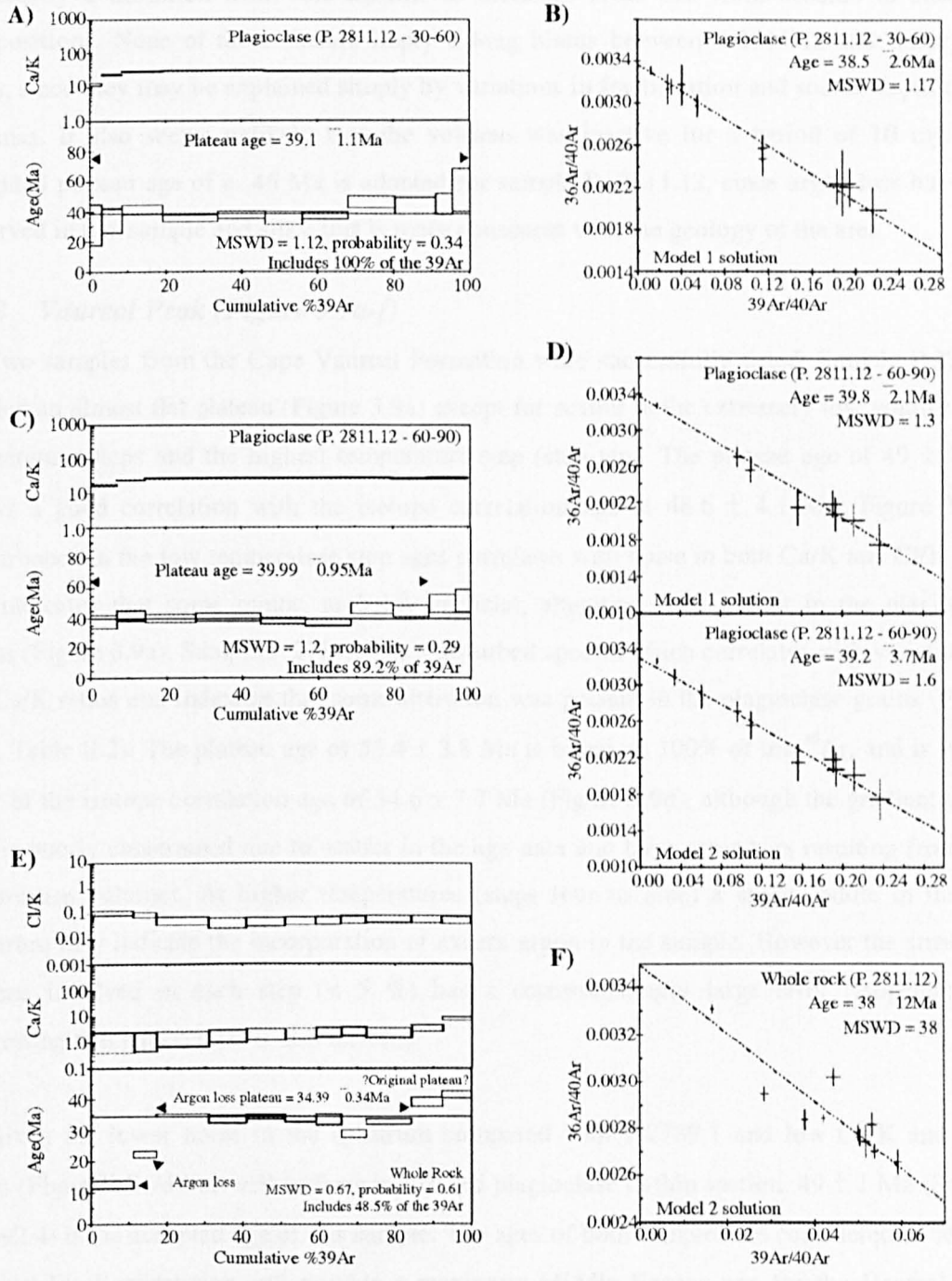

Figure 3.8. $^{40}Ar/^{39}Ar$ stepheating spectra Ca/K and Cl/K profiles (where available) and isotope correlation plots for sample P. 2811.12 from Point Hennequin. A-D Plagioclase separate analyses. E-F Whole rock analysis. Arrows indicate steps used to calculate plateau age by isoplot.

If the calculated plateau age of c. 39 Ma is accepted for sample P.2811.12, a long hiatus must be invoked to explain the age difference between this and underlying lavas (e.g. P.2811.21, P.2807.6b, P.2809.4). A sedimentary horizon of < 10 m thickness separates this lava from the other samples, which represents an extrusion hiatus, but there is no evidence for long term exposure of the volcanic surface, such as a major erosional unconformity or extensive palaeosol

development (Smellie *et al.*, 1984). The transition from underlying lavas to P. 2811.12 is also marked by a transition from calc-alkaline to tholeiitic lavas and from basaltic to andesitic compositions. None of these factors imply a long hiatus between P.2811.12 and underlying lavas, since they may be explained simply by variations in fractionation and source depth of the magmas. It also seems unlikely that the volcano was inactive for a period of 10 my. The weighted plateau age of c. 46 Ma is adopted for sample P. 2811.12, since argon loss has been observed in this sample and since this is more consistent with the geology of the area.

3.7.3 Vaureal Peak (Figure 3.9a-f)

Two samples from the Cape Vaureal Formation were successfully dated. Sample P.2792.4 yielded an almost flat plateau (Figure 3.9a) except for scatter in the extremely low volume, low temperature steps and the highest temperature step (step ten). The plateau age of 49 ± 1 Ma shows a good correlation with the isotope correlation age at 48.6 ± 4.1 Ma (Figure 3.9b). Disturbance in the low temperature step ages correlates with noise in both Ca/K and Cl/K plots and indicates that some minor, probably surficial, alteration was present in the plagioclase grains (Figure 3.9a). Sample P.2789.1 has a disturbed spectra which correlates with variations in the Ca/K ratios and indicates that some alteration was present in the plagioclase grains (Figure 3.9c, Table II.2). The plateau age of 55.4 ± 3.8 Ma is based on 100% of the ^{39}Ar, and is within error of the isotope correlation age of 54.6 ± 7.7 Ma (Figure 3.9d), although the gradient of the plot is poorly constrained due to scatter in the age data and large error bars resulting from low gas release volumes. At higher temperatures (steps four to nine) a slight saddle in the age spectrum may indicate the incorporation of excess argon in the sample. However the small gas volume involved in each step (< 5 %) has a correspondingly large error (Appendix II), suggesting that data scatter is also an issue.

Given the lower noise in the spectrum compared with P.2789.1 and low Ca/K and Cl/K ratios (Figure 3.9c/d), as well as fresher textured plagioclase in thin section, 49 ± 1 Ma (Sample P.2792.4) is the accepted age of this sample. The ages of both samples are considered to be ages of crystallisation/eruption and provide a maximum Middle Eocene age for the Vaureal Peak flora.

Dating of the Vaureal Peak lavas produced equivocal results (Figure 3.9e-f). Neither of the $^{40}Ar/^{39}Ar$ analyses from sample P.2799.1 produced appreciable quantities of gas (Appendix II). The calculated ages were anomalous (between 0 - 270 Ma), either because of isotopic resetting or the large error resulting from the low gas release (Appendix II). A mean K-Ar age of 35 ± 2 Ma was also calculated for the sample based on two sample runs within error (Table 3.5), and is therefore the only available age data for the Vaureal Peak lavas and the only constraint for the minimum age of the Vaureal Peak flora. This date is highly tentative since the $^{40}Ar/^{39}Ar$

analyses yielded total gas ages of ~ 66 Ma, which should coincide with the K-Ar data (Appendix II).

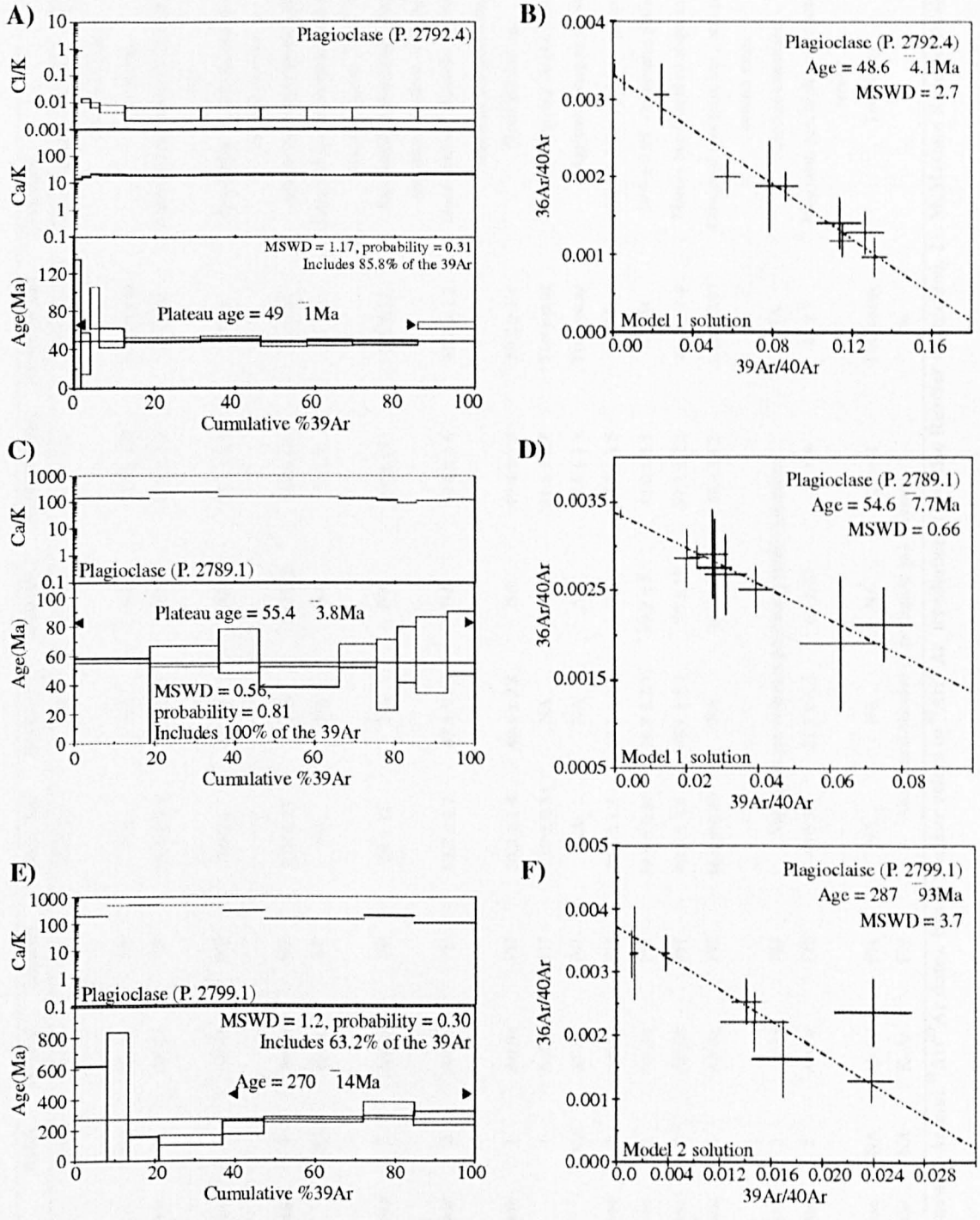

Figure 3.9. 40Ar/39Ar stepheating spectra Ca/K and Cl/K profiles (where available) and isotope correlation plots for lavas from A-D the Cape Vaureal Formation and E-F the Vaureal Peak Lavas. Arrows indicate steps used to calculate plateau age by isoplot.

Sample	Phase	Batch	Method	Locality	Plateau Age	Isochron 1	Isochron 2	Total Gas Age	Accepted Age	Comments
P.2788.6	WR	1	Ar/Ar	VP	27 ± 1.4	NA	27 ± 11	31.8 ± 1.6	27 ± 1.4	Good plateau, correlates with isotope correlation age
P.2788.6	WR	NA	K-Ar	VP	NA	NA	NA	21.0 ± 1.0	Too young	Too young
P.2789.1	Plagioclase	1	Ar/Ar	VP	55.4 ± 3.8	54.6 ± 7.7	NA	50.9 ± 7.3	Too old	Disturbed spectrum, P. 2792.4 is better age
P.2792.4	Plagioclase	1	Ar/Ar	VP	49 ± 1	48.6 ± 4.1	NA	50.7 ± 2.3	49 ± 1	Good plateau. Age assigned to Cape Vaureal Formation
P.2799-1A-D	Plagioclase	1	Ar/Ar	VP	270 ± 14	NA	287±93	229 ± 48	Too old	Age unviable given field relations
P.2799-1A-D	WR	NA	K-Ar	VP	NA	NA	NA	35 ± 2	35 ± 2	Assigned age of Vaureal Peak lavas but uncertain given $^{40}Ar/^{39}Ar$
P.2799-1A-D	Plagioclase	2	Ar/Ar	VP	28 ± 11	NA	NA	66 ± 13	?28 ± 11	Age based on extremely discordant spectrum but close to K-Ar date
P.2807.6b	Plagioclase	2	Ar/Ar	PH	42.2 ± 1.2	42.5 ± 2.6	NA	40.8 ± 1.6	42.2 ± 1.2	Good plateau? Possible Ar loss at low and high temperatures
P.2809.4	Plagioclase	1	Ar/Ar	PH	50.2 ± 1.4	49.1 ± 2.8	NA	49.4 ± 3.3	50.2 ± 1.4	Good plateau age
P.2811.12	WR	1	Ar/Ar	PH	34.39 ± 0.34	NA	38 ± 12	31.5 ± 0.4	Too young	Too young Argon loss
P.2811.12	WR	NA	K-Ar	PH	NA	NA	NA	29.6 ± 1.7	Too young	Age too young as above
P.2811.12 (30-60)	Plagioclase	2	Ar/Ar	PH	39.1 ± 1.1	38.5 ± 2.6	NA	40.3 ± 1.5	46 Ma	39.1 ± 1.1 – minimum plateau age
P.2811.12 (60-90)	Plagioclase	2	Ar/Ar	PH	39.9 ± 0.95	39.8 ± 2.1	39.2 ± 3.7	42.0 ± 1.1	46 Ma	39.9 ± 0.95 – minimum plateau age
P.2811.21	Plagioclase	1	Ar/Ar	PH	49.6 ± 2.4	48.1 ± 5.7	53 ± 18	52.2 ± 2.8	49.6 ± 2.4	Plateau but disturbed steps and Ca/K
P.2814.4B	Plagioclase	1	Ar/Ar	PH	46.4 ± 0.83	NA	46.4± 7.7	49.4 ±4.2	46.4 ± 0.83	Disturbed spectrum but good plateau in central steps
P.3031.LH	Plagioclase	2	Ar/Ar	FH	Negligible gas volumes producing erratic spectrum				NA	No age constraint
P.3031.4L	Plagioclase	2	Ar/Ar	FH	40 ± 3	21.2 ± 6.7	65 ± 27	52 ± 4	40 ± 3	Minimum age, high temperature steps erratic
P.3031.4L	Plagioclase	NA	K-Ar	FH	NA	NA	NA	29 ± 2	Too young	Too young
P.3031.4U	Plagioclase	NA	K-Ar	FH	Abandoned because of negligible gas volumes				Na	

Table 3.6. Comparative table of new K-Ar and $^{40}Ar/^{39}Ar$ dates. Batch number refers to $^{40}Ar/^{39}Ar$ irradiations (1 = Riso Reactor unshielded, 2 = McMasters Reactor shielded).

3.8 Implications of new K-Ar and $^{40}Ar/^{39}Ar$ age data

3.8.1 Fossil Hill

Relative dating suggests that the Fossil Hill flora is Late Palaeocene to Eocene age (section 3.3). This is the first attempt to date the sediments rather than the underlying volcanics of the Great Wall Bay Submember (Shen, 1999) at Fossil Hill. The crystal rich plant-bearing tuff sample, P.3031.4L, from Unit Four (Xue *et al.*, 1996) of the Great Wall Bay Submember yields a highly disturbed age spectrum at higher temperatures, possibly resulting from alteration of groundmass plagioclase. A highly tentative maximum age of crystallisation, 40 ± 3 Ma, is suggested on the basis of three low temperature, high precision steps, comprising nearly 60 % of the ^{39}Ar released from the sample (Figure 3.6c). This is consistent with relative dating (Figure 3.3). Given that the flora was deposited in an active volcanic environment, this age could probably be applied to the entire section at Fossil Hill, since the period of deposition is likely to have been smaller than the precision errors of the age data. Further dating of the Fossil Hill sequence is required to validate this age data.

3.8.2 Point Hennequin

The strata at Point Hennequin are now dated between 44 - 49 Ma based on the weighted average age data, while the strict plateau ages (Ludwig, 1998) at 1σ level give a broader age range of 39 - 50 Ma. A Middle Eocene age is proposed for the entire sequence, based on the weighted average ages that are considered to be valid, given the evidence for argon loss in the younger samples. This supports previous interpretations of the sequence by Smellie *et al.* (1984). K-Ar analyses published by Birkenmajer *et al.* (1983), that suggest an Upper Oligocene age for the upper section of the sequence are likely to reflect the argon loss identified here.

The new age data imply a Middle Eocene age for the Dragon Glacier and Mt. Wawel floras rather than the current Upper Oligocene age (Zastawniak *et al.*, 1985; Birkenmajer and Zastawniak, 1989a, 1989b). A Middle Eocene age is also inferred for the newly described Smok Hill flora. The Mt. Wawel and Dragon Glacier floras are currently considered to be the only post-Polonez glaciation floras in West Antarctica (Birkenmajer, 1997; Dingle and Lavelle, 1998b), also making them the youngest West Antarctic terrestrial flora. Instead the new age data implies that the floras are pre-glacial and therefore no post-glacial floras are present in West Antarctica.

3.8.3 Vaureal Peak

The maximum age of the Vaureal Peak flora, based on dating of the underlying Cape Vaureal Formation lavas, is c. 49 Ma. Tentative K-Ar data suggests an age of c. 35 Ma for the overlying Vaureal Peak lavas, but the erroneous dates produced by $^{40}Ar/^{39}Ar$ dating for this

sample suggest isotopic resetting. Further dating is required to constrain the age of the overlying lavas.

3.9 Summary

$^{40}Ar/^{39}Ar$ dating in this study demonstrates that alteration and isotopic resetting has affected the strata from Fossil Hill, Point Hennequin and Vaureal Peak to some extent. Four new K-Ar dates have been presented for samples from the Vaureal Peak, Point Hennequin and Fossil Hill areas. None of the K-Ar dates match closely with the $^{40}Ar/^{39}Ar$ dating or with inferred field relations, demonstrating the unsuitability of the K-Ar method at these localities. $^{40}Ar/^{39}Ar$ step-heating spectra provide both an alternative means to date the strata on King George Island and an explanation for the spurious K-Ar ages. Step heating spectra show low temperature, anomalously young step ages, that can be interpreted in terms of loss of radiogenic argon (e.g. sample P.2811.12 whole rock dates, Figure 3.8). This would be undetectable through the K-Ar method and would result in erroneous K-Ar ages. The three floras are dated as roughly contemporaneous and Middle Eocene in age. The position of these floras is shown relative to the stratigraphy of Birkenmajer (1987; 1997) in Figure 3.10.

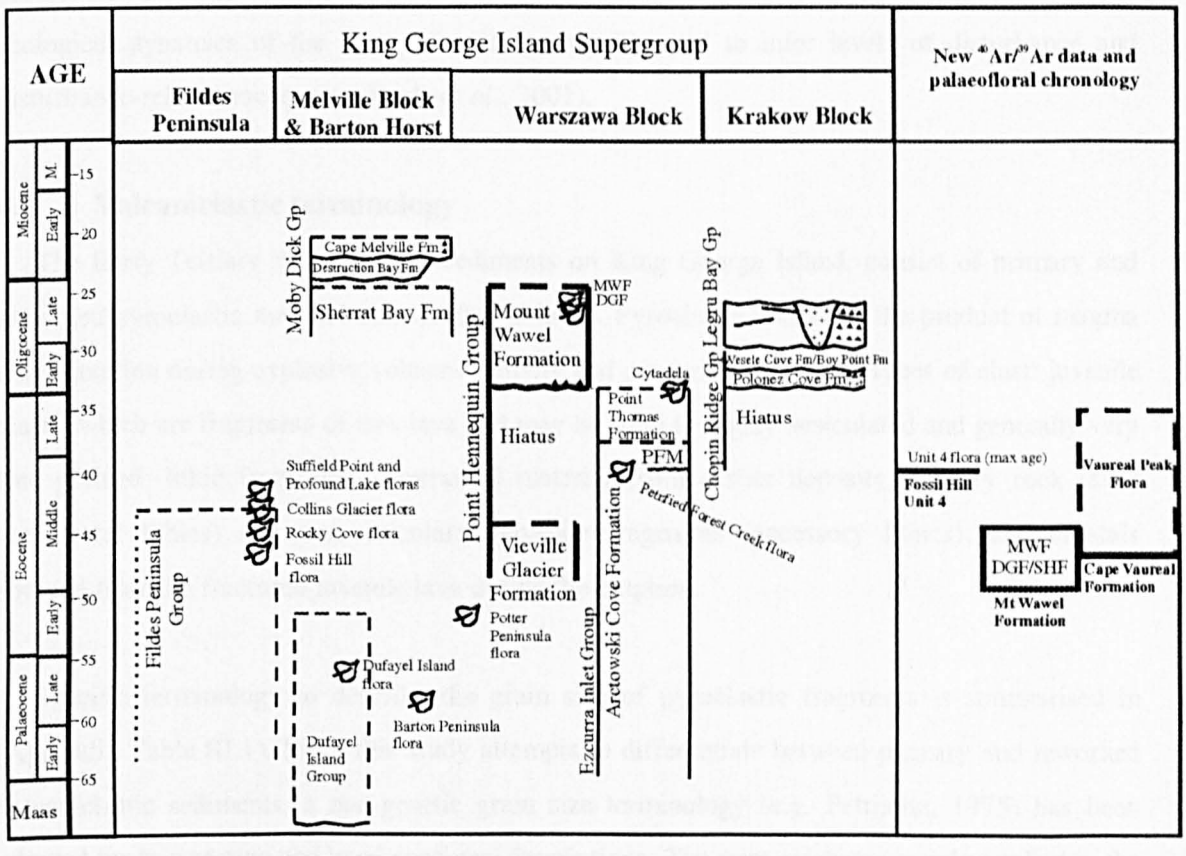

Figure 3.10. Birkenmajer (1987, 1997) stratigraphies modified with new K-Ar and 39Ar-40Ar data. The co-occurrence of the Point Hennequin floras (Dragon Glacier, Smok Hill and Mt. Wawel floras) with other Middle Eocene floras, such as the Fossil Hill flora and ?the Vaureal Peak flora increases the known diversity of the Middle Eocene flora but implies that there is no post-Oligocene (Polonez) glaciation flora. The Point Hennequin and Fossil Hill floras were originally considered to be of different composition due to climate change (Birkenmajer and Zastawniak, 1989a), but since they are now broadly contemporaneous, new models are required to explain the variations in composition. PFM – Petrified Forest Creek Member. MWF –Mt. Wawel Fm, DGF – Dragon Glacier Fm. Timescale recalibrated to Cande and Kent (1992, 1995).

Chapter 4 Sedimentology

4.1 Introduction

Plant-bearing volcaniclastic sequences on King George Island comprise variable proportions of primary volcanic material (scoria, glass shards and less commonly pumice) and basic to intermediate lithic clasts, crystals (plagioclase, clinopyroxene and opaque grains). The depositional history of these sediments has received little attention, probably as a function of the relatively poor exposure and the thin, discontinuous nature of the sediments.

In this chapter the sedimentology of the Tertiary plant-bearing localities is discussed and is interpreted in terms of: i) the mechanisms and environment of deposition, ii) the degree of sediment reworking and iii) proximity to volcanic vents. These three factors help to define the growth-environment of the Tertiary vegetation. They are also qualitative indicators of the ecological dynamics of the flora, since they may be used to infer levels of disturbance and disturbance-related succession (Poole *et al.*, 2001).

4.2 Volcaniclastic terminology

The Early Tertiary volcaniclastic sediments on King George Island, consist of primary and reworked pyroclastic material and weathered lavas. Pyroclastic rocks are the product of magma fragmentation during explosive volcanic activity and comprise three main types of clast: juvenile clasts, which are fragments of new lava and may be solid to highly vesiculated and generally very fine grained; lithic fragments - entrained material from earlier deposits, country rock lavas (accidental lithics) and non-vesiculated juvenile fragments (accessory lithics); and crystals sourced from the fractured juvenile lava during the eruption.

Specific terminology to describe the grain size of pyroclastic fragments is summarised in (Appendix Table III.1). Since this study attempts to differentiate between primary and reworked volcaniclastic sediments, a non-genetic grain size terminology (e.g. Pettijohn, 1975) has been adopted for thin section and hand specimen descriptions. The term epiclastic is only applied in the strict sense of 'lithic clasts and crystals weathered from a pre-existing rock' as opposed to the 'any particle of ash or rock reworked by water' (e.g. Fisher and Smith, 1991).

Pyroclastic deposits have a complex structure and distribution since they are produced by a combination of pyroclastic fall, flow and surge mechanisms (Appendix Table III.2) (Fisher and Schmincke, 1984; Cas and Wright, 1987). With increasing age volcaniclastic deposits become more complex, because the variability of the primary sediments is enhanced by rapid reworking and resedimentation in fluvio-lacustrine settings, or by mass wasting processes (e.g. debris avalanches, lahars). Pyroclasts such as pumice and volcanic glass, are prone to alteration and degradation and in certain conditions may be unrecognisable in the geological record (Fiske, 1969). In addition, lavas and tuffs may be difficult to differentiate in the field having a similar colour and composition, especially when welded. The ability to differentiate between primary and reworked sediments in volcaniclastic terrains is important for studies of vegetation dynamics, because plants preserved in primary volcanic deposits are direct evidence of volcanic disturbance of the palaeovegetation. The abundance of non-volcanic clasts and epiclasts within a sample (e.g. biogenic, chemical sedimentary and authigenic constituents), as well as sedimentary textures may be used to infer the degree of reworking of volcaniclastic sediment (Appendix Table III.1) (Fisher and Schmincke, 1984; Cas and Wright, 1987; D'Atri *et al.*, 1999). Major enrichment in crystals is a good indicator of reworking because crystal-rich deposits usually require a concentrating mechanism (Cas and Wright, 1987).

In the same context, the proximity of the sedimentary deposit or basin to the volcanic centre also has implications for disturbance dynamics, since raised levels of disturbance and consequently floral turnover are inferred for vegetation growing close to a vent (Poole *et al.*, 2001). Vent proximal sequences are distinguished in having a high proportion of lava flows to sedimentary deposits, while distal deposits have a greater proportion of non-volcanic, epiclastic and pyroclastic sediments, with subordinate lavas (Vessel and Davies, 1981; Mathisen and Vondra, 1983; Smith, 1988; Hackett and Houghton, 1989; Riggs and Busby-Spera, 1990). This information is crucial for accurate palaeoclimatic interpretations, because floral variations attributed to climate change could equally be explained in terms of volcanic-induced plant succession.

4.3 British Antarctic Survey archived plant-bearing sediments

Detailed sedimentological data is lacking for the BAS archived collections of material from King George Island. In this study, hand specimen and thin section data has been used to supplement field data. Sedimentological descriptions for the BAS archived collections are given in Table 4.1. A summary of the thin section descriptions is presented in Appendix Table III.3 (all localities defined in Chapter Two).

Age	Locality	Field Observations	Description	Thin section	Interpretation
Palaeocene	Barton Peninsula P.2145	Horizontally stratified mudstones and siltstones*. Probably equivalent to Units 9 and 10, described by Del Valle *et al.* (1984). Overlain by lapilli tuffs and volcaniclastic debris flows (Willan and Armstrong, in press).	Purple resedimented, fine siltstone to granule conglomerate, normally graded. Poorly sorted, angular, matrix supported and weakly laminated to bedded. Possible current ripples. **Leaf fossils are impressions/ mineralised impressions.**	P2145.2: Plagioclase dominated crystal-rich tuffaceous sandstone with fine tuffaceous matrix	Fluvial deposition is implied by the channelised nature of the outcrop (Del Valle *et al.*, 1984). The sediment is therefore considered to be resedimented. A medial volcanic setting is inferred based on the abundance of crystals in thin section, while the upper volcanic sequence with welded tuffs and lavas is more proximal in nature.
Palaeocene	Dufayel Island G.53, G.312	Waterlain tuffs in a 20 m thick sequence of sediments from the lowermost Dalmor Bank Formation (Birkenmajer, 1980) Sediments are capped by an unconformity, which is overlain by massive lava flows (Bibby, 1961; Birkenmajer, 1980).	Massive green, fine grained siltstone to medium grained sandstone. Well sorted, angular to subrounded, clasts. Occasional 1 – 2 mm thick laminae, defined by slight colour and grain size changes. Coarser grained laminations may truncate earlier surfaces. **Leaf macrofossils preserved as whole impressions with some fine venation detail and partially mineralised impressions.**	G.53: Unwelded, sideromelane dominated ash tuff. Matrix and clasts strongly smectised and calcitised. Some chlorite is present	Abundant fine grained sideromelane suggests that this is a primary, distal air fall tuff. Faint lamination may reflect fluctuations in the eruption strength or possibly deposition through a water column e.g. into a lake setting and slight reworking. This might also explain the intense alteration observed in the samples.
?Early Oligocene	Platt Cliffs G.47, G.309, G.319	Collected below a buttress ~ 80 m above sea level from a sequence of lavas and tuffs (Bibby, 1961) at the same locality as the Cytadela flora of Birkenmajer and Zastawniak (1989).	Green poorly compacted, friable, weakly laminated to massive, siltstone. Rare coarse granule clasts. Poor to moderately sorted, angular to subrounded, matrix to clast supported. Grading is common in hand specimens but way-up data is lacking. Laminae are slightly undulose, ?as a result of differential compaction or possible flow structures. Vesicles ~ 1 mm in diameter are common. **Organic material is scattered throughout the matrix. Rare woody fragments are present in the matrix with some preserved cellular structure. A single fern fragment is preserved in vertical ?in-situ orientation (G.47.16).**	G.309.14: Section dominated by glass shards. Post-depositional alteration is common. Chlorite, smectite and calcite frequently form rim cements while zeolite occurs as a late stage pore fill.	Primary distal air fall ash deposit based on the abundance of volcanic glass in thin section, although the dominance of lavas with only thin tuffaceous intervals in the sequence (Bibby, 1961suggests a more proximal environment. Vesicular tuffs are commonly formed by hydroclastic eruptions (e.g. phreatomagmatic base surges of maar volcanoes), usually only 2 – 6 km from the source vent (Fisher and Schmincke, 1984). Volcanic mud rains can also develop vesicles (Fisher and Schmincke, 1984). The Platt Cliff sediments lack the internal cross bedding that typically accompanies base surge deposits, therefore a mud rain origin is inferred. Poorly developed lamination and the high orientation of leaf fossils to bedding suggests high sedimentation rates.

Table 4.1. Summary sedimentary field-, hand specimen and thin section data for the BAS archived plant-bearing sediments (listed alphabetically). * D Armstrong (BAS) unpublished field notes.

Age	Locality	Field Observations	Description	Thin section	Interpretation
	Platt Cliffs G.50	From the same locality as G.47, G.309, G.319	Tuffaceous siltstones to sandstones, faintly laminated. **Leaves preserved parallel and perpendicular to bedding. Some leaves have a post-depositional coating of actinolite.**	G.50.12: Glass shard-rich medium to coarse sandstone.	Abundant glass in thin section suggests a primary airfall deposit. Coarseness of sediment suggests a medial to distal setting.
Eocene	Potter Peninsula P.232 Impression flora	Moraine specimens	Poorly laminated, subangular to subrounded siltstone to fine sandstone. Truncation of laminae suggests an erosional flow regime. Sample P.232.14 appears to show the basal contact of this unit, grading from a green coarse-very coarse, angular, moderate to poorly sorted sandstone into the overlying purple lithology. This is not the green lithology described below. A single, small, vertical burrow is preserved in sample P.232.23. **Plants fossils are preserved bed parallel or occasionally perpendicular to bedding (e.g. P.2145.8).**	P.232.26: Lithic and crystal dominated, with rare scoriaceous clasts. Poorly sorted, clast supported.	Both of the Potter Peninsula lithologies are contain abundant epiclastic material implying reworking. However, the angularity of the grains suggests short transport distances, such that a medial to distal setting is inferred. The relatively fine grain size of the sediment, rare bioturbation and poor lamination suggests a lacustrine or possible flood plain environment. Despite a distinct similarity in colour with sediments from Barton Peninsula, the lithologies are compositionally distinct.
Eocene	Potter Peninsula Compression flora	Moraine specimens	Yellow-brown angular, poorly sorted, medium to coarse, normally graded sandstone, with rare rounded pumice clasts (< 21 mm); Greenish brown, friable, faintly laminated, very fine siltstone; **Carbonised plant compressions are preserved subparallel or parallel to bedding.**	P.232.70I: Grey-green ?faintly laminated to massive fine grained lithic and crystal rich sandstone.	Normal grading suggests waning flow deposition e.g. as a sediment gravity flow, although the presence of pumice pebbles in the yellow brown ?basal sandstone, may imply low energy lacustrine suspension fallout with settling of larger waterlogged pumice grains.
?ME	Suffield Point P.1174	Moraine specimens	Grey brown, thinly bedded, extremely fine grained tuffaceous sediments with **matted, petrified plant material.**		Fine grain size and lamination suggests a distal air fall tuff
?Middle Eocene	Vaureal Peak[1] P.2799	Vaureal Peak is a small inlier of basic volcanics and interlayered sediments, within the older Cape Vaureal Formation. The sequence is divided into four main sedimentary units, which are the product of sediment gravity flows and fluvial sedimentation.	The fossil-bearing horizon is a thin sequence of thin bedded, pale green granule conglomerate, fine to medium sandstone and fissile muddy diamictite. Several thin (sub cm) coaly lenses are present. **Leaf impressions and mineralised impressions are preserved in a basal sandstone unit, of mass flow origin, probably occupying a small erosional hollow. Leaves preserved as impressions (± mineralised), parallel and perpendicular to bedding, sometimes as mats.**	P.2799.19: Basaltic andesite-lithic dominated sandstone with plagioclase and opaque oxide grains. Fe-oxide staining defines some of the laminae. Pyrite is present on some fresh surfaces.	Mass flow deposit. The roundness of the grains, presence of abundant lithic clasts and poor representation of primary volcanic grains such as scoria, indicates that the lithology is resedimented and has experienced moderate to high transport distances and weathering. A medial to distal volcanic setting is inferred.

Table 4.1. Continued. ME – Middle Eocene. 1 – Field notes provided by JL Smellie (BAS).

4.4 Field data

Four sedimentary localities were studied in detail during the 1999 summer field season on King George Island - Collins Glacier, Fossil Hill, Point Hennequin and Rocky Cove. At Collins Glacier, *in-situ* fluvio-lacustrine tuffaceous sediments of the Middle Eocene, Rocky Cove Submember yielded a small flora of leaves and wood fragments approximately 30 m to the south east of the Collins Glacier flora locality (Table 4.2) (Poole *et al.*, 2001). Exotic blocks in the marginal moraines of Collins Glacier yielded a few samples of a previously undescribed, siliceous, plant-bearing lithology (Table 4.2). The sediments of Fossil Hill were mapped using a modified version of the lithostratigraphy proposed by Shen (1994, 1999) and Xue *et al.* (1996) (Table 4.3), and are interpreted in terms of the hypothetical depositional environment (Table 4.4). The exotic plant-bearing blocks from the Dragon Glacier flora at Point Hennequin are subdivided into six facies (DGF-1 – DGF-6) which are grouped as two facies associations (DGF-a – DGF-b) (Table 4.5), and the newly described Smok Hill flora is placed in a separate facies (Smok-1). A brief description of the poorly exposed, *in-situ* sediments of Mt. Wawel is presented (Table 4.5). At Rocky Cove a short stratigraphic sequence of plant-bearing tuffaceous sediments from the Middle Eocene, Rocky Cove Submember is discussed and the implications for the depositional environment are considered (Figure 4.1; Table 4.7).

Site	Description	Interpretation
P.3023	**Silicified wood fragments up to 40 cm long by ca. 30 cm diameter** found in an ochre coloured, modern clay outwash, weathered out from underlying tuffaceous sediments of P.3025 type (Poole *et al.*, 2001).	Abundant juvenile material suggests a primary pyroclastic deposit, but enrichment in plagioclase crystals suggests reworking. The coarseness of the sediment (<5 mm) suggests high energy conditions. Wedged sediment geometries may imply channelised fluvial sedimentation. The high proportion of sediment to lavas suggests a distal setting. The abundance of silicified wood suggests a taphonomic control ?channel lag deposition or accumulation in a sedimentary basin such as a lake.
P.3025	Minimum 2 m thick sequence of grey-green to brown (weathered white), poorly sorted, siltstones to matrix supported breccias (< 5 mm av. 2 mm). The sediments are bedded (0.1 - 0.5 m thick) and dip generally eastwards. Variable dips are observed where the sediments drape the underlying lavas. The upper contact is not exposed. Clasts comprise pebble grade angular to subangular juvenile volcanic material and granule grade subhedral crystals of clinopyroxene and plagioclase. Several thin beds of organic-rich siltstone are present in the lower part of the sequence. Beds appear to wedge out towards the underlying topographic high. **Dispersed plant material and partially silicified wood is present in the upper metre of the sequence. Wood and leaves are segregated into different horizons but there is no apparent pattern to the distribution.**	
P.3028	P.3028 is a finely-laminated, grey siliceous silt. **Excellently preserved plant material, including araucarian cone scales, a single well preserved angiosperm leaf and fragments of ?*Equisetum*.**	The extremely fine grain size of the sediment suggests that it may be a distal siliceous air fall ash deposit.
P.3019 /20/21/ 22/27	Fossil-bearing exotic blocks sourced beneath the glacier, dominantly weathered from tuffaceous sediments of the Middle Member (Smellie *et al.*, 1984) that dip beneath the glacier. **Poorly preserved carbonised and silicified wood and rare carbonised leaf fragments are typical.**	

Table 4.2. Fossiliferous lithologies from the Collins Glacier *in-situ* sediments and from moraines.

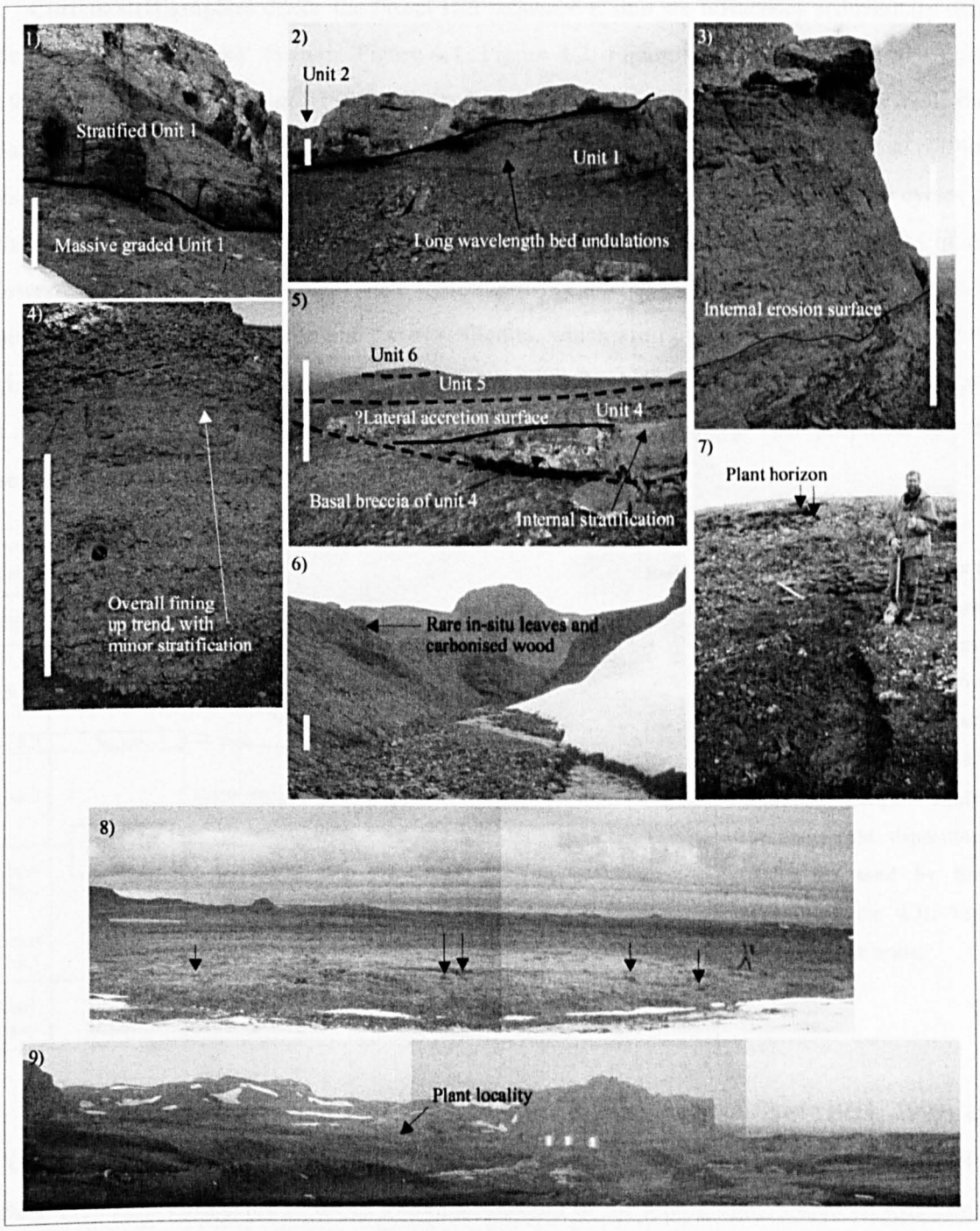

Figure 4.1. Sedimentary sequences from Fildes Peninsula. 1) - 6). Fossil Hill. 1). Unit 1, upper and lower division. Looking east. 2). Upper Unit 1. Flat area at top is Unit 2 boundary. 3). Close up of upper division of Unit 1 showing faint stratification and internal erosion surfaces. 4). Representative section of Unit 2 showing cyclic coarse breccia to sandstone normally graded beds. 5). View looking East of summit of Fossil Hill. Prominent bed in the foreground is the basal breccia of Unit 4 (note thinning to the east). This is overlain by featureless green/grey iron stained deposits of Unit 5 and by Unit 6. 7). - 8). Collins Glacier area. 7). In-situ wood and leaf locality P.3025 looking north west. Beds dipping towards the reader. 8). Panoramic view of P.3025 wood locality, several larger pieces of fossil wood are highlighted. 6) and 9). Rocky Cove.6). Rio Madera river gully, looking west. Exposures on both sides of the river. view of Rocky Cove with approximate locality of the plant beds and Rio Madera (hidden by topography), looking north (silvery objects are large oil tanks). White scale bar ~ 1 m.

4.5 Fossil Hill

Current stratigraphies divide the Fossil Hill sequence is into six tuffaceous sedimentary units deposited in 'layer-cake' fashion (Figure 4.1; Figure 4.2; Figure 4.3; Table 4.3) (Li and Shen, 1990; Shen, 1994; Xue *et al.*, 1996). The sediments are collectively termed the Great Wall Bay Submember of the Fossil Hill Member of the Fildes Formation (Chapter 3). Xue *et al.* (1996) used petrographic analysis and X-ray diffraction studies to divide the sequence into two cycles on the basis of post-depositional mineral formation (Table 4.3). The coarse volcaniclastics of the lower cycle (Units One to Three) were hydrothermally altered to produce laumontite, analcite, albite, and interlayered chlorite and montmorillonite, which are rare or absent in the upper cycle (Units Four to Six) (Xue *et al.*, 1996). An intermontane fluvio-lacustrine setting (Covacevich and Lamperein, 1970), with pyroclastic volcanism and seasonal flooding was proposed for the sequence (Shen, 1994; Xue *et al.*, 1996).

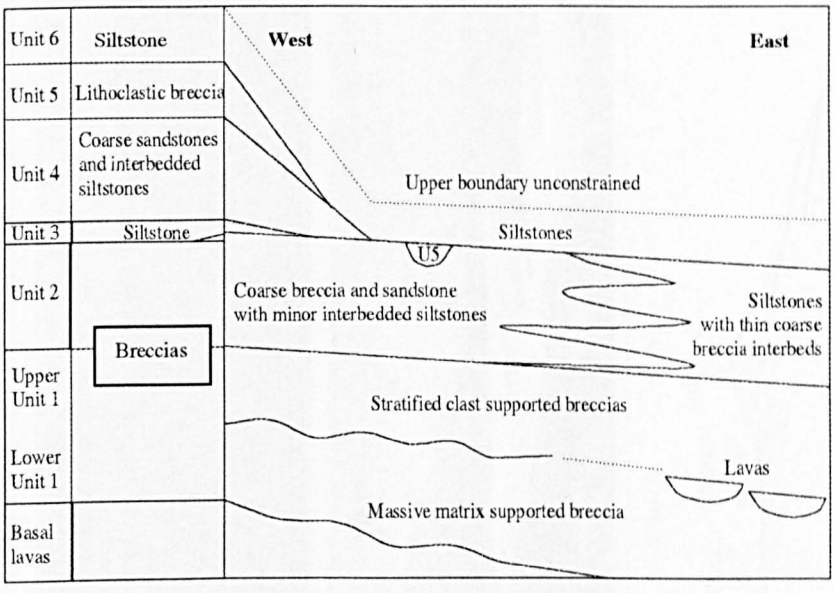

Figure 4.2. Schematic representation of the Fossil Hill sedimentary sequence according to this study viewed from the south. Laterally discontinuous bed geometries argue against the layer cake depositional model proposed by Shen (1994) (Figure 4.3). Units are to relative scale.

Based on field observations the lithostratigraphic unit divisions of Shen (1994, 1999) and Xue *et al.* (1996) have been adopted, with the following modifications: The layer cake model of Shen (1994), is considered to be an oversimplification of the stratigraphy, based on evidence of discontinuous strata such as Unit Three to Five; Unit Three is defined as the single thin dark grey tuffaceous siltstone and the new Unit Two incorporates the lower part of Unit Three; small outcrops of composite lapilli are present, intermediate between the basal lava succession and Unit One; no evidence of continuity was found for the two coal beds identified in Unit 5 (Shen, 1994), instead they are interpreted as large fragments of carbonised wood. These modifications are illustrated schematically (Figure 4.2) and in cross sections (Figure 4.3), to show the relative distribution of the sediments at Fossil Hill and the discontinuous nature of Units Three, Four and Five. This data is the basis for the new geological map of Fossil Hill presented at the end of this section in Figure 4.5.

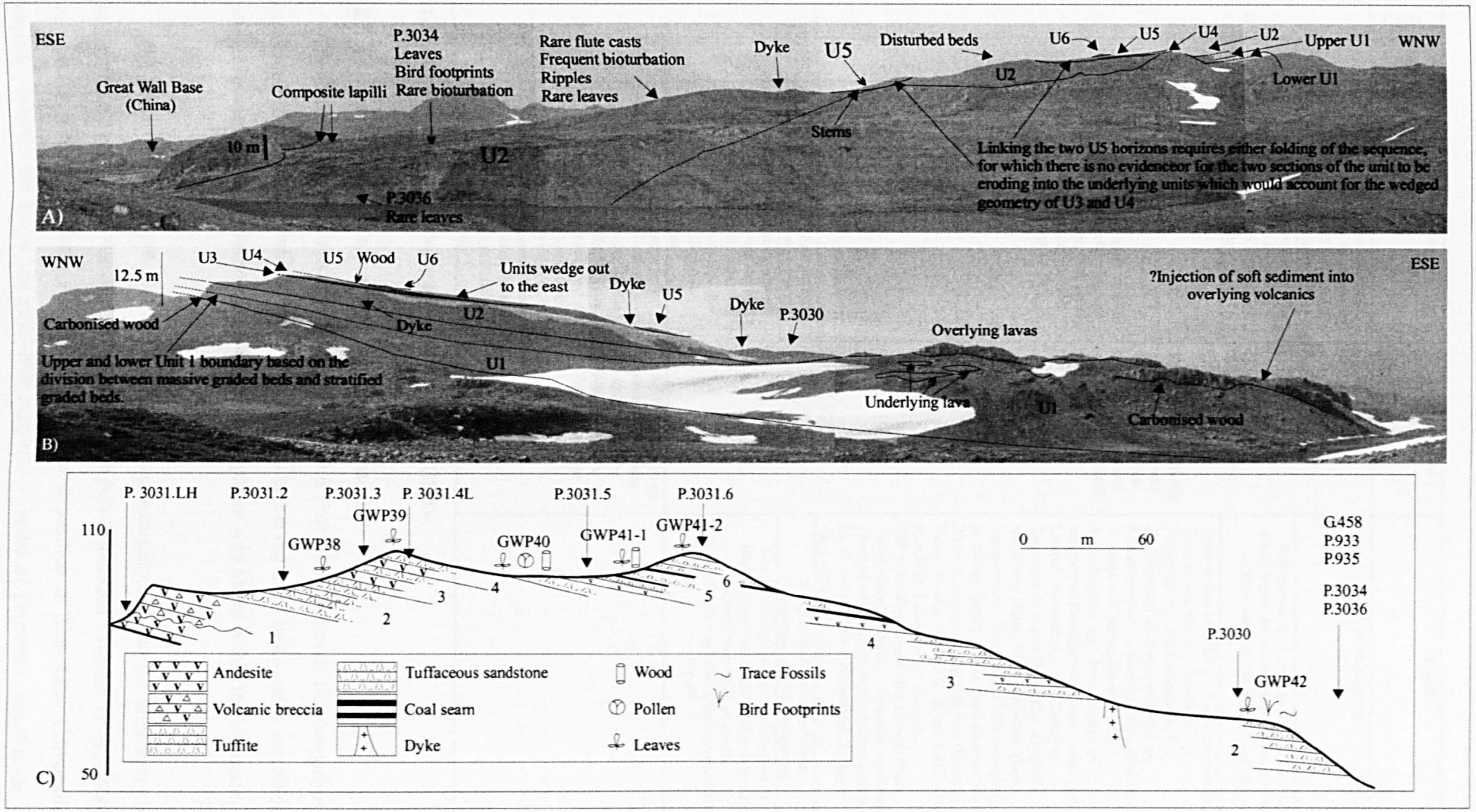

Figure 4.3. Panoramic views of Fossil Hill showing unit (U) divisions. A). North side of Fossil Hill. B). South side of Fossil Hill. C). Cross section of Fossil Hill, viewed from the south, according to Shen (1994).GWP numbers signify Chinese fossil localities, P. numbers are thin section numbers (Appendix III). NB: The Shen (1994) cross section uses a layer cake stratigraphy, whereas the new interpretation suggests that the beds wedge out from west to east as well as from south to north. The panoramic photos have slight curvature.

Cycle	Unit	Description	Interpretation	Fossils	
II	6	Dark grey, thin to medium bedded tuffaceous fine grained sandstone and siltstone with laminated structure, top not observed	Deposition of a diluvial fan, or intermontane lake sedimentation affected by seasonal flooding and volcanic activity	*Nothofagus* sp.	>1 m
	5	Yellow-greyish, thin bedded tuffites and tuffaceous fine sandstone, interbedded with two bituminous coal seams		*Nothofagus* sp., Lower coal seam 6 – 7 cm thick, Upper seam horizontally discontinuous, contains impressions of wood and leaves	1.5 m
	4	Interbedded brown-greyish thin- to medium bedded andesitic breccias and tuffaceous siltstone, with purple greyish and green-greyish level lamination		Spore-pollen assemblage: *Lygodiosporites* spp., *Concavisporites* sp., *Cyathidites* sp., *Trisaccites* sp., *Phyllocladidites* sp., *Podocarpites* sp., *Araucariacites* spp., *Nothofagidites cranwelliae*, *Nothofagidites cf. N. fuegiensis* Menendez et Caccvari, *Nothofagidites* spp., *Proteacidites* cf. *P. stippulatus* Partridge and *Proteacidites* spp. Leaves: *Osmunda* sp., *Gleichenia* sp., *Thyrsopteris shenii* Zhou et Li, *Alsophila antarctica* Christ, *Dion antarctica* Zhou, *Araucaria* sp., *Podocarpus* (*Dacrycarpus*) *tertiarius* (Berry) Florin, *Papuacedrus shenii* Zhou, *Nothofagus subferruginea* (Dusen) Tanai, *N. oligophlebia* Li, *N.* sp., *Caldcluvia mirabilis*, *Pentaneurum dusenii*, *?Myrtiphyllum* bagualense, Rhoophyllum Nordenskjoeldi Dusen, ? Oreopanax guinazui, *Lomatia mirabilis*, *Dicotylophyllum elegans* Li, *D. latitrilobatum* Zastawniak, *D.* spp., *Carpolithus* spp.	2.5 m
I	3	Bedded, dark grey and purple brown tuffites and tuffaceous siltstone		Fragments of leaves and stems *Podocarpus* sp., *Nothofagus* sp.	1 m
	2	Grey purple, bedded, zeolitised tuffites, tuffaceous coarse sandstone and fine conglomerate with mud-cracks[1], wave ripple marks, rain prints[1], and fine rhythmic laminations		Leaves *Nothofagus* sp., *Podocarpus* sp., Bird footprints *Antarctichnus fuenzalidae* Covacevich and Lamperein Trace fossils – tubular, spiral and reticulate types*	2.5 m
	1	Brown grey stratified volcanic breccias and coarse pyroclasts, with coarse level and cross stratification. Breccia small to medium in size, subangular, mainly composed of purplish andesite and greyish black basaltic andesite. Contains clasts from the underlying andesite and unconformably overlies andesites of the Palaeocene Agate Beach Formation	Rapid deposition in an intermontane basin formed after the volcanic eruptions of Agate Beach age ?Debris flow		4 m

Table 4.3. Fossil Hill stratigraphy according to Xue *et al.* (1996).

4.5.1 Depositional history of the Fossil Hill sequence

The Great Wall Bay Submember of the Fossil Hill Formation at Fossil Hill comprises 6 units consisting of tuffaceous sediments. Plant material is preserved in all units and is considered to be allochthonous since no evidence of palaeosol development was found within the sequence.

The Fossil Hill sediments rest on an erosional unconformity cut into the underlying basaltic-andesitic lavas of the Lower Member of the Fossil Hill Formation (Smellie *et al.*, 1984). This suggests a period of erosion and incision prior to deposition of Unit One. Composite lapilli deposits between the lavas and sediments supports a model of precursor, small-scale volcanic

activity (Fisher and Schmincke, 1984; Cas and Wright, 1987) prior to deposition of Unit 1. Unit One is a thick (3 - 4 m) debris flow that unconformably overlies the basic-intermediate lavas of the Lower Member (Smellie *et al.*, 1984) (Figure 4.4; 1 – 2). The NW-SE elongation of the unit and NNW-SSE palaeocurrents, indicated by clast imbrications, suggest that the debris flow was topographically controlled, possibly infilling a palaeovalley cut into the underlying lavas. To the south of Fossil Hill the lower part of the unit is overlain by blue-grey plagiophyric lavas which are sometimes injected by the sediment, suggesting broadly coeval extrusive volcanism.

Unit	*Description*	*Interpretation*	*T(m)*
6	Finely laminated crystal rich siltstone with thin sandstone interbeds. **Plant impression fossils reported by Shen (1994).**	Lacustrine suspension fallout deposits.	> 1
5	Two incised bodies of grey crystal and lithic rich sandstones **with dispersed carbonised plant fragments.**	Possible fluvial deposits.	<1.5
4	Laterally discontinuous crystal- and basic-intermediate lithic-rich tuff, with large scale low angle stratification, ?lateral accretion surfaces. **Moderate to poorly preserved angiosperm and gymnosperm shoot impressions preserved in upper part of section.**	Origin uncertain. Possible lateral accretion surfaces suggest fluvial deposition but might also represent sheet flow deposition of a large body of primary tuffaceous material. Alteration could result from deposition of primary ash into a water body.	2.5
3	Laterally discontinuous grey crystal-rich mudstone and siltstone. **Abundant plant material with rare organic preservation.**	Organic rich sediment gravity flow.	< 0.5
2	Bedded coarse crystal rich sandstones and breccias to fine grained at the western end of Fossil Hill to laminated, rippled, bioturbated mudstone dominated at the east end of Fossil Hill. **Well preserved dispersed impressions, bird footprints and bioturbation at east end of Fossil Hill.**	Hyperconcentrated flow deposits interbedded with low energy shallow lacustrine sediments.	3
1	No basal exposure, matrix supported breccia, becoming stratified and clast supported in the upper section of the deposit. NNW-SSE palaeocurrent. **Carbonised wood present in the upper portion of the deposit.**	?Cold debris flow, possibly channelised by palaeotopography. Upper section ?normal stream flow deposition or waning phase of debris flow.	4 - 5
	Rare, localised outcrops of composite lapilli. **No fossils.**	Small scale strombolian/phreatomagmatic activity of cinder cones or maars. Proximal volcanism.	<1.5
Base	Basic – intermediate lavas of the Lower Member, Fildes Formation (Smellie *et al.*, 1984)		-

Table 4.4. Modified lithological divisions and interpretations of the depositional environments of the Great Wall Bay Member at Fossil Hill. The unit thickness and continuity of the Units Two to Five differ from previous interpretations of Shen (1994) and Xue et al., (1996). T – thickness. Detailed field notes are included in Appendix III.

There is no evidence for sedimentation, prior to deposition of Unit 1, although pyroclastic stripping has been known to remove the substrate to bedrock (e.g. Mt. St Helens in 1980; Spicer, 1989). This suggests a causal relation between the debris flow deposit and the initiation of lacustrine sedimentation. In modern volcanic environments, pyroclastic volcanism often results in the reorganisation of pre-existing drainage systems and the formation of new depositional basins (Spicer, 1989; 1991; Burnham, 1994). Evidence of palaeoflow parallel to

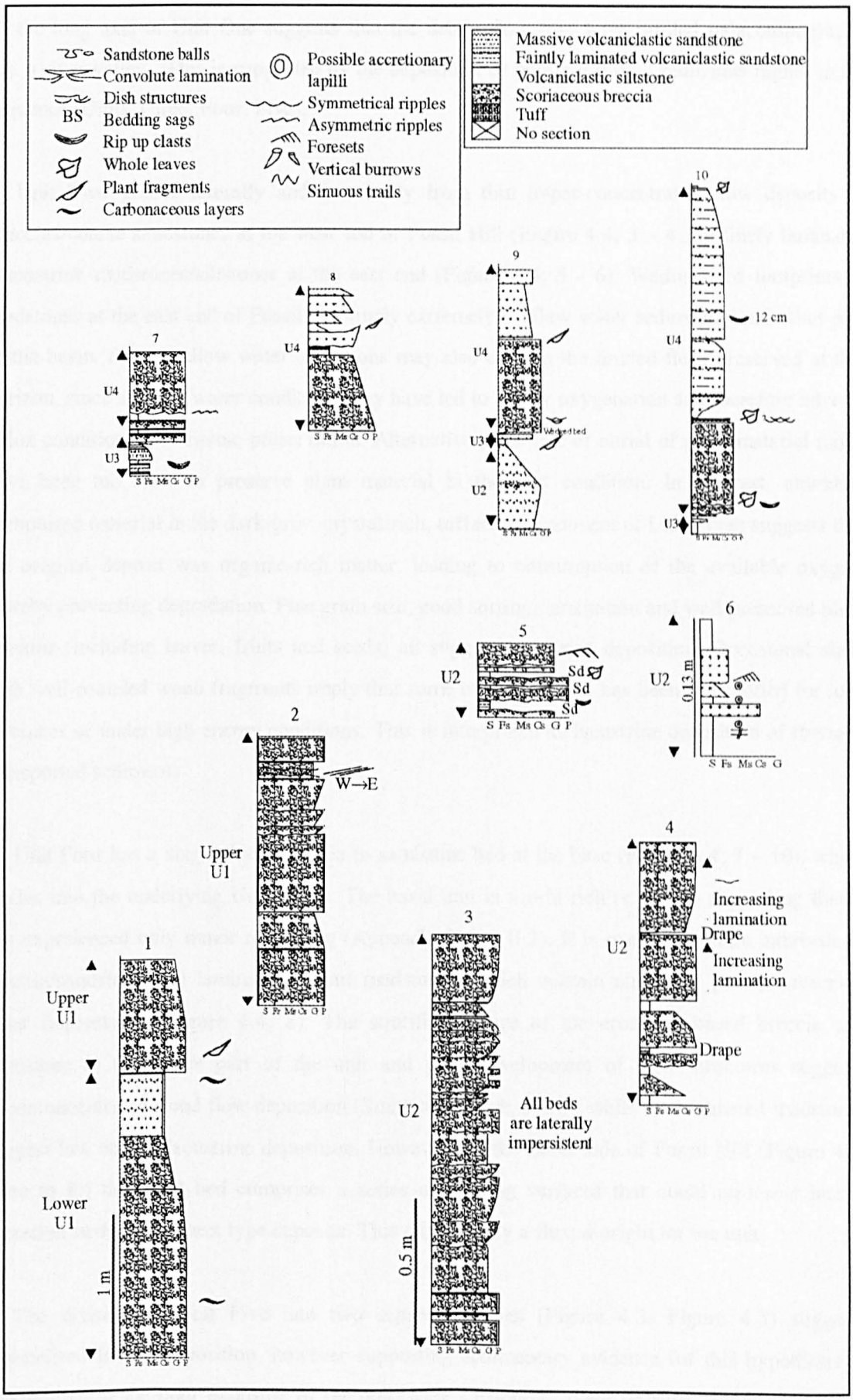

Figure 4.4. (1 – 6) Log sections of Unit One and Unit Two. 1 – 3 are from the west end of Fossil Hill. 4, 5 and 6 are from the east end of Fossil Hill. (7 – 10) Log sections of Units Two to Four. All logs use 0.5 m scale in log 3, except where otherwise highlighted. Only log 6 fully illustrates the fine grained division of Unit Two because surfaces were not commonly available to map these units. The sequence shows an overall fining up trend.

the long axis of Unit One suggests that the debris flow may have infilled palaeotopography e.g. a river valley. This is supported by the deposition of possible fluvial sediments higher in the sequence (Units Three, Four, Five).

Unit Two grades laterally and ?vertically from thin hyper-concentrated flow deposits of breccias/coarse sandstones at the west end of Fossil Hill (Figure 4.4; 3 – 4), to finely laminated ?lacustrine mudstones/siltstones at the east end (Figure 4.4; 5 - 6). Wading bird footprints in mudstones at the east end of Fossil Hill imply extremely shallow water sedimentation in that part of the basin. Such shallow water conditions may also explain the limited flora preserved at this horizon, since shallow water conditions may have led to highly oxygenation and therefore adverse redox conditions for organic preservation. Alternatively the rate of burial of plant material might have been too slow to preserve plant material in the best condition. In contrast, abundant carbonised material in the dark-grey, crystal-rich, tuffaceous sediment of Unit Three suggests that the original deposit was organic-rich matter, leading to consumption of the available oxygen, thereby preventing degradation. Fine grain size, good sorting, lamination and well preserved plant remains (including leaves, fruits and seeds) all suggest lacustrine deposition. Occasional slabs with well-rounded wood fragments imply that some of the material has been transported for long distances or under high energy conditions. This is interpreted as lacustrine deposition of fluvially transported sediments.

Unit Four has a single thick, breccia to sandstone bed at the base (Figure 4.4; 7 – 10), which erodes into the underlying Unit Three. The basal unit is scoria rich (< 40 %) suggesting that it has experienced only minor reworking (Appendix Table II.2). It is overlain by thin interbeds of breccia/sandstone and laminated fallout mudstones, which contain numerous poorly preserved plant impressions (Figure 4.4; 8). The stratified nature of the erosively based breccia and sandstone in the lower part of the unit and poor development of flow structures suggests hyperconcentrated flood flow deposition (Smith and Lowe, 1991), while the laminated mudstones suggest low energy lacustrine deposition. However, on the north side of Fossil Hill (Figure 4.5: close to 8:) the basal bed comprises a series of dipping surfaces that could represent lateral accretion surfaces or sheet type deposits. This might imply a fluvial origin for the unit.

The division of Unit Five into two separate bodies (Figure 4.3, Figure 4.5) suggests channelised fluvial deposition, however supporting sedimentary evidence for this hypothesis is lacking due to the poor exposure of the unit. Rare carbonised plant remains, dominantly stem-material, are present in the unit, which also suggests higher energy, less favourable, conditions of deposition. Unit 6 comprises purple-red laminated mudstones with thin interbeds of coarse

sandstones very similar in structure and composition to sediments from the upper part of Unit Two and are interpreted as lacustrine suspension fallout deposits with inputs of coarse grained sediments ?turbidites.

4.5.2 Implications for the local vegetation

Contemporaneous deposition of lavas with the Unit One debris flow, and evidence of small scale volcanic activity, inferred from composite lapilli deposits, suggests that the sediments were deposited close to an active volcanic vent. These deposits follow a period of erosion marked by the erosional unconformity at the base of the Fossil Hill sequence (Shen, 1994; Xue *et al.*, 1996).

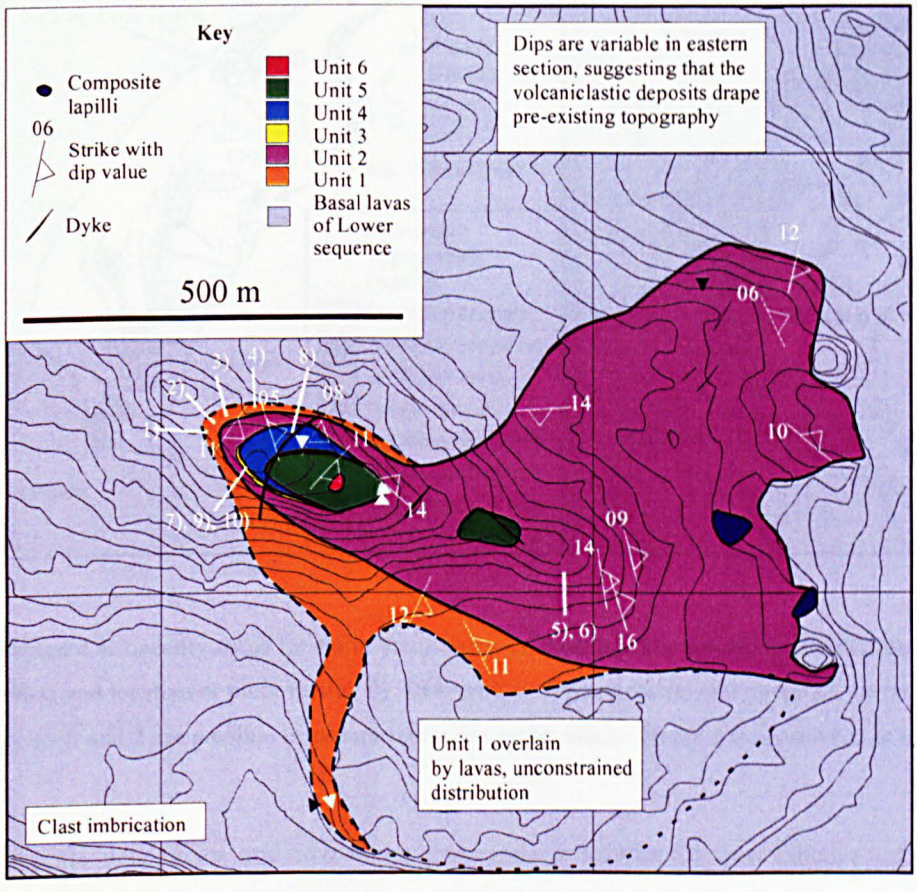

Figure 4.5. Geological map of the Great Wall Bay Submember of the Fildes Formation at Fossil Hill. Bracketed numbers indicate location of sedimentary logs in Figure 4.4.

High levels of floral turnover are inferred for the local vegetation, due to volcanism-related disturbance. Carbonised wood fragments preserved in the basal debris flow may support a model of pyroclastic forest, and soil, stripping similar to that observed at Mt. St. Helens (Burnham and Spicer, 1986; Spicer, 1989, 1991). In this context, plants fossils from the lower part of the sequence (Unit 2) could be interpreted as climax vegetation preserved after the initial volcanism, whilst fossil material from higher in the sequence (units Three and Four) is more likely to represent successional vegetation. However, evidence for partitioning of different vegetation strata in the modern record, suggests that the pattern of distribution is likely to be more complex (Burnham and Spicer, 1986).

4.6 Point Hennequin

Exotic fossiliferous blocks are found concentrated in terminal moraines along the northern margin of Dragon Glacier (Figure 4.6, Figure 4.7). The paucity of fossiliferous material along the margins of the Vieville and Wanda glaciers, to the south and north respectively, suggests that the eroded source beds originated at, or close to, the 'neck' of Dragon Glacier, a view shared by other workers of this area (Birkenmajer, 1981). Certainly the source beds originate less than 5 km distant which is where the present day ice divide occurs in the Krakow ice field (JL Smellie pers. comm., 2001).

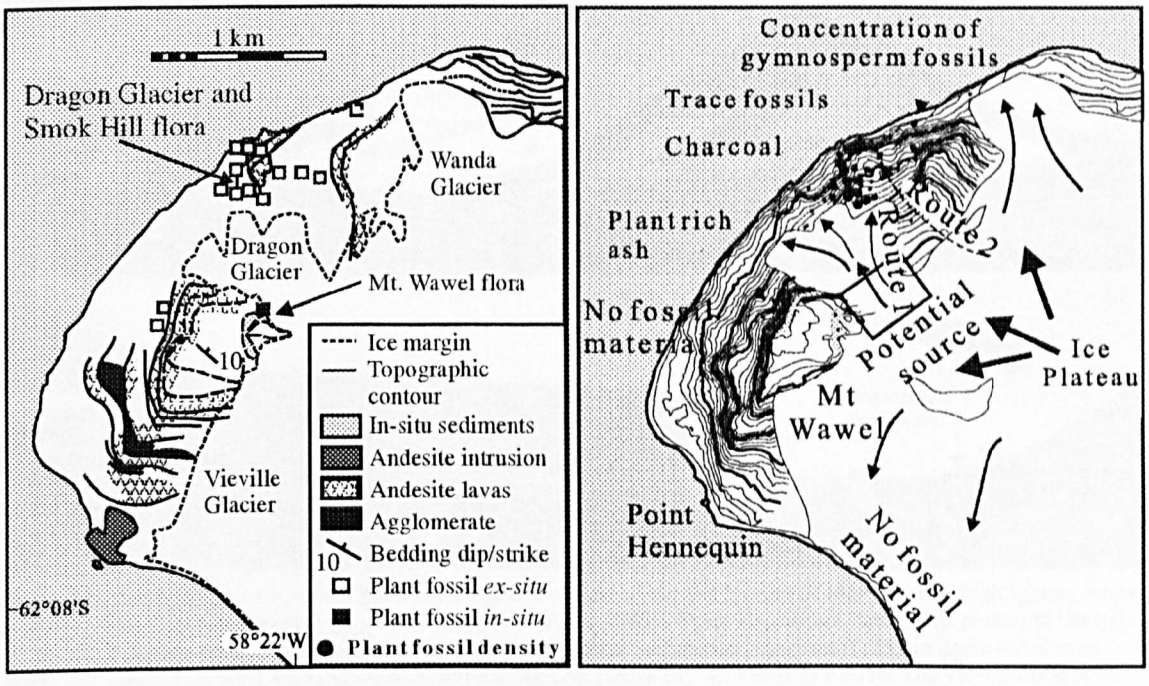

Figure 4.6. Locality maps for Point Hennequin showing A). The geology of Point Hennequin (Smellie *et al.*, 1984) and location of plant fossils, B). Distribution of plant fossils and potential source area of exotic blocks. Route 1 and 2 are possible transport routes for exotic blocks. Route 1 is considered to be the likely pathway.

The six new facies and two facies associations for the Dragon Glacier sediments (Figure 4.8, Figure 4.9, Figure 4.10) have been summarised in Table 4.5. They are commonly gradational in nature, suggesting that the exotic blocks sample through a complete fluvial–lacustrine section, from terrestrial fluvial/shoreline lacustrine sequences (facies association DGF-a) to relatively deeper water, lacustrine facies (DGF-b) (Figure 4.9). The subaqueously deposited tuffaceous sandstones of these two facies associations (Table 4.5) are interpreted as lacustrine rather than brackish or marine deposits due to the lack of any preserved marine organisms and the abundance of palaeosols and plant material. Cyclical development of palaeosols, defined by alternating rootlet beds, and symmetrically wave rippled horizons (facies DGF-2) suggests fluctuating water

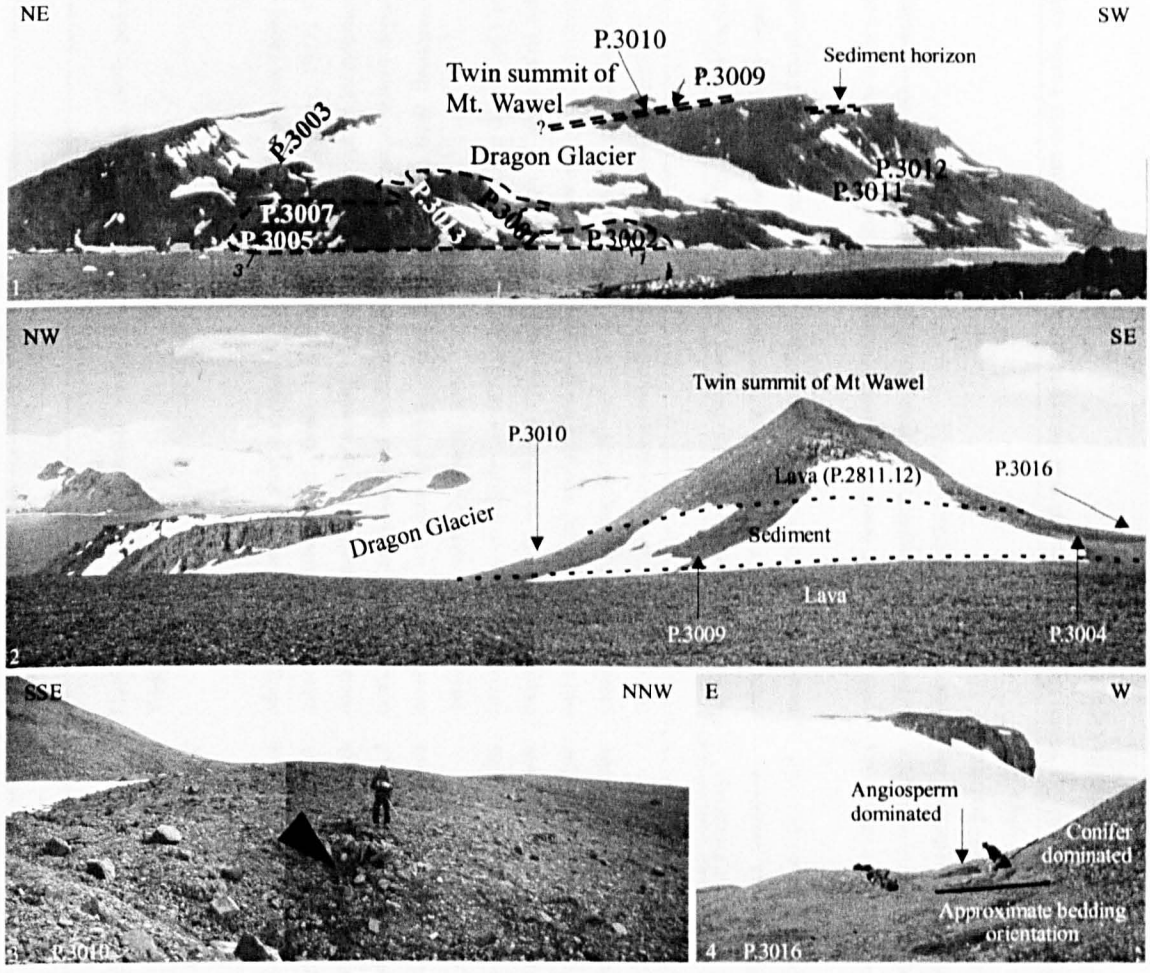

Figure 4.7. Sedimentary localities of Point Hennequin. 1). View of the south coast of Martell Inlet, highlighting major plant fossil localities and sedimentary horizons (photo Dutra, 1990).(Point Hennequin itself is off picture to the right). 2). Twinned summit area of Mt.Wawel and the *in-situ* Mt. Wawel sedimentary horizon (L.232 in Zastawniak *et al.*, 1985), 3). Locality P.3010, showing plant-bearing sediments (arrowed). 4). Locality P.3016. The view is oblique to the strike direction.

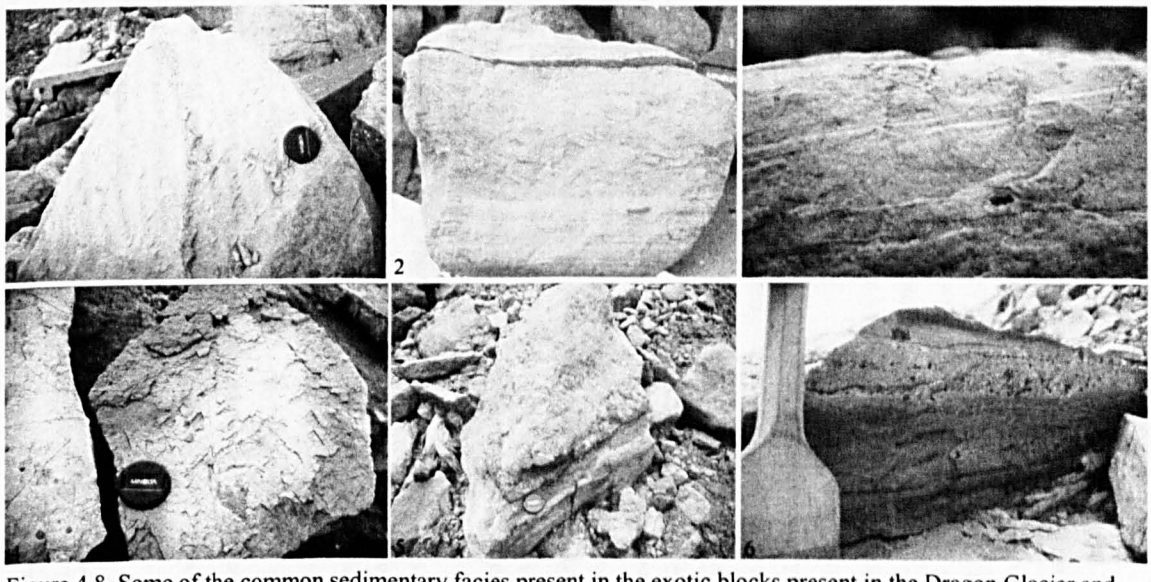

Figure 4.8. Some of the common sedimentary facies present in the exotic blocks present in the Dragon Glacier and Smok Hill area at Point Hennequin. 1). DGF-1. Slab with asymmetric ripples. 2) - 3). DGF-4. 2). Small dewatering folds. Block approximately 20 cm high. 3). Laminated slab with dewatering dish structures. 4). DGF-6. Pale brown ash fall tuffs with poorly preserved leaf impressions. 5) - 6). DGF-3 coarse scoriaceous breccia with large carbonised wood fragment. 6). Airfall tuff, capping a scoriaceous deposit. Lens cap approximately 5 cm wide, chisel approximately 20 cm long.

Facies	Description	Interpretation
	Facies association DGF-a. Subaerial to shallow lacustrine volcaniclastic sediments	
DGF-1	Blue grey to grey-brown coarse tuffaceous sandstones to tuffaceous conglomerates with interbedded tuffaceous siltstones, unidirectional flow structures and internal erosion surfaces. Massive to normally graded, with microscours and rare flute casts. Asymmetric current ripples are common. **Plant material is generally rare except for rootlets, which often arise from the upper part of the sandstone beds.**	Fluvial deposits and/or possible overbank sediments (cf Smith, 1987; Nakayama and Yoshikawa, 1997).
DGF-2	Dark grey to light brown, well sorted, normally graded, fine grained tuffaceous siltstone, interbedded with coarse grained tuffaceous sandstone, specimens capped by massive mudstone. Fine siltstone drape. Laminated to bedded. Some samples show cyclic development of symmetrical wave ripples and rootlets on a centimetre scale. Vertical (length 1 – 4 mm) and horizontal roots (length <120 mm, width<4 mm). Trackways and burrows present on the draped surfaces. Horizontal trackways are frequently associated with symmetrically wave-rippled horizons. **Leaf fossil remains are occasionally preserved in the troughs of wave ripples. Plant material is rare in rootlet horizons.**	Marginal lacustrine and shoreline palaeosol deposits with slack water mudstone drapes and subsequent bioturbation (cf. Smith, 1987; Nakayama and Yoshikawa, 1997). Oxygenated conditions are implied by the scarcity of plant fossils and abundant bioturbation. Samples lacking rootlets are interpreted as slightly deeper water, distal shoreline deposits. Cyclic development of rootbeds and wave rippled horizons suggests rapid fluctuations in water depth (cf Spicer, 1989; Burnham, 1994).
DGF-3	Scoria dominated breccia with rare plant compressions. Poorly sorted granule to small pebble, matrix supported scoria breccia. Clasts angular to rounded. Normally graded to massive. Cryptocrystalline groundmass with fine glass shards and microcryst plagioclase and pyroxene. Long axis clast alignment. Rootlets are sometimes present in the upper portion of deposits. Fine to coarse grained laminated tuffs with impact sags sometimes overlie scoria deposits. **Plant fossils comprise leaf fragments, carbonaceous layers, a single small fruit and rare charcoalified wood.**	Subaerial primary or slightly reworked, scoria flow (pyroclastic) deposit (cf Carey, 1991). Suggests small-scale strombolian type eruption or collapse of an eruption column. The laminated tuffs may be the upper section of the flow unit but are more likely to represent an airfall ash and scoria deposit (cf Carey, 1991). The development of palaeosol characteristics i.e. rootlets and lack of subaqueous textures is interpreted as subaerial deposition.
	Facies association DGF-b. Non-marginal Lacustrine sediments.	
DGF-4	Light brown and grey laminated tuffaceous siltstones to coarse tuffaceous sandstones with soft sediment deformation. Moderate to well sorted. Laminated to medium bedded. Soft sediment deformation includes dish structures, sandstone balls, small scale compaction faults and convolute bedding. Dewatering and ?slump folds vary in scale from < 0.1 – 0.5 m. **Plant fossils rare.**	Reworked tuffaceous sandstones. The scale of discrete folds up to 0.5 m long suggests a basin slope setting with loading of unstable lacustrine sediments caused by rapid sediment accumulation and/or possible synsedimentary volcanotectonic activity (cf Breitkreutz, 1991).
DGF-5	Light brown, grey-green, pink and grey, normally graded tuffaceous siltstones to coarse grained tuffaceous sandstones. Laminated to bedded. Sometimes rhythmically laminated defined by changes in colour and grain size. Laminations defined by alternations of massive tuffaceous sandstone, siltstone and massive or laminated siltstone/mudstone. The asymmetric current ripples. Rare rounded pebbles of cryptocrystalline brown, red and green plagioclase-rich scoriaceous coarser laminae often truncate underlying laminated siltstones and grade normally into laminated siltstones.	Low to moderate energy lacustrine sediments. Rhythmically laminated sediments may indicate seasonal cyclicity or cyclic deposition of normally graded microturbidites (cf e.g. Nakayama and Yoshikawa, 1997).

Table 4.5. Sedimentary facies descriptions for the Dragon Glacier, Smok Hill and Mt. Wawel sediments in which the fossil material was derived (modified from Hunt and Poole, submitted). Facies are DGF-1, DGF-3, DGF-4, DGF-6 are illustrated in Figure 4.8. All DGF-facies are presented as logs in Figure 4.9.

Facies	Description	Interpretation
DGF-5 Cont.	Occasional clasts (<63 mm) occur as isolated poorly sorted clasts. **Plants are most abundant in these sediments and occur in discrete planes, sometimes as dense mats but generally as scattered leaves. Alternating angiosperm rich leaf horizons and debris dominated horizons with abundant conifer shoots are common in many samples.**	
DGF-6	Pale yellow brown tuffs, dominated by low vesicularity-highly fragmented glass shards with diffuse contacts between laminae. Moderate to excellent preservation of abundant plant material.	Probable hydroclastic deposits suggested by high fragmentation of glass shards, lacustrine conditions indicated by diffuse contacts due to bioturbation (Fisher and Schmincke, 1984; Cas and Wright, 1987).
Smok Hill flora facies		
Smok-1	**Pale green, moderate to well sorted, angular, medium to coarse, massive to weakly laminated sideromelane-rich tuff.** Plant fossils comprise a mineralised monotypic leaf assemblage preserved in non bed-parallel orientations, with a single possible stem fragment.	Distal primary or slightly reworked air fall ash deposit. The low vesicularity of the sideromelane fragments suggests a hydroclastic origin.
Mt. Wawel in-situ sediments		
MW-1 P.3004	Highly weathered white to pale green, fine to medium sandstone. The samples were scattered in a line following the course of the gully in which P.3016 outcrops and are potentially in-situ or, at least, weathered only a short distance from their original position, although glacial transportation from an unknown source bed cannot be ruled out. **Plant fossils comprise very poorly preserved impressions mineralisations of angiosperm leaves.**	
MW-2 P.3016	Three small mounds of extremely friable, massive, fine grained, brownish green, siltstone (min 1.6 m thick). The outcrops are heavily fractured, and coated by a purplish-black ?manganese or Fe- oxide. A thin band of orange iron stained clay ?bentonite defines a weak bedding plane (142 / 20 NE). **Plant remains are discrete horizons approximately 20 cm apart and comprise craspedodromously veined, toothed angiosperm leaves, ferns and coniferous shoots. A small coalified layer was identified in the south eastern and central mounds (~ 1.5 m apart), suggesting that the material is continuous and in-situ.**	Low energy sedimentation. The ?bentonite horizon represents possible deposition of volcanic ash. Coalified material could represent leaf litter and palaeosol development, but there are no obvious palaeosol textures (e.g. mottling, rootlets) and a lag deposit, seems more likely.
MW-3 P.3010 P.3009	Coarse sandstone grading to fine massive bluish grey to grey-brown siltstone. The upper section yields well preserved carbonised plant remains. The basal part of the section contains rare poorly sorted juvenile volcanic clasts (10 – 100 mm diameter). A minor erosional surface separates the basal and upper section of the sequence.. The upper fossiliferous layer shows some taphonomic segregation, with stem material preserved close to the erosion surface while leaves and stems are found ~ 100 mm above this horizon.	The generally fine grain size and decreasing grain size up section suggests deposition under moderate to low energy and decreasing energy conditions. There is no evidence for unidirectional flow structures and/or channelisation that would indicate fluvial transport, suggesting that this may be a lacustrine or deposit.

Table 4.5. Continued. Mt. Wawel facies (MW) are stated with locality numbers. Outcrops are pictured in Figure 4.7.

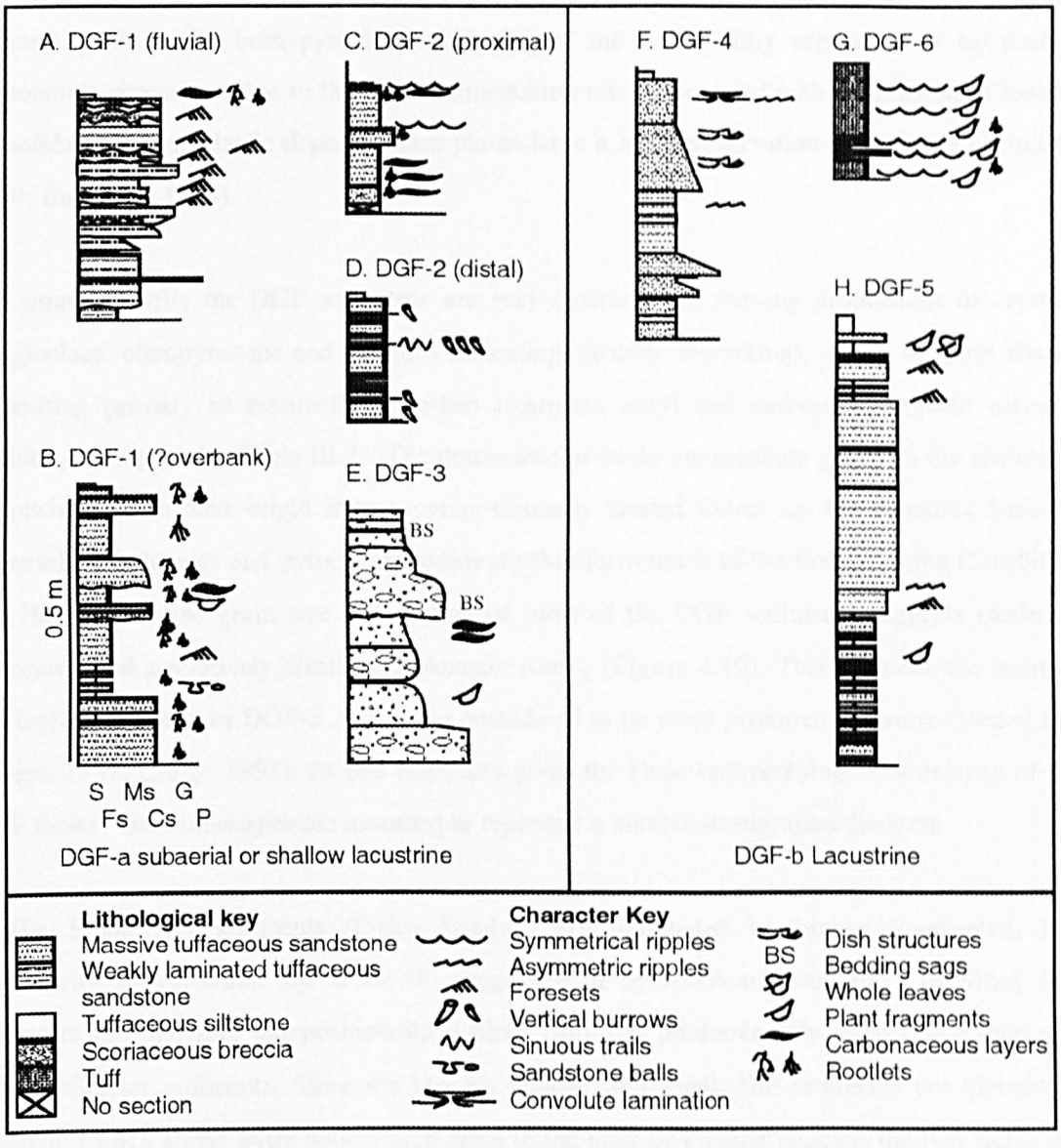

Figure 4.9. Sedimentological logs of Point Hennequin facies associations (Hunt and Poole, submitted). Scales given for DGF-1 apply to all logs. A, Fluvial deposits. B, Possible overbank/floodplain deposits. C, shoreline lacustrine deposits. D, Distal shoreline deposits. E, Coarse subaerial scoria flow (base) to scoria fall (top) deposit. F, Basin slope to delta plain sediments with soft sediment deformation. G, Fine grained subaqueous ash fall deposit. H, Laminated basin plain sediments with good plant preservation. For hypothetical palaeoenvironmental setting of facies, refer to Figure 4.10.

levels possibly resulting from draining and refilling of an ephemeral lacustrine basin. This interpretation is also supported by the absence of a well-developed lacustrine fauna except for rare trackways and burrows (facies DGF-2; Appendix III; Birkenmajer, 1981).

A small microflora comprising only terrestrial palynomorphs, also implies a terrestrial setting (Duan and Cao, 1998; G. Harrington pers. comm., 2001). In modern environments, active pyroclastic volcanism and the resulting high sedimentation rates leads to damming of local drainage networks and the formation of ephemeral lacustrine basins (Figure 4.10; Spicer, 1989). Local subsidence and basin formation due to construction of the volcanic edifice is also common.

In either case, local, often ephemeral, depositional basins are created that preserve organic material produced by both pyroclastic stripping of the surrounding vegetation or by normal taphonomic processes. Due to the high sedimentation rates associated with the erosion of loosely consolidated volcaniclastic deposits these plants have a high preservation potential (e.g. Spicer, 1989; Burnham, 1994).

Compositionally the DGF sediments are very similar, with varying proportions of crystals (plagioclase, clinopyroxene and opaques indicating variable reworking), scoria or glass shards (indicating primary or minimally reworked sediments only) and carbonised organic material (Tables 4.5; Appendix Table III.2). The dominance of basic-intermediate grains in the sediments is consistent with their origin from a compositionally limited source i.e. the abundant basic to intermediate volcanics and pyroclastic sediments that form much of the Eocene strata (Smellie *et al.*, 1984). The fine grain size and sorting of most of the DGF sediments suggests moderate reworking and a relatively distal volcaniclastic source (Figure 4.10). This excludes the coarser, scoriaceous deposits of DGF-3, which are considered to be more proximal in nature (Vessel and Davies, 1981; Carey, 1991). At this time, and given the close sedimentological similarity of the DGF facies, these lithologies are assumed to represent a similar stratigraphic horizon.

The Smok Hill sediments (facies Smok-1) are dominated by highly fragmented, low vesicularity sideromelane (up to 70 %) suggestive of hydrovolcanic activity. The Smok Hill sediments are therefore compositionally distinct from the predominantly reworked crystal-rich Dragon Glacier sediments. Since the Dragon Glacier and Smok Hill sediments are thought to originate from a single small source area close to the neck of Dragon Glacier, the two floras are interpreted as stratigraphically, rather than laterally, distinct. In studies of the modern El Chichon volcano, Mexico (Burnham and Spicer, 1986; Burnham, 1994), certain sections of the vegetation strata were found preserved in different lithologies at different intervals in the volcaniclastic sequence that might be interpreted as separate stratigraphic horizons if preserved in the fossil record. This possibility cannot be excluded for the Smok Hill flora, but the lack of conifer remains such as Araucariaceae and Podocarpaceae that are likely to have constituted part of the canopy vegetation, and are present in the Dragon Glacier Flora argues against this scenario. The fine grain size of Smok-1 suggests a relatively distal source, which is also consistent with the medial to distal setting inferred for the Dragon Glacier sediments.

The *in-situ* Mt. Wawel sediments are poorly exposed but can be divided into two facies, a lower coarse grey tuffaceous sandstone and upper fine grey-green siltstone (Table 4.5). The grey sandstone preserves carbonised plant fragments including seeds and a single cone scale, while

poorly preserved impressions are present in the upper siltstone. These sediments are lateral equivalents to sediments found in the Mt. Wawel cliff face (JL Smellie, pers. comm., 2001; Appendix III). Due to the poor exposure the depositional environment of the sequence is uncertain, although the sequence probably represents fluvio-lacustrine sedimentation.

Previous interpretations of the sediments at Dragon Glacier have been limited to brief descriptions of the range of lithologies present. Birkenmajer (1980, 1981) described pelitic and psammitic tuffs, shaley sandstones and shale, including fine-grained sandstone, siltstone and clayshale triplets from the moraine samples. Birkenmajer (1981) tentatively suggested that the latter were varves. No other evidence has been found for glacial sedimentation in the Dragon Glacier or Mt. Wawel sediments but the possibility of seasonal rhythmic sedimentation cannot be excluded. Sun-cracked surfaces were described by both Barton (1964a) and Birkenmajer (1981) in the Dragon Glacier sediments and used as evidence in support of ephemeral lake conditions. However the supposed cracks are extremely regular and show no evidence of post-formation infilling by other sediments. Red-orange iron oxide staining is concentrated along the cracks suggesting that they were related to fluid flow, possibly as a result of diagenesis.

The location and distance to the volcanic centre that sourced both the lavas and the pyroclastic sediments deposited at Point Hennequin remains unknown (Hunt and Poole, submitted). Evidence from the sequence as a whole is equivocal. Less than 40 m of thin volcaniclastic sediment intercalations, predominantly agglomerate with subordinate reworked tuffaceous material (Birkenmajer, 1981; Smellie *et al.*, 1984), are present in the 300 m sequence at Point Hennequin which is otherwise lava dominated (Jardine, 1950; Smellie *et al.*, 1984). This suggests a proximal setting, while the reworked Dragon Glacier sediments suggest a medial to distal setting (except facies DGF-3/DGF-6). The easterly dip of the volcanic pile at Point Hennequin implies a source vent to the west, possibly between Point Hennequin and Point Thomas 5-6 km distant (Figure 2.1; JL Smellie pers. comm., 2001).

In summary, the available sedimentological evidence derived from fossiliferous exotic blocks from the Dragon Glacier and Smok Hill localities suggests a medial to distal volcanic source (Figure 4.10). Reworked volcaniclastic sediments that suggest low levels of volcanic disturbance and were probably deposited in an ephemeral lacustrine basin dominate the Dragon Glacier sediments. In contrast the Smok Hill sediments are a primary ash fall deposit, possibly derived from hydrovolcanic activity and imply high levels of disturbance. The poorly exposed tuffaceous sediments of the Mt. Wawel flora (Zastawniak *et al.*, 1985) are of equivocal orgin but the low morphotype diversity of the flora tends to suggest a high disturbance setting.

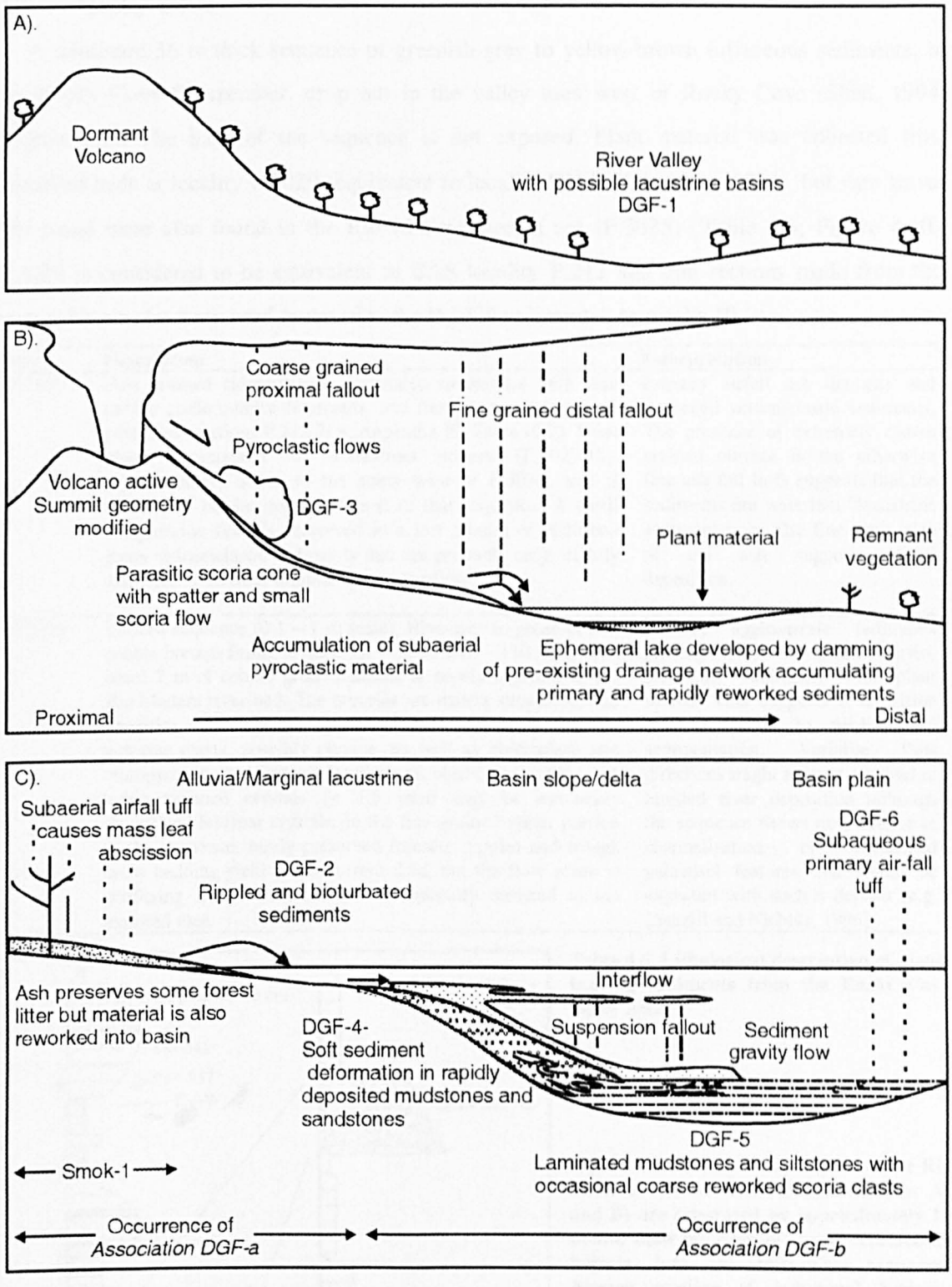

Figure 4.10. Palaeoenvironmental reconstruction of Point Hennequin (from Hunt and Poole, submitted). Schematic representations of facies distribution and the likely mechanism for sedimentation at Point Hennequin. A, hypothetical forest environment prior to volcanism. B, syn-volcanic and post-volcanic phase, primary pyroclastic sedimentation deposits large volumes of material that is quickly resedimented into the existing and/or newly formed ephemeral lacustrine basin(s). C, schematic cross section of the proposed lacustrine setting relevant to the syn-volcanic phase and for the early post-volcanic phase (modified from clastic sedimentation model proposed for oligotrophic lakes in Talbot and Allen, 1996). See text for further details on facies and numbering.

4.7 Rocky Cove

A minimum 36 m thick sequence of greenish-grey to yellow-brown tuffaceous sediments, of the Rocky Cove Submember, crop out in the valley area west of Rocky Cove (Shen, 1994) (Figure 4.1). The base of the sequence is not exposed. Plant material was collected from disturbed beds at locality P.3029 (equivalent to locality GWP 48 in Shen, 1994), but rare leaves and wood were also found in the Rio Madera stream cut (P.3035) (Table 4.6; Figure 4.10). P.3029 is considered to be equivalent to BAS locality P.212 and thin sections made from this material have also been used to describe the P.3029 sediments (Appendix III.2).

Site	Description	Interpretation
P.3029	Fine grained sideromelane dominated sandstones with rare pebble grade pumice fragments, and fine grained crystal-rich siltstones (sections P.212.7/.8; Appendix III, Table III.2). Faint planar laminations are sometimes present (P.3029.15). Approximately 30 m to the south west of P.3035, and is inferred to be the uppermost part of that sequence. A small compression flora is preserved in a low mound of disturbed green volcaniclastic sediments that are probably only slightly displaced from their original in-situ location.	Primary airfall ash deposits and reworked volcaniclastic sediments. The presence of extremely coarse grained pumice in the otherwise fine ash fall tuffs suggests that the sediments are waterlain ?lacustrine sedimentation. The fine grain size of the ash suggests distal deposition.
P.3035	Bedded sequence (0.1 – 1 m scale). Blue-grey to green-brown cobble breccia fining to siltstone (< 0.19 mm – 110 mm). The basal 7 m of cobble grade material is poorly exposed in the Rio Madera river bed. The breccias are matrix supported, and comprise extremely fine grained brown and green juvenile volcanic clasts, possibly pumice, as well as plagioclase and clinopyroxene bearing red ?scoriaceous clasts. Green-blue soft cubic twinned crystals (< 1.5 mm) may be extremely chloritised feldspar crystals. In the fine grained upper portion of the sequence, rarely preserved foresets, ripples and trough cross bedding yield palaeocurrent data, but the flow sense is confusing since structures are orthogonally oriented to the exposed face.	Primary agglomerate sediments grading into reworked fluvio-lacustrine sediments with plant fossils. This suggests a transition from proximal to medial/distal sedimentation. Variable flow directions might support a model of braided river deposition although the sequence shows no evidence of channelisation or associated palaeosol features that would be expected with such a deposit (e.g. Cantrill and Nichols, 1996).

Table 4.6. Lithological description of plant-bearing sediments from the Rocky Cove valley area.

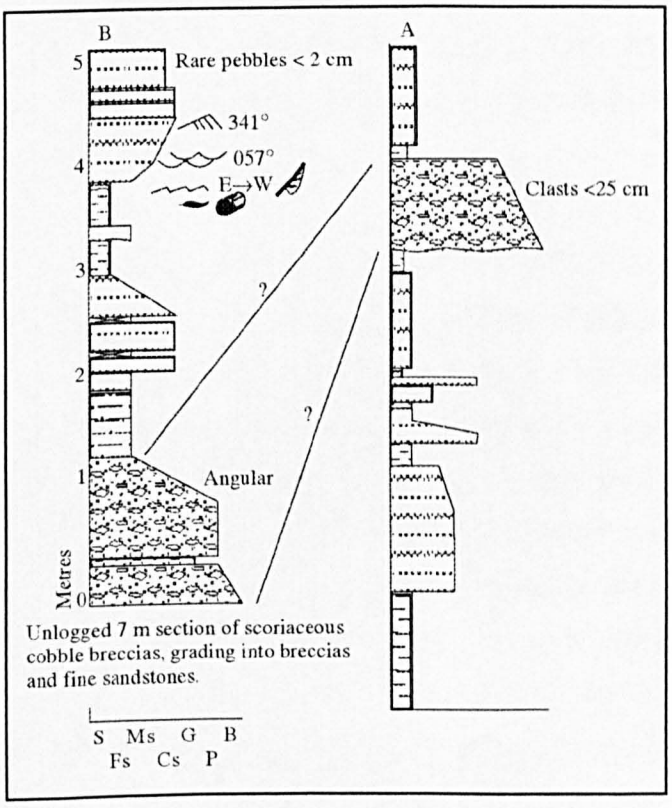

Figure 4.11. Sedimentary logs from the Rio Madera stream cut (P.3035). Sections A) and B) are separated by approximately 10 m and show an input of coarse scoriaceous breccia into the tuffaceous sequence. Normal grading of individual horizons suggests deposition under waning flow conditions. Palaeocurrent data for the upper section of the sequence yield conflicting signals but a general east-west flow sense is suggested. Poorly preserved plant material only, has been found in the uppermost part of the section. The disturbed plant-bearing sections at P.3029 occur at the uppermost part of the section. Grain size and vertical scales are the same for both sections.

The Rocky Cove Submember comprises both primary, glassy ash fall sediments and reworked tuffaceous sediments (Table 4.6). Agglomerates in the lowermost section of the Rio Madera stream pass upwards into fine grained tuffaceous sediments with occasional palaeocurrent markers (Figure 4.11). This suggests a transition from primary pyroclastic flow deposition to the fluvio-lacustrine sediments preserved in the upper part of the sequence. Plant material is confined to the uppermost fluvial-lacustrine section (Figure 4.1: 9; Figure 4.11) and could represent the remains of vegetation disturbed by volcanism. The thickness of sediments suggests a medial or distal setting although the agglomerate deposit suggests a more proximal setting.

4.8 Conclusions

The Lower Tertiary sediments described in this chapter comprise primary ash fall deposits and reworked fluvio-lacustrine and ?sediment gravity flow deposits, which all originate from a terrain governed strongly by volcanic activity. Separate sedimentary terrains are represented by fluvial sediments (e.g. Barton Peninsula) and by lacustrine sediments (Dragon Glacier flora), however the origin of some sedimentary units is enigmatic. Many of the sediments (Dufayel Island, Platt Cliffs, Rocky Cove) have sedimentary characteristics that suggest fluvial and/or lacustrine deposition but without field studies it is not possible to determine their origin. In the case of the Collins Glacier sediments, a fluvio-lacustrine origin is suggested but the lack of clear sedimentary textures mean that further interpretations are not viable. The sediments are interpreted as forming a complete spectrum of vent proximal to distal deposits. There is no apparent spatial or temporal pattern to the deposits. Figure 4.12 shows the hypothetical setting of the fossiliferous sediments in terms of their distance from a volcanic centre (NB: the actual palaeoenvironment of KGI comprises numerous volcanic centres). Disturbance levels are greatest for vegetation growing closest to the vent.

The terms proximal, distal and medial are useful concepts for visualising the palaeoenvironment of a fossil flora and categorising the level of disturbance experienced by a flora, however caution is required in applying this concept. In many cases the sedimentary data and sequence data are consistent in suggesting the proximity of the volcanic centre e.g. Barton Peninsula, Collins Glacier, Rocky Cove and Vaureal Peak (Figure 4.12). On the basis of grain size and composition the Dufayel Island sediment is considered to be a distal air fall tuff, but the dominance of lava in the sequence (Birkenmajer and Zastawniak, 1986) suggests a vent proximal location. This could be explained in terms of deposition of material from a distant volcanic eruption into the proximal zone of a volcano. Alternatively it might be explained as a small-scale eruption of a vent that deposited distal-type material in its own proximal zone.

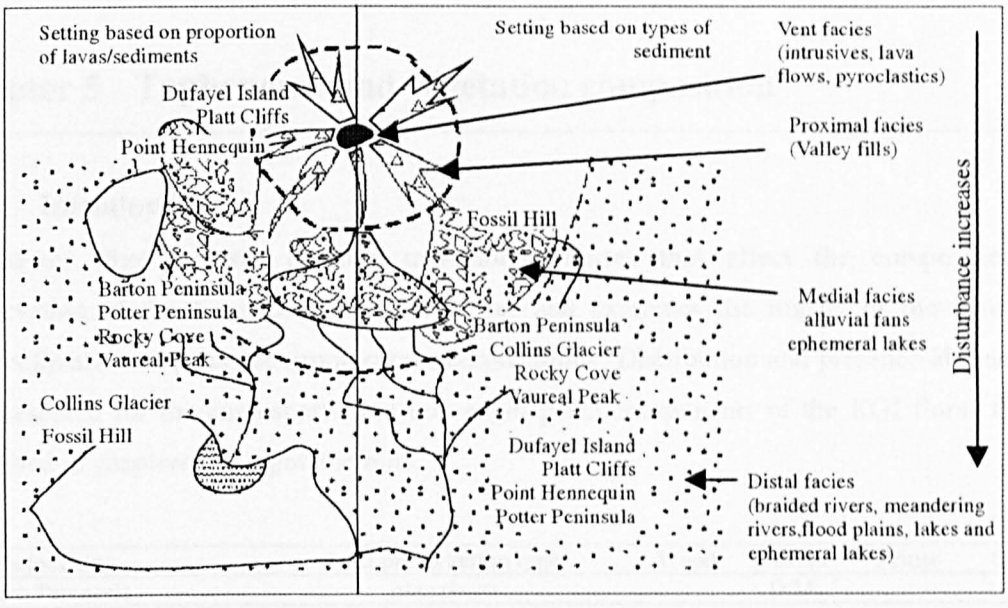

Figure 4.12. Sedimentary localities in relation to the volcanic vent (base map after Vessel and Davies, 1981; Mathisen and McPherson, 1991). Note that the placement of some floras changes according to whether the whole sequence is used to determine the proximity of the flora to a vent or whether this is determined on the nature of the fossiliferous sediment alone.

The disturbance model proposed by Poole *et al.* (2001) implies that floras proximal to a volcano are likely to be low diversity. However, the two most diverse flora localities on King George Island, may represent vegetation growing close to the source of volcanism – Fossil Hill and Point Hennequin (Figure 4.12). This is interpreted in the case of Fossil Hill as volcanic preservation of the pre-volcanic vegetation. At Point Hennequin, evidence of both volcanically preserved leaves and leaves preserved in reworked sediments suggests that the pattern is more complex and that elements of pre-volcanic and syn-volcanic vegetation are preserved together. In conclusion, the majority of the vegetation growing on King George Island during the Lower Tertiary probably originated from disturbed, or periodically disturbed, volcanogenic terrains.

Chapter 5 Taphonomy and vegetation composition

5.1 Introduction

Chapter Five assesses possible taphonomic biases that affect the composition and preservation of the King George Island floras and examines the impact of this data upon palaeoclimatic and palaeoenvironmental interpretations. Distribution and presence-absence data are presented for the angiosperm and non-angiosperm components of the KGI floras that are described in chapters six, eight and nine.

Flora locality	Leaf preservation type	Wood	Leaves	Fruits	Seeds
Barton Peninsula	Impression		D/M		
Collins Glacier (moraines)	Compression	*	D		
Collins Glacier (in-situ)	Compression	x	D		
Cytadela flora	Compression		M	x	
Dragon Glacier	Compression	x	D/M	x	x
Dufayel Island	Impression		M		
Fossil Hill Unit 2	Impression Mineralisation		D		
Fossil Hill Unit 3	Compression	x	M	x	x
Fossil Hill Unit 4	Impression		D/M		
Fossil Hill Unit 5	Compression	x	D		
Fossil Hill Unit 6	Impression		D		
Platt Cliffs	Impression and Mineralisation with amphibole		M		
Mt. Wawel	Compression	x	D/M		x
Potter Cove	Compression	x	M/D		
Potter Cove	Impression		?D		
Profound lake	Impression	x	M	x	
Rocky Cove	Compression	x	D/M		x
Smok Hill	Mineralised impression	x	D/M		
Vaureal Peak	Impression		M		

Table 5.1. Preservation style and types of organs preserved in the King George Island floras. *Silicified wood (Zhang and Wang, 1994; Poole et al., 2001). D – dispersed leaves, M – leaf mats, X – present.

5.2 Style and types of organ preservation

Plant organs collected from King George Island include wood, leaves fruits and seeds (Table 5.1). Fragmented and whole angiosperm leaves are the dominant macrofossil type preserved in the floras. This contrasts with silicified and/or carbonised wood fragments which are relatively rare, although locally abundant (e.g. Collins Glacier) (Table 5.2). Leaf fossils are preserved either as carbonised compressions lacking cuticle, as pure impressions, and as mineralised impressions. Rare organic preservation is indicated in the Fossil Hill flora by occasional poorly preserved fragments of fluorescing cuticle. Leaf remains are preserved as dispersed organs and as leaf mats. The greatest diversity of plant organs occurs in the carbonised compression floras, in particular the Dragon Glacier flora and Fossil Hill Unit 3 floras (Table 5.1 and Table 5.2). This may be a result of selective preservation, although there may also be an identification bias

towards the compression floras, which are more readily identified in field and hand specimens because of their dark coloration.

The Platt Cliffs and Smok Hill floras represent two unusual preservation styles. Leaves of the Platt Cliffs flora, are coated with a layer of blackish-green actinolite. Both the sediment and leaves are coated, suggesting that the mineral is a post-depositional alteration feature. The Smok Hill flora, from Point Hennequin, comprises pale green mineralisations but in this case the coating is confined to the leaves themselves and may represent a non-pervasive alteration product related to pre-abscission ash coating (Spicer, 1989, 1991).

Flora locality	Grain size	Bryophytes	Ferns	Broadleaf conifers	Conifer shoots	Angiosperms (large fragments)	Fruits	Seeds	Woody stems	Wood	Plant debris
Barton Peninsula	S/MS		*			***			**		**
Collins Glacier (moraines)	FS		*		*	*	*		**	***	
Collins Glacier (in-situ)	MS/G		*		*	*					**
Cytadela (G.47, 309, 319)	FS/G		*	***		**	*				***
Dragon Glacier	FS/P		***	***	***	***	**	**	***	*	***
Dufayel Island	FS/MS		*			***			*		***
Fossil Hill Unit 2	FS			*	***	***			*		
Fossil Hill Unit 3	S/FS	*	***	**	**	***	***	*	***		***
Fossil Hill Unit 4	G		**	***	**	**			**		***
Fossil Hill Unit 5	CS					**			***		***
Fossil Hill Unit 6	FS					*					
Platt Cliffs (G.50)	MS/CS			*		**					
Mt. Wawel	S	*	*			*		***	***		***
Potter Cove Compression	FS		***	***							
Potter Cove Impression	MS/P		*			**					**
Profound lake	FS		*	*		**	*		***		
Rocky Cove	FS/G		***	?*		**	*	***			***
Smok Hill	MS/CS					**			*		
Vaureal Peak	FS/CS		***			***					***

Table 5.2. Types of plants occurring in each flora. Grain size, S – siltstone, FS – fine sand, MS – medium sand, CS – coarse sand, G – gravel, P – pebble. *Rare, **Common, ***Abundant. Plant debris refers to small angiosperm fragments (< 25 % lamina), and includes coniferous fragments when they are present in the flora.

5.3 Presence/absence data for the King George Island floras

The following tables summarise the presence-absence data for the all plant organs from King George Island that are described in this study (Table 5.3; Table 5.4; Table 5.5). Since the floras are predominantly clustered in the Middle Eocene, this data has not been arranged in terms of changing biodiversity gradients over time. In general terms though, the flora is lower in diversity in the Palaeocene (Dufayel Island flora, Barton Peninsula flora) and Late Eocene – earliest Oligocene (Cytadela and Platt Cliffs flora) and most diverse in the Middle Eocene (all other floras). This diversity trend is also reflected in the sample size variation over time and could simply be an artefact of the relative sample sizes.

Locality	Barton Peninsula	CG moraines	Cytadela	Dragon Glacier	Dufayel Island	Fossil Hill U2	Fossil Hill U3	Fossil Hill U4	Mt. Wawel	PC impression	Platt Cliffs	Rocky Cove	Smok Hill	Vaureal Peak
Entire margined leaves														
1.1. *Dicotylophyllum washburni*				25		1		14				2		
Morphotype 1.2				1										
Morphotype 1.3					1									
Morphotype 1.4				5										
Morphotype 1.5				2										
Morphotype 1.6					1						2			
1.7. Dicotylophyllum duseni						4		3				1		
Morphotype 1.8											1			
Morphotype 1.9			1								4			
Morphotype 1.10								3						
?Lauriphyllum nordenskjoldii				4				2						
Morphotype 1.12								7						
Morphotype 1.13					2									
Morphotype 1.14				1										
Morphotype 1.15										1				3
Morphotype 1.16				1										
Morphotype 1.17			3											
Morphotype 1.18														1
1.19. *Ficophyllum skuaensis*	1													
Morphotype 1.20				3								1		
Morphotype 1.21				1										
Morphotype 1.22											6			
Morphotype 1.23				1										
Morphotype 1.24				2										
1.25. *Symplocos commutatifolia*										2				
Morphotype 1.26	1													
Morphotype 1.27														1
Toothed margined leaves														
2.1 Cunoniaceae				61										
2.2 Cunoniaceae						1								
2.3. Cunoniaceae *'Fildesia pulchra'*						1		6						
2.4 cf. *Lomatia*				5		3	1	1						
Morphotype 2.5							1							
Morphotype 2.6				1										
Morphotype 2.7										1				
Morphotype 2.8				1										
Morphotype 2.9				8					2					
2.10. *Monimiophyllum antarcticum*						3		2						
Morphotype 2.11	3													
Morphotype 2.12										5				
Morphotype 2.13						2		3						
Morphotype 2.14								1						
Morphotype 2.15						9								
Morphotype 2.16			3		4									
Morphotype 2.17					2									
Morphotype 2.18					5									
Morphotype 2.19											5			
Morphotype 2.20			1		1									
Morphotype 2.21								2						
Morphotype 2.22				3										
Morphotype 2.23												1		
Morphotype 2.24							4							
Morphotype 2.25							2							

Table 5.3. Presence-absence data for the angiosperm component of the King George Island vegetation. PC – Potter Cove. CG – Collins Glacier.

Locality	Barton Peninsula	CG moraines	Cytadela	Dragon Glacier	Dufayel Island	Fossil Hill U2	Fossil Hill U3	Fossil Hill U4	Mt. Wawel	PC impression	Platt Cliffs	Rocky Cove	Smok Hill	Vaureal Peak
Morphotype 2.26						2								
Morphotype 2.27												1		
Morphotype 2.28						1		1						
Morphotype 2.29				7										
Morphotype 2.30								1						
Morphotype 2.31						2								
Morphotype 2.32				1										
Morphotype 2.33		1												
Morphotype 2.34							1							
Morphotype 2.35									1					
Morphotype 2.36				1										
Morphotype 2.37				1					1					
Morphotype 2.38				1										
2.39. *Nothofagus dicksoni*				1										
2.40 *N.* sp. 1				6										
2.41 *N.* sp. 2				1										
2.42 *N.* sp. 3	2									14				
2.43 *N.* sp. 4				5										
2.44 *N.* sp. 5				2										
2.45 *N.* sp. 6				3										
2.46 *N.* sp. 7				3										
2.47 *N.* sp. 8									1					
2.48 *N.* sp. 9			1											
2.49 *N.* sp. 10				1				1		1				18
2.50 *N.* sp. 11				18									3	
2.51 *N.* sp. 12				9										
2.52 *N.* sp. 13			1											2
2.53 *N.* sp. 14				2										
2.54 *N.* sp. 15				7										
2.55 *N. oligophlebia*					6		17	2						
2.56 *N.* sp. 16				6										
2.57 *N.* sp. Juvenile 1				2										
2.58 *N.* sp. Juvenile 2				2										
Total specimens	7	1	10	203	22	29	26	50	5	24	18	7	3	23
Total morphotypes	4	1	6	37	8	11	6	15	4	6	5	6	1	5

Table 5.3. Continued. Total specimens - Number of specimens examined per morphotype, Total types = Total number of morphotypes per flora. Note that only the Dragon Glacier and Fossil Hill floras have morphotype diversity greater than 10. Combining the flora from Units Two, Three and Four gives a total of 22 morphotypes, not 33 morphotypes, since some specimens are common to more than one flora. Data not summarised for Collins Glacier *in-situ*, Profound Lake, which have not been described because of the poorly preserved fragmentary nature of the floras. Potter Cove compression not included because it does not contain angiosperm remains. Total number of angiosperm specimens = 428. Total number of morphotypes = 85, 27 entire margined morphotypes, 58 toothed margined morphotypes of which three specimens are ?juvenile. NB: Only three King George Island floras have more than 10 morphotypes.

5.4 Diversity of the floras

The KGI floras are generally low in diversity, with less than ten angiosperm morphotypes per locality, excepting the Dragon Glacier and Fossil Hill floras, which have 37 and 22 morphotypes respectively. The Dragon Glacier flora is by far the most abundant flora in terms of total plant specimens (305; including all plant organs) (Tables 5.3: Table 5.4) and diverse flora in terms of plant types (61: including all plant organs). This is likely to be related in part to the large size of the collection, and the greater length of time spent examining this flora. The Potter Cove compression flora is the only KGI flora that does not contain any angiosperm remains, although angiosperms are present in the Potter Cove impression flora.

Locality	Barton Peninsula	CG In-situ	CG moraines	Cytadela	Dragon Glacier	Dufayel Island	Fossil Hill U2	Fossil Hill U3	Fossil Hill U4	Mt. Wawel	PC impression	PC compression	Platt Cliffs	Profound Lake	Rocky Cove	Smok Hill	Vaureal Peak
Non-angiosperms (Chapter 8)																	
Bryophyte type 1								1									
Bryophyte type 2										1							
Equisetum					2												
Lophosoria sp.												?4			1		
Thyrsopteris shenii					1												
Fertile fern type 1	1				2			1									6
Gleichenia sp.								5									
Fern sp. 1															1		
Fern sp. 2															1		
Fern sp. 3					2												
Fern sp. 4										1							
Fern sp. 5					4												
Fern sp. 6								1			1						
Fern sp. 7				2	14			7				9					
Dioon antarctica							7	1									
[E]*Araucaria* sp. 1		1						?2									
[C]*Araucaria* sp. 2				4													
[C]*Araucaria* sp. 3										1							
[CBI]*Araucaria* sp. 4					17												
Papuacedrus shenii					2		1	1	10								
Cupressoid type 1					3		4										
Acmopyle antarctica							7										
?Podocarpus sp. 1.				37	1	?1		2					1				
?Podocarpus sp. 2.												3					
?Podocarpaceous root					1												
Lanceolate keeled leaf							1										
Awl leaf sp. 1					16		5		1								
Conifer shoot sp. 1							1	1									
Conifer shoot sp. 2					15		3										
Conifer shoot sp. 3					3			3									
Conifer shoot sp. 4							4		1								
Number of specimens	1	1	0	43	83	?1	33	25	12	3	1	16	1	0	3	0	6
Total types	1	1	0	3	14	1	10	8	2	3	1	3	1	0	3	0	1
Fertile Material (Chapter 9)																	
?Araucaria pichileufensis			2					5		1							
Araucaria cone axis					2												
Cone sp. 1					1												
Cone sp. 2				1													
Cone sp. 3					6												
Cone sp. 4														1			
Fertile organ sp. 1							7										
Fertile organ sp. 2					8												
Fertile organ sp. 3					3												
Fertile organ sp. 4					1												
Fertile organ sp. 5					1		1										
Fertile organ sp. 6					1												
Fertile organ sp. 7					1												
Fertile organ sp. 8							2										
Isolated seed sp. 1					2												
Isolated seed sp. 2															1		
Isolated seed sp. 3															2		
Isolated seed sp. 4															1		
Isolated seed sp. 5															1		
Isolated seed sp. 6					1												
Isolated seed sp. 7															1		
Isolated seed sp. 8					1												
Number of specimens	0	0	2	1	28	0	10	5	0	1	0	0	0	1	6	0	0
Total types	0	0	1	1	12	0	3	1	0	1	0	0	0	1	5	0	0

Table 5.4. Presence-absence data for the non-angiosperm vegetation present in the King George Island floras. CG – Collins Glacier. PC – Potter Cove. Fossil Hill Units Five and Six not included because the poorly preserved carbonised stem and leaf fragments flora has not been described. [E] – *Araucaria* sect. *Eutacta*, [C] – *Araucaria* sect. *Columbea*, [CBI] – uncertain whether *Columbea/Bunya* or *Intermedia* section of *Araucaria*. Total bryphyte types = 2. Total conifer types =

5.5 Composition of the floras

An assemblage of 428 angiosperm leaves, comprising 85 morphotypes (Table 5.5), has been examined during this study. The angiosperms are divided into 27 entire margined and 58 toothed margined morphotypes. Three of the angiosperm morphotypes (morphotypes 2.26, 2.57 and 2.58) are considered to be juvenile, with possible affinities to other leaf morphotypes and are therefore excluded from palaeoclimatic analyses in Chapter 10. A further two leaves are considered to be herbaceous (morphotypes 1.5 and 2.7) and are also excluded from the analyses, which are based on woody dicotyledonous taxa (Chapter 10; Wilf *et al.*, 1998b).

Number of specimens used to define morphotypes	% of morphotypes described
1 – 5	71 %
5 – 15	22 %
>15	7 %

Table 5.5. Number of specimens used to define morphotypes. Ideally the number of specimens used to define a morphotype should be 25 – 100 with cuticular data and fine scale venation detail (Dilcher, 1974).

The number of specimens used to define particular morphotypes in this study varies from more than 15 to only a single specimen. Dilcher (1974) considered that 25 – 100 specimens, cuticular data and fine scale venation detail were necessary to adequately define a taxon, however this is not available in many of the floras which comprise less than 20 specimens in total. Cuticular data is also not available. Therefore the morphotypes are considered to be initial groupings that may be synonymised with further research and the collection of more complete and better preserved specimens. This may be particularly true of the Nothofagaceae specimens, which can be difficult to group morphologically without cuticular data (Hill, 1991b). Morphotypes defined by a single specimen in this study are considered to have particularly distinct lamina form and venation architecture (For further discussion see Chapter 6). It should be noted that multiple synonymies in the flora would present a false impression of diversity. This in turn might effect palaeoclimate analyses that require a minimum of 16 morphotypes (MAP analyses; Wilf *et al.*, 1998) and 20 morphotypes (CLAMP and leaf margin analyses). Grouping all of the nothofagaceous leaves in the Dragon Glacier flora, for example, would reduce the diversity of the flora by approximately one-third (although this is still above the 20 morphotype limit).

The entire margined angiosperm morphotypes are mostly grouped as form genera (e.g. *Dicotylophyllum dusenii* Zastawniak and *Dicotylophyllum washburni*) or morphotypes. Based on gross morphology and venation, affinities are suggested with the Eucryphiaceae, Lauraceae, Monimiaceae, Myrtaceae, Sterculiaceae and Symplocaceae. Less certain affinities are suggested with the Araliaceae, Cochlospermaceae, Proteaceae, Smilicaceae and Winteraceae. The dominant form in terms of specimens is *D. latitrilobatum* (42 specimens), which also has a broad distribution (Dragon Glacier, Fossil Hill, Rocky Cove).

The toothed margined angiosperm morphotypes are also mostly grouped as morphotypes. Nothofagaceous leaves dominate the flora as a whole (19 morphotypes = 22 % of the toothed and entire flora), in terms of both numbers and distribution. A strong cunoniaceous element is suggested by leaves with affinities to *Weinmannia* L., and *Cunonia* L., and the *Schizomerieae* tribe of the Cunoniaceae (morphotypes 2.1; 2.2; 2.3). The Proteaceae is considered to be present on the basis of leaves attributed to *Lomatia* R. Br., *Knightia* Sol. Ex R. Br. Possible leaves of the Araliaceae, Eucryphiaceae, Cochlospermaceae, Myricaceae, Monimiaceae and Sterculiaceae are also present. A single possible fragment of a *Gunnera* L., leaf is present.

The non-angiosperm component of the leaf flora comprises two possible bryophytes (new records for King George Island), one type of *Equisetum*, eleven fern morphotypes (including Gleicheniaceae, Lophosoriaceae, *Thyrsopteris shenii* Zhou and Li) and one cycad. Four types of *Araucaria* spp, belonging to the sections *Eutacta* and *Columbea* have been described in addition to the *Papuacedrus shenii* Zhou and Li (Cupressaceae), indeterminate Cupressaceae foliage, three types of Podocarpaceae (including *Acmopyle antarctica* Florin), a podocarpaceous root and a further six types of conifer foliage with uncertain familial affinities. Two types of araucarian cone material (sect. *Eutacta*), four types of conifer cone and sixteen fruits/seeds are also present.

5.6 Taphonomy of the BAS archived floras (summary table)

Locality	Description	Interpretation
Barton Peninsula P.2145	Fragmentary leaves preserved in coarse fluvial sandstones. Plant impressions/mineralised impressions are preserved from bed parallel to vertical orientation, but most are deposited subparallel to bedding. There are no coniferous remains and only rare ferns are preserved.	Fragmentation of leaf material and the coarse nature of the sediment suggests moderate transport and/or energy conditions, which is consistent with the fluvial interpretation of the deposits and the absence of more delicate fern specimens. Lack of conifer and fern material could be related to taphonomy or reflect local vegetation conditions.
Cytadela G.47, G.309, G.319	Lacustrine vesicular ash fall tuff with carbonised compressions of angiosperm and podocarpaceous leaves and rare ferns alongside a single three dimensionally preserved cone (Cone sp. 2). The assemblage is dominated by stenophyll foliage of *Podocarpus* sp. 1. Leaf remains are predominantly fragmented with a bias towards central and apical leaf fragments.	The three dimensional nature of the cone suggests a relatively uncompacted sediment, an interpretation supported by retention of the original vesicularity. Fragmentation of the leaves implies that the material underwent transport prior to deposition in a lacustrine setting. This is consistent with the abundance of stenophyll *Podocarpus* sp. 1. leaves that suggest a water's edge habitat (Wolfe and Upchurch, 1987).
Dufayel Island G.53	Lacustrine airfall tuff with entire and fragmented leaves, often forming leaf mats. Conifers absent and ferns are rare. Angiosperm leaves are sometimes convexly curved and can cut across bedding surfaces, otherwise preserved subparallel to bedding. Plant-arthropod traces are common. Fragmentation has affected leaves all leaves larger than notophyll size class.	The lack of rooted material and understorey pteridophyte vegetation suggests that this assemblage is allochthonous rather than an *in-situ* leaf litter deposit. Consequently the absence of conifers and low numbers of fern specimens is likely to result from taphonomic processes rather than the original vegetation composition. Fragmentation of larger leaf sizes suggests a size sorting taphonomic processes.
Platt Cliffs G.50	Tuffaceous sandstone with parallel to subparallel leaf impressions that are sometimes preserved with a layer of actinolite as a post-depositional feature. Leaves are often complete or partially fragmented in the mesophyll size class, although long leaves up to 12 cm are sometimes preserved whole. Stenophyll leaves dominate this assemblage.	The preservation of extremely long leaves in this deposit suggests rapid low energy deposition close to the vegetation source. The dominance of stenophyll leaves suggests a water's edge bias but this contradicts the scarcity of toothed leaves in this assemblage (Wolfe and Upchurch, 1987). However long leaves are also characteristic of canopy vegetation, which might imply preferential sampling of the vegetation strata. Unusually for King George Island the flora contains no *Nothofagus*-type *leaves*.

Table 5.6. Taphonomic and palaeoenvironmental interpretation of the archived BAS collections.

Locality	Description	Interpretation
Potter Cove compression flora P.232,	Fine to coarse tuffaceous fluvio-lacustrine sandstone dominated by sterile and fertile fern foliage and broad leafed ?podocarpaceous conifers with no angiosperm remains. Leaves preserved parallel to bedding.	The fine grain size of the sediment suggests low to moderate energy conditions of deposition. The absence of angiosperm material is surprising given their abundance in all other floras on the island and could reflect the original composition of the vegetation. Angiosperm fossils have been recorded from nearby localities (Barton Peninsula flora, Potter Cove impression flora) suggesting that the lack of angiosperms may reflect taphonomic processes.
Potter Cove impression flora P.232	Angiosperm dominated flora with a small fern component, conifers absent. Preserved in a fluvial-lacustrine volcaniclastic siltstone to fine sandstone with rare bioturbation. The leaf remains are generally highly degraded ?fragmented and are generally no larger than microphyll in size although a single ?greater than mesophyll sized leaf of ?*Gunnera* is present.	Low energy sedimentation inferred from the fine grain size and by the preservation of a possible fragment of the herbaceous taxon Gunnera. Oxygenated ?shallow water conditions are inferred from the infrequent burrows. The leaves are degraded as a result of long transport distances or degradation prior to burial, ?fluvial transport followed by lacustrine deposition.
Profound Lake flora P1174	Pale white to brown tuffaceous sediment. Generally very poorly preserved impressions of matted angiosperm, fern and conifer leaves along with a single cone.	This flora is included for completeness and the presence of Cone sp. 4. The fine grain size of the tuffaceous sediment suggests that it is an ash fall deposit ?preserving leaf litter.
Vaureal Peak P.2799	Medium to fine grained fluvial volcaniclastic sandstones with a low diversity flora (Hunt and Smellie, work in progress) comprising five angiosperm taxa and ferns, many of the slabs are dominated by a single nothofagaceous angiosperm morphotype (Morphotype 2.48). The leaves are frequently preserved as mats, with poorly preserved overlapping sections of lamina suggesting *in-situ* decay following deposition.	The abundance of a single nothofagaceous species in these fluvial sandstones can be explained either in terms of 1). a *Nothofagus*-dominated local forest environment; 2) by a nearby source of *Nothofagus* leaves (e.g. a tree overhanging the water body); or 3) as a function of leaf toughness, with such leaves being more durable and less prone to degradation.

Table 5.6. Continued

5.7 Taphonomy of the Collins Glacier in-situ flora P.3025

Fragmentary angiosperm remains (not described) and a single *Araucaria* sect. *Eutacta* shoot remains preserved in fine to coarse tuffaceous sandstones. Leaves are oriented parallel to bedding and widely dispersed. Large woody stems are preserved at separate levels within the same bed.

Interpretation Fragmentation of leaf material suggests moderate energy/transport distance and the association of large stem fragments suggests relatively high energy conditions. Smellie *et al.* (1984) interpreted the sediments as fluvial-lacustrine sediments. The nearby Collins Glacier flora (Poole *et al.*, 2001) is a glacial outwash deposit with abundant large wood fragments (up to 0.4 – 0.3 m long). The concentration of wood in one locality suggests taphonomic sorting processes. Wood is particularly common in both fluvial channel lag and lacustrine deposits (Behrensmeyer and Hook, 1992; Burnham, 1994), and combined with evidence of high energy sedimentation locally, supports a fluvial origin for the sediments.

5.8 Taphonomy of the Collins Glacier moraine flora P.3028

A single entire angiosperm leaf (Morphotype 2.33) and *Araucaria* sect. *Eutacta* cone scales are preserved in a finely laminated siliceous matrix.

Interpretation Siliceous ash fall deposit or biochemical precipitate induced by abundance of silica during a volcanic phase (Spicer, 1989; 1991). Excellent preservation of dispersed organs suggests a very low energy lake setting preserving the nearby lake margin flora. No in-situ material similar to this has been recorded from King George Island, therefore it seems likely that the material originates from an unidentified source bed beneath Collins Glacier.

5.9 Taphonomy of the Fossil Hill flora

5.9.1 Locality P.935, P.3034, P.3036, Fossil Hill Unit Two

Dispersed sometimes clustered entire and fragmentary leaves preserved in well laminated fine siltstones. Occasional small vertical, and sinuous horizontal, bioturbation (Yang and Shen, 1999). The siltstones are interbedded with plant-free high energy coarse sandstones and breccias. Angiosperms dominate the flora but fragmentary conifers and rare ferns are also present. Bird footprints occur in closely spatially related sediments. Large plants such as *Lomatia* fronds (Morphotype 2.4, Chapter 6) are fragmentary and none of the preserved leaf material exceeds notophyll size class. Whole leaf preservation is limited to microphyll sized leaves.

Interpretation Preservation of bird footprints suggests extremely shallow water, highly oxidising conditions, which would have resulted in the removal of organic material, although this seems at odds with the low levels of bioturbation observed at outcrop (Yang and Shen, 1999). Preferential degradation of particular leaf species in leaf litter has been observed experimentally (Ferguson, 1985; Titchener, 1999) and could explain the absence of plant species that are abundant at higher levels in the sequence (Units Three to Six). The bird footprints and planar lamination also imply conditions of fairly low energy and cohesive substrates. According to Behrensmeyer and Hook (1992) footprints are common features of floodplain and ephemeral lake deposits, which supports sedimentological interpretations of the Fossil Hill sequence as a shallow ephemeral lacustrine deposit.

Preservation of complete microphyll leaf specimens but only fragmentary larger plant parts, such as *Lomatia* fronds, suggests transport, fragmentation and preferential size sorting of the material prior to deposition. The combination of low energy lacustrine sediments with coarser sandstone deposits suggests a tranquil environment with periodic higher energy phases. In this context the occasional coarse influxes of sediment are likely to represent increased discharge conditions, perhaps as a result of seasonal flooding. Given the generally low energy conditions the fossil plants are likely to represent lake margin vegetation, with occasional inputs of plant material from more distant localities during the higher energy periods.

5.9.2 *Locality P.3032, Fossil Hill Unit Three*

Thin siltstone, rarely coarse sandstone, with limited areal distribution. Abundant bed parallel preservation of carbonised angiosperm fruits (cupules), seeds and leaves, in addition to fragments of fern pinnae, coniferous foliage and leaf and stem debris. Conifer shoots often comprise fragments with several branches. Delicate organs such as bryophytes and leaves with setaceous and spinose apices are present. Occasional slabs comprise well-rounded woody fragments, without leaf material. Entire leaves fall in the microphyll size class, larger leaves of estimated original mesophyll size, are fragmentary (e.g. *N. oligophlebia*; Li, 1994). Large leaves (>microphyll) are generally fragmented but smaller leaves are preserved complete.

Interpretation The organic preservation of this material suggests reducing conditions possibly resulting from consumption of available oxygen due to high rates of organic deposition. The diversity of organ types in this flora is only equalled at Point Hennequin but the diversity of angiosperms is relatively low. Mixing of plant material from different sources is probably common in Unit Three, since the transport distance of rounded wood fragments can be extremely high, whereas delicate organs, such as moss remains, are likely to have been derived from a nearby source. Large leaves (>microphyll) are generally fragmented but smaller leaves are preserved complete probably implying preferential fragmentation of larger organs and possible transport-related size sorting factors. Few of the leaves preserved in this deposit are present in Unit Two or Four and ferns are both better preserved and more abundant. The grain size of the sediment suggests moderate energy deposition ?fluvial transport. Ferguson (1985) suggested that the presence of leaves and cupules in the same deposit indicated an autochthonous assemblage due to differential settling rates, although the cupules in Unit Three cannot be related to a particular leaf morphotype at present.

5.9.3 *Locality P.3031, Fossil Hill Unit 4*

Normally-graded, erosive based coarse breccias with fine siltstone intercalations grading to fine siltstones that preserve generally fragmented angiosperm leaf and conifer specimens. Orientation to bedding variable and leaves are often distorted ?due to compaction. Occasional large (mesophyll) fragments are preserved but rare. A single specimen of araucariaceous shoot was found in an vertical orientation, ?growth position at the base of the sequence, however no associated rooting structure was observed. Compound angiosperm leaves are occasionally preserved intact. Most of the plant material preserved in Unit Four is found in the fine grained, upper section, of the deposit, although occasional leaf fragments are found at lower levels in silty intercalations.

Angiosperm remains are dominant in Unit Four but ferns are rare. Conifers shoots present in other horizons are also rare, although bilaterally flattened cupressoid conifer leaves are

abundant in this unit that only occur rarely in Unit 2 and as a single specimen in the Dragon Glacier flora. *Nothofagus* species are also absent from this deposit.

Interpretation The coarse grain size of Unit Four suggests high energy deposition, conversely the fine upper siltstones imply very low energy conditions – a waning flow sequence. Intercalation of small lenses of siltstone suggests that the deposit may be internally more complex resulting from more than a single event. The presence of an araucariaceous shoot in life position might represent a juvenile plant, moreover it could imply that soil formation had occurred between deposition of Unit Three and Unit Four. However the seeming absence of associated pedogenic structures or root systems precludes this interpretation. The angiosperm leaf remains are fragmentary suggesting moderate to high transport distances and/or high energy deposition but the fragments are often twisted on the bedding surface, perhaps suggesting that the leaves had dried out slightly prior to preservation and this might imply shorter transport distances. Alternatively differential compaction of the mixed sediments might have resulted in distortion of the leaf material.

The combined leaf and sedimentary data suggest a high energy flood event with deposition of plant material in the waning flow phases, ?settling out of the water column under lower energy conditions. Compound leaves with up to three attached microphyll leaflets are also found within this unit (Morphotype 2.3), which suggests very low energy deposition conditions that are difficult to reconcile with the coarse nature of the sediment or a nearby vegetation source and rapid deposition. The lack of *Nothofagus* sp. in this deposit and incorporation of rare leaf morphologies such as Morphotype 2.31 may suggest a different source vegetation or widely different taphonomic conditions during and/or after deposition of each of the Fossil Hill units. If the unit was deposited during a single flood event, the organic material might be extremely diluted relative to the sediment mass deposited. Unlike the depositional conditions of Unit Three, this might favour more oxygenating conditions and degrade delicate material preserved in the underlying horizon. This could explain the absence of ferns in the deposit.

5.9.4 Locality Fossil Hill Unit Five

Coarse volcaniclastic sandstones with abundant poorly preserved carbonised stems and unidentifiable leaf fragments. Basally erosive.

Interpretation Moderate to high energy/transport distance leading to high fragmentation.

5.9.5 Locality Fossil Hill Unit Six

Interbedded siltstones and coarse sandstones similar in colour and architecture to Unit Two with rare fragmentary impressions of *Nothofagus* sp. (?*N. oligophlebia*) leaves (Shen, 1994).

Interpretation Lower energy deposition in a standing water body is inferred on the basis of the fine grain size and planar laminations but fragmentation of leaf material and coarse breccia intercalations suggests some transport/higher energy deposition of plants prior to deposition.

5.9.6 Summary of Fossil Hill floras

The Fossil Hill floras show no evidence for autochthonous deposition such as *in-situ* rootbeds, or coal horizons (although cf. Shen, 1994). The flora changes in preservation style and composition through the section, from impression floras in Units Two and Four to a carbonised compression flora in Unit Three. Units Two and Four have a similar preservation style, sedimentary lithology and have six angiosperm morphotypes (27 % of the flora) in common. In contrast Unit Three flora has only one angiosperm morphotype (4 %) common to both of the other floras and the sedimentary style is different. The similar composition of the Unit Two and Unit Three floras (Table 5.7) suggests that a preservational bias may be affecting the flora.

	Unit 2	Unit 3	Unit 4	All Units
Unit 2	12	1	6	-
Unit 3	1	6	1	-
Unit 4	6	1	15	-
All Units	-	-	-	1

Table 5.7. Table showing the number of shared morphotypes per Fossil Hill flora. Units Two and Four are most similar having six out of the 22 morphotypes in common.

Two models may explain the changes in diversity observed between Units Two and Four and Unit Three: Firstly, that the differences in sedimentary lithology imply differences in depositional and/or ?redox conditions, such that certain leaves are preferentially preserved whilst others are degraded; Secondly, that the floras represent more than one source vegetation. The inclusion of delicate elements in the Unit Three flora, such as moss axes (Chapter 8), that are absent in the other floras suggests that initial depositional conditions may have been a factor. However, incorporation of taxa not present in the other horizons could also argue for a different vegetation source. The lack of entire margined angiosperm leaves in the Unit Three flora suggests a water's edge bias (Upchurch and Wolfe, 1987; Wolfe and Upchurch, 1987), which combined with evidence of delicate organ preservation, could be interpreted as preferential sampling of the Fossil Hill lake margin flora. In this context the Unit Two and Unit Three floras would represent a more distal vegetation that had been transported ?fluvially to the area, a model that is consistent with the fragmentation of material in these units.

Some support for the distal vegetation model is offered by a vegetation dynamics model (Poole *et al.*, 2001) as described in Chapter Four. Fossil plant material preserved in the Unit Two flora would represent high diversity vegetation growing in pre-volcanism conditions, that was destroyed by the volcanic eruption that led to debris flow deposition. The Unit Three flora (Table 5.3) would then represent an impoverished post-disturbance successional vegetation and Unit Four would represent a return to pre-disturbance 'climax' vegetation conditions. Some support is given to this model by the composition of Unit 3, which comprises *Nothofagus* sp.

(Li, 1994), ferns with a *Blechnum* L. morphology (Chapter 9) and gleicheniaceous ferns (Zhou and Li, 1994a) that are known post-disturbance colonisers (Veblen and Ashton, 1978; Veblen and Lorenz, 1987; Veblen *et al.*, 1977, 1981). *Gunnera*, another disturbance coloniser is also present in the pollen record (Torres and Meon, 1990); although the stratigraphic position of their samples is uncertain.

Either of these models is supported by the available sedimentary taphonomic data, although the lack of stratigraphic constraint of the sequence prevents an assessment of the length of time taken to deposit the sequence. The erosional nature of the base of Unit Four suggests that there is a depositional lag time between the two units, which might favour the vegetation dynamics model. Consequently, palaeoclimatic interpretations that combine the flora of Units Two and Four may be more appropriate for analyses, rather than a whole flora approach.

5.10 Taphonomy of the floras from Point Hennequin

The plant-facies associations of the Dragon Glacier, Mt. Wawel and Smok Hill floras are described in Chapter 4 (Table 4.5). This section presents further observations on the variations in plant distribution observed at Point Hennequin.

5.10.1 Locality P.3007 and P.1404 Dragon Glacier flora (Figure 4.7)

Two sediment types were recovered from this locality: 1). Typical pink and grey laminated plant-bearing lacustrine siltstones and sandstones of the Dragon Glacier flora (DGF-5; Chapter 4). No angiosperms are preserved but homogeneous sized broad-leaved coniferous remains of *Araucaria* sp. 4, Awl leaf sp. 1 and fragmentary ferns and woody are present; 2). Light brown primary lacustrine tuff (DGF-6) with extremely fine diffuse lamination and bed parallel angiosperm preservation (Morphotype 2.50 and Morphotype 2.51).

Interpretation There seems to be no obvious reason for the abundance of conifer remains and lack of the angiosperms in the pink and grey lacustrine sediments of P.3007, since angiosperms are preserved in similar sediments elsewhere at Point Hennequin. The dispersed nature of the leaves and the homogeneous fragment size suggests sorting prior to deposition and distal deposition, relative to the site of growth. The thick conifer leaves preserved at P.3007 have high post-deposition preservation potential, however the incorporation of relatively delicate fern material suggests that a diagenetic rather than taphonomic sorting process may have removed angiosperm remains. Alternatively the different buoyancy potential/settling velocity/entrainment properties of the conifer and fern remains could have resulted in their deposition in a different region of the basin relative to the angiosperm remains (Spicer, 1989). The nature of the original vegetation is equivocal without an *in-situ* horizon to study. In modern South American floras, vegetation at higher altitudes becomes progressively dominated by araucarian conifers (Veblen

et al., 1996), which might imply sampling of two distinct elements of the vegetation. However the mixture of conifer and angiosperm material in the majority of the Dragon Glacier flora (i.e. 5.10.2), suggests that the conifer-dominated layers represent taphonomically distinct intervals, as opposed to sampling of a heterogeneous vegetation.

5.10.2 Locality P.236, P.1404 (in part), P.2810, P.3001 – P.3007, P.3013, P.3015, Dragon Glacier flora (DGF-5)

Plants preserved as carbonised compressions include angiosperms (whole leaves and fragments), ferns (fragments), *Equisetum* (internode fragments), conifers (Araucariaceae broad leaves, Podocarpaceae, and Cupressaceae fragments), fruits, seeds, fragments of araucarian cone axes, large carbonised wood fragments (extremely rare), small ?charcoalified wood fragments (rare), rootlets. Based on observations of individual exotic moraine blocks, the plant assemblages vary between: 1). Conifer-poor, angiosperm whole leaf and leaf fragment assemblages, and 2). debris beds with abundant tough conifer shoot fragments and individual scale leaves. Leaves are generally preserved parallel to bedding.

The dominant angiosperm is *Nothofagus* with several evergreen and deciduous species present (Chapter 6; based on presence/absence of plicate vernation; Hill and Read, 1991). *Nothofagus* spp. co-occur most commonly with other leaf types. The next most abundant leaf types are Morphotype 1.1 (with sterculiaceous affinities) and Morphotype 2.1 (with affinities to *Weinmannia*). Morphotype 2.1 is over-represented by virtue of the compound nature of the leaf (see section 5.12). A complete range of leaf size classes is present from larger than mesophyll sized leaves to nanophyll leaves, although the mesophyll leaves are always fragmented (except in the case of P.3001.177).

Interpretation The abundance and diversity of plant material in the Dragon Glacier flora suggests a diverse source vegetation. Alternations of debris/conifer-rich beds with angiosperm dominated leaf beds suggests that there may be more than one vegetation source, variations in the supply of plant material to the depositional basin or sampling of heterogeneous vegetation within the catchment area. According to Ferguson (1985) debris beds are indicative of lowland environments where low gradients create abundant obstacles for trapping debris. Horizons dominated by robust conifer shoots and conifer leaf debris suggest long distance transport from distal, possibly upland areas, whilst the well preserved angiosperm dominated horizons may represent a local source vegetation. It seems likely that the apparent switch between different vegetation sources is related to seasonal variations in fluvial transport or availability of leaf material. In this context, debris beds represent year-round background organic deposition, while the angiosperm dominated beds may represent autumnal mass abscission beds, where the background debris sedimentation is extremely diluted.

The angiosperm-dominated beds could also result from preferential sorting, concentration and deposition (as P.3007 above) or event deposition i.e. due to volcanism (Spicer, 1989, 1991). Event deposition seems unlikely in this horizon (in contrast to the P.1404 Smok Hill flora) given the generally fine grain size and reworked nature of the sediment, which is more consistent with pre-disturbance vegetation. However, volcanic events might have provided a large volume of leaf material for preservation and hot pyroclastic ash, that can remove epicuticular waxes, might explain the absence of cuticular material in the flora (Spicer, 1989; 1991). This may also explain the absence of insect fossils despite their common representation from trace fossil data (Chapter 7). Small charcoalified fragments in the assemblage are also suggestive of volcanically related forest fires synchronous with deposition of the leaf beds. If the assemblage is the result of a catastrophic event then the flora is likely to be highly representative of the local vegetation (Spicer, 1991).

Size sorting is evident from the presence of fragmented mesophyll leaves, but complete notophyll and smaller leaves might have preferentially removed mesophyll sized leaves, which were present in the original flora but are now represented only by large fragments (borderline notophyll – mesophyll size class). Some transport or degradation is therefore considered to have affected the angiosperm leaf assemblage as well and the deposit is considered to be either allochthonous or para-autochthonous. Such large leaves are likely to be shade leaves and have a generally low preservation potential (Spicer, 1989).

5.10.3 Locality P.3010, Mt. Wawel in-situ flora

Blue-grey volcaniclastic siltstone with abundant plant debris. Small fern and angiosperm fragments (< microphyll) are relatively scarce. A single complete nothofagaceous leaf of Morphotype 2.47 is present. Seeds, a leaf of *Araucaria* sp.2 (sect. *Columbea*), an *Araucaria* sect. *Eutacta* cone scale and fragments of moss are also present. The moss is associated with a woody stem and may have been epiphytic, although there is no evidence for attachment. Plant remains are preserved parallel and subparallel to bedding.

Sediments representing a small lacustrine delta were observed in the upper section of the Mt. Wawel cliff face and the sediment collected from this locality is considered to be equivalent to the *in-situ* flora (J. Smellie, pers. comm., 2000).

Interpretation The relatively fine sediment grain size suggests low energy deposition. This is also consistent with the preservation of delicate mossy axes, although mosses are buoyant and can be transported over a reasonable distance (Spicer, 1989). However, the remainder of the flora is highly fragmented, suggesting higher energy conditions. The blue-grey colour of the

sediment might indicate hydromorphic soil conditions, although colours are easily modified during diagenesis (Behrensmeyer and Hook, 1992). The flora has elements in common with the moraine flora (e.g. Morphotype 2.37 and Araucariaceae remains) but the small size of the flora prevents detailed comparisons. A lacustrine/ephemeral lacustrine interpretation for the deposits is suggested by the presence of a lacustrine delta.

5.10.4 Locality P.1404 Smok Hill flora

A single morphotype of nothofagaceous leaf Morphotype 2.50 (Chapter 6) and rare stem fragments are preserved in the medium to coarse grained, green, shard and crystal rich tuff of P.1404. All leaves are microphyll size class, complete or nearly complete and preserved as green mineralisations. Leaves are oriented parallel to 45° to bedding.

Interpretation The green mineralised fossils are interpreted as leaves prematurely abscised due to lack of light caused by ash coating (Burnham and Spicer, 1986). The mineralisation would probably have occurred post-burial. The leaves therefore reflect event deposition. The homogenous size of the leaf fossils does not reflect the average leaf size of this morphotype, therefore it seems likely that a specific component of the vegetation is being sampled, e.g. smaller canopy rather than larger shade leaves (cf. Burnham and Spicer, 1986; Spicer, 1989, 1991). The lack of any other morphotypes preserved in these sediments may imply that the flora sampled is *Nothofagus*-dominated and in this context might represent a post-disturbance successional vegetation (Poole *et al.*, 2001; Hunt and Poole, submitted), although the sample size is extremely small and may not necessarily be representative (n = 24).

5.11 Taphonomy of the Rocky Cove flora P.3029

Abundant fragmented and dispersed angiosperm and fern macrofossils, with rare delicate ferns (Fern sp. 1 and Fern sp. 2), conifers and seeds preserved in lacustrine tuffs and fluvial sandstones. Leaves do not exceed microphyll size class except for a single specimen from the mid section of the Rio Madera stream cut (P.3035).

Interpretation The preservation of delicate ferns suggests a local vegetation source or low energy conditions of deposition. Conversely most of the angiosperms are fragmented and the dominance of small leaf sizes suggests transport or higher energy deposition. This may imply extremely localised deposition of plant material close to its source.

5.12 Taphonomic biases based on leaf morphology

5.12.1 Compound leaf bias

Based on studies of modern vegetation, Burnham (1989) suggested that compound leaves may be over-represented in fossil floras because they break down into their constituent leaflets (Ferguson, 1985). Sixty one specimens (30 % of specimens) of Morphotype 2.1 were described from Point Hennequin but these may comprise parts of fewer than ten leaves, since compound leaf P.3001.46 consists of at least 6 leaflets (Chapter 6). Since the leaflets are dominantly microphylls 43 (70.5 %) and nanophylls 18 (29.5 %) the whole flora is biased towards the microphyll size class by the incorporation of this taxon. This has implications for specimen based mean annual precipitation and leaf size indices that are on the proportion of leaves in particular size classes (Chapter 10). A further 9 toothed margined morphotypes from the Dufayel Island, Fossil Hill Unit 2 and Fossil Hill Unit 4 floras may also be compound (Table 5.7). However, fewer than these leaves are not present in sufficient numbers to bias the flora in similar fashion to Morphotype 2.1.

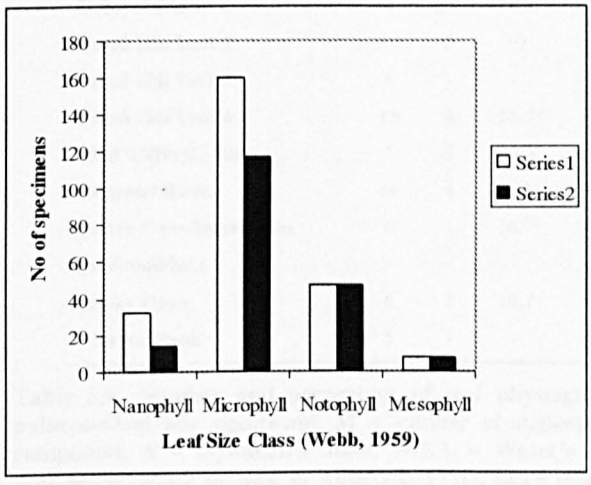

Figure 5.8. Illustration of skewed size class distributions in the Dragon Glacier flora, Point Hennequin when compound leaflets are included. The skewed series 1 include compound leaf Morphotype 2.1, series 1 exclude this data to define a more Gaussian distribution. This is only considered to be a problem in the Dragon Glacier flora since compound leaves are inferred to be rare in other KGI floras. Leaf size class counts are based on estimated leaf areas of all leaves including fragments and whole leaves.

5.12.2 Taphonomic biases drawn from leaf physiognomy

Toothed margined, stenophyll (l:w >4:1) and compound leaves show an ecological preference for water's edge habitats in the modern environment, and are thus more likely to be preserved (Dilcher, 1973; Upchurch and Wolfe, 1987; Burnham, 1989). These leaves may therefore be over represented in a fossil assemblage. Emarginate apices are correlated with subhumid climates, but are also characteristic of canopy vegetation (Wolfe and Upchurch, 1987; Klich, 2000). Acuminate apices are common in environments with high precipitation, and are also characteristic of understorey vegetation. These characters are all present in the KGI fossil assemblages but are hard to quantify in terms of an overall palaeoenvironmental-taphonomic signal. The low morphotype diversity of the individual floras means that interpretations may be unrepresentative of the entire original flora. The interpretations below and in Table 5.8 are therefore treated as first approximations.

Stenophyll vegetation is particularly abundant in the Platt Cliffs (G.50) flora. The associated Cytadela flora is also dominated by stenophyll foliage of *Podocarpus* sp. 1, which is a suggested streamside taxon based on comparison with modern South American Podocarpaceae

(Chapter 8). The high morphotype diversity of the Dragon Glacier flora suggests that the 11 % stenophyll vegetation may be a true water's edge signature, and is consistent with interpretations of the flora as a fluvio-lacustrine assemblage. The Platt Cliffs flora is the only flora in which an emarginate apexed (Morphotype 1.22) leaf is present. Subhumid climates have been proposed for the Upper Cretaceous Zamek flora (Zastawniak, 1994) but are not considered to affect the Tertiary flora (Birkenmajer and Zastawniak, 1989), therefore the emarginate apexed leaf is interpreted as part of the canopy vegetation.

Locality	M#	S#	S %	Cm #	Cm %	A#	A %	W.E.I.	Em#	Em %	Ac #	Ac %
Barton Peninsula	4	1	25	-	-	1	25	88	-	-	-	-
Collins Glacier (moraines)	1	-	-	-	-	-	-	-	-	-	-	-
Cytadela (G.47, 309, 319)	6	2	33.3	-	-	-	0.0	100	-	-	-	-
Dufayel Island	8	1	12.5	-	-	-	-	38	-	-	-	-
Fossil Hill Unit 2	10	5	50	2	20	3	33.3	207	-	-	1	10
Fossil Hill Unit 3	6	-	-	-	-	1	16.7	8.3	-	-	-	-
Fossil Hill Unit 4	15	4	26.7	-	-	1	6.7	83	-	-	1	6.7
Platt Cliffs (G.50)	5	3	60.0	-	-	1	20.0	190	1	20	-	-
Dragon Glacier	36	4	11.1	1	2.8	5	13.9	46	-	-	-	-
Potter Cove Impression	6	1	16.7	-	-	1	16.7	58	-	-	-	-
Profound lake	-	-	-	-	-	-	-	-	-	-	-	-
Rocky Cove	6	1	16.7	-	-	1	16.7	58	-	-	-	-
Vaureal Peak	5	-	-	-	-	-	-	-	-	-	1	20

Table 5.8. Number and percentage of leaf physiognomic features present in the floras listed, that are palaeoecologically significant. M – number of angiosperm morphotypes in the flora, S – stenophyll, Cm – compound, A – asymmetric base, W.E.I. – Water's edge index (higher values = a greater water's edge vegetation signal; defined in Appendix IV.1), Em – emarginate, Ac – acuminate, # - number. Stenophyll and compound leaves suggest a water's edge bias (Upchurch and Wolfe, 1987; Wolfe and Upchurch, 1987), Asymmetric bases are characteristic (but not definitive) of a compound morphology (Dilcher, 1973), Emarginate apices are linked to subhumid environments (Upchurch and Wolfe, 1987), Acuminate apices suggest understorey vegetation or high precipitation (Upchurch and Wolfe, 1987).

Riparian vegetation may screen vegetation further from the streamsides, which presents a further potential source of bias in fossil assemblages (Burnham, 1989). Ferguson (1985) suggested that compound leaves almost certainly dropped straight on to the water. He also found that even large forest trees would not contribute leaf material to a river or stream side if they were more than 50 metres from the water's edge, suggesting that fossil floras are generally biased towards stream side vegetation (Drake and Burrows, 1980). The exceptions to this rule are areas affected by event deposition such as pyroclastic volcanism (Burnham and Spicer, 1986; Spicer, 1989; Burnham, 1994). For example, the eruption of Mt. St Helens deposited large volumes of leaf material in stream point bar deposits and other sediment traps (Spicer, 1989). This is a possible scenario for floras on King George Island, with material being trapped in ephemeral lacustrine basins e.g. the Dragon Glacier flora (Poole *et al.*, 2001).

5.13 Summary

The taphonomy and physiognomic characteristics of the King George Island floras support models of fluvial and lacustrine sedimentary palaeoenvironments on King George Island during the Palaeocene and Eocene. The floras are considered to be allochthonous based on the absence of palaeosol features, except for the Dragon Glacier flora, where alternating rootlet and wave ripple beds imply some *in-situ* plant growth. However, no *in-situ* trunks have been found that would support major palaeosol development.

The KGI flora, described here, comprises 428 angiosperm leaves representing 85 morphotypes (Table 5.5), 27 entire margined and 58 toothed margined. Three angiosperm morphotypes (2.26, 2.57 and 2.58) are considered to be juvenile and two (1.5 and 2.7) are considered to be herbaceous. The KGI floras are generally low in diversity, with fewer than ten angiosperm morphotypes per locality, excepting the Dragon Glacier (37) and Fossil Hill (22) floras. The two Palaeocene floras described here (Dufayel Island and Barton Peninsula) differ in angiosperm composition from the Eocene floras, suggesting that the vegetation of KGI changed during the Palaeocene – Eocene interval, perhaps as a result of the changing climate. The two Palaeocene floras are less diverse in terms of conifer morphotypes than the Eocene floras, contrary to previous interpretations (Askin, 1992), although this could be a function of the small sample size of the Palaeocene floras.

The composition of the floras across KGI is heterogeneous. Floras from Fildes Peninsula (Rocky Cove, Fossil Hill, Collins Glacier) have a similar composition and have some similarities with the Point Hennequin floras (e.g. angiosperm morphotypes - *Dicotylophyllum washburni, cf. Lomatia* and conifer morphotypes - *Araucaria* sect. *Eutacta, Papuacedrus* and possible podocarps). However, floras from the Barton Peninsula, Dufayel Island and Platt Cliffs areas, which have a limited similarity, are distinct compositionally from the Point Hennequin and Fildes Peninsula flora in having a different range of araucarian types (e.g. *Araucaria* sp. 2 and 4), an abundance of *?Podocarpus* sp. 1, and only a single angiosperm species in common (*N.* sp. 10). The Vaureal Peak flora bears limited similiarity to the Cytadela and Point Hennequin floras. The lack of similarity between the floras as a whole suggests that they originate from different initial vegetation types, although without continuous sedimentary horizons it is not possible to determine whether this is a result of a vegetational heterogeneity. Poor geochronological control, also prevents a detailed examination of the vegetation composition over time. At present the Fildes Peninsula, western Admiralty Bay and Point Hennequin form three compositionally distinct

Chapter 6 Angiosperm morphotype analysis

6.1 Introduction

The angiosperm leaf macrofossils preserved in the King George Island floras are described using leaf venation architecture. The leaves are primarily assigned to morphotypes, for use in physiognomy-based palaeoclimatic analyses (Chapter 10). Taxonomic affinities of the leaves are discussed where possible. The distribution of the leaves and their associations are described in Chapter 5. Appendix Table V.1 summarises the list of specimens and morphotypes present at each locality.

6.2 Techniques

Specimens with organic preservation were examined for cuticle using both an Olympus SC-35 (SZH-DA) stereomicroscope with a high objective lens (University of Leeds), and a Leitz microscope, housing a high pressure mercury vapour bulb (100 watts) for fluorescence microscopy (Department of Plant and Animal Sciences, Sheffield University). Ordinary light microscope examination of the specimens revealed no cuticular remains, but limited fluorescence was observed in some gymnosperm specimens from Fossil Hill. The fluorescing cuticles were not studied further because they were highly degraded. Future work using an environmental chamber might reveal further detail of the cuticles (M. Collinson pers. com., 2002).

Leaf venation and tooth architecture were drawn and photographed using a stereomicroscope with camera and camera lucida attachments. Photographs were also taken by the University of Leeds Photographic Services using manual and digital SLR cameras. Fossil surfaces were immersed in ethanol and studied with low angle lighting to enhance surface texture. Incident lighting was not standardised to the top left of specimens because several light directions were often required to maximise differences in surface relief or contrast in venation patterns. A blue filter was found to highlight the venation detail more clearly for microscope photography than plain yellow light.

6.3 Descriptive Terminology

Leaf architectural nomenclature used here is based on the Manual of Leaf Architecture (MLA) (Leaf Architecture Working Group, 1999) and Hickey (1973, 1979). Tooth architectural descriptions follow the system of Hickey and Wolfe (1975) and the MLA. The morphotypes have been grouped in a hierarchical fashion based on characteristics of margin type, leaf

organisation and lower order venation (Table 6.1). Leaf drawings used to support morphotype descriptions are presented in Appendix V.

Size class data is expressed in terms of the Runkaier (1934) definition as modified by Webb (1959) and uses the size class overlays of the Leaf Architecture Working Group (1999). Estimates of leaf area are based on the formula 'area = 2/3 length x width' (Cain and Castro, 1959), except for leaves with an approximately square lamina, in which case 'area = length x width' was considered to be more appropriate. In most descriptions the percentage of leaves of each size class is stated in addition to the actual number of leaves counted (e.g. Pole, 1993), otherwise the size class range of morphotype is stated. Many of the leaf fossils are incomplete, therefore length, width and area measurements are stated as minimum values or estimated values where reasonable constraint of the original lamina shape is available. Where there is reasonable constraint of the lamina margins, width estimates assume that the lamina is symmetrical and the total width = 2 x half width. Length estimates are more arbitrary and rely on using the trend of the preserved margin to interpret the size and shape of the leaf. Such estimates become increasingly difficult with smaller leaf fragments and is generally inappropriate, or highly subjective, if less than c. 50 % of the original lamina is preserved, unless that fossil fragment comprises a large section of the leaf margin. The large quantity of specimens to be examined in the toothed leaves category has meant that leaf measurements have not been expressed for every specimen, instead some descriptions are based on the most complete specimens preserved. The leaves are listed in the material examined category to give an estimate of the diversity and distribution of each morphotype.

1. Entire margined leaves	
1a[1]. Palmately lobed	(1.1 – 1.3)
1a[2]. Pinnately lobed	(1.4 - 1.5)
1a[3]. Non-lobed	
1b[1]. Acrodromous veined leaves	(1.6 – 1.8)
1b[2]. Brochidodromous veined leaves	(1.9 – 1.22)
1b[3]. Peltate/orbicular leaves	(1.23)
1b[4]. Eucamptodromous veined leaves	(1.24 – 1.27)
2. Toothed leaves	
2a[1]. Leaf organisation pinnately compound	(2.1 - 2.2)
2a[2]. Leaf organisation palmately compound	(2.3)
2a[3]. Leaf organisation appears simple	
2b[1]. Leaf pinnately lobed	(2.4)
2b[2]. Leaf palmately lobed	(2.5 - 2.7)
2b[3]. Leaf non-lobed	
2c[1]. Acrodromous venation	(2.8)
2c[2]. Pinnate venation	
2d[1]. Semicraspedodromous secondary venation	(2.9 – 2.25)
2e[1]. Possible juvenile foliage	(2.26)
2d[2]. Craspedodromous secondary venation	(2.27 – 2.38)

Table 6.1. Hierarchical table summarising the main morphological divisions of the King George Island floras studied during this project. 1a – lobing, 1b – secondary venation, 2a – leaf organisation, 2b – lobing, 2c – primary venation, 2d - secondary venation.

Counts of total leaf populations are based on fragmented as well as complete leaves. Secondary divergence angles were standardised and defined as the angle between the primary vein and a secondary vein at 50 % of its length. The number and degree of completeness of specimens used to define each morphotype is stated in the description. The degree of completeness is defined as: Small fragment < 50 % of lamina; Large fragment 50 – 75 % lamina; Near complete > 75 % lamina; Complete > 90 % of lamina.

6.4 Taxonomic interpretations

The method adopted for taxonomic identifications was based on initial reference to the synoptic key and tooth architectural studies of Hickey and Wolfe (1975) and the Southern Hemisphere fossil literature (biased greatly towards New Zealand and Australia), early works from Seymour Island (Dúsen, 1908) and southern South America (Dúsen, 1899; Berry, 1928, 1938), and reference texts, such as Klucking (1986; 1987; 1988; 1989; 1991; 1992; 1995; 1997), Christophel and Hyland (1993), Heywood (1993), Salmon (1986). Modern plant distributions were obtained from Mabberley (1997). In addition, the modern composition of cool to warm temperate Southern Hemisphere forests has also been used as an index for possible plant families and genera that may have been present in Antarctica (e.g. Veblen *et al.*, 1996). This has inevitably been biased, towards *Nothofagus* dominated forests, since *Nothofagus* is a dominant element in the Tertiary fossil record (Chapter 2).

Previous macrofossil collections from the Antarctic Peninsula and southern South America generally lack cuticle and tertiary or higher order venation, which are important taxonomic features (Dilcher, 1974). Detailed leaf architecture descriptions are often lacking for this material and the descriptions often lack a sound systematic basis. In addition, detailed modern records of the South American floras are lacking and older references date back to the 19th century, when the generic and familial affinities are sometimes questionable and plants are often misidentified as Northern Hemisphere genera. A solid database of morphological characters is therefore lacking. This is particularly pertinent when describing taxa that have conservative leaf morphologies such as the Lauraceae, Cunoniaceae (*Weinmannia* and *Schizomerieae*), Proteaceae and for the Nothofagaceae, which are extremely difficult to differentiate without cuticle data (B Hill, pers. comm., 2000).

Herbarium material of southern cool- and warm- temperate plants has also been examined from collections in the Royal Botanic Gardens, Kew and two internet facilities - the web collection of the Smithsonian Institute (http://digilib.si.edu) and the Australian National Botanical Gardens (http://www.anbg.gov.au/anbg/), as well as living material from the Royal Botanic Gardens, Edinburgh, and the Thorpe Perrot Arboretum, Yorkshire.

1. Entire margined morphotypes

1a[1]. Palmately lobed leaves

1.1. Dicotylophyllum washburni n. sp., Hunt (Figures 6.1:1-5)

1963 *Sterculia washburni* Berry 1928, Orlando (p. 632)

1986 *Sterculia* cf. *S. washburni* Berry 1928, Czajkowski and Rösler (p. 103, plate 2, figs 9, 10)

1989 *Dicotylophyllum latitrilobatum* Birkenmajer and Zastawniak (p. 76, plate II, figs 1, 2, 5)

1990 *Dicotylophyllum latitrilobatum* Birkenmajer and Zastawniak, Torres (plate 16, fig 2)

1990 *Sterculia washburni* Berry 1928, Li and Shen (p. 154, plate 1, fig 5)

Material examined: Dragon Glacier flora *Complete* P.3001.5, P.3013.44. *Near complete* P.3001.4, .51, .64, .128, .182, .184; P.3013.3, .9, .13, .20. *Large fragment* P.236.7; P.3001.53, .159; P.3013.9, .16, .43. *Small fragment* P.3001.53, .82, .89.1, .157; P.3002.1; P.3013.29, .162. Fossil Hill U2 *Near complete* P.935.13; Fossil Hill U4 *Near complete* G.458.3, P.3031.7, .11, .22. *Large fragment* G.458.1a/b; P.3031.97, .2, .5, .16, .18, .30, .38, .39. *Small fragment* P.3031.95. Rocky Cove *Small fragment* P.3029.2, .17.

Differential characters: Trilobed leaves with three actinodromous suprabasal primary veins and two basal secondary veins. Long normal petiole when preserved.

Description: Leaf organisation appears simple. Lamina palmate elliptic, symmetrical. Lamina length min 13 - 90 mm, width min 26 – 122 mm, length:width ratio 0.43:1 - 1.44:1. Area min 312 – 3413.33 mm^2. Microphyll = 19 (45 %), notophyll = 20 (48 %) mesophyll = 3 (7 %). Apex symmetrical odd-lobed acute or obtuse acuminate, rarely convex. Apical angle 30° - 110°. Base symmetrical, obtuse, convex, concavo-convex to cordate basal angle 90° - 135°. Normal petiole, attached marginally, length 21 - 23 mm, width 0.6 – 1 mm (P.3001.162 and P.3001.184). Good blade-petiole separation. Petiole often at an angle to the midrib. Margin entire. *Venation* primary vein category suprabasal actinodromous, secondaries weak brochidodromous. *Primary* thickness weak to moderate. Course often curved and/or sinuous, rarely straight. The midvein and one pair of fine secondary veins arise close to the leaf base. *Secondary* min 5 - 8 opposite to alternate secondaries diverging at a narrow to right angle 29° - 90°. Thickness is moderate to fine. Divergence angle decreases toward base. Spacing increases towards base. Loop forming branches join superadjacent secondaries at an acute to right angle. One pair of simple agrophic veins. Weak intersecondaries. *Tertiary* vein category opposite to alternate percurrent. Tertiaries form a series of arches exmedially on basal pair of primary veins. *Fourth order* vein category regular polygonal reticulate. *Fifth order* vein category regular polygonal reticulate and is the highest vein order observed. Areoles 4 or more sided. *Lobes* acute and angular, principal veins are primaries, course central, origin direct. Specimen P.935.13 has a single lateral lobe. *Leaf Rank* 2r/3r.

Remarks: Trilobed lamina morphology with actinodromous triple branching primaries defines these leaves as the form species *Dicotylophyllum latitrilobatum* (Birkenmajer and Zastawniak, 1988). The incorrect synonymisation of the specific epithet has required that the

form be renamed as *Dicotylophyllum washburni*. It is one of the most abundant leaf forms present in the BAS collections and is a common component of the KGI flora (Orlando, 1963; Czajkowski and Rosler, 1986; Troncoso, 1986; Birkenmajer and Zastawniak, 1988, 1989; Li and Shen, 1989; Zastawniak, 1990). The material is distinguished from *Sterculia washburni*, which has a four lobes, a cuneate base morphology, more acute secondary divergence angle and less well organised tertiary venation. The specimens are easily distinguished from *S. patagonica* Berry, which have a pentalobed morphology, more acute secondary divergence angle and less well organised tertiary venation. *S. guinazui* Berry has greater incision of the lobe sinuses and attenuated lobe apices, the apical portion of the leaf also has a more acuminate form. Berry's (1928) descriptions were based on comparisons with *S. diversifolia* Don (Barton, 1964). The material is not considered to group with *Sterculia washburni* but is consistent with the description of *Dicotylophyllum washburni* therefore this name takes precedence.

Palmate leaves with basal actinodromous venation occur in the palmate Dilleniidae (Hickey and Wolfe, 1975), which is consistent previous interpretations of Sterculiaceae. However trilobed morphologies are also present in several other families e.g. Cochlospermaceae (*Cochlospermum*), Euphorbiaceae and Tiliaceae. Leaves from these families possess one or two shared characters, for example trilobed shape *or* triple branching primary *or* agrophic veins but the Sterculiaceae has the only leaves studied that possess all of these features. Herbarium specimens of *Brachychiton populneus* Schott., and Endl. (Sterculiaceae) at the RBG Kew Herbarium are more consistent in lamina shape, low order (primary and secondary) venation, and a less pronounced lobe sinus with the King George Island leaves than *S. diversifolia*. These leaves also possess a petiole at an angle to the midrib. It is important to note that herbarium specimens of modern *Brachychiton* Schott., and Endl., show immense variability in leaf morphology at the generic and species levels, ranging from unlobed elliptic forms to a pentalobed form.

Morphotype 1.2 (Figure 6.1: 6)

Material examined: Dragon Glacier *Near complete* P.3001.36.1a/b.

Differential characters: Trilobed leaf with pinnate brochidodromous venation. Lobing is reduced and highly incised, and the leaf has poor margin-petiole separation.

Description: Leaf arrangement appears simple. Lamina symmetrical and palmate trilobed, margin entire and slightly enrolled. Lamina length min 67 mm, est. 80 mm, width min 45 mm, est. 50 mm, length:width ratio 1.6:1. Area est. 2667 mm^2. Notophyll = 1 (100 %). Apex acute ?asymmetrical, estimated angle 41°. Base obtuse, symmetrical decurrent concavo-convex, basal angle min 100°. Petiole marginal, length min 3 mm, width 1mm. *Venation* pinnate weak

brochidodromous. *Primary* thickness moderate. Course straight becoming zigzag apically. One primary originates at leaf base. *Secondary* min 12 subopposite to alternate moderate secondaries diverging at a narrow to moderate acute angle 41°- 60°. Divergence angle decreases toward base, spacing increases abruptly towards base. Weak intersecondaries. One pair of simple agrophic veins. *Tertiary* veins rare ?percurrent. *Lobes* highly attenuated, indentation to midvein 4 mm. Deep, rounded sinus. Leaf rank 1r/2r.

Remarks: Morphotype 1.2 is differentiated from *Dicotylophyllum washburni* in having a suprabasal pair of secondaries, rather than a triple suprabasal primary, less distinct blade petiole separation, a deeply notched lobe sinus and a much greater length to width ratio. The preservation of the leaf is poor, in particular of the margin and further research may reveal closer links to *D. latitrilobatum* (e.g. based on the morphological variability observed in sterculiaceous genera).

Morphotype 1.3 (Figure 6.1: 7)

Material examined: Dufayel Island *Large fragment* G.53.8(24).

Differential characters: ?Pentalobed entire margined leaf with actinodromous basal primaries.

Description: Leaf organisation appears simple. Lamina ?elliptic, probably symmetrical. Lamina length min 49 mm est. 55, width min 49 mm est. 98 mm. Area est. 3593.33 mm^2. Notophyll = 1 (100 %). Apex not preserved, probably odd-lobed acute and convex. Base partly preserved, basal angle ?obtuse, base shape hastate or truncate. Petiole attachment marginal. Margin entire. Palmately pentalobed. *Venation* Primary vein category actinodromous or possibly palinactinodromous, secondary vein category not preserved. *Primary* weak. Estimated 5 primary veins and 2 primary branches originating at or near base of leaf. Leaf rank uncertain.

Remarks: Birkenmajer and Zastawniak (1986) described a similar sized, pentalobed leaf from the Dufayel Island flora, which they compared with *Cochlospermum* Kunth. The two leaves appear very similar but the preservation. Similar pentalobed leaf fragments have also been described from the Late Cretaceous Zamek Formation as 'pentalobophyll (Araliaephyll)' by Zastawniak (1990, 1994) and *Sterculiaephyllum australis* (Dutra 1997). It is possible that these leaves are all related. In addition, the pentalobed lamina and palinactinodromous venation resembles that of *Sterculia patagonia* (e.g. Berry 1938). Cantrill and Nichols (1996) assigned pentalobed leaves from Lower Cretaceous sequences on Alexander Island to form species *Araliaephyllum quinquelobatus* Cantrill, but this leaf differs in having strong, near dichotomising, abaxial branching of the primaries.

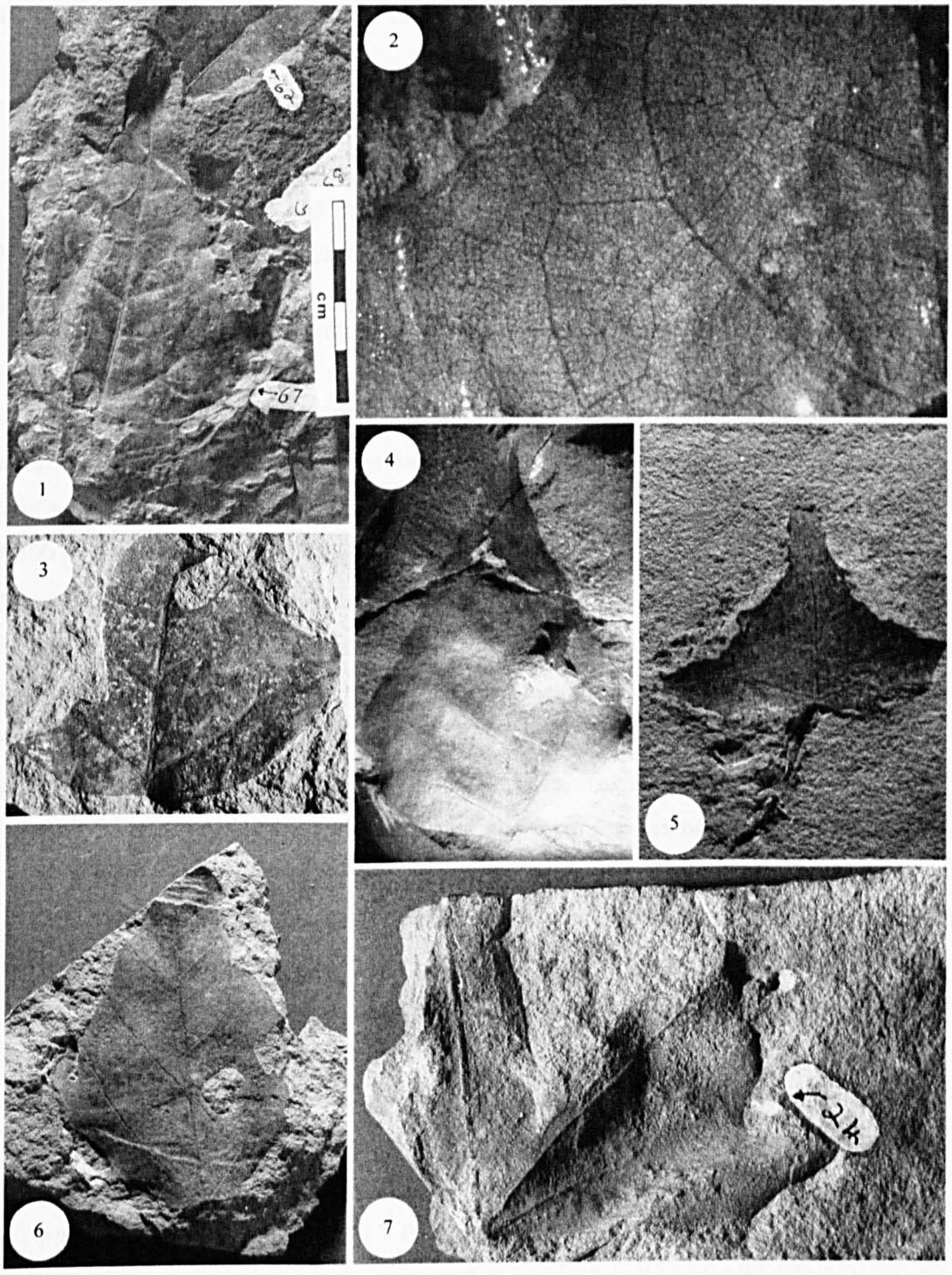

Figure 6.1. Palmately lobed morphotypes. (1) - (5) Morphotype 1.1. *Dicotylophyllum washburni*. (1). G.458.3. x1.2. (2). Fine scale reticulated venation. P.236.7. 5. x3.7. (3). P.3001.51. x1.5. (4). Specimen with indistinct lobes. P.935.13. (5). Angled petiole characteristic of modern *Brachychiton* sp. P.3001.5a. x1. (6). Morphotype 1.2. P.3001.36.1. x0.87. (7). Morphotype 1.3. G.53.8. x1.14.

The preservation of this specimen is too poor to support a taxonomic assignment but pentalobed palmate leaves, with basal actinodromous venation occur in the palmate Dilleniidae (e.g. Cochlospermaceae Passifloraceae and Sterculiaceae) (Hickey and Wolfe, 1975), which supports previous interpretations of a *Cochlospermum* or Sterculiaceae affinity.

1a^2. Pinnately lobed leaves

Morphotype 1.4 (Figure 6.2: 1 - 6)

Material examined: Dragon Glacier *Near complete* P.3001.67. *Large fragment* P.3001.89. *Small fragment* P.3001.64, .114, .133.

Differential characters: Pinnatisect leaf with pinnate craspedodromous venation, tertiary veins are weak brochidodromous.

Description: Leaf organisation appears simple, regular odd pinnately lobed. Lamina symmetrical, elliptic to ovate. Based on near complete specimen P.3001.67, lamina length 62 mm, width 25 mm, length:width ratio 2.48:1. Area est. 1033.33 mm^2. Based on P.3001.67 and P.3001.89, microphyll = 2 (50 %). Apex acute convex, apical angle estimated 40°. Base acute decurrent, basal angle estimated 50°. Petiole normal, attachment marginal. Margin entire. *Venation* pinnate craspedodromous. *Primary* thickness stout. Course is curved and sinuous. *Secondary* estimated 13 alternate moderate secondaries diverging at narrow to wide acute angle 37° - 52°. Divergence angle uniform, vein spacing appears regular. Intersecondary veins are trend to the lobe sinus and combine with a tertiary to form an arch that joins the basally adjacent secondary. *Tertiary* veins are both reticulated and form a series of arches. *Fourth order* vein category regular polygonal reticulate. *Fifth order* vein category regular polygonal reticulate. Higher order venation unresolved. Areoles ?4 or more sided. Marginal ultimate venation ?looped. Lobe sinus rounded. Secondary veins terminate in apex of lobe, which is rounded to slightly angular. Lobe indentation to midvein 2 – 11 mm.

Remarks: The entire margined pinnatisect morphology of this leaf differentiates it from all angiosperm leaf fossils in Tertiary sequences of the Antarctic Peninsula. Pole (1992) referred a leaf form with similar gross, lobed morphology from the Cretaceous Otago flora, New Zealand, to *Nothofagus praequercifolia* (Ett.) Pole, but the material lacks tertiary or higher order venation. None of the modern entire margined *N.* sp. are lobed and lobing is rare in any of the toothed forms (South American *N. antarctica* (Forster f) Oersted and *N. glauca* (Phil.) Krasser sometimes have a near lobed margin). Lobed forms are also rare in the fossil record and where present are toothed, for example the Tasmanian *N. microphylla* Hill and *N. lobata* Hill and the New Zealand *N. melanoides* (Pole, 1992), none of which have intersecondary veins trending to the lobe sinus. The sinus depth of *N. praequercifolia* is also visibly less than in morphotype 1.4.

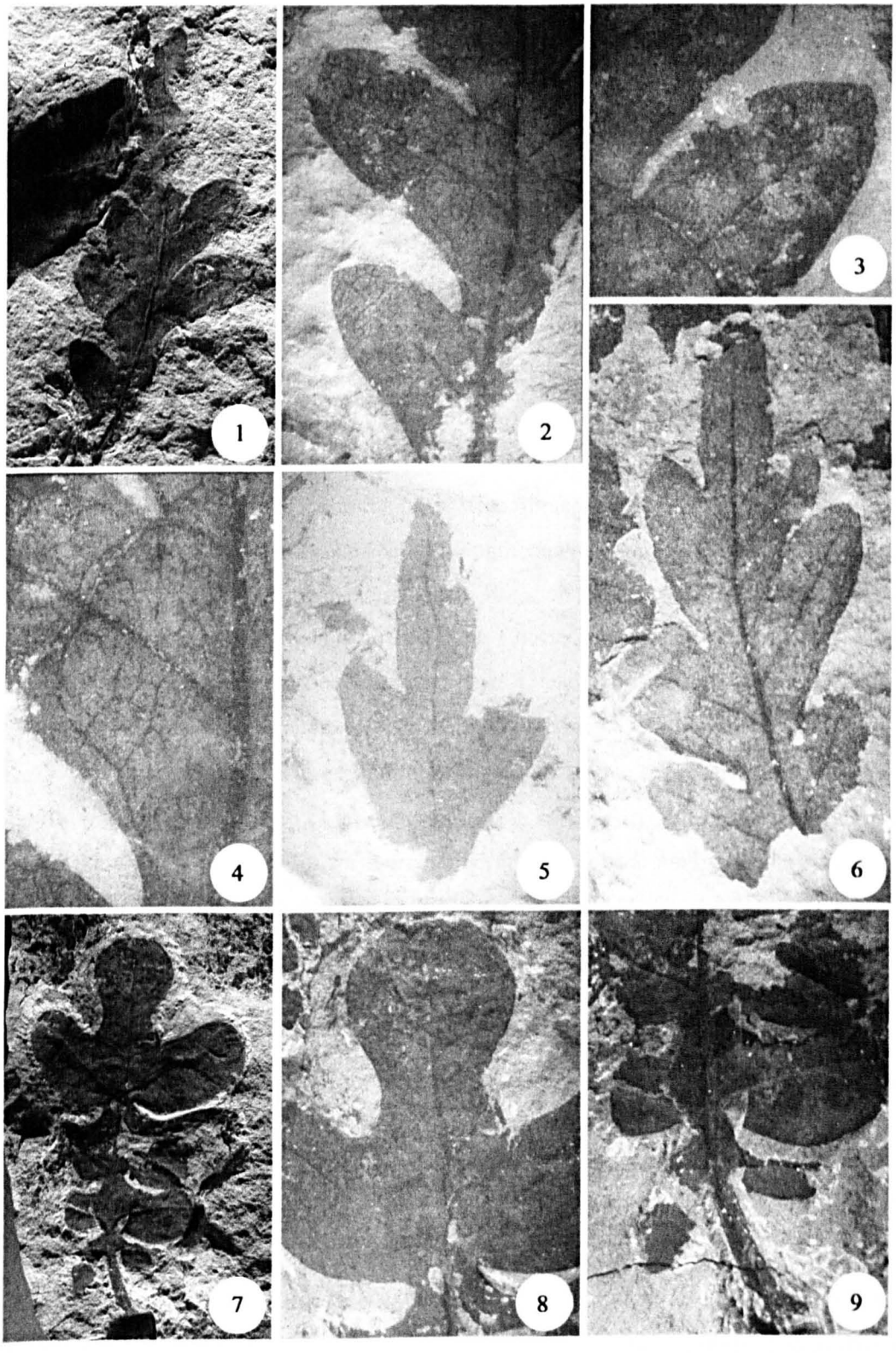

Figure 6.2. Pinnately lobed leaves. (1) - (6) Morphotype 1.4. (1). P.3001.67. x1.2. (2) and (4). Detail of higher order venation in P.3001.67. x2.5, (3). Tooth architecture in P.3001.67. x2.8. (5). Apical fragments P.3001.133. x3.8. (6). P.3001.89. x2.6. (7) - (9) Morphotype 1.5. P.3001.187. (7) x0.8. (8). Apical lobe. x2.25. (9). Detail of swollen petiole base x2.25.

Pinnately lobed entire margined leaves are not specifically discussed by Hickey and Wolfe (1975) but they are present in a number of orders including the Fagales and the Proteales. This leaf also resembles entire margined forms of *Lomatia* R. Br. (Proteaceae) (G Jordan, pers. comm., 2001), and shares the character of an intersecondary that branches towards the sinus. More complete specimens are required to support this comparison.

Morphotype 1.5 (Figures 6.2: 7 - 9)

Material examined: Dragon Glacier *Near complete* P.3001.187.1. *Large fragment* G.9.54 (housed in Swedish Museum of Natural History).

Differential characters: Entire margined pinnatisect leaf with deeply incised, rounded lobes, which increase in size apically. Pinnate venation. Thick ?sheathing petiole.

Description: Lamina organisation appears simple, regular odd pinnately lobed. Lamina obovate, symmetrical. Lamina length 55-62 mm, width min 37-46 mm, length:width ratio 1.34:1 – 1.49:1. Estimated leaf area 1901.33 mm^2. Notophyll = 2 (100 %). Apical lobe rounded, apical angle odd lobed obtuse 98°. Hastate base, wide obtuse, basal angle 260°. Lobes indented 1-25 mm to midvein. Petiole marginal, petiole length min 16 mm, width max 4 mm. Petiole winged, swollen at base ?sheathing. Margin entire. *Venation* pinnate craspedodromous. Primary thickness 1 mm, vein size 2.2 % and is termed stout. Course is curved and slightly sinuous. One primary originates at the leaf base. *Secondary* min 13 subopposite to alternate secondaries diverging at a moderate to wide acute angle 52°-95°. Angle increases toward base, basal pair are obtuse 95°. Thick secondaries diverge into lobes, moderate to fine secondaries present in apical lobe ?could potentially be classed as tertiary veins. Vein spacing irregular. Intersecondary veins are present but weak. *Tertiary* veins form brochidodromous loops around secondary and tertiary veins. *Fourth order* veins dichotomising. *F.E.V's* not observed. *Other features* leaf surface is creased and a crater-like trace is present in the apical-most right hand lobe.

Remarks: A single pinnately lobed leaf illustrated but not described by Birkenmajer and Zastawniak (1988) has the same pinnate rounded lobes, secondary venation and is of a similar size to morphotype 1.5 and is therefore considered to belong to the same morphotype. No modern or fossil specimens with even a superficial similarity were found to compare with this morphotype.

Some elliptic entire margined leaves have a juvenile lobed state during ontogeny and this leaf could represent such a growth stage (B. Stannard, pers. com., 2000). The herbaceous Plumbaginaceae has multiple lobed leaf morphologies, such as *Limonium* Miller (Statice), however this is a predominantly Northern Hemisphere genus and the apical lobe of the leaf is larger, ~ 50 % of the lamina, compared to c. 25 % of the lamina in morphotype 1.5. In addition, the secondary venation bifurcates towards the margin rather than forming brochidodromous

loops (Heywood, 1998). Some ferns, in particular the Polypodiaceae have pinnatisect fronds and sheathing petioles, however the presence of at least 4 well defined and regular vein orders supports an angiosperm rather than a fern classification for this leaf.

1a[3]. Non-lobed leaves

1b[1]. Acrodromous veined leaves

Morphotype 1.6 (Figures 6.3: 1 - 2)

Material examined: Platt Cliffs *Complete* G.50.6(36, 37). Dufayel Island *Large fragment* G.53.25.

Differential characters: Elliptic leaves with pinnate suprabasal acrodromous venation. Secondaries are indistinct, higher order venation scarcely visible.

Description: Lamina organisation appears simple. Lamina elliptic, symmetrical. Lamina length 33 – 75 mm, width 15 – 42, length:width ratio 1.71 – 2.2. Microphyll = 2 (67%), notophyll = 1 (33 %). Area est. 330 – 2100 mm^2 . Apex acute convex, apical angle 66° - 88°. Base acute to obtuse concavo-convex to decurrent, basal angle 67° - 92°. Petiole marginal. Margin entire. *Venation* pinnate suprabasal acrodromous. *Primary* thickness moderate to massive. ?One primary and 4 - 6 secondary veins arise at or close to the leaf base. *Secondary* 4 - 6 fine to moderate secondary veins running to leaf apex. Vein spacing uncertain, vein angle acute 18° – 31°. *Tertiary* venation (G.53.25) ?opposite percurrent. Vein angle to primary perpendicular, vein angle ?uniform. No higher order venation preserved.

Remarks: Barton (1964) considered this morphotype to be monocotyledonous based on the parallel venation, however there is insufficient venation detail to support this interpretation because at this scale of resolution, the venation pattern could equally be described as pinnate basal acrodromous dicotyledonous leaf. Morphotype PPT13 (App. 39; Kennedy, 1998) from the Palaeocene of New Zealand is similar in length and secondary vein architecture, but the preservation of this leaf is also poor and no taxonomic affinities were suggested.

Entire margined leaves with perfect acrodromous venation are present in the parts of the Magnoliidae subclass (Hickey and Wolfe, 1975). Suprabasal acrodromous venation is particularly common in the Lauraceae (e.g. *Cinnamomum* Schaeffer and *Lindera* Thunb), however without cuticular characters it is not possible to assign a leaf morphotype to a particular lauraceous genus (Hill, 1986). The number of secondary veins terminating in the apex (four to six) seems to be unusual in combination with the venation style and might be taxonomically significant. *Ripogonum scandens* J.R. et G. Forst. (Smilacaceae) described by Pole (1993) from the Miocene Manuherika Group, New Zealand has a similar morphology with

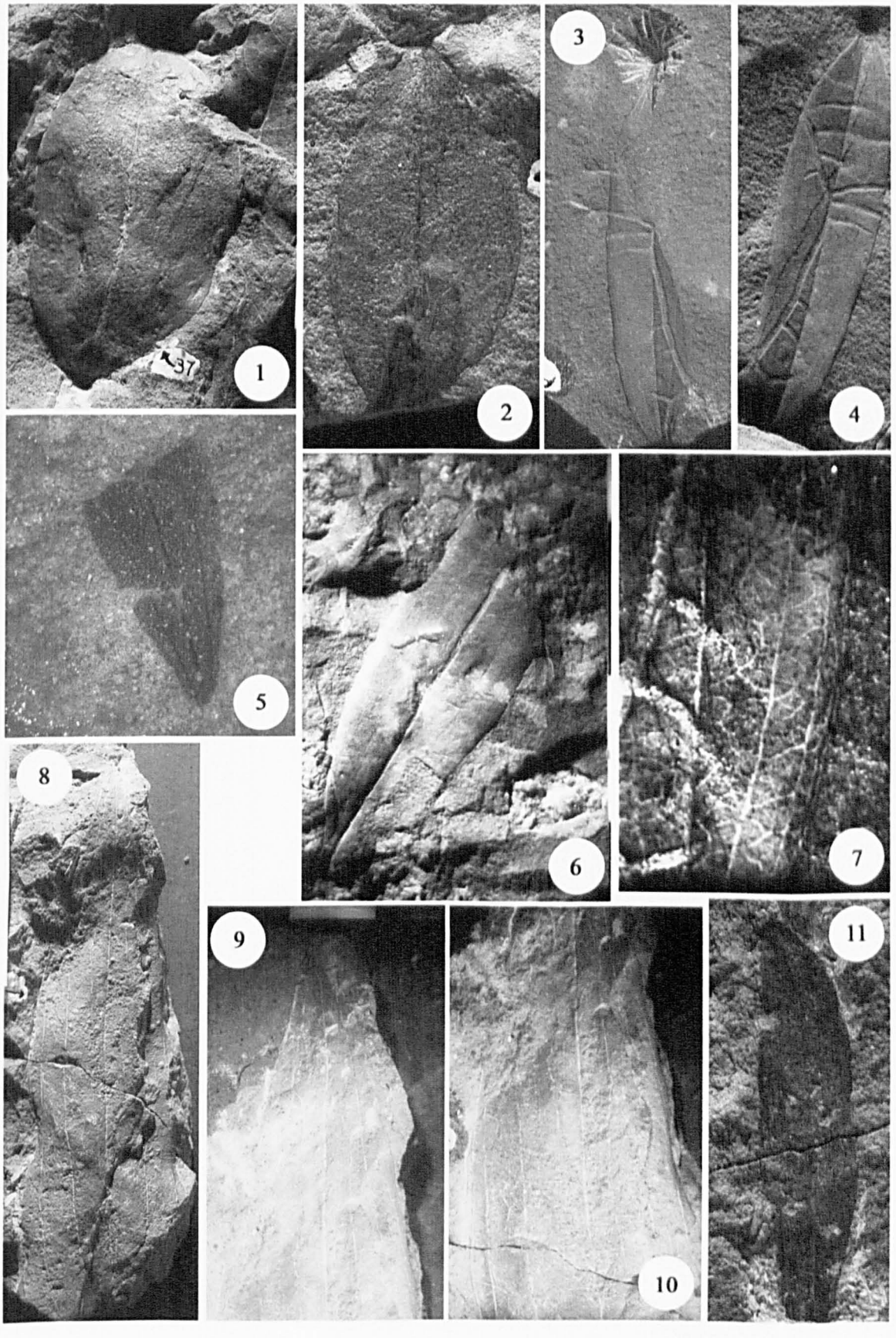

Figure 6.3. (1) - (2) Morphotype 1.6. (1). G.50.6(37). x0.8. (2). G.53.25. To scale. (3) - (7) Morphotype 1.7. x1. (3). P.935.23a. (4). P.935.23b. x1.3. (5). P.212.12. x2. (6). P.3031.60. x2. (7). Venation detail of P.935.23. x3. (8) - (10) Morphotype 1.8. G.50?(35). x0.5. (9). Detail of leaf apex. x0.8. (10). Detail of venation. x0.8. (11). Morphotype 1.9. G.309.18. x1.4.

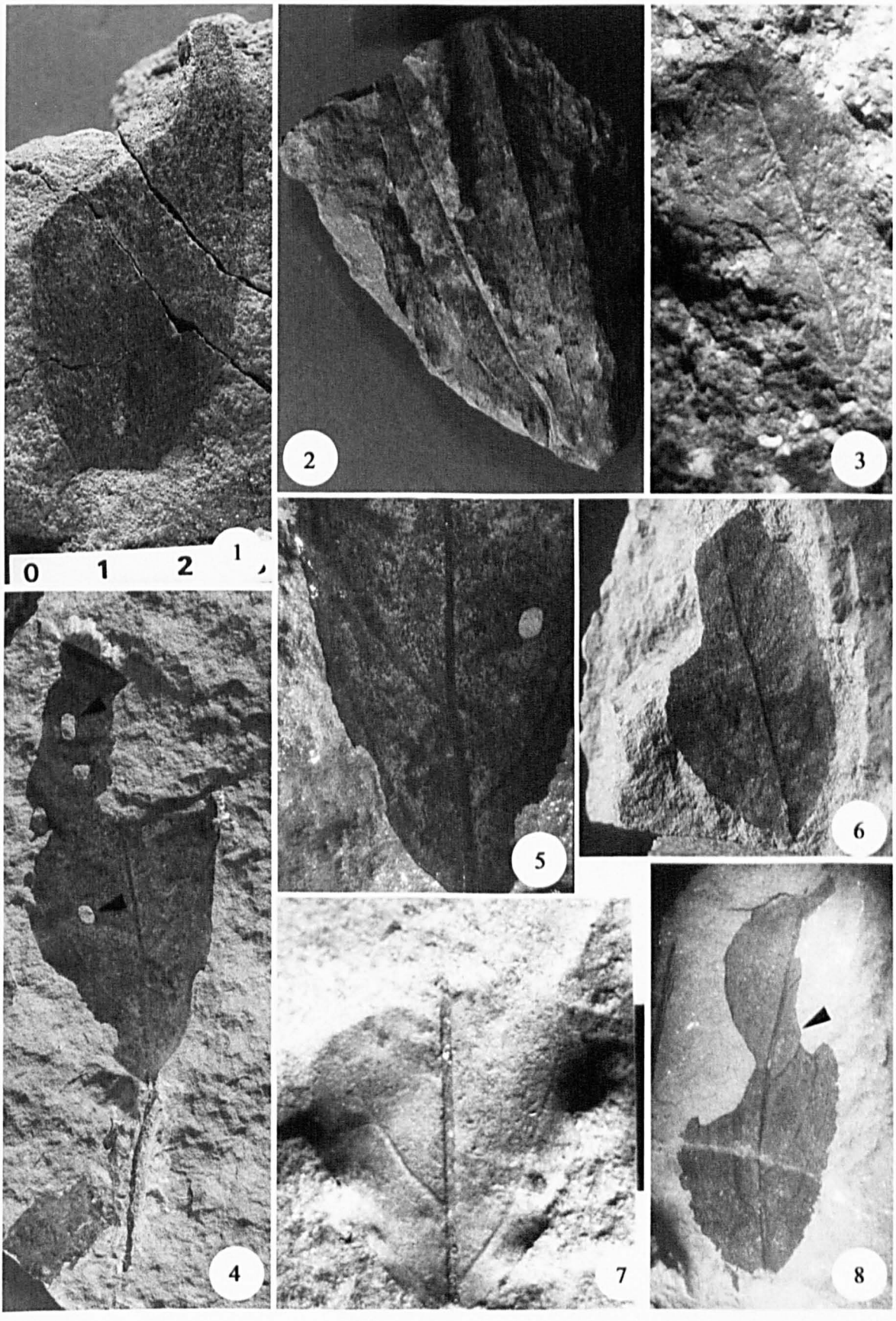

Figure 6.4. (1) - (2) Morphotype 1.9. (1). G.50.19. 1 cm scale bar. (2). G.50.5.1 (right) and G.50.5.2 (left). x0.6. (3). Morphotype 1.10. P.3031.47.x2.2. (4) - (8) Morphotype 1.11. (4). P.3013.7, note small elliptical traces with thin rim of reaction tissue (arrowed). x1. (5). Detail of basal venation. P.3013.7. x1.5. (6). P.3001.209. x1.9. (7). P.3031.70. x3. (8). P.3001.169, note marginal feeding trace (arrowed). x2.2.

up to ten secondaries terminating at the apex, a thick primary vein and relatively fine secondaries convex to slightly attenuated apices and bases as observed in morphotype 1.6. *R. scandens* differs in having strong secondary branching in the mid-portion of the lamina.

1.7. *Dicotylophyllum australe* n. sp., Hunt (Figure 6.3: 3 - 7)

1986 *Miconiiphyllum australe* Dusén, Czajkowski and Rösler (p. 101, plate 1, figs 3, 5)

1989 *Dicotylophyllum duseni* Zastawniak, Birkenmajer and Zastawniak (p. 79, plate V, figs 1, 1a, 2, 3)

1989 *Miconiiphyllum australe* Dusén, Li and Shen (p. 131 - 132, plate II, fig 5, 5a)

1990 cf. *Smilax duseni* Torres, (plate 17, figs 3, 4)

1994 *Pentaneurum duseni* Li, (p. 167, plate 5, figs 3, 3a, plate 6, figs 5, 5a)

Material examined: Fossil Hill U2 *Large fragments* P.935.17, .22, .23a/b, .25, Fossil Hill U4 *Large fragments* P.3031.60, .4, .71. Rocky Cove *Small fragment* P.212.12.

Differential characters: Oblong to lanceolate leaves with five basal acrodromous secondaries. Intersecondary venation is reticulated. Apex attenuated to a drip tip.

Description: Lamina organisation simple. Lamina oblong to lanceolate, symmetrical. Lamina length 60 - 90 mm, width 8 – 24 mm, length:width ratio 2.63:1 – 4.62:1. Area est. min 210 – 1280 mm^2. Microphyll = 7 (100 %). Apex acute ?acuminate, apical angle 30° - 42°. Base acute, concave to decurrent, basal angle 42° - 46°. Petiole marginal. *Venation* basal acrodromous. *Primary* thickness moderate to stout. *Secondary* vein category basal acrodromous with 4 secondary veins converging towards the leaf apex. *Tertiary* vein category mixed opposite and alternate percurrent, angle to primary acute to obtuse, increasing basally. Course sinuous. *Fourth order veins* ?anastamosing. Marginal ultimate venation looped. Leaf rank 2r/3r.

Remarks: This leaf morphotype was originally referred to *Miconiiphyllum australe* (Melastomataceae) (Czajkowski and Rösler, 1986; Li and Shen, 1989) by comparison with a single leaf fragment from Seymour Island. However, the extremely small size of that fragment (< 20 % of the lamina) means that any comparison must be tentative at best (Birkenmajer and Zastawniak, 1989), and is insufficient to group the material with *M. australe*. Birkenmajer and Zastawniak (1989) erected the form species *Dicotylophyllum duseni* Zastawniak to resolve this problem. However, the specific epithet of Dúsen has priority, therefore the leaf should be assigned to *Dicotylophyllum australe*. Li (1994) assigned the leaves to *Pentaneurum dusenii* Li (Melastomataceae), based on the primary venation pattern, suggesting that the leaf comprised five primary veins. Using the definition of the Leaf Architecture Working Group (1999) these leaves actually possess a single primary vein and four acrodromous secondary veins, or two acrodromous secondaries and two exmedial composite secondaries formed by tertiary loops. In addition, this morphology is conservative and common to several families including the Melastomataceae, Lauraceae (*Cinnamomum*), the Smilicaceae (e.g. *Smilax*), Anisophyllaceae and Myrtaceae (e.g. *Rhodamnia* Jack.). On this basis it is not considered that the criteria of Li

(1994) adequately relate these specimens to the Melastomataceae and the material is referred to the form species *D. duseni.*

Morphotype 1.8 (Figure 6.3: 8 - 10)

Material examined: Platt Cliffs *Large fragment* G.50? (35).

Differential characters: Lanceolate entire margined leaf with primary acrodromous venation.

Description: Lamina organisation appears simple. Lamina elliptic, symmetrical. Length min 105 mm, width 33 mm, length:width ratio min 3.18:1. Area est. 2310 mm^2. Mesophyll = 1 (100 %). Apex acute convex or straight, apical angle 30°. Base and petiole not preserved. *Venation* primary suprabasal acrodromous. *Primary* thickness weak. 5 primaries diverge at a narrow acute angle. *Secondary* vein category regular polygonal reticulate. *Tertiary* vein category ?dichotomising. *F.E.V's* 2 or more branched.

Remarks: The lanceolate morphotype 1.8 is distinguished from morphotype 1.7, suprabasal branching and true multiple primaries. The lamina is also extremely large (mesophyll), although size is not a sound taxonomic character (Dilcher, 1974). The leaf was described as a monocotyledon by Barton (1964, 1965), who stated that the leaf did not possess any distinguishing characteristics. A monocotyledonous interpretation is possible but the leaf has suprabasal acrodromous venation rather than classic parallelodromous monocot venation and similar leaves are present in some angiosperm families (Lauraceae, Myrtaceae), therefore more venation detail and a complete specimen are required to confirm that the leaf is a monocot.

$1b^2$. Brochidodromous veined leaves

Morphotype 1.9 (Figures 6.3: 11 and Figure 6.4: 1 - 2)

Material examined: Platt Cliffs *Near complete* G.50.5.1/.2, .19, .(35), Cytadela *Near complete* G.309.18.

Differential characters: Elliptic leaves with a stout primary vein and fine opposite secondaries.

Description: Leaf organisation appears simple. Lamina elliptic, symmetrical. Lamina length 38 – 140 mm, width 12 – 26 mm, length:width ratio 2.69:1 – 5.45:1. Area 400 – 2166.66 mm^2. Microphyll = 2 (50 %), notophyll = 2 (50 %). Apex not preserved, appears acute convex, apical angle est. 35° – 43°. Base acute convex, basal angle 38° - 53°. Petiole marginal length 13 mm, width 2 mm (G.50.5), flares slightly at base. Leaf fossils comprise a thick layer of carbonised material suggesting that they were originally coriaceous. *Venation* pinnate. *Primary* thickness moderate to stout. *Secondary* venation too poorly preserved to suggest category, possibly brochidodromous from curvature of veins in specimen G.309.18. Where preserved secondaries are opposite to subopposite. *Tertiary* rare veins have reticulated appearance.

Remarks: Morphotype 1.9 is a poorly constrained grouping based on nearly complete leaves that lack venation detail. The group might be further subdivided on the basis of the high length to width ratios observed in specimens G.50.5a/b relative to the lower length to width ratios of G.50.19 and G.309.18. The large leaf size and high length:width ratio might also be a taxonomically significant character. However, without further venation detail the leaves have been grouped in order to present a minimum estimate of diversity. A single unidentified leaf of similar size and morphology to G.50.19 and G.309.18 was described from Eocene erratics in McMurdo Sound (Pole *et al.*, 2000), but the preservation of the leaf is so poor that any affinities are uncertain.

Elliptic leaves with brochidodromous secondary venation are common in the Magnoliidae subclass (Hickey and Wolfe, 1975). The leaves are too poorly preserved to suggest closer affinities, although several New Zealand genera *Pseudowintera* (Winteraceae), *Beilschmiedia* (Lauraceae) and *Mida* (Santalaceae) and the Australian *Tasmanica* and *Drimys* (Winteraceae) have similar elliptic laminas with thick primary veins, poorly defined secondaries and high length:width ratios. The thick texture of the preserved compressions (G.50.19 and G.309.18) suggests that they may have been coriaceous evergreen taxa.

Morphotype 1.10 (Figure 6.4: 3)

Material examined: Fossil Hill U4 *Large fragments* P.3031.34, .47, .70.

Differential characters: Elliptic leaves with decurrent brochidodromous venation and base.

Description: Leaf organisation appears simple. Lamina symmetrical, elliptic. Lamina length min 30 – 45 mm, width min 11 – 16 mm, length:width ratio 2.25:1 – 4.09:1. Area 220 - 330 mm^2. Microphyll = 3 (100 %). Apex not preserved, possibly acute convex, est. apical angle 50° – 65°. Base acute decurrent, basal angle. Petiole not preserved, insertion marginal. Margin entire. *Venation* pinnate weak brochidodromous. *Primary* thickness moderate to stout. *Secondary* min 3 – 6 moderate and subopposite to alternate secondary veins diverging from midvein at a narrow to moderate acute angle 28° – 50°. Vein angle irregular, spacing irregular. *Tertiary* vein category ?opposite percurrent, sinuous to convex, increasing basally.

Remarks: Elliptic leaves have previously been described from Fossil Hill (Li, 1994) but the leaves described here differ in having decurrent, opposite secondary branches, as opposed to normal opposite branching (e.g. *Dicotylophyllum* sp. 1, *D.* sp. 7, *D.* sp. 10; Li, 1994).

Elliptic entire margined leaves with pinnate weak brochidodromous venation are common in the Magnoliidae (Hickey and Wolfe, 1975). Decurrent secondary veins are characteristic of leaves of low rank (LAWG, 1999). *Nectandra acutifolia* (R. and P.) Mez. (Lauraceae) possesses

exmedially ramified brochidodromous loops and concavo-convex curvature of the secondary venation, moderate to strong intersecondary veins and broad secondary spacing in the mid to apical portion of the lamina, suggesting possible affinities with the Lauraceae.

1.11. *?Lauriphyllum nordenskjöldii* Dusén 1908 (Figure 6.4: 4 - 8)

Material examined: Dragon Glacier *Near complete* P.3013.7. *Large fragment* P.3001.80, .169, .209. Fossil Hill U4 *Large fragment* G.458.1.2. *Small fragment* P.3031.70.

Differential characters: Elliptic entire margined leaf with secondary vein spacing basally. Long narrow petiole.

Description: Leaf organisation appears simple. Lamina elliptic symmetrical. Lamina length min 29 - 72 mm. Lamina width min 11 - 34 mm. Length:width ratio min 2:1 – 2.73:1. Estimated leaf area min 220 - 1632 mm^2. Microphyll = 6 (100 %). Apex acute convex, apical angle 60° - 71°. Base convex, basal angle 66 - 70°. Petiolar attachment marginal (P.3013.7), petiole length min 38 mm, width ~1 mm. Petiole inflected at an angle of 165°, slightly thickened close to abcission point suggesting insertion point for second leaf. Margin entire. *Venation* pinnate and weak brochidodromous. *Primary* thickness weak to moderate. Course is curved or slightly sinuous. One primary originates at the leaf base. *Secondary* min 7 - 11 alternate moderate secondaries diverging at narrow to wide acute angle 36° - 86°. Angle decreases smoothly toward base. Vein spacing is irregular. Weak intersecondary veins. *Tertiary* veins obtuse, angle decreasing exmedially.

Remarks: Morphotype 1.11 is divisible into two subgroups, represented by the larger leaf P.3013.7 and the smaller leaves P.3001.81, .169 and .209. Size class is an extremely plastic characteristic of leaf morphology (Dilcher, 1974) and was therefore considered to be insufficient to separate the otherwise similar leaves. The leaves are referred to *Lauriphyllum nordenskjöldii* Dusén, a supposed lauraceous leaf, which has an elliptic lamina and similar broadly spaced basal secondaries that decrease abruptly apically. Other elliptic leaves are present in the Fossil Hill flora (Li, 1994) but these differ in having oppositely paired and evenly spaced secondaries (e.g. *Dicotylophyllum* sp. 10). *Anona infestans* Berry (1938) has similar secondary venation but is distinguished by a short petiole.

Elliptic leaves with weak brochidodromous venation are common in numerous groups within the Magnoliidae subclass (Hickey and Wolfe, 1975). Such leaves are common in the modern Lauraceae family, which lends support to the interpretations of Dusén (1908). Cuticular data is required to identify the Lauraceae (Hill, 1986) but the broad spacing of the secondaries in the mid portion of the lamina and close spacing of the basal secondaries is a feature present in *Ocotea* Aublet, *Notaphoebe* Griseb., *Neolitsea* Merr., and *Cinammomum*.

1.12. *Dicotylophyllum* sp. 10 Li 1994 (Figure 6.5: 1 - 4)

?1986 *Hydrangeiphyllum affiné* Dusén 1899, Czajkowski and Rosler (p.103, plate II, fig 14)

1986 *Sapindus* L. sp., Troncoso (p.39, plate 3, fig 24)

1994 *Dicotylophyllum* sp. 10, Li (p.159, fig 12, p. 160, plate 8, fig 1)

Material examined: Fossil Hill U4 *Large fragments* P.3031.9, .12, .21, .35, .51, .52, .56 .69.

Differential characters: Elliptic to lanceolate leaves with convex bases. Secondary veins not decurrent. Basal secondaries opposite.

Description: Lamina organisation appears simple. Lamina elliptic to lanceolate and symmetrical. Length min 25 – 50 mm, width 14 – est. 28 mm, length:width ratio 1.56:1 – 3.31:1. Area est. 266.66 – 933.33 mm^2. Microphyll = 8 (100 %). Apex only partly preserved (P.3031.51), acute straight or convex, apical angle est. 28°. Base convex, basal angle 62° - 83°. Petiole not preserved. *Venation* pinnate weak brochidodromous. Primary vein thickness weak to stout. *Secondary* min 5 – 9 secondaries diverging at a moderate acute angle 41° – 84°. One pair of agrophic veins observed in some specimens (e.g. P.3031.21). Vein spacing variable, generally increasing towards base, vein angle decreasing towards base. ?Weak intersecondaries. Tertiary vein category not preserved.

Remarks: Morphotype 1.12 is grouped with *Dicotylophyllum* sp. 10 based on the combination of a prominent basal pair of opposite secondaries and alternate apical secondaries, and a convex base. This also differentiates the material from the alternately veined *Lauriphyllum nordenskjöldii* and from the toothed form *Rhoophyllum nordenskjöldii* Dusén (Czajkowski and Rösler, 1986; Li, 1994), which has opposite secondaries over most of the lamina. This also differentiates the fossil leaves from *Thunbergia* sp. which only has opposite secondaries (Torres, 1990). The material is otherwise too poorly preserved to suggest taxonomic affinities. The original descriptions by Czajkowski and Rosler (1986) and Troncoso (1986) are based on poorly preserved material that does not justify a generic assignment given the conservative nature of elliptic brochidodromous leaves. Therefore this material is assigned to the form species *Dicotylophyllum* sp. 10 (Li, 1994).

Morphotype 1.13 (Figure 6.5: 5 - 6)

Material examined: Dufayel Island *Large fragments* G.53(20)a/b, .27(21).

Differential characters: Lanceolate leaf with secondary spacing decreasing basally. Prominent lateral agrophic secondaries. Strong opposite and alternate percurrent tertiaries.

Description: Leaf organisation appears simple. Lamina ?symmetrical, ?elliptic. Length min 75 mm, width min 30 mm, length:width ratio min 2.5:1. Area 1500 mm^2. Notophyll = 2 (100 %). Apex not preserved. Base convex to rounded, basal angle 62° - 83°. Margin entire. Petiole marginal, length 4 mm, width 1 mm (G.53.1.1). *Venation* pinnate weak brochidodromous. *Primary* thickness moderate. Course straight. *Secondary* min 7 - 8 moderate, opposite to ?alternate secondaries diverge at narrow to moderate acute angle 35 – 56°. Course curved within

the margin and following margin trend. Angle decreasing abruptly basally. Angle with superadjacent secondary wide obtuse. Spacing uncertain ?greatest at base. Agrophic veins simple. Intersecondaries moderate to strong. *Tertiary* vein category mixed opposite and alternate percurrent. Course sinuous or straight. Thickness moderate to thick. Angle to primary obtuse, increasing exmedially. *Fourth order* vein category uncertain possibly forming a reticulated network. *Marginal ultimate venation* appears looped. Leaf rank 2r. *Other* spherical traces are present in the mid portion of the lamina, two traces occurring close to the primary and one closer to the margin which also overlaps a secondary vein.

Remarks: Barton (1964) suggested that the leaf was similar to *Phyllites* sp. 2 described by Dúsen (1908) from the Tertiary of Seymour Island and suggested affinities with the modern *Lauraceae*. Barton (1964) noted that the insertion point of the basal secondaries was distinctly higher and the base was more strongly cordate than *Phyllites* sp. 2. This may be a typographic error, since the figure reference given by Barton (1964) refers to *Phyllites* sp. 3, and *Phyllites* sp. 2 has a decurrent base and no obvious ramification of the brochidodromous secondary venation. In any case the tertiary and higher order venation in *Phyllites* sp. 3 is not prominent, suggesting that it was originally fine in comparison to the primary and secondary venation, which contrasts distinctly with the strong tertiary venation of morphotype 1.13. The spacing of the veins is similar to *Lauriphyllum nordenskjöldii* (Dúsen, 1908) but the leaves can be distinguished from morphotype 1.13 by the lack of strong tertiary and higher order venation. Morphotypes 11 and 21 of Hayes (1999) from the Cretaceous of James Ross Island are also similar. Hayes' (1999) morphotype 11 has a more acute base and a narrower angle of secondary divergence, but the leaf is otherwise similar in size, venation style and lamina morphology. Hayes (1999) considered the venation style to be acrodromous, however the "arches" that she described do not terminate in the apex and in two specimens (Figure 5.10:b, 5.10:c; p144; Hayes, 1999) clearly recurve to join a superadjacent secondary, which constitutes brochidodromous venation. Morphotype 21 has a similar lamina shape but is differentiated from morphotype 1.13 in having at least 5 pairs of secondaries that are more closely spaced and secondaries that join at an approximate right angle rather than the obtuse angle observed in morphotype 1.13. Zastawniak (1994) described similar laurophyll morphotypes from the Late Cretaceous Zamek flora on KGI, however the preservation is fragmentary and does not support detailed comparisons. *Dicotylophyllum* sp. 2 (Figure 8: 4 & 5; Plate 4: 1; pages 131 and 163; Zastawniak, 1994) appears to have a similar broadly spaced pair of basal secondary veins and convex tertiaries. Unfortunately the resolution of the plates is insufficient for more detailed comparison.

By comparison with fossil material Morphotype 1.14 has a lauraceous morphology and is similar to both *Dicotylophyllum* sp. 2 (Zastawniak, 1994) and Morphotype 21 of Hayes (1999).

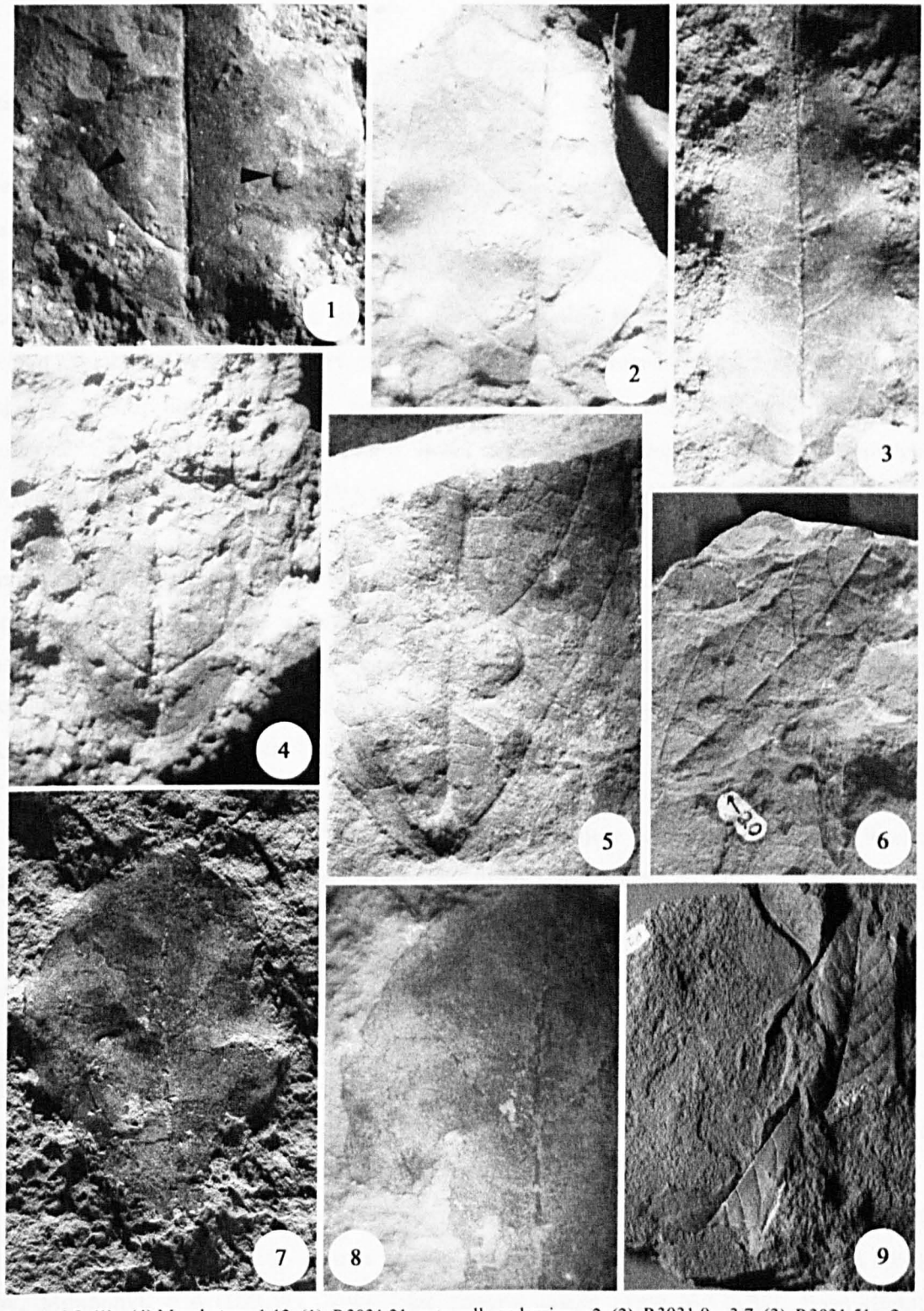

Figure 6.5. (1) - (4) Morphotype 1.12. (1). P.3031.21, note galls on lamina. x2. (2). P.3031.9. x3.7. (3). P.3031.51. x2. (4). P.3031.56. x3. (5) - (6) Morphotype 1.13. (5). G.53(20)a, note galls preserved in right intercostal areas. x1.7. (6). G.53(20)b. x0.7. (7) - (8) Morphotype 1.14. (7). P.3013.21. x1.1. (8). Detail of secondary venation. x2. (9). Morphotype 1.15. P.2799.6.1 (uppermost) and P.2799.6.2 (lowermost). x0.8.

Elliptic leaves with pinnate brochidodromous venation are present in the modern Magnoliidae (e.g. Laurales, Magnoliales and Illiciaceae), Caryophyllidae, Dilleniidae and Hamamelidae (Hickey and Wolfe, 1975), supporting a possible lauraceous origin for the leaf.

Morphotype 1.14 (Figure 6.5: 7 - 8)

Material examined: Dragon Glacier *Large fragment* P.3013.21.

Differential characters: Elliptic leaf with a prominent suprabasal pair of secondaries.

Description: Leaf organisation appears simple. Lamina elliptic, ?symmetrical. Length min 55 mm, width min 42 mm, length-width ratio min 0.95:1. Area 1540 mm^2. Notophyll = 1 (100 %). Apex not preserved, apical angle estimated 95°. Base convex, basal angle 105°. Petiole marginal, not preserved. Margin probably entire. Venation pinnate weak brochidodromous. *Primary* thickness weak. *Secondary* min 8 moderate to thick secondaries diverge at 35° - 90°, angle decreasing abruptly basally, spacing increasing abruptly basally. Intersecondary veins moderate. One pair lateral agrophic veins. Basal secondary bifurcates in addition to ramifying loops. Higher order and marginal ultimate venation not resolved. Leaf rank 2r/3r.

Remarks: Morphotype 1.14 is similar to morphotype 1.13 in having elliptic lamina with a prominent pair of agrophic secondaries but it can be distinguished by strong branching of the basal secondaries. In addition morphotype 1.14 has less pronounced curvature of the mid-lamina secondaries and the basal secondaries appear to more branch strongly towards the superadjacent secondary and closer to the leaf base than in morphotype 1.13.

Elliptic leaves with pinnate brochidodromous venation are present in the modern Magnoliidae (e.g. Laurales, Magnoliales and Illiciaceae), Caryophyllidae, Dilleniidae and Hamamelidae (Hickey and Wolfe, 1975), supporting a possible lauraceous origin for the leaf.

Morphotype 1.15 (Figures 6.5: 9 and 6.6: 1 - 2)

Material examined: Potter Cove impression flora *Small fragment* P.232.17.4. Vaureal Peak *Large fragment* P2799.2.1,.6.1,.2.

Differential characters: Elliptic leaves with thick secondaries. Basal secondaries are slightly more acute and irregular than apical secondaries.

Description: Leaf organisation appears simple. Lamina narrow-elliptic, symmetrical. Length est. 94 - 96 mm, width est. 26 - 30 mm, length:width ratio 3.2 – 3.62. Area est. 1629.33 - 1920 mm^2. Microphyll = 4 (100 %). Apex acute convex, apical angle 41° - 55°. Base slightly asymmetrical, acute convex, basal angle 42° - 46°. *Venation* Primary pinnate weak brochidodromous. *Primary* thickness weak to moderate. Course straight. *Secondary* min 5 – 11 (est. 14) pairs of moderate secondaries diverging at a moderate to wide acute 40° - 73° Spacing

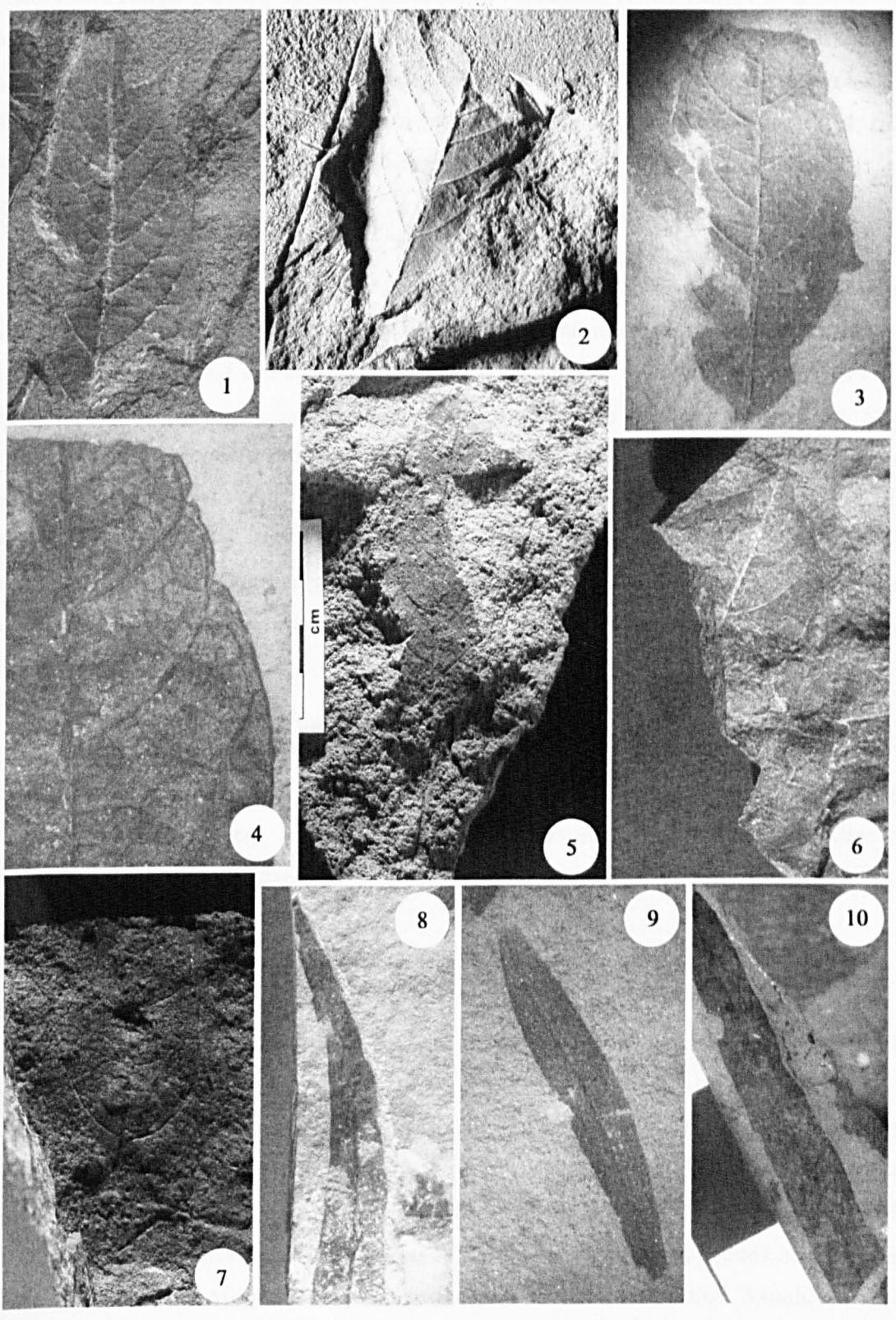

Figure 6.6. (1) - (2) Morphotype 1.15. (1). P.2799.6.1. x1.4. (2). P.2799.2.1. x1.4. (3) - (4) Morphotype 1.16. (3). P.3001.43. x1.6. (4). Detail of venation. x3.2. (5). Morphotype 1.17. G.309.1. (6). Morphotype 1.18. P.2799.14.1. x1.5. (7). Morphotype 1.19. x0.7. (8) - (10) Morphotype 1.20. (8). P.2810.3.1. x1. (9). P.212.11. x2. (10). P.3001.42.2. All scale bars have 1 cm gradations.

uniform or increasing basally, divergence angle decreasing exmedially. Course curves abruptly near the margin, joining superadjacent secondary at an acute angle. Strong intersecondaries. *Tertiary* vein category mixed opposite and alternate percurrent, course convex or sinuous, vein angle to primary perpendicular or obtuse, angle increasing basally. *Fourth order* vein category regular polygonal reticulate. *Fifth order* vein category regular polygonal reticulate. Areoles 4 or more sided. *Sixth order* veins are highest order present. Single F.E.V observed to be 2 or more branched. Highest excurrent fifth order. Marginal ultimate venation consists of a ?looped. Leaf rank 3r.

Remarks: There is no whole leaf preservation of this morphotype, although the two leaf fragments preserved on P.2799.6 are very similar in size and morphology and it is tempting to suggest that they are base and apex of the same leaf (Figure 6.5: 9). The conservative nature of this leaf morphology means that it is comparable to a number of fossil species from South America, such as *Nectandra* spp. (Orlando, 1964; Berry, 1938), *Cassia* L. spp. (Leguminosae), *Embothrium* Forster and Forster f., spp., and *Hoffmannia protagaea* Engel., (Proteaceae) (Berry, 1938), *Remijia* DC spp., and *Cephalanthus* L. spp. (both in the Rubiaceae). Of these *Cephalanthus glabratifolius* Berry and *Hoffmania protagaea* have a more acute pair of basal secondaries and opposite branching secondaries, suggesting affinities with the fossil Rubiaceae and Proteaceae.

By reference to modern herbarium material and leaf atlases, the entire margined elliptical leaf type with brochidodromous venation is perhaps the most conservative leaf morphology, occurring in many modern southern temperate families including, but not exclusive to, Lauraceae, Sapindaceae, Winteraceae, Myrtaceae and Proteaceae.

Morphotype 1.16 (Figure 6.6: 3 - 4)

Material examined: Dragon Glacier flora *Large fragment* P.3001.43.

Differential characters: Elliptic leaves with secondary vein spacing that increases basally. Thick percurrent tertiary veins.

Description: Leaf organisation appears simple. Lamina ?symmetrical, ?elliptic (margin trend could indicate small lobes but probably a preservational feature). Length min 40 mm est. 80 mm, width min 22 mm, length:width min 1.82:1. Area est. 1540 mm^2. Notophyll = 1 (100%). Apex appears acute convex, apical angle est. 64°. Base not preserved suggested acute convex. Petiole not preserved. Margin entire, course irregular due to preservation. *Venation* pinnate weak brochidodromous. *Primary* thickness stout. *Secondary* min 11 moderate to thick secondaries diverge from midvein at a moderate to wide acute angle 52° - 73°. Angle variable, decreasing basally. Spacing sometimes irregular, generally increasing uniformly towards base. Course rarely irregular, curved apically close to margin. Intersecondaries strong often composite

from tertiaries. *Tertiary* vein category mixed opposite and alternate percurrent, angle increasing exmedially. Fourth order vein category ?reticulated. Higher order venation not clearly preserved. Marginal ultimate venation appears looped. Leaf rank 2r.

Remarks: Morphotype 1.16 is differentiated from morphotype 1.15 by the increase in secondary spacing towards the leaf base. This characteristic is also present in the elliptic, brochidodromous leaves of *Anona infestans* and *Rubiacites chameliifolia* Berry (Rubiaceae) (Berry, 1938) but these leaves lack the strong tertiary venation of morphotype 1.16. More complete specimens are required for further comparisons.

Morphotype 1.17 (Figure 6.6: 5)

Material examined: Platt Cliffs (Cytadela) *Large fragment* G.309.1, .17, .10.

Differential characters: Elliptic leaves with irregular secondaries that are closely spaced in the basal portion of the lamina. Strong intersecondaries. Long thick petiole.

Description: Leaf organisation appears simple. Lamina ?symmetrical, elliptic. Length min 69 mm est. 74 mm, width min 26 mm est. 34 mm, length:width est. 2.85:1. Area est. 1677.33 mm^2. Notophyll = 3 (100 %). Apex not preserved, appears convex, apical angle est. 68°. Base acute convex, basal angle est. 75°. Petiole marginal, length 31 mm width 1.8 mm, base slightly swollen (G.309.1). Margin entire. *Venation* pinnate weak brochidodromous. Primary thickness stout. *Secondary* min 8 secondaries diverging at an acute angle 50° - 63°. Spacing regular to irregular, vein angle variable. Occasional strong intersecondaries. *Tertiary* vein category not preserved.

Remarks: The thick petiole, large lamina size and weakly developed (almost eucamptodromous) brochidodromous venation of this morphotype suggests affinities with the Magnoliidae (Hickey and Wolfe). Such a thick petiole is not typical of the Lauraceae.

Morphotype 1.18 (Figure 6.6: 6)

Material examined: Vaureal Peak *Small fragment* P2799.14.1.

Differential characters: Elliptic leaf with fine secondaries and an acuminate apex.

Description: Leaf organisation appears simple. Lamina ?wide elliptic, ?symmetrical. Lamina length min 45 mm, width est. 30 mm, length:width ratio min 1.18:1. Area 900 mm^2. Notophyll = 1 (100 %). Apex acute, acuminate, apical angle ~ 80°. Base not preserved. Petiole not preserved. Margin entire. *Venation* pinnate weak brochidodromous. *Primary* thickness weak. *Secondary* min 7 fine secondaries, diverging at a wide acute angle 60° - 73°, course is curved abruptly, joining superadjacent secondaries at an acute angle, some loops show ramification with tertiary loops. One intersecondary present. *Tertiary* vein category alternate

percurrent, course sinuous, obtuse angle to primary vein. Higher order venation not preserved. Leaf rank 2r/3r.

Remarks: The leaf is considered to be entire margined, however the possibility of toothing in the absent basal region of the lamina cannot be excluded. The poor preservation of the specimen does not allow detailed morphological comparisons. An apical fragment of a leaf also with an acuminate apex, fine secondaries and weak brochidodromous venation was described by (Figure 3d, p78; Greenwood *et al.* 2000) from the Neogene Yallourn Clays, Australia, but no taxonomic affinities were suggested. Fine brochidodromous secondaries and acuminate apices are also found in *Anona infestens*, *Allamanda crassostipitata* Engelhardt and *Ficus patagonica* Berry from the Rio Pichileufu flora of Argentina (Berry, 1938), but increased basal spacing is only present in *A. infestans*, which is also of a similar size. The closest affinities are therefore with *A. infestans* or possibly with the Yallourn Clays specimen.

1.19. *Ficophyllum skuaensis* Dutra and Batten (Figure 6.6: 7)

2000 Dutra and Batten, (p.11, fig 5a)

Material examined: Barton Peninsula *Large fragment* P.2145.3.

Differential characters: Ovate leaf with irregular coursed opposite secondaries.

Description: Leaf organisation appears simple. Lamina ?asymmetrical ?ovate. Length min 75 mm, width min 36 mm, length:width min 2.08:1. Area min 1800 mm^2. Mesophyll = 1 (100 %). Apex not preserved, appears convex, apical angle est. 52°. Base not preserved. Petiole probably marginal. Margin entire, with irregular course. *Venation* pinnate weak brochidodromous. *Primary* thickness stout. *Secondary* min 6 moderate secondaries diverging at a moderate to wide acute angle 50° – 68°. Vein spacing irregular, variability of divergence angle uncertain due to size of fragment. Strong intersecondaries. *Tertiary* vein category opposite percurrent, course convex or sinuous, angle to primary ?increasing basally. Higher order venation not preserved. Leaf rank 1r/2r. *Other features* spherical traces present on mid portion of lamina.

Remarks: The poor organisation of the secondary venation, irregular margin course, strong perpendicular intersecondaries, and strongly curved secondaries are characteristic of *Ficophyllum skuaensis* from the Upper Cretaceous Half Three Point Formation, Skua Bay, Fildes Peninsula (Dutra and Batten, 2000).

Morphotype 1.20 (Figure 6.6: 8 - 10)

Material examined: Rocky Cove *Complete* ?P.212.11. Dragon Glacier *Large fragment* P.2810.3.1, P.3001.28. *Small fragment* P.3001.166.

Differential characters: Stenophyll leaves with a strong primary and very fine secondaries which form a weak intramarginal vein.

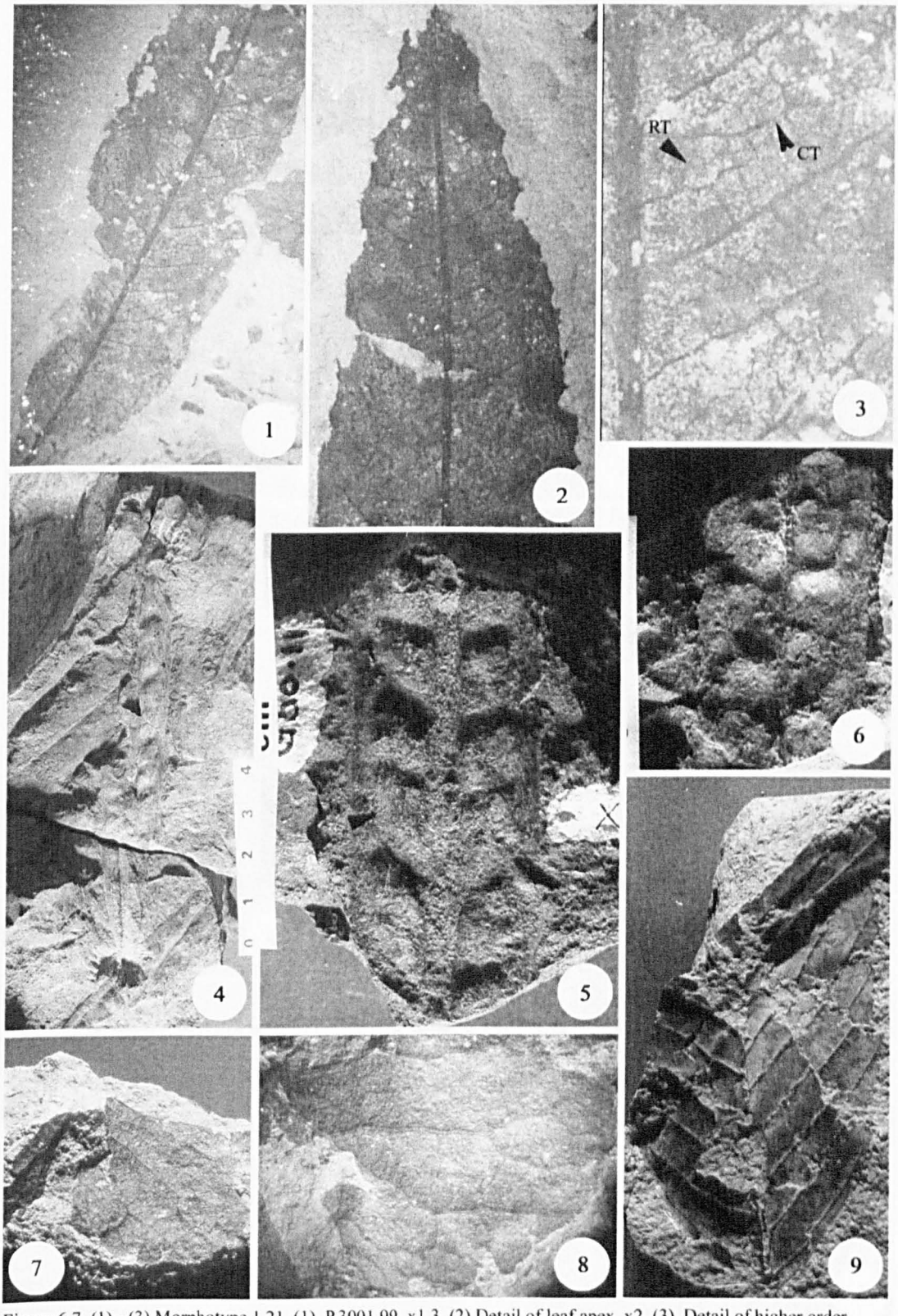

Figure 6.7. (1) - (3) Morphotype 1.21. (1). P.3001.99. x1.3. (2) Detail of leaf apex. x2. (3). Detail of higher order venation showing composite intersecondary venation and reticulate tertiary venation. x3.4. (4) - (6) Morphotype 1.22. (4). G.50.21, note inflated intercostal areas (1 cm graduated scale). (5) Detail of lamina, G.50.11. x1.4. (6). Detail of lamina with small areas of lamina inflated exmedial to the main intercostal areas, G.50.8. x1.4. (7) - (8) Morphotype 1.23. (7). P3001.111. x0.8. (8). Detail of venation, note thickness of secondaries. x1.2. (9). Morphotype 1.24. P.3007.1. x0.7.

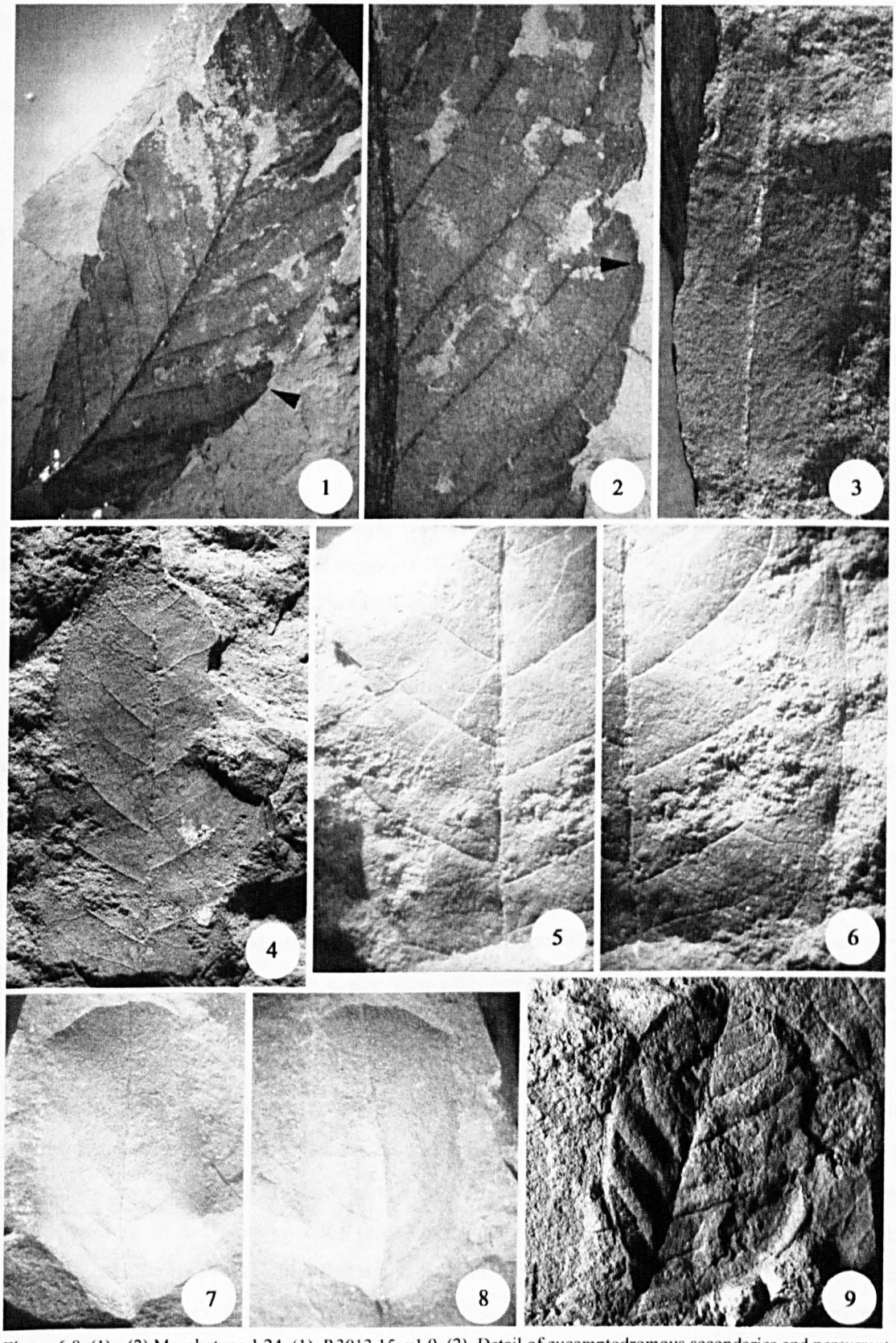

Figure 6.8. (1) - (2) Morphotype 1.24. (1). P.3013.15. x1.9. (2). Detail of eucamptodromous secondaries and percurrent tertiary venation (PT). Note the margin has a tooth like appearance due to tearing of the lamina along the secondary venation (arrowed). (3) - (6) Morphotype 1.25. (3). P.232. (4). P.232.12a. x0.9. (5). P.232.12b. x1.8. (6). P.232.12b. x1.8. (7) - (8) Morphotype 1.26. Part and counterpart of P.2145.8. x1.6. (9). Morphotype 1.27. P.2799.1.2. x1.3. Note lamina is enrolled (arrowed) and is more undulose on left side of lamina.

Description: Lamina organisation appears simple. Lamina ovate or oblong, symmetrical. Based on P.2810.3, lamina length min 67 mm, width min 12 mm, length:width ratio min 5.58:1. Area min 40 - 536 mm^2. Microphyll = 4 (100 %). Apex acute, ?straight, apical angle estimated 15°. Base ?acute convex, basal angle 8° (P.3001.166). Margin entire and slightly revolute. *Venation* pinnate ?weak brochidodromous. *Primary* thickness moderate. Course curved. *Secondary* 22 fine secondaries diverging at an acute angle 40 - 84° (P.2810.3.1). Secondaries ?converge at margin to form an intramarginal vein. *Other features* marginal damage with reaction tissue (P.2810.3.1).

Remarks: Stenophyllous leaves with intramarginal veins are common in the Myrtaceae. Although the secondary venation is generally extremely well organised and regular in that genera, while morphotype 1.20 is rather irregular secondaries. The poor preservation of the secondaries prevents close comparison of the morphotype with particular myrtaceous genera.

Morphotype 1.21 (Figure 6.7: 1 - 3)

Material examined: Dragon Glacier *Large fragment* P.3001.99.

Differential characters: Stenophyll leaf with moderate secondaries and strong intersecondaries, moderate to wide acute angle of secondary vein divergence.

Description: Leaf organisation appears simple. Lamina elliptic, symmetrical. Lamina length min 89 mm, width min 17 mm, length:width ratio 5.24:1. Estimated leaf area 1008.67 mm^2. Microphyll = 1 (100 %). Apex acute, ?convex, apical angle est. 35°. Base, ?convex, basal angle est. 42°. Margin entire. *Venation* pinnate weak brochidodromous. *Primary* thickness stout. Course straight. *Secondary* min 26 moderate secondaries diverging at moderate to wide acute angle 52° - 73°. Courses are curved. Angle uniform, spacing uniform. Strong intersecondaries. *Tertiary* vein category random to regular polygonal reticulate. *Fourth order* vein category regular polygonal reticulate. *Fifth order* vein category dichotomising and is the highest vein order present. Areolation 4 – 5 sided. F.E.V.s unbranched to 1 branched.

Remarks: Weak brochidodromous venation, strong intersecondaries, moderate to wide acute angle of secondary divergence and an elliptic lamina are characteristic of modern leaves of *Eucryphia moorei* F. Muell., from Australia (e.g. Dickison, 1978; Hill, 1991a). These features are also present in the Apocynaceae (e.g. *Cerbera manghas* B. Gray) but the tertiary veins ramify towards the midvein (Christophel and Hyland, 1995). Cuticular characters are required to identify leaves of *Eucryphia* (Hill, 1991a), however *Eucryphia* is commonly associated with *Nothofagus* in modern and ancient forests (Hill, 1991a), and eucryphiaceous wood has been identified from contemporaneous deposits on King George Island (Poole *et al.*, 2001), so by deduction foliar remains of *Eucryphia* could be present in the macrofossil record.

Morphotype 1.22 (Figure 6.7: 4 - 6)

Material examined: Platt Cliffs *Near complete* G.50.21, .22. *Large fragment* G(38). *Small fragments* G.50.8, .11, .17.

Differential characters: Stenophyll oblong leaf with thick secondaries and prominently convex intercostal areas. Apex emarginate.

Description: Leaf organisation appears simple. Lamina symmetrical, oblong. Based on G.50.21/G.50.22, length < 120 mm, width min 15 - 21 mm. Length:width ratio 9.3:1. Area 396.66 – 1065.33 mm^2. Min microphyll = 3 (50 %). Notophyll = 2 (33 %). Apex retuse (emarginate), apical angle 132°. Base cuneate, basal angle 18°. Margin appears entire. Marginal petiole, length min 6 mm, width 1.1 mm (G.50(38)). *Venation* Primary vein category pinnate, ?1 primary vein and 2 secondaries arising close to leaf base. Primary vein thickness massive. *Secondary* vein category eucamptodromous or weak brochidodromous, min 9 – 11 secondaries diverging at a moderate acute to obtuse angle 50° - 92°. Vein spacing uniform. Vein angle uniform. Weak intersecondaries. Intercostal areas are inflated. *Tertiary* vein category opposite percurrent rarely mixed opposite and alternate percurrent. Vein course convex or sinuous, angle to primary obtuse, increasing basally. Higher order venation is uncertain.

Remarks: Elongate entire margin leaves with weak brochidodromous venation are common to many families (Hickey and Wolfe, 1975). However, the Myrtaceae (pinnate Dilleniidae) is the only family in which I have observed inflation of the intercostal area e.g. *Lophomyrtus* sp.

Several features of this morphotype are more typical of leguminous pods, than angiosperm leaves - an extremely wide primary vein, bilateral symmetry (G.50.17) and inflated intercostal areas. However several specimens are distinctly asymmetrical (G(38) and G.50.21/22) and there is no evidence for large fruiting bodies, a calyx, or placental remains, therefore this plant organ is identified as a leaf. The presence of an emarginate apex is unusual since it has not been reported from other macrofossil localities on King George Island. Alternatively the folding of the lamina might be a result of plant – arthropod interactions e.g. a form of leaf galling or a taphonomic effect, for example, desiccation of the lamina prior to preservation.

$1b^3$. Festooned brochidodromous venation

Morphotype 1.23 (Figure 6.7: 7 - 8)

Material examined: Dragon Glacier *Small fragment* P. 3001.111.

Differential characters: This morphotype is defined by the festooned brochidodromous venation, thick secondary veins and strong relief compared to the thin lamina.

Description: Lamina fragmented, symmetry not preserved, shape ?ovate or peltate. Fragment length min 32 mm, width min 50 mm. Area est. 1066.67 mm^2. Mesophyll = 1 (100

%). Base ?cordate or lobate. Apex not preserved. The leaf margin is poorly preserved and apparently entire except for a single rounded and enrolled sinus, although parts of the margin are potentially crenulated. *Venation* Primary vein category not preserved ?pinnate. *Secondary* vein category ?festooned brochidodromous, loops are angular and formed from bifurcating secondary veins. Min 3 secondary veins with a separation angle of approximately 45°. Secondaries dichotomise towards the margin. *Intercostal areas* quite deeply impressed. *Tertiary* vein category ?regular polygonal reticulate. Higher order venation unclear. Marginal ultimate venation looped, possibly as a fimbrial vein. Leaf rank 1r.

Remarks: The angular style of the secondary vein curvature is similar to the *Nymphaeaphyll* morphotype described by Crabtree (1987) and in this sense also resembles *Paranymphaea proteaefolia* Berry from the upper Cretaceous of Patagonia (Berry, 1937).

Entire margined leaves with festooned brochidodromous venation are present in some orders of the Magnoliidae subclass e.g. the Magnoliales (Hickey and Wolfe, 1975). *Hausmannia papilio* (Cantrill, 1995), described from the Cretaceous of Alexander Island has both entire or crenate margined states and the crenations could relate to the 'notches' described in this morphotype. However *Hausmannia papilio* tends to have square areolation whilst this morphotype has hexagonal areolation (D. Cantrill, pers. com., 2001), supporting an angiosperm rather than a fern classification.

1b[4]. Venation eucamptodromous

Morphotype 1.24 (Figures 6.7: 9 and 6.8: 1 - 2)

Material examined: Dragon Glacier *Large fragments* P.3007.1, P. 3013.15.

Differential characters: Elliptic leaf with strongly percurrent tertiaries and eucamptodromous secondaries.

Description: Leaf organisation appears simple. Lamina symmetrical to slightly asymmetrical, elliptic. Length min 58 – 115 mm, width min 22 - 76 mm, length:width ratio min 1.51:1 - est. 2.64:1. Area est. min 851 - 5826 mm^2. Microphyll = 1 (50 %). Mesophyll = 1 (50 %). Base ?asymmetrical, convex, basal angle 45° - 86°. Apex not preserved appears convex, estimated apical angle 53° (P.3013.15). Margin entire. Intercostal areas curved concavely, possibly as a result of vernation. *Venation* pinnate weak brochidodromous. *Primary* vein thickness moderate to stout. Course straight or slightly curved. *Secondary* min 14 – 22, moderate to thick, alternate secondaries, diverge at narrow to wide acute angle 29° - 65°. Angle uniform or increasing basally. Spacing regular to irregular, narrow intercostal area between basal secondaries and leaf margin. Intersecondaries absent. *Tertiary* vein category opposite percurrent rarely mixed opposite and alternate percurrent. Vein course convex or sinuous, angle

to primary obtuse, increasing basally. Tertiary veins particularly well defined. Higher order vein category uncertain. Leaf rank 3r/4r.

Remarks: Morphotype 1.24 is considered to be an entire margined leaf, however the poorly preserved leaf margins are also suggestive of toothing in the two specimens assigned to this morphotype. The tooth-like projections comprise intersections of the secondary veins with the damaged margin. Although the possibility of semi-craspedodromous venation cannot be ruled out, until further specimens are discovered this leaf morphotype is considered to be entire margined.

The combination of entire margin, uniform secondary venation angle, eucamptodromous secondary venation and percurrent tertiary veins is found in parts of the Magnoliidae subclass e.g. in the Magnoliales and Illiciales (Illiciaceae) (Hickey and Wolfe, 1975). If the leaf was determined to have toothed margins it could be grouped within the subclass Hamamelididae in the Eucommiales, Fagales, Betulales and Leitnerales or within the Cunoniaceae. *Geissois* Labill., (Cunoniaceae) has a similar gross morphology, strong percurrent tertiary venation and also attains a large adult size (D. Greenwood pers. comm, 2001). The slight plicate vernation of specimen P.3013.15 and the strongly percurrent tertiaries might suggest an affinity with deciduous species of the Nothofagaceae.

1.25. *Symplocos commutatifolia* Berry 1938 (Figure 6.8: 3 - 6)

1938 Berry (p. 124, plate 48, figs 3, 4)

Material examined: Potter Cove impression flora *Large fragments* P.232.12a/b.

Differential characters: Elliptic leaf with secondary vein angle increasing basally. Strong intersecondaries. Tertiary veins strongly percurrent. Secondaries sometimes dichotomising.

Description: Leaf organisation appears simple. Lamina elliptic, ?symmetrical. Lamina length min 82 mm, est. 110 mm, width 46mm, length:width ratio 2.39:1. Area 3373.33 mm^2. Notophyll = 1 (100%). Apex not preserved ?acute convex, angle est. 50°. Base not preserved ?acute convex, angle est. 60°. Margin entire. Petiole not preserved. *Venation* pinnate weak brochidodromous. *Primary* thickness moderate. *Secondary* min 10 moderate secondaries diverge at a moderate acute angle 51° - 70°. Vein angle increasing abruptly towards base, spacing variable. Secondaries occasionally branch apically and basally towards the margin. Secondaries join superadjacent secondaries at an acute to wide obtuse angle (near eucamptodromous). *Tertiary* vein category opposite percurrent, rarely mixed opposite and alternate percurrent, course convex to sinuous, vein angle to primary obtuse decreasing exmedially. *Quaternary* veins poorly preserved, possibly forming incomplete marginal loops.

Remarks: The large size and eucamptodromous venation, slightly irregular secondary course, abrupt increase in secondary vein divergence angle at the leaf base and irregular abaxial branches are features of *Symplocos commutatifolia* (Symplocaceae) from the Rio Pichileufu flora (Berry, 1938). The lamina size of 105 mm, and the number of secondary vein pairs (eight to nine) are also consistent with this identification. Pole (1993) described a similar eucamptodromous leaf morphotype with affinities to *Sloanea* L. sp. cf. *S. magnifolia* (Manu-18, p. 126 – 127; Pole, 1993), eucamptodromous venation branching at a similar wide acute angle to morphotype 1.25, but the leaf differs in having common strong intersecondaries, a distinctly thicker primary and a lack of abaxial branching. The secondaries are also more organised in Manu-18. The leaf is therefore assigned to *S. commutatifolia*. Berry (1938) based his identification on the modern species *S. commutata* Brand from Brazil. Specimens and illustrations of modern *Symplocos* were not available for comparison, therefore although the morphotype is confidently placed into the species *Symplocos commutatifolia* erected by Berry (1938) the assignment to the modern taxon is equivocal.

Morphotype 1.26 (Figure 6.8: 7 - 8)

Material examined: Barton Peninsula *Large fragment* P.2145.8.

Differential characters: Elliptic leaf. Secondaries are irregularly spaced with a variable course.

Description: Leaf organisation appears simple. Lamina elliptic or possibly ovate, ?asymmetrical. Length min 32 mm, width min 18 mm, length:width ratio min 1.78:1. Microphyll = 1 (100 %). Apex not preserved. Base not preserved. Margin appears entire, although poorly preserved. *Venation* pinnate weak brochidodromous. *Primary* thickness stout. *Secondary* min 13 moderate secondaries diverge at a narrow to moderate acute angle 40° - 62°. Angle ?decreasing apically, although variable, spacing variable. Course variable. Secondaries curve to meet superadjacent secondaries at an acute angle. Intersecondaries present. Tertiary veins rarely preserved, opposite percurrent with convex course, obtuse angle to primary ?increasing exmedially. Higher order and marginal ultimate venation not preserved. Leaf rank 1r/2r.

Remarks: Disorganised secondary venation is a defining characteristic of this morphotype and is a feature of leaves of the first rank (Hickey, 1977), typically in the Magnoliales. Similarly disorganised venation is also present in the Australian Clusiaceae (*Garcinia mestonii* B. Hyland) (Christophel and Hyland, 1993), but these leaves form a weak intramarginal vein and join the superadjacent secondaries at a wide obtuse angle.

Morphotype 1.27 (Figure 6.8: 9)

Material examined: Vaureal Peak *Large fragment* P2799.1.2a.

Differential characters: Elliptic to lanceolate leaf with an enrolled margin frequent intersecondary veins and an undulose lamina. Secondary vein course highly variable.

Description: Leaf organisation appears simple. Lamina symmetrical, wide elliptic. Length min 40 mm, width min 24 mm, length:width ratio 1.66:1. Area min 640 mm^2. Microphyll = 1 (100 %). Apex not preserved, ?convex. Base asymmetrical, acute convex, basal angle 71°. Petiole thickened relative to primary vein. Margin ?entire, although not well preserved. Margins enrolled, lamina undulose. Mineralised leaf has a coriaceous texture. *Venation* pinnate weak eucamptodromous. *Primary* thickness weak. *Secondaries* min 17 moderate secondaries, diverging at moderate acute angle 45° - 60°. Secondaries thin rapidly towards margin and are sometimes branched, spacing irregular, vein angle approximately uniform but lower on sinistral portion of lamina. Weak intersecondaries. *Tertiary* vein category weakly percurrent, angle to primary ?obtuse.

Remarks: Morphotype 1.27 is unusual in having an enrolled margin, an undulose lamina, a feature only seen elsewhere in morphotype 1.22, and irregular vein spacing and branching. The irregular nature of the undulation suggests that it is does not result from plicate vernation, which is usually regular. Inflated intercostal areas are present in the Myrtaceae family (e.g. *Lophomyrtus*), however this leaf lacks (or has not preserved) the intramarginal vein that normally characterises the Myrtaceae. The affinities of the leaf are uncertain.

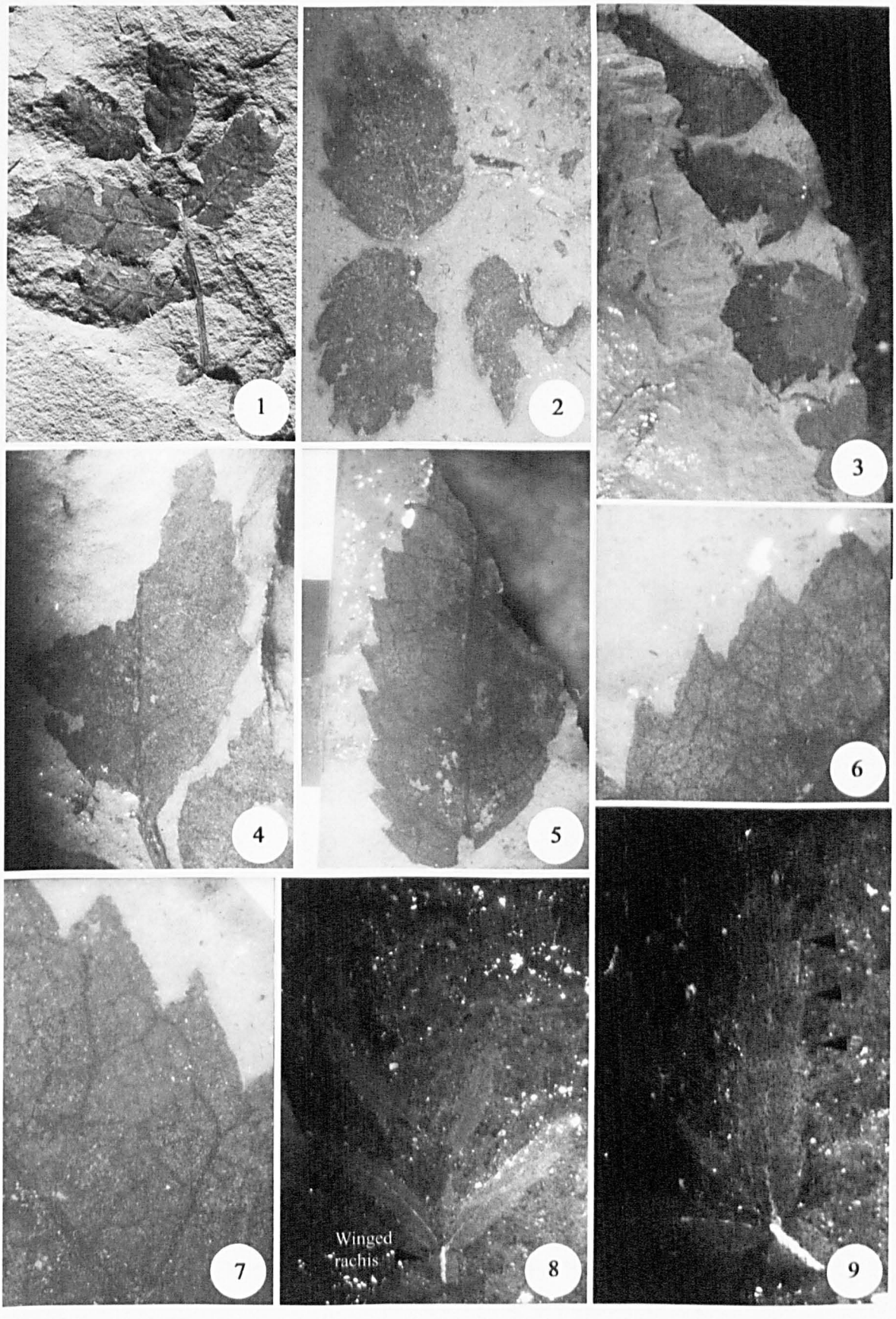

Figure 6.9. (1) - (7) Morphotype 2.1. (1). P.3001.46. x1.2. (2). P.3001.158. x4. (3). P.3001.168. x1.8. (4). P.3001.116. x2.5. (5). P.3001.202a. x3.5. (6). Detail of tooth architecture, showing branching of the secondary close to the sinus with one vein trending apically and the other to the apex. x7. (7) Detail of tooth architecture and venation. P.3001.202b. x9.5. (8) - (9) Morphotype 2.2. (8). Fragment of pinnately compound leaf. P.3034.41. x2. (9). Individual leaflet, showing toothed margin (arrowed). x3.7.

2. Toothed margined morphotypes

2a[1]. Leaf organisation pinnately compound

Order Rosales

2.1. Family Cunoniaceae (Figure 6.9: 1 - 7)

Material examined: Dragon Glacier *Near complete* P.2810.5.1, .5.3, .7, .17.3, .18, .22.1, .28.1; P.3001.1.1-.2, .2.1-.3, .22, .28, .29.1/.2/.3, .30, .45, .46.1/.2/.3/.4/.5/.6, .47a/b, .55, .58.3, .60.1/.2/.3, .65, .81, .110.1/.2/.3/.4/.5, .116.1/.2/.3, .118, .120, .126, .134, .153, .158.1/.2/.3, .168.1/.2/.3/.4, .166, .172, .178, .202, .210, .231.

Differential characters: Imparipinnate compound leaves. Leaflets with a convex, often asymmetric, base and an elongate apex. Venation semicraspedodromous. Tooth type cunonioid.

Description: Leaf attachment opposite. Leaf organisation odd pinnate, at least once pinnate with at least eight leaflets. Lamina generally ovate but also elliptic or oblong. Length min. 8 - 42 mm, width min. 5.5 - 22 mm. Terminal leaflet larger than laterals (P.3001.116). Length:width ratio min1.09:1 - 3.3:1. Area min 36 - 574 mm^2. Nanophyll = 30 (51 %), microphyll = 49 (45.5 %). Apex acute straight to ?convex, apical angle 35° - 46°. Base generally asymmetric rarely symmetrical, convex, rarely cordate, basal angle 63° - 111°. Margin serrate. Petiole if present is normal and short, max length 1 mm, max width 0.8 mm. Rachis ribbed (P.3001.46, P.3001.110, P.3001.116) min length 18 - 61 mm, min width 0.5 - 2 mm. *Venation* pinnate semicraspedodromous. *Primary* thickness weak to massive. Course straight or curved apically. *Secondary* min 5 - 22 secondary opposite to alternate veins, diverging from midvein at a moderate to wide acute angle 40°- 84°. Divergence angle increases abruptly towards base, spacing irregular to regular. Basal secondaries rarely bifurcated. Intersecondaries strongly developed, sometimes difficult to differentiate from secondaries. *Tertiary* vein category alternate percurrent. *Fourth order* vein category regular polygonal reticulate. *Fifth order* vein category dichotomising. Areoles weakly to moderately well developed, 5 or more sided. F.E.V's absent to two or more branching. Marginal ultimate venation possibly looped. *Teeth* 1 order, 2 - 4 teeth/cm, regular spacing. Apex acute angular, shape CC/CV, CV/CV, or base FL, rarely RT/CV. Sinus acute angular and glandular. The deflected principal vein course central or slightly apical, with one branch entering tooth and one branch running across the sinus base to connect with apical secondary defines a cunonioid tooth. Accessory veins looped.

Remarks: The individual leaflets of Morphotype 2.1 are grouped with isolated leaves (leaflets) referred to *Cupania* L., by Dutra (1997a) and Zastawniak (1981), based on the distinctive concavo-convex tooth shape, high length to width ratio and semicraspedodromous venation.

Imparipinnate leaves, with leaflets that have pinnate semicraspedodromous venation and cunonioid teeth are present in the Rosidae, Asteridae and rosid leafed Asterids, (Hickey and Wolfe, 1975). Imparipinnate leaves are particularly common in the Sapindaceae (D. Greenwood, pers. comm., 2001), a family that is strongly represented in modern South America but the ribbed rachis and an elongate terminal leaflet is characteristic of the Cunoniaceae (R. Barnes pers. comm., 2001), in particular *Weinmannia* and *Cunonia* (Carpenter and Buchanan, 1993). The presence of multicellular trichome bases distinguishes *Weinmannia/Cunonia* but without cuticular data the assignment of a leaf macrofossil to *Weinmannia/Cunonia* is particularly difficult and may not be possible without reproductive structures (Barnes *et al.*, in press). On this basis the material is considered to be cunoniaceous, with strong affinities to *Weinmannia/Cunonia*. This identification is also supported by the presence of two species of *Weinmannioxylon* Petriella in the Upper Cretaceous sequences of Livingston and James Ross Islands (Poole *et al.*, 2000a).

2.2. Family Cunoniaceae (Figure 6.9: 8 - 9)

Material examined: Fossil Hill U2 *?Large fragment* P.3034.41.1-.4.

Differential characters: Pinnately compound leaf with a winged rachis. Leaflets arranged in opposite pairs diverging at ~ 45°. Leaflets are stenophyllous and serrate margined.

Description: Lamina pinnately compound, terminal arrangement not preserved. Four leaflets are preserved in two opposite pairs. Rachis sheathed, sheathed thickness 3 mm, unsheathed thickness 1 mm. Minimum length of fragment measured along rachis 24 mm. Single leaflet lamina symmetrical, base asymmetrical. Length min 16 mm, width min 3 mm, length:width ratio 5.33:1. Nanophyll = 4 (100 %). Apex not preserved, apical angle est. acute 30°. Base convex, basal angle 32°. Margin serrate. *Venation* pinnate ?craspedodromous. *Primary* thickness moderate. *Secondary* min 3 fine to moderate secondaries diverge at an moderate to wide acute angle 51° - 71°. Course appears regular, spacing not observed. Higher order venation not preserved. Leaf rank uncertain. *Teeth* 1 order of teeth, min 2 teeth/cm, 1 tooth/cm. Spacing decreases apically. Shape FL/CC – RT/CC. Sinus and apex angular. Teeth appear non glandular but may be due to poor preservation.

Remarks: Pinnately compound leaves with a winged rachis between successive leaflets diagnose *Weinmannia* and *Cunonia* in the Cunoniaceae (Barnes *et al.*, in press and cf. comments on Morphotype 2.1) but cuticular data is required to separate the two genera. The Cunoniaceae family have cunonioid teeth however the preservation of P.3034.41 is too poor to determine the specific tooth type (Hickey and Wolfe, 1975). The material is distinguished from morphotype 2.1 by the thick winging of the rachis.

Inorganic leaf macrofossils from the Oligocene Cethana deposits (Tasmania), with architectural similarities to extant *Weinmannia* and *Cunonia* were placed in the form species *Weinmanniaphyllum bernardii* (Carpenter and Buchanan, 1993) because the morphological overlap between the fossil forms could not be resolved in the absence of cuticular data. Barnes *et al.* (in press) argued that *W. bernardii* probably incorporates two or three separate taxa based on leaf architecture. One form with long thin leaflets that leave the rachis at a narrow angle may be consistent with morphotype 2.4 herein but the angle of branching is less than 30° according to Barnes *et al.* (in press) rather than 40° - 50° observed in morphotype 2.4.

2a^2. Palmately compound leaves

Family Cunoniaceae

Tribe Schizomerieae

2.3. *Fildesia pulchra* Rohn, Rosler and Czajkowski (Figure 6.10: 1 - 4)

1987 *Fildesia pulchra* Rohn, Rosler and Czajkowski (p.13, figs 4, 5)

1988 *Dicotylophyllum* sp. 1 Li and Song (p.401, fig 5, plate I, figs 1, 1a)

1989 Dicotyledonous leaf Birkenmajer and Zastawniak (p. 76, plate II, figs 3 - 4)

1990 *Banksia antarctica* Torres (plate 16, figs 5, 7)

1994 *Dicotylophyllum* sp. 2 Li (p. 157, fig 9, plate 8, fig 2, plate 9, figs 2, 2a, 2b, 3

Material examined: Fossil Hill U2 *Small fragment* P.935.10, Fossil Hill U4 P.3031.43.1, .53, .82, .64, .51, .36.

Differential characters: Trifoliate leaves with stenophyllous leaflets, teeth glandular and spinose. Secondary venation disorganised, tertiaries are a similar thickness to the secondaries.

Description: Leaf organisation palmate trifoliate. Lamina ?symmetrical, base symmetrical. Lamina length 69 mm, width 11 mm, length:width ratio 6.27:1. Leaflets microphyll = 4(100%). Apex ?straight, apical angle acute 18°. Base straight possibly decurrent, basal angle acute 32°. Margin crenate. Leaflets are sessile. No petiole preserved. *Venation* pinnate semicraspedodromous. *Primary* thickness massive, raised . Course straight. *Secondary* min 17 thick secondaries diverge at a moderate acute to right angle 58° - 90°. Course irregular. Vein angle and spacing very variable. Secondary veins are difficult to distinguish from intersecondaries and from tertiaries. *Tertiary* random reticulate. *Fourth order* dichotomising. *Areolation* poor to moderately developed, areoles 5 or more sided. *F.E.V's* unbranched to two or more branched. Marginal ultimate venation fimbrial vein. Leaf rank 1r. *Teeth* 1 order, 5 teeth/cm, ~1 teeth/secondary, spacing ~regular. Teeth are defined by a small curvature of the margin. Indentation to midvein ~0.1 mm. Sinus obtuse, angular to rounded. Teeth are glandular and appear spherulate. Principal vein course generally apical. Origin deflected, formed by a small ?secondary branch or tertiary vein, which trends across the sinus and is difficult to differentiate from the tooth apex.

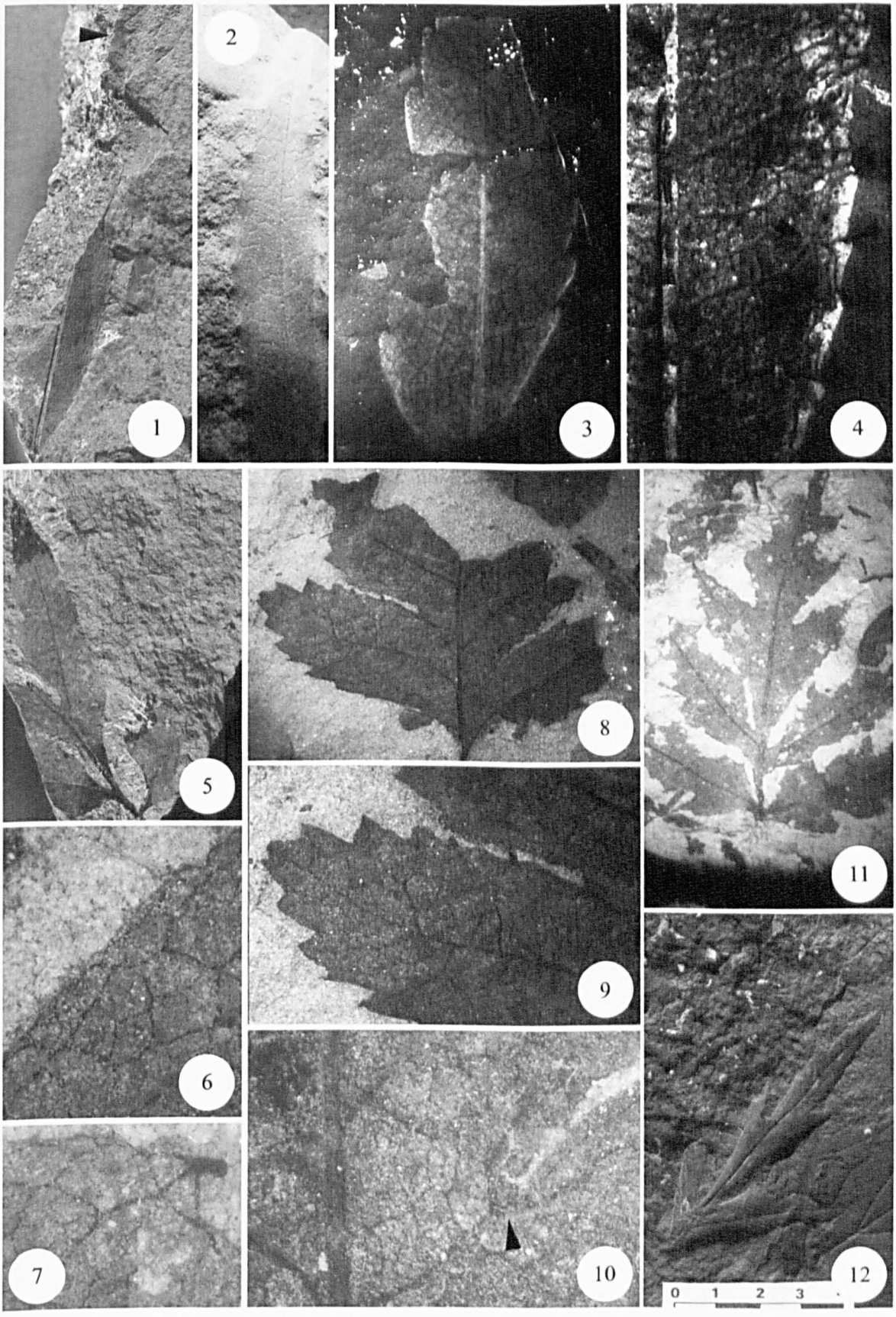

Figure 6.10. (1) - (4) Morphotype 2.3. (1). Elongate leaf, apex arrowed. P.3034.51. x1.1. (2). P.935.10. x1.8. Elongate leaf showing irregular secondary venation. (3). Broad, shorter leaf with ragged asymmetrical base suggesting detachment from a palmate leaf. P.3034.36. x4.2. (4). P.3034.51. Detail of venation and cunonioid teeth, showing branching of secondary sending a vein to the tooth and apically. Note that the thickness of the tertiaries is similar to that of the secondary veins. x4.9. (5) - (12) Morphotype 2.4. *Lomatia* sp. (5). P.3001.59. x0.9. (6). Detail of venation. x8. (7). Detail of tooth apex. x8. (8). P.3001.110. x2.3. (9). Detail of toothed lobe. x4.4. (10). Detail of strong intersecondary vein branching towards sinus. x10. (11). G.9.3. x1.6. (12). P.3034.3a. x0.6.

Remarks: The thick, raised midvein, irregular secondary venation and loosely reticulated tertiaries define this material as isolated leaflets of the palmate to trifoliate leaf *Fildesia pulchra* (Rohn *et al.*, 1987). Rohn *et al.* (1987) compared *Fildesia pulchra* to *Myrica* L. (Myricaceae). Although palmately trifoliate, toothed leaves with pinnate venation are sometimes present in the Hamamelididae they are not characteristic of the Myricales and as such are inconsistent with this interpretation (Hickey and Wolfe, 1975). This morphology also argues against the proteaceous affinity suggested by Torres (1990). The raised, pronounced midvein, irregular secondary venation and tooth architecture are more typical of the Cunoniaceae (e.g. Barnes and Rozefelds, 2000).

The variable leaf morphology, irregular secondary vein course, fimbrial vein, poor to moderately developed areolation and spherulate glandular tooth apices are all characteristic features of the Schizomerieae tribe of the Cunoniaceae. The leaves most resemble the modern *Ceratopetalum* Sm., and *Platylophus* D Don (R Barnes, pers. comm., 2001). On this basis the form species *Fildesia pulchra* is considered to be most similar to the Schizomerieae tribe of the Cunoniaceae. Cuticular data is required to refine this assignment.

2a^3. Leaf organisation simple

2b^1. Leaf pinnately lobed

Order Proteales

Family Proteaceae

Subfamily Grevilleoideae

2.4. cf. *Lomatia* R. Brown 1810 (Figure 6.10: 5-9)

Material examined: Dragon Glacier *Small fragments* G.9.3, P.3001.59, .166, .110, ?.117. Fossil Hill U2 P.3034.3.1, .59, .66. Fossil Hill U3 P.3032.19. Fossil Hill U4 *Small fragment* P.3031.21.2.

Differential characters: Strong pinnatisect dissection of the lamina, prominent glandular teeth and well developed reticulation of the higher order venation.

Description: Leaf organisation pinnately lobed. Lamina symmetrical - asymmetrical. Lamina length min 46 - 64 mm. Lamina width min 35 - 43 mm. Estimated leaf area 1319 – 1493 mm^2. Lobe size class notophyll = 2 (66 %). Margin serrate. *Venation* pinnate craspedodromous. *Primary* thickness moderate. Course curved to sinuous. *Secondary* min 5 - 10 subopposite-alternate secondaries diverge at 35°-79° av. 54° angle decreases smoothly toward apex but with an abrupt increase in the upper 4 secondary veins (P. 3001.59). Thickness is moderate. Vein spacing regular – irregular. Strong intersecondaries trend to lobe sinus and branch to combine with tertiary veins. *Tertiary* veins form a series of loops basally and apically along secondary. *Fourth order* veins regular polygonal reticulate. *Fifth order* dichotomising.

Areoles 5 or more sided. F.E.V's appear two or more branched. Marginal ultimate venation looped. Teeth estimated 4 - 9 per lobe. Apex angular, sinus angular to rounded (P.3001.59). Teeth glandular, sinus rounded (P. 3001.59). Tooth type rosoid or chloranthoid. Principal veins are tertiaries except for apical teeth, which are served by secondaries. Accessory veins looped. Lobes incised 16 – 24 mm to midvein leaving only a thin sheath of lamina along midvein, except P.3001.110, which is only incised by ¾ of its width. *Other features* Single elliptical non-marginal trace with reaction tissue (P.3001.59).

Remarks: The strong pinnatisect dissection and toothing of the lamina is a characteristic of the genus *Lomatia* (Proteaceae), which has a broad southern hemisphere distribution in both the modern and fossil records (South America, Australia and Tasmania) (Hill and Carpenter, 1988). Morphotype 2.4 comprises macrofossils from Point Hennequin and from Fossil Hill and may represent several species of the same genus based on the extremely variable foliage character of modern and fossil *Lomatia* (Jordan *et al.*, 1998). *Lomatia antarctica* (Orlando, 1964) and *L. mirabilis* (Li, 1994) have been described from Fildes Peninsula but the genus has not previously been described from Point Hennequin. Berry (1938) erected the species *L. preferruginea* Berry to describe leaves similar to *L. ferruginea* (Cav.) R. Br., from Rio Pichileufu. These fossils differ in having greater incision of the lobes than morphotype 2.4.

Lomatia sp. are defined on the basis of cuticular data and are difficult to identify without this information (R Hill, pers. comm., 2000), however the basic morphology of *Lomatia* leaves varies between species, such as the degree of lamina dissection, thickness of the lamina sheathing the midvein and degree of dissection of individual lobes. In terms of lamina form Morphotype 2.4 is similar to the modern *Lomatia fraseri* (Sm.) R. Br., from Australia, the fossil genus *Euproteaciphyllum* (Jordan *et al.*, 1998) from Eocene – Early Oligocene deposits in Tasmania. Given the difficulty of assigning taxa to *Lomatia* sp., in the absence of cuticle this leaf is best described as cf. *Lomatia* sp.

2b^2. Palmately lobed leaves

Morphotype 2.5 (Figure 6.11: 1)

Material examined: Fossil Hill U3 *Small fragment* P.3032.59.

Differential characters: Trilobed leaf with sinuses indented to the midvein to less than the width of the apical lobe. Margin toothed.

Description: Lamina palmate. Length min 52.5 mm, width min est. 82.6 mm, length:width ratio est. 0.64:1. Area est. 2891 mm^2. Mesophyll = 1 (100 %). Venation actinodromous camptodromous.

Remarks: Based on the shape and style of lobing observed in the fossil material, this leaf is same as the toothed leaf *?Oreopanax guinazui* Berry (Araliaceae) (Li, 1994). It can be differentiated from the palmately lobed morphotype 1.1 by the greater incision of the lobe sinuses, which forms a near right angle rather than an obtuse convex curve and by the presence of marginal serrations.

Morphotype 2.6 (Figure 6.11: 2 - 3)

Material examined: Dragon Glacier *Large fragment* P.3001.4.1.

Differential characters: Leaf with actinodromous venation comprising five basal primaries. Tertiary venation is thick and concentrically oriented with respect to the top of the petiole.

Description: Leaf organisation appears simple. Lamina palmately lobed (wide elliptic), ?symmetrical. Length min 41 mm, width min 37 mm. Length:width ratio min 1.11:1. Area 1011.33 mm^2. Notophyll = 1 (100 %). Apex potentially straight. Base appears to be obtuse, truncate but could be peltate, lobate or cordate. No margin preservation but toothed by comparison with Zastawniak *et al.* (1985). Petiole may be present but cannot be conclusively linked with fossil. *Venation* palinactinodromous camptodromous with 5 primary veins originate from the ?leaf base. *Primary* thickness moderate. Course straight becoming sinuous apically. *Secondary* min ?17 opposite to subopposite veins, diverging from primaries at narrow acute angle 31° - 51°. Divergence angle decreasing apically. Spacing decreases apically. *Tertiary* vein category mixed opposite and alternate. Course convex. Vein angle to primary obtuse, increasing exmedially. *Fourth order* vein category regular polygonal reticulate. *Fifth order* vein category dichotomising and highest order present. Areoles well developed and 4 or more sided. F.E.V's absent to 2 or more branched. Leaf rank 3r.

Remarks: This prominent actinodromous venation and alternate percurrent tertiaries supports a grouping with more complete leaves described as *Cochlospermum* sp. Zastawniak *et al.* (1985). According to Zastawniak *et al.* (1985) these are possible pentalobed leaves with a toothed margin and actinodromous camptodromous venation. The leaves may be differentiated from other palmately lobed leaves, such as *Oreopanax guinazui* and Morphotype 1.1. by the strong percurrent tertiary venation and the greater number of lobes. Zastawniak *et al.* (1985) compared the leaves to *Cochlospermum* sp. *C. previtifolium* Berry based on venation characteristics. However, the leaf size is markedly smaller than the specimens described by Berry (1935, 1938), but leaf size is highly variable and a poor criteria for separating taxa (Dilcher, 1974). Birkenmajer and Zastawniak (1986) described a leaf from the Palaeocene Dufayel Island flora as aff. *Cochlospermum* but the tertiaries are less well defined and it is unlikely to be the same morphotype.

Leaves with palmate venation and venation oriented concentrically with respect to the top of the petiole are present in the palmate Dilleniidae, which is consistent with the interpretation of *Cochlospermum* sp., but could also apply to other taxa e.g. *Ribes* L. (Saxifragales) (Ribusoideae), Elaeocarpaceae, Tiliaceae, Sterculiaceae, Bombacaceae (Hickey and Wolfe, 1975).

Morphotype 2.7 (Figure 6.11: 4)

Material examined: Potter Cove impression flora *?Small fragment* P.232.17.

Differential characters: Leaf at least bilobed. Teeth CC-CC shaped with angular apices. Venation mixed craspedodromous. Apex attenuated.

Description: Lamina organisation appears simple. Lamina palmately lobed, shape and symmetry uncertain ?wide elliptic or ovate. Length min 87 mm, width min 71 mm, length:width min 1.23:1. Fragment area min 4118 mm^2. ?Megaphyll = 1 (100 %). Apex (of lobe fragment) straight, apical angle acute 38°. Base not preserved. Margin serrate. *Venation* ?palinactinodromous semicraspedodromous. *?Primary* (thickest vein) weak. *Secondary* min 11 fine to moderate secondaries diverge at a moderate to wide acute angle 52° - 74°. Angle variable generally decreasing basally, spacing increasing basally. Intersecondaries weak. *Tertiary* vein category alternate percurrent. Higher order venation not preserved. Leaf rank ?2r. *Teeth* 1 order, < 1 tooth/cm, spacing uncertain. Apex angular, sinus rounded. Principal vein central, origin ?direct. No glands observed. Tooth indentation to midvein 6 mm.

Remarks: This leaf is a fragment of a larger lobed leaf and the main vein may not be the primary vein in the leaf. Lobed leaves of this size are not present in the King George Island flora. *Sterculia patagonica* and *Cochlospermum* sp. in the Rio Pichileufu flora (Berry, 1938) are lobed and have a similarly large lamina, but the divergence angle of the secondaries is generally more acute in *S. patagonica* and *C.* sp. generally have smaller teeth that are more apically directed.

Semicraspedodromous venation, lobing and strong toothing is a characteristic of *Gunnera* L. sp. (Gunneraceae) a modern, dominantly southern hemisphere, herbaceous taxon (Brickell, 1998) that is also present in the Tertiary pollen record of King George Island (Torres and Meon, 1990). The incomplete nature of the specimen prevents detailed comparisons but the preservation of even part of a large herbaceous leaf would be unusual, because the leaves are prone to decaying *in-situ* rather than being transported for burial. At this level of preservation the leaf has affinities with *Gunnera*, Sterculiaceae and Cochlospermaceae but the level of preservation prevents a positive identification.

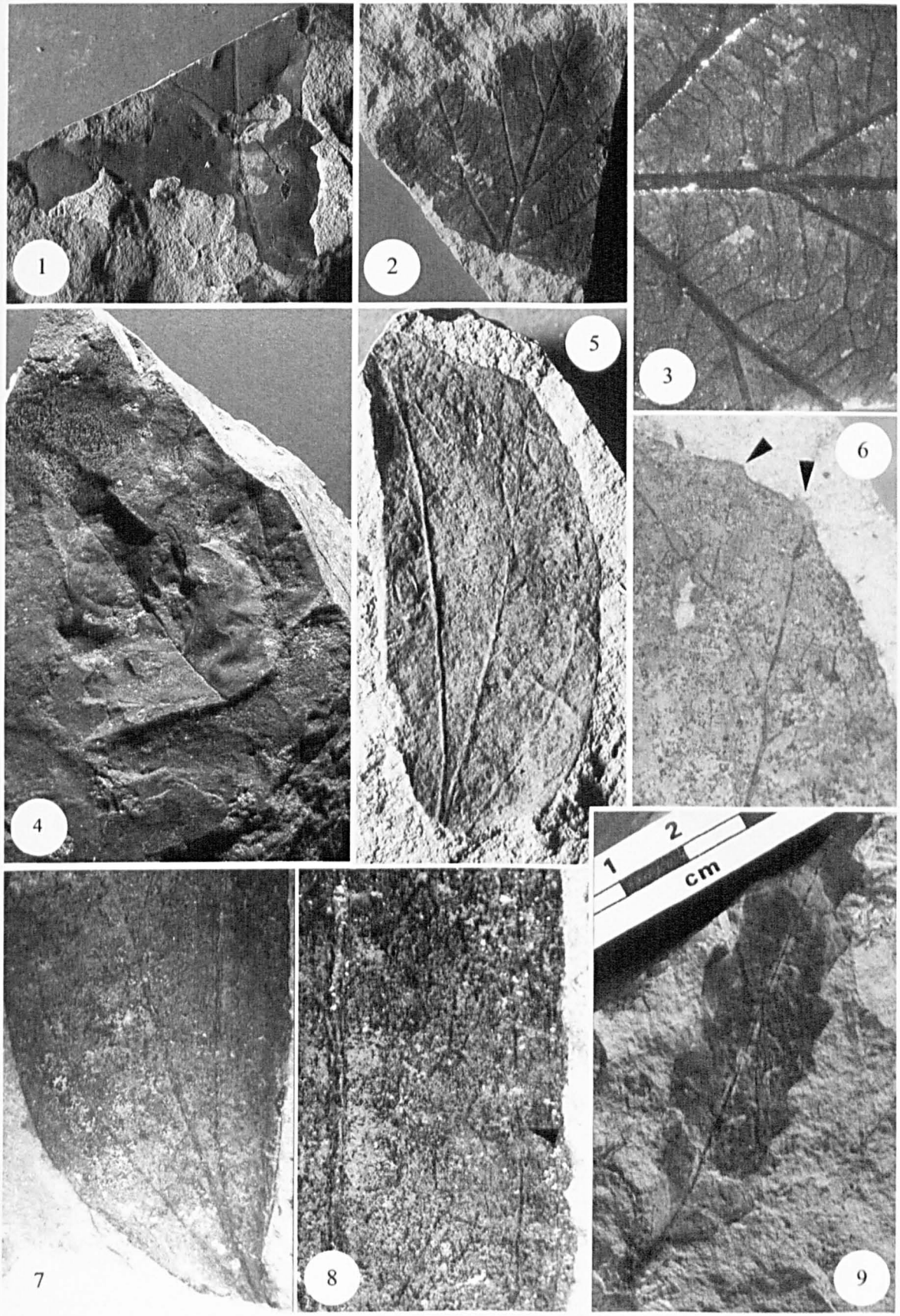

Figure 6.11. (1). Morphotype 2.5. P.3032.59. x1.1. (2) - (3) Morphotype 2.6. (2) P.3001.4. x0.95. (3). Detail of alternate percurrent venation. x2.9. (4). Morphotype 2.7. P.232.17. x1.6. (5 - 8) Morphotype 2.8. (5). P.3001.50.1a. x1.3. (6). Detail of toothed apical margin (arrowed). x3.8. (7). Detail of base. P.3001.50.1b. x3.1. (8). Detail of composite marginal vein and loose reticulation. x7.4. (9). Morphotype 2.9. P.3001.109. Note prominent Scale bar 1 cm graduated.

2b[3]. Leaf non-lobed

2c[1]. Acrodromous venation

Morphotype 2.8 (Figure 6.11: 5-8)

Material examined: Dragon Glacier *Near complete* P.3001.50a/b.

Differential characters: Oblong asymmetrical leaf with 3 suprabasal acrodromous primaries. Small teeth are present on the apical margin of the leaf.

Description: Leaf organisation appears simple. Lamina oblong, asymmetrical with base and apex skewed to one side. Lamina length min 55 mm. Lamina width 23 mm. Length:width ratio 2.39:1. Area est. 843.33 mm^2. Microphyll = 1 (100 %). Apex acute, ?complex, apical angle estimated 60°. Base concave or decurrent, basal angle estimated 45°. Margin crenate. *Venation* suprabasal acrodromous. *Primary* three stout primaries. Course curved, primaries branch at an acute to obtuse angle. *Secondary* converge close to margin to form two composite secondary veins, which follow the leaf margin. *Tertiary* vein category ?regular polygonal reticulate. Leaf rank ?2r. *Teeth* 2 teeth present on apical margin, comprising two smooth crenations. Apices asymmetric and obtuse. Principal vein is a primary branch, course central.

Remarks: No similar leaves are present on King George Island or elsewhere in W. Antarctica. The asymmetric base may suggest a pinnately compound morphology. The combination of a toothed margin, oblong lamina and acrodromous venation is unusual, but is present in the modern Eucalyptus stellulata (Klucking, 1988) (Myrtaceae) and Acacia flavescens Cunn. ex Benth. (Mimosaceae) (Christophel and Hyland, 1993). E. stellulata differs in being entire margined. Acacia flavescens has glandular teeth, which are not apparent in Morphotype 2.8, however the marginal preservation of the fossil material is quite poor and glandular teeth may have been destroyed during preservation.

Leguminous leaves have been reported from King George Island and Seymour Island (Dúsen, 1908; Birkenmajer and Zastawniak, 1986; Troncoso, 1986) but all of these descriptions are based on entire margined leaves with brochidodromous venation and are not comparable to morphotype 2.8.

2d[1]. Leaves with semicraspedodromous venation

Morphotype 2.9 (Figures 6.11: 9 and 6.12: 1-5)

Material examined: Dragon Glacier *Almost complete* P.3001.109. *Large fragments* P.3001.104, .189, .234, .283, P.3013.26. *Small fragments* P.3013.5, .32. Mt. Wawel in-situ *Large fragment* P.3010.11a/b, .12.

Differential characters: Lanceolate stenophyllous leaves. Strongly toothed margin. Tooth type rosoid or spinose. Secondaries semicraspedodromous. Tertiaries strongly reticulated.

Description: Leaf organisation appears simple. Lamina oblong, base asymmetrical (P3001.109). Lamina length min 29 - 68 mm. Lamina width min 10 - 20 mm. Length:width ratio 1.61:1 – 4.19. Estimated leaf area min 336 – 906.67 mm^2. At least microphyll = 10 (100 %). Apex straight, apical angle 20° - 30°. Base complex and decurrent, basal angle 40° - 43°. Petiole winged, attachment marginal petiole length min 4 mm, winged thickness 1.5 mm (P.3001.109). Margin serrate. *Venation* pinnate and craspedodromous to weakly semicraspedodromous. *Primary* thickness weak to stout. Course is straight or curved. *Secondary* min 16 secondaries, diverging at a narrow to wide acute angle 42° - 70°. Angle decreases slightly toward base. Weak intersecondaries. *Tertiary* vein category regular polygonal reticulate. *?Fourth order* veins regular polygonal reticulate. Fifth order veins dichotomising. Areoles well developed, 4 or more sided. F.E.V's unbranched to 2 or more branched. Marginal ultimate venation looped. *Teeth* 1 order, 2 teeth/cm in middle 50 % of the leaf, spacing approximately regular. Apex angular shape FL/FL, FL/CV. Sinus angular. Indentation to midvein 0.5 - 4 mm. Teeth glandular. Principal vein course central to apical, origin deflected. Tooth type cunonioid or possibly spinose (P.3001.109).

Remarks: The toothing and venation architecture are similar to *Lomatia* sp. However, the presence of a petiole, differentiates this leaf from a *Lomatia* lobe fragment. The tertiary reticulation is also more strongly developed in this material. In gross morphology, these leaves are almost identical to the modern *Knightia excelsa* from New Zealand. *K. excelsa* also has weakly developed semicraspedodromous venation strongly reticulated tertiaries and pronounced marginal serration with a rounded sinus. *K. excelsa* has a somewhat more angular base than the specimens described here but the petiole is equally thick. Toothing in *K. excelsa* sometimes becomes less pronounced apically.

The form species *Knightiophyllum andreae* (Dúsen) Zastawniak was erected by Doktor *et al.* (1996) to describe lanceolate semicraspedodromous leaves with cunonioid teeth from Seymour Island. However, the lamina is much broader, and has less pronounced toothing, than either *K. excelsa* or Morphotype 2.9 and it is considered that Morphotype 2.9 is more similar to *K. excelsa* than *K. andreae.*

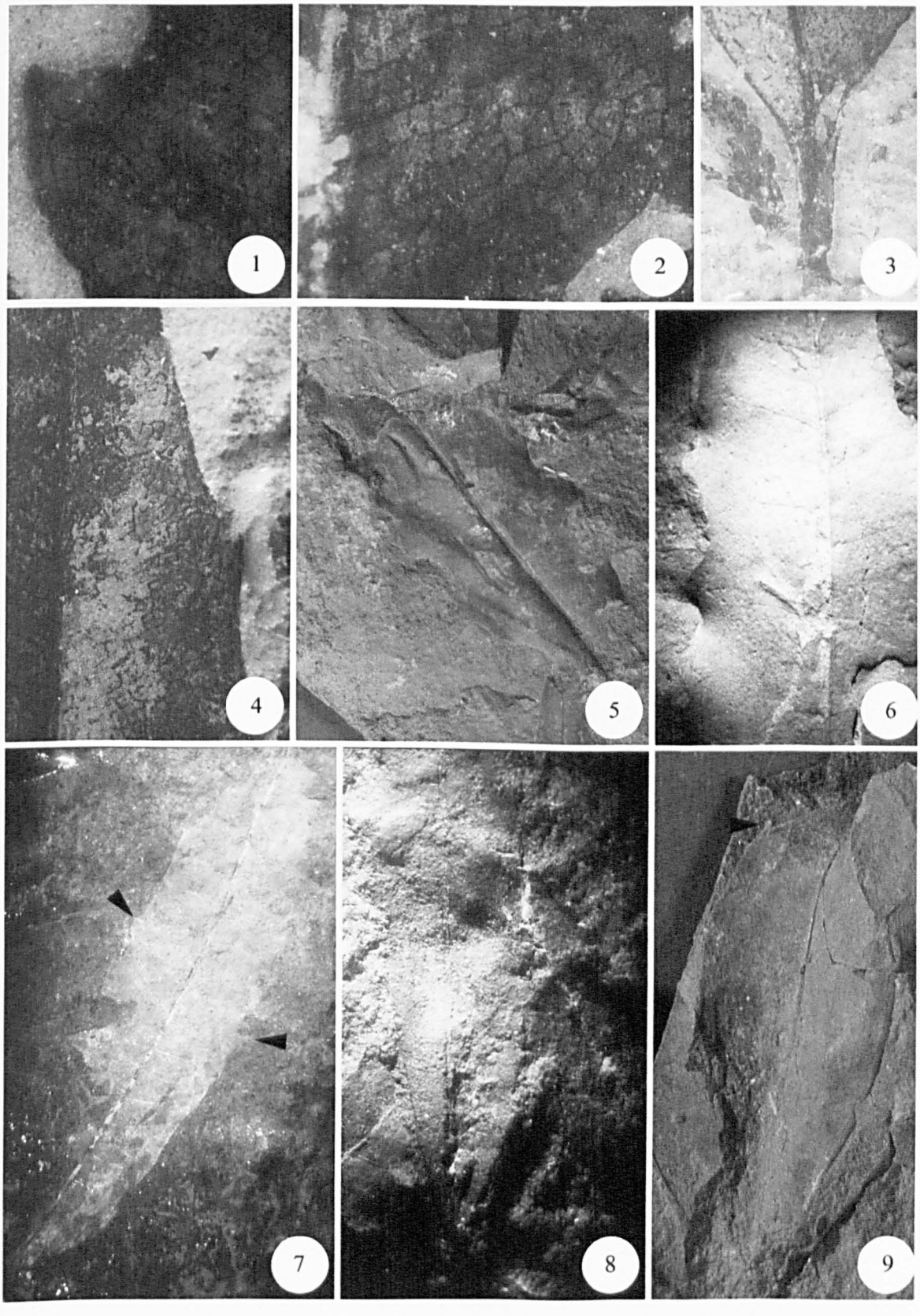

Figure 6.12. (1) - (5) Morphotype 2.9. (1). Tooth detail. P.3001.109b. x8. (2). Detail of reticulate tertiary venation. x8.5. (3). Detail of slightly asymmetric petiole. x4.3. (4). Specimen with less pronounced toothing. P.3001.104. x4.8. (5) - (6). 2.10. *Monimiophyllum antarcticum*. (5). Detail of specimen, showing undulose margin and strongly indented midvein P.935.27. x0.8. (6). Mid lamina fragment of morphotype 2.10 with detail of weak secondaries, that have a slightly undulose course. P.935.17. x1.2. (7). Morphotype 2.11. Showing indistinct marginal teeth (arrowed). P.2145.10. x1.6. (8). Morphotype 2.12. P.232.24. x2.1. (9). Morphotype 2.13. Showing small apical teeth (arrowed). P.935.12. x1.1.

2.10. *Monimiophyllum antarcticum* Birkenmajer and Zastawniak (Figure 6.12: 5 - 6)

1986 cf. *Knightia andreae* Dúsen, Troncoso (p. 12, plate 2, figs 18, 19)

1986 *Dicotiledonea* indet, Czajkowski and Rösler (p.10, fig 2, 11)

1989 *Monimiophyllum antarcticum* Birkenmajer and Zastawniak (p. 82, plate VI, figs 1A, 1B.)

Material examined: Fossil Hill U2 *Large fragments* P.935.17, .25, Fossil Hill Unit 4 *Large fragments* P.3031.63, .79.

Differential characters: Margin undulose with pronounced toothing. Secondary venation opposite to subopposite, branching at a wide acute or right angle. Leaves are sometimes paired.

Description: Leaf organisation appears simple. Lamina symmetrical, base slightly asymmetric, oblong. Lamina length min 78 mm, width min 28 mm, length:width ratio min 2.79:1. Area up to 2184 mm^2. Microphyll = 2 (50 %), notophyll = 2 (50 %). Apex not preserved. Base convex, basal angle acute 61°. Margin serrate. Petiole marginal not preserved. *Venation* pinnate semicraspedodromous. Primary stout. Secondary min 13 fine to moderate secondaries diverge at a moderate to wide acute angle 58° - 80°. Angle variable, spacing variable. Tertiary and higher order venation not preserved. Leaf rank ?2r/3r. Teeth 1 order, ?1 tooth/cm, spacing regular. Shape CC-FL, sinus rounded, apex angular. Indentation to midvein 3 mm. Principal vein is a secondary branch. Course central, origin deflected.

Remarks: Morphotype 2.10 has previously been assigned to *Knightia andreae* (Proteaceae) (Dúsen, 1908; Troncoso, 1986; Dutra, 1989) but can be distinguished from this leaf by tooth architecture and lamina shape (Birkenmajer and Zastawniak, 1989). The leaves differ from morphotype 2.9, also compared to *K. excelsa* in having numerous closely spaced secondaries.

Morphotype 2.11 (Figure 6.12: 7)

Material examined: Barton Peninsula *Large fragments* P.2145.7, .10.1/2.

Differential characters: Stenophyll leaves with semicraspedodromous secondaries diverging at right angles to the midvein. Intersecondaries common. Teeth angular with a rounded sinus and apices oriented almost parallel to the midvein.

Description: Lamina organisation appears simple. Lamina symmetrical, base ?asymmetric, elliptic. Length min 51 – 80 mm, width 14 – 21 mm, length:width ratio min 3.64:1. Area 476 – 952 mm^2. Microphyll = 3 (100 %). Apex straight, apical angle acute 20°. Base ?decurrent or complex, basal angle acute 32°. Margin serrate. *Venation* pinnate semicraspedodromous. *Primary* thickness weak to stout. *Secondary* min 18 moderate secondaries diverge at a moderate to wide acute angle 58° - 83°. Angle and spacing fairly regular. Intersecondaries strong. *Tertiary* venation opposite percurrent with a sinuous course, approximately parallel to midvein. Teeth ?2 orders, < 1 tooth/cm, spacing irregular. Shape CC-CV. Sinus rounded apex angular. Principal vein configuration not preserved.

Remarks: *Fagara serrata* (Berry, 1938) is also similar to morphotype 2.11 with small distinctly rounded tooth sinuses although it has a more acute secondary divergence angle.

Morphotype 2.12. (Figure 6.12: 8)

Material examined: Potter Cove impression *Large fragment* P.232.24.1, .24.2, .24.3. *Small fragment* P.232.24.4 .29.

Differential characters: Elliptic leaf with minute teeth directed apically and wide acute to right angle secondary veins. No intersecondaries. No teeth in the basal third of the leaf.

Description: Leaf organisation appears simple. Lamina ?symmetrical, elliptic, base slightly asymmetrical. Lamina length 57 - 65 mm, width 12 -13 mm, length:width 4.75 - 5:1. Area est. 456 - 563.33 mm^2. Microphyll = 5 (100 %). Apex convex, apical angle acute 35°. Base convex, basal angle 37°. Margin serrate. Petiole length min 2 mm, width 1 mm, slightly flared at base. *Venation* pinnate semicraspedodromous possibly craspedodromous. *Primary* thickness moderate. *Secondary* min 5 fine to moderate secondaries diverge at a wide acute angle 75° - 78°. Spacing and angle variability uncertain. Higher order venation not preserved. Leaf rank uncertain >1r. *Teeth* 1 order, ?1 tooth/secondary, spacing irregular. Shape ST-CV, CV-CV. Sinus and apices angular. Indentation to midvein 0.2 mm.

Remarks: Despite a similar gross morphology these leaves are distinguished from Morphotype 2.11 by the angularity of the sinuses and the absence of teeth basally. The leaves are too poorly preserved for detailed comparison.

Morphotype 2.13 (Figure 6.12: 9 and Figure 6.13: 1 - 2)

Material examined: Fossil Hill U2 *Large fragment* P.935.12, .22. Fossil Hill U4 *Near* P.3031.55 *Large fragment* ?G.458.1.3, *Small fragment* P.3031.109.

Differential characters: Obovate leaves. No teeth in the basal two thirds of the leaf. Teeth small and angular. Secondary venation curvature extremely angular.

Description: Leaf organisation appears simple. Lamina symmetrical and obovate. Length min 55 mm, width 30 mm, length:width ratio 1.83:1. Microphyll = 3 (60 %), notophyll = 1 (20 %). Apex not preserved ?convex, apical angle 71°. Base decurrent, basal angle 92°. Margin serrate. *Venation* pinnate semicraspedodromous. *Primary* thickness stout. Course sinuous *Secondary* min 5 - 7 moderate secondaries diverge at a narrow to moderate acute angle 42 - 65°. Course curved, forming angular loops with superadjacent secondaries. Spacing variable, angle decreasing basally. Intersecondaries moderate. *Tertiary* veins ?opposite percurrent and forming ramified loops around secondaries. Higher order vein categories not preserved. Leaf rank 2r. Teeth restricted to apical portion of lamina. 1 order, 1 tooth/cm. Spacing irregular. Shape CC-CV, ST-CC. Principal vein originates from a ramified loop of tertiary order.

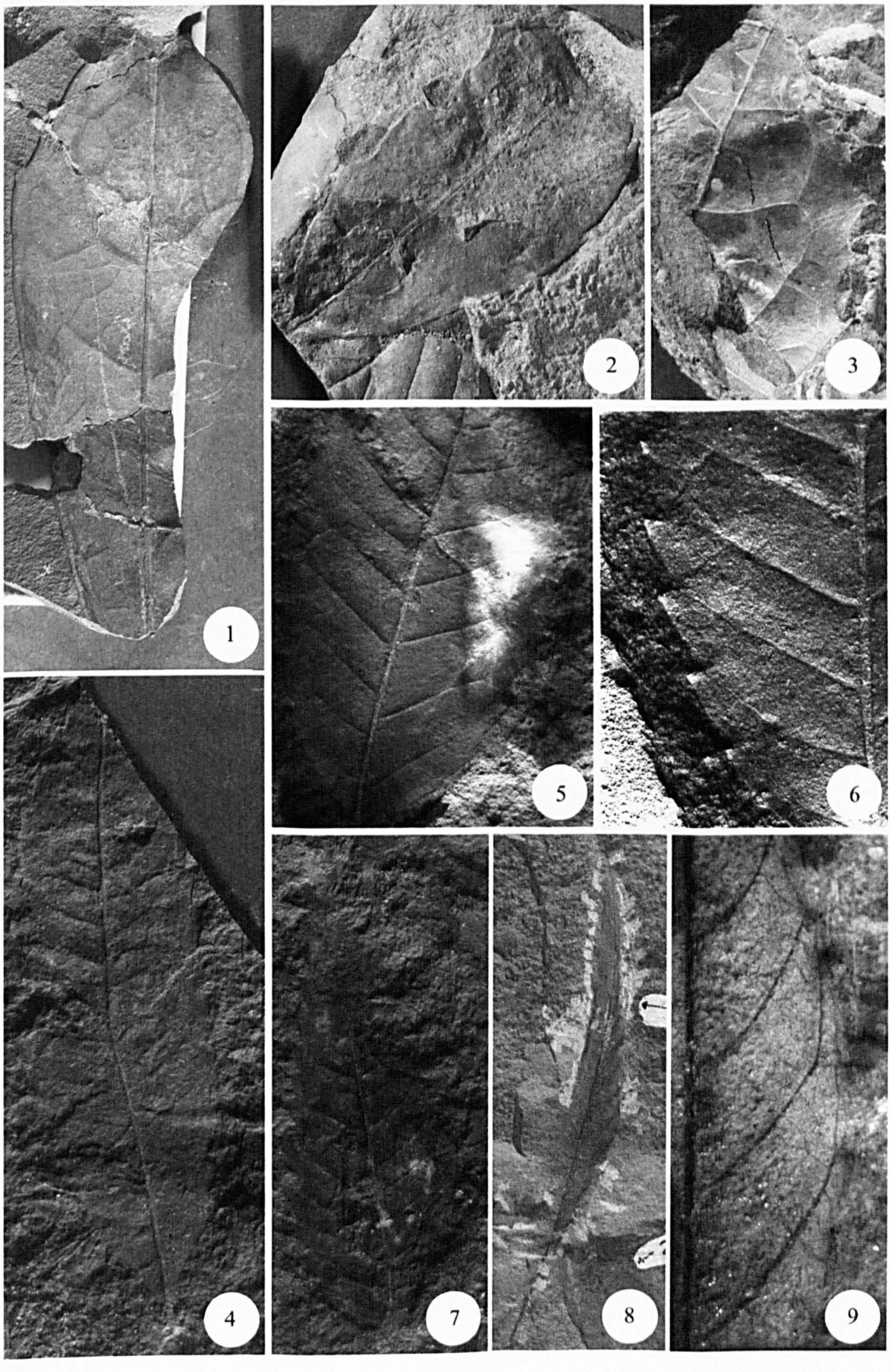

Figure 6.13. (1) - (2) Morphotype 2.13. (1). P.935.12. x1.1. (2). P.3031.55. x1.2. (3). Morphotype 2.14. x1.6. (4) - (7) Morphotype 2.15. (4). P.3034.3.6. x1.7. (5). P.3034.3.5. x1.8. (6). Detail of venation and tooth architecture. P.3034.3.5. x2.8. (7). P.3034.3.4. x1.2. (8) - (9) Morphotype 2.16. (8). G.53.25.2(5). x0.9. (9). Detail of marginal venation. x4.7.

Remarks: Morphotype 2.12 is similar in obovate form to *Lomatia serrulata* Dúsen and *L. seymourensis* Dúsen (p. 28, plate 1, figs 1,2). However, *Phyllites* sp. 2 (Dúsen, 1908, p.28, plate 1, fig 15; Troncoso, 1986, p.39, plate 3, fig 32) has both the obovate form, in addition to angular pinnate brochidodromous venation. Morphotype 2.12 is tentatively grouped with *Phyllites* sp. 2. Angular brochidodromous secondary venation with fine ramified loops towards the margin a feature present in the Australian Proteaceae e.g. *Carnarvonia araliifolia* (Christophel and Hyland, 1995). However these leaves are distinguished by a decurrent rather than rounded base. Semicraspedodromous toothed leaves are present in the Myricales, Dilleniales, Rosidae and the Rosid-leafed Asterids (Hickey and Wolfe, 1975), which would support a proteaceous grouping but is not definitive.

Morphotype 2.14 (Figure 6.13: 3)

Material examined: Fossil Hill U4 *Small fragment* G.458.2.1.

Differential characters: ?Ovate serrate margined leaves, with a series of ramified loops towards the margin.

Description: Leaf organisation appears simple. Lamina symmetry uncertain. Length min 40 mm, width est. 42 mm, length:width ratio min 0.95:1. Microphyll = 1 (100 %). Apex and base not preserved, apical angle est. 80°. Margin serrate. *Venation* pinnate semicraspedodromous. *Primary* thickness weak. *Secondary* min 5 moderate secondaries branch from midvein at a moderate to wide acute angle 54° - 72°. Angle ?decreasing abruptly basally. Spacing appears to increase apically. Curvature of secondaries is rounded angular. Basal-most secondary has ramified loops. Loops join superadjacent secondaries at an obtuse angle. *Tertiary* vein category opposite percurrent, obtuse angle to primary, course concave or sinuous. No higher order venation observed. Marginal venation ?unlooped, with veins terminating randomly at the margin. Leaf rank 2r. *Teeth* 2 orders, 2/cm. Spacing ?regular. Shape CV-CV. Sinus rounded, apex angular – right angled to wide acute. ?Non glandular apices. Principal vein course apical or central, origin deflected from secondary loop or ramified loop.

Remarks: Barton (1964) grouped this leaf with the Morphotype 1.1, although there is no evidence for toothing in any other specimens of that morphotype. Tooth-like projections are present on some specimens of Morphotype 1.1 but these are shown to be an artefact of variable margin preservation when the specimens are prepared. The leaf has similar secondary venation to *Rhoophyllum nordenskjöldii* (Araliaceae) (Li, 1994) but is distinguished in having near dentate teeth and a lower length to width ratio.

Morphotype 2.15 (Figure 6.13: 4 - 7)

1986 ?*Myrica* L. Czajkowski and Rösler (p.103, plate II, fig 8, 12, 13, 15)

Material examined: Fossil Hill U2 *Near complete* P.3034.3.4, .3.6. *Large fragments* P.3034.3.3, .3.5, P.3034.22, P.3034.25, P.3034.37, P.3034.55b, P.3034.68.

Differential characters: Lanceolate leaves with a saw-like serrate margin. Teeth are uniformly spaced and shaped. Tooth size decreases towards the leaf base.

Description: Leaf organisation appears simple. Lamina symmetrical, base ?asymmetric, shape ovate to obovate. Length min 87, width min 26, length:width ratio min 3.35:1. Microphyll = 8 (89 %), notophyll = 1 (11 %). Apex straight, apical angle 61°. Base convex to decurrent, basal angle 44 - 80°. Margin serrate. No petiole preserved. *Venation* pinnate semicraspedodromous to craspedodromous. *Primary* thickness moderate. *Secondary* min 11 - 23 moderate secondaries diverge at a narrow to moderate acute angle 44° - 70°. Secondaries bifurcate close to margin to form angular loops with the adjacent secondaries. Angle decreasing basally, spacing irregular. Weak intersecondaries. *Tertiary* vein category poorly reserved, ?regular polygonal reticulate or alternate percurrent. *Fourth order* venation forming a reticulum. No higher order venation preserved. Leaf rank ?2r/3r. *Teeth* 1 order, 1 tooth/secondary, 3 teeth/cm, spacing usually regular. Shape CC-CV. Indentation to midvein 1.5 – 2 mm. Principal vein origin deflected, course apical.

Remarks: The leaves of Morphotype 2.15 are occasionally found in pairs, which might suggest a compound leaf form. Czajkowski and Rosler (1986) suggested that the material was related to *Myrica* (Myricaceae) based on comparisons with Berry (1938) and Dúsen (1908). Semicraspedodromous veined leaves with serrate margins are present in the Myricales, Dilleniales, Rosidae and the Rosid-leafed Asterids (Hickey and Wolfe, 1975). Compound leaves are present in the Myricales, which supports the interpretations of Czajkowski and Rosler (1986).

Morphotype 2.16 (Figures 6.13: 8 - 9 and 6.4: 1 - 2)

Material examined: Dufayel Island *Large fragments* G.53.25.2(5), .30.2, .30.3, G.312.12. Cytadela (Platt Cliffs) *Large fragments* G.47.3(40), .9(45), G.309.17.

Differential characters: Lanceolate leaf with high length:width ratio. Secondary veins gradually recurve apically towards the leaf margin. Teeth serrate to dentate. Cuneate bases.

Description: Leaf organisation appears simple. Lamina symmetrical, lanceolate. Length min 64 – 78 mm, width min 11 - 15 mm, length:width ratio min 4.27:1 - 4.59:1. Microphyll = 7 (100 %). Apex acute straight, apical angle 18°. Base poorly preserved (G.53.25(5)) with a long narrow petiole < 17 mm in length but this may be a result of damage to the leaf base skeletonising the midvein. Margin serrate. *Venation* pinnate semicraspedodromous. *Primary* thickness weak. *Secondary* min 26 moderate secondaries diverge at a narrow to wide acute

angle 44° - 68°. Angle decreasing basally. Spacing increasing basally. *Tertiary* vein category opposite percurrent, course variable, angle to primary obtuse ?increasing basally. Higher order vein categories not preserved. *Leaf rank* ?2r/3r. *Teeth* 1 tooth/secondary, 4 teeth/cm, spacing irregular. Shape CC-FL, CV-CC. Sinus angular, apex angular. ?Simple apices. Principal vein origin deflected, course apical.

Remarks: Morphotype 2.16 comprises Barton's (1964) Ezcurra Inlet leaf form 2 and part of his Dufayel Island simple leaf forms 1 and 2, which he referred to *Myrica mira* Berry (Myricaceae) and to *Cupania* sp. (Sapindaceae) respectively. The remainder of Dufayel Island leaf form 2 is merged with Dufayel Island leaf form 1 to form morphotype 2.18. This includes the only example of a compound leaf for Dufayel Island leaf form 2 (G.53.6(3) and consequently there is no direct evidence for a compound morphology in Morphotype 2.16. A long narrow petiole may be present in specimen G.53.25.2(5) (Figure 6.13: 8), although the poor preservation of the leaf base makes it difficult to distinguish the margin-petiole separation. Morphotype 2.16 differs from the morphotype 2.18 in having a lower angle of secondary divergence, greater recurving of the secondaries towards the margin and increased spacing basally.

These leaves are distinguished from *Cupania* spp. which have a lower length to width ratio and often more rounded tooth apices (Berry, 1938). The small marginal serrations, semicraspedodromous venation and lanceolate leaf shape of Morphotype 2.16 are very similar to that of *M. mira*. Semicraspedodromously veined leaves with serrate margins are present in the Myricales, (Hickey and Wolfe, 1975), which supports this interpretation. However, this combination of features is also common in the Rosidae (Hickey and Wolfe, 1975).

Morphotype 2.17 (Figure 6.14: 3)

Material examined: Dufayel Island *Near complete* G.53.6.1(18). *Small fragment* G.312.2.2.

Differential characters: Elliptic leaf with a decurrent base. Strong intersecondaries. Margin serrate.

Description: Lamina organisation appears simple. Lamina symmetrical elliptic. Length 84 mm, width 37 mm, length:width 2.27:1. Area 2072 mm^2. Notophyll = 2 (100 %). Apex convex, apical angle acute 62°. Base decurrent or concavo-convex, basal angle acute 63°. Petiole marginal, partly preserved length 2 mm, width 3 mm. Margin serrate. *Venation* pinnate ?semicraspedodromous. *Primary* thickness stout. *Secondary* min 11 moderate secondaries diverge at a narrow to moderate acute angle 32° -56°. Spacing decreasing basally, angle decreasing basally. Intersecondaries weak. *Tertiary* vein category percurrent, rarely alternate percurrent. Angle to primary obtuse, increasing basally. Higher order venation not preserved.

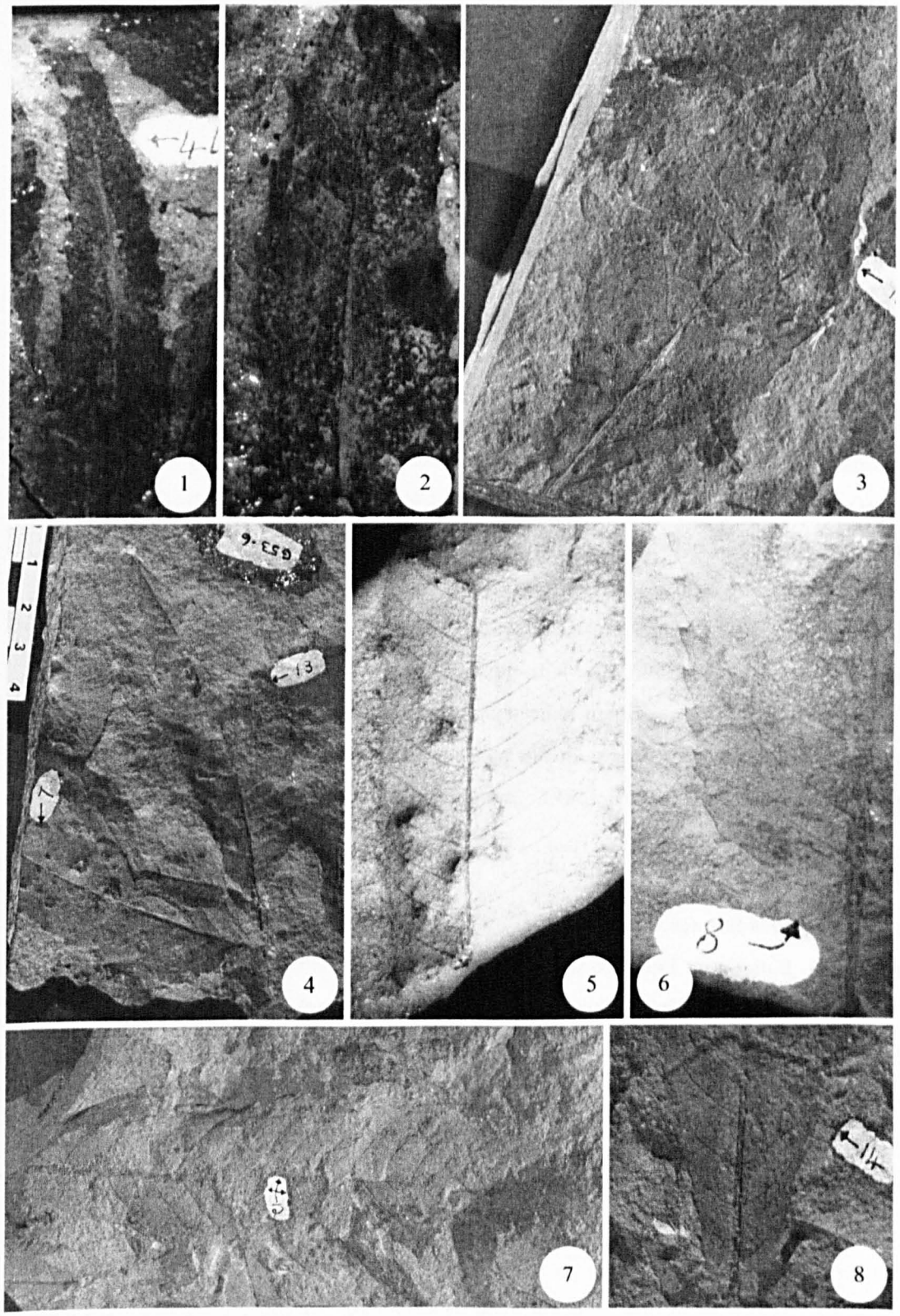

Figure 6.14. (1) - (2) Morphotype 2.16. (1). G.47. (44). x1.5. (2). G.47.9(41). G.47.(42). x3.4. (3). Morphotype 2.17. G.53.6.1(18). x1.2. (4) - (8) Morphotype 2.18. (4). Two leaves of morphotype 2.18 showing possible pinnate arrangement. G.53.6.2(7) and G.53.6.2(13). x1.25. (5). G. 53.1.2. x2.5. (6). G.312.15. x2.5. (7). G.53.6.4(12). x0.6. (8). Asymmetric leaf base of morphotype 2.18. G.53.6.5(14). x0.8.

Leaf rank 2r/3r. *Teeth* ?1order, ?2 teeth/cm, ?2 teeth/secondary. Spacing uncertain. Shape ST-FL some teeth may be formed by a rounded inflection in the margin. Principal vein configuration appears to be formed from a secondary, course central, origin ?deflected. Indentation to midvein 1.2 mm.

Remarks: Pole (1993) illustrated several leaves with affinities to *Elaeocarpus/Sloanea* of the Elaeocarpaceae from the Miocene of New Zealand. These leaves are similar in having semicraspedodromous venation with higher order looping external to the secondary veins and in the wide acute to obtuse angle of the tertiary veins to the primary. The tooth architecture is also similar with rounded inflections, although the leaves described by Pole (1993) have spine-like glands that are not present, or preserved, in Morphotype 2.17. Morphotype 2.17 also has fewer secondary veins and ?larger teeth.

Barton (1964) compared the leaf to ?*Laurelia* Juss sp. (Monimiaceae) based on the venation and form of the modern Chilean *L. aromatica* (Poir). *Laurelia guinazui* from Rio Pichileufu (Berry, 1938) is more lanceolate with smaller serrations, whilst *L. insularis* (Dúsen, 1908) is more elongate, with less pronounced serrations and less constantly upcurved secondaries. Also in the Monimiaceae, *Tetrasynandra* Perkins sp. (Monimiaceae) from Australia also have a similar form and semicraspedodromous venation, although the teeth are distinctly smaller. Basal agrophic secondaries are present in most of the Australian monimiaceous forms illustrated by Christophel and Hyland (1993) a feature not present in this morphotype. The New Zealand *L. novae-zealandiae* has prominent toothing (Salmon, 1986), but the number of teeth per secondary is much greater than in morphotype 2.19.

Semicraspedodromous leaves are common to both the Elaeocarpaceae and Monimiaceae, but the two families can be differentiated by the tooth style, theoid and monimioid, respectively (Hickey and Wolfe, 1975). Unfortunately the marginal serrations are too poorly preserved to distinguish glands or tooth architecture. Palaeocene wood assigned to *Atherospermoxylon* Kräusel (Monimiaceae) with affinities to *Daphnandra* Benth., *Doryphora* Endl. and *Laurelia novae-zealandiae,* has been described from the Cross Valley Formation on Seymour Island (Poole and Gottwald, 2001), which suggests that *Laurelia* may have been present in the Early Tertiary of West Antarctica supports a possible monimiaceous origin for this leaf.

Morphotype 2.18 (Figure 6.14: 4 - 8)

Material examined: Dufayel Island *Large fragment* G.53(1), .6.2(7), .6.2(13), .6.3(12).1.2, .29.2, .31, G.312.2.1, 10.1, .15.

Differential characters: Lanceolate to elliptic leaves with >30 wide acute secondaries. Secondary loops extremely angular. Margin serrate with acute ?glandular apices and sinuses.

Description: Leaf organisation appears simple. Lamina ?symmetrical, obovate or elliptic. Length min 45 mm, width min 17 – 40 mm, length:width ratio min 2.65:1. Microphyll = 6 (67 %), notophyll = 2 (22 %), mesophyll = 1 (11 %). Apex not preserved. Base cuneate, basal angle est. 36°. Margin serrate. Petiole not preserved. Venation pinnate semicraspedodromous. *Primary* thickness stout. Secondary min 11 moderate secondaries diverge at a narrow to moderate acute angle 42° – 53°. Angle uniform, spacing uniform. No higher order venation preserved. Leaf rank ?2r/3r. Teeth 2 orders, 4/cm, 2-3 teeth/secondary, spacing irregular. Shape CC-RT, ST-FL. Indentation to midvein 0.2 – 1 mm. Sinus angular, apex angular. Apices of two basal teeth are darkened and pointed and may be spinose.

Remarks: Barton (1964) divided the leaves grouped here as morphotype 2.18 into two groups (Dufayel Island form 1 and form 2) based on lamina size and the distinctively outward directed tooth apices but noted the similarity between the two leaf forms. Since lamina size is a poor criteria for distinguishing taxa (Dilcher, 1974) these two groups have been combined, since

they appear to differ only in their size and degree of preservation. Specimen G.53.6(3) and G.53.6(7) appear to be arranged as part of a compound leaf with G.53.6(7) as the terminal leaflet. However the attachment point of the 'leaflets' is not preserved and the compound nature of the leaf cannot be verified.

Barton (1964) compared Dufayel Island leaf form 1 to *Allophyllus graciliformis* (Sapindaceae) from the Tertiary Rio Pichileufu assemblage, although none of those leaves exhibited such a high secondary divergence angle. Barton (1964) also suggested affinities with *Salix newtonii* (Salicaceae) and with *Phyllites* sp. 1 described by Dúsen (1908) but the resolution of Dúsen's illustrations is too poor to support this interpretation and on these criteria is equally similar to *Phyllites* sp. 7. Leaf form 2 was compared to *Banksia* (Proteaceae) and to *Myrica mira* (Barton, 1964). The possible pinnate morphology of this leaf morphotype and the semicraspedodromous venation support a possible origin within the Myricaceae (Hickey and Wolfe, 1975).

Morphotype 2.19 (Figure 6.15: 1 - 2)

Material examined: Platt Cliffs *Large fragment* G.50.1 (48), .6(49), .6.2(52),.6.4(51), .6.5(50).

Differential characters: Elliptic leaves with a decurrent base. Small serrate teeth. Basal pair of acute secondaries, strong intersecondaries.

Description: Leaf organisation appears simple. Lamina ?symmetrical, ?elliptic, base slightly asymmetric. Lamina length min 33 – 73 mm, width min 15 – 26 mm, length:width min 2.2:1. Area 330 mm^2. Microphyll = 2 (67 %), notophyll = 1 (33 %). Apex ?convex, apical angle est. acute 67°. Base decurrent or concave, basal angle acute 63°. Margin serrate. Petiole marginal

length 2 mm, width 1 mm. Venation pinnate semicraspedodromous. Primary weak. Secondary min 8 secondaries diverge at a narrow to wide acute angle 26° - 78°. Angle variable. Spacing increases basally. Higher order venation not preserved. Leaf rank ?2r. Teeth 1 order, 1 tooth/secondary, min 2 teeth/cm, spacing uncertain. Shape ST-RT, CC-ST. Indentation to midvein 0.1 mm. Principal vein configuration uncertain.

Remarks: This morphotype was classed as 'mainly, if not wholly entire' by Barton (1964; p. 125), who consequently compared the morphotype with entire margined rather than toothed leaves. Based on the presence of teeth, this leaf is classed as toothed margined and Barton's (1964) interpretations for this leaf are not considered further. *Fagara serrata*, from the Rio Pichileufu flora is similarly elongate and has a strong intersecondary veins but the poor preservation prevents more detailed comparisons.

Morphotype 2.20 (Figure 6.15: 3)

Material examined: Dufayel Island *Large fragment* G.53.(17). Cytadela (Platt Cliffs) *Large fragments* G.47.5.

Differential characters: Lanceolate leaves with a crenate margin.

Description: Lamina organisation appears simple. Lamina ?symmetrical, ?elliptic. Length min 45mm, width 14 mm, length:width ratio 3.21:1. Area 420 mm^2. Microphyll = 2 (100 %). Apex, base and petiole not preserved. Margin crenate. *Venation* pinnate semicraspedodromous. *Primary* thickness stout. Course straight. Secondary min 11 moderate subopposite to opposite secondaries diverging at a moderate to wide acute angle 56° - 70°. Angle uniform, spacing irregular. No higher order venation preserved. Leaf rank ?2r. Teeth 1 order, 2 teeth/cm, 1 tooth/secondary, spacing irregular. Apex shape CV-CV, CC-CV. Sinus and apex rounded. Principal vein origin deflected with main vein joining superadjacent secondary, course eccentric apical.

Remarks: Barton (1964) classed this morphotype as Dufayel Island leaf form 3 but did not make any comparative analysis of the specimen due to its poor preservation. *Myrica nordenskjöldii* (Dúsen, 1908) has a similar decurrent base and saw-like serrations but the poor preservation prevents more detailed comparison.

Morphotype 2.21 (Figure 6.15: 4)

Material examined: Fossil Hill U2 *Large fragment* G.458.2.2 *Small fragment* ?G.458.1.4.

Differential characters: Stenophyll oblong leaf with widely spaced semicraspedodromous secondaries that diverge at an approximate right angle.

Description: Lamina organisation appears simple. Lamina elliptic to oblong, symmetrical. Length min. 48 - 72 mm, width min.16 mm. Length:width ratio 4.5:1 (G.458.2.2). Microphyll = 2 (100 %). Apex not preserved ?straight, angle acute 30°. Base poorly preserved ?decurrent.

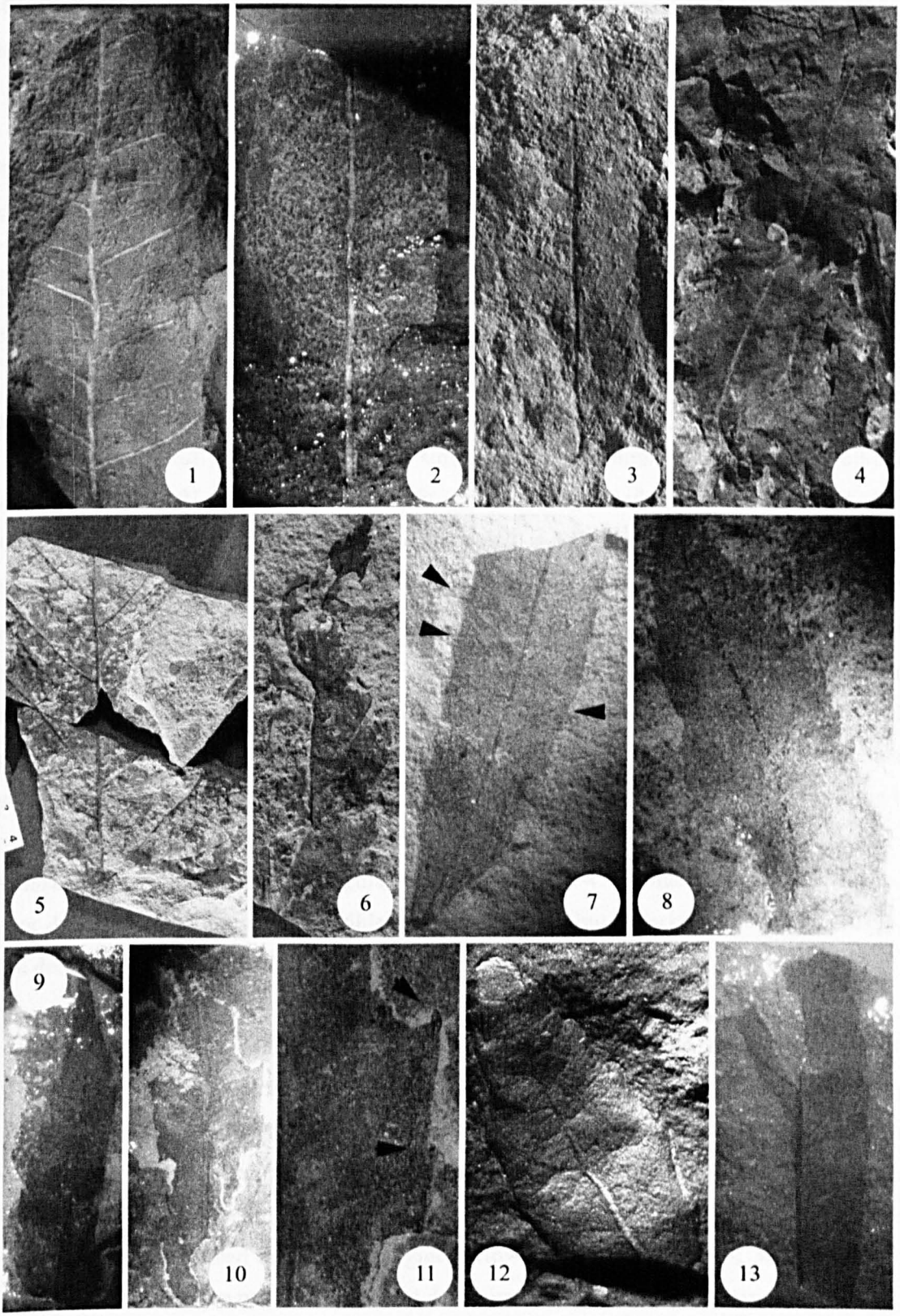

Figure 6.15. (1) - (2) Morphotype 2.19. (1). G.50.1(48). x1.7. (2). G.50.6.2. x2.1. (3). Morphotype 2.20. G.53(17). x1.8. (4). Morphotype 2.21. G.458.2.2. x1.2. (5) - (6) Morphotype 2.22. (5). P.2810.12.1. x0.5. (6). Single fragment with marginal serrations preserved. P.3001.57.1. x0.7. (7). Morphotype 2.23. Marginal crenations arrowed. x2. (8) - (9) Morphotype 2.24. (8). P.3032.24. x1.6. (9). P.3032.4.1. x3.8. (10) - (11) Morphotype 2.25. (10). P.3032.80. x1.6. (11). Detail of glandular apex (arrowed). x4. (l2). Morphotype 2.26. x6.3. (13). Morphotype 2.27. P.212.10. x1.8.

Petiole not preserved, marginal. Margin serrate. *Venation* pinnate semicraspedodromous. *Primary* massive, straight. *Secondary* min 10 secondaries diverging at a wide acute angle 66 – 90° and recurving abruptly close to the margin. Spacing irregular, possibly decreasing towards the base. Loop forming veins join at a wide obtuse angle.

Remarks: This material is very poorly preserved but resembles material described as *Phyllites* sp. 4 (Torres, 1990) and *Rhoophyllum nordenskjoeldi* by Li (1994), in terms of venation architecture.

Morphotype 2.22 (Figure 6.15: 5 - 6)

Material examined: Dragon Glacier *Large fragments* P.2810.12.1; P.3001.57.1, .195.

Differential characters: Lanceolate leaves with basal agrophic secondaries, serrate margin and darkened glandular teeth. Strong alternate percurrent tertiaries.

Description: Leaf organisation appears simple. Lamina incomplete, lanceolate or elliptic. Lamina length min 91 - 110 mm, width min 36 – 80 mm, length:width min 1.38:1 - 2.52:1. Area 1092 – 5866.67 mm^2. Microphyll = 1 (33%), notophyll = 1 (33%), mesophyll = 1 (33%). Apex straight acute, apical angle 34° (P.3001.57.1). Base convex cuneate to convex, basal angle acute to obtuse est. 58° - 120°. Petiole marginal, not preserved. Margin serrate. *Venation* pinnate semicraspedodromous. *Primary* thickness moderate. *Secondary* min 5 – 7 moderate secondaries diverge at narrow to moderate acute angle 26° - 55°. Angle smooth decrease towards base. Vein spacing increases towards base. 1 pair of simple agrophic veins. *Tertiary* vein category alternate percurrent. *Fourth order* veins regular polygonal reticulate. *Fifth order* veins ?dichotomising or regular polygonal reticulate. Areolation ?5 or more sided. Leaf rank 3r. Teeth 1 order, 1 tooth/secondary in apex, spacing ?regular, shape ST-RT, CV-CV. Sinus angular, apex angular. Apex darkened glandular with a possible chloranthoid tooth but is darkened not clear, principal vein deflected. Course central.

Remarks: Morphotype 2.22 is unusual in the large size of lamina (at least mesophyll). Although much of the material does not have margin preservation, a toothed apex is preserved in P.3001.57.1 hence its inclusion as a toothed margin morphotype. The strong secondary and tertiary venation of Morphotype 2.22 is present in *Magnoliidaephyllum birkenmajeri* (Zastawniak, 1994) from the Cretaceous Zamek Formation, which she considered to be brochidodromously veined and entire margined. However, no leaf bases of *M. birkenmajeri* were preserved, which would have allowed for comparisons of the characteristic large basal agrophic loops that are present in this morphotype. No other similar material was found for comparison, although this is partly a function of the poor preservation.

Toothed leaves with pinnate venation and basal agrophic secondaries are common in the Hamamelididae and the Magnoliidae, although the secondaries are congested in the Hamamelididae (Hickey and Wolfe, 1975), which suggests that a grouping with the Magnoliidae is more appropriate.

Morphotype 2.23 (Figure 6.15: 7)

Material examined: Rocky Cove *Large fragment* P.3029.14.

Differential characters: Elliptic leaf with one pair of acute basal secondaries, divergence angle increasing apically. Moderate to strong intersecondaries. Minute teeth.

Description: Leaf organisation appears simple. Lamina shape ?elliptic, symmetrical, base slightly asymmetric. Length min 32 mm, width 10 mm, length:width ratio min 3.2:1. Area min 213.33 mm^2. Microphyll = 1 (100 %). Apex not preserved. Base complex or convex, basal angle acute 36°. Margin dentate. *Venation* pinnate semicraspedodromous. *Primary* vein thickness weak. Course curved. *Secondary* min 12 moderate secondaries diverge at a narrow to moderate acute angle 21° – 60°. Angle decreasing abruptly basally with one pair of acute basal secondaries. Spacing irregular, increasing basally. Course irregular. Weak intersecondaries. Loops join superadjacent secondaries at an obtuse angle. *Tertiary* vein category uncertain. Higher order venation not preserved. Leaf rank ?2r.

Remarks: The minutely toothed margin, semicraspedodromous venation and small leaf size of Morphotype 2.23 are similar to *Dicotylophyllum elegans* from Fossil Hill (Li, 1994), however the preservation of the leaves is too poor for further comparison.

Morphotype 2.24 (Figure 6.15: 8 - 9)

Material examined: Fossil Hill Unit 3 *Large fragments* P.3032.4.1, P.3032.90. *Small fragments* P.3032.58, P.3032.24.

Differential characters: Lanceolate leaf with an irregular serrate margin. Convex base and an attenuated apex.

Description: Leaf organisation appears simple but asymmetric bases in some specimens may indicate compound leaf type. Length min 51 mm, width 17 mm, length:width min 3:1. Microphyll = 4 (100 %). Apex symmetrical straight, apical angle acute ? Base convex, sometimes asymmetric, basal angle ? Margin serrate. Petiole not preserved but possibly attached direct to rachis. *Venation* pinnate semicraspedodromous. *Primary* vein course curved, thickness 0.5 mm, size 2.94 % and is termed stout. No agrophic veins observed. Number of basal veins uncertain due to preservation. *Secondary* min 14 moderate secondaries diverge at a narrow to moderate acute angle 43 – 66°. Angle irregular ?due to preservation. Loop forming veins join superadjacent secondaries at an acute angle. Higher order venation not preserved. Leaf rank ?2r.

Teeth simple, ?1 – 2 teeth per secondary, 2 teeth/cm. Spacing regular. Shape FL-FL, CC-FL. Apex and sinus angular. Apices occasionally darkened, possibly glandular. Principal vein course central, origin direct.

Remarks: Morphotype 2.24 is similar to *Dicotylophyllum* sp. 3 (Li, 1994) in having semicraspedodromous secondary venation with loop forming branches meeting superadjacent secondary veins at acute angles but differs in having more pointed tooth apices and a higher density of teeth per secondary. The toothing of Morphotype 2.24 is also more irregular.

Morphotype 2.25 (Figure 6.15: 10 - 11)

Material examined: Fossil Hill Unit 3 *Small fragment* P.3032.80.1/.2.

Differential characters: ?Narrow elliptic leaf with a thick primary and serrate margin. Tooth type setaceous (with an opaque bristle or cap, thickened proximally, not fused firmly with the remaining tooth substance).

Description: Leaf organisation appears simple. Lamina narrow elliptic, ?symmetrical. Length 36 mm, width 13 mm, length:width ratio min 2.77:1. Area 312 mm^2. Microphyll = 2 (100 %). Apex not preserved, base ?acute convex. Margin serrate. *Venation* pinnate ?craspedodromous. *Secondary* preservation rare, no higher order venation. Leaf rank uncertain. *Teeth* 1 order, 2/cm, ?1 per secondary, spacing ?regular. Tooth shape ?RT-ST, sinus ?rounded. Apex setaceous.

Remarks: There are no previous records of leaves with setaceous teeth from King George Island. The lamina shape and venation is the same as morphotype 2.24, suggesting that they may be related. Setaceous apices are likely to have a low preservation potential being deciduous and not fused to the lamina. Deciduous seta are common in the Theaceae and Ochnaceae (Hickey and Wolfe, 1975).

2e[1]. Possible juvenile semicraspedodromously veined leaves

Morphotype 2.26 (Figure 6.15: 12)

Material examined: Fossil Hill Unit 2 *Large fragment* P.3034.61, P.3036.2.

Differential characters: Leptophyll elliptic leaf with sinuous primary vein. Teeth have a deep sinus with rounded to pointed apices.

Description: Leaf organisation appears simple. Lamina ovate ?symmetrical, base slightly asymmetric. Length min 10 mm, width min 4.5 mm, length:width ratio min 2.22:1. Area min 30 mm^2. Nanophyll = 2 (100 %). Apex convex, apical angle acute 64°. Base not preserved. Margin serrate. Venation pinnate semicraspedodromous. *Primary* thickness weak. *Secondary* min 6

moderate secondaries diverge at a moderate acute angle 49° - 70°. Angle decreasing basally, spacing increasing basally. Higher order venation not preserved. Leaf rank 2r/3r. *Teeth* 1 order,

1 tooth/secondary, spacing regular. Shape CC-CV, RT-CV. Sinus angular, apex angular to slightly rounded. Principal vein is a secondary.

Remarks: This leaf morphotype has not previously been described from King George Island. The small size (leptophyll) of the leaf suggests that it may be a juvenile form.

2d^2. Craspedodromous venation

Morphotype 2.27 (Figure 6.15: 13)

Material examined: Rocky Cove *Small fragment* P.212.10.

Differential characters: Elliptic or obovate leaf with 1 order of serrate teeth. Vein angle decreases towards base, secondary course irregular.

Description: Leaf organisation appears simple. Lamina shape ?elliptic to obovate. Length min 34 mm, width min 13 mm est. 22 mm, length:width ratio min 1.55:1. Area min 498.66 mm2. Microphyll = 1 (100 %). Apex and base not preserved, probably acute. Margin serrate. *Venation* pinnate craspedodromous. *Primary* thickness weak. Course straight. Secondary min 10 moderate secondaries diverge at a narrow to moderate acute angle 36° - 55°. Angle ?decreasing abruptly basally. Spacing variable. Course variable. Rare intersecondaries. No higher order venation preserved. Leaf rank 1r/2r. *Teeth* 1 order, 3/cm, 1 tooth/secondary, spacing irregular. Apex shape ?CC-CV but very poorly preserved. Sinus ?rounded.

Remarks: This leaf is similar in form to Morphotype 2.23 but is distinguished by the craspedodromous venation and serrate teeth.

Morphotype 2.28 (Figure 6.16: 1)

Material examined: Fossil Hill U2 *Large fragment* P.935.27.Fossil Hill U4 *Large fragment* G.458.2.3(57),

Differential characters: Stenophyll lanceolate leaf with minutely serrate margin.

Description: Leaf organisation appears simple. Lamina ?symmetrical, lanceolate to elliptic. Length min 52 mm, width 12 mm, length:width ratio min 4.33:1. Microphyll = 2 (100 %). Apex appears straight, apical angle acute est 31°. Base complex, basal angle acute, basal angle 50°. Petiole not preserved. Margin serrate. Venation pinnate ?craspedodromous. Primary thickness moderate. Secondary and higher order venation rarely preserved. Leaf rank uncertain. Teeth 4/cm, 1-2 orders, spacing irregular. *Other features* large irregular traces focussed on midvein (P.935.27), 38 spherical galls in mid portion of lamina (G.458.2.3(57)).

Remarks: The low angle of secondary vein divergence combined with a lanceolate lamina is present in the *Dicotylophyllum* sp. 3 (Li, 1994) although the teeth are less defined than in that morphotype and it also has semicraspedodromous venation (Li, 1994).

Morphotype 2.29 (Figure 6.16: 2 - 4)

Material examined: Dragon Glacier *Almost complete* P.3013.10. *Large fragments* P.3001.91.1/.2/.3/.4, P.3013.26. *Small fragment* P.3029.13.

Differential characters: Ovate to elliptic leaf with large serrate CC-ST teeth and a decurrent base. ?Whorled arrangement. Strong primary venation and weak, barely visible secondaries.

Description: Leaf organisation appears simple. Lamina ovate (lanceolate) to elliptic or ovate, base asymmetrical. Lamina length 33 - 80 mm. Lamina width 15 - 61mm. Length:width ratio 1.02:1 - 3.64:1. Area est. 550 – 2521.33 mm^2. Microphyll = 6 (86 %), notophyll = 1 (14 %). Apex straight or convex acute to obtuse, apical angle 12° - 108°. Base decurrent, basal angle 36° - 68°. Petiole may be present but cannot be differentiated from decurrent base. Margin serrate. *Venation* is pinnate ?craspedodromous, possibly semicraspedodromous. *Primary* moderate to stout. Course is straight. One primary originates at the leaf base. *Secondary* min 2 – 3 fine to moderate secondaries diverge at a narrow to wide acute angle 41° - 72°. Angle and spacing variability uncertain, possibly loop forming in apex. *Teeth* 1 or 2 orders, ?1 per secondary, 2 - 3 teeth/cm in middle 50 % of the leaf, spacing regular to irregular. Apex angular, shape CC-ST, CC-CV, FL-CV/RT, CV-ST. Sinus angular. Apices ?non-glandular. Indentation to midvein 2 mm.

Remarks: The distinctive tooth style of this leaf is similar to Morphotype 2.4 implying that the leaves could be detached lobes but specimens P.3001.90.1-3 appear to have a whorled or palmately compound organisation rather than being part of a pinnatisect leaf. In addition the number of teeth present in this morphotype >14 is higher than in Morphotype 2.4 (<12 teeth per lobe). The tooth morphology is also similar to Morphotype 2.30 but the teeth are more widely spaced, have more pointed apices and the apex of the leaf is highly attenuated, suggesting that the leaves are not the same.

Dúsen (1908) described two leaves with decurrent bases from the Tertiary of Seymour Island, which he referred to *Lomatia* (*L. seymourensis* and *L. serrulata*) but neither of the leaves possess the well defined toothing present in morphotype 2.29. The two leaf types are also obovate rather than elliptic.

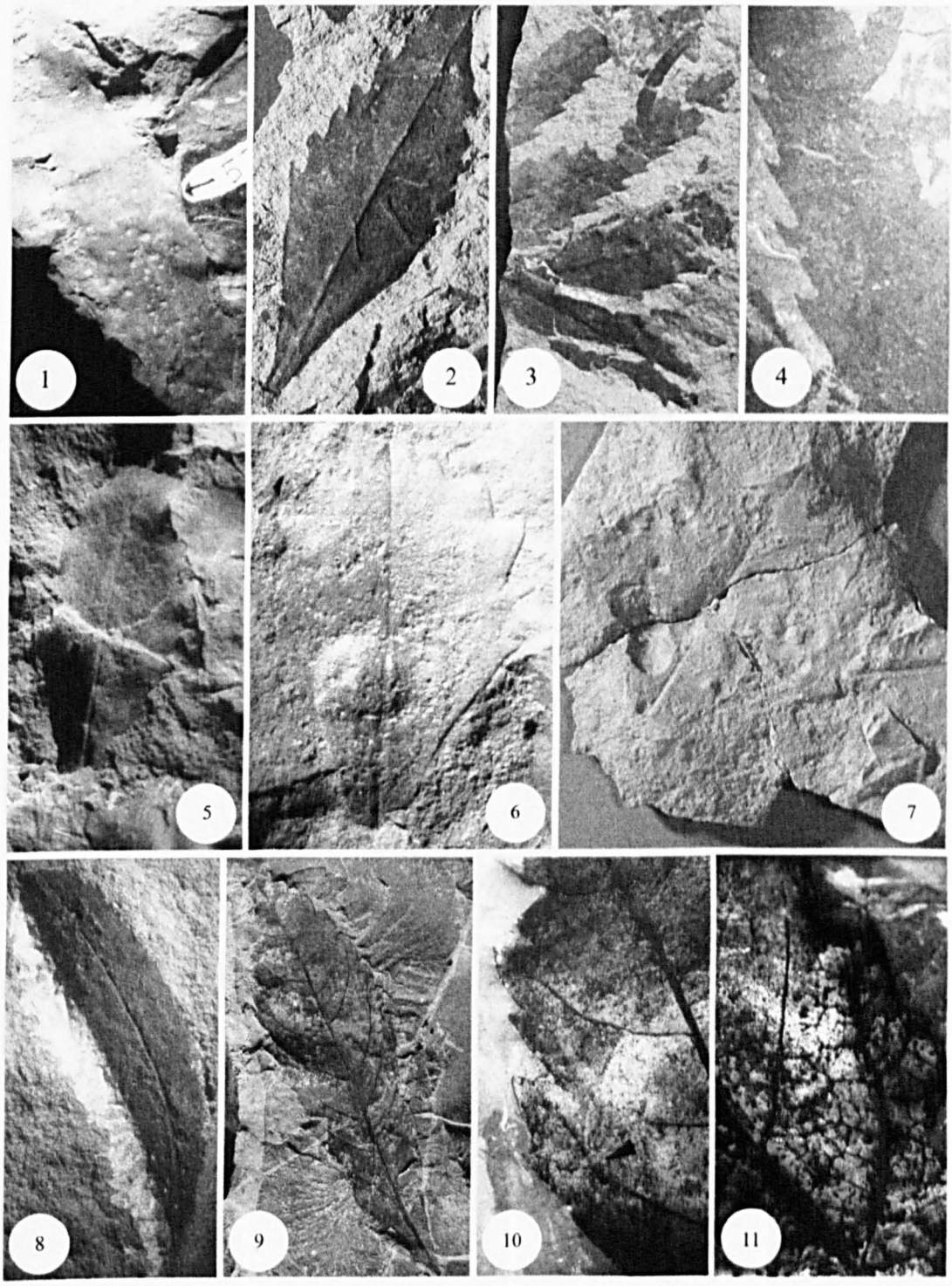

Figure 6.16. (1). Morphotype 2.28. G.458.2.3(57). x1.3. (2) - (4). Morphotype 2.29. (2). P.3013.10. x1.5. (3). Inferred whorled arrangement of leaves. P.3001.91. x0.7. (4). P.3001.91.2b. x 1.8. (5). Morphotype 2.30. G.458.1.5. x1.7. (6) - (7). Morphotype 2.31. (6). P.935.27. x1.8. (7).P.935.25. x0.8. (8). Morphotype 2.32. P.3001.44. x1.7. (9) - (10). Morphotype 2.33. (9). P.3028.2. x1.1. (10). Detail of marginal serrations. Showing abaxial branching of secondaries that terminate in the secondary teeth. x4.4. (11). Detail of venation. x4.9.

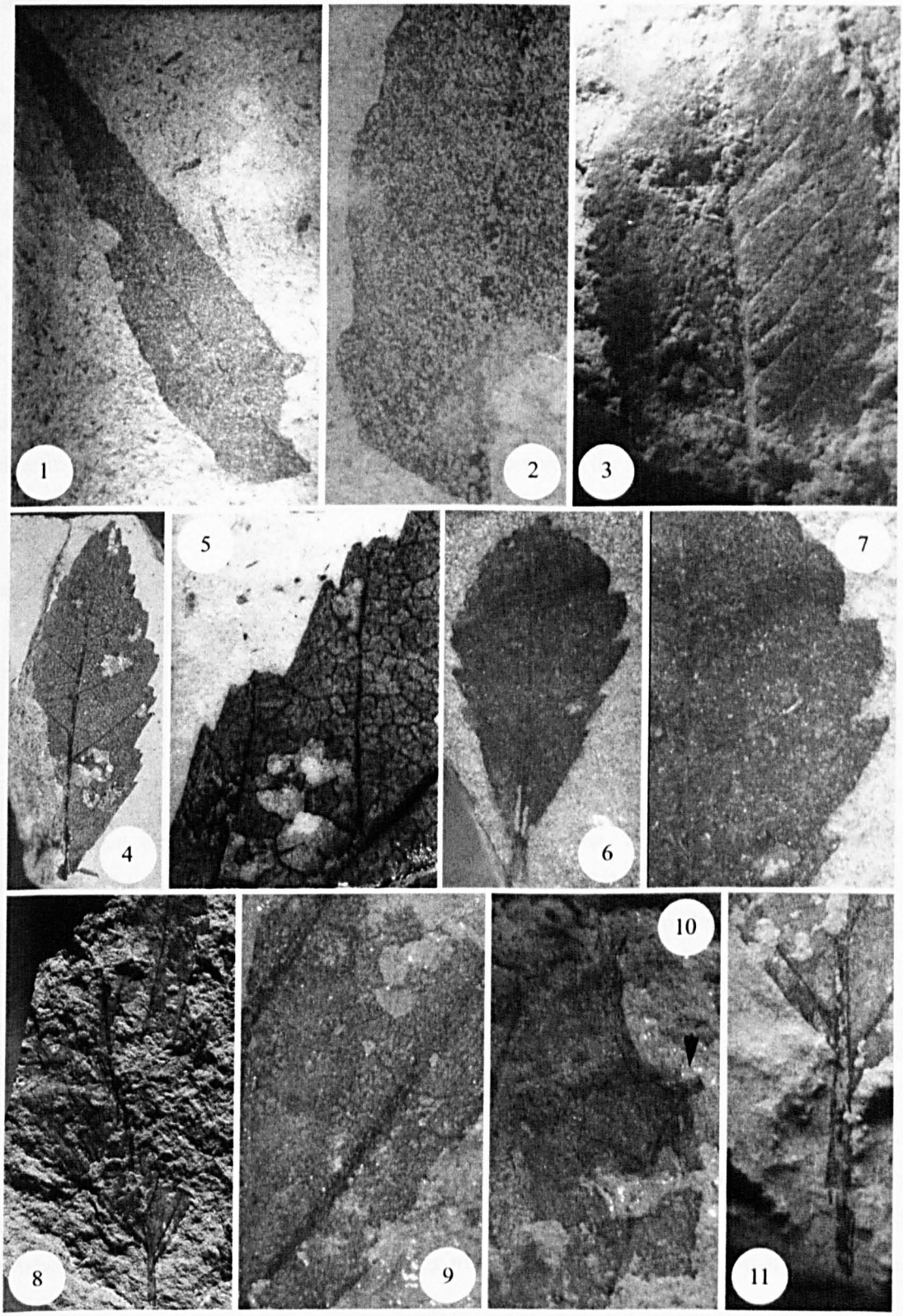

Figure 6.17. (1) - (2) Morphotype 2.34. (1). P.3032.60. x1.6. (2). Detail of venation and margin. x5.7. (3). Morphotype 2.35. P.3011.1. x2.1. (4) - (5) Morphotype 2.36. (4). P.3001.83a. x2.4. (5). P.3001.83b. Detail of margin and higher order venation. x5.5. (6) - (7) Morphotype 2.37. (6). P.3001.36.2. x3.1. (7). Detail of margin. x7. (8) - (11) Morphotype 2.38. (8). P.3013.17. x1.1. (9). Detail of venation. x4.5. (10). Detail of tooth architecture. x5.5. (11). Detail of petiole. x4.1.

Morphotype 2.30 (Figure 6.16: 5)

Material examined: Fossil Hill U4 *Near complete* G.458.1.5.

Differential characters: Serrate margined leaf with an attenuated apex and a decurrent base.

Description: Lamina organisation appears simple. Lamina ?symmetrical lanceolate. Length min. 53 mm, width min. 15 mm. Length:width ratio min. 3.5:1. Microphyll = 1 (100 %). Apex straight, attenuated, acute, apical angle 12°, base acute decurrent 46°. Margin serrate. *Venation* pinnate ?craspedodromous. *Primary* weak, course sinuous. Rare secondaries, with a straight course but marginal behaviour not preserved. *Teeth* Regular spacing, 3 – 4 teeth/cm, shape CV-CV, apices angled towards lamina.

Remarks: This leaf is differentiated from morphotype 2.32 by the smaller CV-CV shaped teeth, although there is otherwise a strong similarity between the leaves in lamina form, further collecting from this area may find further similarities between the leaf types.

Morphotype 2.31 (Figure 6.16: 6-7)

Material examined: Fossil Hill U2 *Large fragments* P.935.27, .25.

Differential characters: Obovate leaves with a decurrent base, strong primary and poorly preserved fine secondary venation. Large teeth confined to the apical margin of the leaf.

Description: Leaf organisation appears simple. Lamina obovate, symmetrical. Length min. 33 – 62 mm, width min 25 – 61 mm, length:width ratio min. 1.02:1 - 1.32:1. Microphyll = 1 (50 %), notophyll = 1 (50 %). Apex obtuse convex, apical angle 108°, base decurrent, acute 68°. Apical margin toothed. *Venation* pinnate ?craspedodromous. *Primary* moderate thickness, course straight. Teeth prominent FL-RT, CC-RT with slightly rounded apices. Spacing irregular, sinus angular. No glands observed. 2 – 5 mm indentation to midvein.

Remarks: Morphotype 2.31 is differentiated from morphotypes 2.32 and 2.33 by the lack of an elongate apex and a wider tooth apical angle. This morphotype is not found elsewhere on King George Island or in West Antarctica. No leaf base is preserved and therefore the leaf might be a fragment of a pinnately compound leaf such as *Lomatia*, however there is no venation evidence to support this interpretation. The leaf apex is also greatly suppressed compared to any of the forms attributed to *Lomatia* (e.g. Li, 1994) and the *Lomatia* lobes are generally asymmetric towards close to their base with the midvein skewed to the apical margin of the leaf base.

In the modern record *Hoheria angustifolia* (Salmon, 1998) (Malvaceae) has a juvenile form with apical toothing and a decurrent base, with a thick petiole, however the leaves are much smaller than those described here.

Morphotype 2.32 (Figure 6.16: 8)

Material examined: Dragon Glacier *Near complete* P.3001.44.

Differential characters: Very poorly preserved leaf which is distinct in having a very high length:width ratio and minute serrations.

Description: Leaf organisation appears simple. Lamina ?obovate or elliptic, ?symmetrical. Length min 46 mm, width 8 mm. Length:width ratio min 5.75:1. Area estimated 245.33 mm^2. Microphyll = 1 (100 %). Apex acute, apical angle 26°. Base acute, basal angle 30°. Margin serrate. *Venation* pinnate craspedodromous. *Primary* vein thickness stout. Course slightly sinuous and curved. One primary vein originates at leaf base. *Secondary* one secondary vein observed, diverging from midvein at narrow acute angle 22°. Toothing 1 order, 4 teeth/cm in middle 50 % of leaf, spacing regular. Teeth simple, indentation to margin 0.2 mm. Shape st/cv, angular sinus.

Remarks: On the basis of the high length:width ratio and minute toothing the leaf is similar to *Proteaceiphyllum linearis* (Carpenter and Jordan, 1997) and some *Banksiaephyllum* sp., although these fossils are identified on the basis of cuticular features rather than leaf architecture. The leaf is also similar to morphotype 2.2 from Fossil Hill, but there is no evidence of any attachment to a winged rachis and insufficient venation detail to compare the leaves more closely.

Morphotype 2.33 (Figure 6.16: 9 - 11)

Material examined: Collins Glacier Moraines *Complete* P.3028.2a/b.

Differential characters: Elliptic leaf with a long decurrent base and a serrate margin, 1 – 2 teeth/secondary.

Description: Leaf arrangement appears simple. Lamina lanceolate, symmetrical. Length 72 mm, width 21 mm. Length:width ratio 3.43:1. Area 1008 mm^2. Microphyll = 1 (100 %). Apex acute convex, apical angle 51°. Base acute decurrent, basal angle 38°. No petiole preserved. Margin toothed. *Venation* pinnate craspedodromous. *Primary* thickness stout. Course curved. *Secondary* min 20 opposite to alternate veins, diverging from primary at narrow acute angle 41° - 66° av. 55°. Divergence angle increasing apically. Spacing greatest in upper 3/4 of the lamina. Intersecondaries are weakly developed. *Tertiary* vein category alternate percurrent. Vein angle to primary obtuse, increasing apically. *Fourth order* veins regular polygonal reticulate. *Fifth order* veins ?dichotomising. *F.E.V's* ?twice branching. *Marginal Ultimate Venation* uncertain. Leaf rank ?1r. *Teeth* 1 - 2 orders. 2 teeth/cm in the mid 50 % of the leaf. *Spacing* irregular. *Tooth shape* ST/ST, FL/CV. *Sinus* angular. *Apex* simple. *Principal vein course* central. *Origin of vein* deflected with one vein running to the superadjacent sinus or a superadjacent tooth, crossing the sinus. Accessory veins not observed.

Remarks: In spite of the distinct appearance of this leaf, no corresponding modern or fossil leaves were found for comparison.

Morphotype 2.34 (Figure 6.17: 1 - 2)

Material examined: Fossil Hill Unit 3 *Large fragment* P.3032.60.

Differential characters: Tapering lanceolate leaf with indistinct basal crenations. Base straight. Strong primary and indistinct secondaries.

Description: Leaf organisation appears simple. Lamina ?symmetrical, lanceolate. Length 55 mm, width min 14 mm, length:width ratio 3.93:1. Microphyll = 1 (100 %). Apex straight, apical angle acute 15°. Base convex, basal angle 41°. Margin crenate. No petiole preserved. *Venation* pinnate ?craspedodromous. *Primary* thickness stout. Course sinuous *Secondary* venation poorly preserved, min 6 fine to moderate secondaries diverge at a narrow to wide acute angle 32° - 74°. Apparent low diversity of secondary veins. Vein angle variability uncertain ?decreasing abruptly basally. Spacing ?regular. *Tertiary* and higher order vein category uncertain. Margin darkened possibly representing a fimbrial vein. Rank ?1r/2r. *Teeth* rounded, ?1 order, spacing uncertain. Indentation to midvein 0.7 mm. Apex shape not defined by MLA categories, concave apical sinus with a convex basal side. Sinus ?rounded. Principal vein is a secondary, origin direct, course eccentric apically.

Remarks: This morphotype has not been described from King George Island previously. Hayes' (1999) Morphotype 2 is similar in having indistinct toothing, a relatively high l:w ratio (1.98:1), broadly spaced secondaries and a tapering apex. Hayes' (1999) morphotype has three to five actinodromous primaries and brochidodromous secondary veins, whilst this leaf appears to be pinnate craspedodromous. On this basis the two leaves cannot be grouped, however, the resolution of the higher order venation in this leaf is extremely poor.

Morphotype 2.35 (Figure 6.17: 3)

Material examined: Mt Wawel *Large fragments* P.3011.1a/b.

Differential characters: Elliptic leaf with prominent CV-RT, FL-RT teeth. Secondaries irregular and bifurcating/branching towards the margin. Teeth glandular possibly spinose or rosoid.

Description: Leaf organisation appears simple. Lamina ?symmetrical, elliptic. Lamina length min 36 mm est. 44 mm, width 19 mm, length:width est. 2.32:1. Area min 456 mm^2. Microphyll = 1 (100 %). Apex appears convex from margin trend, apical angle est. acute 72°. Base not preserved. Margin serrate. *Venation* pinnate craspedodromous. *Primary* thickness stout. *Secondary* min 22 moderate secondaries diverge at a narrow to moderate acute angle 44° - 56°. Angle uniform or increasing slightly towards the base, spacing variable, course variable.

Secondaries frequently branch towards the margin. *Tertiary* veins rare, percurrent, course convex, angle to primary obtuse. Higher order venation not preserved. Leaf rank 1r/2r. Teeth 1 order, ~5 teeth/cm, 1-2 teeth/secondary, spacing regular. Shape ST-CV, FL-CV. Sinus angular. Apices darkened towards leaf apex (where preservation is better). One apex appears spinose or chloranthoid, with a triangle of fused darkened material.

Remarks: Morphotype 2.35 bears a superficial resemblance to Morphotype 2.1, but differs in having craspedodromous, not semicraspedodromous secondary venation, disorganised, irregular coursed branching secondaries and spinose/rosoid teeth rather than cunonioid teeth. These features are characteristic of the Chilean endemic *Eucryphia glutinosa* Cav. (Eucryphiaceae) (Dickison, 1978; Hill, 1991a), however the identification of foliar material of *Eucryphia* sp. is dependent on cuticular data which is not available for this morphotype (Hill, 1991a). *Eucryphiaceous* wood has been found in coeval deposits on KGI (Poole *et al.*, 2001), therefore leaves of *Eucryphia* may be present in fossil assemblages.

Morphotype 2.36 (Figure 6.17: 4 - 5)

Material examined: Dragon Glacier *Almost complete* P.3001.83.a/b.

Differential characters: Elliptic leaf with two pairs of acute basal secondaries. Margin serrate with three teeth per secondary. Fimbrial vein. Base straight and acute. 5 orders of venation.

Description: Leaf arrangement appears simple. Lamina elliptic, ?symmetrical. Length 26mm, width 11mm. Length:width ratio 2.36:1. Area estimated 190.67 mm^2. Microphyll = 1 (100 %). Apex acute, estimated apical angle 61°. Base acute, estimated basal angle 64°. Petiole absent or not preserved. Margin crenate. *Venation* pinnate craspedodromous. *Primary* weak. Course slightly curved. *Secondary* 12 secondary alternate veins, diverging from midvein at narrow to wide acute angle 36° - 78° av. 59.6°. Divergence angle greater on left side of lamina and decreasing basally with an abrupt decrease in the basal secondaries. Two pair of acute basal secondaries. *Tertiary* vein category regular polygonal reticulate. Vein angle to primary is obtuse, angle increasing exmedially. *Fourth order* dichotomising. Areoles well developed, 4 or more sided. F.E.V's where observed are unbranched to 2 or more branched. Marginal ultimate venation probably looped, forming a fimbrial vein. Leaf rank 2r/3r. *Teeth* 2-3 teeth per secondary, size varies irregularly. Basal four intercostal areas have 3 orders of teeth upper intercostal areas have 2 orders of teeth. 7 teeth/cm in middle 50% of leaf. Spacing irregular. Tooth shape cc/cv, st/cv, apex rounded. Sinus shape rounded, rarely angular. Tooth indentation to margin 0.2-0.8mm. Teeth glandular. Principle vein is formed by a secondary branch. Course of principal vein is eccentric, running basal to tooth axis of symmetry. Origin of principal vein

deflected, secondary vein bifurcating to connect with an apical and basal secondary. Principal veins in subordinate teeth. Accessory veins not observed. Tooth type ?chloranthoid.

Remarks: This leaf type has not been described from King George Island. The cuneate base is suggestive of a compound leaf morphology, although there are no complete specimens to support this. According to Hickey and Wolfe (1975) pinnately veined leaves with chloranthoid teeth are present in the Magnoliidae and Hamamelididae. In the Hamamelididae the secondaries are congested towards the leaf base, which is not the case in this specimen, suggesting affinities with the Magnoliidae (e.g. Chloranthaceae or Illiciales).

Morphotype 2.37 (Figure 6.17: 6 - 7)

Material examined: Dragon Glacier *Large fragment* P.3001.36.2. Mt. Wawel *Small fragment* P.3010.4a.

Differential characters: Obovate leaf with a decurrent base. Secondaries have an irregular course. Margin serrate with CV-ST apices, that are darkened and glandular.

Description: Leaf organisation appears simple. Lamina ?asymmetrical, shape obovate or elliptic. Lamina length min 21 mm, width min 11 - 13 mm, length:width min 1.54:1 - 1.91:1. Area min 154 mm^2. Microphyll = 2 (100 %). Apex not preserved. Base appears decurrent, basal angle acute 41° - 57°. Petiole marginal, winged thickness 1.1 mm. Margin serrate. Venation pinnate craspedodromous. *Primary* thickness massive. Course straight. One primary vein and two secondaries originate at the leaf base. Secondary min 15 alternate to subopposite secondary veins diverging at a narrow acute to right angle 30° - 90°. One pair acute basal secondaries, otherwise angle smoothly increases toward base, spacing irregular, thickness increasing apically, fine to moderate. Weak intersecondaries. Tertiary veins poorly preserved ?percurrent. Leaf rank ?1 r. Teeth ?1 order, 1 – 2 teeth/secondary, spacing irregular. Apex angular, shape CC/CV, CV/RT, sinus angular. Teeth glandular. Principal vein course eccentric, origin deflected one branch entering tooth apically and one trending to sinus. Darkened ?glandular on apical side. Teeth increase in size apically. Indentation to midvein 0.2-1.1 mm.

Remarks: No similar leaves were found to compare with this morphotype.

Morphotype 2.38 (Figure 6.17: 8 - 11)

Material examined: Dragon Glacier *Large fragment* P.3013.17.

Differential characters: ?Obovate leaf, broadly spaced serrate teeth apically, no teeth in the basal three quarters of the leaf.

Description: Leaf arrangement appears simple. Lamina obovate, ?symmetrical. Length min 55 mm, width min 33 mm. Length:width ratio 1.67:1. Area min 1210 mm^2. Microphyll = 1 (100 %). Apex not preserved, margin trend suggests acute convex or truncate. Base acute, asymmetric, basal angle 63°. Petiole winged, thickness 1 mm, winged thickness 1.1 mm, length

min 11 mm. Petiole flares slightly towards base. Margin serrate. *Venation* pinnate craspedodromous. *Primary* thickness moderate. Course slightly sinuous. One primary vein and two secondary veins originate at leaf base. *Secondary* min 9 secondary alternate veins, diverging from midvein at a narrow angle 21° - 34°. Divergence angle greater on right side of lamina but otherwise uniform. Secondary vein course mirrors the margin trend. Spacing uniform or increasing towards base. *Tertiary* vein category regular polygonal reticulate, to alternate percurrent. Vein angle to primary perpendicular to obtuse, showing slight increase basally. *Fourth order* vein category regular polygonal reticulate. *Fifth order* vein category dichotomising and highest order present. Areoles moderately well developed and 5 or more sided. F.E.V's absent to 2 or more branched. Marginal ultimate venation ?looped. Leaf rank 2r/3r. *Teeth* one order, 1 tooth per secondary, ?angular apex, ?rounded sinus, indentation to margin min 1 mm. Principal vein course ?central. Origin of principal vein deflected, one secondary branch trends to the tooth, one trends apically following margin course. Accessory veins looped. No teeth in basal portion of leaf.

Remarks: The laterally directed tooth style is more typical of *N. plicata*, as is the low angle of secondary divergence (Scriven *et al.*, 1995). This is also consistent with the cuneate base shape and low angle of secondary divergence. The modern species *Atherospermum moschatum* Lab. V. of the Atherospermataceae family also possesses an obovate lamina morphology and secondary venation that mirrors the margin trend, although the secondary divergence angle is greater than in this morphotype. *Atherospermoxylon* has been described from the Tertiary of Seymour Island (Poole and Gottwald, 2001), therefore Atherospermataceae leaves may be present in the flora.

6.5 Nothofagaceae and forms attributed to Nothofagaceae

Morphotype 2.39 (Figure 6.19: 1 - 2)

1899 *Fagus dicksoni* Dúsen. (p. 95, plate 8, fig 14 – 16)

1908 Dúsen (plate 1, fig 12)

1937b Berry (p.93, plate 18, fig 1)

1986 Nothofagus dicksoni *(Dúsen) Tanai* (p. 523, Text-fig 8, g, p. 577, plate 13, fig 4, 8, 13, 17)

Material examined: Dragon Glacier *Large fragment* P.3007.16.

Differential characters: Ovate leaves characterised by a deeply toothed, almost lobed margin with large CV-CV teeth.

Description: Leaf arrangement appears simple. Lamina ?elliptic, symmetrical. Length min 35 mm, width min 22 mm. Length:width ratio min 1.59:1. Area min 513.33 mm^2. Microphyll = 1 (100 %). Apex acute, convex, apical angle 75°. Margin serrate toothed. *Venation* pinnate

craspedodromous, possibly semicraspedodromous in apex of leaf. *Primary* moderate. Course straight. *Secondary* min 15 secondary alternate to subopposite veins, diverging from midvein at moderate to wide acute angle 45° - 70° av. 57.14°. Divergence angle increases slightly towards base. Thickness is moderate to fine. Spacing irregular. *Tertiary* veins weakly percurrent, obtuse angle to primary. Prominent percurrent tertiaries cross intercostal area basally of sinus. Higher order venation not preserved. Leaf rank ?2r. *Teeth* 1 - 2 teeth per secondary vein, 3 teeth/cm, spacing irregular. Number of teeth increases from 1 per secondary in apical region to (compound) 2 per secondary in mid/basal region. Apex shape CV/CV, apex rounded points, sinus angular. Teeth indentation to midvein ~3 mm. Non-glandular teeth. Principal vein is a secondary vein, subordinate teeth served by a secondary branch. Accessory veins ?looped.

Remarks: The distinctive lobate teeth and pinnate craspedodromous venation are characteristic of *Nothofagus dicksoni* (Tanai, 1986). Tanai (1986) differentiated the leaf from *Fagus dicksoni* Dúsen by the presence of large elongate teeth, secondary veins centrally entering the teeth and a thick fimbrial vein along the margin. Tanai (1986) instead suggested affinities with the New Zealand *N. fusca* (Hook f.) Oerst., and *N. truncata* (Colenso) Cockayne. The fimbrial vein also allowed *N. dicksoni* to be distinguished from *N. simplicidens* Dúsen.

None of the descriptions of *N. dicksoni* mention abaxial branching of the secondary veins or the slightly irregular secondary course that is observed in specimen P.3007.16. Dúsen's (1899) 'Magellansländer' flora also included two forms assigned to the Araliaceae - *Rhoophyllum nordenskjöldi* Dúsen and *R. serratum* Dúsen. *Rhoophyllum serratum* is a palmately lobed toothed leaf, with a similar tooth style to *F. dicksoni* and it is possible that this morphotype might represent an apical fragment of *R. serratum*. However, no leaf bases are preserved for comparison and since there is no actual evidence for a palmate lamina in this morphotype, the leaf is considered to be most similar to *N. dicksoni*. However, this type of prominent serrated margin is not present in any of the modern species of *Nothofagus*, therefore this leaf morphotype is considered to have been placed in the wrong genus by Tanai (1986). Re-examination of the leaf within the context of the Fagaceae is required.

Leaves of the Nothofagaceae are generally characterised by uniform pinnate craspedodromous venation, percurrent tertiary venation, open looped or fimbrial marginal venation, freely ending veinlets that branch up to several times and a compound toothed margin (Romero and Dibbern, 1986; Hill and Read, 1991). A sinuous primary vein that is deflected after each secondary branch is often present (Hill, 1991b). This excludes the *Brassospora* subgenus, which is now endemic to New Caledonia and New Guinea, which has semicraspedodromous or brochidodromous venation and may be toothed or entire margined. Plicate vernation is exclusive and unique to deciduous species of modern *Nothofagus* (Hill *et*

al., 1996), therefore fossils which exhibit plicate vernation (or can be related to plicately folded leaves) are interpreted as deciduous. However, cladistic analyses suggests that the deciduous character has arisen numerous times in the history of Nothofagus and is not therefore an evolved, taxonomically significant character.

Family Nothofagaceae

Nothofagus Blume 1851

2.40 *Nothofagus* sp. 1 (Figure 6.18: 3 - 7)

Material examined: Dragon Glacier *Near complete* P.3001.131, .140, *Large fragment* P.3002.2; P.3001.155, .157; P.2810.18.

Differential characters: Ovate leaves with a sinuous primary. Margin almost lobed. Teeth have one primary tooth and a smaller secondary tooth with a rounded triangular since. Base often asymmetrical with a short slightly inflated petiole. Tertiaries are concentric with respect to the top of the petiole.

Description: Leaf arrangement appears simple. Lamina ovate, base asymmetrical. Length min 19 – 29 mm, width min 15 – 22 mm. Length:width ratio 0.90:1 - 1.71:1. Area estimated min 210 - 328.67 mm^2. Microphyll = 6 (100 %). Petiole normal to slightly inflated, marginal, thickness 0.6 - 0.7 mm, length min 4 - 25 mm. Margin serrate. *Venation* pinnate craspedodromous. *Primary* moderate to stout. Course straight to zigzag. One primary vein and four secondaries originate near the leaf base. *Secondary* min 11 - 15 alternate to subopposite secondary veins diverging at a narrow to wide acute angle 28°-90°. Angle smoothly increasing toward base, spacing regular or irregular, thickness fine to moderate. *Tertiary* veins opposite percurrent, rarely alternate percurrent. Course convex and/or sinuous, angle to primary obtuse, increasing basally. *Fourth order* alternate percurrent. Fifth order dichotomising. Areoles well developed. F.E.V's two or more branched. Marginal venation not observed. Leaf rank 3r/4r. *Teeth* 2 orders. 5 teeth/cm. Spacing regular. Indentation to midvein 0.5 - 2 mm. Apex angular, shape ST/ST or CV/ST, sinus angular to slightly rounded. Teeth non-glandular. Principal veins are second order, course central to basal, origin direct. Lower order teeth are served by secondary branches. Accessory veins ?joining with principal vein.

Remarks: The characteristic margin shape of this morphotype is similar to several *N.* sp. illustrated by Tanai (1986), in particular *N. variabilis* Dúsen. However, *N. variabilis* has a fimbrial vein and the tertiary venation is irregularly percurrent, sinuous or forking (Tanai, 1986), whilst the tertiary venation of this morphotype is strongly opposite percurrent. *Nothofagus microphylla* (Hill, 1991b; Scriven and Hill, 1996) from the Oligocene of Tasmania is comparable in size, base shape, number of secondaries, the apical decrease in secondary divergence angle and the high degree of primary sinuosity. The margin is also similar in being

almost lobed and having a double serration. The closest affinities of this leaf are with *N. microphylla.*

Nothofagus microphylla was moved from subgenus *Lophozonia* to *Nothofagus* on the basis of cuticular data not available for the original morphological description of the leaves (Scriven and Hill, 1996). The species was also subdivided into two groups, those leaves that conformed to the original morphological grouping and the new species *N. martinii* Scriven and Hill, which had plicate vernation and different cuticular characters (Scriven and Hill, 1996). Scriven and Hill (1996) also considered *N. microphylla* and *N. lobata* Hill to be the product of heterophyllous shoots. This morphotype conforms to the original morphological description of *N. microphylla* and shows no evidence for the plicate vernation of *N. martinii. Nothofagus microphylla* was considered to have affinities with *N. cunninghamii* (Hill, 1991b), a leaf of the *Lophozonia* subgenus, while *N. lobata*, the alternative leaf morphology of this species was compared to *N. nitida* (subgenus *Nothofagus*).

2.41 *Nothofagus* sp. 2 (Figure 6.18: 8 - 10)

Material examined: Dragon Glacier *Complete* P.3001.100.

Differential characters: Ovate microphyllous leaf. with a crenate, lobate margin. Primary vein is sinuous. Petiole almost double the width of the primary vein.

Description: Leaf organisation appears simple. Lamina ovate symmetrical. Lamina length 18 mm. Lamina width 11 mm. Length:width ratio 1.64:1. Estimated leaf area 132 mm^2. Leptophyll = 1 (100 %). Apex acute convex, apical angle 76°. Base obtuse convex, basal angle 94°. Petiolar attachment marginal, petiole is short and inflated, length 1.2 mm, width 0.8 mm. Margin is lobed, 1 - 2 mm indentation to margin and crenate. *Venation* pinnate and craspedodromous. *Primary* vein width at the leaf midpoint is 0.1 mm. The vein size is 0.9 % and is termed weak. Course zigzag, deflected after each secondary branching. One primary vein and two secondary veins originate at the leaf base. *Secondary* 13 subopposite to alternate secondaries diverging at narrow acute angle 28° - 48°. Basal secondaries are prominently bifurcating. Thickness is moderate. Vein spacing is approximately uniform with a slight increase towards the apex. Intersecondary veins are present but weak. *Tertiary* vein category alternate percurrent, course is sinuous. Vein angle to primary obtuse angle 100° - 150°, angle increases exmedially. *Fourth order* veins are regular polygonal reticulate. *Fifth order* veins are dichotomising and the highest order veins present. Areoles well developed and 4 or more sided. F.E.V's absent to 2 or more branched. Tertiaries are highest excurrent. Marginal ultimate venation ?incomplete loops. Teeth 1-2 orders. 12 teeth/cm. 4-5 teeth per secondary. Tooth spacing approximately regular. Teeth occur on apical and basal portion of lobes. Basal tooth shape cv/cv to cv/st. Apical tooth shape cv/st to st/st. Sinus angular. Tooth apex often darkened ?glandular. Apical termination of tooth is ?cassidate, dillenioid. Course of vein entering tooth is

central. Secondary vein enters principal tooth, secondary branches enter subordinate teeth. Accessory veins are looped or enter subordinate teeth. Leaf rank 3r.

Remarks: The lamina of this morphotype shows no evidence of plicate vernation suggesting that it is an evergreen form. Of the fossil *Nothofagus* species *N. crenulata* has the greatest similarity in terms of secondary venation, toothing style and petiole thickness, although the low resolution of the illustrations in Tanai (1986) makes detailed comparisons difficult. Tanai (1986) highlighted the affinities of *N. crenulata* Dúsen to *N. antarctica* (Forst) Oerst, in contrast to Dúsen (1899) who suggested affinities with *N. cunninghamii* (Hook f.) Oerst., and *N. betuloides* (Mirb.) Oerst.

The lobate toothed margin and relatively disorganised higher order venation are typical of the modern South American *Nothofagus antarctica* (subgenus *Nothofagus*), with the exception that the secondaries of *N. antarctica* generally terminate in the 'lobe' sinus rather than in the apex (Romero, 1980b; Hill and Read, 1991). This variation from the modern form might indicate an inaccurate identification or an evolutionary trend. However, one specimen illustrated by Romero (1980b; Figure 2, number 1) has a very irregularly toothed margin with secondaries that trend roughly to the apex of the lobate margin. Tanai (1986) considered *N. crenulata* from Chile to be closely related to *N. antarctica*, and this species does have sinuses vascularised by secondary veins. Alternatively the Nothofagaceae are known to hybridise and this variation from the normal form of *N. antarctica* form might represent an ancient hybrid or cline (Hill and Read, 1991). Poole (1987) reported hybrids with *N. pumilio* (Poepp. & Endl.) Oerst., in areas where the two species overlapped. This hypothesis is supported by the more ordered tertiary venation of this morphotype, which is more like *N. gunnii* (Hook f.) Oerst., and *N. pumilio* in character.

Other similar modern leaves include *N. obliqua* (Mirb.) Oerst., which has a lobate margin and branches apically and basally into subordinate teeth, although these are much less pronounced than in this morphotype or *N. antarctica*. The close affinities of this morphotype to both fossil species related to *N. antarctica* and to the modern species itself suggests that it belongs in the *Nothofagus* subgenus and is probably related to N. antarctica itself. Cuticular data is required to draw further comparisons.

2.42 *Nothofagus* sp. 3 (Figure 6.19: 1 - 2)

Material examined: Barton Peninsula *Small fragments* P.2145.1, .6.1. Potter Cove impression *Small fragments* P.232.15.1/.2/.3, .19.1, .21, .23, .25.1/.3-.6, .27.1/.2/.3, .28.

Differential characters: Elliptic or ovate leaves with a high density of secondary veins. Strongly percurrent tertiaries. Lamina often asymmetric. Angular plicate vernation.

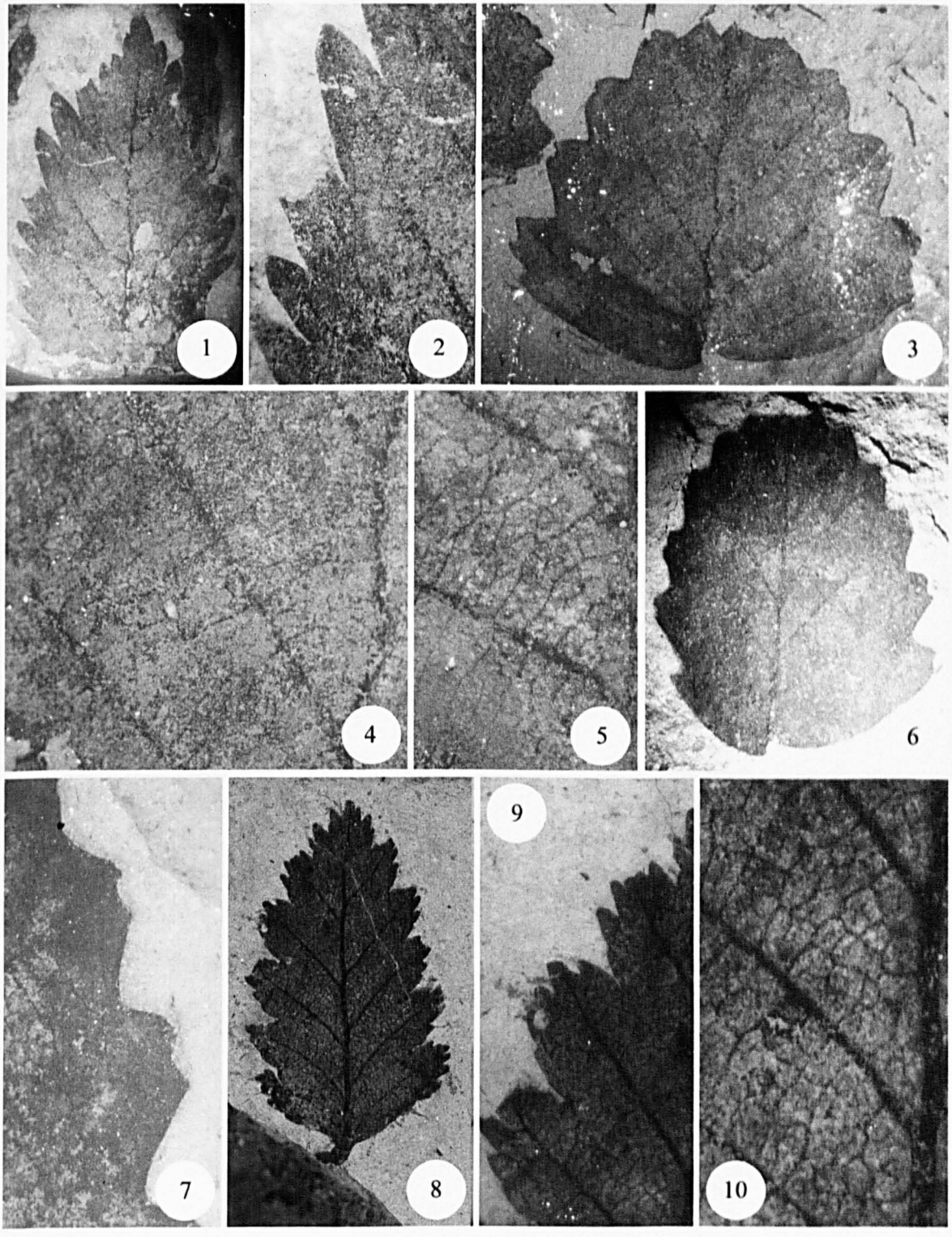

Figure 6.18. (1) - (2) Morphotype 2.39. (1). P.3007.16. x1.6. (2). Detail of marginal serrations. x5. (3) - (7). Morphotype 2.40. (3). P.3001.140.1. x2.7. (4). Detail of venation. x8.3. (5). P.3001.57.2. x9.4. (6). P.3001.131. x2.3. (7). Detail of margin. x5.7. (8) - (10). Morphotype 2.41. (8).P.3001.100. x3. (9). Detail of tooth architecture. x7.7. (10). Detail of venation. x4.2.

Description: Lamina organisation appears simple. Lamina ?symmetrical, ovate. Length min. 43 - 84 mm, width est. 34 - 60 mm. Length:width ratio est. min 2.7:1 - 1.3:1. Microphyll = 9 (56 %), notophyll = 6 (38 %), mesophyll = 1 (6 %). Apex convex acute 43°. Base convex wide acute 78°. Lamina has angular plicate vernation. Margin serrate. *Venation* pinnate craspedodromous. *Primary* weak. *Secondary* up to 27 secondaries in subopposite to opposite pairs. Divergence angle narrow acute 21° - 40°, increasing smoothly towards base. Secondary veins sometimes recurve apically. Spacing increases apically otherwise uniform. *Tertiary* thick opposite or mixed opposite and alternate percurrent, Convex to concave course. Perpendicular or obtuse to midvein. No higher order or marginal venation. *Teeth* two teeth per secondary vein, two orders. Shape CC-CV Sinus rounded. Principal vein enters teeth basally to centrally with a branch trending to the superadjacent secondary.

Remarks: This leaf has previously been described from Barton Peninsula (Tokarski *et al.*, 1987; Figure 8a/e). This morphotype has identical lamina and secondary venation form to *Nothofagus densi-nervosa* (Dúsen, 1899). Specimen P.232.25.1, has a similar style of decurrent secondary branching and angular plicate vernation to *N. magellanica* Engelhardt in Dúsen (1908) and should perhaps be separated as a different morphotype.

2.43 *Nothofagus* sp. 4 (Figure 6.19: 3 - 4)

Material examined: Dragon Glacier *Complete* P.3001.49. *Near complete* P.2810.22. 3. *Large fragment* P.2810.7, ?.22.4.

Differential characters: Ovate to elliptic leaves with angular plicate vernation. Up to 29 subopposite to alternate secondaries. Uniform spacing. Margin crenate, two orders of teeth and up to four teeth/secondary.

Description: Leaf organisation appears simple. Lamina ovate, symmetrical. Length min 31 - 38 mm, width 15 - 17 mm. Length:width ratio min 2.07:1 - 2.24:1. Area min 310 - 430.67 mm^2. Microphyll = 5 (100 %). Margin crenate. Plicate vernation. *Venation* pinnate craspedodromous. *Primary* thickness stout. Course slightly deflected after secondary branches. *Secondary* min 26 - 27 secondary alternate veins, diverging from midvein at narrow acute angle 45° - 94°. Divergence angle increases abruptly towards base. Angle may be greater on one side of lamina. Spacing regular. *Tertiary* veins not observed. *Teeth* 2 - 3 orders of teeth, 2-3 teeth per secondary, 12 teeth/cm, spacing irregular. Apex shape rounded, sinus rounded. Teeth non-glandular. Principal vein enters tooth basally rarely centrally. Venation of lower order teeth not preserved.

Remarks: Morphotype 2.43 is differentiated from Morphotype 2.42 in having a higher angle of secondary divergence and less curvature of the secondaries. It also lacks the strongly

percurrent tertiaries of 2.42. No good margin preservation has been found in Morphotype 2.42 to aid comparison of the leaves but further studies might be able to group these two morphotypes. The crenate teeth with basally eccentric vascularisation in Morphotype 2.43 is characteristic of *Nothofagus densinervosa* (Tanai, 1986; Plate 12, Figure 11). Leaves described as *N. pulchra* Dúsen from Seymour Island may also be related to this morphotype, although the preservation is too poor for close comparison (Tanai, 1986). According to Tanai (1986) *N. densinervosa* is closely related to the South American *N. pumilio* (subgenus *Nothofagus*). *N. alpina* lacks the distinctive tooth architecture of *N. densinervosa* but has the most similar lamina form to *N. densinervosa* of any of the modern *N.* sp (Hill, 1991b).

2.44 *Nothofagus* sp. 5 (Figure 6.19: 5 - 8)

Material examined: Point Hennequin *Large fragment* P.3001.74. .125.2.

Differential characters: Ovate leaf with narrow basal intercostal areas. Secondary veins branch close to the margin trending to apical and basal subordinate teeth. Lowermost secondaries are convex up, more apical secondaries become more concave.

Description: Leaf organisation appears simple. Lamina ovate, ?symmetrical. Length min 56 mm, width min 29 mm est. 42 mm, length:width ratio min 1.33:1. Area est. 1568 mm^2. Microphyll = 2 (100 %). Apex convex, apical angle ??. Base convex, basal angle ??. Margin crenate. Petiole marginal. *Venation* pinnate craspedodromous. *Primary* moderate thickness, course curved. *Secondary* min 11 moderate alternate secondaries diverge at a narrow to moderate acute angle 22° – 54°. Angle more acute on left side due to preservation. Angle smoothly increasing towards base. Spacing abruptly decreases between basal secondaries and

margin. Course curved, decurrent branching at leaf base. No intersecondaries. 1 pair of simple agrophic veins. Tertiary venation ?mixed opposite and alternate percurrent. Course sinuous, angle to primary obtuse, increasing basally. Fourth order venation regular polygonal reticulate, poor differentiation from tertiaries. Areolation well developed, 5 or more sided. F.E.V's unbranched – 2 or more branched. Darkened margin possibly indicates a fimbrial vein. Leaf rank 2r/3r. Teeth 2 orders, 3 – 5/secondary, 5/cm, spacing irregular. Shape CV-CV, FL-CV. Sinus rounded, apex rounded. Slight darkening at apex may indicate glands. Principal vein is a secondary or a secondary branch. Course central or apical. Origin direct or deflected. Accessory veins not preserved.

This morphotype strongly resembles *Nothofagus hillii* Dutra (1997), in having reduced basal intercostal areas, basally decurrent secondary branching that becomes normal apically and a similar number of teeth per secondary. The specimen described by Dutra (1997) is too poorly preserved to compare the distinctive tooth style with a lobe-like margin that has one tooth apical

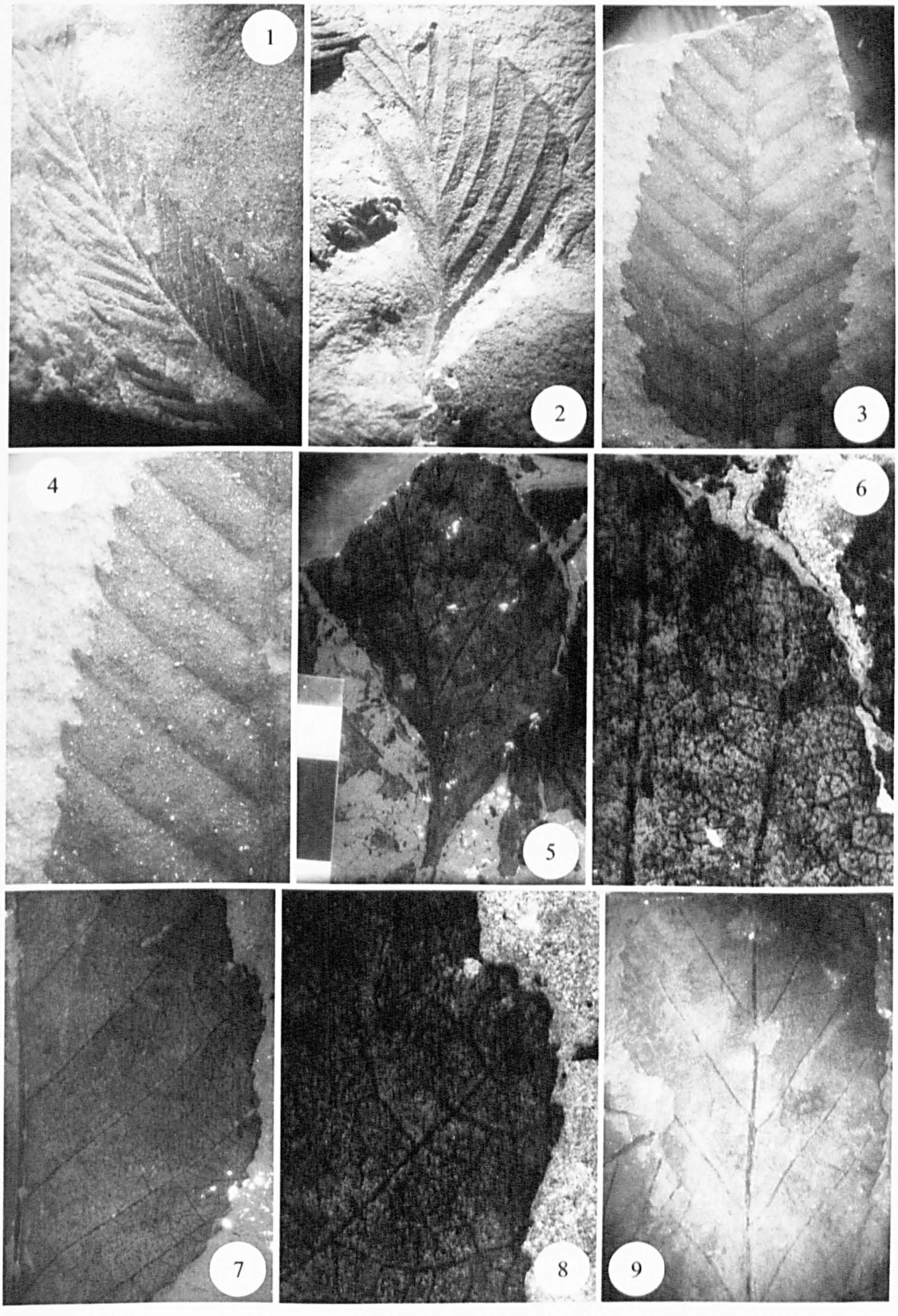

Figure 6.19. (1) - (2). Morphotype 2.42. (1). P.232.21. x1.6. (2). P.232.25. x1.6. (3) - (4) Morphotype 2.43. (3). P.3001.49b. x2.5. (4). Detail of marginal crenations. x3.8. (5) - (8) Morphotype 2.44. (5). P.3001.125.2. x1.6. (6). Detail of marginal crenations. x4.2. (7). P.3001.74. x1.9. (8). Detail of marginal venation and tooth architecture. x5.2. (9). Morphotype 2.45. x1.8.

to the principal tooth and several subordinate basal teeth. The apical and basal branching of the secondary veins into subordinate teeth in this morphotype is present in the modern South American *N. obliqua* and *N. glauca* (Romero, 1980; Plate 1, 4 and 6) suggesting affinities with the *Nothofagus* subgenus.

2.45 *Nothofagus* sp. 6 (Figures 6.19: 9 and 6.20: 1)

Material examined: Dragon Glacier *Large fragments* P.3001.88, .106. *Small fragment* P.2810.5.1.

Differential characters: Elliptic leaf with ~four small acute serrations per secondary. Secondary vein angle uniform, secondaries send a strong branch apically prior to entering the tooth.

Description: Leaf organisation appears simple. Lamina ?elliptic to ovate, ?symmetrical. Length min 21-81 mm, width min 10-50 mm. Length:width ratio estimated min 1.17-1.62:1. Area min 140 mm^2. Microphyll = 2 (66 %), notophyll = 1 (30 %). Margin serrate. *Venation* pinnate craspedodromous. *Primary* thickness weak. Course straight. *Secondary* min 7 secondary alternate veins, diverging from midvein at narrow acute angle 50° - 64°. Divergence angle greater on right side of lamina and decreasing towards base. Spacing regular. *Tertiary* vein category ?percurrent. Vein angle to primary ?obtuse. Marginal ultimate venation possibly looped. *Teeth* dark glandular, apex angular, shape RT/RT, sinus angular. Possibly mucronate, similar to salicoid tooth type but preservation too poor to define.

Remarks: The distinctive margin style of this morphotype is characteristic of *Nothofagus lobata* (Hill, 1991b), but Morphotype 2.45 differs in having at least 12 secondary veins, compared to the maximum 10 of *N. lobata*. The tertiary venation of both leaves is weakly percurrent and they are of a similar size. No higher order venation details were provided by Hill (1991b) for more detailed comparisons.

2.46 *Nothofagus* sp. 7 (Figure 6.20: 2 - 4)

Material examined: Dragon Glacier *Complete* P.3001.114.2. *Near complete* P.3001.37, .144.

Differential characters: Ovate microphyllous leaves with angular plicate vernation. Secondaries branch within margin to enter marginal teeth. Higher order venation poorly preserved.

Description: Leaf organisation appears simple. Lamina ovate, symmetrical. Length min 12 - 28, width 12 - 23 mm. Length:width ratio min. 1:1 – 1.22:1. Area min 104 - 429.33 mm^2. Nanophyll = 1 (33%), microphyll = 2 (67 %). Margin crenate. Plicate vernation. *Venation* pinnate craspedodromous. *Primary* vein thickness weak. Course deflected after secondary branching. *Secondary* min 12 – 14 secondary alternate veins, diverging from midvein at narrow to moderate acute angle 40° - 69°. Divergence angle increases abruptly towards base. Spacing

regular. *Tertiary* veins not observed. Teeth 1 – 2 orders of teeth, 2 – 3 teeth per secondary, 9 teeth/cm, spacing regular. Apex shape rounded FL/CV – CV/CV, sinus rounded - angular. Apex ?non-glandular. Secondary vein appears to branch equally into two main teeth.

Remarks: Rounded angular plicate vernation, small leaf size and secondary veins branching close to the margin are characteristics of two modern deciduous *Nothofagus* sp. - *N. gunnii* and *N. pumilio* (although plicate vernation is not considered to be a taxonomically significant character). Although Morphotype 2.46 has a similar margin to *N. pumilio* the teeth are less pronounced and more regular than *N. pumilio* suggesting that it is more similar to *N. gunnii* (Hill and Read, 1991). The leaves of morphotype 2.46 also differ from the mature foliage of *N. gunnii* because they do not possess the characteristic large, rounded triangular teeth. In contrast juvenile foliage of *N. gunnii* has a marginal morphology similar to *N. pumilio* (Hill, 1984; Hill and Read, 1991) and concave up secondaries both characters which occur in this morphotype.

According to Tanai (1986) the free ending veinlets of both modern species are unbranched or once branched, this is clearly not the case in the specimens illustrated by Hill and Read (1991; p. 52, Figures 43 – 51) which branch up to several times, a feature which can be observed in the fossils (Figure). *N. gunnii* appears to have more organised tertiary venation than *N. pumilio* but this detail is not available in the fossils. Possible strong basal secondary branches in specimen P.3001.137 are also present in juvenile N. gunnii and to a lesser extent in N. pumilio.

Although this morphotype has affinities with both *N. pumilio* and *N. gunnii*, the closest morphological similarity seems to be with the juvenile *N. gunnii* (e.g. Hill and Read ,1991; Figure 48), therefore it is grouped with the *Fuscospora.* Cuticles of *N. gunnii* are extremely thin, which may explain the poor preservation of these fossils.

2.47 *Nothofagus* sp. 8 (Figure 6.20: 5 - 6)

Material examined: Mt. Wawel *Near complete* P.3010.6a/b.

Differential characters: Ovate leaf. Margin serrate, apices CC-CC, FL-CC. One order of teeth.

Description: Leaf organisation appears simple. Lamina ovate to elliptic, ?symmetrical, base asymmetric. Length 21 mm, width 17 mm, length:width ratio 1.24:1. Microphyll = 1 (100 %). Apex convex, apical angle obtuse 98°. Base convex, basal angle obtuse 102°. Petiole marginal. *Venation* pinnate craspedodromous. *Primary* thickness weak. *Secondary* min 15 opposite-alternate moderate secondaries diverge at a narrow to moderate acute angle 30° - 54°. Angle increasing smoothly towards base. Spacing decreases towards base. Intercostal area between basal secondaries and margin greatly reduced. Weak intersecondaries. Tertiary and higher order venation not preserved. Leaf rank 3r. Teeth 1 orders, 1 tooth/secondary, spacing regular. Shape

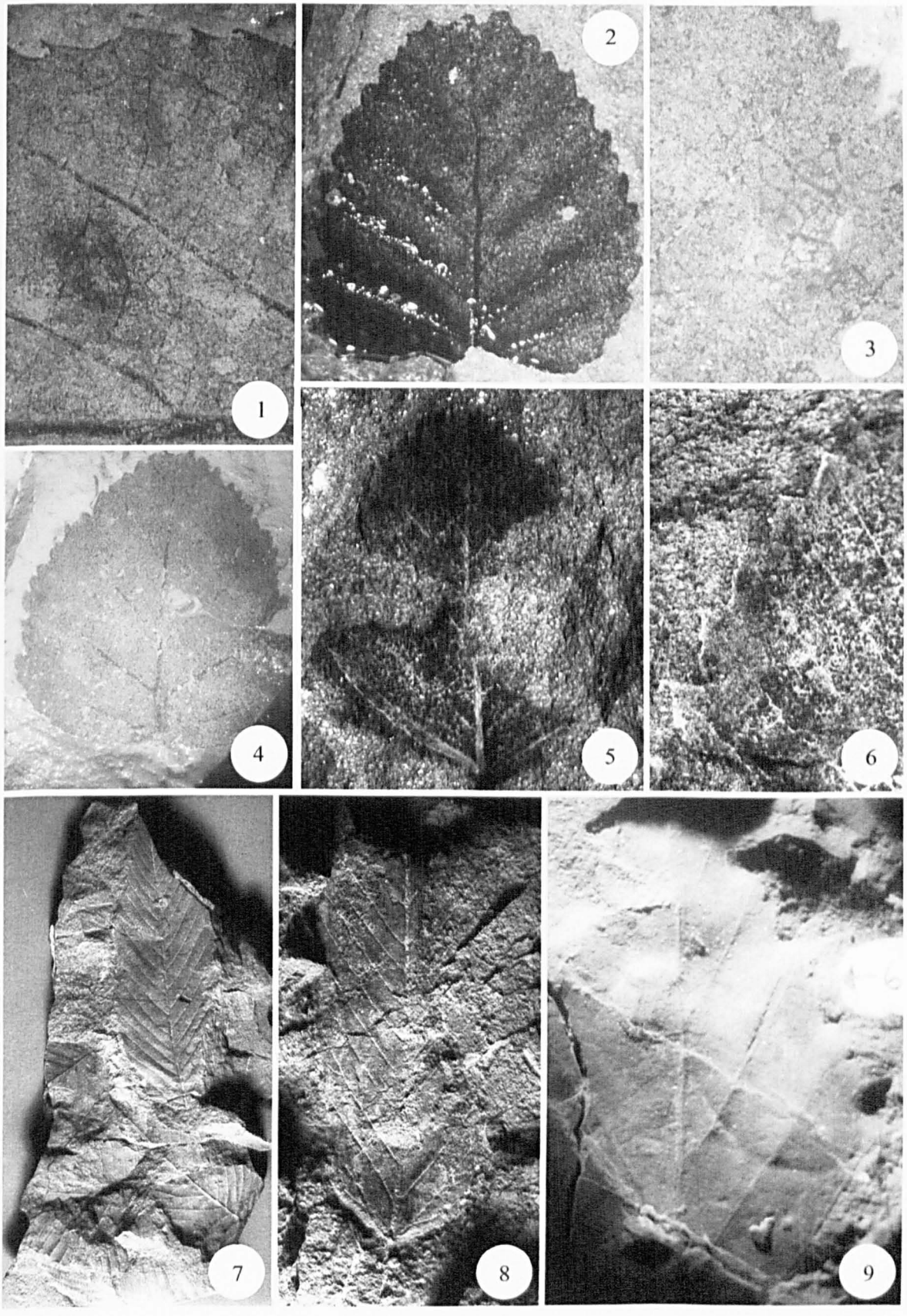

Figure 6.20. (1). Morphotype 2.45. Detail of marginal serrations. x5. (2) - (4) Morphotype 2.46. (2). P.3001.114. x4.8. (3). Detail of higher order venation. P.3001.137. x.6. (4). P.3001.137. x1.7. (5) - (6) Morphotype 2.47. (5). P.3010.6. x2.9. (6). Detail of marginal serration. x4. (7) - (8) Morphotype 2.48. (7). P.2799.8.1. x0.4. (8). P.2799. 28. x1. (9) Morphotype 2.49. G.458.1.1. x2.2.

ST-CC, CV-RT. Sinus shape angular to slightly rounded. Apex ?simple. Principal vein course central, origin direct.

Remarks: The leaf is has very similar lamina shape, size and secondary venation style to *N. variabilis* Dúsen (e.g. Tanai, 1986; Plate 14, Figure 12). The leaf margin appears to be dominantly uniserrate rather than doubly serrate but this may be due to the poor level of preservation. Marginal whitening observed in morphotype 2.47 may be the well developed fimbrial vein described by Tanai (1986). Two of the leaves illustrated as *N. variabilis* by Romero and Dibbern (1986; Plate 1, Figures 5 and 6) and one illustrated by Tanai (1986; Plate 14, Figure 11) actually resemble *N. microphylla* (Hill, 1991b) in their margin shape and there may be some overlap between these species.

Tanai (1986) considered that *N. variabilis* was most similar to the New Zealand *N. fusca,* differing from the South American forms in having secondary veins that terminated in the sinus rather than apex of the marginal serrations. In contrast, Romero and Dibbern (1986) suggested affinities with *N. glauca* and *N. obliqua* based on lamina shape, margin and venation characteristics. The presence of a possible fimbrial vein, differentiates Morphotype 2.47 from these latter two species (Hill and Read, 1991) and supports the interpretation of Tanai (1986). This leaf is grouped with *N. variabilis.*

2.48 *Nothofagus* sp. 9 (Figure 6.20: 7 - 8)

Material examined: Cytadela (Platt Cliffs) *Small fragment* G.309.15. Vaureal Peak *Large fragments* P2799.1-3, .5-6,.8-11, .13, .15-18, .20, .22-23, .26-28.

Differential characters: Ovate leaves with up to 36 secondary veins diverging at a narrow to moderate acute angle. Secondaries occasional branch abaxially, especially the basal pair.

Description: Lamina organisation appears simple. Lamina lanceolate to ovate symmetrical, length min. 26 - 110 mm, width min. 13 - 40 mm. Microphyll = 15 (88 %), Notophyll = 2 (12 %). Apex acute, apical angle 40 - 51°. Base symmetrical, convex, base angle wide acute 65-78°. Petiole normal, minimum length min. 12 mm width 1.5 mm. Margin serrate. *Venation* pinnate craspedodromous. *Primary* moderate to stout, course straight or slightly curved. *Secondary* minimum 7-18 sub-opposite pairs of secondary veins; narrow to wide acute divergence angle 40 - 60°, uniform or decreasing apically; secondaries are moderate thickness, course straight; secondaries may branch especially in basal pair. straight non-paired secondary veins. *Secondaries* occasionally branch towards the margin, particularly in the basal pairs. *Tertiary* rare weakly percurrent tertiaries with a moderate acute angle of divergence. No higher order vein detail observed. *Teeth* indentation to midvein ~1mm, two orders of teeth, spacing and

number of teeth uncertain due to poor margin preservation (?4 per cm), tooth shape straight acuminate, ?rounded sinus, tooth apical angle acute, teeth are simple.

Remarks: The extremely high number of secondary veins and the regular nature of the craspedodromous venation are typical of *Nothofagus subferruginea* (Dúsen) Tanai, although the margin is not sufficiently well preserved to determine whether the leaves possess the characteristic double serration. This morphotype also differs in having a larger lamina (length < 110 mm, width < 40 mm). *N. subferruginea* is one of the most frequently described fossil leaf morphologies from King George Island but these associations are generally based on incompletely preserved leaves with little margin preservation, and the leaves often don't conform to Tanai's (1986) description of a leaf with a doubly serrate margin. For example, Troncoso (1986) described craspedodromous leaves with compound teeth with ?up to four teeth/secondary which he referred to *N. subferruginea* as did Li (1994; Plate 1, Figure 4; Plate 2, Figure 1(b). At least one of figured leaves is more suggestive of a double serration (Li, 1994; Plate 1, Figure 1a), although only a few of the leaves described by Li (1994) conform to the minimum 10 subopposite veins (Li, 1994; Plate 1, Figure 4) (Tanai, 1986). This morphotype is therefore similar to *N. subferruginea*

2.49 *Nothofagus* sp. 10 (Figures 6.20: 9 and 6.21: 1)

Material examined: Dragon Glacier *Small fragment* P.3001.172. Fossil Hill U4 *Large fragment* G.458.1.1. Potter Cove Impression *Small fragment* P.232.20.1.

Differential characters: Ovate leaves with doubly serrate margins. ?Angular teeth with shape CC-CV, CC-RT. Sinuses rounded. Secondaries recurve apically before entering teeth. ?Partially developed fimbrial vein.

Description: Leaf arrangement appears simple. Lamina ovate to elliptic, ?symmetrical. Length min 35 mm, estimated width 30 mm. Length:width ratio min 1.17:1. Area min 700 mm^2. Microphyll = 6 (67 %), notophyll = 2 (22 %), mesophyll = 1 (11 %). Apex and base not preserved. Margin serrate. *Venation* pinnate craspedodromous. *Primary* thickness stout, course straight. *Secondary* min 12 alternate secondary veins, diverging from midvein at a narrow acute angle 26° - 36°. Divergence angle uniform, spacing uniform. Higher order venation not preserved.

Remarks: Doubly serrate margins are present in *Nothofagus subferruginea*, *N. magelhaenica* (Engelhardt) Dúsen and *N. variabilis*. All of these species differ from morphotype 2.49 in having much broader tooth apices that are oriented at a more obtuse angle to the margin. The Australian species *N. moorei* (F. v. Muell.) Krasser has similar apically oriented marginal serrations to this morphotype as well as a partially formed fimbrial vein. No higher order venation is preserved in the fossils for further comparison. *N. moorei* is the only

similar leaf to this morphotype, suggesting that the leaves have affinities with the subgenus *Lophozonia.*

2.50 *Nothofagus* sp. 11 (Figures 6.21: 2 - 11)

Material examined: Dragon Glacier *Near complete* P.2810.18, P.3001.11, .84, .132, .136, .148, .170. *Large fragments* G.9.2, ?.3; P.3001.8, .38, .42, .89.1, .112, .131, .164, .168. *Small fragment* P.3001.139. Smok Hill *Complete* P.1404.17, .19, .20.1.

Differential characters: Highly variable ovate to obovate leaves with a convex base and crenate to serrate margins. Angular plicate vernation. Secondary angle increasing basally, course often concave, recurving apically towards margin. Up to 5 teeth per basal secondary.

Description: Leaf organisation appears simple. Lamina ovate to obovate, symmetrical, base occasionally asymmetrical. Length 32 – 34 mm, width 19 mm estimated 36 mm, length:width ratio 0.94:1. Size class microphyll to notophyll. Apex acute to obtuse convex, apical angle 100°. Base convex to concavo-convex, basal angle acute to obtuse 80° - 98°. Petiole is marginal. Petiole thickness 0.5 mm, length up to 6 mm. Margin crenate to slightly serrate. *Venation* pinnate craspedodromous. *Primary* thickness weak to moderate. Course curved or straight and often deflected after secondary branches. One primary vein and min 2 secondary veins originate at the leaf base. *Secondary* min 7 – 16 secondaries secondary veins, diverging from midvein at narrow to moderate acute angle 12° - 46°. Angle increasing smoothly basally. Basal intercostal area reduced in size relative to other intercostals. Vein spacing ?uniform or increasing towards base. No intersecondaries. Secondaries become more concave/recurved basally. Branching style straight apically, decurrent basally. Tertiary loops form along basal secondaries. *Tertiary* vein category mixed opposite and alternate percurrent, course straight to sinuous, obtuse angle to primary, increasing basally. Tertiaries somewhat concentric around top of petiole. *Fourth order* vein category alternate percurrent. *Fifth order* vein category ?regular polygonal reticulate or dichotomising. *Areolation* well developed, 4 - 5 sided. *F.E.V's* unbranched to 2 or more branched. Leaf rank 3r/4r. *Teeth* < 3 orders, 2 – 6 teeth/secondary, 4 teeth/cm,, spacing irregular. Shape CC-CV, CV-CV or ST-CV. Sinus angular to slightly rounded, apex rounded. Tooth indentation to margin 0.2 - 1.1 mm. Apex ?glandular. Principal vein is a secondary or secondary branch. Course of secondary in principal tooth is central or basal, merging with a darkened sinus ?incomplete fimbrial vein. Origin of vein direct, secondary branches enter subordinate teeth. Accessory veins ?incomplete. Sinus is darkened ?glandular and actual termination of secondary vein in principal tooth is often difficult to resolve.

Remarks: The lamina shape of this morphotype is highly variable from ovate to more obovate forms and the main grouping is based on the presence of compound crenations, percurrent tertiary venation and an increased number in the basal margins. Plicate vernation is not observed in all leaves, but a faint curvature is often observed in the intercostal areas of

leaves that lack this character. This is one of the dominant leaf morphologies present at Point Hennequin (besides morphotypes 1.1 and 2.1).

This morphotype possesses some features of *N. variabilis* Dúsen, such as increasing secondary divergence towards the base, and a broad convex or cordate base but the tooth style is less angular. Specimens P.3001.8 and P.3001.139 with a distinctive obovate morphology bear a strong resemblance to *N. johnstonii* (Hill, 1983; Hill, 1991b), which is comparable in size, variability of lamina shape, number of secondary veins and tooth architecture. The leaves also have a high number of serrations on the basal margin. The leaf apices are not spinose but may be glandular and *N. johnstonii* is not described as having plicate vernation (Hill, 1983). Since *N. johnstonii* is closely related to *N. cunninghamii* which does not have plicate vernation.

N. alesssandri Espinosa has the closest lamina shape to this morphotype as well as percurrent tertiary venation that is concentrically arranged with respect to the top of the petiole, but it also has a greater number of secondary veins and reduced teeth (Romero, 1980; Hill and Read, 1991). The morphotype cannot be satisfactorily grouped with any of the modern or ancient fossil *N.* sp. *N.* johnstonii shares many architectural features but lacks the plicate vernation of this morphotype. The teeth are also more distinctly serrate. Based on comparisons with *N. johnstonii* the leaf is grouped with the *Lophozonia* subgenus.

2.51 *Nothofagus* sp. 12 (Figure 6.22: 1 - 9)

Material examined: Dragon Glacier Near complete ?P.3001.93, .108, .128, .157, .177, P.3013.30. Large fragment P.3001.90, P.3007.5, .9.

Differential characters: Ovate to lanceolate leaf with a basal pair of agrophic secondary veins. Tertiaries are strongly percurrent. Margin serrate up to 5 teeth/secondary. Principal tooth terminating in a swollen glandular apex. Secondaries branch apically and basally close to margin to join with tertiary veins branching from the adjacent secondary or to terminate in a subordinate tooth.

Description: Leaf organisation appears simple. Lamina ovate, symmetrical. Length min 60 - 142 mm, width up to est. 44 - 74 mm, length:width ratio 1.92:1. Area est. up to 7005.33 mm^2. Microphyll to mesophyll. Apex straight, apical angle acute to obtuse 48° - 96°. Base obtuse convex, basal angle est. 102° - 110°. Margin serrate. Petiole marginal. *Venation* pinnate craspedodromous. *Primary* thickness moderate. Course straight. *Secondary* min 13 - 20 moderate alternate secondaries, diverge at a narrow to moderate acute angle 24° - 61°. Angle increasing smoothly basally. Spacing uniform or greater in mid portion of lamina. 1 pair of simple agrophic veins may be present. No intersecondaries. *Tertiary* vein category mixed opposite and alternate percurrent. Vein course straight to sinuous. Vein angle to primary obtuse, increasing exmedially basally. *Fourth order* vein category alternate percurrent. *Fifth order* vein

category ?dichotomising but possibly regular polygonal reticulate with the 6th order veins dichotomising. *F.E.V's* unbranched to 2 or more branched. *Areolation* well developed 4 – 5 sided. *Marginal ultimate venation* ?looped. *Leaf rank* 4r. *Teeth* 3 - 5 teeth/secondary, 3 orders, 7 teeth/cm, spacing regular to irregular. Tooth shape RT-CV, CC-RT CC-CV, ST-CC. Sinus rounded, apex angular to rounded, glandular. Tooth type uncertain, secondary vein expanded in apex like a dillenioid tooth. Principal vein is a secondary, course central to basal, origin direct, accessory veins ?looped or incomplete. Secondaries become sinuous towards the tooth. Secondary branches converge from the abaxial and adaxial sides of two adjacent secondaries and then branch to serve the subordinate teeth. Indentation to midvein 1 – 6 mm.

Remarks: This morphotype is unusual in its size range (length 30 – 140 mm) and in the good marginal preservation. The leaves are probably related to previous pinnate craspedodromous leaves described as *N.* sp from Point Hennequin (Zastawniak, 1981; Zastawniak *et al.*, 1985) but many of these leaves lack marginal characters. The venation, margin architecture and number of teeth in this morphotype are comparable to *N. johnstonii* Hill and *N. tasmanica* Hill from the Oligocene of Tasmania, although the largest leaf of *N. johnstonii* is 5.2 mm and of *N. tasmanica* is 9 cm (Hill, 1983). The tooth configuration of *N. johnstonii* (Hill and Read, 1991) with a large principal tooth oriented at 30° – 40° to the midvein and the second subordinate tooth oriented nearly at right angles to the midvein is sometimes apparent in *N. johnstonii.* More detailed comparisons are not possible due to the small size of the leaf images.

The swollen termination of the secondary vein in the principal tooth resembles the dillenioid and platanoid tooth types described by Hickey and Wolfe (1975). This might imply closer affinities of this morphotype to the Hamamelidales, Dilleniaceae or Actinidiaceae.

2.52 *Nothofagus* sp. 13 (Figure 6.22: 10)

Material examined: Cytadela (Platt Cliffs) *Small fragment* G.309.15. Vaureal Peak *Large fragments* P2799.8, .27.2.

Differential characters: Obovate leaves with frequent branching of the secondary veins and prominent intersecondaries. Margin at least doubly serrate, with up to four teeth/secondary.

Description: Leaf organisation appears simple. Lamina elliptic to obovate, symmetrical. Length min 40 - 55 mm, width est. 30 - 36 mm, length:width ratio 1.33:1 – 1.53:1. Area 1222 – 1621 mm^2. Notophyll = 2 (100 %). Base and apex absent. Apex ?convex. Base ?acute convex, midvein 0.75 - 1 mm. Shape ST-ST, ST-CV. Angular sinus, apical angle acute. Principal vein is a secondary or a secondary branch. Course ?slightly eccentric, apical. Origin direct.

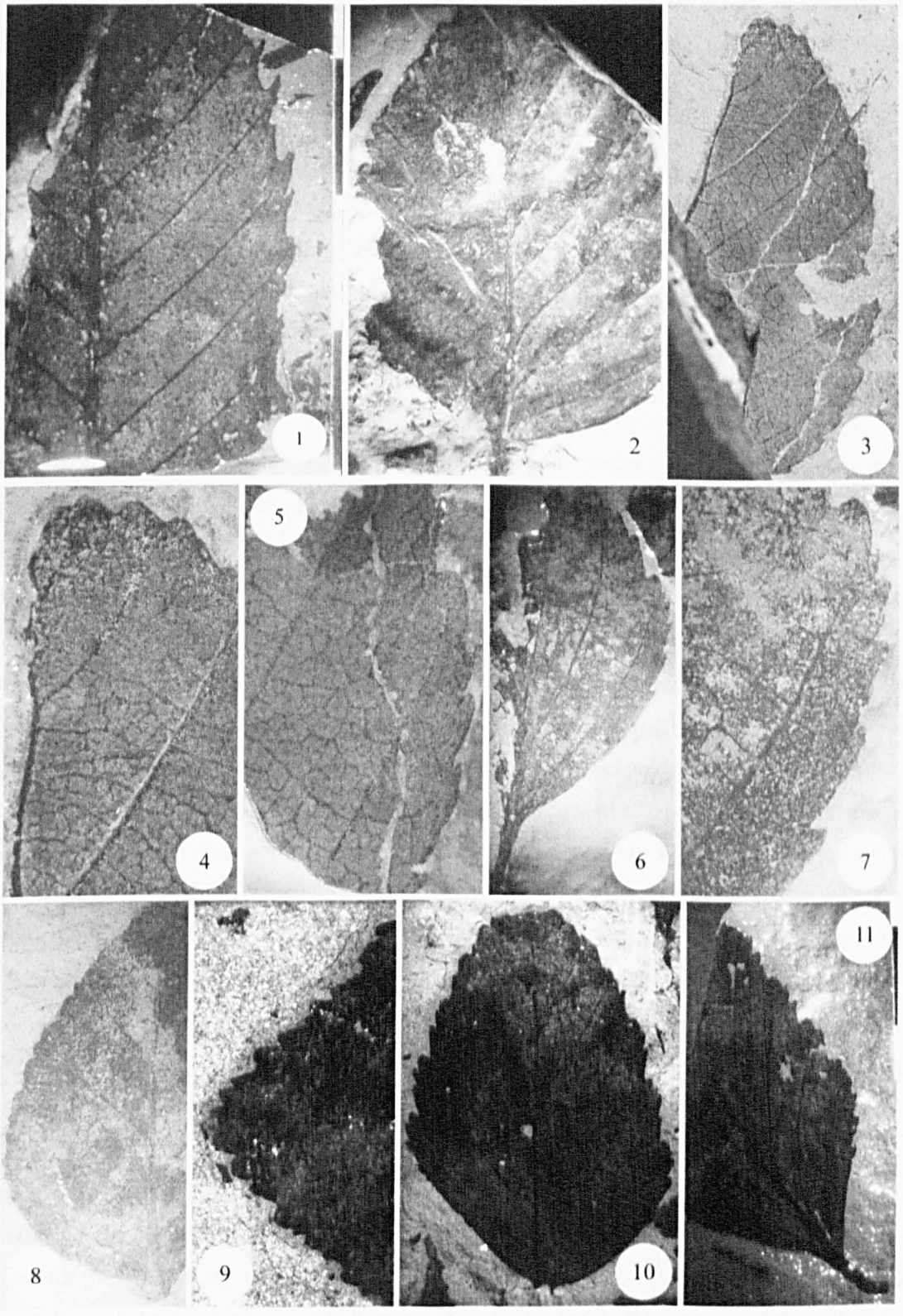

Figure 6.21. (1). Morphotype 2.49. P.3001.172. (2) - (11) Morphotype 2.50. (2). P.3001.131. x1.6. (3). P.3001.38. x2.4. (4). Detail of apex. x5.8. (5). Detail of basal margin crenations for comparison with P.3001.8. x5.5. (6). P.3001.8. x1.8. (7). Detail of basal margin crenations. x5. (8). P.3001.57.3b. x2.6. (9). Apical detail. P.3001.3. x7. (10). P.3001.42.3. x2.8. (11). P.3001.25. x1.5.

Remarks: These leaves are from the same locality as leaves assigned to Morphotype 2.48, that is similar to *N. subferruginea,* but differ in having an obovate to elliptic lamina, frequent abaxial branches of the secondary veins and strong intersecondaries and multiple rather than the double serrations of Morphotype 2.48.

2.53 *Nothofagus* sp. 14 (Figure 6.23: 1 - 4)

Material examined: Dragon Glacier *Almost complete* P.3001.47, .64.

Differential characters: Elliptic leaf with high length:width ratio, pinnate craspedodromous to eucamptodromous venation and plicate vernation. Tertiaries percurrent. 2 orders of serrate teeth with up to four teeth/secondary.

Description: Leaf organisation appears simple. Lamina elliptic, symmetrical or asymmetrical. Length min 48 - 68 mm, width min 20 mm. Length:width ratio 2.4:1 - 3.4:1. Area min 640 – 906.67 mm^2. Microphyll = 2 (100 %). Apex ?acute convex, slightly asymmetric (P.3001.47), estimated apical angle 48° - 53°. Base acute, slightly asymmetric, estimated basal angle 45° - 48°. Petiole absent. Margin serrate toothed. Rounded plicate vernation. *Venation* pinnate craspedodromous to eucamptodromous. *Primary* stout. Course curved. One primary vein and ?two secondary veins originate at leaf base. *Secondary* min 20 - 22 secondary opposite to alternate veins, diverging from midvein at narrow to moderate acute angle 21° - 47°. Divergence angle sometimes greater on one side of lamina. Angle ~uniform or decreasing apically. Spacing uniform. *Tertiary* vein category opposite percurrent. Vein angle to primary obtuse, increasing basally. Higher order venation not preserved. *Leaf rank* ?3r. *Teeth* very poorly preserved. ?3 teeth per secondary vein. Teeth non-glandular. Principal vein not observed.

Remarks: The slightly irregular secondary vein course of P.3001.64 and the absence of plicate vernation in that specimen suggest that the leaf may be more closely allied with morphotype 2.45. However, P.3001.64 has tertiaries that have an increasing angle to the primary exmedially rather than a decreasing angle to the primary and the tertiaries are also more strongly percurrent. P.3001.64 also has more rounded teeth than Morphotype 2.45.

The low angle of secondary vein divergence and plicate vernation of this morphotype is very similar to the deciduous Eocene *Nothofagus plicata* Scriven, McLoughlin and Hill, from Australia (Scriven *et al.*, 1995; McLoughlin, pers comm 2001). However *N. plicata* only has one order of teeth and craspedodromous venation rather than the multiple teeth and craspedodromous to eucamptodromous venation of this morphotype. The two leaf types cannot therefore be grouped. Dutra (1997) also described leaves with affinities to *N. plicata* although basal angle 49°. Petiole absent. Margin serrate. *Venation* pinnate craspedodromous. *Primary*

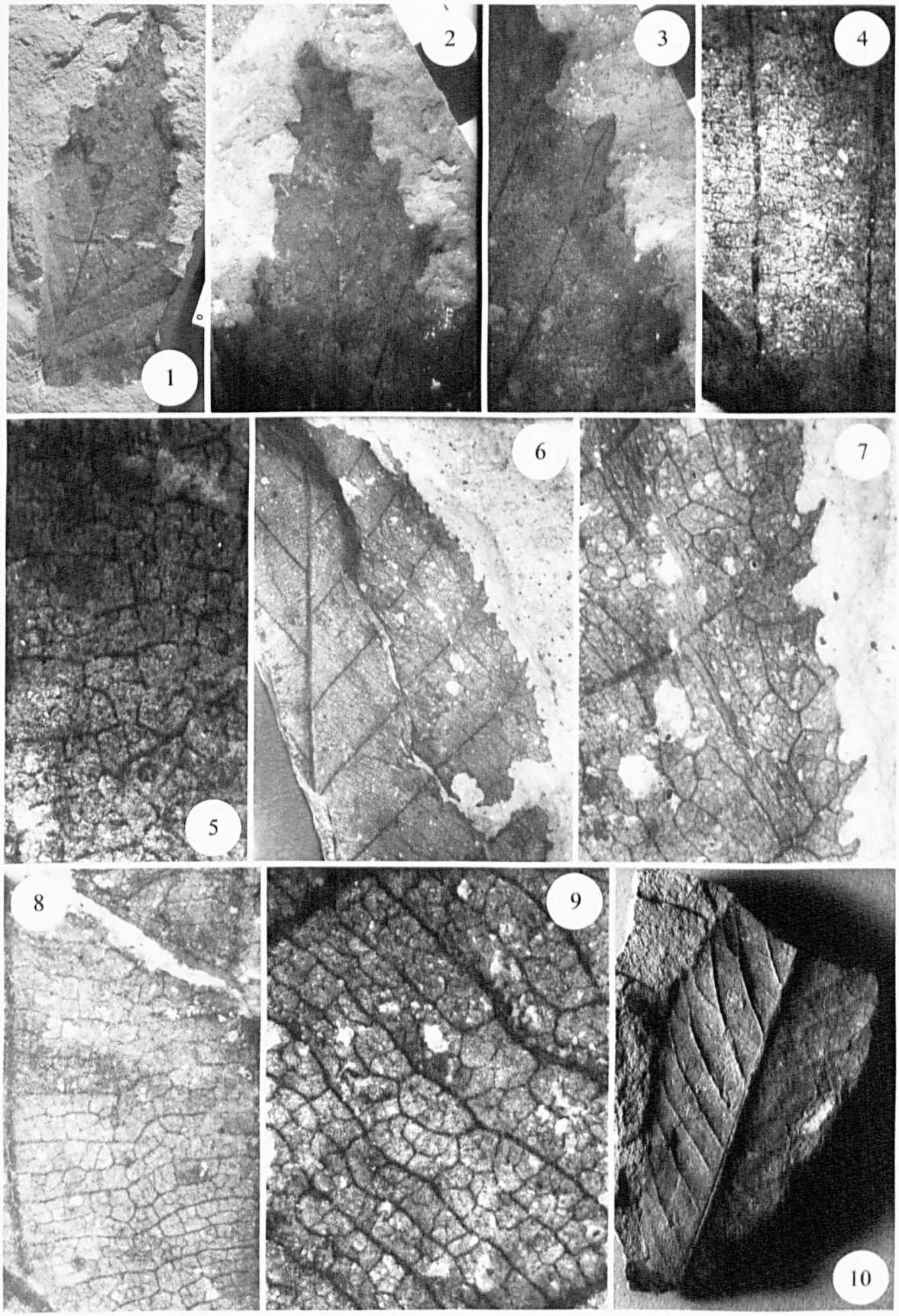

Figure 6.22. (1) - (9). Morphotype 2.51. (1). P.3001.177. x0.5. (2). Detail of apex. x1.5. (3). Detail of marginal serrations. x2.3. (4). Detail of tertiary and higher order venation. x1.6. (5). Areolation and F.E.V's. x6.8. (6). P.3001.90. x1.7. (7). Detail of marginal serrations for comparison with (3). x5.3. (8). Detail of percurrent tertiary venation. x6.4. (9). Detail of areolation and F.E.V's. x10.5. (10). Morphotype 2.52. P.2799.8.2. x0.9.

thickness massive. Course straight. *Secondary* min 9 moderate secondaries diverge at a narrow to moderate acute angle 30° - 50°. Subopposite to alternate. Angle increasing basally, slightly recurved towards margin. Spacing varies. *Tertiary* veins opposite percurrent, convex and nearly perpendicular to midvein, angle increasing exmedially. Higher order venation not preserved. Leaf rank 2r. Teeth, 2 orders, ~ 4 teeth/secondary, 3 teeth/cm, regular spacing, indentation to the leaves had no margin preservation and a higher density of secondary veins than the illustrations of Scriven *et al.* (1995).

2.54 *Nothofagus* sp. 15 (Figure 6.23: 5 - 9)

Material examined: Dragon Glacier *Near complete* P.3001.6, .151. *Large fragment* P.2810.20.2, P.3001.7, .58, P.3002.5.2. *Small fragment* P.2810.18.

Differential characters: Elliptic leaves with a decurrent base. A fine pair of basal secondaries are present close to the basal margin. Slender, slightly winged petiole. Margin crenate with secondaries entering the teeth basally.

Description: Leaf organisation appears simple. Lamina symmetrical ovate to elliptic. Lamina length min 22 - 50 mm. Lamina width 18 - 25 mm. Length:width ratio 1.22:1 - 2.38:1. Area estimated 264 - 700 mm^2. Microphyll = 7 (100 %). Petiole winged, marginal attachment, length 3 - 13 mm, width 0.5 - 1 mm. Margin crenate. *Venation* pinnate craspedodromous. *Primary* weak to moderate. *Secondaries* min 7 - 15 secondaries diverging at a narrow to moderate acute angle 8° - 52°. One pair of acute basal secondaries, otherwise vein angle uniform, veins recurved apically near to margin. *Tertiary* vein category mixed opposite and alternate percurrent, course sinuous. Vein angle to primary obtuse and uniform. *Fourth order* vein category regular polygonal reticulate. *Fifth order* vein category dichotomising and highest order present. Areolation well developed, 5 or more sided. *F.E.V's* absent to 2 or more branched. Margin darkened (P.2810.20.2), suggesting fimbrial vein. Leaf rank 2r. *Teeth* 1 order of teeth, 4 teeth/cm, 2 – 3 teeth per secondary vein, spacing irregular. Shape CC-CV. Sinus rounded, apex rounded. Margin crenate with secondaries entering the teeth basally.

Remarks: Margin preservation is generally poor in Morphotype 2.54, and the small size of the teeth mean that the leaves are easily mistaken for ragged entire margins. P.3002.5.2 is grouped with this morphotype but differs from the normal morphology in having subopposite to opposite secondaries rather than the usual subopposite to alternate secondaries. The leaves are very similar to Morphotype 2.50 in terms of shape, size and having several teeth in the basal margin of the leaf and percurrent tertiary venation. Morphotype 2.54 is distinguished by a more lobate margin, straight branching, rather than decurrent, secondaries, low sinuosity of the primary vein and more strongly percurrent tertiary venation.

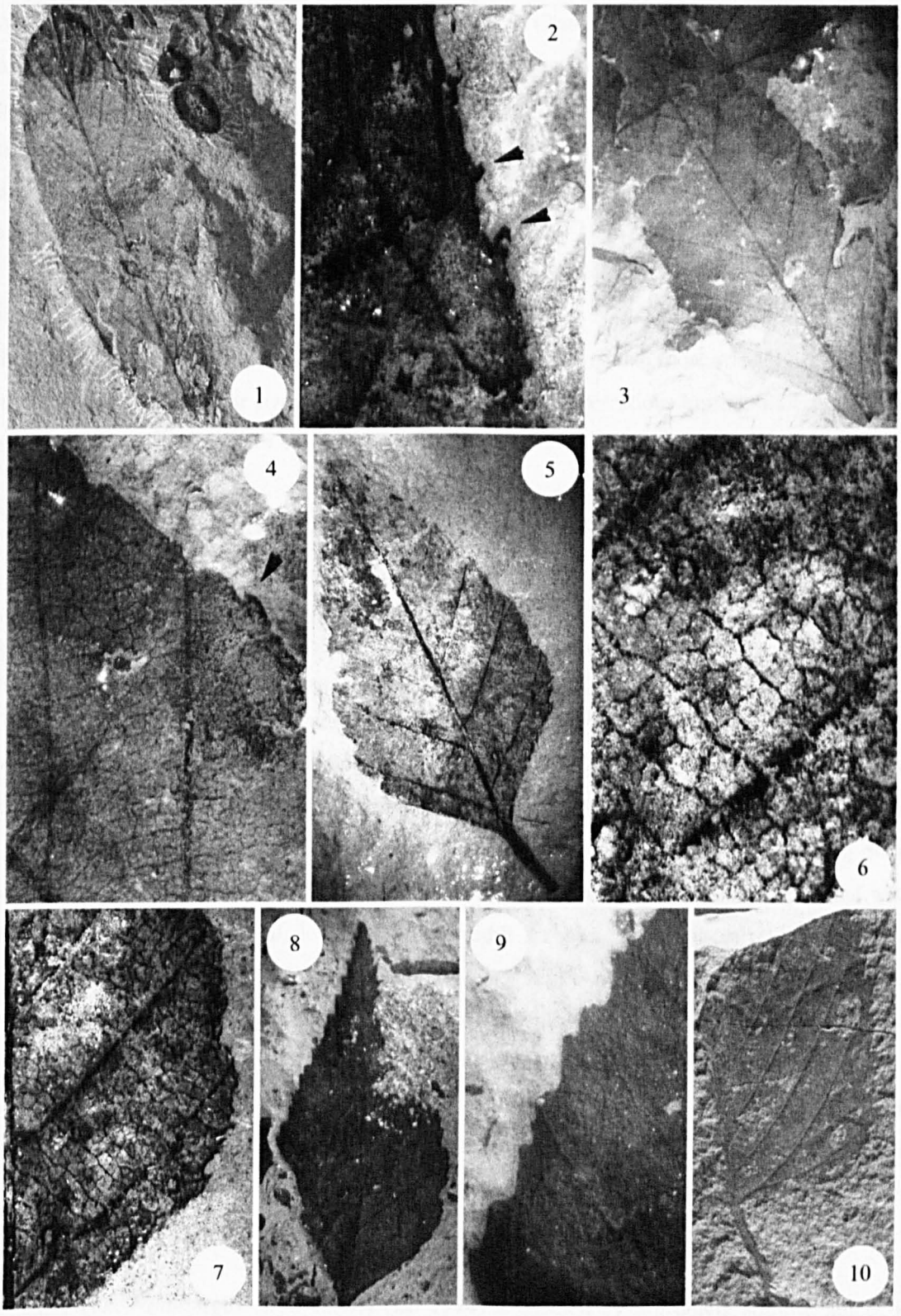

Figure 6.23. (1) - (4) 2.53. *N.* sp. 14, (1). P.3001.47. x1.1. (2). Detail of marginal serration and craspedodromous/ eucamptodromous venation. x5.7. (3). P.3001.64. x1.8. (4). Detail of marginal serration. x6.8. (5) - (9). 2.54. *N.* sp. 15, (5). P.3001.6. x1.8. (6). Detail of higher order venation. x9. (7). Detail of venation and margin. x3.8. (8). P.3001.151.1. x1.9. (9). P.3001.151.1. x7.1. (10). Morphotype 2.55. P.3032.21. x0.7.

In morphotype 2.54 the tertiary angle to the primary also decreases, rather than increases exmedially. No close morphological similarity was found with any of the fossil species of *Nothofagus* but *N. simplicidens* and *N. gonzalezi* (Tanai, 1986) both have similar tooth architecture, with a secondary vein entering the tooth basally and recurving apically towards the tooth apex. Both species are distinct from Morphotype 2.54 because they lack the distinctive trullate lamina shape. *N. johnstonii* from the Oligocene of Tasmania is similar in shape, number and angle of secondary veins and in having a reduced basal intercostal area but has a much smaller lamina (Hill, 1991b).

In terms of lamina shape Morphotype 2.54 is most similar to *N. nitida* (Hill and Read, 1991) but they lack the abundant basal branches. The tertiary venation is also more strongly percurrent. *N. nitida* does have a similar size, elongate apex and marginal serrations but this morphotype has a greater number of secondary veins.

Morphotype 2.55 (Figure 6.23: 10 and Figure 6.24: 1 - 4)

1994 *Nothofagus oligophlebia* Li (pl. 3, figs, 2, 2a, 3, 3a)

Material examined: Dufayel Island *Large fragment* G.53.24. *Small fragment* G.53.6.2(7),.9, .11, .22, .?(22). Fossil Hill Unit 3 *Large fragment* P.3032.15, .21, .58.1, .64.1. *Small fragment* P.3032.2, .25.1/.2, .38, .57, .58.2/.3/.4/.5, .64.2, .72, .78, .85. Fossil Hill Unit 4 *Large fragment* P.3031.77, .55.

Differential characters: Ovate leaves with a truncate base. Basal pair of simple agrophic secondaries. Margin serrate, compound with at least 3 orders of teeth and darkened apices, which sometimes terminate in distinct spines. Sinus between every two adjacent teeth rounded.

Description: Described by Li (1994) with the following amendments: Length min 50 mm est. 100 mm, width min 34 mm, est 68 mm. Microphyll to mesophyll. Petiole marginal with a thin wing of lamina material, length 21 mm, width 2.2 mm. Agrophic veins branch up to 5 times, with branches terminating at margin. *Primary* vein becoming sinuous apically. *Tertiary* veins percurrent with an obtuse angle to the primary, angle increasing basally (P.3032.64.1). Fourth order vein category regular polygonal reticulate. Fifth order vein category dichotomising. Areolation well developed 4 – 6 sided (P.3032.25). F.E.V's ?2 or more branched. Leaf rank 3r/4r. *Teeth* 3 orders, 3 teeth/cm, spacing irregular. Shape CC-ST, FL-FL. Spine thick with a woody texture, length < 3 mm. Indentation to midvein < 4 mm. Principal vein secondary or a secondary branch, course eccentric basally, origin direct or deflected.

Remarks: *Nothofagus oligophlebia* (Li, 1994) is defined by prominent spinose apices and basal agrophic secondaries. Many of the leaves that are grouped in Morphotype 2.55 do not actually have spines but are similar in all other characteristics of venation and lamina. The

absence of spines is suggested to indicate taphonomic rather than taxonomic factors, because spines are easily detached. This is supported by the presence of occasional spines on some leaves and could imply that the spines were deciduous. On this basis, many or all of the craspedodromously veined *Nothofagus* leaves from Fossil Hill referred to *N. subferruginea* may actually belong to this species (Troncoso, 1986; Li and Shen, 1989; Torres, 1990; Li, 1994). In any case, several of the descriptions of *N. subferruginea* from Fossil Hill are of leaves with multiple toothing (up to 4 serrations per secondary), which is inconsistent with Tanai's (1986) description of the doubly serrate *N. subferruginea* (Li, 1994). The small fragments from Dufayel Island assigned to this morphotype also lack spines but are associated with the spinose specimen G.53.24.

Li (1994) suggested that the leaf bore superficial similarities to *N. variabilis* Dúsen from the Early to Middle Eocene Brush Lake Formation (Dúsen, 1899; Tanai, 1986). There is no evidence of spinose apices in *N. variabilis* and the leaves are also much smaller and lacking in agrophic secondaries. *N. betulifolia* Dutra (Dutra, 1997) is also similar to this morphotype in having abaxially branching secondaries and multiple toothing (but not spines). The margin morphology of the leaf is different from any other modern or fossil Nothofagaceae specimens that I have studied and is actually more similar to *Paracarpinus chaneyi* (Manchester and Crane, 1987) an extinct betulaceous leaf from the Oligocene John Day Formation, Oregon. *Paracarpinus. chaneyi* differs only in having a larger number of secondaries 12 – 18, rather than 12 – 14 and Li (1994) suggests that *N. oligophlebia* has reticulated rather than percurrent tertiaries and up to four agrophic secondaries rather than two to three agrophic secondaries.

Craspedodromous venation, large lamina size, ovate to shape and toothed margins are all characteristics of *Nothofagus* sp. but although serrations are common in many *N.* sp. spines are not present in any other fossil or modern *N.* sp. Fossil leaf types that have more pronounced apices e.g. *N. subferruginea* also tend to have one to two teeth per secondary rather than three to four teeth per secondary (e.g. P.3032.21). Spinose apices are present in some Fagales but also in the Ranunculidae, Hamamelidaceae, Flacourtiaceae, Meliosmaceae (Hickey and Wolfe, 1975) and it is therefore possible that these leaves do not group with the Nothofagaceae.

2.56 *Nothofagus* sp. 16 (Figure 6.24: 5)

Material examined: Dragon Glacier *Large fragments* P.2810.1, P.3001.64.5, .89, .163, .181, .186.

Differential characters: Lamina with two pronounced crenations per secondary and a large sinus. Crenation shape CC-CV. The leaf has extremely narrow basal intercostal areas. Secondary veins are alternate and uniformly spaced, possibly recurving towards the margin. Tertiary veins are weak and weakly percurrent.

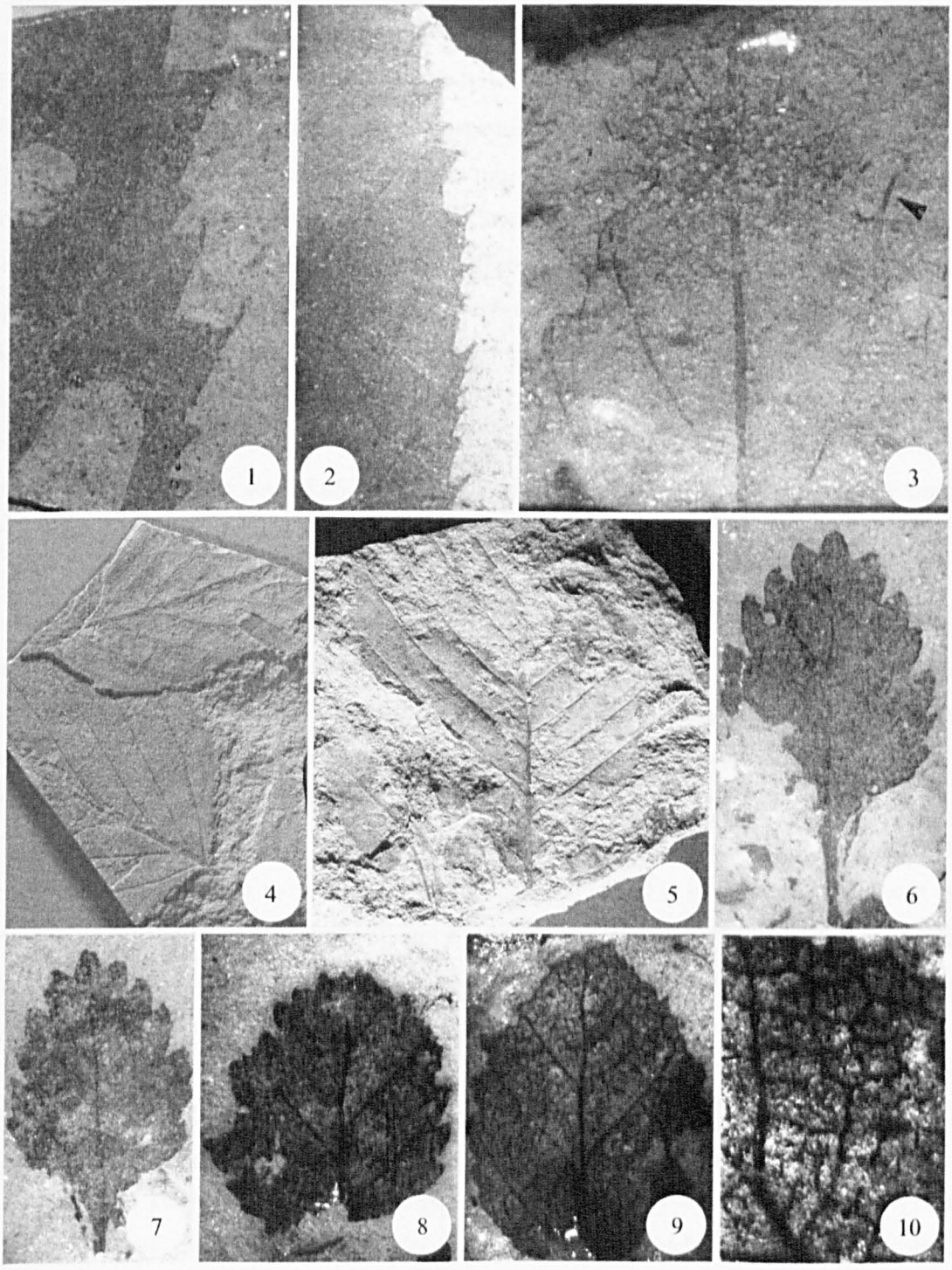

Figure 6.24. (1) - (2) Morphotype 2.55. (1). Detail of marginal teeth with spinose apices, note elliptical traces. P.3032.21. x3.2. (2). P.3032.15. x6.1. (3). G.53.24. x3.6. (4). P.3032.64. x0.6. (5). 2.56. *Nothofagus* sp. 16, P.3001.186. x0.6. (6) - (8). 2.57. *Nothofagus* Juvenile sp. 1, (6). P.3001.42.1a. x4.1. (7). P.3001.42.1b. x3.7. (8). P.3001.140. x4.2. (9) - (10). 2.58. *Nothofagus* Juvenile sp. 2, (9). G.9.3.2. x3.9. (10). Detail of venation. x7.7.

Description: Leaf organisation appears simple. Lamina ovate, symmetrical. Length min 39 – 64-105 mm est. 220 mm, width min 20-90 est. 110 mm. Length:width ratio min 1.32:1 – est. 2:1. Area min 520 – 2126.67 mm^2. Microphyll = 2 (33%), notophyll = 2 (33%), mesophyll = 2 (33%). Apex acute straight, angle 40° – 60°. Base convex to cuneate/complex, basal angle 60°-100°. Margin crenate. *Venation* pinnate craspedodromous. *Primary* thickness weak to stout. Course straight or slightly sinuous. *Secondary* min 12 – 15 subopposite to opposite secondaries diverging at a narrow acute angle 32° - 55°. Secondaries rarely decurrent. Spacing uniform. Basal intercostal areas narrower than others. Secondaries branch exmedially towards margin. *Tertiary* vein category mixed opposite and alternate percurrent. Vein angle to primary obtuse, increasing basally. *Fourth order* vein category regular polygonal reticulate. *Fifth order* veins dichotomising. *Areoles* well developed. *F.E.V's* 2 or more branched. *Leaf rank* 3r. *Teeth* ?2 orders. 2-3 teeth/secondary, 4 teeth/cm. Spacing irregular. Principal vein is a secondary, subordinate teeth fed by secondary branches. Origin of principal vein deflected, one secondary branch entering tooth and one branch directed

Remarks: Leaves of mesophyll size are extremely rare in the fossil record of King George Island. Only *N. subferruginea, N. tasmanica* and *N. simplicidens* have leaf lengths approaching those of morphotype 2.56, but none of these species has a similar width and *N. simplicidens* is single serrate. The leaves may therefore represent outsized leaves of *N. tasmanica* or *N. subferruginea* (similar to leaves from Vaureal Peak , P.2799) or a completely different species. *N. subferruginea* does have a reduced basal intercostal area and regular craspedodromous venation that matches this morphotype and the tertiary venation is weakly percurrent with thin veins. According to Hill (1983) and Hill and Read (1991) *N. tasmanica* has 1 – 3 glandular teeth per secondary, but no glands have been observed in this morphotype due to poor margin preservation.

2.57 *Nothofagus* Juvenile sp. 1 (Figure 6.24: 6 - 8)

Material examined: Dragon Glacier *Near complete* P.3001.42.1, .140.1.

Differential characters: Ovate microphyllous leaves with a decurrent base and pinnate craspedodromous venation. Petiole slender. Secondary veins branch close to margin, with the abaxial branch terminating at a tooth and the secondary vein recurving apically to terminate in another tooth. Teeth are large relative to the lamina size and have rounded apices.

Remarks: The small lamina size relative to tooth size and poor margin-petiole separation of this morphotype suggests that the leaf may be juvenile. The presence of several teeth in the basal intercostal area of specimen P.3001.140.1 (Figure 6.24: 8) suggests a possible relationship with morphotype 2.50, which also has an abundantly toothed basal margin and an ovate form.

The tooth shape is distinctive, with large rounded triangular apices that resemble the modern *N. fusca* and *N. truncata* but the secondary divergence angle is more variable. The central or basal course of the principal vein is also present in *N. truncata*. *N. antarctica* (in Hill and Read, 1991) possesses similarly distinct rounded teeth with intersecondary veins and secondaries that branch close to the margin. The suggested affinities of the leaf are ancestral to the subgenera *Nothofagus* or *Fuscospora*.

2.58 *Nothofagus* Juvenile sp. 2 (Figure 6.24: 9 - 10)

Material examined: Dragon Glacier *Near complete* G.9.3.2, P.2810.18.2.

Differential characters: Ovate nanophyll leaves with ?craspedodromous venation. Strong intersecondaries. Tertiaries thick, reticulated. Fourth order veins dichotomising.

Remarks: The poor vein organisation and small size of this morphotype suggest that it is a juvenile leaf form.

Chapter 7 Traces on leaves

7.1 Introduction

An abundant and diverse range of trace fossils on leaves are preserved in the leaf macroflora of King George Island. These include traces resulting from possible plant-arthropod interactions, plant-fungal interactions and mechanical damage. There are no published records of leaf traces from the Antarctic fossil record, although Hayes (1999) documented several types of traces from James Ross Island in her PhD thesis. The traces represent a new source of palaeoenvironmental data for KGI. The aim of this chapter is catalogue the types of insect traces present in the flora, in order to provide a complete overview of the KGI palaeoenvironment.

7.2 Methodology

The traces documented in this chapter have been described using the terminology of Scott *et al.* (1994) and Lang *et al.* (1995), and have been categorised according to their location on the lamina, whether marginal or non-marginal and by the presence or absence of wound reaction tissue (Table 6.1). Wound reaction tissue is induced by damage caused to living leaf material (Scott *et al.*, 1992), and is an important characteristic because it indicates that a trace formed prior to abscission. Reaction tissue is identified as a darkened, thickened rim of material trace rim in fossils that have organic preservation, but is less obvious in leaves that are only preserved as impressions. In the latter type of trace a change in the colour of the impression surface suggests that reaction tissue is present.

Leaf traces can be formed by plant-arthropod interaction, fungi and by mechanical action. Plant-arthropod interactions may be grouped according to the nature of the trace e.g. whether for feeding or for shelter. Feeding traces may be divided into three categories: wounding, feeding and mining (Scott *et al.*, 1992). These traces may be marginal or non-marginal and wound reaction tissue is a pre-requisite for their identification, since detritivory and bioturbation can mimic the morphology of leaf traces (Scott and Titchener, 1999; Titchener, 2000). Leaf mining is a specialised form of feeding trace in which the trace maker feeds within the leaf tissue (Lang *et al.*, 1995). Feeding traces are often non-specific and consequently the identification of a trace-making organism is complex, such that many traces cannot be definitively linked to any one trace maker (Titchener 1999). Non-marginal traces without reaction tissue are difficult to interpret and may relate to leaf feeding or abscission of galls. Sheltering behaviour of arthropods results in the formation of galls, a physiological response induced in leaf tissues in

the immediate vicinity of an invasive parasite (Scott *et al.*, 1992; Scott *et al.*, 1994). Galls are defined as the positive or negative manifestations of growth and abnormal differentiation induced on a plant by an animal or plant parasite (Meyer, 1987). Skeletonisation of the leaf lamina may result from preferential feeding patterns or during biodegradation (Titchener, 2000).

Mechanical damage in the canopy is largely related to wind damage. Wind induced lesions, for example may be formed by the abrasion of leaves rubbing together (MacKerron, 1976; Wilson, 1980). Leaves are also subjected to mechanical degradation during post-abscission, transport.

7.3 Trace morphology data

Trace morphology data is summarised in Table 7.1 and is illustrated in Figures 7.2 – 7.5. Figure 7.1 provides a brief summary of the distribution and proportion of trace types.

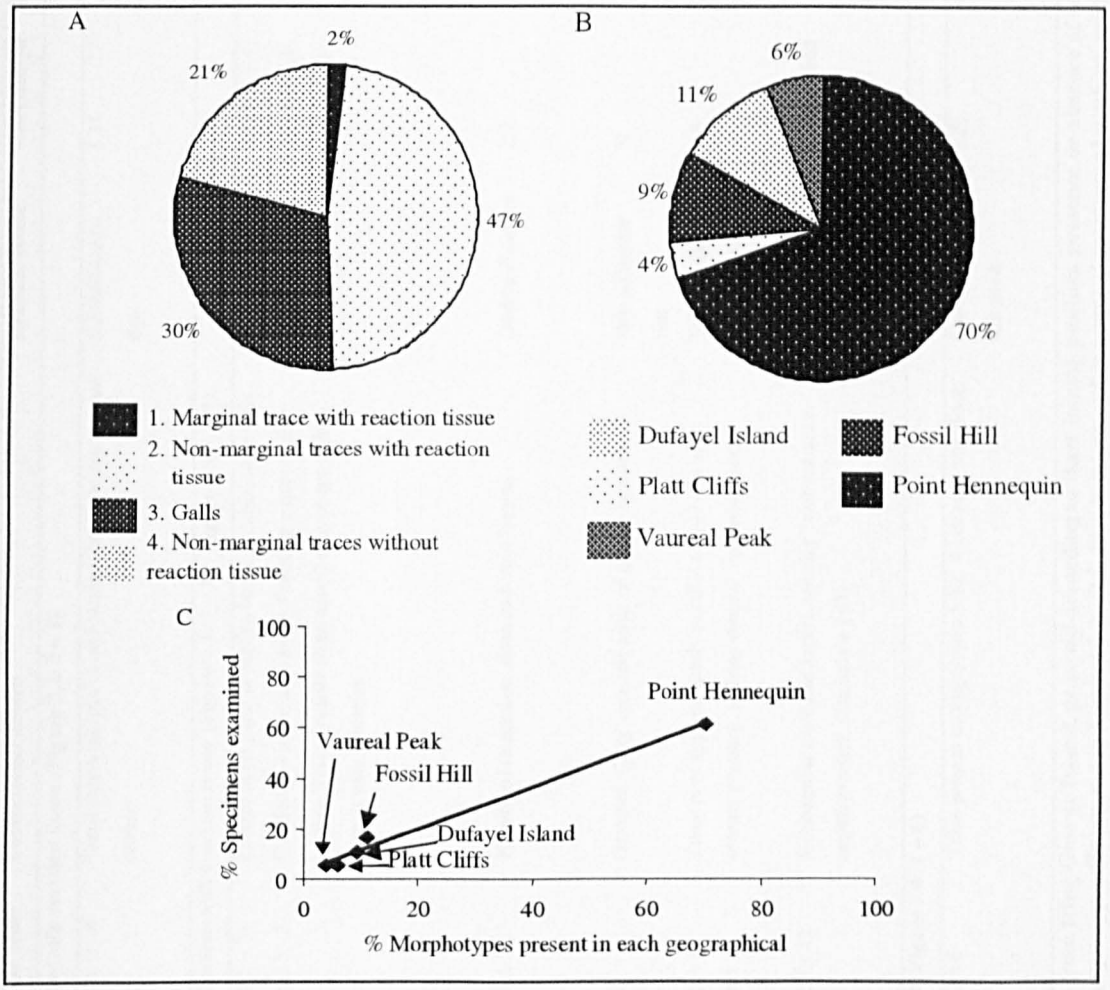

Figure 7.1. Breakdown of leaf trace types and distributions in the King George Island floras. A) Proportion of traces falling into particular morphotypes expressed as a percentage of the total number of traces found in the whole of the King George Island flora., B) Percentage of traces present at each locality, C. Plot of % specimens examined vs. % morphotypes present in each locality, the plot is poorly constrained but suggests that greater sample size and/or better preservation state is directly correlated with the number of leaf traces, resulting in taphonomic bias towards Point Hennequin.

Type	Shape	Size (mm)	Course/other details	Reaction tissue	Morphotype	Interpretation	Material examined
	1. Marginal traces with reaction tissue (Figure 7.2: 1 – 2)						
1.	Continuous	5 x 0 - 4	Trace enters margin in mid lamina, irregular course and outline.	Submillimetre rim.	1.11	Marginal feeding trace.	Dragon Glacier P.3001.169
	2. Non-marginal traces with reaction tissue (Figure 7.2: 3 – 10; Figure 7.3: 1 – 7)						
2.1	Elliptic to rounded rectangular	0.5 – 16 x 0.5 - 5	Present in all parts of lamina but less common basally. Confined to intercostal areas. Forming a hole in the lamina. Traces radiate from apical side of secondary branch with midvein.	Submillimetre - millimetre rim.	1.1, 1.2, 1.4, 1.6, 1.9, 2.1, 2.3, 2.8, N.	Non-marginal feeding trace.	Cytadela (Platt Cliffs) G.309.18. Dragon Glacier P.2810.5.1, P.3001.7.2, P.3001.10, P.3001.12.1, P.3001.28, P.3001.36.1, P.3001.46, P.3001.52, P.3001.59, P.3001.89, P.3001.180, P.3007.5, P.3013.5, P.3013.7, P.3013.9. Fossil Hill Unit 3 P.3032.25, P.3032.4, P.3032.14. Platt Cliffs G.50.1,
2.2	Elliptic, areolar	1 x 1	?Confined to areoles. Base and mid lamina.	Darkened circles.	2.7.	Non-marginal feeding trace ?sap sucking, or fungal damage.	Dragon Glacier P.2810.20.2, P.3001.89.
2.3	Elliptic	4	Oriented along upraised folds of plicate vernation.	Submillimetre rim.	N.	Mechanical damage due to leaf rubbing.	Dragon Glacier P.3001.42.3
2.4	?linear	5 – 20 x 1 - 4	Trace runs approximately parallel to midvein and crosses primary, sinuous course. ?possible frass.	Submillimetre rim. Globular textured,	2.8	Linear leaf mine.	Dragon Glacier P.3001.81, P.3013.9.
2.5	Blotch	30 x 11	Rectangular trace that tapers apically ?exit/entrance, negative relief (?strictly a gall)	Entire trace darkened	Unidentified fragment	Large leaf mine	Dufayel Island G.53.30.
	3. Galls (Figure 7.3: 8 – 9; Figure 7.4: 1 – 8)						
3.1	Roughly spherical	7 x 6	Trace present on uppermost lobe. Lamina is undulose.	Lamina shape distorted.	1.5,	Gall.	Dragon Glacier P.3001.58.2, P. 3001.187.

Table 7.1. Leaf traces from King George Island, grouped according to their lamina position, presence or absence of reaction tissue and by abnormal manifestations of growth on the lamina. Leaf trace morphotypes illustrated in Figures 7.2 - 7.5. Size is expressed in terms of maximum length vs. maximum width. Co-traces - co-occurring traces, M N° - trace morphotype number.

Type	Shape	Size (mm)	Course/other details	Reaction tissue	Morphotype	Interpretation	Material examined
3.2	Doughnut like.	0.5 – 10 x 5 – 1	Doughnut shaped. Sometimes overlapping. Concentrated basally but larger infrequent traces occur in more apical sections of the leaf, often concentrated close to midvein. Specimens single except for multiple traces on P.3001.44.	Lamina thickened.	2.1, 2.34	Spot gall.	Dragon Glacier P.3001.28, P.3001.44, P.3001.110.3, P.3001.120.
3.3	Round	4 - 8	Positive and negative spherical swellings in all parts of lamina. Swellings sometimes interrupted by venation (P.2799.6). Perfectly rounded trace in P.3031.81. No associated colour change.	Lamina inflated.	N, 1.12, 1.13, 1.15.	Gall	Dufayel Island G.53.?(20), G.53.6(18), Fossil Hill Unit 4, Vaureal Peak P.2799.6, P.2799.7, P.2799.10, P.3031.21, P.3031.81.
3.4	Elliptic	3 - 10	Traces occur in all parts of the lamina. Positive or negative relief.	Entire trace darkened.	1.6, 2.?	Gall.	Dufayel Island G.53.?(1), G.53.25(23), G.312.10.
4. Non-marginal traces without reaction tissue (Figure 7.5: 1 - 10)							
4.1	Elliptic, areolar.	1 - 1.5 x 1 – 2	Confined to areoles, which have skeletonised appearance but maintain form.	None but lamina lighter coloured.	2.43 and N. type.	Preferential feeding trace or leaf rotting.	Dragon Glacier P.3001.83, P.3001.140.
4.2	Elliptic, areolar.	0.1 x 0.1	As subtype 2.1 but traces consist of a series of smaller areole shaped traces, clustered as a single trace. The trace appears to radiate from the apical side of the secondary branch with the midvein.	None.	N.	Preferential feeding trace.	Dragon Glacier P.3001.10, P.3001.42.4, P.3001.52
4.2	Lamina thinning.		Trace occurs over all parts of lamina.	None but Lamina lighter in colour	2.1, N.	Possibly related to weathering but may be evidence of leaf rotting.	Dragon Glacier P.3001.8, P.3001.52, P.3001.61, P.3001.180.
4.3	Spherical – elliptic.	4 – 9	Intercostal, as type 2.1 but without reaction tissue.	None	N.	Uncertain, similar morphology to feeding traces	Dragon Glacier P.3007.16, P.3032.21,

Table 7.1. Continued.

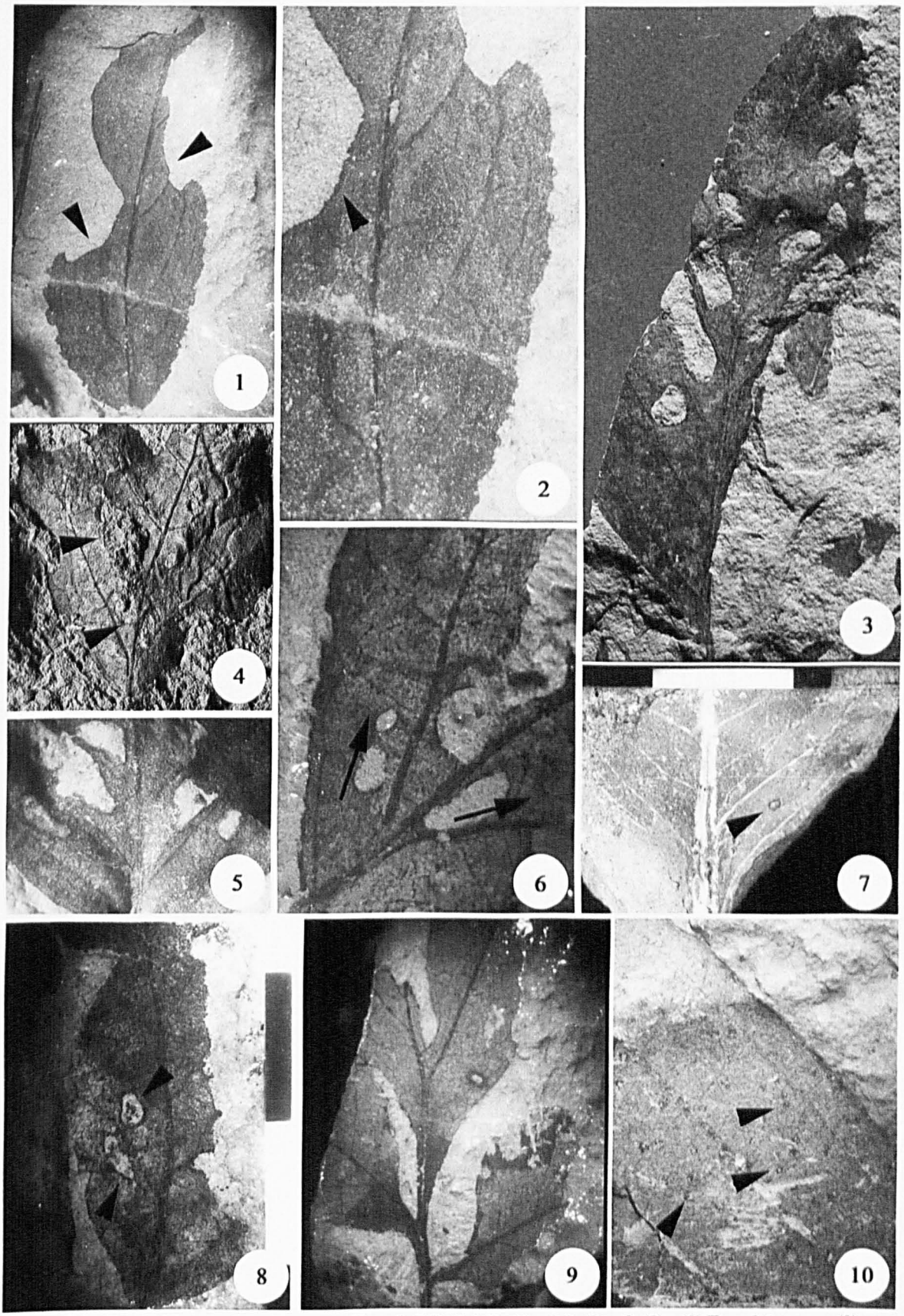

Figure 7.2. (1) - (2) Marginal feeding trace Type 1. P.3001.169. (1). x2.3. (2). x9. (3) - (9) Type 2.1 traces. (3). P.3001.10 to scale. (4). P.3013.9. x1.8. Note possible linear mine (Type 2.4) on right side of lamina. (6). Detail of traces. x4. (5). P.3001.7.2. x3. (7). g.50.1. x2.25. Trace appears to be focussed on a single areole.(8). P.3007.5a. x2.75. (9). P.3001.59. x1.6. (10). P.3001.89. Basal fragmentof a leafwith darkened spheres of trace type 2.2.

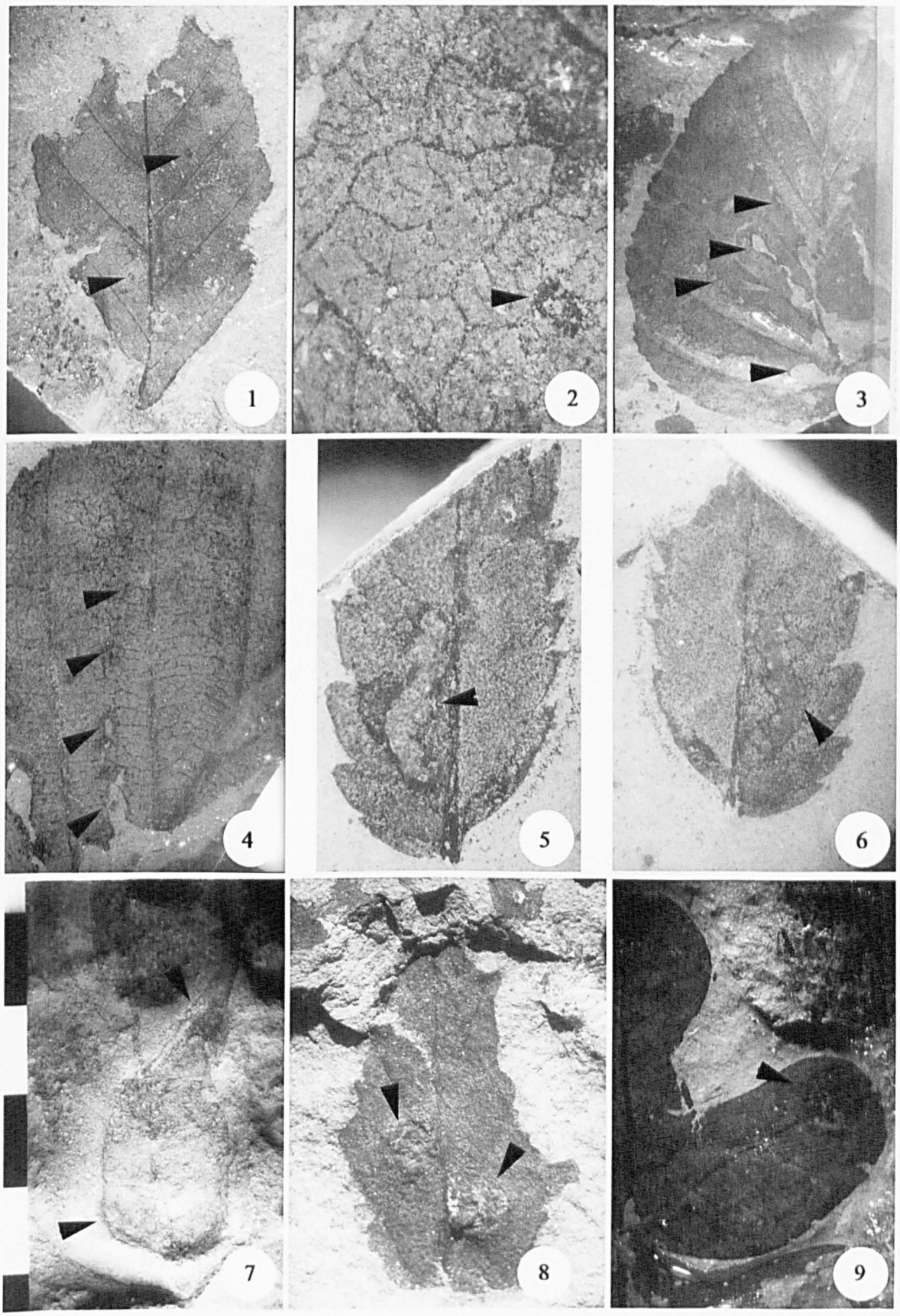

Figure 7.3. (1) - (2) Trace type 2.2. P.2810.20. x3 and x10 respectively. (3) - (4) Trace type 2.3 possible leaf abrasion traces. Note concentration of reaction tissue along plicate fold. P.3001.42.3. x1.6 and x4 respectively. (5) - (6) Trace type 2.4, possible leaf mine, note lighter material ?frass in trace. P.3001.81a/b. x8. (7). Trace type 2.5, possible leaf mine with funnel shaped exit/entrance pore. (8) - (9) Trace type 3.1. Small leaf galls with low relief. (8). P.3001.58.2. x3. (9). P.3001.187. x1.5.

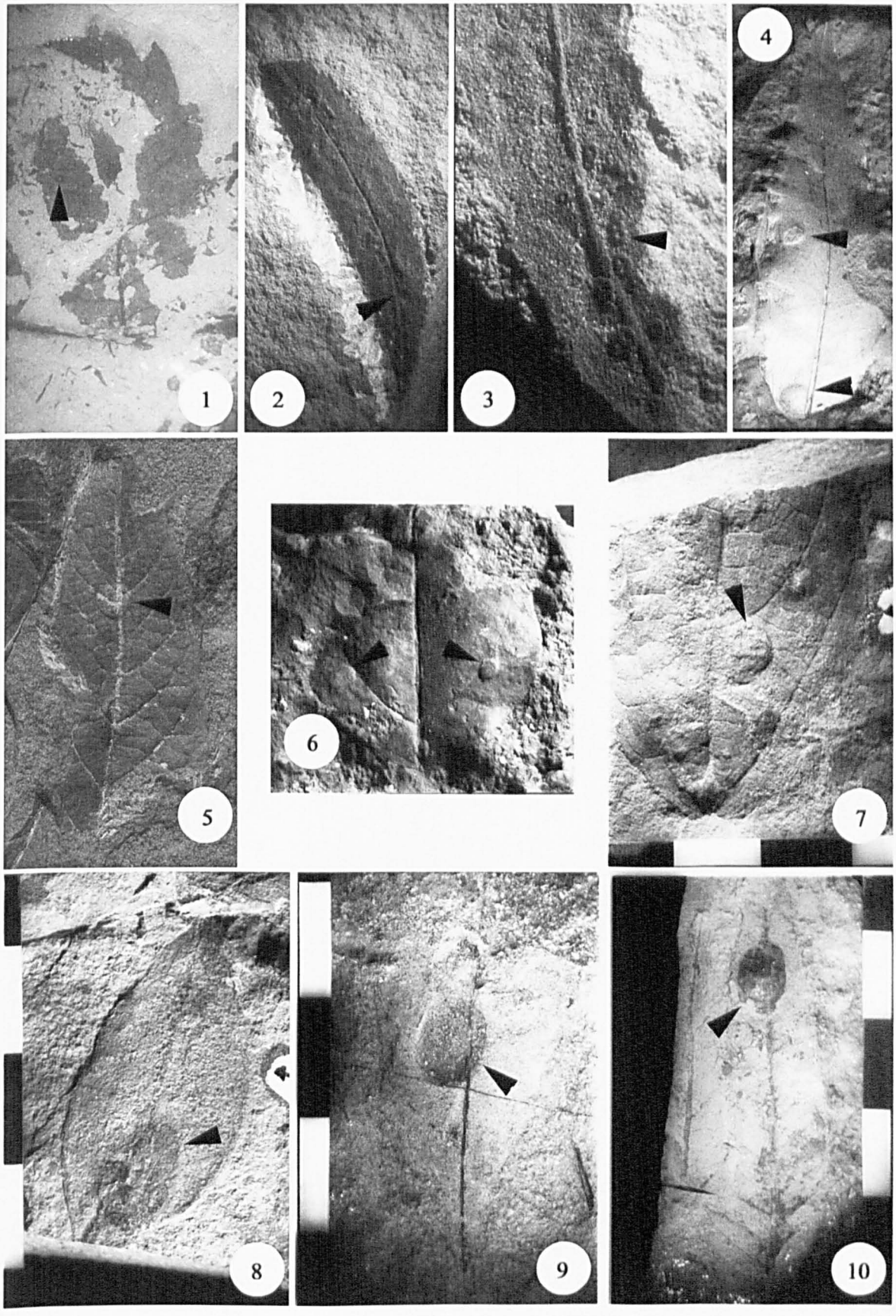

Figure 7.4. (1) - (3) Trace type 3.2, spot galls. (1). P.3001.110.2. x2. (2). P.3001.44a. Extremely abundant galls which frequently overlap (negative counterpart). x1.6. (3). P.3001.44b. Detail of galls (positive counterpart). x5. (4) - (7) Trace type 3.3. (4). Large spherical protrusion at leaf base. P.3031.81. x1.6. (5). Lamina swelling which has been obstructed by secondary venation. P.2799.6. To scale. (6). P.3031.21. x3. (7). G.53.?(20). (8) - (10). Trace type 3.4. Note darkened colour of traces. (8). G.53.25(23). All scale bars are 10 mm graduated.

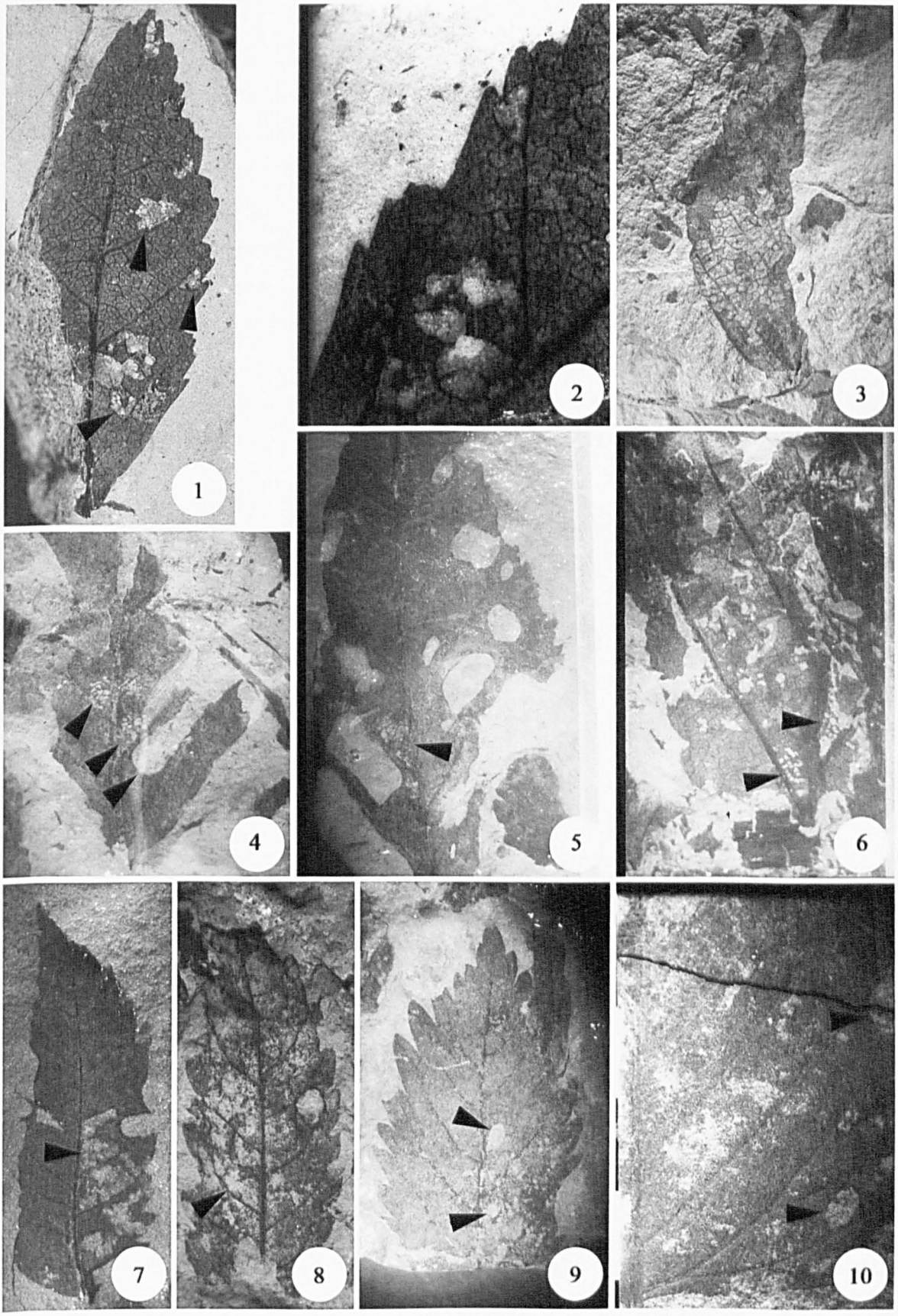

Figure 7.5. (1) - (3) Trace type 4.1. (1). P.3001.83. x3. (2). Detail of thinned lamina and lighter coloured tissues. (3). Intense skeletonisation of lamina in P.3001.140. x2. (4) - (6) Trace type 4.2. Note combination of larger traces in addition to small areole related traces. (4). P.3001.42.2. (5). P.3001.10. x1.8. (6). P. P.3001.50.2. To scale. (7) - (8). Thinning of leaf lamina, also associated with trace type 2.1. (7). P.3001.52. x2. (8). P.3001.180. x 2.7. (9) - (10) Trace type 4.3. (9). P.3007.16. x1.5. (10). P.3032.21. To scale.

7.4 Discussion

This is the first collection of traces on leaves from Antarctica. Traces occur in all of the King George Island floras except the Collins Glacier (P.3025) and the Profound Lake (P.1174) floras, both of which comprise fewer than 10 leaf specimens, suggesting that their absence is related to sample size rather than environmental factors. The Dragon Glacier flora has the greatest diversity of traces, many of which are specific to that locality.

Traces comprise marginal and non-marginal feeding traces, possible fungal or sap-sucking traces, rare leaf mines, mechanical damage related to leaf abrasion and several forms of leaf galling. No other types of trace were observed. The dominant trace type preserved is a non-marginal trace with reaction tissue (37 % of traces), interpreted as the result of phytophagic activity (Figure 7.1 and Figure 7.2 (3) – (9)). Traces were most commonly found on morphotype 2.1 and on nothofagaceous leaf forms, both of which are abundantly preserved in the fossil record, suggesting a preservational bias resulting on the large number of leaves preserved. Chewing and biting feeders that produce such traces are commonly the result of *Coleptera* and *Lepidoptera* but they are also present in the *Orthoptera* and *Hymenoptera* (Schoonhoven *et al.*, 1998). It is therefore suggested that at least one of these groups is represented by the leaf traces. Skeletonisation (trace type 4.1) commonly results from larval feeding of the *Hymenoptera*, *Lepidoptera* and *Coleoptera* (Stephenson, 1991). Galls are less specific, resulting from the interaction of bacteria, fungi, nematodes and mites and insects (Titchener, 2000). In the insects group alone there are 13000 types of gall inducers (Titchener, 2000). No taxon specific traces were observed, although future collections may clarify this point since some of the traces were found only as single examples on single specimens.

The abundance and diversity of traces present in the Dragon Glacier flora may be a result of sample size and preferential collecting bias (e.g. Figure 7.1), but it could also be related to the style and quality of the organic preservation. Alternatively, the local environment could have possessed a greater number of trace forming organisms. Given that many of the traces specific to the Point Hennequin flora affect the tertiary and higher order venation, it seems likely that in floras where tertiary vein preservation is rare or absent e.g. the Dufayel Island, Vaureal Peak and Fossil Hill (P.3031) floras, there may be a significant preservational bias. Some traces, for example Gall subtype 3.1, were only observed in morphotypes that are specific to Point Hennequin, again suggesting preservational and/or sample size biases. One final point is that insect trace-makers are adversely affected by volcanism, since sharp volcanic glass particles damage the cuticle of the insect, leading to its eventual demise (Spicer, 1989). Abundant traces in a flora could therefore be used as evidence to suggest a pre-volcanic vegetation. No mechanical damage traces were observed that could be related to volcanic activity.

Chapter 8 Non-angiosperm foliage

8.1 Introduction

The aim of Chapter 8 is to catalogue the non-angiosperm component of the King George Island vegetation that was studied in this project, and to provide a preliminary taxonomic/morphotype analysis of the flora. The flora comprises fern genera and gymnosperms including Araucariaceae, Cupressaceae and Podocarpaceae in addition to a new record of two possible bryophytes. In addition to foliar material, roots of probable podocarpaceous affinity are also present in the assemblage. All of the organs described here are summarised in Table 5.4.

8.2 Systematic palaeobotany

Division ?Bryophyta

Bryophyte sp. 1(Figure 8.1: 1)

Material examined: Fossil Hill Unit 3 P.3032.4.3.

Description: One clump of axes (min 22), which radiate from a central point. Axes have multiple branches diverging at ~35° - 54°. Axes up to 12 mm long by 0.3 mm wide, bearing ?leaves along the entire length of the axes. Preservation of axes too poor to distinguish leaf morphology.

Remarks: None of the axes have sufficient preservation to distinguish particular features of leaf morphology, although the irregular surface texture of the strands suggests that they are leafy. It is not possible to distinguish whether the axes are dorsiventrally flattened and might possibly group with the liverworts. The radiating nature of the axes is suggestive of a moss with an epiphytic habit (A. Newton pers. comm., 2001).

Bryophyte sp. 2 (Figure 8.1: 2)

Material examined: Mt. Wawel flora P.3010.5.

Description: Three small ?unbranched axis bearing linear lanceolate leaves. Axis length up to 15 mm by 1.3 mm. Total length of axes unconstrained. Leaves up to 2 mm long by 0.2 mm wide. Leaves appear to cluster at intervals along the axes. Distinct midrib. Leaf margin entire, apices acute. No detail of leaf venation was observed.

Remarks: The leafy axes, with microphylls bearing a single vein are typical of the mosses but the axes lack cellular detail and taxonomically significant morphological characters, therefore affinities with the fern allies (Lycopodiales, Selaginellales) cannot be excluded. The genus *Muscites* (Cantrill 2000) was erected to describe small unbranched moss axes from Cretaceous sediments on Snow Island, South Shetlands but *M. antarcticus* differs in having leaflets continuously along the axes.

Division Sphenophyta

Genus *Equisetum* L. (Figure 8.1: 3 - 5)

Material examined: Dragon Glacier flora G.9.6, .18a.

Description: Length of stems preserved up to 60 mm, width up to 6 mm. Nodes 32 mm apart, sheath length 7 mm. Internodes longitudinally ridged, 8 ridges. Leaflets acute angular, length 2 mm.

Remarks: The longitudinally ridged stem fragments, partitioned by nodes, define aerial portions of mature sporophytes of *Equisetum*. *Equisetum* is relatively rare in the King George Island flora and the specimens described here are those described by Barton (1964, 1965). Rare *Equisetum* stems have previously been described from Point Hennequin (Zastwaniak, 1981), and the Lower Tertiary Block Point assemblage (Dutra, 1989a).

Division Tracheophyta

Class Filicopsida

Family Lophosoriaceae

Genus ?*Lophosoria* C. Presl. (Figure 8.1: 6-8)

Material examined: Potter Cove compression P.232.40, .55 (fertile), ?.56, ?.57. Rocky Cove P.3029.28.

Description: Preserved fragments of frond at least 100 mm long, at least bipinnate. Primary rachis up to 3 mm wide. Primary pinnae alternate and distichous, up to 41 mm long diverging at a wide acute angle 68° – 70°. Primary pinnae spaced 14 mm apart. Secondary pinnae alternate and distichous, 5 – 6 mm long, diverging at a moderate acute angle 58° – 60°, spaced 2 – 3 mm apart and bearing an average of 8 pinnules. Lamina wing lacking. Pinnules sessile, elliptic to rounded and up to 1 mm long by 1 mm wide, diverging at a moderate acute angle 58° – 61°. Pinnules strongly concave. Venation not observed. Fragments of dehisced sporangia, are associated with some pinnules (Figure 8.1: 7-8). Annulus elliptic, up to 0.4 mm diameter. No spores or paraphyses were observed with these specimens.

Remarks: Fern fronds with semicircular or rhomboidal pinnules are characteristic of the form genera *Gleichenites* Goeppert and *Lophosoria* (Cantrill, 2000). None of the fronds described here preserve the arrested bud axil characteristic of the Gleicheniaceae and the diagnostic spores *Cyatheacidites* (Dettmann, 1986) that would define *Lophosoria* are lacking. However, fragments of stalked sporangia and the revolute pinnule margin suggest affinities with *Lophosoria* rather than the Gleicheniaceae. *Lophosoria quadripinnata* (Gmel) Chr. has been described from the pollen record of Fildes Peninsula by Torres and Meon (1993) but the pinnules of that species are significantly larger (12 x 4 mm) than the material described here. *Lophosoria cupulatus* Cantrill, previously described from Cretaceous sequences on Snow Island (Cantrill, 1998, 2000), has smaller pinnules and is similar in having moderate to wide acute insertion of the pinnae, although the pinnule number is lower (8 rather than 12 pinnules per pinna in these specimens).

Family incertae

Fertile fern sp. 1(Figure 8.1: 6 - 7)

Material examined: Dragon Glacier flora P.3013.10. 4.

Description: Pinnule fragments up to 6 mm long bearing at least two terminal sori on a narrow axis 0.1 mm wide. Sori obovate up to 1.5 mm wide.

Remarks: Given the fragmentary nature of these specimens it is difficult to relate them to either fossil or extant material. However fertile pinnae with terminal sori are present in two genera described from the Antarctic Peninsula – *Aculea bifida* Douglas present in the Snow Island (Cantrill, 2000) and *Thyrsopteris shenii* Zhou and Li, from Fossil Hill (Zhou and Li, 1994). The specimens are distinguished from *A. bifida* in having club-like obovate sori rather than globose sori, which are a characteristic feature of *T. shenii* (Zhou and Li, 1994), suggesting affinities with that species.

Fertile fern sp. 2 (Figure 8.1: 10-11)

Material examined: Fertile axes Vaureal Peak P2799.12, .19, .21, .24, .26.1, .27. Sterile foliage Barton Peninsula P.2145.2. Dragon Glacier flora P.2810.13. P.3001.35a/b. Fossil Hill Unit 3 P.3032.82.

Description: Preserved frond length 24 - 27 mm, total length unknown, at least once pinnate. Pinnules 3 - 4 mm long, 2 - 2.5 mm wide, arising at 50° - 70°. Single unbranched midvein. Pinnule margin interrupted by elliptical to reniform structures. 0.5 - 1 mm long, 0.1 - 0.5 mm wide, 0 - 2 elliptical structures present on both the basal and apical margins of the pinnule. Sterile foliage is essentially the same but frond lengths 25 - 55 mm, at least bipinnate. Primary pinnae 39 mm long, 1 mm wide, bearing at least 7 secondary pinnae. Secondary pinnae distichous, 7 - 11 mm apart, arising

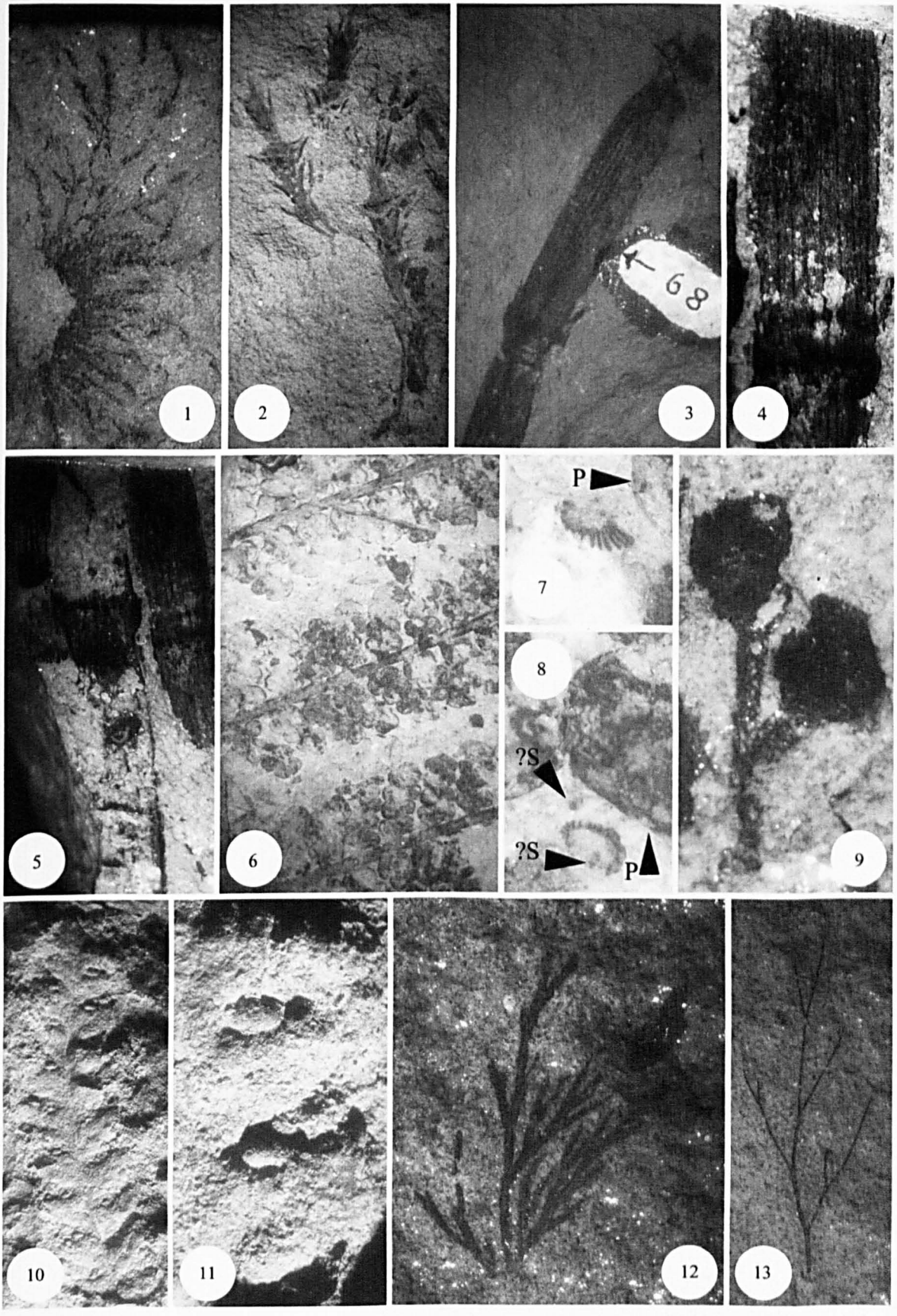

Figure 8.1. (1). Bryophyte sp. 1. P.3032.4.3. x2.4. (2). Bryophyte sp. 2. P.3010.5. x2.8. (3) - (5). *Equisetum* (3). G.9.6. x1.3. (4). Detail of node. G.9.18b. x3.5. (5). *Equisetum*. G.9.18b. x1.8. (6) - (8). *Lophosoria* sp. P.232.55. (6). Fertile frond. x.1.8. (7) - (8). Fragments of annuli. P - pinnule margin, ?S - ?spores. x24. (9). Terminal sori of *Thyrsopteris shenii*. P.3013.10. x10.9. (10) - (11) Fertile fern sp. 1. (10). P.2799.19. x1.9. (11). Detail of probable sori. x8. (12). Fern sp. 1. P.3029.21. x3.3. (13). Fern sp. 2. P.3029.19. x4.1.

acutely 35° - 43° (av. 41°) at least 16 mm long. Pinnules 1.9 - 5.2 mm long, 1.9 - 2.6 mm wide, arising at 43° - 66°. Sterile foliage differs only in the lack of elliptic structures. Variable preservation gives the impression of toothing in some specimens.

Remarks: The elliptic structures present on the pinnule margins of Fertile Fern type 1 are probably sori, however the poor preservation of the specimens prevents discrimination of which lamina surface is exposed. The elliptic structures may be the expression of an object from the reverse side of the lamina. The cupped shape of the pinnules and the similarity in size of the elliptic structures to the receptacles of *Lophosoria cupulatus* Cantrill, suggest that these fronds might be related to *Lophosoria.* However the number of pinnules per pinna is significantly higher in Fertile Fern type 1, which has up to 18 pinnules compared to a maximum of 12 in *L. cupulatus.*

Sterile Foliage

Fertile foliage is required to identify separate fern species. However, obvious gross morphological divisions have been made here based on venation and margin characters of sterile foliage.

Family Incertae

Fern sp. 1 (Figure 8.1: 11)

Material examined: Rocky Cove P.3029.21.

Description: Deeply dissected fern foliage with linear uninerved pinnules. Preserved frond length up to 17 mm by 0.4 mm wide, total frond length unknown. At least ?bipinnate. Pinnae distichous. Pinnae producing at least 9 pinnules, each 3 – 4 mm long by up to 0.4 mm wide.

Remarks: Sphenopterid-like fossil fern foliage with narrow needle-like pinnules was placed in three genera *Aculea* Douglas, *Alamatus* Douglas and *Amanda* Douglas (Douglas, 1973). These genera have similar vegetative morphology but differ in the arrangement and position of their sori (Cantrill, 1996). Similar *in-situ* fern foliage was described from the Cretaceous of Alexander Island by Jefferson (1981) and Cantrill (1996). Cantrill (1996) compared finer more delicate fronds to *Aculea*, for which he erected the new genus *A. acicularis* Cantrill, more robust forms were assigned to *Alamatus bifarius.* Sphenopteris sp. A with thick uninerved pinnae is most similar to *Alamatus bifarius.*

Fern sp. 2 (Figure 8.1: 12)

Material examined: Rocky Cove P.3029.19.1a/b, .19.2.

Description: Delicate bifurcating fronds. Preserved frond length 14 mm by <1 mm wide, total frond length unknown. Midvein <0.1 mm thick. At least bipinnate.

Remarks: The uninerved fronds of Fern *sp. 2* are similar to those of *Aculea acicularis* (Cantrill, 1996, 2000; see above), however the frond is only a small fragment of the original plant and further collecting of this material is required to support these comparisons.

Fern sp. 3 (Figure 8.2: 1 – 2)

Material Examined: Dragon Glacier flora P.236.11. P.3001.117. P.3013.12.

Description: Preserved frond min 34 - 48 mm long by min 12 - 22 mm wide. Total frond length unknown. Single unbranched midvein thickness 0.5 - 0.8 mm. Closely spaced veins arising from midvein at an acute angle 52° - 88° average 82° (P. 3013.12), becoming more acute towards apex, veins dichotomise at least once to twice towards margin. Margin ?toothed.

Remarks: Fern *sp. 3* is defined by the closely spaced, multiple dichotomising veins that branch from the midvein and possible marginal toothing (P.3013.12). This combination of features is present in *Phyllopteroides* Medwell spp., (Osmundaceae) (Cantrill and Webb, 1986; McLoughlin *et al.*, 1995). The more oblong pinnule shape of specimen P.236.11 is consistent with *Phyllopteroides lanceolata* Walkom from the Lower Cretaceous of eastern Australia, although the vein divergence angle is lower in *P. lanceolata* and other *P.* spp. illustrated by Cantrill and Webb (1986), being generally <45° as opposed to 52° - 88°.

Straplike fern fronds with irregular margin course ?toothing and several vein dichotomies were described from Fossil Hill by Zhou and Li (1994) and assigned to the Osmundaceae. These fronds have a greater angle of secondary venation than the *Phyllopteroides* sp. discussed above and are therefore similar to this morphotype. The bifurcating venation is also present in *Cladophlebis biformis* Drinnan and Chambers, although most of the species described by Drinnan and Chambers (1986) have shorter pinnules around 10 mm in length which are more wedge shaped. *Marattia* Sw. (Marattiaceae) and *Blechnum* L. (Blechnaceae) also have simple strap-like fronds with bifurcating venation.

Fern sp. 4 (Figure 8.2: 3)

Material examined: Mt. Wawel flora P.3010.17.

Description: Ovate pinnule, preserved length min 11 mm, width 6 mm. Total length unknown. Single unbranched midvein thickness 0.01 mm. Veins arise from midvein at a moderate acute angle

48° - 55° and dichotomise at least once towards margin. Margin toothed. Teeth 1 order (rarely 2 orders), spacing regular. Shape RT-CV, CC-CV. Sinus and apex angular.

Remarks: Toothed margins and dichotomising venation suggest affinities with *Phyllopteroides* spp. a common fern present in Cretaceous Australian sequences e.g. McLoughlin *et al.* (1995). Dichotomising venation distinguishes the leaf from *Phyllocladus* Rich (e.g. *P. hypophyllus* Hook), which otherwise has a superficial resemblance in terms of margin morphology and lamina shape.

Fern sp. 5 (Figure 8.2: 4 - 5)

Material examined: Dragon Glacier flora P.236.9, .15. P.3001.141a/b, .234. P.3013.24.

Description: Fronds with undivided blade-like pinnules. Preserved frond lengths min 22 - 44 mm, total frond length unknown, at least once pinnate. Single midvein occasionally branched at 54° - 80°. Pinnules alternate, rarely subopposite. Pinnule length up to 8 - 15 mm by 1.5 - 3 mm wide, arising at 44° - 90° av. 66.7°. Pinnule venation alternate to subopposite, arising at 56° - 64°, ?unbranched. Pinnule indented to 0.2 mm from midvein. Pinnule margin entire, apex acute.

Remarks: The small blade-like pinnules of these fronds is similar to *Cladophlebis biformis* (Drinnan and Chambers, 1986), although the frond fragments preserved here lack the typical dichotomising venation.

Fern sp. 6 (Figure 8.2: 6)

Material examined: Fossil Hill Unit 3 P.3031.89. Potter Cove impression flora P.232.34.

Description: Fragments of large fronds with long undivided bladelike pinnules. Fronds at least once pinnate at least 139 - 160 mm long. Midrib up to 1 mm wide, rachis 3.8 mm wide. At least 14 alternate, distichous pinnules, diverging from midvein at 74° - 90°. Pinnules fragmentary at least 30 mm long by 7 – 8 mm wide. Pinnule venation not preserved. Pinnule margin appears entire.

Remarks: Troncoso (1986) assigned straplike alternate pinnules with ?petiolate bases to *Blechnum* sp. This morphotype is distinguished from the specimens illustrated by Troncoso (1986) in having a pinnatifid morphology with a winged, non-petiolate, rachis. Pinnatifid fronds are present in a number of genera including *Blechnum* (Blechnaceae) and *Polypodium* L. (Polypodiaceae) but the specimens presented here lack diagnostic features that would differentiate between these genera.

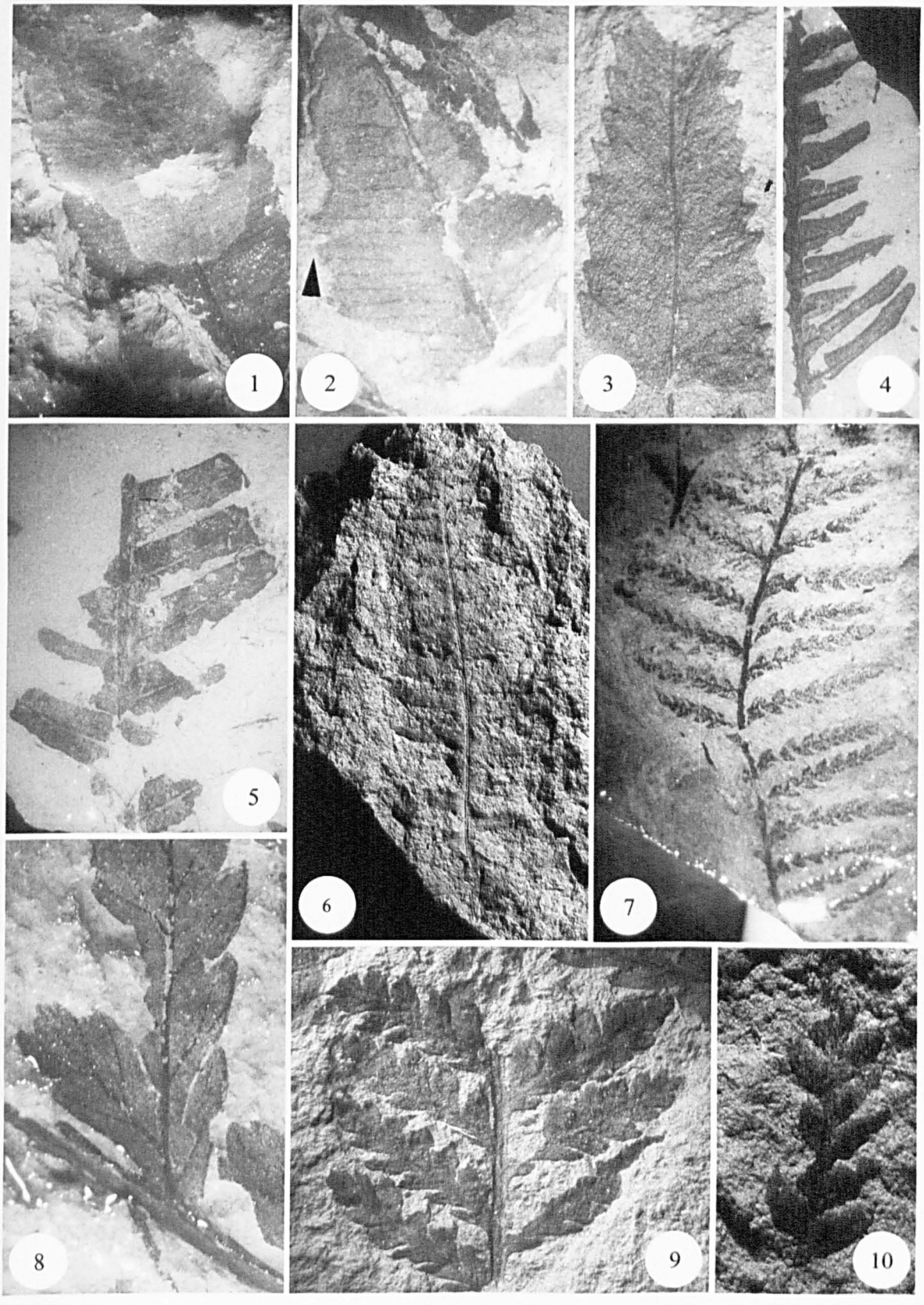

Figure 8.2. (1 - 2) Fern sp. 3. (1). P.3013.12. x1.6. (2). Example of marginal indentations ?toothing and multiply dichotomising venation. P.3001.117. x3.8. (3). Fern sp. 4. P.3010.17. x5.6. (4) - (5) Fern sp. 5. (4). P.3001.141.1a. x2. (5). P.3001.141.1b. x4.9. (6) Fern sp. 6. P.232.34. x0.48. (7). *Gleichenia* sp. P.3032. x1.9. (8) - (9). Fern sp. 7. P.236.1a. (8). Detail of pinnule venation and toothing. x2.5. (9). Frond fragment. x2.5. (10). Fragment of sterile foliage of Fertile fern sp. 1. P.2810.13. x2.

Family Gleicheniaceae

Gleichenia sp. (Figure 8.2: 7)

Material examined: Fossil Hill Unit 3 P.3032.23, .70, .71, .77, .79.

Description: Preserved frond lengths up to 55 mm by 0.2 mm wide. Pinnae alternate up to 20 mm long. Pinnae spaced regularly 3 – 4 mm, diverging at a moderate to wide acute angle 54° - 88°. Pinnules 0.5 – 1 mm long by 0.8 – 1 mm wide. Pinnules alternately arranged. Pinnule shape triangular or slightly falcate, apices acute less frequently obtuse.

Remarks: Zhou and Li (1994) identified fern foliage from Fossil Hill as *Gleichenia* Sm., sp. on the basis of pseudodichotomous branching of the rachis and faintly preserved arrested bud axils, which are characteristic of the Gleicheniaceae (Cantrill, 2000). The distinctive triangular to falcate pinnule morphology of these fossil specimens is characteristic of *Gleichenia* Sm., sp. (Gleicheniaceae), described by Zhou and Li (1994) from Fossil Hill. Fronds described as cf. *Pecopteris* from the Palaeocene Cross Valley Formation (Dusén, 1908) and *Gleichenia* sp. from Fossil Hill (Czajkowski and Rosler, 1986) are comparable in size and frond morphology and are likely to belong to the same morphotype.

Fern sp. 7 (Figure 8.2: 8 - 9)

Material examined: Cytadela flora (Platt Cliffs) ?G.47.16. ?G.309.4. Dragon Glacier flora G.9.7. P.236.1a/b, .14. P.3001.17, .35a/b, 71, .147, .197. P.3008.3. P.3010.16, P.3013.10.3, .18, .24, .44. Fossil Hill Unit 3 P.3032.23, .74, .75, .85, .87, .88, .124. Potter Cove compression flora P.232.7, .10, .37, ?.43, .44, .54, .58, ?.61, .68.

Description: Fronds with variably highly divided pinnae, having a prominently branched midvein (Figure 8.2: 8). Preserved frond lengths 17 - 69 mm, total frond length unknown. At least bipinnate. Apical fronds have poorly divided pinnae (e.g. P.236.1a), division becomes more pronounced basally (P.3001.35). At least 7 - 21 secondary pinnae, length 2 – 27 mm. Secondary pinnae alternate and distichous, 1 – 6 mm apart, arising acutely 53° - 60° av. 57° (P.236.1a). < 18 pinnules per secondary pinnae, length 2 – 5 mm, width 1 - 2.5 mm, arising at 43° - 65° av. 49.8° (P.236.1a). Single branched midvein, up to 7 branches which terminate in serrations (P.236.1a). Pinnule margin toothed 0 - 5 serrations/pinnule, apex acute 62° - 80° (P.236.1a). Pinnule venation alternate, veins sometimes dichotomising towards tooth apices. Toothing less pronounced or absent in pinnules on proximal side of pinnae.

Remarks: These are the most common fern macrofossils in the King George Island floras and are grouped with specimens described as *Culcita macrocarpa* Presl. (cf. Dicksoniaceae) by Dutra and

Batten (2000), that also have a rounded triangular pinnule shape, pinnule venation and divergence angle.

Division Cycadophyta

Order Cycadales

Family Zamiaceae

Genus *Dioon*

Dioon antarctica Zhou and Li 1994 (Figure 8.3: 1)

Material examined: Fossil Hill Unit 2 P.3034.3.6, .4, .10, .24, .46, .69.2, .84. Fossil Hill Unit 3 P.3032.46.

Description: Small fronds with distichous pinnae. Fragment length up to 107 mm, pinnule length 5 – 6 mm by 2 – 4 mm wide. Pinnules opposite to subopposite, triangular to wedge shaped with slightly imbricated base. Pinnules with 4 - 5 parallel veins, which terminate in marginal teeth.

Remarks: The parallel veined pinnules with toothed margins are characteristic of *Dioon* (Dion) *antarctica* described by Zhou and Li (1994). Zhou and Li (1994) related their material to the modern *Dioon* Lindley on the basis of these characters as well. Specimen P.3034.3.6 is 2.3x longer than the largest specimen described by Zhou and Li (1994) but does not differ in any other aspect from their original description.

Division Coniferophyta

Order Coniferales

Family Araucariaceae

Araucaria sp. 1. sect. *Eutacta* (Figure 8.3: 2)

Material examined: Collins Glacier in-situ P.3025.7. Fossil Hill Unit 3 P.3032.80, ?.93.

Description: Axis with spirally arranged leaves. Fragment length 30 mm. Leaf length 5 – 7 mm, ?width 0.8 – 1.5 mm wide, leaves are keeled. Length:width ratio 4.1 – 6.25:1. Leaves bilaterally flattened, triangular, tapering towards a ?rounded apex. Leaves diverging at a narrow acute angle 24° – 41°, spreading and incurved distally. Apex acute. No petiole. Margin entire no evidence of thickening. Venation not observed. Insertion not observed.

Remarks: Helically arranged keeled leaves occur in a number of genera including *Araucaria*, *Dacrydium*, *Microcachrys* and *Podocarpus* (Offler, 1984). The association of *Araucaria* section *Eutacta* cone-scales with this foliage (at Fossil Hill) suggests that the material belongs to the

Araucaria section *Eutacta* rather than one of the other genera. The distally incurved, bilaterally flattened triangular leaves with a low divergence angle are similar to those of the modern *Araucaria cunninghamii* Ait. in Sweet, but *A. cunninghamii* differs in having smaller leaves with a lower length:width ratio.

Barton (1964) described araucarian foliage from the Admiralen Peak flora, which differs from these specimens, only in having slightly longer leaves (up to 1 cm). Barton (1964) considered that the leaf arrangement, shape and size of the fossil species was similar to *Araucarites ruei* Sew., from the Kerguelen Islands and to the modern *A. rulei* Muell., from the New Hebrides but closer comparisons were limited by the lack of cuticular data in the fossil specimens. Triangular, tapering leaves are also present in the Early Eocene *A. readiae* (Hill and Bigwood, 1987) from Tasmania and to the Early Cretaceous *A. falcatus* (Cantrill, 1992) from Australia. *Araucaria* sp. 1 are differentiated from *A. readiae* that has a broader leaf base (Hill and Bigwood, 1987), and *A. falcatus* which has leaves oriented at a greater angle to the stem. The leaves of *A. pichileufensis* Berry are also of a similar size and shape, although Berry (1938) could not confirm the presence of a keel on the leaves.

Araucaria sp. 2 sect. *Columbea* (Figure 8.2: 3 - 4)

Material examined: Cytadela flora (Platt Cliffs) G.47.10(30), G.309.17.1(29), 17.2(28), 17.3.

Description: Isolated multiveined lanceolate bifacially flattened leaves. Bases and apices tapering. Length up to 85 mm, width up to 20 mm. Orientation of leaves uncertain, due to lack of leaf base preservation.

Remarks: This is the largest multiveined unkeeled leaf type present in the King George Island flora. Large and broad leaves, which taper both apically and basally, are characteristic of *Agathis* spp., and leaves of the *Araucaria* sections *Columbea.* Leaves of *Agathis* spp., are petiolate distinguishing them from the specimens described here. Barton (1964) compared these leaves to *Araucaria imponens* Düsen by reference to a leaf from Seymour Island described by Düsen (1908). The material from both floras is consistent in size, lanceolate form and parallel venation. Düsen (1908) based his interpretations on the recent *A. bidwilli* Hook, although these leaves have rostrate apices (Offler, 1984) and the bases do not taper to the same degree as the fossil specimens.

Berry (1938) described parallel-veined lanceolate, inequilateral and often falcate leaves, that taper proximally and distally, as *Zamia tertiaria* Engelhardt, however there is no discussion of his reasons

for this classification. His illustrations, although faint, suggest a possible adnate, decurrent leaf base, rather than a petiolate base that would define cycadalean foliage.

Araucaria sp. 3 ?sect. *Columbea* (Figure 8.3: 5)

?Araucaria nathorsti Dusén 1899

Material examined: Mt Wawel flora P.3010.9.2.

Description: Leaf bilateral, triangular, with margins slightly convex. Length 10 mm, width 7mm, length:width ratio 1.43:1. Apex convex, apical angle acute 80°. Base convex, basal angle obtuse 109°. Margin entire. Venation parallelodromous with a minimum of 8 pronounced veins converging apically.

Remarks: The broad attachment and lack of a prominent keel in this specimen suggests that the leaf belongs to either the *Intermedia*, *Columbea* or *Bunya* sections rather than the *Eutacta* section (Hill and Bigwood, 1987). In shape the leaf resembles the Middle to Late Eocene *Araucaria hastiensis* Hill and Bigwood, from Tasmania, but the venation of that leaf is much less distinct. The fossil specimens are also similar in size and shape to *Araucaria nathorsti* Dusén 1899, from the section *Columbea* (Menendez and Caccvari, 1966) from the Tertiary of Argentina, which also have pronounced parallel venation. The fossil specimens are therefore considered to be morphologically most similar to *A. nathorsti*.

Araucaria sp. 4 (Figure 8.3: 6)

Material examined: Dragon Glacier flora P.1404.16, .27.2, P.2810.17.1. P.3001.1.2, .198, .215. P.3005.3. P.3007.1, .3 -.8, .10.2-6, .15, .20. P.3013.27.

Description: Elliptic to oblong, strongly bifacially flattened leaves with parallel veins. Probable spiral arrangement, spacing uncertain (P.2810.7.1). Leaves appear to spread a wide acute angle from the axis. Length 17 – 34 mm, width 6 - 12.5 mm. Length:width ratio 1.82:1-5.6:1. Apex and base convex rounded, angle wide acute 80°. Base tapers slightly. Margin entire. Veins vary in strength, with elongate specimens having more pronounced ribs.

Remarks: Large elliptic, unkeeled multiveined leaves are present in the sections *Columbea*, *Bunya* and *Intermerdia*. A similar lamina shape is also present in proximal leaves of *Wollemia nobilis* (Jones et al., 1995) (Wollemi Pine) but the fossil specimens differ in tapering more towards the base (Chambers *et al.*, 1998). The variation in vein strength between the elliptic and more elongate specimens suggests that this group may require further subdivision, but it could simply

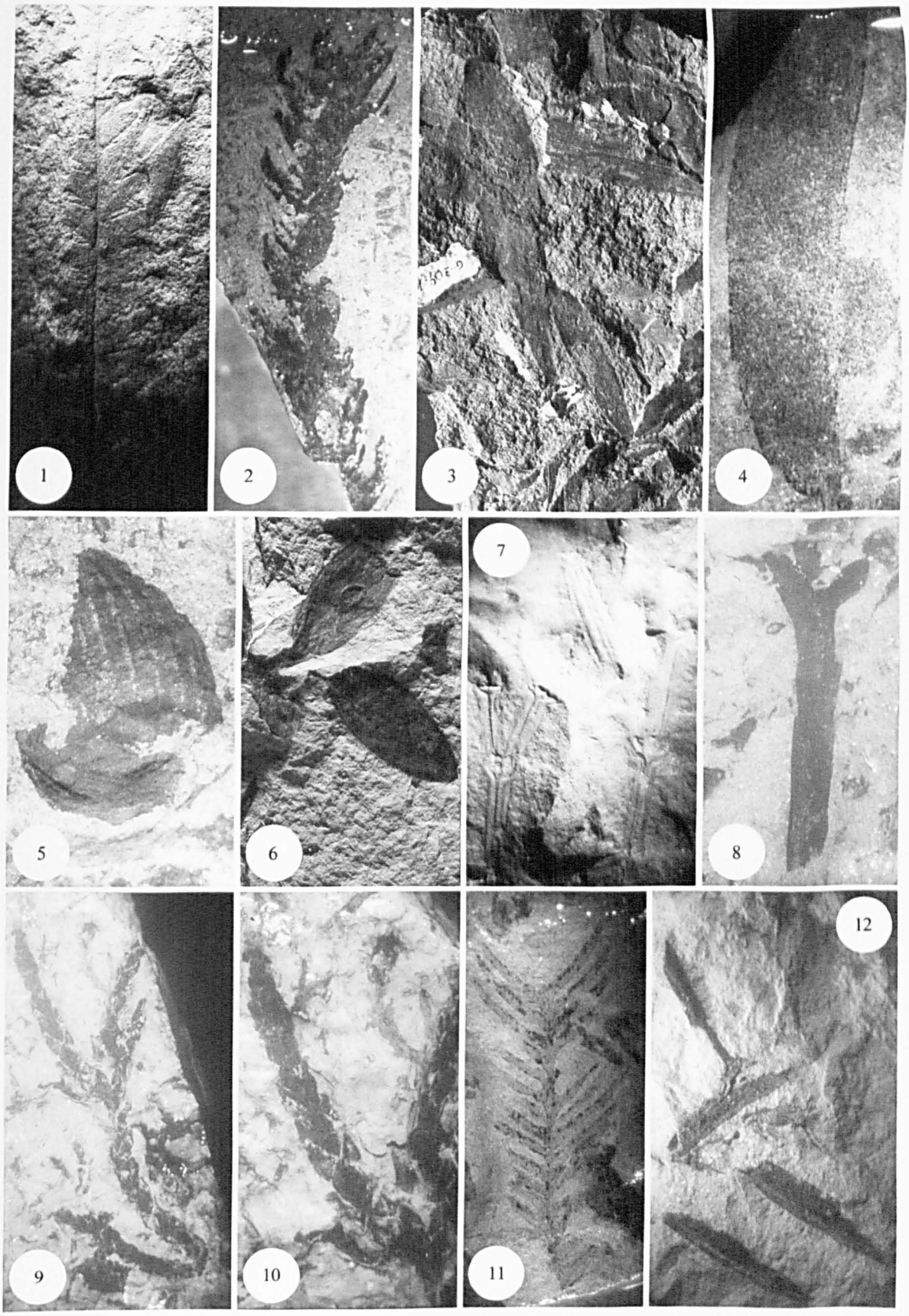

Figure 8.3. (1). *Dion antarctica*. P.3034.69.2. x2.3. (2). *Araucaria* sp. 1. P.3032.80. x2.6. (3) - (4). *Araucaria* sp. 2. (3). G.309.17. x0.65. (4). G.47.10. x1.8. (5). *Araucaria* sp. 3. P.3010. 9. 2. x4.9. (6). *Araucaria* sp. 4. P.2810.17.1. x1.3. (7) - (8). *Papuacedrus shenii*. P.3031.84. x1.78. (8). Fragment of bilaterally flattened leaf pair, fused margin arrowed. P.3001.58. (9) - (10). Cupressoid sp. 1. P.3001.188. (9). x1.87. (10). x3.64. (11). *Acmopyle antarctica*. P.3032.72. x1.59. (12). Awl leaf sp. 1. P.2810.17.2. x1.26.

relate to differences in leaf maturity since the leaves in the Araucariaceae family are perennial and remain on the branches for a number of years (Cantrill, 1992).

Family Cupressaceae

Genus *Papuacedrus shenii* Zhou and Li 1994 (Figure 8.3: 7 - 8)

(pl. 1, figs 1, 1a, text figs, 1a-d)

Material examined: Dragon Glacier flora P.3001.58. Fossil Hill Unit 2 P.3034. Fossil Hill Unit 3 P.3032.89. Fossil Hill Unit 4 P.3031.2, .36, .41, .84, .87, .88, .92, .93, .97, .109.

Description: Fragments of leafy shoots comprising one pair of opposite bilaterally flattened leaves and a second pair of opposite bifacially flattened leaves. Shoots up to 44 mm, sometimes branching by insertion of a second shoot. Bilaterally flattened leaves up to 15 mm long by up to 4 mm wide, tapering to 1.5 mm adaxially. Bifacially flattened leaves up to 1 mm long by 0.2 mm wide. The adaxial termination of the bilaterally flattened leaves is flared and tapering.

Remarks: The alternate opposite pairing of bifacially and bilaterally flattened leaves in these specimens is characteristic of *Austrocedrus* Florin and Bout., *Libocedrus* Endl., and *Papuacedrus* Li (Cupressaceae) (Whang and Hill, 1999). Zhou and Li (1994b) assigned identical foliage from the same beds at Fossil Hill to *Papuacedrus shenii* Zhou and Li. Subsequently, Hill and Brodribb (1999) considered that the generic affinities were difficult to determine due to the lack of organic preservation in the fragmentary material described by Zhou and Li (1994). However, Whang and Hill (1999) noted that fusing of alternately pairs of bifacially and bilaterally flattened leaves occurs only in *Papuacedrus*, a feature used to distinguish the species by Zhou and Li (1994b).

Cupressoid sp. 1 (Figure 8.3: 9 – 10)

Material examined: Dragon Glacier flora ?P.3001.50b, .179.2, .188. Fossil Hill Unit 2 ?P.3034.29.1-.4.

Description: Fragments of multiply branched leafy shoots with oppositely paired scale leaves. Shoot length up to 49 mm by 2 mm wide, tapering slightly distally. Rhomboidal/awl shaped leaves up to 2 mm long by 1.2 mm wide, closely apressed. Main branch gives rise to two branches which give rise to several other branches. Leaf type does not vary between branches. Individual branches often short 15 – 17 mm long.

Remarks: The alternate opposite arrangement of the scale leaves on these leafy shoots is characteristic of the Cupressaceae.

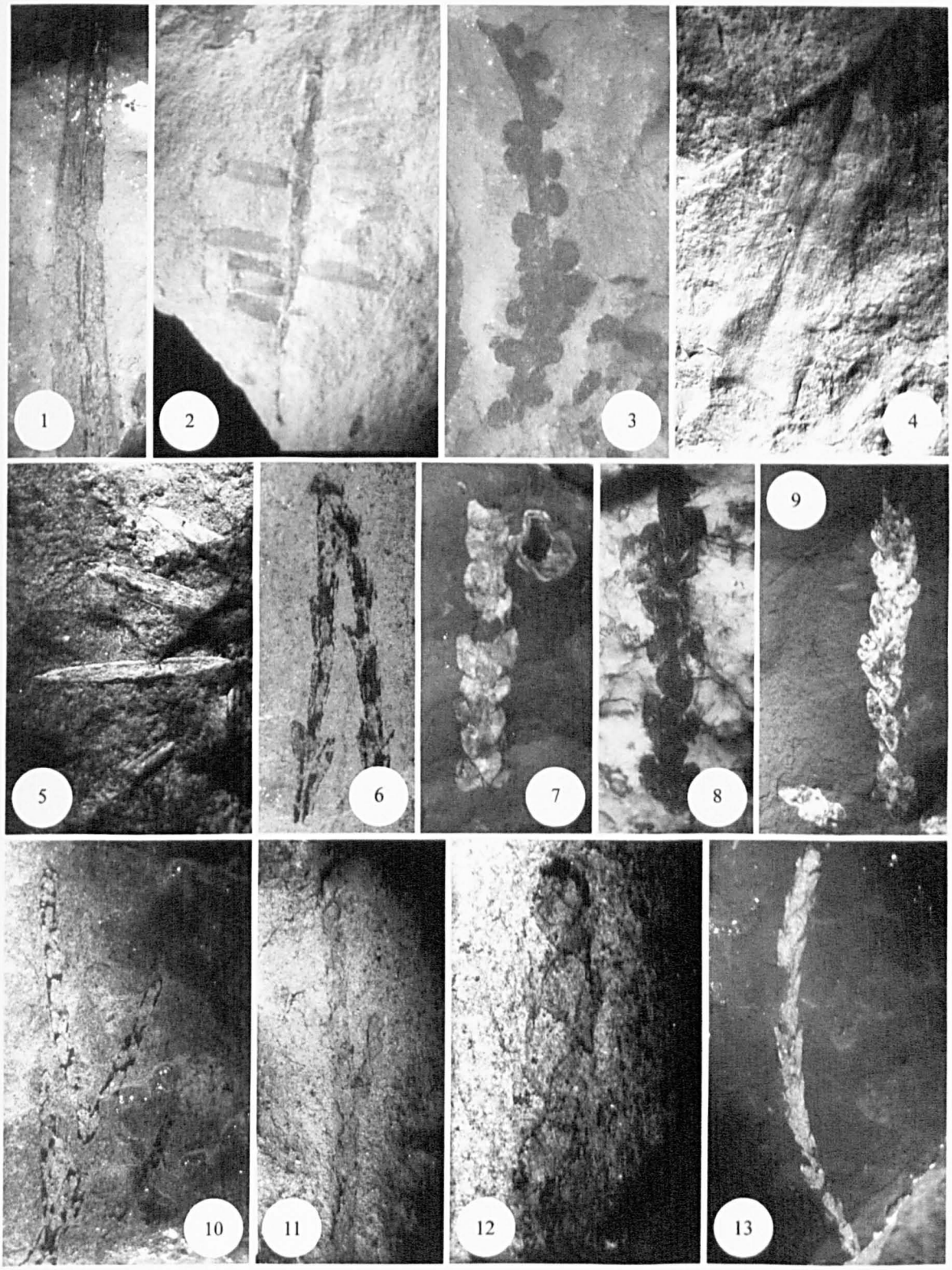

Figure 8.4. (1). *?Podocarpus* sp. 1. G.47.3. x1.7. (2). *?Podocarpus* sp. 2. P.232.70ii. x2. (3). Podocarpaceous root. P.3001.208. x6.8. (4). Lanceolate keeled leaf sp. 1. P.3034.71. x1.4. (5). Awl leaf sp. 1. P.3031.38.2. x3.65. (6) Conifer shoot sp. 1. P.3032.89. x4. (7) - (9). Conifer shoot sp. 2. (7). P.3034.36b. x5.42. (8). P.3001.188.2. x5.2. (9). P.3034.36a. x4.4. (10) - (12). Conifer shoot sp. 3. P.3032.68. x1.6. (10). Branching axis. x1.7. (11). Detail of shoot. x1.86. (12). Detail of terminal shoot. x5.67. (13). Conifer shoot sp. 4. P.3032.28. x2.15.

Family Podocarpaceae

Genus *Acmopyle*

Acmopyle antarctica Florin (Figure 8.3: 11)

Material examined: Fossil Hill Unit 3 P.3032.20, .51, .68, .69, .72, .76, .81.

Description: Small axes with bilaterally flattened, alternate and distichously arranged leaves. Axes length up to 62 mm, thickness 0.5 - 1 mm. Leaves up to 11 mm long 1.5 – 2 mm wide. Leaf base decurrent and slightly imbricate, apex acute, tapering. Leaves diverge at a moderate acute angle 45° - 54°. Margins entire.

Remarks: These specimens were assigned to *Acmopyle antarctica* by Li and Zhou (1994) based on morphological similarities with *Phyllites* sp. 4, from the Palaeocene Cross Valley Formation samples of Dusén (1908). *Phyllites* sp. 4 was later reassigned to *A. antarctica* by Florin (1940), based on the close gross morphological similarity with *Acmopyle pancheri* (Brongn et Gris) Pilger.

Genus ?*Podocarpus* sp. 1 (Figure 8.4: 12 and Figure 8.4: 1)

Material examined: Cytadela flora (Platt Cliffs) G.47.1.1-.10, .3.1-.10. G.309.2, .3.1-.7, .7, .16.1-.7, .19. Dragon Glacier flora P.3001.179. Dufayel Island ?G.53.26. Fossil Hill Unit 3 P.3032.27, .89. Platt Cliffs ?G.50.20.

Description: Fragmentary strap-like leaves with a high length:width ratio and a single pronounced midvein. Length up to 50 mm, width up to 5.5 mm. Length:width ratio may be up to 22.5:1. Up to seven less pronounced ribs 0.1 - 0.7 mm thick occur in addition to the midvein. Margin entire. Base, absent.

Remarks: These leaves are unusual in having an extremely high length:width ratio and a long lamina (>5 cm). Elongate leaves with a strong midrib are common within the Podocarpaceae, e.g. *Dacrycarpus* (Endl) Laubenf., *Prumnopitys* Phillippi, *Retrophyllum* Page and *Podocarpus* L'Herit. ex. Pers. Of these, *Podocarpus* sp. tends to have the highest leaf length to width ratios (Hill and Brodribb, 1999), therefore these leaves are assigned to *Podocarpus*. The leaf bases, which are an important characteristic for grouping this leaf morphology, are not preserved. The Chilean *Podocarpus selignus* D. Don has similarly high length:width ratios to the fossil material, a comparison also noted by Barton (1964) with his "*P. saligna*". A tentative grouping with *P. selignus* is therefore suggested.

?Podocarpus sp. 2 (Figure 8.4: 2).

Material examined: Potter Cove compression flora P.232.46, .49, .70ii.

Description: Thick axes with ?distichously arranged straplike, multiveined leaves. Axis fragments up to 75 mm long by up to 1.5 mm thick. Leaves bilaterally flattened at least 22 mm long by 2 – 3.5 mm wide. Leaves apressed to axis, slightly imbricate. Leaves diverge at a moderate to wide acute angle 48° – 90°. Entire margined.

Remarks: Distichous straplike leaves are common in many genera of the Podocarpaceae e.g. *Prumnopitys, Dacrycarpus* and *Podocarpus* although most of these leaves have a strong midrib. Without cuticular data the leaves are simply assigned to the Podocarpaceae.

?Podocarpaceous root (Figure 8.4: 3)

Material examined: Dragon Glacier flora P.3001.208.

Description: Nodular root. Roots 9 mm long by 0.2 mm wide. Two opposite rows of swollen spherical nodules constricted at the point of attachment, 0.4 – 0.5 mm diameter. Nodules closely spaced, occasionally overlapping.

Remarks: Nodular roots that are constricted in at the point of attachment are present in the Taxodiacaeae and Podocarpaceae (Cantrill and Douglas, 1988). Taxodiaceous plants have not been described from King George Island, whilst the Podocarpaceae is a common element of the flora, therefore by deduction the roots are more likely to be podocarpaceous.

Family incertae

Lanceolate keeled leaf sp. 1 (Figure 8.4: 4)

Material examined: Fossil Hill Unit 2 P.3034.71.

Description: Fragment of a lanceolate multiveined keeled leaf with a truncate, slightly concave base. Minimum 46 mm long by 10 mm wide. Keel 1 mm wide.

Remarks: The unusual truncate base of this leaf is probably due to abscission from the stem portion of the lamina, or it might imply direct adpression to the stem. The strong midrib and shape of this leaf are common in the Podocarpaceae although there is no evidence of two dimensional flattening and twisting of the lamina that might be expected in the distichous fronds of this family. *Libocedrus yateenensis* (Cupressaceae) has keeled leaves that are not two dimensionally flattened and are also lanceolate shaped (Hill and Brodribb, 1999), suggesting a possible affinity.

Awl leaf sp. 1 (Figure 8.4: 1).

Material examined: Dragon Glacier flora P.2810.17.2. P.1404.27.1. P.3001.2, .19. P.3007.7.1, .10.1 .15, .19 - .20, .87, 131.2, 139.2. P.3013.28, .31, .34. Fossil Hill Unit 2 P.3034.23, .26, .45, .58, .75. Fossil Hill Unit 4 P.3031.38.2.

Description: Small axes bearing ?spirally arranged awl shaped, sometimes concave, keeled leaves. ?Alternate or whorled arrangement. Length 10 - 20 mm av. 13 mm, width 1 - 5 mm av. 3.0 mm. Length:width ratio 3.4:1-7:1. av. 5.1:1. Apex acute and angular. Keel < 0.1 - 0.8 mm. Keel emerges through apex to form a spine, length 0.2 – 1 mm (e.g. P.3001.28). Leaves diverge from stem at a wide acute angle 70° – 90°. Sheathing stem for approximately 3 mm. Margin entire.

Remarks: The group of leaves presented here may represent two different species essentially the division between the narrower and shorter P.2810.17.2 and P.3032.23 and the remaining specimens. The former are the only two specimens that show some of their original arrangement on the branch, but differ in no other feature (without cuticular data). Li and Shen (1990) assigned the Fossil Hill specimens of this material to *Podocarpus* sp. 1, however keeled awl shaped leaves with a concave adaxial surface are present in the Araucariaceae, Podocarpaceae and Taxodiaceae and spines occur in mature examples of these groups (Cantrill, 1992). Cuticular data is necessary to differentiate among these families. The leaves are similar in size and gross morphology to *Podocarpus nubigenia* and *Saxegotheca conspicua* (Podocarpaceae). The smaller and narrower leaves of P.2810.17.2 and P.3032.23 are more similar to *Prumnopitys andini* (Podocarpaceae).

Conifer shoot sp. 1 (Figure 8.4: 6).

Material examined: Fossil Hill Unit 2 P.3034. Fossil Hill Unit 3 P.3032.89.

Description: Fragments of long leafy shoots with spirally arranged leaves. Shoot length up to 35 mm, width up to 1.1 mm. Leaves up to 8 mm long by up to 0.2 mm wide. Leaves linear with an expanded distal portion and imbricate, ?oppositely paired.

Remarks: Coniferous shoots with spirally arranged foliage are common to a number of coniferous genera and without cuticular data it is impossible to relate these specimens to a particular genus. The possible opposite pairing of these leaves is similar to *Papuacedrus shenii* (Zhou and Li, 1994) but these leaves are generally shorter and thicker than the material included here. The pairing suggests cuppressoid affinities.

Conifer shoot sp. 2 (Figure 8.4: 7-9)

Material examined: Dragon Glacier flora G.9.3.2. P.236.20b. P.2810.11, 18.5. P.3001.3.2, .53, .99.2, .162.2, .179.2, .181.2, .184.2, .189, .234. P.3007.18. P.3013.24. Fossil Hill Unit 2 P.3034.28, .29, .43.

Description: Fragments of leafy shoots with helically arranged imbricate leaves. Shoot length up to 41 mm long by up to 2 mm wide. Occasional branches. Leaves are rounded triangular with a low length:width ratio, 1.5 mm long by up to 1 mm wide. Spirally arranged around axis.

Conifer shoot sp. 3 (Figure 8.4: 10-12)

Material examined: Dragon Glacier flora G.9.3.3. P.2810.23.1. ?P.3001.187.4. Fossil Hill Unit 3 P.3032.68, .91, .143.

Description: Fragments of branching leafy shoots with helically arranged leaves. Shoots up to 90 mm long by 2 mm wide, branches up to 30 mm long. Branch angle narrow acute 18° – 38°. Leaves rhomboidal, closely apressed, 2.5 mm long by 1.5 mm wide.

Conifer shoot sp. 4 (Figure 8.4: 13)

Material examined: Fossil Hill Unit 2 P.3034.28.1, 32, 42, .43. Fossil Hill Unit 4 P.3031.

Description: Fragments of leafy shoots with helically arranged leaves. Shoots up to 31 mm long by 1.1 mm wide. No branches observed. Leaves closely apressed, triangular, 3 mm long by 0.5 mm wide.

Remarks: These shoots are described as *Podocarpus tertiarius* by Zhou and Li (1994).

Chapter 9 Fertile organs

9.1 Introduction

Collections of reproductive material from the King George Island flora are relatively limited, comprising rare araucarian cone material (Barton, 1964), fertile fern axes (Li and Shen, 1992; Torres and Meon, 1993; Zhou and Li , 1994) and angiosperm and podocarp seeds (Zastawniak *et al.*, 1985; Troncoso, 1986; Dutra, 1989). During the 1999 field season, 35 fern, gymnosperm and angiosperm fertile organs were collected from Fossil Hill, Point Hennequin and Rocky Cove (Figure 2.1). The aim of this chapter is to document the large body of fertile material present in the King George Island floras and to provide a preliminary taxonomic/systematic arrangement of the material. Fertile fern axes are discussed in Chapter 8, since they are also associated with sterile foliage. All of the organs described here are summarised in Table 5.4.

9.2 Systematic Palaeobotany

Division Coniferophyta

Family Araucariaceae

Araucaria sect. *Eutacta* Cone scale (Figure 9.1:1 - 4)

?Araucaria pichileufensis Berry 1938

Material examined: Collins Glacier moraines P.3028.1a/b, .3a/b. Fossil Hill Unit 3 P.3032.7, .83.4, .86, .17.1/.2. Mt. Wawel flora P.3010.9.1.

Description: Ovuliferous cone scale. Up to 25 mm long, winged width up to 24 mm, unwinged up to 12 mm, cuneate in shape, tapering towards point of attachment. Distal spine up to 4 - 7 mm long. Wings are often absent due to preservation, where preserved they are thin and almost papery and have a distinct sinus to either side of the seed complex (P.3028.1a/b).

Remarks: Distal spines are characteristic of *Araucaria* sect. *Eutacta* (Hill and Brodribb, 1999). A thin winged cone scale referred to *Araucaria pichileufensis* (Berry 1938) also bears a distal spine and has distinct sinuses to either side of the seed complex, similar to those of P.3028.1 (Figure 9.1: 2). On this basis the King George Island specimens are grouped with *A. pichileufensis* sect. *Eutacta.* Berry (1938) grouped araucarian foliage together with his isolated cone scales, although the material was not intimately associated. Similar foliage is also found in the King George Island flora, which might support this grouping (Chapter 8).

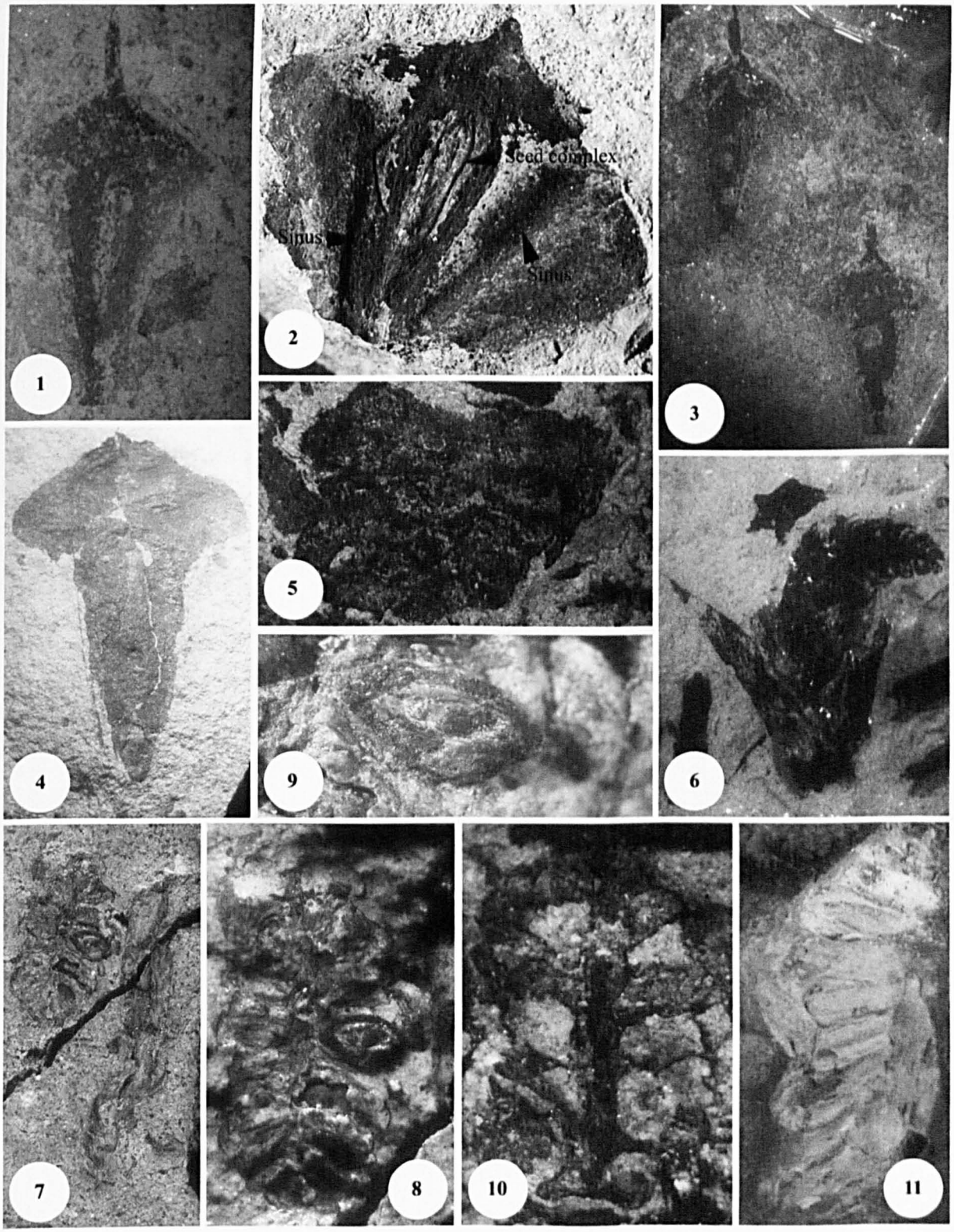

Figure 9.1. (1) - (4) *Araucaria pichileufensis* cone scales. (1). P.3032.7. x2.5. (2). P.3028.1.a. x4.3. (3). P.3032.17. x1.6. (4). P.3010.9.1 x5.5. (5). Fragment of *Araucaria* cone axis. P.3001.187. x3.6. (6). Cone sp. 1. P.3001.12.1. x6.9. (7) - (9) Cone sp. 2. Cytadela (Platt CliffsG.47/G.309). (7). Cone and associated branch material. x3. (8). Detail of cone. x5.7. (9). Detail of ovule. x16.4. (10). Cone sp. 3. P.3001.187.2. x10.6. (11). Cone sp. 4. P.1174.6. x2.3.

Araucaria Seed cone axis (Figure 9.1: 5)

Material examined: Dragon Glacier flora P.3001.117.2, .187.

Description: Fragment of cone axis. 8 mm long by 16 mm wide. Scars depressed, rhomboidal, spirally arranged.

Remarks: Two sections of *Araucaria* are present at Point Hennequin, foliage of *Araucaria nathorsti* (sect. *Columbea*) (Chapter 8) and a cone scale belonging to the *Araucaria* sect. *Eutacta* (see above), and are both considered to be possible origins of the cone axis.

Cone sp. 1 (Figure 9.1: 6)

Material examined: Dragon Glacier flora P3001.12.1.

Description: Microsporangiate pollen cone, with two awl shaped leaves proximally. No shoot preserved. Cone 5 mm long by up to 2 mm wide, tapering distally. Cone comprises a thick central axis bearing helically at least 16 microsporophylls.

Cone sp. 2 (Figure 9.1: 7 - 9)

Material examined: Cytadela flora (Platt Cliffs) G.47/G.309.

Description: Ovuliferous cone, with an associated leafy axis with triangular leaves. Cone length 9 mm, width 4.5 mm. Minimum ?10 elliptic ovules. Associated leafy axis 16 mm long by 2.5 mm wide. Leaves triangular, spreading from the axis and incurving distally. 2 – 3 mm long, width at least 0.5 mm. ?unkeeled, ?spirally arranged.

Remarks: A single type of ?*Podocarpus* foliage dominates the Platt Cliffs flora, suggesting that this cone might be related to the genus.

Cone sp. 3 (Figure 9.1: 10)

Material examined: Dragon Glacier flora P.3001.1.3, 12.2, 41, .139.1/2, .187.3.

Description: Fragmentary remains of ?microsporangiate pollen cones. Fragmentary cones up to 6 mm long by up to 2.5 mm wide. Fragments do not appear to taper distally. Cones comprises a thick central axis bearing helically at least 10 sporophylls.

Cone sp. 4 (Figure 9.1: 11)

Material examined: Profound Lake P.1174.6.

Description: Fragment of ovuliferous cone with no associated stem. Cone length minimum 20 mm by at least 10 mm wide. Minimum six ovules preserved attached to thick axis 1 mm thick.

Fertile organ sp. 1 (Figure 9.2: 1-11)

Material examined: Fossil Hill Unit 3 P.3032.95.1/.2/.3/.4/.5/.6/.7.

Description: Woody capsules < 1 cm long. Valve 9 - 10 mm long by 7 mm wide. Four organs clustered together suggesting an original grouping. Four broad valves enclose one larger, and one smaller, pair of basally fused fruits (Figures 9.1: 5-11). The larger pair of fruits appears to have developed at the expense of the smaller pair. The peduncle is thick and woody, 2 - 3 mm long by 4 mm wide, possibly swollen at its base. Two small ?lamellae are present at the base of the organ/top of the peduncle and are deeply incised (Figure 9.2: 5), no glands are apparent. Valve gape suggested by sediment infill in mid apical portion of specimen P.3032.95.3. Valves split for the whole length of the organ (Figure 9.2: 1). Internal face of valve is divided by a ridge (Figure 9.2: 4).

Remarks: Hill (1991) described five species of *Nothofagus* cupule from the Oligocene Little Rapid River deposit, Tasmania. Two of the species *N. glandularis* Hill and *N. bulbosa* Hill, have four valves, and a similar morphological character to Fertile organ sp. 1, including a large peduncle and woody valves. However, the arrangement of the fruits in two basally fused pairs differentiates these organs from *Nothofagus*. The organs are also similar to terminal Cupressaceae cones (R. Hill pers. comm., 2001), but there is no associated branch material to support this identification. More complete and 3 dimensionally preserved specimens are necessary for interpretations.

Fertile organ sp. 2 (Figure 9.2: 12 and 9.3: 1 - 4)

Material examined: Fossil Hill Unit 3 P.3032.4.1, .2, .18, .39, .48, .65, .142, .137.

Description: ?Cupules < 1.5 cm long, with a possible 4 – 6 slender valves. Fruits are absent. Valves are elongate with a high length:width ratio min. 8.6:1 - 10:1. 8 – 10 mm long by 1 – 2 mm wide. Valves gape to ~70 – 82 % of cupule length. Peduncle well developed and comparatively thick relative to the width of the cupule (35 - 42.5 % of the cupule width). 3 – 4 mm long by 2 mm wide.

Remarks: The structure of these organs with four to six valves suggests that the organs are cupules. Cupules are unique to the Fagaceae and Nothofagaceae. *N. dombeyi, N. alpina, N. moorei, N. menziesii, N. cunninghamii, N. betuloides* and *N. nitida* have similar slender elongate cupules. Fused cupule valves and variable valve numbers are common in *N. dombeyi*, which could explain the variable number of valves. The peduncle is well developed in the fossil specimens, a feature present in *N. alpina* and *N. betuloides* but not in *N. menziesii*. However, Hill and Read (1991) noted that valve number and appearance were not taxonomically important features, highlighting the importance of valve lamellae and the arrangement of the

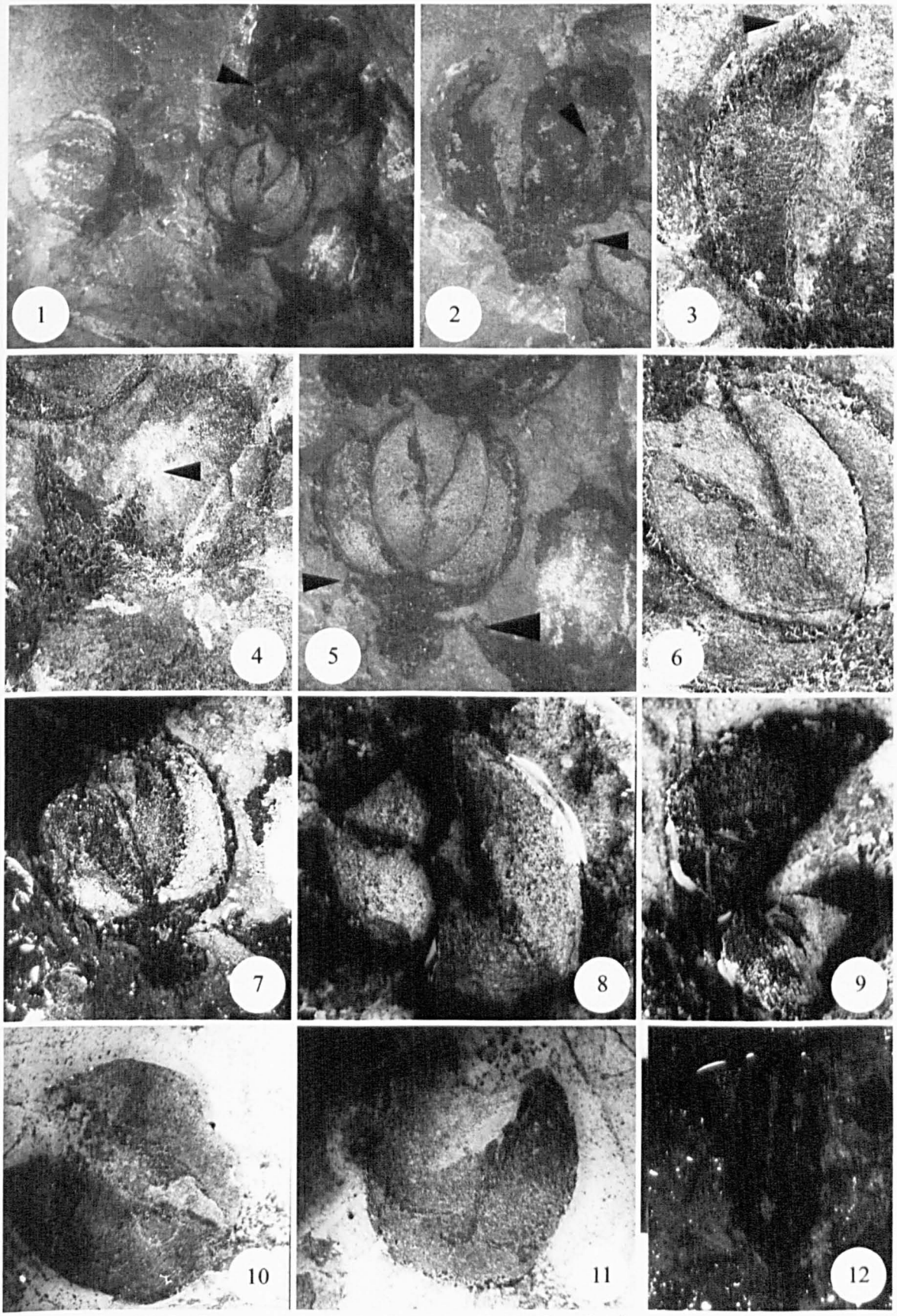

Figure 9.2. (1) - (11). Fertile organ sp. 1. (12). Fertile organ sp. 2. (1). View of main organ cluster, valve gape arrowed. P3032.95. x1.9. (2). ?External surface of valves and possible lamellae (arrowed). P.3032.95.1. x2.7. (3). Detail of valves with possible apical lamellae (arrowed). P.3032.95.1. x5.3. (4). Internal surface of valve. Two valves are observed in cross section. P.3032.95.2. x4. (5). Organ with two paired fruits preserved and incised basal lamellae (arrowed). P.3032.95.3. x3.5. (6). Detail of surface of fruits. P.3032.95.3. x5.6. (7).Basal pair of fruits after removal of upper pair. x3.5. (8). Isolated upper pair of fruits showing fused base. x5.6. (9). Underside of upper pair of fruits, showing darkened layer of organic material. x5.5. (10). Underside of basal pair of fruit. x5.6. (11). P.3032.95.3. x5.6. (12). Fertile organ sp. 2. P.3032.4.2. x 3.1.

fruits within the cupule. Material with better preservation is therefore required to make further comparisons. A further possibility is that the valvate structures are actually parts of a dehiscent capsule, such as the capsules attached to the infloresence Fertile organ sp. 4.

Fertile organ sp. 3 (Figure 9.3: 5 - 6)

Material examined: Dragon Glacier flora P.3001.1, P.3001.29, P.3001.151.1a/b.

Description: Lamina elliptic, symmetrical. Length min 8 - 11 mm, width 8 – 14 mm. Length:width ratio min. 0.57:1 - 1.14:1. Area est. 37.33 -74.67 mm^2. Nanophyll = 3 (100 %). Apex truncate, apical angle 106° - 138°. Base truncate, basal angle 105° - 155°. Apical margin serrate. No petiole preserved. *Venation* best described as flabellate, with a series of branching primary veins diverging from base to terminate in apical teeth. *Primary* veins 7 – 8, thickness ~ 0.1 mm. Course ziz-zag. *Secondary* ?weak brochidodromous (P.3001.151.2), diverging from primaries at moderate to wide acute angle 59 - 74° (P.3001.151.2). *Teeth* possible 2 orders, up to 11 teeth, spacing ~regular, indentation 1 – 2 mm. Apices ?simple. Apex rounded, shape flexuous-flexuous to convex-convex, sinus angular.

Remarks: These organs are differentiated from leaves by the absence of a petiole, midvein or well defined venation system in any of the specimens. Stipules and/or bracts have similar morphologies but are not well documented.

Bracts are common in the Betulaceae (Crane, 1981). The Betulaceae has not previously been reported from Antarctica in the macro- or microfloral record. However, leaves with betulaceous and nothofagaceous character have been found in the King George Island flora (e.g. Fossil Hill Unit 3; Chapter 6) (Dutra, 1997). Broad, squat bracts with a toothed apical margin are found in *Corylus* L. in the *Coryleae* tribe of the Betulaceae (e.g. Crane, 1981). More complete specimens are required to make further interpretations of this material but the material may represent evidence of a primitive taxon with a betulaceous rather than nothofagaceous character on King George Island (Dutra, 1997).

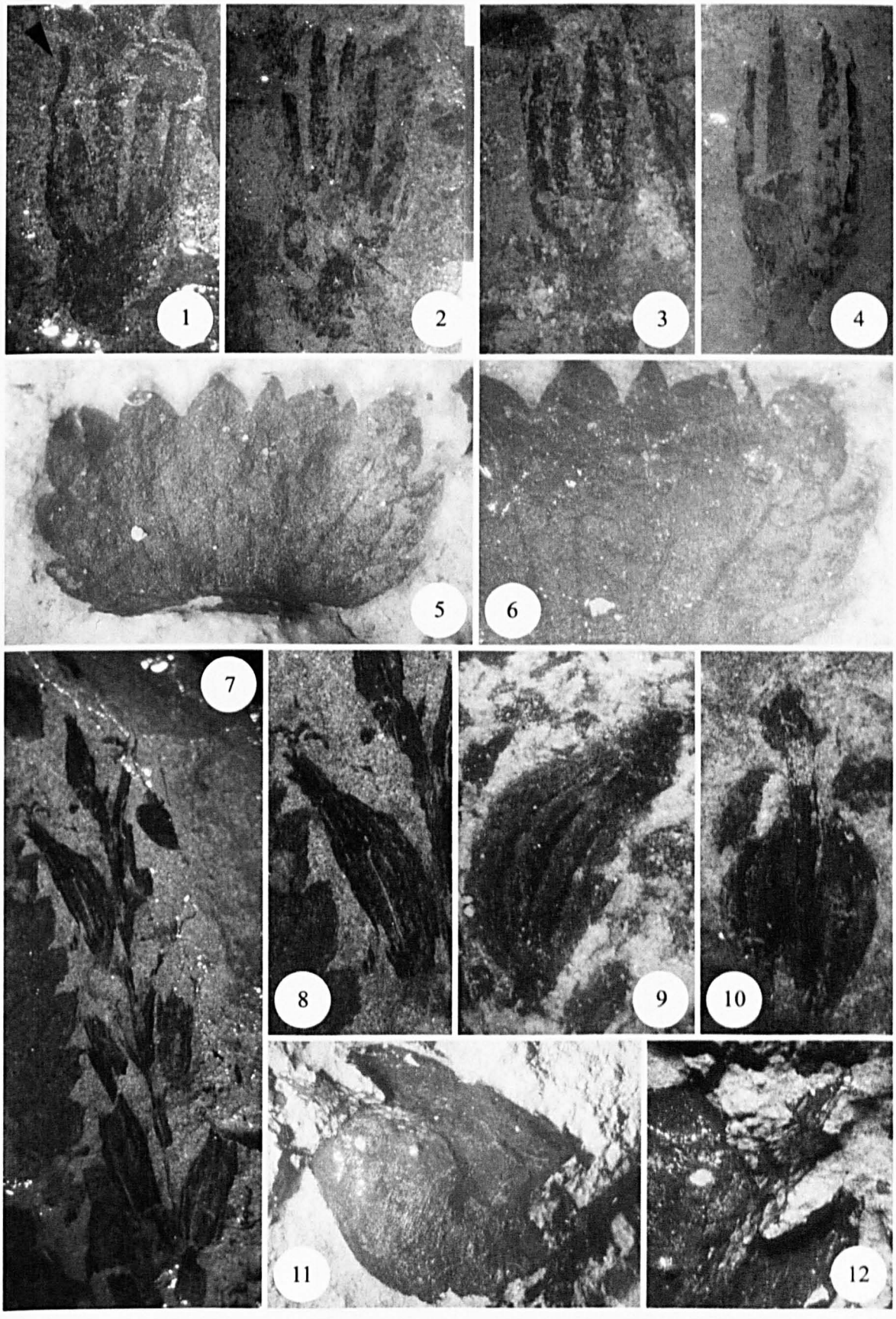

Figure 9.3. (1) - (4) Fertile organ sp. 2. (1). Fertile organ sp. 2 P.3032.39. x3.2. (2). P.3032.65. x3.6. (3). P.3032.4.1. x2.9. (4). P.3032.18. x3.3. (5) - (6) Fertile organ sp. 3. (5). ?Bract with apical margin serration, irregular venation and a flattened basal ?apression zone. P.3001.151a. x4.8. (6). Detail of venation and marginal serration. x7.4. (7) - (8). Fertile organ sp. 4. (7). P.3001.61. x2. (8). Detail of fruit, with ?remains of flower parts. x3.3. (9). Fertile organ sp. 5. P.3001.172.2. x9.5. (10). Fertile organ sp. 5. ?Capsule. P.3001.83.1. x5. (11) - (12) Fertile organ sp. 6. (11). P.3001.10.2. x1.6. (12). Detail of ?follicle. x1.9.

Organ morphotype	Flora and locality	Description
Fertile organ sp. 4 (Figure 9.3: 7-8)	Dragon Glacier flora P.3001.61.	Inflorescence, axis slightly curved. A minimum of 12 oppositely arranged ?quadrilocular capsules are present on the preserved axis (min. 14 inferred from the arrangement). Fragments of flower parts or apical teeth may be present. Length of individual capsules min. 5 - 11 mm, width 3 mm. Length of inflorescence min. 61 mm. Similar in appearance to capsules from racemose infloresence of *Eucryphia lucida*, but differs in having an extremely short pedicel, no evidence of septicidal dehiscence and a smaller potential valve number (Barnes and Jordan, 2000).
Fertile organ sp. 5 (Figure 9.3: 9-10)	Dragon Glacier flora P.3001.172.2. Fossil Hill Unit 3 P.3032.83.1.	Isolated capsules. Length 9 mm, width 4 mm. Differs in having a central structure that emerges apically through the central portion of the capsule, ?possibly the remains of the flower, e.g. an ovary and stigma. Alternatively, might represent germinating parts. Morphology suggests that they are related to Fertile organ sp. 4.
Fertile organ sp. 6 (Figure 9.3: 11-12)	Dragon Glacier flora P.3001.10.2.	Rounded rectangular shaped pod. Length 2.9 mm, width 22 mm. Internal ?follicle length min. 10 mm, width 3 mm. Surface has transverse ribs. Number of seeds uncertain.
Fertile organ sp. 7 (Figure 9.4: 1)	Dragon Glacier flora P.236.21.	One hemisphere of a fruiting body with a concave surface, suggesting an original rounded morphology. Width 20 mm. Internal surface is ornamented with a series of ridges running from the base and converging apically. Ridges are rarely connected by fine perpendicular ridges, which define ~ rectangular areoles.
Fertile organ sp. 8 (Figure 9.4: 2-3)	Fossil Hill Unit 3 P.3032.83.2/3.	Elliptic seed with an aperture in the mid section, which could be preservational but the regularity of the opening might indicate circumscissile dehiscence. Part of a style is preserved at capsule apex. Minimum 13 ribs. Length 5 - 7 mm, width 3 - 4 mm.
Isolated seed sp. 1 (Figure 9.4: 4-5)	Dragon Glacier flora P.3013.25, P.3013.35.	Ovate flattened seeds with studded marginal ornament. A small elliptical aperture is present at the narrow apex of the seed, which is also thickened relative to the broader base. Length 7 mm, width 4 – 5 mm.
Isolated seed sp. 2 (Figure 9.4: 6)	Rocky Cove P.3029.37.	Elliptic lenticular seeds. Length 5 mm, width 3 mm.
Isolated seed sp. 3 (Figure 9.4: 7)	Rocky Cove P.3029.18, P.3029.39.1.	Rounded triangular seeds. No relief. Length 3 – 7 mm, width 1.5 – 5 mm.
Isolated seed sp. 4 (Figure 9.4: 8)	Rocky Cove P.3029.38.	Seed with smooth central division. Length 9 mm, width 7 mm.
Isolated seed sp. 5 (Figure 9.4: 9)	Rocky Cove P.212.14.	Elliptic seed with a minimum of 10 small longitudinal ridges. Length 5 mm, width 3 mm. Apical portion of seed divided.
Isolated seed sp. 6 (Figure 9.4: 10)	Dragon Glacier flora P.3010.10.	Spherical lenticular seed, flattened marginally, thickened centrally. Length 6 mm, width 6 mm.
Isolated seed sp. 7 (Figure 9.4: 11)	Rocky Cove P.3029.4.	Spherical lenticular seed. Width 3 – 5 mm. Possibly related to seed type 7.
Isolated seed sp. 8 (Figure 9.4: 12)	Dragon Glacier flora P.3001.47.	Large elliptic lenticular seed. Length 9 mm, width 5 mm, height min 1.5 mm. Flattened marginally, thickened centrally.

Table 9.1. Summary descriptions of fertile material present in the BAS King George Island fossil collections.

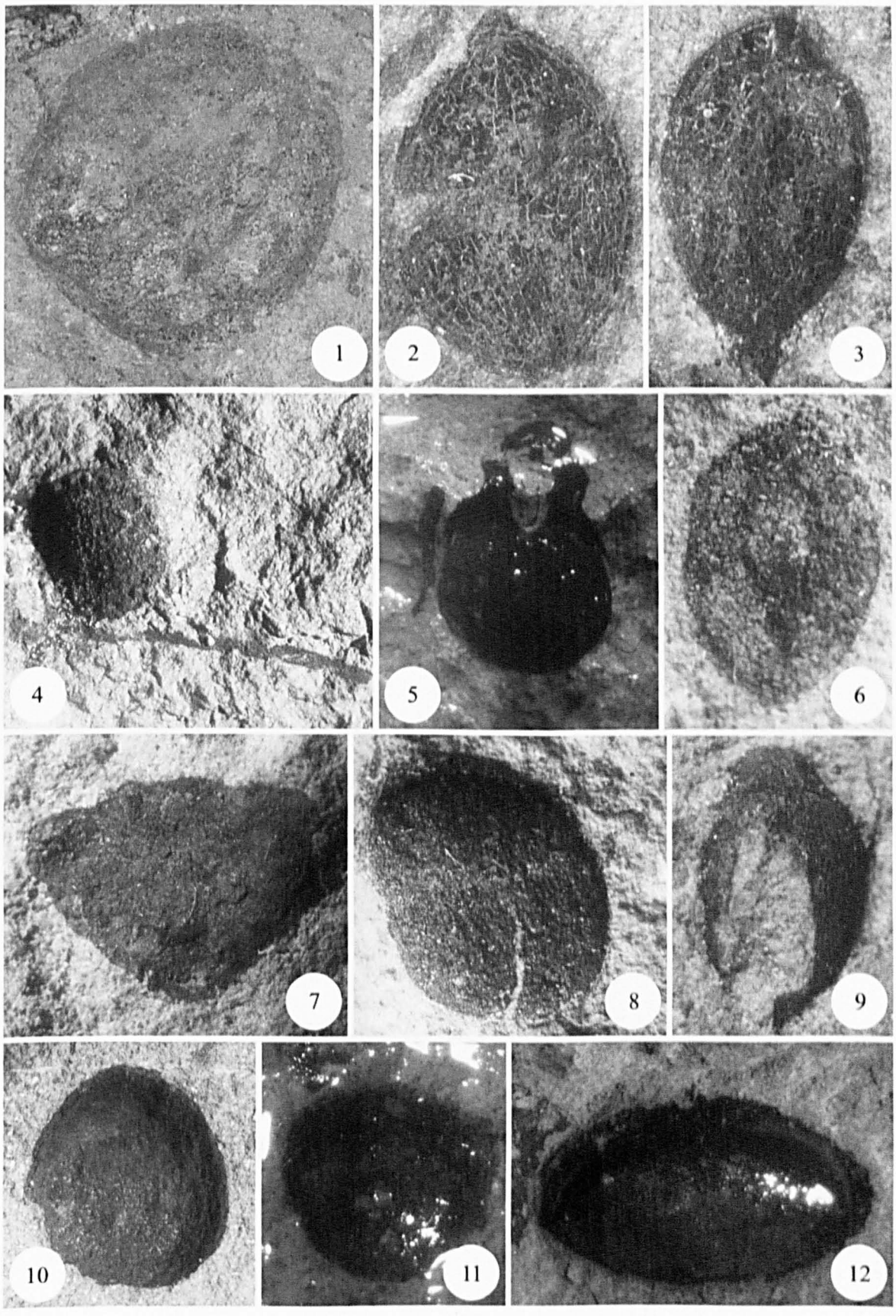

Figure 9.4. (1). Fertile organ sp. 7. P.236.21. x2.9. (2) - (3) Fertile organ sp. 8. (2). P.3032.83.1. x8.4. (3). P.3032.83.2. x11. (4) - (5) Isolated seed sp. 1. (4). P.3013.35 x6.3. (5). P.3013.25. x6. (6). Isolated seed sp. 2. P.3029.37. x9.5. (7). Isolated seed sp. 3. P.3029.18. x8.3. (8). Isolated seed sp. 4. P.3029.38. x5.1. (9). Isolated seed sp. 5. P.212.14. x9.2. (10). Isolated seed sp. 6. P.3010.10. x6.1. (11). Isolated seed sp. 7. P.3029.4. x7. (12). Isolated seed sp. 8. P.3001.47. x6.2.

Chapter 10 Palaeoclimate analyses

10.1 Introduction

Plant macrofossil palaeoclimatic analyses are based on the uniformitarian assumption that modern relationships between vegetation and climate can be extrapolated into the past using particular physiognomic characteristics of fossil leaf assemblages (Chaloner and Creber, 1990). Qualitative nearest living relative (NLR) analyses extrapolate the modern climatic tolerances of a plant to its fossil relative. Semi-quantitative methods use the functional morphology of leaves to infer climatic parameters. This chapter discusses the available palaeoclimate techniques and assesses the climatic inferences drawn from the King George Island floras based on both qualitative and semi-quantitative methods. The data is used to support and constrain palaeoenvironmental models.

10.2 Leaf morphological features used in palaeoclimate analyses

10.2.1 Leaf margin analysis

The relationship between the proportion of dicotyledonous species with entire margined leaves to mean annual temperature (MAT) was recognised early in the last century (Bailey and Sinnott, 1915, 1916). Toothed margined leaves are rare in wet and dry tropical, subtropical and arctic forest environments (Dilcher, 1973; Wing *et al.*, 2000) while non-entire margined leaves dominate in warm to cool temperate forests. The functional basis of the leaf margin-MAT correlation is still debated, but teeth may serve an advantageous photosynthetic function during the early phases of lamina development, although this is probably counterbalanced at a later stage by transpirational water loss through the teeth (Wing et al., 2000).

Wolfe (1979) expressed the leaf margin-MAT relationship as a simple linear regression (SLR), correlating an increase of 3 % entire margined species with an approximate MAT increase of 1° C for Northern Hemisphere leaves. Wolfe (1979) considered that 1° C increase per 4 % increase in entire margined leaves, was more appropriate for the modern Southern Hemisphere, since the vegetation has a predominance of evergreen taxa with entire margined leaves. This is not considered to be representative of the Paleogene Antarctic floras, which have a high proportion of deciduous toothed margined taxa, like those of the Northern Hemisphere floras, as evidenced by the presence of abundant *Nothofagus* sp., with the plicate vernation character (Hill, 1991). Precision errors are ± 5° C for an assemblage of >29 species and ± 10° C with 20 – 29 species. Correlations based on small fossil floras with less than 20 species are invalid because of the large precision errors (Wolfe and Upchurch, 1987). In studies of Late

Cretaceous floras Boyd (1994) considered that a sample size of less than 30 angiosperm species was unrepresentative of climatic conditions unless the flora was originally impoverished. Alternative simple linear regressions have been developed, based on Wolfe's (1979) and other databases (Greenwood, 1992; Wing and Greenwood, 1993; Wilf, 1997; Wilf *et al.*, 1998; Wiemann *et al.*, 1998) (Table 10.1).

MAT(°C) SLR	Error	Modern database	Author
(0.25 x %entire) + c	-	Humid to mesic East Asian forests	Wolfe (1979) suggested that a 4 % increase in entire margined species equated to a 1° C increase in MAT
(0.306 x %entire) + 1.141	$r^2 = 0.983$ P <0.001 S.E = ±0.788°C	Humid to mesic East Asian forests	Wing and Greenwood (1993) based on Wolfe (1979) data
(0.286 x %entire) + 2.24	$r^2 = 0.76$ P <0.0005 S.E = ±2.0°C	Temperate and tropical floras of North and South America	Wilf (1997)
(0.291 x %entire) – 0.266	$r^2 = 0.76$ P < 0.0005 S.E = ±3.4°C	CLAMP database (Wolfe, 1993)	Wilf (1997)
(0.244 x %entire) + 3.25	$r^2 = 0.84$ P < 0.0005 S.E = ±2.1°C	CLAMP database (Wolfe, 1993) with 32 coldest winter sites removed	Wilf (1997)
(0.22 x %entire) + 4.4	$r^2 = 0.75$, S.E. not stated	Australian floras	Wiemann *et al.* (1998) based on Greenwood (1992) data

Table 10.1. Summary of SLR equations used to derive MAT (°C) estimates based on the relationship of the proportion of entire margined species in a flora to MAT (°C). Wilf (1997) suggested that a minimum error of ± 2° C should be applied to the regressions to account for collection bias errors or a binomial sampling error if that value was larger: $\sigma[MAT] = c\sqrt{P(1-P)/r}$, where c is the MAT regression slope, R^2 – coefficient of determination, P - % entire margined species, S.E. – standard error.

The leaf margin-MAT relationship has two underlying assumptions. Firstly that the fossil assemblage represents non-successional, climax vegetation and secondly that a valid leaf margin/temperature scale is applied (Wolfe and Upchurch, 1987). Artificially low temperature estimates may result from sampling vegetation of disturbed habitats e.g. streamsides that are biased towards toothed margined leaves (Greenwood, 1992), although this bias is minimised by estimates based on >29 species (Wolfe, 1979). MAT estimates of disturbed habitats are therefore likely to represent minimum values, which is particularly relevant to King George Island, where volcanic activity is probably responsible for major floral turnover and disturbance (Poole *et al.*, 2001). Burnham *et al.* (2001) found that modern streamside vegetation systematically underestimated MAT by 2.5° - 5° C due to the bias of lianoid species with toothed leaves in lakeside and riverside samples. MAT estimates from the fossil record are therefore likely to underestimate palaeotemperatures. A sample of less than 30 species was found to give highly variable MAT estimates but 29 – 36 samples were found to give the best MAT constraint with a ± 2° C standard error (Burnham *et al.*, 2001). Jordan (1997) found that

MAT was systematically and significantly overestimated by 6° - 11.3° C for modern Australian and New Zealand floras using the methods of Wolfe (1979) and Wing and Greenwood (1993). Mean annual rainfall (MAR) was also found to be underestimated by c. 400 mm for Australasian sites (Jordan, 1997). However, both sites were physiognomically distinct from the CLAMP database of Wolfe (1993), suggesting a physiognomic division between the modern Northern and Southern Hemisphere databases.

Multiple linear regression (MLR) approaches use a combination of physiognomic variables to predict climatic parameters (Wing and Greenwood, 1993; Gregory, 1994; Gregory and McIntosh, 1996; and see summary in Wiemann *et al.*, 1998). Many of the regressions are derived from the CLAMP character set (Wolfe, 1993; 1995), based on significance levels of statistical correlations between leaf morphological characters and climatic parameters. Wiemann *et al.* (1998) concluded that reducing the number of variables used in MLR models improved the accuracy of analyses because uncertainty in scoring techniques and removal of characters, unimportant in climate prediction, reduced precision errors. However, the underlying assumption of interdependence of climatic parameters in these multivariate analyses is considered to be inappropriate, given that some character states vary in response to more than one climatic variable (e.g. margin state varies with humidity and temperature) (Jordan, 1997; R. Spicer, pers. comm., 2001).

10.2.2 Leaf size

Leaf size is strongly coupled to the physical environment and therefore leaf size is a character that can be used to interpret climatic signals from fossil assemblages (Dilcher, 1973; Dolph and Dilcher, 1980; Wolfe and Upchurch, 1987). In modern vegetation, leaf size (and morphology) varies as a function of temperature and humidity, with large leaves occurring in warm humid environments and smaller leaves dominating cool dry environments. Insertion height within the canopy is also important (Wolfe and Upchurch, 1987; Klich, 2000). Klich (2000) found that sun leaves of *Elaeagnus angustifolia* (Russian Olive) are generally smaller and slender rather than larger, more ovate shade leaves, morphological features that are adaptive advantages to climatic conditions. Wolfe (1985) found that high latitude Cretaceous and Tertiary floras are characterised by large leaf size which probably results from a combination of low incidence sunlight, warm growing season temperatures and long summer day length.

Leaf length has been used to categorise leaf size in several studies of Australian vegetation (Christophel and Greenwood, 1988; Greenwood, 1992, 1996; Hill, 1992). Wolfe and Upchurch (1987) used the Leaf Size Index (LSI) to express this feature of leaf morphology (Equation 10.1) In calculations of LSI, leaves that fall into more than one size category are included in the larger size class (Wolfe and Upchurch, 1987). This is significant because fragmentation of leaf

material prior to preservation tends to favour smaller leaf sizes (Ferguson, 1985) and may produce an artificially small LSI estimate for fossil assemblages (Wolfe and Upchurch, 1987). This bias may be reduced by thorough collecting and assessment of the taphonomic history of a fossil assemblage. In the King George Island floras large leaves (mesophyll or greater) are rare but 10 cm wide fragments of leaves, identifiable to morphotype level (Chapter 5) suggest that the larger size classes were originally present in the flora and that estimates of LSI will be systematically lower than expected.

$$\text{Leaf size index} = \frac{4MC + 3ME + 2NO + 1MI - 100}{2}$$

MC = % Macrophyllous/larger species
ME = % Mesophyllous species
NO = % Notophyllous species
MI = % Microphyllous species

Equation 10.1

The relationship between leaf area and mean annual precipitation has been discussed in numerous studies (Dilcher, 1973; Dolph and Dilcher, 1979; Givnish, 1984; Wilf, 1997; Wilf *et al.*, 1998a, 1998b; Jacobs, 1999). Leaf area is a function of both temperature and humidity such that warm and cool dry climates have a high proportion of small entire leaves whereas warm and cool wet climates have a larger leaf size. Wilf *et al.* (1998b) summarised this relationship with the equation:

$$\ln(\text{MAP}) = 0.548\text{MlnA} + 0.768$$

where MAP (cm), $r^2 = 0.760$, S.E. = 0.359, MlnA - mean of the natural logs of the species leaf areas (mm^2).

The equation makes no adjustment for the taphonomic removal of large leaves, which may be significant in the King George Island and other floras. Wing and Greenwood (1993) derived MAP regressions that incorporate the percentage of large leaves (Mesophyll I or larger) (Wilf *et al.*, 1998b). However since this leaf size class has been preferentially removed from the KGI floras, this equation has not been applied (Chapter 5).

10.2.3 Leaf shape

Several features of leaf shape have palaeoclimatic and palaeoenvironmental significance. Attenuated leaf apices or drip tips are common in humid environments, where they are thought to accelerate the draining of moisture from the lamina, to retard the growth of epiphytes (Spicer, 1990). Stenophyllous vegetation (l:w ratio ≥4:1) tends to occur on stream-sides (Richards, 1952). Retuse apices are typical of subhumid or canopy vegetation (Upchurch and Wolfe, 1987).

Using correspondence analysis (CA) of the CLAMP database Wolfe (1995) found that the percentage of lobed leaves in a flora showed a strong, non-linear correlation with mean annual

temperature (Spicer and Wolfe, 1999). Lobed species were found to be absent or infrequent in megathermal vegetation (>20°C), to increase in mesothermal vegetation (13° – 20°C) and reaches a maximum between 4° - 12° C in warm microthermal vegetation (<13°C). Canonical correspondence analysis can be used to demonstrate covariant relationships (Spicer and Wolfe, 1999), for example samples with high percentages of compound teeth were also found to have high proportions of lobed leaves (Figure 10.1). Lobed and compound leaves are characteristic of understorey or successional vegetation and may signal taphonomic bias in climate signals (Upchurch and Wolfe, 1987; Spicer, 1990). Cordate based leaves occur in successional vegetation as light gap colonisers or they indicate a lianoid habit (Upchurch and Wolfe, 1987).

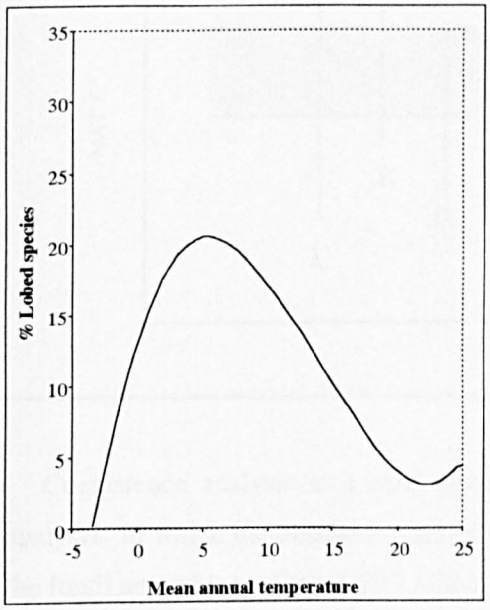

Figure 10.1. Plot of lobed species vs. mean annual temperature. Lobing is absent or infrequent in megathermal vegetation (MAT > 20°C), increases in mesothermal vegetation (MAT 13° - 20°C) and reaches a maximum between 4° – 12°C in warm microthermal vegetation (MAT <13°C). Redrawn from Spicer and Wolfe (1999).

10.2.4 Leaf texture

Megathermal and mesothermal climax vegetation is dominated by thick coriaceous, xeromorphic leaves that are usually evergreen. In microthermal climax vegetation and successional mesothermal vegetation deciduous vegetation is predominant with thin hygromorphic leaves (Upchurch and Wolfe, 1987). This is difficult to quantify in impression floras and tentative at best in these carbonised plant fossils, that lack original organic material.

10.3 Nearest Living Relative analyses (NLR)

Nearest living relative analyses are based on the uniformitarian assumption that the modern climatic tolerances of plants can be extrapolated to fossil taxa with known taxonomic affinity to derive palaeoclimatic parameters for fossil assemblages (Chaloner and Creber, 1990; Mosbrugger, 1999). At a basic level NLR analyses use a single fossil taxon or a suite of taxa to infer palaeoclimates, for example *Nothofagus* is used to infer temperate climates and the Lauraceae are generally considered to be subtropical. The NLR approach is age dependent, since taxonomic assignment is more difficult in older floras that may only be identified to the

genus (at best), or family level. At the family level the analysis may be meaningless given the wide potential range of climatic tolerances (Spicer, 1990). NLR comparisons are therefore limited by understanding of the fossil flora and of the particular assemblage of taxa (Dilcher, 1973; Mosbrugger, 1999). Sedimentary environment and taphonomy are also important, because the range of plants that are preserved may be unrepresentative of the original flora. For example, Mosbrugger (1999) highlighted the abundance of evergreen taxa in peat, as opposed to clastic environments, as a function of leaf persistence and adaptation to nutrient-poor soils.

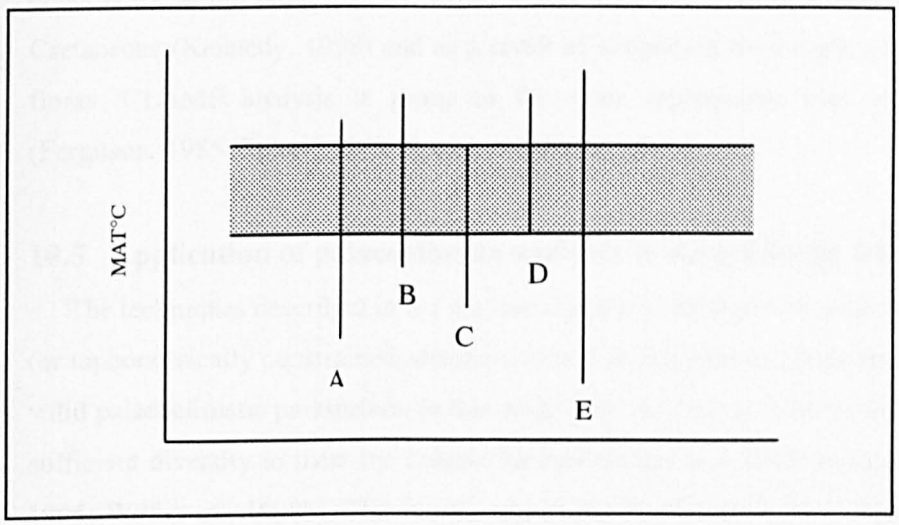

Figure 10.2. A coexistence plot for MAT. Individual MAT ranges are plotted for the fossil taxa A – E. The shaded area denotes the interval of coexistence, which is considered to be the best estimate of MAT for the fossil flora (after Mosbrugger, 1999). Other climatic parameters may also be plotted in this fashion.

Coexistence analysis is a semi-quantitative technique, developed from taxon-based NLR analyses, in which the climatic range of modern taxa are used to delimit a climatic window for the fossil assemblage (Figure 10.2) (Mosbrugger, 1999). The limitations and requirements of the method are the same as with the single taxon approach - correct identification of the fossil taxa, conservation of climatic tolerances over the geological past and accurate constraint of modern climatic tolerances. The method has been developed in a web-based format by T. Utescher at the University of Bonn, Germany (http://www.palaeoflora.de/).

10.4 CLAMP analysis

The Climate Leaf Analysis Multivariate Programme (CLAMP) was developed by Wolfe (1993, 1994, 1995) as a method for obtaining climatic parameters from simultaneous analysis of multiple physiognomic characters. In the CLAMP methodology each leaf species in a fossil assemblage is scored for 31 character states that are features of lamina shape, size and tooth architecture and the whole flora is then compared to a modern database of vegetation sites with known climatic parameters (Wolfe, 1993, 1995; Spicer and Wolfe, 1999; see also http://tabitha.open.ac.uk /spicer/CLAMP/Clampset1.html). According to the position of the flora in 'character space', climatic parameters may be inferred for the fossil assemblage.

CLAMP is only valid for leaf assemblages comprising more than 20 species (Herman and Spicer, 1996, 1997; Kennedy, 1998). With less than 20 species, the precision errors for the method increase exponentially. The CLAMP database is strongly biased towards the Northern Hemisphere, since it is based predominantly on samples of Northern Hemisphere vegetation (Spicer and Wolfe, 1999). In addition, the modern Australian and New Zealand floras are somewhat anomalous being physiognomically distinct from the Northern Hemisphere vegetation (Jordan, 1997; Spicer and Wolfe, 1999). This is interpreted as a result of high endemicity in the New Zealand flora, which has been geographically isolated since the Late Cretaceous (Kennedy, 1998) and as a result of adaptation to drought and fire in the Australian floras. CLAMP analysis is prone to the same taphonomic bias as leaf margin analysis (Ferguson, 1985; Spicer, 1989; Spicer and Wolfe, 1999).

10.5 Application of palaeoclimate analyses to King George Island floras

The techniques described in the previous sections highlight the need for a large and unbiased (or taphonomically constrained) database of leaf physiognomic characters to derive accurate and valid palaeoclimatic parameters. In this study only the Dragon Glacier and Fossil Hill flora have sufficient diversity to meet the criteria for leaf margin and MAP analyses (Wolfe, 1979, 1993, 1995; Wilf *et al.*, 1998b). This is only true of the Fossil Hill flora if floras from Units Three to Four are combined. The Dragon Glacier flora is the only assemblage that is sufficiently diverse, in its own right, for CLAMP analyses. However, there is also a potential for time averaging in the Dragon Glacier flora, because the moraine blocks cannot be definitively attributed to the same stratigraphic horizon. The leaf size data used in the size analyses is summarised for the Dragon Glacier and Fossil Hill floras in Appendix VI.

10.6 Leaf margin analysis results

Table 10.2 summarises the results of simple linear regression analyses for the Dragon Glacier and Fossil Hill floras using the available regression equations (Table 10.1). The different regression equations yield estimates that vary by only 1.7° C. The Southern Hemisphere regression line (Wolfe, 1979; Spicer and Parrish, 1993) is not included in the average values or in the maxima and minima for reasons discussed earlier (Section 10.2.1).

Two MAT estimates were derived from the Dragon Glacier flora. The first is based on the total number of morphotypes present in the flora, while the second excludes possible herbaceous and juvenile taxa from the analyses and is therefore considered to be more appropriate. The average MAT results from the analyses are 11.01° and 10.58° C respectively.

Mean annual temperature estimates were derived from the Combined Fossil Hill flora (Units Two, Three and Four), which comprises 22 morphotypes and excludes one juvenile form

(Chapter Five). Fossil Hill Units Two and Four (both constituting less than the minimum 20 species required by Wolfe, 1971), were also analysed for comparison with the combined Fossil Hill flora. A fourth estimate is based on the description of the Fossil Hill flora by Li (1994). Li (1994) did not specify which stratigraphic horizon the flora originated from, but the material illustrated comprises both compressions (e.g. Unit Three flora) and impressions (e.g. Units Two and Four floras), therefore it is likely to represent material from the entire flora, and should be equivalent to the Combined Fossil Hill flora (Table 10.2). Unit Three is not analysed on its own because the flora comprises only six entire margined specimens, and would give a meaningless MAT value.

Locality	Dragon Glacier*	Dragon Glacier**	Fossil Hill Unit 2	Fossil Hill Unit 4	Combined Units 2, 3, 4	Li (1994) flora
#Morphotypes	37	34	11	15	22	20
%Entire	31.00	29.41	18.18	33.33	23.00	40.00
LMA[1]	10.63	10.14	6.70	11.34	8.18	13.38
σ	2.36	2.39	3.56	3.72	2.75	3.35
LMA[2]	11.11	10.65	7.44	11.77	8.82	13.68
σ	2.20	2.23	3.33	3.48	2.57	3.13
LMA[3]	11.26	10.80	7.53	11.94	8.93	13.88
σ	2.24	2.27	3.38	3.54	2.61	3.19
LMA[4]	10.81	10.43	7.69	11.38	8.86	13.01
σ	1.88	1.91	2.84	2.97	2.19	2.67
LMA[5]	11.22	10.87	8.40	11.73	9.46	13.20
σ	1.70	1.72	2.56	2.68	1.97	2.41
LMA[6]	7.75	7.35	4.55	8.33	5.75	10.00
σ	1.93	1.95	2.91	3.04	2.24	2.74
Range min	10.63	10.14	6.70	11.34	8.18	13.01
Range max	11.26	10.87	8.40	11.94	9.46	13.88
Average	11.01	10.58	7.55	11.63	8.85	13.43

Table 10.2. Summary of mean annual temperature data (°C) derived from the Dragon Glacier flora at Point Hennequin (Hunt and Poole, submitted) and the Fossil Hill flora. *total DGF flora, **flora excluding possible herbaceous and juvenile taxa. Mean annual temperature derived from leaf margin analysis (LMA) using the formulae of [1]Wing and Greenwood (1993) based on Wolfe (1979); [2]Wilf (1997) based on temperate and tropical floras of North and South America; [3]Wilf (1997) based on the CLAMP dataset of Wolfe (1993); [4]Wilf (1997) based on the CLAMP dataset with the 32 coldest months removed; [5]Wiemann *et al.* (1998) based on Greenwood (1992); [6]Southern Hemisphere scale LMA not included in average MAT value (see text for details), using an increase in 4 % entire margined species to equate to an increase in 1°C (Wolfe, 1979). #Morphotypes = morphotypes. %Entire = %entire margin leaves used in analyses. LMA = leaf margin analysis. σ = binomial sampling error. Standard errors are quoted in Table 10.1, but a minimum standard error of ± 2° C is suggested where the binomial sampling error is less than this value (Wilf, 1997);

Mean annual temperature values derived from the Fossil Hill floras have a broad range of over 7° C from 6.70° – 13.88° C. However, the Unit Four and the Li (1994) flora, which are the two most diverse floras and therefore should provide the most precise estimates, are within binomial sampling error. This suggests that the higher temperature estimates (11.63 – 13.43° C) may be more representative mean annual temperature values. The low estimate from the

combined Fossil Hill Units flora is likely to be a result of bias, due to the incorporation of the low diversity Unit Three flora, which is composed entirely of toothed margined leaves.

Leaf margin analysis MAT of c. 10.6° C for the Middle Eocene Dragon Glacier flora is in agreement with Middle Eocene nearest living relative analyses. These suggest MAT of 10 - 12° C based on comparisons with the Valdivian rain forests (Birkenmajer and Zastawniak, 1986; Poole *et al.*, 2001). The Dragon Glacier flora MAT is also in agreement with Eocene $\delta^{18}O$ shallow marine palaeotemperature data (7.9° - 11.7° C), derived from benthic bivalves from the La Meseta Formation of Seymour Island, (Ditchfield *et al.*, 1994). Comparative studies of the wood flora from the James Ross Basin tentatively suggest Late Paleocene-Early Eocene MAT of between 7 - 15°C (I Poole pers. comm., 2001), which also support these palaeotemperature estimates.

Leaf margin analysis of the Fossil Hill flora yields mean annual temperatures of c. 7.6° – 13.4° C, which is slightly higher than that of the contemporaneous Dragon Glacier flora, although the MAT values are still in agreement with nearest living relative comparisons. The MAT data is also within error of the $\delta^{18}O$ palaeotemperature data of Ditchfield *et al.* (1994). Both the analyses for the floras suggest a warm microthermal climate.

10.7 Leaf size analyses

Mean annual precipitation and leaf size indices were calculated for the Dragon Glacier and Fossil Hill floras following the methodology of Wilf *et al.* (1998b) (Appendix Table VI.1 – VI.3) and Wolfe and Upchurch (1987) respectively. Sample size and low diversity factors that affect leaf margin analyses also apply to MAP analyses, since the fit of regression line is considered to be poor when there are fewer than 16 morphotypes (Wilf *et al.*, 1998b). The Dragon Glacier and Fossil Hill floras are consequently the only floras with sufficient diversity for valid analysis. LSI values calculated from small floras with low morphotype diversity are likely to be unrepresentative, due to the potential bias resulting from preservation of a small cross section of the vegetation. Preferential removal of the larger leaf size classes (Chapter 5) implies that the LSI calculated here are minimum values.

Species based MAP estimates were made for both the Dragon Glacier and Fossil Hill floras. Analyses of the Dragon Glacier flora suggest MAP of 1039.1 mm. The Fossil Hill flora has a similar MAP range of c. 1058 – 1408 mm, although the higher diversity floras are at the lower end of this range c. 1058 - 1087 mm. Previous nearest living relative comparisons have suggested MAP of 2000 – 4000 mm (Birkenmajer and Zastawniak, 1986, 1989; Poole *et al.*, 2001) based on comparisons with the Valdivian rain forests. Recent estimates of the Valdivian rainforest MAP parameters suggests average MAP of 2064, with a range of 900 – 2500 mm

(Ogha, 1987). The values derived from both floras are therefore at the lower range of precipitation values. However, the observed taphonomic bias towards smaller leaf size classes (Chapter 5) implies that the new estimates are minimum, rather than maximum values.

Locality/flora	Morphotypes	LSI	MAP mm	S.E+ve	S.E-ve
Fossil Hill Unit 2	11	27.27	1132.0	488.9	341.4
Fossil Hill Unit 3	6	41.67	1408.1	608.1	424.7
Fossil Hill Unit 4	15	23.33	1087.9	469.9	328.1
Fossil Hill combined	22	22.74	1058.9	457.3	319.4
Fossil Hill (Li, 1994)*	20	25.00	1139.0	492.0	344.0
Dragon Glacier**	36	27.95	1039.1	501.2	350.0

Table 10.3. Summary of leaf size indices (LSI) and mean annual precipitation (MAP) values (mm) based on numbers of specimens for the Dragon Glacier and Fossil Hill floras. Estimates based on Fossil Hill Units Two Three and Four individually do not meet the minimum morphotype diversity required for these analyses, although they exceed the minimum 16 species required when combined (Fossil Hill combined flora). The positive and negative standard errors (SE) for the MAP analyses are not equal because they are derived using a log function (Wilf *et al.*, 1998b). Fossil Hill Li (1994)* - Li (1994) did not specify whether his size class estimates were species or specimen based. Dragon Glacier flora excluding herbaceous and juvenile taxa.**

Systematic name	Forest type	Abbr	LSI^1	LSI^2
Mesophyll vine forest	Tropical rainforest	MVF	81.25	83.75
Semi-evergreen mesophyll vine forest	Tropical rainforest	SEVF	50	-
Simple mesophyll vine forest	Warm temperate rainforest	SMVF	52.5	62.5
Notophyll vine forest	Subtropical rainforest	NVF	51.25	58.75
Araucarian vine forest	Subtropical rainforest	AVF	50	43.75
Simple notophyll vine forest	Warm temperate rainforest	SNVF	45	45
Araucarian microphyll vine woodland	Subtropical rainforest	AVW	40	25
Microphyll vine woodland	Subtropical rainforest	MVW	25	25
Semi-evergreen vine thicket	Subtropical rainforest	SEVT	25	-
Deciduous vine thicket	Tropical rainforest	DVT	36.25	-
Microphyll mossy forest	Cool temperate	MMF	2.5	3.75
Microphyll mossy thicket	Cool temperate	MMT	0	0

Table 10.4. Leaf size indices of the Australian rainforest subformations defined by Webb (1959). LSI^1 leaf size index based on median numbers of species, LSI^2 based on median number of specimens. Dashes indicate absence of data.

Leaf size indices were calculated for Fossil Hill (22.74 – 41.67 av. 28.0) and Dragon Glacier flora (27.95). Leaf size index data is lacking for Tertiary Southern Hemisphere floras but modern data has been collected by Webb (1959) (Table 10.4; Figure 10.4) and Greenwood (1992) from the Australian rainforests. The LSI data presented here is similar to values derived from subtropical and cool temperate elements of the Australian rain forests, both in terms of leaf size index and the proportion of species attributed to each leaf size category (Table 10.4). Although the taphonomic bias towards smaller leaf size classes in the fossil floras should not be disregarded, there appears to be an overall dominance of the microphyll and notophyll leaf size classes, with subordinate mesophyll sized leaves (Figure 10.4). Most of the floras are of similar size class distribution to the semi-evergreen vine thicket, deciduous vine thicket, microphyll mossy forest and microphyll mossy thicket subformations of the Australian rain forests (Figure 10.3; Table 10.4) (Webb, 1959). However, none of the forest categories have a similar percentage of entire margined leaves and the potential climatic data derived from these comparisons is ambiguous, ranging from cool temperate to tropical rainforest. It is interesting to

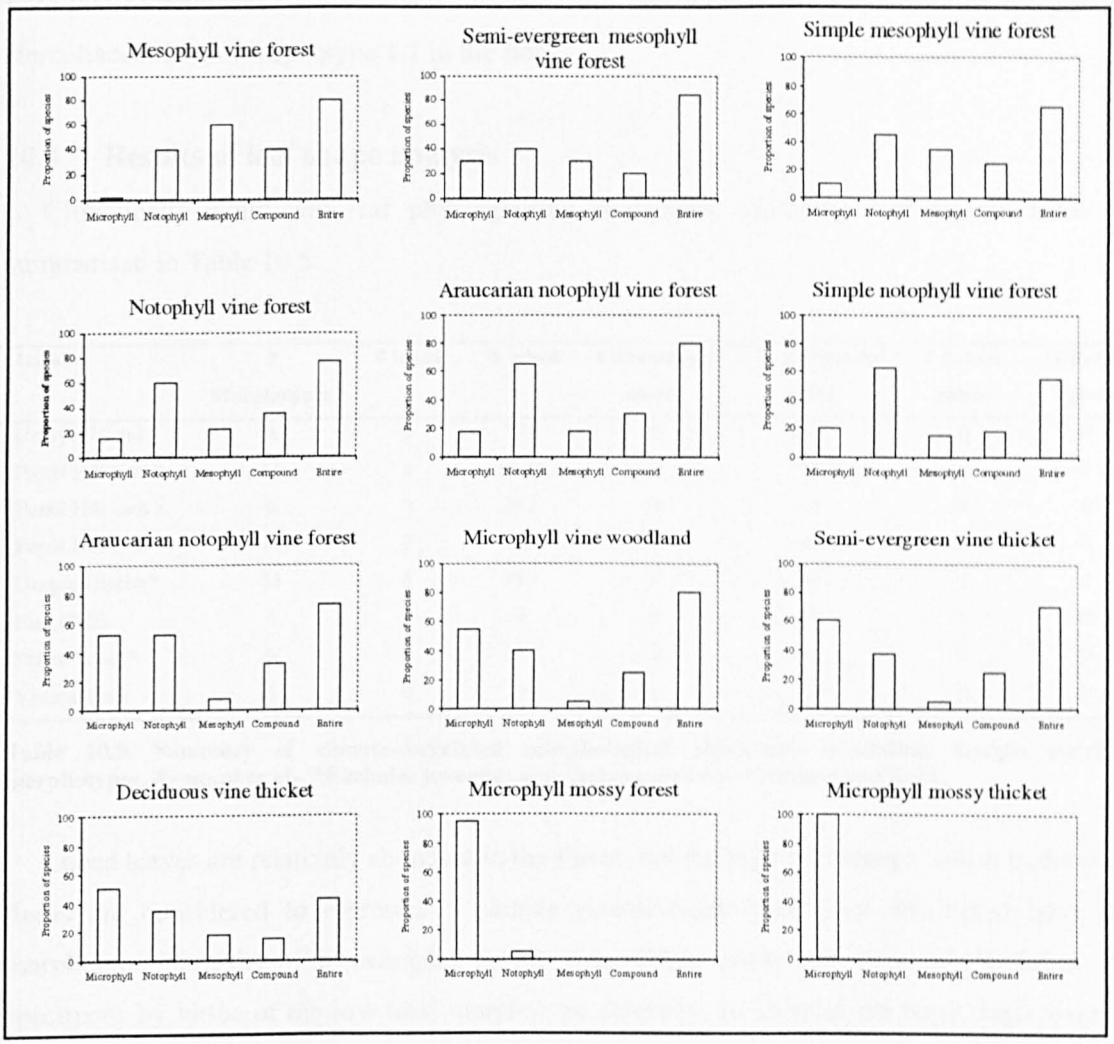

Figure 10.3. Range of leaf size classes, proportions of compound species and proportion of entire margined species in each flora for different Australian forest types, also including percentages of entire margined and compound species. Data replotted from Webb (1959), using median values rather than data ranges e.g. 5 – 25 % microphyll = 15 % microphyll in this figure.

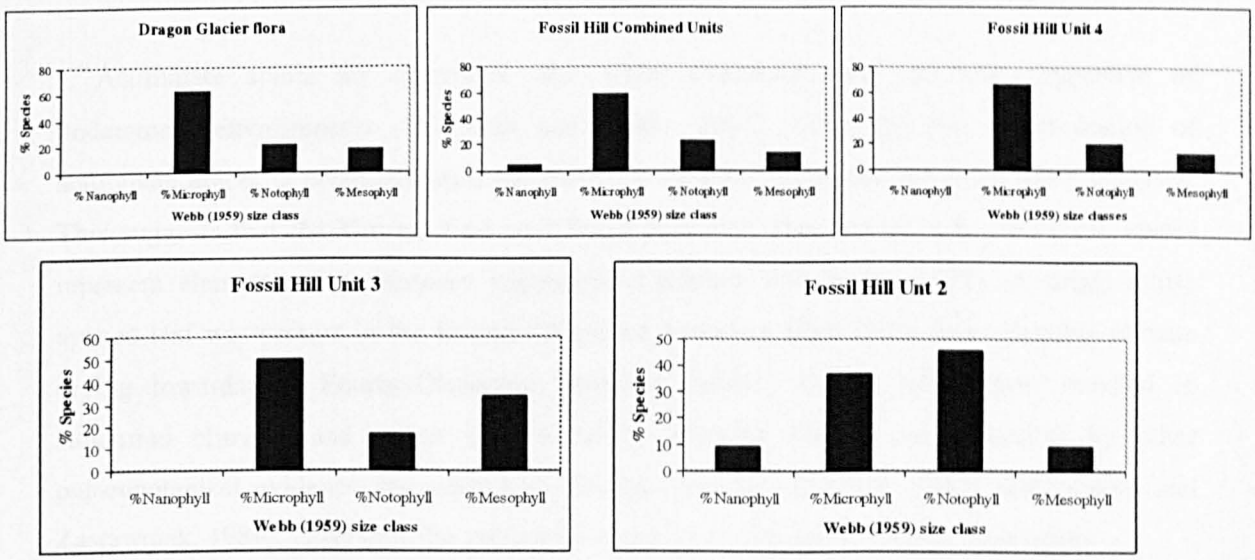

Figure 10.4. Species based leaf size class distribution in the Dragon Glacier and Fossil Hill floras. Note that the x-axis scale is not the same as in Figure 10.3.

note that Sterculiaceae are common in the SEVT, considering the abundance of the possible sterculiaceous leaf Morphotype 1.1 in the flora.

10.8 Results of leaf shape analysis

Climatically significant leaf physiognomic characters, excluding leaf margin state, are summarised in Table 10.5.

Locality	# Morphotypes	# lobed	% lobed	# Acuminate apices	% Acuminate apices	# Retuse apices	% Retuse apices
Dufayel Island	8	1	12.5	0	0	0	0
Fossil Hill Unit 2	11	2	18.18	1	9.09	0	0
Fossil Hill Unit 3	6	2	33.3	0	0	0	0
Fossil Hill Unit 4	15	2	13.3	1	6.7	0	0
Dragon Glacier*	34	6	16.7	0	0	0	0
Platt Cliffs	5	0	0	0	0	1	20
Potter Cove**	6	1	16.7	0	0	0	0
Vaureal Peak	5	0	0	1	20	0	0

Table 10.5. Summary of climate-correlated morphological characters (excluding margin state) in morphotypes. # - number of-. *Excludes juveniles and herbaceous taxa. **Impression flora.

Lobed leaves are relatively abundant in the floras, but the high percentage values in the some floras are considered to represent a sample size/diversity bias since the floras have low morphotype diversity. For example, Fossil Unit Three comprises over 30 % lobed leaf specimens by virtue of the low total morphotype diversity. In contrast the large, high diversity Dragon Glacier flora with a high proportion of lobed specimens seems to reflect original vegetation composition and supports the warm microthermal climate estimates (Spicer and Wolfe, 1999) based on leaf margin analysis.

Acuminate apices are correlated with water availability and are also suggestive of understorey environments (Upchurch and Wolfe, 1987). Generally low representation of acuminate apices is consistent with the moderate rainfall values derived from MAP analyses. This suggests that the Vaureal Peak and Fossil Hill Unit Four leaves with acuminate apices represent elements of understorey vegetation (Upchurch and Wolfe, 1987). A single retuse apexed leaf was present in the Eocene-Oligocene boundary Platt Cliffs flora. Possible climate drying towards the Eocene-Oligocene boundary (Dutra, 1997a), might have resulted in subhumid climates and retuse apexed forms, although this is not supported by other palaeobotanical evidence for moist Late Eocene climates (Stuchlik, 1981; Birkenmajer and Zastawniak, 1989). Otherwise the leaf might represent an element of canopy vegetation.

10.9 Results of nearest living relative analyses

Nearest living relative analyses of the King George Island floras were based on both single taxon-based comparisons as well as coexistence analysis (CA). Co-existence analyses were provided by T Utescher (University of Bonn) and are summarised in Table 10.6. Single taxon-based nearest living relative analyses are presented in Table 10.7.

Modern taxon	MAT° C	CMM° C	WMM ° C	MAP mm
Acmopyle sp.[1]	23.30 – 23.90	17.20 - 20.10	26.10 - 26.70	1143 – 1778
Araucaria sect. *Eutacta*[1,2]	13.80 - 26.50	6.60 - 26.10	20.40 - 28.10	815 - 2740
Cupressaceae[1,2]	8.20 - 26.50	5.50 - 26.10	11.20 - 27.00	787 - 4486
Podocarpus sp.[1,2]	11.00 - 27.70	1.70 - 27.00	15.10 - 28.80	652 - 3151
Brachychiton populneus[1,2]	14.80 - 27.20	9.20 - 21.80	19.90 - 30.60	352 - 954
Cunoniaceae (Schizomerieae) Ceratopetalum Anodopetalum[1]	12.20 – 26.80	7.80 - 25.30	16.30 - 27.80	652 - 2099
Eucryphia glutinosa[2]	7.70 - 13.00	1.60 - 9.10	9.20 - 18.00	574 - 4486
Eucryphia moorei[2]	12.20 – 17.40	7.80 - 11.80	16.30 - 24.40	352 - 1205
Knightia excelsa[1,2]	12.40 - 15.20	8.10 - 10.80	16.40 - 19.60	1242 - 1250
*Nothofagus*** [1,2]	7.70 – 12.20	1.60 - 7.80	9.20 - 16.30	574 - 1982
Weinmannia sp.[1]	8.50 – 27.70	1.80 - 27.00	14.30 - 31.20	200 - 3151
Dragon Glacier	14.8 – 15.2	9.2 – 10.8	20.4 – 27.0	815 – 954, 1242 - 1250
Fossil Hill flora	13.8 – 26.5	7.8 – 25.3	20.4 – 27.0	815 - 2099

Table 10.6. Modern taxa used in coexistence nearest living relative analyses (CA). MAT – mean annual temperature, CMM – Cold month mean, WMM – Warm month mean, MAP – Mean annual precipitation *based on *Austrocedrus*, *Libocedrus*, and *Papuacedrus*. **N. antarctica, N. pumilio, N. gunnii*. 1 – used in Fossil Hill CA analysis, 2 – used in Dragon Glacier CA analysis. CA results are expressed as maxima and minima. Analyses performed by T. Utescher. Standard coexistence analyses incorporate more than 20 taxa and the statistical uncertainty surrounding this analyses is increased by the small sample size.

The CA-analyses for both the Dragon Glacier and Fossil Hill flora yielded higher MAT values than leaf margin-MAT analyses. The contrast is marked in the Dragon Glacier flora, for which a MAT 2 – 3° C higher is predicted. The Fossil Hill flora MAT (minima) is in agreement with the leaf margin analysis, which supports that interpretation. MAP estimates show a better correlation, although the range of possible values is extremely broad and does not offer a better resolution of the palaeoclimatic parameters. The suggested bias towards toothed margined forms in the fossil floras has already been highlighted as a possible factor in underestimates of regression-based MAT (Burnham *et al.*, 2001).

Single taxon based nearest living relative analyses yield a broad range of mean annual temperature and precipitation estimates (Table 10.6 and Table 10.7) that are broadly consistent with simple linear regression approaches (Section 10.2). The assemblage as a whole is dominated by leaves referred to the Nothofagaceae, suggesting prevailing temperate climates and growth conditions that were not water-limited.

Eucryphia sp. and the Nothofagaceae suggest temperate climates, but the remainder of the vegetation used in the analyses consists of taxa with broad, temperate to subtropical, and even tropical, climatic ranges. Actual mean annual temperature ranges are poorly resolved

Taxon	Inferred NLR*	Locality	Modern distribution	Climatic range	Altitudinal range	Habit/Habitat	Source data
NON-ANGIOSPERMS (Chapter 8)							
Lophosoria sp.	*L. quadripinnata*	Rocky Cove Potter Peninsula	S. America, Mexico	MAT 8° - 22°C MAP 195 – 1997 mm	S.L – 3800 m	Cloud forests, Paramo thickets, alpine grasslands.	Cantrill (1998)
Thyrsopteris shenii	*Thyrsopteris elegans*	Fossil Hill Unit 3	Juan Fernandez Islands	MAT 16°C MAP 935 mm			Li (1994)
Assorted Araucariaceae *Araucaria* sp.	*Araucaria* sp.	Fossil Hill Unit 3 Fossil Hill Unit 4 Collins Glacier	South Hemisphere S. Am	Cool temperate to tropical. MAT 11-26°C MAP 850 – 4000 mm	600 – 1800 m Often at higher altitudes >1000 m and at the treeline	Emergent and/or canopy evergreen trees. Often on steep slopes and ridge tops. Often in moist habitats but also present in drier areas. *A. heterophylla* occurs at sea level on Norfolk Island.	Veblen *et al.* (1995) Enright (1995) Armesto (1995) Veblen *et al.* (1995)
Assorted Podocarpaceae Podocarpaceae	Podocarpaceae	Dragon Glacier Fossil Hill Unit 4 Platt Cliffs Potter Cove	Southern Hemisphere to Japan and Central America	Temperate to tropical	S. Am Coastal lowlands to >600 m Aus <1800 m	Emergent or canopy trees. Often in wetter sites. Tropical Australasian forms are common in montane forests and may be dominant at higher altitudes >3000 m.	Gibson *et al.* (1995) Enright (1995) Armesto (1995) Veblen *et al.* (1995)
Papuacedrus shenii Cupressaceae	*Austrocedrus*[1] *Libocedrus*[2] *Papuacedrus*[3]	Fossil Hill Unit 4	S. Chile, Argentina/New Caledonia, NZ/New Guinea (Tasmania in the Tertiary)	Temperate to tropical [1]Able to withstand xeric conditions MAP 500 - 1700 mm	[1]900 – 1800 m [2]1450 – 1600 m [3] 600 – 3900 m	[1]Evergreen trees often not overlapping with *Nothofagus*. [2]Forms subalpine timberline with podocarps and angiosperms. [3]Stunted forms at altitude.	Enright (1995) Jaffre (1995) Armesto (1995) Veblen *et al.* (1995)
ANGIOSPERMS							
Dicotylophyllum washburni	*Brachychiton* sp.	Dragon Glacier Fossil Hill Unit 4	Australia, New Guinea	Temperate to tropical	Near sea level	Bottle trees. Require moderate moisture (Webb, 1959)	
Morphotypes 1.10, 1.11, 1.12, 1.13, 1.14	Lauraceae	Dragon Glacier Dufayel Island Fossil Hill	Pantropical and pansubtropical, less commonly temperate	Tropical and warm	Lowland to montane rain forests	Evergreen trees and shrubs, rarely parasitic twiners	
Morphotype 1.21	*Eucryphia moorei*	Dragon Glacier	SE Australia	Cool temperate		Evergreen trees and shrubs	Hill (1991)
Morphotype 2.35	*Eucryphia glutinosa*	Dragon Glacier	Chilean endemic	Cool temperate	250 – 900 m	Winter deciduous	Hill (1991)
Morphotype 2.1/2.2	*Weinmannia-Cunonia*	Dragon Glacier Fossil Hill Unit 4	Broad Southern Hemisphere Ex. Africa and Australia	Temperate to tropical	Uplands	Tree or small shrub in cloud or upland montane forests.	Barnes *et al.*,
Morphotype 2.3	Schizomerieae	Fossil Hill Unit 4	New Guinea, Australia, Tasmania, South Africa				
Morphotype 2.4 *Cf. Lomatia* sp.	*Lomatia* sp.	Fossil Hill Unit 2 Fossil Hill Unit 3	Australia, South America	Temperate to pantropical		Small trees and shrubs, wet forests, possibly on low nutrient soils	Carpenter & Hill (1994)
Morphotype 2.10	*Knightia excelsa*	Dragon Glacier Fossil Hill Unit 2	New Zealand, North Island and Marlborough in South Island	Temperate to subtropical		Tree up to 40 m high	Salmon (1998)
2.40 – 2.58, excl. 2.55 Nothofagaceae	Nothofagaceae	All floras	South America, Australia	Dominantly temperate forests	All altitudes up to 2500 m	Canopy tree, some cold tolerant species (< -22°C)	Hill *et al.* (1996) Donoso (1996)

Table 10.7. Palaeoclimatic parameters based on nearest living relative comparisons of the morphotypes described in this study (Distribution and habit data also obtained from Mabberly, 1997 and Heywood, 1998). *Not confirmed by cuticle, based on gross morphology – shape, secondary/tertiary venation, margin state. Inferred NLR's are sometimes based on inferred taxonomic affinities and are therefore tentative.

8° - 26° C. Mean annual precipitation values also have a broad range from 195 – 4000 mm, although several taxa with overlapping MAP tolerances (Cupressaceae, *Lophosoria* and *Thyrsopteris*) suggest a more restricted MAP range c. 195 – 1997 mm, which is consistent with MAP values obtained from the leaf size analyses. The single taxon-based NLR methods dominantly suggest the Palaeocene to Eocene flora of King George Island grew under temperate climates. The Palaeocene to Eocene flora of the southern South America-Antarctic Peninsula region has previously been interpreted as a 'Palaeoflora mixta', that comprises elements of both modern subantarctic and subtropical vegetation (Romero, 1986; Markgraf et al., 1996). Therefore the occurrence of warmer subtropical to tropical elements in the flora does not imply highly elevated mean annual temperatures. Instead it may suggest a climatic regime sufficient to support temperate vegetation and more thermophilic taxa at the lower threshold of its climatic range.

10.10 Results of CLAMP analysis

CLAMP analyses were undertaken for the Dragon Glacier flora (Table 10.8), which satisfies the minimum diversity criteria for the method (Section 10.4). The Dragon Glacier flora constitutes a test case for this method, because it has not previously been used in the Antarctic and it was uncertain whether the Antarctic flora would plot within the framework of the Northern Hemisphere biased CLAMP database. The Dragon Glacier flora was scored for 31 leaf characters using scoresheets from the CLAMP website (Section 10.4) (Appendix VI; Table VI.5). The data was then added to the CLAMP-144 and CLAMP-173 vegetation database, the latter including the 'subalpine nest' a group of 20 anomalous outlying samples from the analysis of Wolfe (1993). These outliers came from regions with climates that had a WMM temperature of less than 16° C and CMM of less than 3° C floras and reduce the resolution of the method (Spicer and Wolfe, 1999), unless the flora analysed is also adapted to cold, subalpline climates. The vegetation databases were then analysed simultaneously with corresponding meteorological databases using CANOCO software (e.g. Ter Braak, 1988). The results obtained using the two datasets do not show a dramatic variation (Table 10.8) but the standard deviation of the residuals is lower for the CLAMP-144 dataset, therefore this dataset has been used.

	σ	Dragon Glacier[1]	σ	Dragon Glacier[2]
MAT	1.17	10.55° C	1.72	9.23° C
WMM	1.58	19.01° C	1.80	18.67° C
CMM	1.88	2.56° C	2.54	0.59° C
GROWSEAS	0.70	6.47 months	0.85	5.83 months
GSP	33.59	884.6 mm	31.80	783.6 mm
MMGSP	3.69	93.7 mm	3.67	96.6 mm
3-WET	14.03	425.3 mm	13.81	406.0 mm
3-DRY	9.30	126.3 mm	8.99	168.6 mm
RH	7.36	60.52 %	8.17	61.56 %
SH	0.90	4.88 %	0.98	5.48 %
ENTHALPY	0.32	29.73	0.35	29.72

Table 10.8. CLAMP results for the Dragon Glacier flora. σ – standard deviation of residuals. 1 – CLAMP-144 dataset, 2 – CLAMP-173 dataset (including subalpine nest). WMM – warm month mean, CMM – cold month mean, GROWSEAS – Length of the growing season, GSP – Growing season precipitation, MMGSP – Mean monthly growing season precipitation, 3-WET/3-DRY – precipitation in the three wettest/driest months, RH – Relative humidity SH.

The CLAMP results shows a strong similarity to MAT values derived from leaf margin analysis of the Dragon Glacier flora and provide further support for warm microthermal Middle Eocene climates. Interestingly, the cold month mean estimates suggest a lack of freezing conditions at this latitude during the Middle Eocene. The MAP values are lower, but within error of values predicted by size class analyses.

CLAMP analyses are not suitable for floras from disturbed settings since the composition of the flora is not in equilibrium with its surroundings. Chapter three demonstrated that the composition of the Dragon Glacier plant-bearing sediments and the diversity of the flora suggest minimal disturbance and therefore a flora appropriate for CLAMP analysis.

The CLAMP results do not replicate the high MAT values predicted by co-existence analysis, but the CLAMP method can be affected by same taphonomic biases as the simple linear regression analyses, although this should be minimised by the relatively large sample size of the Dragon Glacier flora. However, coexistence analysis may also be biased by the incorporation of modern taxa, which have a climate minimum that is a high mean annual temperature. The weight of the evidence argues against the high temperatures suggested for MAT by CA and instead supports the lower MAT range of 8° – 10°C.

Parameter	Dragon Glacier	Fossil Hill combined	Fossil Hill (Li, 1994)	VRF
MAT°C	-	-	-	11.7, 10 - 12
LMAT°C	10.14 – 10.87, 10.58	8.18 – 9.46, 8.85	13.01 – 13.88, 13.43	-
CLAMP MAT°C	10.55	-	-	-
CA-MAT°C	14.8 – 15.2	13.8 – 26.5	-	-
CLAMP-CMM°C	2.56	-	-	-
CA-CMM°C	9.2 – 10.8	7.8 – 25.3	-	-
CLAMP-WMM°C	19.01	-	-	-
CA-WMM°C	20.4 – 27.0	20.4 – 27.0	-	-
Actual MAP mm	-	-	-	900 - 4000
LMAP mm	1039.1	1058.9	1139.2	-
CLAMP-MAP mm	884.6	-	-	-
CA-MAP mm	815 – 954, 1242 - 1250	815 - 2099	-	-
LSI (dimensionless)	27.95	22.74	25.00	-

Table 10.9. Summary of palaeoclimatic data from this study for the three floras that meet the required minimum morphotype diversity. LMAT – leaf margin analysis MAT. VRF – Valdivian rain forest climate data based on Birkenmajer and Zastawniak (1986) and Ogha (1987). All other terms defined previously.

10.11 Summary

Palaeoclimatic parameters based on leaf physiognomy, nearest living relative and CLAMP analysis have been assessed in Chapter 10. Palaeoclimatic data has also been derived from the datasets presented by Li (1994). The Middle Eocene Dragon Glacier and Fossil Hill floras are the only KGI floras with sufficient diversity for valid palaeoclimatic analyses using semi-

quantitative foliar physiognomic methods. Low diversity floras that incorporate taxonomically identifiable elements, with known climatic range, support nearest living relative based climatic comparisons e.g. *Lophosoria* in the Potter Cove compression flora.

Nearest living relative analyses support previous interpretations of warm microthermal, temperate climates on KGI during the Palaeocene and Eocene (Birkenmajer and Zastawniak, 1989; Cao, 1992, 1994; Li, 1992, 1994; Duan and Cao, 1998; Poole *et al.*, 2001).

Mean annual temperature data for the Middle Eocene Dragon Glacier and Fossil Hill flora derived from simple linear regression, leaf size class and CLAMP analyses are within error of previous climatic interpretations for the Palaeocene and Eocene based on comparisons with the Valdivian rain forests (Table 10.9) (Birkenmajer and Zastawniak, 1986; Poole *et al.*, 2001). The simple linear regression analyses potentially underestimate MAT due to a preservational bias towards water's edge, toothed margined dominated fossil assemblages. Therefore the MAT values should be treated as minima.

Co-existence analyses produced equivocal results, suggesting distinctly higher MAT values for the floras of 14° - 15° C and 13° - 26° C respectively. The higher MAT values reflect the inclusion of taxa with broad modern climatic tolerances e.g. temperate to tropical. The mixture of subtropical/tropical elements with the temperate vegetation is consistent with the model of Romero (1986) that interprets the Early Tertiary Antarctic Peninsula flora as a 'Palaeoflora mixta' comprising modern subantarctic and subtropical elements. In this context the warm temperate and subtropical signals, from nearest living relative analysis of the flora, do not imply highly elevated temperatures. Instead they suggest incorporation of vegetation elements growing at the cooler extreme of their climatic tolerances, or alternatively that the fossil taxa were adapted to a broader climatic range. This also suggests that MAT values derived from nearest living relative analyses of the flora may be overestimated.

Chapter 11 Discussion

11.1 Introduction

This study presents the first complete overview of the palaeoecology of King George Island that incorporates all of the 20th Century British Antarctic Survey leaf macrofossil collections. The study is based on field research from two areas on King George Island, Point Hennequin and Fildes Peninsula, that together comprise a total of 36 field sites. Field studies included new palaeobotanical collections and geochronological sampling, sedimentary logging and mapping. The field collections were supported by material collected in previous field seasons for BAS, from Barton Peninsula, Dufayel Island, Platt Cliffs, Potter Cove, Profound Lake, Rocky Cove and Vaureal Peak.

In this chapter the above data is synthesised and used to construct palaeoenvironmental models for King George Island. The composition of the vegetation is compared with coeval floras from Gondwana. Palaeoclimatic data is assessed in terms of its impact on Early Tertiary West Antarctic and Southern Hemisphere palaeoclimatic models.

	Palaeocene		Eocene													Eocene – Oligocene boundary	
Locality	Barton Peninsula	Dufayel Island	CG *in-situ*	CG moraines	Dragon Glacier	Fossil Hill U2	Fossil Hill U3	Fossil Hill U4	Mt. Wawel	PC compression	PC impression	Profound Lake	Rocky Cove	Smok Hill	Vaureal Peak	Platt Cliffs	Cytadela
#AS	7	22	*	1	203	29	26	50	5	-	24	-	7	3	23	18	10
#AM	4	8	-	1	37	11	6	15	4	-	6	-	6	1	5	5	6
#CyS	-	-	-	-	-	7	1	-	-	-	-	-	-	-	-	-	-
#CyM	-	-	-	-	-	1	1	-	-	-	-	-	-	-	-	-	-
#CS	-	?1	1	1	60	26	14	12	-	-	3	-	-	-	-	1	41
#CM	-	?1	1	1	9	8	6	2	-	-	1	-	-	-	-	1	2
#FS	1	-	-	-	23	-	14	-	-	1	13	-	3	-	6	-	2
#FM	1	-	-	-	5	-	4	-	-	1	2	-	3	-	1	-	1
#ES	-	-	-	*	2	-	-	-	-	-	-	-	-	-	-	-	-
#EM	-	-	-	-	1	-	-	-	-	-	-	-	-	-	-	-	-
#BS	-	-	-	-	-	-	1	-	1	-	-	-	-	-	-	-	-
#BM	-	-	-	-	-	-	1	-	1	-	-	-	-	-	-	-	-
#FeS	-	-	-	1	28	10	5	-	1	-	-	1	6	-	-	1	1
#FeM	-	-	-	1	12	3	1	-	1	-	-	1	5	-	-	1	1

Table 11.1. Morphotype and specimen diversity for the King George Island floras, showing clustering of floras in the Eocene. # - number of, AS – angiosperm specimens, AM – angiosperm morphotypes, CS/CM – conifer specimens/morphotypes (includes fertile cone material and foliage), FS/FM – fern specimens/morphotypes, ES/EM – *Equisetum* specimens/morphotypes, BS/BM – bryophyte specimens/morphotypes, FeS/FeM – fertile specimens/morphotypes. ?- indicates uncertain identification of an organ. *Fragmentary material not described.

11.2 Tertiary floras of King George Island

The British Antarctic Survey angiosperm macrofossil flora from King George Island comprises a total of 85 morphotypes from 15 localities (Table 11.1). The record includes three possible juvenile morphotypes and two inferred herbaceous taxa. The assemblage is dominated by non-entire margined leaves 58 morphotypes (68 %), with a subordinate number of entire margined morphotypes – 27 (32 %). 54 % of the morphotypes have not previously been described from King George Island. The collection is the largest and most diverse assemblage of fossils described from King George Island to-date and is therefore one of the most diverse Tertiary Antarctic floras. The conifer component of the vegetation comprises 161 specimens placed in 16 morphotypes. Ferns - 11 types and 64 specimens; cycads - one type and eight specimens; Two types of bryophyte, the first described from King George Island are also preserved. Fertile remains - 22 types and 54 specimens. The collection includes the first record of cones, conescales and bryophyte remains for King George Island. A single inflorescence present in the Dragon Glacier flora is the first angiosperm inflorescence from Antarctica (Fertile organ sp. 4; Chapter Nine).

11.3 Composition of the flora

Angiosperm taxonomic comparisons based on leaf venation patterns (Chapter Six), suggest that the Cunoniaceae (*Schizomerieae*, *Eucryphia* and *Weinmannia*), ?*Gunnera*, Lauraceae Monimiaceae, Myrtaceae, Nothofagaceae, Proteaceae, Symplocaceae and Sterculiaceae are present in the flora. Other families that are similar to the leaf morphotypes include the Myricaceae, Cochlospermaceae, Araliaceae, Elaeocarpaceae, and possibly the legumes (morphotype 2.8). Presence-absence and possible presence data is summarised in Figure 11.1. Many of the leaves have conservative morphologies that occur in a broad range of families, for example, pinnate weakly brochidodromous, elliptic to ovate, entire margined leaves, and botanical affinities are therefore difficult to assess. This problem is compounded by the lack of a well-described Tertiary database of floras from the Antarctic Peninsula. In addition, the absence of cuticles from the flora means that all taxonomy must be based on physiognomic characters of the leaf venation. No database of cuticular characters exists at present to substantiate either the morphological groupings or the suggested taxonomic affinities of the leaves, but the widest possible base of modern and fossil material has been studied in order to minimise identification errors or biases.

All of the angiosperm taxa (Chapter Six) have previously been described from the Antarctic Peninsula flora, except for the Symplocaceae and the Schizomerieae tribe of the Cunoniaceae. Unusual elements of the flora are two possible herbaceous taxa - Morphotypes 1.5 and 2.7 (?*Gunnera*). Morphotype 1.5 has not previously been described from King

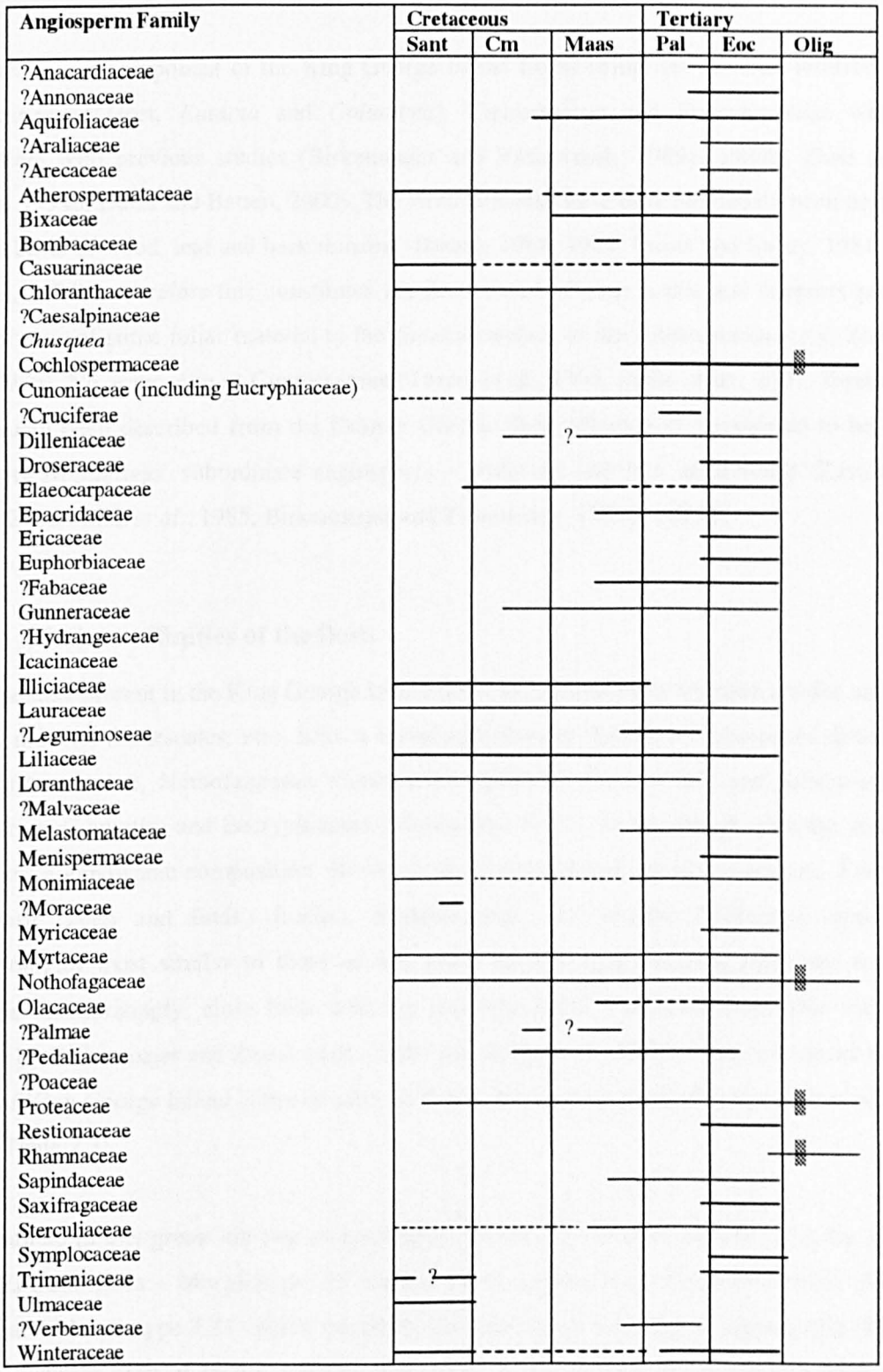

Figure 11-1. Compilation of angiosperm presence and range data from the Antarctic Peninsula based on pollen, leaf and wood fossils (modified from Askin, 1992 with additional range data from Hayes, 1999; Duan and Cao, 1998; Poole *et al.*, 2000b and this study). Plant families present on King George Island are highlighted in bold. Dashed lines show inferred presence. Grey boxes indicate incorrect presence data, based on new 40Ar/39Ar data presented in Chapter Three.

George Island and no fossil or modern analogues were found for the leaf. The possible *Gunnera* fragment, is an extremely unlikely occurrence given that the leaves of herbaceous taxa tend to rot *in-situ* rather than abscise.

The conifer component of the King George Island floras comprises material referred to the Araucariaceae (sect. *Eutacta* and *Columbea*), Cupressaceae and Podocarpaceae which is consistent with previous studies (Birkenmajer and Zastawniak, 1989a, 1989b; Zhou and Li, 1994a, 1994b; Dutra and Batten, 2000). The Araucariaceae have only previously been described on the basis of wood, leaf and bark remains (Barton, 1964, 1965; Lucas and Lacey, 1981; Zhou and Li, 1994b), therefore this constitutes the first record of cone scales and supports previous assignments of some foliar material to the *Eutacta* section of the Araucariaceae (e.g. Zhou and Li, 1994b). No araucarian or Cupressaceae (Torres *et al.*, 1984; Poole *et al.*, 2001) fossils have previously been described from the Dragon Glacier flora, which was considered to be a low diversity *Nothofagus*, subordinate angiosperm – podocarp and fern assemblage (Zastawniak, 1981; Zastawniak *et al.*, 1985; Birkenmajer and Zastawniak, 1989a, 1989b).

11.4 Modern affinities of the flora

The taxa present in the King George Island flora, as inferred from venation studies and from fertile material (conescales, etc), have a broad and disjunct Southern Hemisphere distribution e.g. Araucariaceae, Nothofagaceae, Cunoniaceae (possible *Weinmannia* and *Schizomerieae*), Proteaceae (*Lomatia*) and Eucryphiaceae (Mabberley, 1997). At this broad scale the Antarctic flora has a gondwanic composition. However, the association of possible *Gunnera*, *Eucryphia glutinosa* (Poep and Endl.) Baillon, Symplocaceae, and several *Nothofagus* spp., with morphologies most similar to those of the South American *Nothofagus* subgenus suggests, perhaps unsurprisingly, close links with the southern South American flora. This view was shared by Birkenmajer and Zastawniak (1986) and Poole *et al.* (2001), who considered that the flora of King George Island is floristically similar to the modern Valdivian rain forests (Chapter Two; Table 2.3).

Outliers in this group are two morphotypes with strong affinities to taxa from the modern New Zealand flora - Morphotype 2.9 similar to the proteaceous *Knightia excelsa* (Salmon, 1986) and Morphotype 2.31, which resembles juvenile forms of *Hoheria angustifolia* (Salmon, 1986). Identification of leaves possibly belonging to the modern *Schizomerieae* tribe of the Cunoniaceae is extremely interesting since the genera *Anodopetalum* A. Cunn., *Ceratopetalum* Sm., and *Platylophus* D. Don., do not have a modern South American distribution. These genera occur in Africa, Australia, New Guinea and Tasmania, the latter area also linked with the KGI flora based on similarities between *Nothofagus* spp. Other members of the Cunoniaceae family

have previously been identified in the Antarctic Peninsula leaf, wood and pollen record (Birkenmajer and Zastawniak, 1989a/b; Askin, 1992; Zhang and Wang, 1994; Poole *et al.*, 2000; Poole *et al.*, 2001), although that material is more similar to *Weinmannia, Eucryphia* Cav., and *Caldcluvia,* D. Don., which have Gondwanic distributions.

11.5 Fossil affinities of the flora

Comparison of the KGI flora with other Southern Hemisphere fossil floras also supports interpretations of the flora as broadly gondwanic in nature. *Araucaria* sect. *Eutacta* has a wide distribution in the early Cenozoic fossil record of the Southern Hemisphere, while the sect. *Columbea* is present in the Cenozoic record of Argentina, Australia and the Middle to Late Eocene of Tasmania (Hill and Brodribb,1999). The earliest record of *Libocedrus* (closely related to both *Papuacedrus* and *Austrocedrus*), is from Late Palaeocene sediments of south eastern Australia (Whang and Hill, 1999). The genus is present in the Early Oligocene to at least the earliest Miocene in Tasmania (Hill and Carpenter, 1989). *Acmopyle antarctica* was described by Florin (1940) from the La Meseta Formation on Seymour Island, and is also present from the Palaeocene in Australia and the Early Eocene in Tasmania (Hill and Brodribb, 1999). However, the KGI flora differs from the Australian floras during the late Palaeogene since it does not show a corresponding rise in the abundance of scleromorphic and xeromorphic taxa (Hill, 1990). This trend is linked directly to the northerly drift of the continent into lower latitudes and correspondingly warmer and drier climates (Hill, 1990). Some similarity to the Tasmanian palaeoflora is suggested based on similarities between Morphotype 2.40 and the Oligocene *Nothofagus microphylla* (Hill, 1991b). Strong similarities exist between the KGI floras and fossil specimens from the Palaeocene Cross Valley Formation, Seymour Island (Dusen, 1908), which also contain *Nothofagus*, Proteaceae, Cunoniaceae and Winteraceae in addition to diverse ferns (Askin, 1992). Macrofossil assemblages described from the Eocene La Meseta Formation have been of limited diversity, with a predominance of *Nothofagus* and possible Proteaceae (Case, 1988; Doktor et al., 1994), however recent BAS collections suggest a greater diversity (A. Tosolini, pers. comm., 2002) and pollen assemblages include taxa such as Liliaceae, Aquifoliaceae, Casuarinaceae, Bombacaceae, Loranthaceae and ?Pedaliaceae (Askin, 1998) that have not been recognised in the leaf macrofossil record.

Again several of leaf morphotypes described herein suggest strong similarities to southern South American floras by comparison with *Nothofagus dicksoni, N. variabilis* and *N. densi-nervosa* from the Palaeocene Magellansland flora (Tanai, 1986) and to *Lomatia preferruginea* and *Araucaria* spp., in Berry's (1938) Rio Pichileufu flora. This is consistent with the interpretations of Romero (1986) and Troncoso and Romero (1998) who considered the Antarctic Peninsula to be part of their 'Palaeoflora mixta' – a floral assemblage common to the

southern part of South America and the Antarctic Peninsula that comprised temperate elements such as *Nothofagus,* Proteaceae, Monimiaceae and Cunoniaceae in addition to more tropical/subtropical elements such as Lauraceae and Sterculiaceae.

11.6 Forest structure and palaeoecology

Growing at a paleolatitude of c. 62 °S, these southern high latitude forests would have experienced a growth regime with lengthy periods of winter darkness and prolonged low-angle sunlight during the summer months. The forests contained mixed evergreen along with deciduous elements, as evidenced by *Nothofagus* leaves with characteristic deciduous plicate vernation (Birkenmajer and Zastawniak, 1986, 1988, 1989; Hill, 1991; Hill and Read, 1991; Hunt, 2001). Occasional leaf mats may also provide evidence for mass leaf fall that is associated with deciduousness and frequently associated with modern deciduous vegetation. Forest fire, which could have been associated with volcanic activity, may have occurred on King George Island and is evident at Point Hennequin and Fossil Hill where rare charcoalified fragments have been recovered. Since KGI is on the eastern side of the Pacific where trade winds provide strong orographic rainfall, it is postulated that the Early Tertiary KGI would also have received abundant precipitation, an interpretation supported by leaf size analyses (Chapter Ten).

The dominance of *Nothofagus* spp., in the King George Island flora and its association with ?*Laurelia,* Proteaceae, Cupressaceae, *Araucaria* and fern species (Birkenmajer and Zastawniak, 1988, 1989; Li, 1994) suggests a multistratal forest structure similar to that of the modern Valdivian rainforests (Veblen *et al.,* 1983; 1996). *Nothofagus* spp., would probably have formed a dominant element of the canopy with other angiosperms such as Cunoniaceae, Eucryphiaceae, *Laurelia* spp., podocarps and Lauraceae. Ferns, such as Cyatheaceae, Dicksoniaceae and some Osmundaceae (Poole *et al.,* 2001) and shrubby angiosperms (e.g. Proteaceae) would have formed the understorey (Veblen *et al.,* 1996). One aspect of the modern and fossil vegetation that differs is the presence of abundant ferns. In many areas of modern Valdivian flora the bamboo *Chusquea culeou* Desv., is the sole understorey vegetation, however only one example of bamboo has been found in the microfossil record of King George Island (Stuchlik, 1981). It is suggested that ferns would have filled this niche, since they are common in the fossil flora and a prominent component of the understorey vegetation in the *Nothofagus*-dominated forests in New Zealand and Tasmania (MacPhail *et al,* 1996). The bamboo pollen recorded by Stuchlik (1981) is considered to be Late Eocene to Early Oligocene in age, potentially suggesting that the taxon migrated into the region shortly before the glacial extinction (Dingle and Lavelle, 1998) and did have the opportunity to establish itself as a major vegetation component.

Conifers such as *Araucaria* occur today at higher elevations and along ridges and/or as emergent trees, since it is shade intolerant (Veblen *et al.*, 1983; Hill and Brodribb, 1999). The co-occurrence of *Araucaria* alongside other angiosperms suggests that it fulfilled the latter role in the palaeoforests of King George Island. The Cupressaceae, present in the Fossil Hill and Dragon Glacier floras, are also likely to have been emergents and have a wide ecological range from seasonally dry or xeric to wet and cool temperate (Hill, 1995). Based on the modern altitudinal range of *Luma* and *Eucryphia* associations in the Collins Glacier wood flora Poole *et al.* (2001) considered that the palaeoforest probably grew at low to mid altitudes, possibly on the flanks of local stratovolcanoes.

Interestingly, several taxa present in the flora are both shade intolerant (*Nothofagus* spp., and *Araucaria* sp.) and have regeneration patterns linked to disturbance – *Araucaria* sp., *Nothofagus* sp., and Cunoniaceae (*Weinmannia*) (Veblen *et al.*, 1983; Hill, 1990; Burns, 1993; Carpenter and Buchanan, 1993; Veblen *et al.*, 1996). As part of the late Triassic to Recent Andean – West Antarctic subducting margin (Elliot, 1988; Leat *et al.*, 1995), King George Island has a sedimentary history strongly influenced by volcanism. This would have led to elevated levels of volcanic disturbance. Stratovolcanic activity is recorded by thick sequences of lavas (indicative of proximal locations and high disturbance) with intercalated tuffaceous and epiclastic volcanic sediments (indicative of more distal locations and low disturbance) (Birkenmajer, 1980; Smellie et al., 1984).

Poole *et al.* (2001) highlighted the potential impact of volcanic activity on the KGI flora and used particular assemblages of fossils to suggest high or low levels of volcanic disturbance in the flora. Based on Valdivian rainforests comparisons, low diversity, *Nothofagus*-rich floras equated to highly disturbed habitats, whilst lower diversity, relatively *Nothofagus*-poor floras equated to less disturbed habitats. This is significant because low diversity, *Nothofagus*-rich floras have also been used as indicators of prevailing cold climates, for example, at Point Hennequin (Zastawniak, et al., 1985; Birkenmajer, 1997), whilst the diversity of the assemblage may simply link to vegetation dynamics, implying that climate is not the sole driving mechanism for vegetational composition or diversity on King George Island.

Stratigraphically and geographically preserved vegetation distribution patterns occur at Fossil Hill (Shen 1994), Ardley Island (Orlando, 1964) and in the Collins Glacier Flora (Poole *et al.*, 2001) on Fildes Peninsula. These are evidence for Palaeocene-Eocene ecological disturbance resulting from fluctuating volcanic activity. The sequence at Fossil Hill probably represents a single eruptive phase (Chapter Four and Chapter Five) thus providing evidence for a stratigraphically/temporally changing environment. In the lower part of the sequence and overlying the coarse volcanic debris flow of Unit One, the low diversity Unit Two flora consists

only of *Nothofagus* and podocarps, which is characteristic of high disturbance. Higher up the sequence, in Units Three and Four, floral diversity increases with pteridophytes, conifers - including Araucariaceae, Cupressaceae, Podocarpaceae - and angiosperms, including *Nothofagus*, Proteaceae, Myrtaceae, ?Araliaceae, Anacardiaceae and Cunoniaceae. These latter angiosperm taxa would represent environments of low disturbance. In the uppermost part of the sequence (Units Five and Six) the low diversity *Nothofagus* assemblage suggests a return to high disturbance environments (Cao, 1994; Li 1994).

The Collins Glacier Flora of Middle Eocene age is either contemporaneous or slightly older than the Fossil Hill flora (Smellie *et al.*, 1984). It is preserved in thick tuffaceous and epiclastic sediments characteristic of a more distal location relative to volcanic centre (Vessel and Davies, 1981). As such it should have experienced lower levels of disturbance than the Fossil Hill flora, and this is supported by the floral composition. The presence of *Luma* and *Eucryphia* alongside *Nothofagus*, podocarps and Cupressaceae (Poole *et al.*, 2001) suggests that the flora was relatively diverse and had experienced low or relatively moderate levels of disturbance. On Ardley Island a flora probably coeval with the Fossil Hill flora includes leaves referred to Cupressaceae, Lauraceae, Monimiaceae, Sterculiaceae, Myrtaceae and Proteaceae (Orlando, 1964) and can therefore also be interpreted as a low disturbance vegetation (at least until the time of preservation).

Sedimentary palaeoenvironmental interpretations of the flora localities suggest that all of the floras grew in fluvial-lacustrine settings developed on the volcanic terrain (Chapter Four). These environments were likely to have been extremely dynamic, with loose volcanic ash soils prone to rapid resedimentation. Primary volcaniclastic sediments such as the Smok Hill and Dufayel Island sediments imply direct preservation by volcanic activity, most probably as a result of ash fall deposition, given the moderate to well preserved macrofossil remains (Chapter Four and Chapter Five). The lack of thick sequences of palaeolacustrine sediments suggests that these lakes were ephemeral bodies, possibly created by pyroclastic activity and damming of local drainage networks (Chapter Four; Spicer, 1989).

11.7 Palaeoclimate

In this study a combination of approaches was used to assess the palaeoclimatic signature of the KGI floras. Mean annual temperature and mean annual precipitation data was derived from regression based analyses using leaf physiognomy (Wolfe, 1979; Wing and Greenwood, 1993) and leaf area (Wilf *et al.*, 1998b). This data was supported by coexistence nearest living relative analyses (Mosbrugger, 1999) and by CLAMP analysis of the Dragon Glacier flora (Spicer and Wolfe, 1999).

11.7.1 Mean annual temperature data

Mean annual temperature analysis of the Dragon Glacier flora yielded an average of c. 10.6° C, and c. 8.9° - 13.4° C for the combined Fossil Hill (Units Two – Three) flora and the Li (1994) flora respectively. MAT estimates for the Dragon Glacier flora derived from co-existence nearest living relative analysis are at least 3° – 4° C higher than values derived by simple linear regression and CLAMP methods. This may imply that taphonomic bias has affected these analyses. Taphonomic analyses suggest that some of the floras have a streamside bias. According to Burnham *et al.*, (2001) streamside biased assemblages are likely to underestimate MAT by 2.5° to 5°C, implying that MAT estimates derived from the CA-analyses may be more realistic. However, uncertainty related to the validity of modern and Early Tertiary fossil plant relationships suggest that CA-analysis should be treated as tentative estimates (T Utescher, pers. comm., 2001).

11.7.2. Mean annual precipitation data

Mean annual precipitation estimates based on leaf area data (Wilf et al., 1998b) are c. 1039 mm for the Dragon Glacier flora and c. 1058 – 1139 mm for the Fossil Hill flora. The MAP estimates are considered to be minimum values given the observed bias in the floras towards smaller size classes by fragmentation of larger leaves (Chapter Five). Tentative co-existence nearest living relative analyses suggest mean annual precipitation of 815 – 1250 mm for the Dragon Glacier flora and 815 – 2099 mm for the Fossil Hill flora.

11.7.3 CLAMP analyses

CLAMP has not previously been used to assess Antarctic Peninsula floras because of the limited sample sizes, poor preservation and age (Hayes, 1999), uncertainty in morphological groupings (Hill, 199b) and the uncertainties surrounding the applicability of the method to the Southern Hemisphere flora. This approach is currently being applied to Palaeocene and Eocene floras from Seymour Island (J. Francis and A. Tosolini, pers. comm., 2001). The Dragon Glacier flora with over 30 morphotypes was analysed for 11 climatic parameters (Table 10.8). Using the CLAMP-144 database derived a MAT estimate of 10.6° C, showing excellent correlation with MAT values derived from simple linear regressions. Mean annual temperature is the most accurately predicted climatic variable using the CLAMP method (Kennedy, 1998), which combined with leaf margin analysis strongly supports interpretations of a warm microthermal climate. Growing season precipitation rather than MAP was calculated as 884.6 mm and the cold month mean was predicted as 2.56° C, suggesting a lack of winter freezing conditions, which is consistent with the presence of subtropical elements in the flora, such as the Lauraceae (possible Lauraceae described herein; Birkenmajer and Zastawniak, 1988; 1989).

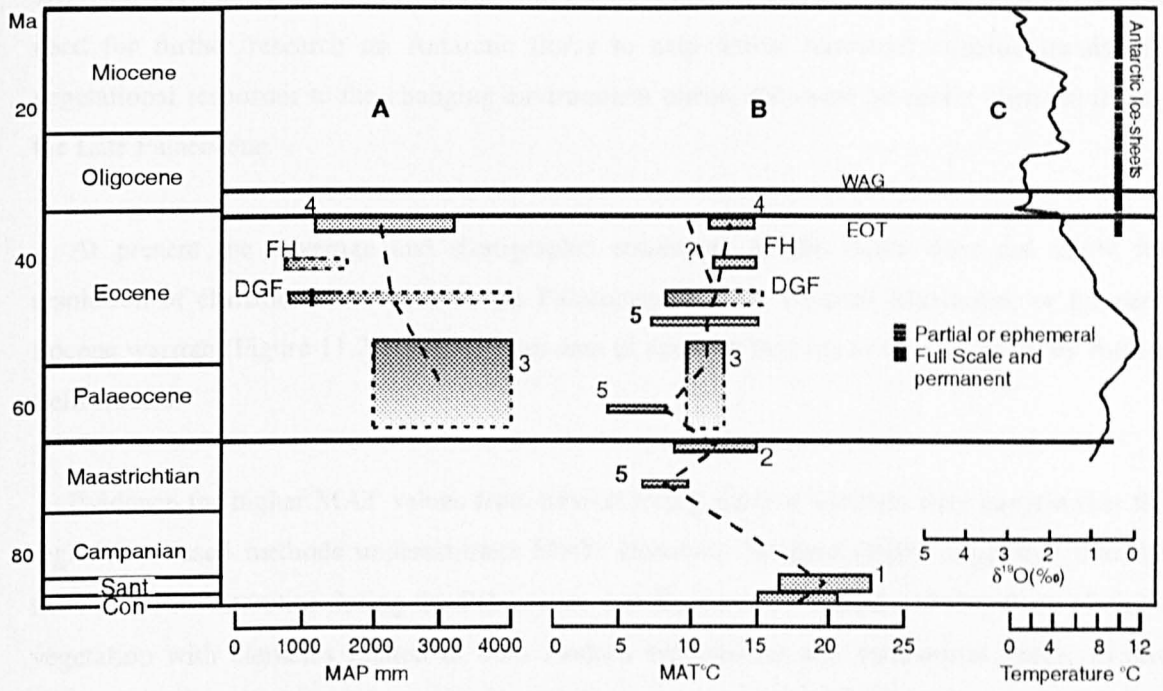

Figure 11-2. Palaeoclimatic parameters for the Late Cretaceous through Miocene Antarctic Peninsula region based on fossil plant assemblages (adapted from Francis and Poole, 2002; and Hunt and Poole, in review). A Estimated mean annual precipitation (MAP, mm); B Estimated mean annual temperature (MAT, °C) derived from leaf and wood macrofossils and floras; C Global $\delta^{18}O$ isotope curve for the latest Cretaceous and Cenozoic (from Zachos *et al.*, 2001) included for comparisons. Data from [1]Hayes (1999) for the Coniacian Hidden Lake Formation (15-20°C), and the early Santonian-early Campanian Santa Marta Formation (16-23°C); [2]Askin (1992); [3]Birkenmajer and Zastawniak (1986); [4]Birkenmajer and Zastawniak (1988, 1989); [5]Francis and Poole (2002); DGF – Dragon Glacier flora, this study. FH – Fossil Hill flora this study. EOT – Eocene-Oligocene Transition (Wilson *et al.*, 1998), WAG - West Antarctic glaciation (Dingle and Lavelle, 1998). Dashed boxes and gradation in shading indicate range of possible geological age due to uncertainties of dating of some sedimentary sequences, or total range in climatic parameter (see text). Black broken lines provide a relative but general trend in MAP and MAT as derived from fossil plant material.

11.7.4 Comparison with contemporaneous climate data

Contemporaneous climate data from the Antarctic Peninsula is plotted with the results obtained here in Figure 11.2. General paleoclimatic inferences based on fossil plant material from the Antarctic Peninsula region (e.g. Birkenmajer and Zastawniak, 1986, 1988, 1989; Askin, 1992; Hayes, 1999; Francis and Poole, 2002) provide evidence for the climate becoming cooler and somewhat drier from the Late Cretaceous into the Tertiary with a temporary increase in temperature during the Maastrichtian-earliest Palaeocene (Figure 11.2). The minimum MAT and MAP estimates presented here reflect a cool to warm temperate climate (c.f. Holdridge, 1967; Whittaker, 1975) prevailing across the northern Antarctic Peninsula region during the mid Eocene. This seems to have preceded a relatively warm, moist phase during the late Eocene (Figure 11.2) prior to the onset of glaciation in the Oligocene. The overall trend in MAT derived from fossil plant material is similar to that from oxygen isotope studies of marine macrofossils and foraminifera from the James Ross Basin (Barrera *et al.*, 1987; Pirrie and Marshall, 1990; Ditchfield *et al.*, 1994) and complements the general trends in the global $\delta^{18}O$ curve given by Zachos *et al.* (2001; redrawn in Figure 6). However, both the terrestrial MAT and MAP values

are relatively poorly constrained during the Late Eocene – earliest Oligocene, highlighting the need for further research on Antarctic floras to help define terrestrial climatic trends and vegetational responses to the changing environment during the onset of cooler climates during the Late Palaeocene.

At present the coverage and stratigraphic resolution of the floras does not allow for resolution of climatic events such as the Palaeocene-Eocene Thermal Maximum, or for peak Eocene warmth (Figure 11.2: C). This is an area of research that needs to be pursued by further field studies.

Evidence for higher MAT values from nearest living relative analyses may suggest that the regression based methods underestimate MAT. However, Romero (1986) suggested that the flora of West Antarctica during the Palaeocene and Eocene represented a 'Palaeoflora Mixta' - vegetation with elements related to both modern subantarctic and subtropical floras. In this context the warm temperate and subtropical signals, from nearest living relative analysis of the flora, do not imply highly elevated temperatures. Instead they suggest incorporation of vegetation elements growing at the cooler extreme of their climatic tolerances, or that the fossil taxa were adapted to a broader climatic range. Consequently nearest living relative analyses are likely to provide a much broader range of climatic tolerances for West Antarctica, than in areas with a more homogeneous, endemic vegetation.

11.7.5 Extrapolation of palaeoclimatic data to the Antarctic mainland

Applying a latitudinal temperature lapse rate of 0.3° C per 1° latitude (Wolfe and Upchurch, 1987; Wing and Greenwood, 1993) to the mean annual temperature data, from the Middle Eocene Dragon Glacier and Fossil Hill floras (10.6° - 13.9° C), implies MAT of 1.6° - 4.9° C for the Middle Eocene South Pole. Applying the same lapse rate to cold month mean values for the Dragon Glacier flora based on CLAMP analysis suggests tentative CMM of – 6° C. Such low MAT and CMM values suggest that ice masses could have formed at the pole during the Middle Eocene. According to Holdridge (1967) this constitutes a polar to cold climate, able to sustain permanent ice masses.

11.7.6 Comparison with modern data

Previous studies of the Palaeocene to Eocene King George Island palaeoclimate have used nearest living relative comparisons with modern temperate Valdivian vegetation (Birkenmajer and Zastawniak, 1986, 1989a, 1989b; Torres, 1990; Poole *et al.*, 2001), to suggest warm microthermal to cool mesothermal climates with MAT of 12 – 14° C and MAP of 2000 – 4000

mm for the Palaeocene and Middle Eocene (Birkenmajer and Zastawniak, 1986). The MAT estimates for both the Dragon Glacier and Fossil Hill floras both are consistent with this interpretation, reflecting a temperate, cool to warm microthermal climate (c.f. Holdridge 1967, Whittaker 1975), prevailing across the Antarctic Peninsula during the Eocene. Mean annual precipitation values are lower than those suggested by Birkenmajer and Zastawniak (1986) but are consistent with more recent Valdivian MAP range data of 900 – 2500 mm (Ogha, 1991).

11.8 Geochronology – implications for stratigraphy and palaeoclimate

The floras of King George Island are the basis for glacial-interglacial models proposed by Birkenmajer (1997), that suggest a decrease in vegetation diversity through the Eocene, extinction in the Early Oligocene and re-establishment in the Upper Oligocene. However, the reliability of the geochronology of the King George Island floras has been questioned (Soliani and Bonhomme, 1994; Willan and Kelley, 1999), which casts doubt on the climatic interpretations based on the floras.

As a whole the fossil floras of KGI appear to converge in age around the Late Palaeocene – Middle Eocene (Chapter 3). This clustering may well reflect increased preservation potential at times of heightened volcanic activity, such as occurred during the Early Eocene at ~52Ma, at 51-45Ma, in the Middle-Late Eocene (44-36Ma) and finally during the Oligocene (31-29Ma) (Willan and Kelley, 1999). Further $^{40}Ar/^{39}Ar$ geochronological studies are required to refine the age constraint of King George Island floras that might support such a tectonic preservation influence. A worst case scenario is that the data reflect homogenisation of the argon isotope ratios during this interval, although at present there is evidence only for moderate argon loss in certain samples (Chapter Three).

$^{40}Ar/^{39}Ar$ geochronology was used to date the Point Hennequin sequence to confirm whether the Mt. Wawel, Dragon Glacier (Zastawniak, 1981; Zastawniak *et al.*, 1985) and Smok Hill floras (Hunt and Poole, submitted) were Late Oligocene in age. The accepted stratigraphy divides the sequence into the Lower Eocene Vieville Glacier Formation and Late Oligocene Mt. Wawel Formation (Birkenmajer, 1981; Birkenmajer *et al.*, 1983). Alternative studies suggest an entirely Eocene age for the sequence (Smellie *et al.*, 1984).

The new $^{40}Ar/^{39}Ar$ data for the Point Hennequin sequence yields an entirely Middle Eocene age, whether the maximum plateau age range (39 - 50 Ma) or the inferred weighted average age range (44 - 49 Ma) is considered (Chapter 3), supporting the interpretations of Smellie *et al.* (1984). A Middle Eocene age is therefore inferred for the fossil floras, which implies that the plants were growing prior to the onset of either East Antarctic (c. 34 Ma) or West Antarctic (c.

30 Ma) glaciation (Dingle and Lavelle, 1998b; Wilson *et al.*, 1998). An older age for the flora is also consistent with the observed higher diversity of the fossil assemblage (Chapters Five and Six), since the flora was growing shortly after the Early Eocene climatic optimum (Zachos *et al.*, 2001). This contrasts distinctly with interpretations cool temperate, post-glacial, low diversity Nothofagaceae-podocarp and fern assemblage interpretations of Zastawniak (1981) and Zastawniak *et al.* (1985) from the same locality. The new age data imply that there are no floras younger in than Eocene-Oligocene boundary age.

Birkenmajer (eg. 1987, 1990, 1997) recognised four glacial phases in the Antarctic Peninsula; the Early Eocene (Kraków Glaciation), Early Oligocene (Polonez Glaciation), Late Oligocene (Legru Glaciation) and Early Miocene (Melville Glaciation). Dingle and Lavelle (1998a) re-evaluated Birkenmajer's (1987, 1990, 1997) glacial chronology using Sr^{86}/Sr^{87} isotope stratigraphy and found evidence for only two major Polonez (c. 30 Ma) and Melville glaciations (c. 23 Ma), with a single intervening Wawel Interglacial. The Wawel Interglacial was based on the absence of glacial deposits and the presence of the only Upper Oligocene flora in West Antarctica - the Mt. Wawel flora. Birkenmajer (1987, 1990, 1997) considered that the KGI flora went extinct during the Polonez Glaciation but re-established itself from refugia at a later stage.

The new Middle Eocene age of the Mt. Wawel flora implies that no West Antarctic flora post-dates the initial West Antarctic, Polonez Glaciation. This scenario may be explained in terms of two alternative hypotheses, firstly that Oligocene and younger fossiliferous strata are present beneath the ice cap, or have been glacially eroded. This is supported by evidence of Oligocene - ?Pliocene vegetation in East Antarctica (Francis and Hill, 1996; Hill and Truswell, 1993; Raine, 1998), that should have acted as a source vegetation for West Antarctic recolonisation. More intriguing is a model of complete extinction in the West Antarctic terrestrial flora following Polonez Glaciation. This latter model has some support from the Late Eocene pollen record of Seymour Island, which diminishes in diversity towards the Eocene-Oligocene boundary. It is possible that the combined effects of Andean and Trans-Antarctic Mountain uplift and climate cooling may have created environmental gradients that exceeded the adaptation ability of the Antarctic Peninsula flora.

Chapter 12 Conclusions

12.1 Conclusions

1. Abundant fossil plants are preserved within Palaeogene volcaniclastic sediments on King George Island. The fossils represent the remains of vegetation growing prior to the onset of Cenozoic glaciation, during a period of globally warm climates.

2. Fifteen floras from King George Island have been examined: The old British Antarctic Survey Collections (part described by Barton, 1965) including; the Palaeocene Dufayel Island and Barton Peninsula floras; the Middle Eocene Fossil Hill, Profound Lake and Rocky Cove floras from Fildes Peninsula; the Middle Eocene Smok Hill and Dragon Glacier floras from Point Hennequin; the Eocene Potter Cove compression and impression floras; the ?Middle Eocene Vaureal Peak flora; and the ?Eocene-Oligocene boundary Platt Cliffs and Cytadela floras from Ezcurra Inlet. This material is supplemented by new collections made in the 1999 field season from; the Middle Eocene Collins Glacier (*in-situ* and moraine), Fossil Hill and Rocky Cove floras from Fildes Peninsula; and the Middle Eocene Dragon Glacier and Mt. Wawel floras from Point Hennequin. The floras are all considered to be allochthonous, since there is no evidence of associated palaeosol development with any of the deposits. The exception is at Point Hennequin, where sediments of the Dragon Glacier flora preserve ?marginal lacustrine rootlet horizons.

3. Leaf fossil assemblages are preserved as carbonised compressions, lacking original organic material, or as impressions (± mineralisations). Leaves are preserved intact and as fragmentary remains. The floras comprise angiosperm, gymnosperm, fern and rare moss remains. Fertile material consists of fertile fern axes, seeds, araucarian cone scales and rare pollen and ovuliferous cones. Trace fossils commonly occur on the leaf laminae and are grouped into four categories according to their position, shape and structure. The traces are interpreted as evidence of plant-arthropod interactions, a single possible fungal damage trace and mechanical damage resulting from wind-induced abrasion.

4. The 428 angiosperm leaf specimens examined in this study, comprise 85 morphotypes – 27 entire margined and 58 toothed margined. Three of the morphotypes are considered to be juvenile and a further two are considered to be herbaceous. Conifers are represented by 161 specimens comprising 16 types; ferns - 11 types and 64 specimens; cycads - one type and

eight specimens; bryophyte remains - two types and two specimens; fertile remains - 22 types and 54 specimens.

5. Leaves referred to *Nothofagus* spp., are a common and dominant element of the angiosperm flora. Based on morphological similarity of fossil leaves to those of modern plants the Proteaceae, and Cunoniaceae are considered to be present in the angiosperm flora. The Myrtaceae, Lauraceae, Monimiaceae, Sterculiaceae, Symplocaceae and Eucryphiaceae are possibly present in the flora described herein. The angiosperm element is combined with *Araucaria* sections *Eutacta* and *Columbea*, the Podocarpaceae and Cupressaceae and a variety of indeterminate fern types. The flora is considered to be most similar in composition to the modern Valdivian rainforests of Chile, however, some elements of the flora such as *Lomatia*, *Schizomeriaeae* (Cunoniaceae) and certain of the *Nothofagus* species are also common in the modern temperate forests of Tasmania.

6. The structure of the forest is interpreted using the modern Southern Hemisphere, and in particular Valdivian rainforests, as a model. In this context the canopy would have comprised mixed *Nothofagus* and other angiosperms (e.g. Eucryphiaceae, Myrtaceae), with emergent Araucariaceae, Podocarpaceae and Cupressaceae. Mid stratal forest composition would have comprised small angiosperm tree or shrubs (e.g. Proteaceae, Cunoniaceae, Sterculiaceae). Ferns and possibly bamboo (as a minor element) would have formed the understorey. During times of high disturbance the canopy would have comprised almost 100 % *Nothofagus* and conifers, whilst other angiosperms would rise to dominate the canopy during periods of low disturbance (Poole *et al.*, 2001).

7. Dating of the fossiliferous sequences from Fossil Hill, Point Hennequin and Vaureal Peak has been questioned, based on evidence of Ar-loss and K-metasomatism (Birkenmajer *et al.*, 1983; Soliani and Bonhomme, 1994; Smellie and Hunt, work in progress). Multiple $^{40}Ar/^{39}Ar$ analyses of the Point Hennequin sequence yield a Middle Eocene age (c. 44 – 49 Ma), and tentative Middle Eocene ages are derived from Fossil Hill (c. 40 Ma) and Vaureal Peak (younger than 49 Ma). This clustering of ages around the Middle Eocene is likely to represent the true age of the strata but the possibility of isotope homogenisation cannot be ruled out, further detailed geochronological studies are required to establish a robust local and regional stratigraphic framework.

8. The King George Island floras were previously thought to decline in diversity from the Eocene onwards as a result of climate cooling and glaciation, with extinction in the Oligo-Miocene (Birkenmajer and Zastawniak, 1989a; Askin, 1992). Modification of the old King George Island palaeobotanical chronology using the new $^{40}Ar/^{39}Ar$ geochronology suggests

that the floras are all Palaeocene to Eocene-Oligocene boundary age. The new age data suggests that there are no post-Oligocene floras in West Antarctica, which implies that the KGI flora went extinct during, or slightly *preceding,* the Oligocene Polonez glaciation (Dingle and Lavelle, 1998b) and did not re-establish itself during the following interglacial periods (Birkenmajer, 1997). The apparent extinction is enigmatic though, since it cannot be determined at present, whether the flora became extinct or if there is no record of younger floras. The stratigraphic section may have been eroded by Pliocene to recent glacial erosion, but a decline in pollen diversity towards the Eocene-earliest Oligocene is observed in the Seymour Island flora (Askin, 1998), which suggests that the whole of the West Antarctic flora declined in diversity towards the Eocene-Oligocene boundary. Future collections need to focus on Oligocene and younger terrestrial sections to determine whether a reduced diversity vegetation existed in Antarctica during post-Polonez Glaciation times.

9. Mean annual temperature data have been derived from the Middle Eocene Fossil Hill and Dragon Glacier floras, which are the only floras to-date that have sufficient morphotype diversity for physiognomy-based palaeoclimatic analyses. Leaf margin and CLAMP analysis methods suggest warm microthermal climates c. 10.5° C for the Dragon Glacier flora (precision error 5°C). Analysis of the Fossil Hill flora also suggests warm microthermal climates c. 8.85° C (precision error 10°C), although distinctly cooler than estimates from the DGF. This variation could reflect the different precision errors relating to numbers of morphotypes used in the analyses, or it might relate to regional climatic variations. In either case, MAT values suggest warm microthermal climates for the Middle Eocene in West Antarctica.

10. Mean annual precipitation data have been derived from the Middle Eocene Fossil Hill and Dragon Glacier floras. MAP of c. 1000 mm is inferred for both floras.

11. The estimated MAT and MAP parameters suggest a climatic range similar to modern temperate Valdivian rain forests from Chile (Ogha, 1991) and are consistent with shallow marine palaeotemperature data from Seymour Island. (Ditchfield *et al.*, 1994).

12. In contrast to previous studies, the variations in diversity and composition of the KGI flora have also been interpreted in terms of ecological dynamics and volcanic disturbance succession. Based on comparisons with the Valdivian rain forests a model of vegetation dynamics (Poole *et al.*, 2001) suggests that low diversity, *Nothofagus*-dominated floras may represent a successional vegetation following volcanic disturbance of the vegetation. High diversity floras, such as the Dragon Glacier flora may represent climax vegetation growing in a low disturbance regime. The basic-intermediate volcaniclastic sediments of KGI can be

divided into 1). primary, or only slightly reworked, pyroclastic sediments and 2). reworked volcaniclastic sediments. Primary pyroclastics are defined by abundant juvenile volcanic material, such as scoria and volcanic glass, and are interpreted as ash fall, and less commonly, ash flow deposits. Reworked sediments are characterised by low proportions of juvenile volcanic material and enrichment in epiclasts and crystals, and are interpreted as fluvio-lacustrine in origin.

13. Primary volcanic sediments, which preserve plant fossils (such as the low diversity Smok Hill and Mt. Wawel floras) are used to indicate volcanic disturbance of the palaeoflora. Reworked sediments that preserve plant fossils (such as the higher diversity Dragon Glacier flora) are used to suggest minimal volcanic disturbance. It should be noted that the Smok Hill flora comprises only 24 specimens and therefore may be low in diversity due to sample size. The vegetation dynamic model has otherwise only been applied to the more diverse floras (Dragon Glacier and Fossil Hill) and those that have a low diversity but high sample size (Mt. Wawel flora in Zastawniak *et al.*, 1985).

14. The Fossil Hill sedimentary sequence comprises six units belonging to the Great Wall Bay Submember in the Lower Member of the Fildes Formation. This is a reconciliation of the stratigraphic schemes proposed by Smellie *et al.* (1984) and Shen (1999). The Fossil Hill units record the development of lacustrine conditions following major volcanism-related debris flow deposition.

15. At Point Hennequin the Dragon Glacier sediments have been divided into six facies that are interpreted in terms of a complete terrestrial fluvial to lacustrine sequence. Primary volcanic ?ashfall sediments with mineralised impression fossils at Smok Hill are grouped as a single separate facies and the Mt. Wawel *in-situ* sediments are interpreted as low energy, lacustrine/ephemeral lacustrine deposits.

12.2 Future Work

- There is a great deal of scope for further research on King George Island. The continual retreat of the ice-margins, for example at Point Hennequin, means that new fossiliferous exotic blocks are constantly being exposed. Continued research and collection at Point Hennequin is required to pinpoint the source of the plant bearing beds. This is crucial to understanding the variations in diversity observed in the Point Hennequin floras that is currently interpreted in terms of vegetation dynamics (e.g. Poole *et al.*, 2001; Hunt and Poole, *submitted*).

- Geochronological studies (Chapter 3) undertaken during this project highlight the need for further dating of the fossiliferous strata on King George Island. Robust geochronological techniques, such as $^{40}Ar/^{39}Ar$ dating, that can detect alteration and isotopic resetting are needed to support, or refute, previous K-Ar dating. A detailed programme of $^{40}Ar/^{39}Ar$ dating across the whole of the Palaeogene strata of KGI is required, for improved stratigraphy and to confirm whether the floras do all cluster in the Eocene. The Dufayel Island and Platt Cliff floras in particular require redating. Until a detailed stratigraphic framework is emplaced, the full climatic and ecological significance of the KGI floras will remain untapped.

- Improved geochronology of the fossil bearing sequences is also required to cross correlate the stratigraphy across King George Island. Currently it is practically impossible to link the strata of Fildes Peninsula, Ezcurra Inlet and Point Hennequin to undertake meaningful studies of the geographical distribution of the palaeovegetation. Volcanic events might be useful in this respect. Recognition of a single large pyroclastic event across the island is required, which could provide a datum. Given the small distances involved (<100 km) it seems likely that such an event could have occurred. Detailed petrographic studies are required to identify such a horizon.

- Further studies are required to establish the taxonomic diversity of the flora. Morphotype identifications provide a first estimate but need to be supported by cuticular studies. Use of an environmental chamber for examining specimens may provide this information. Identification of leaf specific feeding traces might also be useful in this respect.

- In spite of the sedimentary data summarised here, the terrestrial sedimentary history of King George Island is still poorly understood. A project on the sedimentary volcanic history of the island is required, that focuses on palaeoenvironmental and landscape reconstructions.

- CLAMP analysis of the flora, shows good correlation with other physiognomic and nearest living relative analyses, however the basis for CLAMP analysis in the Southern Hemisphere has still not been fully established. South American floras need to be added to the CLAMP database to make it a more representative tool for Southern Hemisphere climate analyses

- Animal and insect fossils are still rare in the floras, despite secondary evidence of their presence (e.g. bird footprints, feeding traces on leaves). Further collecting expeditions are required to establish what happened to this section of the Tertiary KGI ecosystem.

References

Askin RA. 1988a. The Campanian to Paleocene palynological succession of Seymour and adjacent islands, northeastern Antarctic Peninsula. Memoir of the Geological Society of America 169: 131-153.

Askin RA. 1988b. The palynological record across the Cretaceous/Tertiary transition on Seymour Island, Antarctica. Geological Society of America Memoir 169: 155-162.

Askin RA. 1989. Endemism and heterochroneity in the Late Cretaceous (Campanian) to Paleocene palynofloras of Seymour Island, Antarctica: implications for origins, dispersal and palaeoclimates of southern floras. In: Crame JA (ed), Origins and evolution of the Antarctic biota. Geological Society Special Publications 47: 217-226.

Askin RA. 1990. Cryptogam spores from the upper Campanian and Maastrichtian of Seymour Island, Antarctica. Micropaleontology 36: 141-156.

Askin RA. 1992. Late Cretaceous-early Tertiary Antarctic outcrop evidence for past vegetation and climates. Antarctic Research Series 56: 61-73.

Askin RA. 1994. Monosulcate angiosperm pollen from the Lopez de Bertodano Formation (upper Campanian-Maastrichtian-Danian) of Seymour Island, Antarctica. Review of Palaeobotany and Palynology 81: 151-164.

Askin RA. 1997. Eocene - ?Earliest Oligocene terrestrial palynology of Seymour Island, Antarctica. In: Ricci CA (ed), The Antarctic Region: Geological evolution and processes: Terra Antartica Publication, Siena: 993-996.

Askin RA. 2000. Spores and pollen from the McMurdo Sound erratics, Antarctica. In: (eds), Paleobiology and paleoenvironments of Eocene rocks, McMurdo Sound, East Antarctica. Antarctic Research Series 76: 253-260.

Askin RA, Markgraf V. 1986. Palynomorphs from the Sirius Formation, Dominion Range, Antarctica. Antarctic Journal of the United States 21: 34-35.

Askin RA, Spicer RA. 1995. The Late Cretaceous and Cenozoic history of Vegetation and Climate at northern and southern high latitudes: A comparison. In: The effects of past global change on life. Studies in Geophysics, National Research Council, National Academy Press, Washington: 156-173.

Askin RA, Baldoni AM. 1998. The Santonian through Paleogene record of Proteaceae in the Southern South America-Antarctic Peninsula region. Australian Systematic Botany 11: 373-390.

Bailey IW, Sinnott EW. 1915. A botanical index of Cretaceous and Tertiary climates. Science 41. 831-834.

Bailey IW, Sinnott EW. 1916. The climatic distribution of certain types of angiosperm leaves. American Journal of Botany, 3: 24-39.

Barker PF, Burrell J. 1977. The opening of the Drake Passage. Marine Geology 25: 15-34.

Barker PF, Barrett PJ, Cooper AK, Huybrechts P. 1999. Antarctic glacial history from numerical models and continental margin sediments. Paleogeography, Palaeoclimatology, Palaeoecology 150: 247-267.

Barnes RW, Jordan GJ. 2000. *Eucryphia* (Cunoniaceae) reproductive and leaf macrofossils from Australian Cainozoic sediments. Australian Systematic Botany 13: 373-394.

Barnes RW, Rozefelds AC. 2000. Comparative morphology of *Anodopetalum* (Cunoniaceae). Australian Systematic Botany 13: 267-282.

Barnes RW, Hill RS, Bradford JC. 2001. The history of Cunoniaceae in Australia based on macrofossil evidence. Australian Journal of Botany, 49(3): 301-320.

Barron B, Larson B, Baldauf JG. 1991. Evidence for late Eocene to early Oligocene Antarctic glaciation and observations on late Neogene glacial history of Antarctica: Results from Leg 119. Proceedings of the Ocean Drilling Programme Scientific Results 119: 869-891.

Barton CM. 1959. The east coast of Admiralty Bay from Point Hennequin to Ternyck Glacier. F.I.D.S Base G. Admiralty Bay Report (1949). Geology Survey (Archive No AD6/2G/1959/GI), 19 pages.

Barton CM. 1961. The geology of King George Island South Shetland Islands. Preliminary Report of the Falkland Islands Dependencies Survey 12: 18 pages.

Barton CM. 1964a. Significance of the Tertiary fossil floras of King George Island, South Shetland Island. In: Adie RJ (ed). Antarctic Geology. Amsterdam, North Holland Publishing Company: 603 - 608.

Barton CM. 1964b. The geology of King George Island, South Shetland Islands. PhD thesis, University of Birmingham.

Barton CM. 1965. The Geology of the South Shetland Islands. Part 3: The stratigraphy of King George Island. British Antarctic Survey Scientific Reports 44: 33 pages.

Behrensmeyer AK, Hook RW. 1992. Palaeoenvironmental contexts and taphonomic modes. In: Behrensmeyer AK, Damuth JD, DiMichele WA, Potts R, Sues H, Wing SL (eds), Terrestrial Ecosystems through time. Evolutionary palaeoecology of terrestrial plants and animals. The University of Chicago Press, Chicago and London: 568 pages.

Berry EW. 1925. A Miocene flora from Patagonia. Johns Hopkins University, Studies in Geology 6: 183-252.

Berry EW. 1928. Tertiary fossil plants from the Argentine Republic. Proceedings of the US National Museum 70: 1-27.

Berry EW. 1937a. An Upper Cretaceous flora from Patagonia. Johns Hopkins University Studies in Geology 12: 11-31.

Berry EW. 1937b. A Paleocene flora from Patagonia. Johns Hopkins University Studies in Geology 12: 33-50.

Berry EW. 1937c. Eogene Plants from Rio Turbio in the terrtory of Santa Cruz, Patagonia. Johns Hopkins University Studies in Geology 12: 91-97.

Berry EW. 1938. Tertiary flora from the Rio Pichileufu, Argentina. Geological Society of America Special Papers 12: 1-149. 56 plates.

Birkenmajer K. 1980. Tertiary volcanic-sedimentary succession at Admiralty Bay, King George Island (South Shetland Islands, Antarctica). Studia Geologica Polonica, 64: 7-65.

Birkenmajer K. 1981. Lithostratigraphy of the Point Hennequin Group (Miocene volcanics and sediments) at King George Island (South Shetland Islands, Antarctica). Studia Geologica Polonica, 74: 175-197.

Birkenmajer K. 1982. Pliocene tillite-bearing succession of King George Island (South Shetland Islands, Antarctica). Studia Geologica Polonica 74: 7-72.

Birkenmajer K. 1983. Late Cenozoic phases of block-faulting on King George Island (South Shetland Islands, West Antarctica). Bulletin de l'Academie Polonaise des Sciences, Série des Sciences de la Terre 30(1-2): 21-32.

Birkenmajer K. 1988. Tertiary glacial and interglacial deposits, South Shetland Islands, Antarctica: geochronology versus biostratigraphy (a progress report). Bulletin of the Polish Academy of Sciences, Earth Sciences 36: 133-145.

Birkenmajer K. 1989. A guide to Tertiary geochronology of King George Island, West Antarctica. Polish Polar Research 10: 555 -579.

Birkenmajer K. 1990. Geochronology and climatostratigraphy of Tertiary glacial and interglacial successions on King George Island, South Shetland Islands (West Antarctica). Zbl. Geol. Paläont. Teil I: 141 - 151.

Birkenmajer K. 1997. Tertiary glacial/interglacial palaeoenvironments and sea-level changes, King George Island, West Antarctica. An overview. Bulletin of the Polish Academy of Sciences, Earth Sciences 44 No 3: 157 - 181.

Birkenmajer K, Gadzicki A. 1986. Oligocene age of the Pecten conglomerate on King George Island, West Antarctica. Bulletin of the Polish Academy of Sciences, Earth Sciences 34: 219-226.

Birkenmajer K, Zastawniak E. 1986. Plant remains of the Dufayel Island Group (Early Tertiary?), King George Island. South Shetland Islands (West Antarctica). Acta Palaeobotanica 26: 33–108.

Birkenmajer K, Zastawniak E. 1989a. Late Cretaceous – Early Neogene vegetation history of the Antarctic Peninsula sector. Gondwana break-up and Tertiary glaciations. Bulletin of the Polish Academy of Sciences, Earth Sciences 37(1-2): 63-88.

Birkenmajer K, Zastawniak E. 1989b. Late Cretaceous-early Tertiary floras of King George Island, West Antarctica: their stratigraphic distribution and palaeoclimatic significance. In: Crame JA. Origins and evolution of the Antarctic biota. Geological Society Special Publication 47: 227-240.

Birkenmajer K, Narębski W, Nicoletti M, Petrucciani C. 1983. Late Cretaceous through Late Oligocene K-Ar ages of the King George Island Supergroup volcanics, south Shetland Islands (West Antarctica). Bulletin de l'Academie Polonaise des Sciences, Série des Sciences de la Terre 30(3-4): 133-143.

Birkenmajer K, Delitala MC, Narębski W, Nicoletti M, Petrucciani C. 1986a. Geochronology and migration of Cretaceous through Tertiary plutonic centres, South Shetland Islands (West Antarctica): Subduction and hot spot magmatism. Bulletin of the Polish Academy of Sciences, Earth Sciences 34: 139-155.

Birkenmajer K, Delitala MC, Narębski W, Nicoletti M, Petrucciani C. 1986b. Geochronology of Tertiary island arc volcanics and glacigenic deposits, King George Island, South Shetland Islands (West Antarctica). Bulletin of the Polish Academy of Sciences, Earth Sciences 34: 257-273.

Birkenmajer K, Soliani E, Kawashita K. 1989. Geochronology of Tertiary glaciations on King George Island, West Antarctica. Bulletin of the Polish Academy of Sciences, Earth Sciences 37: 27-48.

Birkenmajer K, Soliani E, Kawashita K. 1990. Reliability of potassium-argon dating of Cretaceous-Tertiary island-arc volcanic suites of King George Island, South Shetland Islands (West Antarctica). Zentralblatt für Paläontologie 1: 127-140.

Birkenmajer K, Francalanci L, Peccerillo A. 1991. Petrological and geochemical constraints on the genesis of Mesozoic-Cenozoic magamtism of King George Island, South Shetland Islands (West Antarctica). Antarctic Science 3: 293-308.

Boyd A. 1994. Some limitations in using leaf physiognomic data as a precise method for determining paleoclimates with an example from the Late Cretaceous Pautût Flora of West Greenland. Palaeogeography, Palaeoclimatology, Palaeoecology, 112: 261-278.

Breitkreutz C. 1991. Fluvio-lacustrine sedimentation and volcanism in a Late Carboniferous tensional intra-arc basin, northern Chile. Sedimentary Geology, 74: 173-187.

Brickell C. 1998. A-Z of garden plants. The Royal Horticultural Society. Dorling Kindersley Ltd, London.

Burnham RJ. 1989. Relationships between standing vegetation and leaf litter in paratropical forest: implications for palaeobotany. Review of Palaeobotany and Palynology, 58: 5-32.

Burnham RJ. 1993. Reconstructing richness in the plant fossil record. Palaios 8: 376 – 384.

Burnham RJ. 1994. Plant deposition in modern volcanic environments. Transactions of the Royal Society of Edinburgh: Earth Sciences 84: 275 – 281.

Burnham RJ, Spicer RA. 1986. Forest litter preserved by volcanic activity at El Chichon, Mexico: A potentially accurate record of the pre-eruption vegetation. Palaios 1: 158 – 161.

Burnham RJ, Pitman NCA, Johnson KR, Wilf PW. 2001. Habitat-related error in estimating temperatures from leaf margins in a humid tropical forest. American Journal of Botany 88(6): 1096 – 1102.

Burns BR. 1993. Fire-induced dynamics of *Araucaria araucana-Nothofagus antarctica* forest in the southern Andes. Journal of Biogeography 20: 669-685.

Cain SA, Castro GM de O. 1959. Manual of vegetation analysis: Harper and Row, New York. 325 pages.

Cao L 1989. Late Cretaceous sporopollen flora from Half Three Point on Fildes Peninsula of King George Island, Antarctica. In: Proceedings of the International Symposium on Antarctic Research, China Ocean Press, Tianjin, China: 151-156.

Cao L. 1992. Late Cretaceous and Eocene palynofloras from Fildes Peninsula, King George Island (South Shetland Islands), Antarctica. In: Yoshida Y, ed. Recent Progress in Antarctic Earth Science. Tokyo: Terra Scientific Publishing Company (Terrapus), 363-369.

Cao L. 1994. Late Cretaceous palynoflora in King George Island of Antarctica with reference to its palaeoclimatic significance. In: Shen Y, ed. Stratigraphy and palaeontology of Fildes Peninsula, King George Island. State Antarctic Committee Monograph 3: 85-96.

Cande SC, Kent DV. 1992. A new geomagnetic polarity time scale for the Late Cretaceous and Cenozoic. Journal of Geophysical Research 97: 13918-13951.

Cande SC, Kent DV. 1995. Revised calibration of the geomagnetic polarity timescale for the Late Cretaceous and Cenozoic. Journal of Geophysical Research, 100. 6093-6095.

Cande SC, Kent DV. 1995. Revised calibration of the geomagnetic polarity timescale for the Late Cretaceous and Cenozoic. Journal of Geophysical Research 100: 6093-6095.

Cantrill DJ. 1991. Broad leafed coniferous foliage from the Lower Cretaceous Otway Group, southeastern Australia. Alcheringa 15: 177-190.

Cantrill DJ. 1992. Araucarian foliage from the Lower Cretaceous of southern Victoria, Australia. International Journal of Plant Science 153: 622-645.

Cantrill DJ. 1995. *Hausmannia* Dunker (Dipteridaceae): a pteridophyte from the Cretaceous of Alexander Island. Alcheringa 19: 243-254.

Cantrill DJ. 1996. Fern thickets from the Cretaceous of Alexander Island, Antarctica containing *Alamatus bifarius* Douglas and *Aculea acicularis* sp. nov. Cretaceous Research 17: 169-182.

Cantrill DJ. 1998. Early Cretaceous fern foliage from President Head, Snow Island, Antarctica. Alcheringa 22: 241 – 258.

Cantrill DJ. 2000. A Cretaceous (Aptian) flora from President Head, Snow Island, Antarctica. Palaeontographica Abteilung B: 191 pages and 8 plates.

Cantrill DJ, Douglas JG. 1988. Mycorrhizal conifer roots from the Lower Cretaceous of the Otway Basin, Victoria. Australian Journal of Botany 36: 257-272.

Cantrill DJ, Nichols GJ. 1996. Taxonomy and palaeoecology of Early Cretaceous (Late Albian) angiosperm leaves from Alexander Island, Antarctica. Review of Palaeobotany and Palynology 92: 1-28.

Cantrill DJ, Webb JA. 1987. A reappraisal of *Phyllopteroides* Medwell (Osmundaceae) and its stratigraphic significance in the Lower Cretaceous of eastern Australia. Alcheringa 11: 59-85.

Cape Roberts Science Team. 1998. Miocene strata in CRP-1, Cape Roberts Project, Antarctica. Terra Antartica 5(1): 63-124.

Carey SN. 1991. Transport and deposition of tephra by pyroclastic flows and surges. In Fisher RV, Smith GA (eds), Sedimentation in volcanic settings. Society for Economic Paleontologists and Mineralogists, Special Publication No 45: 39-57.

Carpenter RJ, Buchanon AM. 1993. Oligocene leaves fruit and flowers of the Cunoniaceae from Cethana, Tasmania. Australian Systematic Botany 6: 91-109.

Cas RAF, Wright JV, 1987. Volcanic Successions, Modern and Ancient: Allen and Unwin, London. 528 pages.

Case JA. Woodburne MO, Chaney DS. 1988. A genus of polydolopid marsupial from Antarctica. Geological Society of America Memoir 169: 505-521.

Case JA. 1989. Antarctica: the effect of high latitude heterochroneity on the origin of the Australian marsupials. In: Crame JA (ed), Origins and evolution of the Antarctic biota, Geological Society Special Publication 47: 217 - 226.

Chaloner WG, Creber GT. 1990. Do fossils give a climatic signal? Journal of the Geological Society, London 147: 343-350.

Chambers TC, Drinnan AN, McLoughlin S. 1998. Some morphological features of Wollemi Pine (*Wollemi nobilis*: Araucariaceae) and their comparison to Cretaceous plant fossils. International Journal of Plant Science 159(1): 160-171.

Chapman JL, Smellie JL. 1992. Cretaceous fossil wood and palynomorphs from Williams Point, Livingston Island, Antarctic Peninsula. Review of Palaeobotany and Palynology 74: 163-192.

Christophel DC, Greenwood DR. 1988. A comparison of Australian tropical rainforest and Tertiary fossil leaf beds. Proceedings of the Ecological Society of Australia 15: 139 – 148.

Christophel and Hyland. 1993. Leaf atlas of Australian tropical rain forest trees. CSIRO publications, Victoria. 260 pages.

Cortegmiglia G, Gastaldo P, Terranova R. 1981. Studio di piante fossili trovate nella King George Island delle Isole Shetland del Sud (Antartide), Atti Societá Italiana Sci. Nat. Museo Civ. Stor. Nat. Milano 122: 37-61.

Covacevich V, Hernandez P. 1971. Investigaciones paleontologicas en las islas Shetland del Sur, Antartica. 1970-1971. Bolletin Instituto Antartica Chilena 6: 3-6.

Covacevich V, Lamperein C. 1969. Nota sobre el hallazgo de icnitas fossiles de aves en Peninsula Fildes, Isla Rey Jorge, Shetland del Sur, Antartica. Bolletin Instituto Antartica Chilena 4: 26-28.

Covacevich V, Lamperein C. 1970. Hallazago de icnitas en Peninsula Fildess, Isla Rey Jorge, Archipelago Shetland del Sur, Antartica. Serie Cientifica Instituto Àntartico Chileno 1(1): 55-74.

Covacevich V, Lamperein C. 1972. Ichnites from Fildes Peninsula, King George Island, South Shetland Islands. In: Adie RJ (ed), Antarctic geology and geophysics. Oslo, Universitetsforlaget, 71-74.

Covacevich V, Rich P. 1982. New bird ichnites from Fildes Peninsula, King George Island, West Antarctica. In: Craddock C ed, Antarctic Geoscience, University of Wisconsin Press, Madison: 245-251.

Crabtree DR. 1987. Angiosperms of the northern Rocky Mountains: Albian to Campanian (Cretaceous) megafossil floras. Annals of the Missouri Botanical Garden, 74: 707-747.

Crame JA, Pirrie D, Crampton JS, Duane AM. 1993. Stratigraphy and regional significance of the Upper Jurassic-Lower Cretaceous Byers Group, Livingston Island, Antarctica. Journal of the Geological Society London 150: 1075-1087.

Crane PR. 1981. Betulaceous fossils from the Upper Palaeocene. Botanical Journal of the Linnean Society 83: 103-136.

Crouch EM. 2001. Environmental change at the time of the Palaeocene-Eocene biotic turnover. PhD thesis, Laboratory of Palaeobotany and Palynology, Utrecht University: 216 pages.

Czajkowski S, Rosler O. 1986. Plantas fosseis da Peninsula Fildes; Ilha Rei Jorge (Shetlands do Sul); Morfografia das impressoes foliares. Anais Academia Brasileira de Ciencias Supplemento 58: 99-110.

D' Atri, Pierre D, Lanza R, Ruffini R. 1999. Distinguishing primary and resedimented vitric volcaniclastic layers in the Burdigalian carbonate shelf deposits in Monferrato (NW Italy). Sedimentary Geology 129: 143-163.

Davies RES. 1982. New geological interpretation of Admiralen Peak, King George Island, South Shetland Islands. British Antarctic Survey Bulletin 51: 294-6.

Del Valle RA, Diaz MT, Romero EJ. 1984. Preliminary report on the sedimentites of Barton Peninsula, 25 de Mayo Island (King George Island), South Shetland Islands. Argentine Antarctica. Instituto Antartico Argentino Contribution 308: 121-131.

Denton GH, Prentice ML, Burckle LH. 1991. Cainozoic history of the Antarctic ice-sheet. In: Tinjey RJ (ed), The geology of Antarctica, Oxford University Press, New York: 365- 421.

Dettmann ME. 1989. Antarctica: Cretaceous cradle of austral temperate rainforests? In: Crame JA (ed), Origins and evolution of the Antarctic biota, Geological Society Special Publication 47: 89 - 105.

Dettmann ME, Thomson MRA. 1987. Cretaceous palynomorphs from the James Ross Island area, Antarctica - A pilot study. British Antarctic Survey Bulletin 77: 13 - 59.

Dickison WC. 1978. Comparative anatomy of Eucryphiaceae. American Journal of Botany 65: 722-735.

Dilcher 1973. A palaeoclimatic interpretation of the Eocene floras of southeastern North America. In: Graham A (ed), Vegetation and vegetational history of northern Latin America. Elsevier Publishing Co. Amsterdam. 39-59.

Dilcher 1974. Approaches to the identification of angiosperm leaf remains. Botanical Review 40(1): 1-157.

Dingle RV, Lavelle M. 1998a. Antarctic Peninsular cryosphere: Early Oligocene (c. 30 Ma) initiation and a revised glacial chronology. Journal of the Geological Society London 155: 433-437.

Dingle RV, Lavelle M. 1998b. Late Cretaceous-Cenozoic climatic variations of the northern Antarctic Peninsula: new geochemical evidence and review. Palaeogeography, Palaeoclimatology, Palaeoecology: 215-232.

Dingle RV, McArthur JM, Vroon P. 1997. Oligocene and Pliocene interglacial events in the Antarctic Peninsula dated using strontium isotope stratigraphy. Journal of the Geological Society London 154: 257-264.

Dingle RV, Marenssi SA, Lavelle M. 1998. High latitude Eocene climate deterioration: evidence from the northern Antarctic Peninsula. Journal of South American Earth Sciences 11(6): 571-579.

Dingle RV, Lavelle M. 2000. Antarctic Peninsula Late Cretaceous-Early Cenozoic palaeoenvironments and Gondwana palaeogeographies. Journal of African Earth Sciences 31(1): 91-105.

Ditchfield PW. Marshall JD, Pirrie D. 1994. High latitude palaeotemperature variation: new data from the Tithonian to Eocene of James Ross Island, Antarctica. Palaeogeography, Palaeoclimatology, Palaeoecology, 107: 79-101.

Doktor M, Gazdzicki A, Jerezmanska A, Porebski J, Zastawniak E. 1996. A plant and fish assemblage from the Eocene La Meseta Formation of Seymour Island (Antarctic Peninsula) and its environmental implications. Palaeontologia Polonica 55: 127 - 146

Dolph GE, Dilcher DL. 1979. Foliar physiognomy as an aid in determining palaeoclimate. Palaeontographica Abteilung B, 170: 151-172.

Dolph GE, Dilcher DL. 1980. Variation in leaf size with respect to climate in the tropics of the Western Hemisphere. Bulletin of the Torrey Botanical Club 107(2): 154 – 162.

Douglas JG.1973. The Mesozoic floras of Victoria Part 3. Geological Survey of Victoria Memoir 29: 1-185.

Drinnan AN, Chambers TC. 1986. Flora of the Lower Cretaceous Koonwarra Fossil bed (Korumburra Group), south Gippsland, Victoria. Association of Australasian Palaeotologists Memoir 3: 1-77.

Duan W, Cao L. 1998. Late Palaeogene palynoflora from Point Hennequin of the Admiralty Bay, King George Island, Antarctica with reference to its stratigraphical significance. Chinese Journal of Polar Science 9: 125-132.

Dupre DD. 1982. Geochemistry and 40Ar/39Ar geochronology of some igneous rocks from the South Shetland Islands, Antarctica. MSc thesis, Ohio State University, Columbus: 229 pages.

Dusén P. 1899. Uber die Tertiäre Flora der Magellansländer. Wissentschaftliche Ergebnisse nach den Magellansländern: 87-107 and 12 plates.

Dusén P. 1908. Uber die Tertiäre Flora der Seymour Insel. Wissentschaftliche Ergebnisse der Schwedischen Südpolar Expedition 1(4): 1-27.

Dutra T. 1989a. A tafoflora terciária dos arredores do pontal block, Baía do Almirantado, Ilha Rei George (Arquipelago das Shetland do Sul Península Antártica). Acta Geologica Leopoldensia 28: 45-90.

Dutra T. 1989b. Informações preliminares sobre a tafoflora do Monte Zamek (Bahía do Almirantado Ilha Shetland do Sul), Antártica. Serie Cìentifica Instituto Àntartico Chileno 39: 31-42.

Dutra T. 1997a. History and composition of the paleoflora at King George Island, northern Antarctic Peninsula. PhD thesis. Universidade Federal do Rio Grande do Sul, Porto Alegre, Brazil.

Dutra T. 1997b. Primitive leaves of *Nothofagus* (Nothofagaceae) in Antarctic Peninsula: An Upper Campanian record and a betulaceous more than fagaceous morphological character. In: Actas del IX Congresso Geológico Chileno, Antofagasta: 24-29.

Dutra T, Batten D. 2000. Upper Cretaceous floras of King George Island, West Antarctica and their palaeoenvironmental and phytogeographic implications. Cretaceous Research 21: 181-209.

Elliot DH. 1988. Tectonic setting and evolution of the James Ross Basin, northern Antarctic Peninsula. Geological Society of America Memoir 169: 1988.

Fairon-Demaret et al. 1999. Fossil leaf character states: multivariate analyses. In: Jones TP, Rowe NP (eds), Fossil plants and spores: modern techniques. Geological Society, London: 33-35.

Farquharson GW, Hamer RD, Ineson JR. 1984. Proximal volcaniclastic sedimentation in a Cretaceous back-arc basin, northern Antarctic Peninsula. In: Kokelaar, B.P. and Howell, M. F. (eds), Marginal basin geology. Geological Society of London, Special Publication 16: 219-229.

Fensterseifer HC, Soliani E, Hansen MAF, Troian FL. 1988. Geología e estratigrafía da associação de rochas do setor centro-norte da peninsula Fildes, Ilha Rei George, Shetland do Sul, Antártica. Serie Cìentifica Instituto Àntartico Chileno 38: 29-43.

Ferguson DK. 1985. The origin of leaf assemblages – New light on an old problem, Review of Palaeobotany and Palynology 46: 117 – 188.

Fiske RS. 1969. Recognition and signfiicanc of pumice in marine pyroclastic rocks. Geological Society of America Bulletin 80: 1-8.

Florin 1940. The Tertiary fossil conifers of South Chile and their phytogeographical significance. Kungl. Sv. Vetensk.-Akad. Handl., series 3 number 19: 1-107.

Flower, BP. 1999. Cenozoic deep-sea temperatures and polar glaciation: the oxygen isotope record. Terra Antartica Reports 3: 27-42.

Fisher RV. 1966. Rocks composed of volcanic fragments and their classification: Earth Science Reviews, 1: 287-298.

Fisher RV, Schmincke HU. 1984. Pyroclastic rocks. Springer-Verlag. Berlin Heidelberg. 472 pages.

Fisher RV, Smith GA. 1991. Volcanism, tectonics and sedimentation. In: Fisher RV, Smith GA (eds), Sedimentation in volcanic settings. Special Publications of the Society for Sedimentary Geology, Tulsa, USA: 1-5.

Francis JE. 1986. Growth rings in Cretaceous and Tertiary woods from Antarctica and their palaeoclimatic implications. Palaeontology 29: 665 - 684.

Francis JE. 1996. Antarctic Palaeobotany: Clues to climate change. Terra Antartica 3(2): 135 - 140.

Francis JE. 1991. Palaeoclimatic significance of Cretaceous-early Tertiary fossil forests of the Antarctic Peninsula. In: Thomson MRA, Crame JA, Thomson JW eds, Geological evolution of Antarctica. Cambridge University Press, New York: 623-627.

Francis JE. 1999. Evidence from fossil plants for Antarctic palaeoclimates over the past 100 million years. Terra Antartica Reports 3: 43-52.

Francis JE. 2000. Fossil wood from Eocene high latitude forests, McMurdo Sound, Antarctica. In: (eds), Paleobiology and paleoenvironments of Eocene rocks, McMurdo Sound, East Antarctica. Antarctic Research Series 76: 253-260.

Francis JE, Hill RS. 1996. Fossil plants from the Pliocene Sirius Group, Transantarctic Mountains: Evidence for climate from growth rings and fossil leaves. Palaios 11: 389-396.

Francis J.E. and Poole I. 2002. Cretaceous and Tertiary climates of Antarctica: evidence from fossil wood. Palaeogeography, Palaeoclimatology, Palaeoecology (in press).

Gastaldo RA, Carroll SM, Douglass DP. 1985. A model for the incorporation of plant detritus within clastic accumulating interdistributary bays. Geological Society of America Abstracts Programme 17: 588.

Gastaldo RA. 1989. Preliminary observations on phyto-taphonomic assemblages in a subtropical/temperate Holocene bayhead delta: Mobile Delta, Gulf Coastal Plain, Alabama. Review of Palaeobotany and Palynology 58: 61 - 83.

Givnish TJ. 1984. Leaf and canopy adaptations in tropical forests. In: Medina E, Mooney HA, Vasquez-Yanes C (eds). Physiological ecology of plants of the wet tropics: Tasks for Vegetation Science 12. The Hague, Junk: 51-84.

Gothan W. 1908. Die fossilen Hölzer von der Seymour- und Snow Hill- Insel. Wissentschaftliche Ergebnisse der Schwedischen Südpolar Expedition 1901-1903 3: 1-33.

Greenwood DR. 1992. Taphonomic constraints on foliar physiognomic interpretations of Late Cretaceous and Tertiary palaeoclimates. Review of Palaeobotany and Palynology 71: 149 – 190.

Greenwood DR, Vadala AJ, Douglas JG. 2000. Victorian Paleogene and Neogene macrofloras: a conspectus. Proceedings of the Royal Society of Victoria 112(1): 65-92.

Gregory KM. 1994. Paleoclimate and paleoelevation of the Florissant flora, Front Range, Colorado. Palaeoclimates 1: 23-57.

Gregory KM, McIntosh WC. 1996. Paleoclimate and paleoelevation of the Oligocene Pitch-Pinnacle flora, Sawatch Range, Colorado. Geological Society of America Bulletin 108: 545-561.

Hackett WR, Houghton BF. 1989. A facies model for a Quaternary andesitic composite volcano: Ruapehu, New Zealand. Bulletin of Volcanology 51: 51-68.

Hathway B, Lomas SA. The Upper Jurassic-Lower Cretaceous Byers Group, South Shetland Islands, Antarctica: Revised stratigraphy and regional correlations. Cretaceous Research 19: 43-67.

Hawkes DD. 1961. The Geology of the South Shetland Islands. I. The petrology of King George Island. Falkland Islands Dependencies Survey, Scientific Reports 26:

Hayes P. 1999. Cretaceous angiosperm floras of Antarctica. Ph.D. Thesis, University of Leeds, 1-310.

Hee YC, Soon-Keun C. 1991. Study on the gymnospermous fossil woods from the King George Island. Korean Journal of Polar Research Special Issue, 2(1): 179-185.

Heywood VH. 1998. Flowering plants of the world. Batsford Ltd, London: 335 pages.

Hickey LJ. 1973. Classification of the architecture of dicotyledonous leaves. American Journal of Botany, 60: 17-33.

Hickey LJ. 1977. Stratigraphy and paleobotany of the Golden Valley Formation (Early Tertiary) of Western North Dakota. Geological Society of America Memoir 150: 159.

Hickey LJ. 1979. A revised classification of the architecture of dicotyledonous leaves. In: Metcalfe CR, Chalk L (eds). Anatomy of the dicotyledons (second edition). Oxford, Clarendon: 25-39.

Hickey LJ, Wolfe JA. 1975. The bases of angiosperm phylogeny: vegetative morphology. Annals of the Missouri Botanical Garden 62(3): 538 - 589.

Hill RS. 1983. *Nothofagus* macrofossils from the Tertiary of Tasmania. Alcheringa 7: 169 – 183.

Hill RS. 1984. Tertiary *Nothofagus* macrofossils from Cethana, Tasmania. Alcheringa 8: 81 – 86.

Hill RS. 1989. Fossil leaf, Antarctic Cenozoic history from the CIROS-1 drillhole, McMurdo Sound. DSIR Bulletin New Zealand 245: 143-144.

Hill RS. 1991a. Leaves of *Eucryphia* (Eucryphiaceae) from Tertiary sediments in south-eastern Australia. Australian Systematic Botany 4: 481-97.

Hill RS. 1991b. Tertiary *Nothofagus* (Fagaceae) macrofossils from Tasmania and Antarctica and their bearing on the evolution of the genus. Botanical Journal of the Linnean Society, 105: 73-112.

Hill RS. 1996. The riddle of unique Southern hemisphere *Nothofagus* on south west Pacific islands: its challenge to biogeographers. In Keast A, Miller SE (eds), The origin and evolution of Pacific island biotas, New Guinea to Eastern Polynesia: patterns and processes: 247 - 260.

Hill RS, Bigwood AJ. 1987. Tertiary gymnosperms from Tasmania: Araucariaceae. Alcheringa 11: 325-335.

Hill RS, Carpenter RJ. 1989. Tertiary gymnosperms from Tasmania: Cupressaceae. Alcheringa 13: 89 – 102.

Hill RS, Brodribb TJ. 1999. Southern conifers in time and space. Turner Review No 2. Australian Journal of Botany 47: 639-696.

Hill RS, Read J. 1991. A revised infrageneric classification of *Nothofagus* (Fagaceae). Botanical Journal of the Linnean Society, 105: 37-72.

Hill RS, Scriven LJ. 1995. The angiosperm-dominated woody vegetation of Antarctica: a review. Review of Palaeobotany and Palynology 86: 175 - 198.

Hill RS, Truswell EM. 1993. *Nothofagus* fossils in the Sirius Group, Transantarctic Mountains: Leaves and pollen and their climatic implications. The Antarctic Paleoenvironment: A perspective on global change. Antarctic Research Series 60: 67 - 73.

Hill RS, Harwood DM, Webb PN. 1996. *Nothofagus beardmorensis* (Nothofagaceae), a new species based on leaves from the Pliocene Sirius Group, Transantarctic Mountains, Antarctica. Review of Palaeobotany and Palynology 94: 11 - 24.

Holdridge, L.R., 1967. Life Zone Ecology. Tropical Science Center, San Jose.

Hunt RJ, Poole I. Paleogene West Antarctic climate and vegetation history in light of new data from King George Island. In: Wing S (ed), Causes and consequences of globally warm climates in the Early Paleogene.

Jacobs BF. 1999. Estimation of rainfall variables from leaf characters in tropical Africa. Palaegeography, Palaeoclimatology, Palaeoecology 145: 231 – 250.

Jagmin N.I.B. 1987. Estudo anatômico dos troncos fósseis de Admiralty Bay, King George Island (Península Antárctica). Acta Biologica Leopoldensia, 9(1): 81-98.

Jardine DJ. 1950. Base G. Admiralty Bay Report (1949). Geology Report (F.I.D.Sc Bureau No. 83/50), 31 pages.

Jefferson TH. 1980. Angiosperm fossils in supposed Jurassic volcanogenic shales, Antarctica. Nature 285: 157-158.

Jefferson TH. 1981. Palaeobotanical contributions to the geology of Alexander Island, Antarctica. Ph.D. Thesis, University of Cambridge (Unpublished).

Jones DL. 1987. Encyclopaedia of ferns. An introduction to ferns, their structure, biology and economic importance, cultivation and propagation. British Museum (Natural History). London. 433 pages.

Jones WG, Hill KD, Allen JM. 1995. *Wollemia nobilis*, a new living Australian genus and species in the Araucariaceae. Telopea 6: 173-176.

Jordan GJ. 1997. Contrasts between the climatic ranges of fossil and extant taxa: Causes and consequences for palaeoclimatic estimates. Australian Journal of Botany 45: 465 – 474.

Jordan GJ. 1997. Uncertainty in palaeoclimatic reconstructions based on leaf physiognomy. Australian Journal of Botany 45: 527 – 547.

Kennedy L. 1998. Cretaceous and Tertiary megafloras from New Zealand and their climate signals. PhD thesis, Department of Earth Sciences, The Open University: 262 pages.

Kennett JP. 1977. Cenozoic evolution of Antarctic glaciation, the Circum-Antarctic Ocean and their impact on global paleoceanography. Journal of Geophysical Research 82(27): 3843 - 3860.

Klucking EP. 1986. Leaf venation patterns. Volume 1: Annonaceae. J. Cramer, Berlin. 538 pages.

Klucking EP. 1987. Leaf venation patterns. Volume 2: Lauraceae. J. Cramer, Berlin. 514 pages.

Klucking EP. 1988. Leaf venation patterns. Volume 3: Myrtaceae. J. Cramer, Berlin. 584 pages.

Klucking EP. 1989. Leaf venation patterns. Volume 4: Melastomataceae. J. Cramer, Berlin. 522 pages.

Klucking EP. 1991. Leaf venation patterns. Volume 5: Combretaceae. J. Cramer, Berlin. 436 pages.

Klucking EP. 1992. Leaf venation patterns. Volume 6: Flacourtiaceae. J. Cramer, Berlin. 584 pages.

Klucking EP. 1995. Leaf venation patterns. Volume 7: The classification of leaf venation patterns. J. Cramer, Berlin. 337 pages.

Leaf Architecture Working Group. 1999. Manual of leaf architecture – morphological description and categorization of dicotyledonous and netveined monocotyledonous angiosperms.

Lawver LA, Gahagan LM, Millard FC. 1992. The development of paleoseaways around Antarctica. In: Kennet JP, Warnke DA, (eds), The Antarctic Paleoenvironment: A perspective on global change, Antarctic Research Series 56: 7-30.

Lawver LA, Keller RA, Fisk MR, Strelin JA. 1995. Bransfield Strait, Antarctic Peninsula active extension behind a dead arc. In: Taylor B (ed), Backarc bains: Tectonics and Magmatism: 316-342.

Lawver LA, Gahagan LM. 1998. Opening of Drake Passage and its impact on Cenozoic ocean circulation. Oxford Monographs on Geology and Geophysics, 39: 212-223.

Leaf Architecture Working Group. 1999. Manual of leaf architecture - Morphological description and categorisation of dicotyledons and net-veined monocotyledonous angiosperms. Smithsonian Institution, Washington D.C., USA. 65 pages.

Leat PT, Scarrow JH, Millar IL. 1995. On the Antarctic Peninsula batholith. Geological Magazine 132: 399-412.

Li HM. 1992. Early Tertiary palaeoclimate of King George Island, Antarctica - Evidence from the Fossil Hill Flora. In: Yoshida Y et al (eds), Recent progress in Antarctic Earth Science: 371 - 375.

Li HM. 1994. Early Tertiary Fossil Hill flora from Fildes Peninsula of King George Island, Antarctica. In: Shen Y, ed. Stratigraphy and palaeontology of Fildes Peninsula, King George Island. State Antarctic Committee Monograph 3: 133-171.

Li H, Song D. 1988. Fossil remains of some angiosperms from King George Island, Antarctica. Acta Palaeontologica Sinica 27(4): 399-403.

Li HM, Shen Y. 1989. A primary study of Fossil Hill flora from Fildes Peninsula of King George Island, Antarctica. Acta Palaeontologica Sinica 29(2): 147-153.

Li Z, Liu X. 1992. The geological and geochemical evolution of Cenozoic volcanism in central and southern Fildes Peninsula, King George Island, South Shetland Islands. In: Yoshida Y, ed. Recent Progress in Antarctic Earth Science. Tokyo: Terra Scientific Publishing Company (Terrapus): 487-491.

Li J, Zhen S. 1994. New materials of bird ichnites from Fildes Peninsula, King George Island of Antarctica and their biogeographic significance. In: Shen Y, ed. Stratigraphy and palaeontology of Fildes Peninsula, King George Island. State Antarctic Committee Monograph 3: 223-249..

Longton RE. 1985. Terrestrial habitats - vegetation. In: Bonner WN, Walton DWH (eds), Antarctica: 73 - 105.

Lucas RC, Lacey WS. 1981. A permineralised wood flora of probable early Tertiary age from King George Island, South Shetland Islands. British Antarctic Survey Bulletin 53: 147 - 151.

Lyra CS. 1986. Palinologia de sedimentos Terciários da Península Fildes, Ilha Rei George (Ilha Shetland do Sul Antártica) e Algumas Conciderações Paleoambientais. Anais da Academia Brasileria de Ciências (supplemento) 58: 137-147.

Mabberley DJ. 1997. The Plant Book. A portable dictionary of the vascular plants. Cambridge University Press: 858 pages.

Maldonaldo A, Larter RD, Aldaya F. Forearc tectonic evolution of the south Shetland Margin, Antarctic Peninsula. Tectonics 13: 1345-1370.

Manchester SR, Crane PR. 1987. A new genus of Betulaceae from the Oligocene of western North America. Botanical Gazette 148(2): 263 – 273.

Manos PS. 1997. Systematics of *Nothofagus* (Nothofagaceae) based on RDNA spacer sequences (ITS): Taxonomic congruence with morphology and plastid sequences. American Journal of Botany 84(8): 1137 – 1155.

Markgraf V, Romero E, Villagrán C. 1996. History and palaeoecology of South American *Nothofagus* forests. In: Veblen TT, Hill RS, Read J. eds. The Ecology and Biogeography of *Nothofagus* forests. New Haven and London: Yale University Press, 354-386.

Mathisen ME, Vondra CF. 1983. The fluvial and pyroclastic deposits of the Cagayan Basin, Northern Luzon, Philippines – an example of non-marine volcaniclastic sedimentation in an interarc basin. Sedimentology 30: 369-392.

Mathisen ME, McPherson 1991. Volcaniclastic deposits: Implications for hydrocarbon exploration. In: Fisher RV, Smith GA (eds), Sedimentation in volcanic settings. Special Publications of the Society for Sedimentary Geology, Tulsa, USA: 27-36.

McCarron JJ. Larter RD. 1998. Late Cretaceous to early Tertiary subduction history of the Antarctic Peninsula. Journal of the Geological Society of London 155: 255-268.

McDougall I, Harrison TM. 1999. Geochronology and thermochronology by the 40Ar/39Ar method. Oxford University Press, New York: 212 pages.

McLoughlin S, Drinnan AN, Rozefelds AC. 1995. A Cenomanian flora from the Winton Formation, Eromanga Basin, Queensland, Australia. Memoirs of the Queensland Museum 38(1): 273-313.

Mildenhall DC. Terrestrial palynology, Antarctic Cenozoic history from the CIROS-1 drillhole, McMurdo Sound, Antarctica. DSIR Publications, DSIR bulletin 245: 119-127.

Miller KG, Fairbanks RG, Mountain GS. 1987. Tertiary oxygen isotope synthesis, sea-level history and continental margin erosion. Paleoceanography 2. 1-19.

Nakayama K, Yoshikawa S. 1997. Depositional processes of primary to reworked volcaniclastics on an alluvial plain; an example from the Lower Pliocene Ohta tephra bed of the Tokai Group, central Japan. Sedimentary Geology, 107: 211-229.

Ohga N. 1991. The plant ecology of the cloud forests of the eastern and western slopes of the Andes I. microclimatic conditions of the forests of Bolivia and Chile. In: Nishida (ed), Contributions to the botany of the Andes II. Academia Scientific Book Inc, Tokyo: 12-22.

Orlando HA. 1963. La flora fosil en las imediaciones de la Peninsula Ardley, Isla 25 de Mayo, Islas Shetlans del Sur. Instituto Antartico Argentino. 79: 3-17.

Orlando HA. 1964. The fossil flora of the surroundings of Ardley Peninsula (Ardley Island), 25 de Mayo Island (King George Island) South Shetland Islands. In: Adie RJ, ed. Antarctic Geology. Amsterdam: North Holland Publishing Company, 629-636.

Palma-Heldt S. 1987. Estudio palinologico en el Terciario de islas Rey Jorge y Brabante, territorio insular Antartico. Series Cientifica Instituto Antartico Chileno 36: 59-71.

Pankhurst RJ, Smellie JL. 1983. K-Ar geochronology of the South Shetland Islands, Lesser Antarctica: apparent lateral migration of Jurassic to Quaternary island arc volcanism. Earth and Planetary Science Letters 66. 214-222.

Pettijohn FJ. 1975. Sedimentary Rocks. Harper and Row, New York. 628 pages.

Pirrie D, Marshall JD. 1990. High-paleolatitude Late Cretaceous paleotemperatures: New data from James Ross Island, Antarctica. Geology 18: 31-34.

Pirrie D, Duane AM, Riding JB. 1992. Jurassic-Tertiary stratigraphy and palynology of the James Ross Basin: review and introduction. Antarctic Science 4(3): 259-266.

Pirrie D, Crame JA, Riding JB, Butcher AR, Taylor PD. 1997. Miocene glaciomarine sedimentation in the northern Antarctic Peninsula region: The stratigraphy and sedimentology of the Hobbs Glacier Formation, James Ross Island. Geological Magazine 136(6): 745 - 762.

Pirrie D, Marshall JD, Crame JA. 1998. Marine high Mg calcite cements in Teredolites bored fossil wood: evidence for cool palaeoclimates in the Eocene La Meseta Formation, Seymour Island, Antarctica. Palaios 13(3): 276-286.

Pole M. 1992. Cretaceous macrofloras of Eastern Otago, New Zealand: Angiosperms. Australian Journal of Botany 40: 169-206.

Pole M. 1993. Early Miocene flora of the Manuherikia Group, Journal of the Royal Society of New Zealand 23(4). 426 pages.

Pole M, Hill, RS, Harwood D. 2000. Eocene plant macrofossils from erratics, McMurdo Sound, Antarctica. In: (eds), Paleobiology and paleoenvironments of Eocene rocks, McMurdo Sound, East Antarctica. Antarctic Research Series 76: 253-260.

Poole I, Cantrill DJ. 2001. Fossil woods from Williams Point Beds, Livingston Island, Antarctica: a Late Cretaceous southern high latitude flora. Palaeontology. in press.

Poole, I., and Francis, J. E. (1999). The first record of fossil atherospermataceous wood from the Upper Cretaceous of Antarctica. Review of Palaeobotany and Palynology 107, 97-107.

Poole, I., and Francis, J. E. (2000). The first record of Winteraceae wood from the Cretaceous of Antarctica. Annals of Botany 85, 307-315.

Poole I. and Gottwald H. (2001) Monimiaceae sensu lato, an element of Gondwanan polar forests: Evidence from the Late Cretaceous-early Tertiary wood flora of Antarctica. Australian Systematic Botany 14, 207-230.

Poole, I., Cantrill, D. J., Hayes, P., and Francis, J. E. (2000a). The fossil record of Cunoniaceae: new evidence from Late Cretaceous fossil wood of Antarctica. Review of Palaeobotany and Palynology, 111 (1-2): 127-144.

Poole I., Gottwald H. and Francis J.E. 2000b Illiciaceae, an element of Gondwanan polar forests? Late Cretaceous and Early Tertiary woods of Antarctica. Annals of Botany 86, 421-432.

Poole, I., Richter, H. G., and Francis, J. E. (2000c). Gondwanan origins for *Sassafras* (Lauraceae): evidence from Late Cretaceous fossil wood of Antarctica. International Association of Wood Anatomists Journal in press.

Poole I., Hunt R.J. and Cantrill D.J. (2001) A fossil wood flora from King George Island: ecological implications for an Antarctic Eocene vegetation. Annals of Botany 88, 33-54.

Raine JI. 1998. Terrestrial palynomorphs from Cape Roberts Project drillhole CRP-1, Ross Sea, Antarctica. Terra Antartica 5(3): 539-548.

Read J, Brown MJ. 1996. Ecology of Australian *Nothofagus* forests. In Veblen TT, Hill RS, Read J. eds. The Ecology and Biogeography of *Nothofagus* forests. New Haven and London: Yale University Press, 131-181.

Richards PW. 1952. The tropical rain forest. Cambridge, Cambridge University Press, 450 pages.

Riggs NR, Busby-Spera. 1990. Evolution of a multi-vent volcanic complex within a subsiding arc graben depression: Mount Wrightson Formation, Arizona. Geological Society of America Bulletin 102: 1114-1135.

Roddick JC. 1978. The Application of Isochron diagrams in 40Ar-39Ar Dating: A discussion. Earth and Planetary Science Letters 41: 233-244.

Roddick JC. 1980. The Evolution of excess Argon in Alpine biotites – A ^{40}Ar-^{39}Ar analysis. Earth and Planetary Science Letters 48: 185-208.

Roddick JC. 1983. High precision intercalibration of ^{40}Ar-^{39}Ar standards. GCA 47: 887-898.

Rohn R, Rösler O, Czajkowski S. 1987. *Fildesia Pulchra* gen. et sp. Nov. – Folha fóssil do terciário inferior da Península Fildes, Ilha Rei George, Antártica. Boletim IG-USP. Série Científica 18: 13-16.

Romero EJ. 1980a. Fossil evidence regarding the evolution of *Nothofagus* Blume. Annals of the Missouri Botanical Gardens 73: 276-283.

Romero EJ. 1980b. Arquitectura foliar de las especies SudAmericana de *Nothofagus* Bl. Boletin de la Sociedad Argentina de Botanica, XIX, 1 – 2: 289 – 308.

Romero EJ. 1986. Paleogene phytogeography and climatology of South America. Annals of the Missouri Botanical Garden 73: 449-491.

Romero EJ, Dibbern MC. 1985. A review of the species described as *Fagus* and *Nothofagus* by Dusen. Palaeontographica Abt. B. 123-137.

Runkiaer C. 1934. The life forms of plants and statistical plant geography. Clarendon Press, Oxford. 632 pages.

Scott AC, Titchener FR. 1999. Techniques in the study of plant-arthropod interactions. In: Jones TP and Rowe NP (eds) Fossil plants and spores: modern techniques. Geological Society, London: 310-315.

Scriven LJ, Hill RS. 1996. Relationships among Tasmanian Tertiary *Nothofagus* (Nothofagaceae) populations. Botanical Journal of the Linnean Society 121: 345-364.

Scriven LJ, McLoughlin S, Hill RS. 1995. *Nothofagus plicata* (Nothofagaceae), a new deciduous Eocene macrofossil species, from southern continental Australia. Review of Palaeobotany and Palynology 86: 199 – 209.

Shen Y. 1994. Subdivision and correlation of Cretaceous to Paleogene volcano-sedimentary sequence from Fildes Peninsula, King George Island, Antarctica. In: Shen Y, ed. Stratigraphy and palaeontology of Fildes Peninsula, King George Island. State Antarctic Committee Monograph 3: 1-36.

Salmon JT. 1998. The Reed field guide to New Zealand native trees. Reed books. Auckland. p. 228

Shen Y. 1999. Subdivision and correlation of the Eocene Fossil Hill Formation from King George Island, West Antarctica. Korean Journal of Polar Research 10: 91-95.

Smellie JL, Davies RES, Thomson MRA. 1980. Geology of a Mesozoic intra-arc sequence on Byers Peninsula, Livingston Island, South Shetland Islands. British Antarctic Survey Bulletin 50: 55-76.

Smellie JL, Hunt RJ. Geology of the Vauréal Peak area of King George Island, South Shetland Islands, including the discovery of new ?Middle Eocene flora: Implications for Cenozoic palaeoenvironments and palaeoclimates. Work in progress.

Smellie JL, Pankhurst RJ, Thomson MRA, Davies RES. 1984. The Geology of the South Shetland Islands: VI. Stratigraphy, geochemistry and evolution. British Antarctic Survey, Scientific Report 87: 1-85.

Smith GA. 1986. Coarse-grained nonmarine volcaniclastic sediment: Terminology and depositional process: Geological Society of America Bulletin 97: 1-10.

Smith GA. 1987. The influence of explosive volcanism on fluvial sedimentation: The Deschutes Formation (Neogene) in Central Oregon. Journal of Sedimentary Petrology, 57: 613-629.

Smith GA. 1988. Sedimentology of proximal to distal volcaniclastics dispersed across an active foldbelt: Ellensburg Formation (late Miocene), central Washington. Sedimentology 35: 953-977.

Smith GA. 1991. Sedimentology of proximal to distal volcaniclastics dispersed across an active foldbelt: Ellensburg Formation (late Miocene), central Washington. Sedimentology, 35. 935-977.

Smith GA, Lowe 1991. Lahars: Volcano-hydrologic events and deposition in the debris flow – hyperconcentrated flow continuum. In: Fisher RV, Smith GA (eds), Sedimentation in volcanic settings. Special Publications of the Society for Sedimentary Geology, Tulsa, USA: 59-70.

Smith RIL. 1991. Exotic sporomorpha as indicators of potential immigrant colonists in Antarctica. Grana 30: 313-324.

Soliani E, Bonhomme MG. 1994. New evidence for Cenozoic resetting of K-ar ages in volcanic rocks of the northern portion of the Admiralty bay, King George Island, Antarctica. Journal of South American Earth Sciences 7: 85-94.

Spicer RA. 1989. The formation and interpretation of plant fossil assemblages. Advances in Botanical Research 16: 96-191.

Spicer RA. 1990. Climate from plants. In: Briggs, D.E.G. Crowther (eds), Palaeobiology: A synthesis. Blackwell Scientific Publishing. Oxford: 401 – 403.

Spicer RA. 1991. Plant taphonomic processes. In Allison, PA and Briggs DEG (eds), Taphonomy: Releasing the data locked in the fossil record. Volume 9 of Topics in Geobiology. Plenum Press, New York.

Spicer RA, Parrish JT. 1990. Late Cretaceous-early Tertiary palaeoclimates of northern high latitudes: a quantitative view. Journal of the Geological Society, London 147: 329 - 341.

Spicer RA., Wolfe JA. (1987). Taphonomy of Holocene deposits in Trinity (Clair Engle) Lake, Northern California, Palaeobiology 13: 227 – 245.

Spicer RA, Wolfe JA. 1999. Fossil leaf character states: multivariate analyses. In: Jones TP, Rowe NP (eds). Fossil plants and spores: modern techniques. Geological Society, London: 233-239.

Steiger RH, Jäger E. 1977. Subcommission on geochronology: Convention on the use of decay constants in geo- and cosmochronlogy. Earth Planetary Science Letters 36: 359-362.

Stevens GR. 1989. The nature and timing of biotic links between New Zealand and Antarctica in Mesozoic and early Cenozoic times. In: Crame JA (ed), Origins and evolution of the Antarctic biota, Geological Society Special Publication 47: 141 -166.

Stonehouse B. 1989. Polar Ecology. Blackie, Glasgow: 62 - 105.

Storey BC, Garret SW. 1985. Crustal growth of the Antarctic Peninsula by accretion, magmatism and extension. Geological Magazine 122: 5-14.

Stuchlik L. 1981. Tertiary pollen spectra from the Ezcurra Inlet Group of Admiralty Bay, King George Island (South Shetland Islands, Antarctica). Studia Geologica Polonica, 72: 109-132.

Swenson U, Backlund A, McLoughlin S, Hill RS. 2001. *Nothofagus* biogeography revisited with special emphasis on the enigmatic distribution of subgenus *Brassospora* in New Caledonia.

Talbot MR, Allen PA. 1996. Lakes. In: Reading HG (ed), Sedimentary environments. Processes, facies and stratigraphy. Blackwell Science, Oxford: 83-124.

Tanai T. 1986. Phytogeographic and phylogenetic significance of the Genus Nothofagus Bl. (Fagaceae) in the Southern Hemisphere. Journal of the Faculty of Science, Hokkaido University series IV 21(4): 505-582.

Ter Braak CJF. 1988. CANOCO – a FORTRAN program for canonical community ordination. New York, Microcomputer Power, Ithaca.

Terra Antartica Initial Report on CRP-2/2A. 1999. Chapter 5 – Palaeontology. Terra Antartica 6(1/2): 107-144.

Thomson MRA, Burn RW. 1977. Angiosperm fossils from latitude 70°S. Nature 269: 139-141.

Titchener FR. 2000. Plant arthropod interactions in the Late Tertiary . PhD thesis, University of London. Unpublished.

Tokarski AK. 1989. The Late Cretaceous-Cenozoic structural history of King George Island, South Shetland Islands, and its plate tectonic setting. In: Yoshida Y et al (eds), Recent progress in Antarctic Earth Science:

Tokarski AK, Danowski W, Zastawniak E. 1987. On the age of the fossil flora from Barton Peninsula, King George Island, West Antarctica. Polish Polar Research 8(3): 293-302.

Torres T. 1984. *Nothofagoxylon antarcticus* n. sp., madera fósils del Terciario de la isla Rey Jorge, islas Shetland del Sur, Antártica. Serie Cientifica Instituto Àntartico Chileno 31: 39-52.

Torres T. 1985. Plantas fosiles en la Antarctica. Boletin Antartico Chileno 5: 17-31.

Torres T. 1990. Etude Palaeobotanique du Tertiare des Iles Roi Georges et Seymour, Antarctique. PhD Thesis Université Lyon, 1-210.

Torres T, Lemoigne Y. 1988. Maderas fósiles terciarias de la Formación Caleta Arctowski, Isla Rey Jorge, Antártica. Serie Cientifica Instituto Àntartico Chileno 37: 69-107.

Torres T, Meon H. 1990. Estudio palinologico de Cerro Fosil, peninsula Fildes, isla Rey Jorge, Antartica. Serie Cientifica Instituto Àntartico Chileno 40: 21-39.

Torres T, Meon H. 1993. Lophosoria del Terciario de isla Rey Jorge y Chile Central: origen y dispersión en el hemisferio Sur. Serie Cientifica Instituto Àntartico Chileno 43:17-30.

Torres T, Román A, Deza A, Rivera C. 1984. Anatomiá, mineralogía y termoluminiscencia de madera fósil del Terciario de la isla Rey Jorge, Islas Shetland del Sur. III Congreso Latinoamericano de Paleontologia Brasil 2: 566-574.

Troncoso A. 1986. Nuevas organo-especies en la tafoflora Terciaria Inferior de peninsula Fildes, isla Rey Jorge, Antartica. Serie Cientifica Instituto Àntartico Chileno 34: 23-46.

Troncoso A, Romero EJ. 1998. Evolución de las comunidades florísticas en el extremo sur de Sudamérica durante el Cenofítico. In: Fortunato R, y Bacigalupo N (eds), Proceedings of the VI Congreso Latinoamericano de Botánica. Monographs in systematic botany from the Missouri Botanical Garden 68: 149-172.

Truswell EM. 1990. Cretaceous and Tertiary vegetation of Antarctica: A palynological perspective. In: Taylor TN, Taylor EL (eds), Antarctic Paleobiology: its role in the reconstruction of Gondwana. Springer and Verlag: 71 - 88.

Truswell EM. 1991. Antarctica: a history of terrestrial vegetation. In: Tinjey RJ (ed), The geology of Antarctica, Oxford University Press, New York: 499 - 528.

Upchurch GR, Wolfe JA. 1987. Mid-Cretaceous to early Tertiary vegetation and climate: evidence from fossil leaves and woods. In: Friis EM, Chaloner WG, Crane PR (eds), The origin of angiosperms and their biological consequences. Cambridge University Press: 75-105.

Upchurch GR, Askin RA. 1989. Latest Cretaceous and earliest Tertiary dispersed plant cuticles from Seymour Island. Antarctic Journal of the United States 24(5): 7-10.

Veblen TT, Ashton DH 1978. Catastrophic influences on the vegetation of the Valdivian Andes, Chile. Vegetatio 36: 149-167.

Veblen TT, Lorenz DC. 1987. Post-fire stand development of *Austrocedrus-Nothofagus* forests in northern Patagonia. Vegetatio 71: 113-126.

Veblen TT, Ashton DH, Rubulis S, Lorenz DC, Cortes M. 1989. *Nothofagus* stand development on in-transit moraines, Casa Pangue Glacier, Chile. Arctic and Alpine Research 21: 144-155.

Veblen TT, Ashton DH, Schlegel FM, Veblen AT. 1977. Plant succession in a timberline depressed by vulcanism in south-central Chile. Journal of Biogeography 4: 275-294.

Veblen TT, Burns BR, Kitzberger T, Lara A, Villalba R. 1995. The ecology of the conifers of southern South America. In Enright N, Hill RS (eds), Ecology of the Southern Conifers. Melbourne: Melbourne University Press, 120-155.

Veblen TT, Donoso C, Kitzberger T, Rebertus AJ. 1996. Ecology of Southern Chilean and Argentinean *Nothofagus* forests. In: Veblen TT, Hill RS, Read J. eds. The Ecology and Biogeography of *Nothofagus* forests. New Haven and London: Yale University Press, 293-353.

Veblen TT, Donoso CZ, Schlegel FM, Escobar BR. 1981. Forest dynamics in south-central Chile. 1981. Journal of Biogeography 8: 211-247.

Veblen TT, Hill RS, Read J. 1996. The ecology and biogeography of *Nothofagus* forests. Yale University Press, New Haven and London. 403 pages.

Veblen TT, Schlegel FM, Oltremari JV. 1983. Temperate broad-leaved evergreen forests of South America. In: Ovington JD, ed. Ecosystems of the World 10. Temperate broad-leaved evergreen forests. Amsterdam: Elsevier, 5-31.

Vessel RK, Davies DK. 1981. Non-marine sedimentation in an active fore arc basin. Society of Economic Palaeontologists and Mineralogists. Special Publication No 31: 31-45.

Vizcaino SF, Bond M, Reguero MA, Pascual R. 1997. The youngest record of fossil land mammals from Antarctica; its significance on the evolution of the terrestrial environment of the Antarctic Peninsula during the Late Eocene. Journal of Palaeontology 71(2): 348-350.

Webb LJ. 1959. A physiognomic classification of Australian rainforests. Journal of Ecology 47: 551 – 570.

Whang SS, Hill RS. 1999. Late Palaeocene Cupressaceae macrofossils at Lake Bungarby, New South Wales. Australian Systematic Botany 12: 241-254.

Whittaker, R.H., 1975. Communities and ecosystems. MacMillan Publishers, New York, pp. 385.

Wiemann MC, Manchester SR, Dilcher DL, Hinojosa LF, Wheeler EA. 1998. Estimation of temperature and precipitation from morphological characters of dicotyledonous leaves. American Journal of Botany, 85: 1796-1802.

Wilde MH, Eames AJ. 1952. Th ovule and "seed" of *Araucaria bidwillii* with discussion of the taxonomy of the genus. Annals of Botany (London) 16: 27-47.

Wilf P. 1997. When are leaves good thermometers?: A new case for leaf margin analysis. Palaeobiology, 23: 373-390.

Wilf P. 2000. Late Paleocene – early Eocene climate changes in southwestern Wyoming: Paleobotanical analysis. GSA Bulletin 112(2): 292 – 307.

Wilf P, Beard KC, Davies-Vollum KS, Norejko JW. 1998a. Portrait of a Late Paleocene (Early Clarkforkian) terrestrial ecosystem: Big Multi Quarry and associated strata, Washakie Basin, Southwestern Wyoming. Palaios 13: 514 – 532.

Wilf P. Wing SL. Greenwood DR. Greenwood CL. 1998b. Using fossil leaves as paleoprecipitation indicators: an Eocene example. Geology 26: 203 – 206.

Willan RCR, Kelley SP. 1999. Mafic dike swarms in the South Shetland Islands volcanic arc: Unravelling multiepisodic magmatism related to subduction and continental rifting. Journal of Geophysical Research 104: 23051-23068.

Willan and Armstrong in press

Wilson, G.S., Roberts, A.P., Verosub, K.L., Florindo, F., Sagnotti, L., 1998, Magnetobiostratigraphic chronology of the Eocene-Oligocene transition in the CIROS-1 core, Victoria Land margin, Antarctica: Implications for Antarctic glacial history. Geological Society of America, v. 110, no. 1, p. 35-47.

Wing SL, Greenwood DR. 1993. Fossils and fossil climate: the case for equable continental interiors in the Eocene. Philosophical transactions of the Royal Society of London 341: 243 – 252.

Wing SL, Huiming B, Koch PL. 2000. An early Eocene cool period? Evidence for continental cooling during the warmest part of the Cenozoic. In: Huber BT, MacLeod KG, and Wing SL (eds), Warm climates in Earth history: 197 – 237.

Wise SW, Breza JR, Harwood DM, Wei W. 1991. Paleogene glacial history of Antarctica. In: McKenzie JA, Müller, Weisert H (eds), Controversies in modern geology. Academic Press Ltd, London: 133-171.

Wolfe JA. 1971. Tertiary climatic fluctuations and methods of analysis of Tertiary floras. Palaeogeography, Palaeoclimatology, Palaeoecology, 9: 27-57.

Wolfe JA. 1979. Temperature parameters of humid to mesic forests of eastern Asia and relation to forests of other regions in the Northern Hemisphere and Australasia. U.S. Geological Survey Professional Paper 1106: 37 pages.

Wolfe JA. 1993. A method of obtaining climatic parameters from leaf assemblages. U.S. Geological Survey Bulletin 2040: 71 pages.

Wolfe JA. 1995. Palaeoclimatic estimates from Tertiary leaf assemblages. Annual Review of Earth and Planetary Sciences, 23: 119-142.

Wolfe JA, Upchurch GR. 1987. North American non-marine climates and vegetation during the Late Cretaceous. Palaeogeography, Palaeoclimatology, Palaeoecology: 33-77.

Xue YS, Shen YB, Zhou EJ. 1996. Petrological characteristics of the sedimentary volcanic rocks of the Fossil Hill Formation (Eocene) in King George Island, West Antarctica. Antarctic Research 7(2): 99-117.

Yang SP, Shen YB. 1999. Early Tertiary trace fossils from King George Island, West Antarctica. Acta Palaeontologica Sinica 38(2): 203-217.

Zachos J Lohmann KC, Walker JCG, Wise SW. 1993. Abrupt climate change and transient climates during the Paleogene: a marine perspective. Journal of Geology 101: 191-213.

Zachos J, Pagani M, Sloan L, Thomas E, Billups K. 2001. Trends, rhythms and aberrations in global climate 65 Ma to present. Science 292: 686-693.

Zamaloa MC, Romero EJ, Stinco L. 1987. Polen y esporas de la Formacion La Meseta (Eoceno Superior-Oligoceno) de la isla Marambio (Seymour), Antartida, VII Simp. Argentino Paleobotanico. Actas Paleobot. Palin. Buenos Aires: 199-203.

Zastawniak E. 1981. Tertiary leaf flora from the Point Hennequin Group of King George Island (South Shetland Islands, Antarctica) Preliminary Report. Geological Results of the Polish Antarctic Expeditions 72: 97-112.

Zastawniak E. 1990. Late Cretaceous leaf flora of King George Island, West Antarctica. Proceedings of the Symposium: Paleofloristic and paleoclimatic changes in the Cretaceous and Tertiary. Geological Survey Publisher, Prague: 81-85.

Zastawniak E. 1994. Upper Cretaceous leaf flora from the Blaszyk moraine (Zamek Formation), King George Island, South Shetland Islands, West Antarctica. Acta Palaeobotanica 34(2): 119-163.

Zastawniak E, Wrona R, Gazdzicki A, Birkenmajer K. 1985. Plant remains from the top part of the Point Hennequin Group (Upper Oligocene), King George Island (South Shetlands, Antarctica). Geological Results of the Polish Antarctic Expeditions: 143 - 170.

Zhang S, Wang Q. 1994. Palaeocene petrified wood on the west side of Collins glacier in the King George Island, Antarctica. In: Shen Y, ed. Stratigraphy and Palaeontology of Fildes Peninsula King George Island, Antarctica, State Antarctic Committee Monograph 3. China: Science Press, 231-238.

Zhou Z, Li, H. 1994a. Early Tertiary ferns from Fildes Peninsula, King George Island, Antarctica. In: Shen Y, ed. Stratigraphy and Palaeontology of Fildes Peninsula King George Island, Antarctica, State Antarctic Committee Monograph 3. China: Science Press, 181-207.

Zhou Z, Li H. 1994b. Early Tertiary Gymnosperms from Fildes Peninsula, King George Island, Antarctica. In: Shen Y, ed. Stratigraphy and Palaeontology of Fildes Peninsula King George Island, Antarctica, State Antarctic Committee Monograph 3. China: Science Press, 208-230.

Zhou Z, Li H. 1994c. Some Late Cretaceous plants from King George Island, Antarctica. In: Shen Y, ed. Stratigraphy and Palaeontology of Fildes Peninsula King George Island, Antarctica, State Antarctic Committee Monograph 3. China: Science Press, 91-105.

Zinsmeister WJ. 1982. Review of the Upper Cretaceous-Lower Tertiary sequence on Seymour Island, Antarctica. Journal of the Geological Society London 139: 779-785.

Zinsmeister WJ. 1988. Early geological exploration of Seymour Island, Antarctica. Geological Society of America Memoir 169: 1-17.

Appendix I Locality data

Locality	BAS Station Number	Material	BAS Station Number	Material
Point Hennequin	P.3001	Abundant well preserved leaf remains	P.3009	Fragmentary carbonised material
	P.3002	Rare leaf fragments	P.3010	Leaves (*Nothofagus* sp.)
	P.3003	Rare coalified wood fragments	P.3011	Leaf fragments
	P.3004	Leaves	P.3012	Leaf fragments
	P.3005	Leaves	P.3013	Abundant well preserved leaves
	P.3006	Leaf fragments	P.3014	Leaf fragments (*Nothofagus* sp.)
	P.3007	Leaves (dominantly conifers)	P.3015	Single well preserved angiosperm leaf and abundant trackways
	P.3008	Merged with P.3001	P.3016	Poorly preserved angiosperms/ferns
Fildes Peninsula	P.3017	Fragments of silicified wood	P.3027	Rare fragments of fossil wood
	P.3018	Fragments of silicified wood	P.3028	Rare excellently preserved angiosperm leaf and cone scales
	P.3019	Fragments of silicified wood	P.3029	Fragmentary angiosperm leaves and rare seeds
	P.3020	Poorly preserved fossil wood and stems	P.3030	Occasional leaf material
	P.3021	Poorly preserved fossil wood	P.3031	Abundant leaf impressions, poorly preserved
	P.3022	Fragments of silicified wood	P.3032	Abundant carbonised leaves
	P.3023	Abundant large fragments of well preserved wood	P.3033	Rare silicified wood
	P.3024	Fragments of poorly preserved silicified wood	P.3034	Scattered leaf impressions and bird footprints
	P.3025	In-situ fragmentary leaf fossils and partially silicified wood	P.3035	Rare leaf material
	P.3026	Fragmentary wood and leaf material	P.3036	Rare leaf material

Table I.1. List of station numbers and types of fossil material collected for this study.

Appendix II Geochronological tables and derivation of K-Ar and 40Ar/39Ar ages

II.1 Derivation and interpretation of K-Ar data

The K-Ar method of dating is based on the decay of radioactive 40K. 40K has a dual decay to 40Ca and 40Ar and the branch 40K-40Ar is the basis for the K-Ar technique. In the simple case of an extruded lava, 40Ar is trapped within crystals subsequent to cooling and the accumulated radiogenic argon can then be measured by mass spectrometry. Potassium concentrations are measured using flame photometry. The K-Ar age can be calculated using the measured quantity of 40Ar and the known decay rate of 40K. This is expressed in the potassium-argon age equation (Dalrymple and Lanphere, 1969).

$$t = \frac{1}{\lambda_\varepsilon + \lambda_\beta} \log_e\left[\frac{^{40}Ar_{rad}}{^{40}K}\frac{(\lambda_\varepsilon+\lambda_\beta)}{\lambda_\varepsilon}+1\right] \qquad \text{Equation 1}$$

where t=geological age, $\lambda_\varepsilon = 0.581 \times 10^{-10}$/yr = decay constant for the branch ^{40}K-^{40}Ar, $\lambda_\beta = 4.962 \times 10^{-10}$/yr decay constant for the branch ^{40}K-^{40}Ca.

Substituting for λ_ε and λ_β in equation 1;

$$t = 1.804 \times 10^9 \log_e\left[9.540\frac{^{40}Ar^*}{^{40}K} + 1\right] \qquad \text{Equation 2}$$

40Ar begins to accumulate in the sample only after the closure temperature has been reached. In the case of extrusive volcanics such as lava flows, this is a period of months or years and is numerically insignificant to the final age determination, which has calculated errors on the order of millions of years. 40Ar will only escape from the mineral if it is melted, recrystallised or heated to a sufficiently high temperature to allow diffusion of the argon through the mineral lattice, normally extremely slow given the relatively high atomic radius of 40Ar (1.9Å). Any factors that affect the physical or chemical state of the rock such as heating, weathering and alteration can, at least partially, reset the K-Ar clock. In the case of partial reheating, the measured K-Ar age, dependent on the degree of argon loss, could be anywhere between the time of initial cooling and the time of completion of the heating event.

For 'good' age determinations to be made using the K-Ar method, there are five fundamental assumptions (from Dalrymple and Lanphere, 1969);

- The decay of ^{40}K occurs at a constant rate independent of the chemical or physical environment.
- The proportion of ^{40}K to Ktotal in nature is the same in all materials to which the potassium-argon method is applied.
- There is no extraneous argon in the sample, it is all either radiogenic or atmospheric. Atmospheric argon will be present as a contaminant in the equipment and minerals used for the analyses.
- Any atmospheric ^{40}Ar can be corrected for in the sample being dated. This is assumed to have a composition $^{40}Ar/^{36}Ar = 295.5$.
- The sample has been a closed system since the time of initial cooling (t_0), i.e. there has been no loss or gain of ^{40}K or ^{40}Ar except for that resulting from radioactive decay of the ^{40}K. This assumption is strongly dependent on geologic conditions since t_0. Argon loss or gain results in extraneous age determinations. Gain or loss in argon from the mineral lattice may also cause disruptions in the mineral structure and could result in further argon loss.

Of these Assumptions numbers 3-5 are potentially false for samples from KGI which have potentially experienced isotopic resetting.

In terms of preparation and analysis of samples the three following criteria must be met;

1. A measurable volume of ^{40}Ar must have accumulated in the sample - i.e. the sample must have attained a certain age, a factor also dependent on the resolution of the K-Ar instrumentation.
2. The mineral used in the age determination must be an effective argon trap.
3. Hand specimens and thin sections of dating samples should be unweathered and show no/minimal alteration.
4. Triplicate K-Ar ages are produced for samples and should be internally consistent - i.e. within error. A single age that is either excessively young or old relative to the other duplicated results may be discarded as anomalous.

II.2 Derivation and interpretation of $^{40}Ar/^{39}Ar$ age

The $^{40}Ar/^{39}Ar$ method is a modified version of the K-Ar method in which 39Ar is produced by neutron activation of the 39K during irradiation. The K-Ar age equation (Equation 2) is rearranged and expressed in terms of $^{40}Ar^*$ and ^{39}Ar:

$$\frac{^{40}Ar^*}{^{39}Ar_K} = \frac{^{40}K\lambda_e+\lambda_e'}{^{39}K\ \lambda\ \Delta\int\phi(E)\sigma(E)dE}\ 1\ [(\exp\lambda t) - 1] \qquad \text{Equation 3}$$

where Δ= duration of irradiation, $\lambda_e+\lambda_e'$ = partial decay constants, t = age of sample, $\phi(E)$ = neutron flux at energy E and $\sigma(E)$ = neutron capture cross section at energy E for the $^{39}K(n, p)^{39}Ar$ reaction.

A dimensionless irradiation parameter J may then be substituted in to Equation 3:

$$J = \frac{^{39}K}{^{40}K}\ \frac{\lambda}{\lambda_e+\lambda_e'}\ \Delta\int\phi(E)\sigma(E)dE \qquad \text{Equation 4}$$

Substituting equation 4 into equation 2 gives:

$$\frac{^{40}Ar^*}{^{39}Ar_K} = \frac{(\exp\lambda t) - 1}{J} \qquad \text{Equation 5}$$

Equation 3 may be rearranged in order to calculate the age t of the sample:

$$t = \frac{1}{\lambda} \ln\left(1+J\ \frac{^{40}Ar^*}{^{39}Ar_K}\right) \qquad \text{Equation 6}$$

To calculate the $^{40}Ar/^{39}Ar$ age the J-value must be constrained. However the J-value is dependent on the duration of irradiation, the neutron flux and the neutron capture cross sections, parameters which can be difficult to quantify. By irradiating a sample mineral of known K-Ar age alongside the unknown the integrated fast neutron dose may be monitored and the J-value can be determined using the rearranged form of equation 4.

$$J = \frac{(\exp\lambda t) - 1}{^{40}Ar^*/^{39}Ar_K} \qquad \text{Equation 7}$$

The important implication of the equation 6 is that only the $^{40}Ar^*/^{39}Ar_K$ *ratio* rather than the exact quantity of each gas needs to be known to calculate the age of a sample. $^{40}Ar/^{39}Ar$ age spectra are produced by plotting the apparent $^{40}Ar/^{39}Ar$ age for each temperature step (y-axis) against the cumulative percentage of ^{39}Ar (x-axis). An error of ± one standard deviation (1σ) from the calculated age is indicated by the vertical thickness of each box and does not include the systematic J value error. The method of step heating at progressively higher temperatures produces a series of ages which reflect the internal distribution of ^{39}K and theoretically the presence or absence of alteration in the sample. If the sample has remained in a closed system since the time of initial closure, a concordant age spectrum with a flat 'plateau' should be

produced with steps of approximately equal age, which will be equal to the total gas age. In contrast if the system has remained open or has become open in the intervening period then contamination of the sample may have occurred, resulting in loss of ^{40}Ar, or in the uptake of excess ^{40}Ar and an anomalous age spectrum will be produced.

^{40}Ar loss results in step ages that are disproportionately young (Figure II.1). Assuming simple volumetric diffusion from the sample, the age spectra produced will have increasingly older steps at progressively higher temperatures (the presence of defects in the mineral sample might result in a significant volume of preferential degassing).

Excess $^{40}Ar_E$ results in step ages that are anomalously old (Figure II.2). Typically, discordant age spectra produced by the incorporation of excess argon are 'U-shaped' or 'saddle-shaped', since excess argon tends to be released at both high and low extraction temperatures.

Wartho et al (1996) demonstrated that acid leaching of mineral separates resulted in the removal of ~50% of the total excess ^{40}Ar in samples with minimal loss of $^{40}Ar^*$. This technique has been applied to all of the plagioclase separates discussed in chapter three.

A plateau age is defined for a sample only if it meets a set of criteria (Dalrymple and Lanphere, 1974, Lanphere and Dalrymple, 1978, Berger and York, 1981). The requirements are as follows;

a) The plateau in an age spectrum must consist of at least 3 consecutive steps, which constitute a significant proportion of the ^{39}Ar released from the sample (typically >50%).

b) Within errors all plateau steps must be of the same age.

c) Plateau steps must produce a well-defined line on a $^{36}Ar/^{40}Ar$ versus $^{39}Ar/^{40}Ar$ correlation plot.

The Isoplot/Ex program (Ludwig, 1998) that is used to calculate the ages presented in this chapter employs an algorithm to select a plateau based on the following similar criteria:

1) The plateau has three or more contiguous steps comprising more than 60% of the 39Ar (as default).

2) The probability of fit of the weighted-mean age of the steps is greater than 5%.

3) The slope of the error-weighted line through the plateau ages is not different from zero at 5% confidence.

4) The ages of the outermost two steps for either side of the plateau must not be significantly different (at 1.8σ) than the weighted-mean plateau age (6 or more steps only);

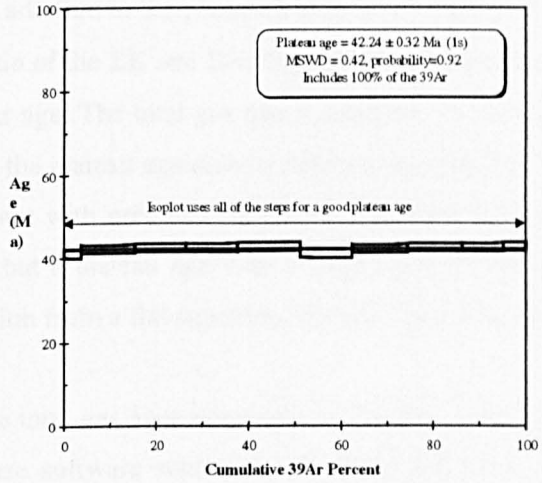

A

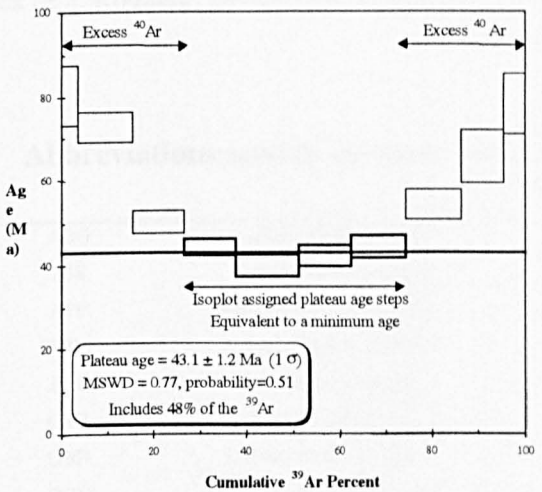

B

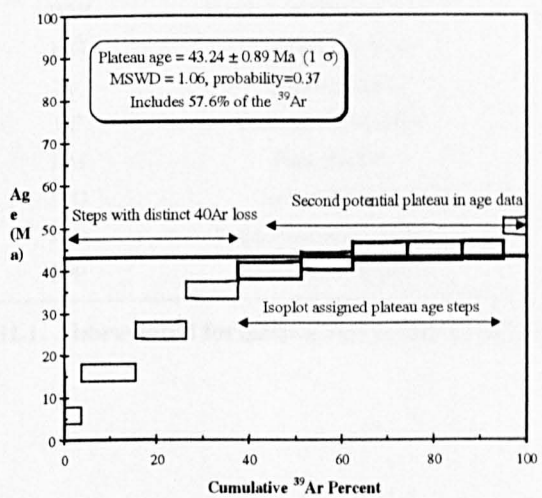

C

Figure II.1. Example step heating spectra showing a) a good plateau age spectrum b) a 'saddle-shaped age spectrum indicating excess ^{40}Ar c) a spectrum which has experienced ^{40}Ar loss, giving rise to artificially young low temperature steps.

5) The outermost 2 steps for either side of the plateau must not have non-zero slopes (at 1.8σ) with the same sign (9 or more steps only).Criteria 4 and 5 are arbitrary, whilst the first three criteria are a minimum statistical requirement. The plateau selection of Isoplot requires interpretation and modification and is not a final rigorous definition of the data being evaluated.

II.3 Isotope correlation plot ages

Extrapolating a best-fit line through an $^{36}Ar/^{40}Ar$ vs. $^{39}Ar/^{40}Ar$ plot using values derived from the plateau age steps produces an $^{40}Ar/^{39}Ar$ age which should correspond to the plateau age. The intersection of the line with the y-axis should be $1/y_{value}$ = ~295, the atmospheric ratio of ^{36}Ar to ^{40}Ar. Significant deviation from this value implies a non-atmospheric source of argon.

The Isoplot/Ex program uses three separate models to regress the $^{40}Ar/^{39}Ar$ versus $^{36}Ar/^{40}Ar$ data on the isotope correlation plot (Ludwig, 1998). If the probability of fit of the initial regression is low, Isoplot attempts to use either the second or third model fit, which weight the data-points using different criteria.

In addition to the plateau and isotope correlation ages, a third date is obtained by measuring the ratio of the ΣK and ΣAr degassed from the sample. A total gas age is therefore equivalent to a K-Ar age. The total gas age is assigned an error based on the analytical errors for each step, whilst the plateau age error is derived from the degree of spread of these steps. Thus a disturbed spectrum with precisely measured individual steps will yield a total gas age with only a small error, but a plateau age with a large error. In specimens with a good plateau age, or minimal deviation from a flat spectrum, the total gas- and plateau ages should be identical.

The total gas ages presented in Chapter 3 and in the following tables were calculated using in-house software written by P. Guise based on algorithms and Fortran code developed by Roddick (e.g. Roddick, 1978, 1980, 1983)(P. Guise, pers comm, 2000).

II.4 Abbreviations used in summary data tables

ABG	Admiralty Bay Group	MHF	Martins Head Formation
AIS	Andean Intrusive Suite	MPF	Mazurek Point Formation
APF	Admiralen Peak Formation	MFM	Mount Flagstaff Member
BBM	Barton Buttress Member	MWG	Mt. Wawel Group
BPF	Boy Point Formation	PCF	Polonez Cove Formation
CSG	Cape Syzerol Group	PPM	Plaza Point Member
DBF	Dalmor Bank Formation	PTF	Point Thomas Formation
DGF	Domeyko Glacier Formation	RPG	Rakusa Point Member
DRF	Dunikowski Ridge Formation	TBH	Three Brothers Hill
EIG	Ezcurra Inlet Group	UPF	Uchatka Point Formation
FF	Fildes Formation	USF	Ullman Spur Formation
HF	Hennequin Formation	VAF	Visa Anchorage Formation
HM	Hala Member	VGF	Vieville Glacier Formation
JHU	Jerzak Hills Unit	VPFT	Vaureal Peak Formation tillite
KPF	Keller Peninsula Formation	WPG	Wegger Peak Group
LPF	Llano Point Member	ZGF	Znosko Glacier Formation

Table II.1. Abbreviated formation and group names used in tables of age data.

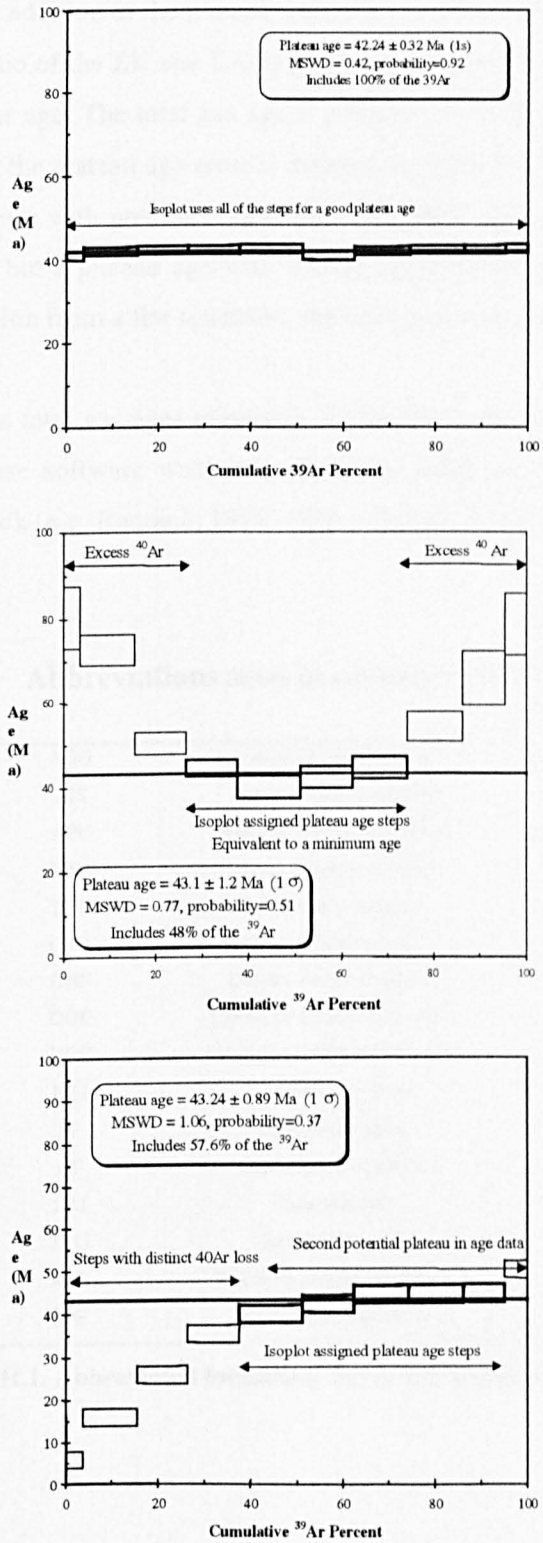

Figure II.1. Example step heating spectra showing a) a good plateau age spectrum b) a 'saddle-shaped age spectrum indicating excess ^{40}Ar c) a spectrum which has experienced ^{40}Ar loss, giving rise to artificially young low temperature steps.

5) The outermost 2 steps for either side of the plateau must not have non-zero slopes (at 1.8σ) with the same sign (9 or more steps only).Criteria 4 and 5 are arbitrary, whilst the first three criteria are a minimum statistical requirement. The plateau selection of Isoplot requires interpretation and modification and is not a final rigorous definition of the data being evaluated.

II.3 Isotope correlation plot ages

Extrapolating a best-fit line through an $^{36}Ar/^{40}Ar$ vs. $^{39}Ar/^{40}Ar$ plot using values derived from the plateau age steps produces an $^{40}Ar/^{39}Ar$ age which should correspond to the plateau age. The intersection of the line with the y-axis should be $1/y_{value}$ = ~295, the atmospheric ratio of ^{36}Ar to ^{40}Ar. Significant deviation from this value implies a non-atmospheric source of argon.

The Isoplot/Ex program uses three separate models to regress the $^{40}Ar/^{39}Ar$ versus $^{36}Ar/^{40}Ar$ data on the isotope correlation plot (Ludwig, 1998). If the probability of fit of the initial regression is low, Isoplot attempts to use either the second or third model fit, which weight the data-points using different criteria.

In addition to the plateau and isotope correlation ages, a third date is obtained by measuring the ratio of the ΣK and ΣAr degassed from the sample. A total gas age is therefore equivalent to a K-Ar age. The total gas age is assigned an error based on the analytical errors for each step, whilst the plateau age error is derived from the degree of spread of these steps. Thus a disturbed spectrum with precisely measured individual steps will yield a total gas age with only a small error, but a plateau age with a large error. In specimens with a good plateau age, or minimal deviation from a flat spectrum, the total gas- and plateau ages should be identical.

The total gas ages presented in Chapter 3 and in the following tables were calculated using in-house software written by P. Guise based on algorithms and Fortran code developed by Roddick (e.g. Roddick, 1978, 1980, 1983)(P. Guise, pers comm, 2000).

II.4 Abbreviations used in summary data tables

ABG	Admiralty Bay Group	MHF	Martins Head Formation
AIS	Andean Intrusive Suite	MPF	Mazurek Point Formation
APF	Admiralen Peak Formation	MFM	Mount Flagstaff Member
BBM	Barton Buttress Member	MWG	Mt. Wawel Group
BPF	Boy Point Formation	PCF	Polonez Cove Formation
CSG	Cape Syzerol Group	PPM	Plaza Point Member
DBF	Dalmor Bank Formation	PTF	Point Thomas Formation
DGF	Domeyko Glacier Formation	RPG	Rakusa Point Member
DRF	Dunikowski Ridge Formation	TBH	Three Brothers Hill
EIG	Ezcurra Inlet Group	UPF	Uchatka Point Formation
FF	Fildes Formation	USF	Ullman Spur Formation
HF	Hennequin Formation	VAF	Visa Anchorage Formation
HM	Hala Member	VGF	Vieville Glacier Formation
JHU	Jerzak Hills Unit	VPFT	Vaureal Peak Formation tillite
KPF	Keller Peninsula Formation	WPG	Wegger Peak Group
LPF	Llano Point Member	ZGF	Znosko Glacier Formation

Table II.1. Abbreviated formation and group names used in tables of age data.

Locality	Sample	Formation	Lithology	Mineralogy	%An	Degree of alteration	Stratigraphic information
Point Hennequin	P. 2807.6b	PHG / Hennequin Fm	?Basaltic-andesite	30% Phenocrysts - 90% Plag, 5% Cpx, <5% Opaque oxides, <1% Opx 70% Groundmass, Dominantly plagioclase with abundant opaques and lesser pyroxene	52	Plagioclase varies from v. fresh and free from inclusions to high % inclusions, exsolution and alteration. Some alteration of groundmass.	Part of Wawel sequence
	P. 2809.4	PHG / Hennequin Fm	Calc-alkaline Andesite lava*	25% Phenocrysts - 80% Plag (50% clusters) 5% Cpx/opx clusters, <2% Opaque oxides 75% Groundmass <90% Plag, <6% Cpx, <2% altered Cpx, <2% Opaque oxides	49	Moderate in groundmass, generally low in phenocrysts Cte rims present on some opx grains Rare v. degraded plag	Maximum age of in-situ Wawel Flora
	P. 2811.12	PHG / Hennequin Fm	Tholeiitic Trachyandesite lava*	15-20% Phenocrysts <95% Plag (30% composite) <40% Cpx, <5% Opaque oxides, <1% Opx 80-85% Groundmass <40% Glass, 60% Plag <5% Cpx, <1% Opaque oxides	43	Some inclusions in plag but generally fresh	Minimum age of in-situ Wawel Flora
	P. 2811.21	PHG / Hennequin Fm	Calc-alkaline Basaltic-andesite lava*	50% Phenocrysts 85% Plag, 15% Cpx <5% altered Cpx, <1% Opaque oxides 50% Groundmass V. fine, <70% Plag, <10% Cpx, <5% Opaque oxides	53.5	Inclusions common in plagioclase < 50% Fresh groundmass	Part of Wawel sequence

Table II.2. Summary mineralogical details for geochronological samples based on thin section data. * based on XRF analyses made available to RH by J Smellie (BAS).

Locality	Sample	Formation	Lithology	Mineralogy	%An	Degree of alteration	Stratigraphic information
	P. 2814.4b	PHG / Hennequin Fm	Calc-alkaline Basaltic andesite lava*	50% Phenocrysts - 90% Plag, 5% Cpx, <5% Opaque oxides, <1% Opx	46	Plagioclase v. fresh, low %inclusions or alteration, rarely has opaque red fracture fill	Age of lavas in Lussich Cove, separated by faulting from remainder of Point Hennequin sequence
				50% Groundmass - 60% Plag, 20% Opaques, <10% Cpx, ?10% Opx/plag			
Vaureal Peak	P. 2789.1	Cape Vaureal Fm	Calc-alkaline Basaltic lava*	35% Phenocrysts - <95% Plag, <10% Cpx 65% Groundmass - <60% Plag, <10% Cpx <2% Opaque oxides, <30% V. fine grained plag	49	Moderate/high alteration Cpx frequently altered to bastite, high %inclusions in plag, also altered	Maximum age of sequence at Vaureal Peak
	P. 2792.4	Cape Vaureal Fm	Calc-alkaline Basaltic lava	As above but finer grained	49	Moderate in groundmass v.low in plag	Maximum age of sequence at Vaureal Peak
	P. 2799.1a-d	Vaureal Peak Lavas	Calc-alkaline Basaltic lava*	40% Phenocrysts - 95% Plagioclase, <5% Alkali fspar, <2% Altered Cpx 60% Groundmass - 75% Plag, <15% Altered Cpx, 10% Opaque oxides	55	Moderate/high Inclusions common in plag phenocrysts ?smectite	Minimum age of Vaureal Peak lavas and the Vaureal Peak flora
Fossil Hill	P. 3031.LH	Fossil Hill Formation (Shen, 1994)	?Basaltic-andesite	<25% Phenocrysts - 97% Plag, 2% Cpx 1% Opx, <1% Opaque oxides <90% Groundmass- <50% Plag, <40% Cpx <15% Opaque oxides	61	Plag phenocrysts and groundmass plag often altered, inclusions common	Maximum age of Fossil Hill sediments
	P. 3031.4L	Fossil Hill Formation	?Basaltic or basaltic andesite	< 60% Phenocrysts - <80% Plag, <40% Cpx ? rare amphibole < 60% Groundmass - highly variable, fine material, comprising plagioclase, cpx, opx, opaque oxides	57.5	Moderate to high groundmass alteration but fresh plagioclase	Maximum age of Fossil Hill sediments

Table II.2. Continued.

Reference	Date	Locality	Strat-gp	Lithology	Sample#	Meth	Phase	Age	Error	Comments-Interpretation
Birkenmajer et al.	1982	Point Hennequin	PHG-MWG	Andesite	A-144	K-Ar	WR	24.5	0.5	
Birkenmajer et al.	1982	Point Thomas	EIG-ACF-RPM	Basaltic andesite	A-202	K-Ar	WR	66.7	1.5	
Birkenmajer et al.	1982	Point Thomas	EIG-HM			Relative				Younger than the Rakusa Pt Fm(A-202)
Birkenmajer et al.	1982	Baranowski Glacier	BGG-LPF	Basaltic andesite	A-195	K-Ar	WR	77	4	
Birkenmajer et al.	1982	Paradise Cove	PCG-UPF	Basalt	A-198	K-Ar	WR	67.7	3.5	Redistribution of K, older than 77+/-4Ma
Birkenmajer et al.	1982a	Wegger Peak	WPG	Diorite	A-224	K-Ar	WR	31.7	0.9	
Birkenmajer et al.	1982a	Dufayel Island	CCG-ZGF	Andesite	A-452	K-Ar	WR	56.8	1.2	
Birkenmajer et al.	1982b	Gdynia Pt, Dufayel Is.	DIG-DBF	Basaltic andesite	A-451	K-Ar	WR	51.9	1.5	
Dupre	1982	Point Hennequin	PHG-MWG	At least two flows from summit	HP 2-04	Ar-Ar	WR	47	2	Total gas age = 47.0Ma, Wtd apparent age = 46.7+/-1.5Ma. Pronounced 'step down' profile
Pankhurst & Smellie	1983	Keller Peninsula	ABG	Andesite	P. 560.1	K-Ar	WR	41	1	
Pankhurst & Smellie	1983	Keller Peninsula	ABG	Andesite	P. 1452.2	K-Ar	WR	44	1	
Pankhurst & Smellie	1983	Keller Peninsula	ABG	Andesite	P. 1454.1	K-Ar	WR	42	1	
Pankhurst & Smellie	1983	Point Hennequin	HF	Andesite	P. 831.2	K-Ar	WR	45	1.0	
Pankhurst & Smellie	1983	Point Hennequin	HF	Andesite	P. 831.3	K-Ar	WR	27	1.0	Not easily interpreted - resetting or unidentified sill intrusion'
Pankhurst & Smellie	1983	Point Hennequin	HF	Andesite	P. 831.3	Rb-Sr	WR	27		Bracketed in text ?unreliable
Pankhurst & Smellie	1983	Point Hennequin	HF	Andesite	P. 831.4	K-Ar	WR	32	2	Not easily interpreted - resetting or unidentified sill intrusion'
Pankhurst & Smellie	1983	Point Hennequin	HF	Andesite	P. 831.5	K-Ar	WR	46	1	Agrees with dates
Pankhurst & Smellie	1983	Point Hennequin	HF	Andesite	P. 831.8	K-Ar	WR	47	1	from N. Fildes and Potter Pen

Table II.3. Summary geochronological data for the Admiralty Bay area.

Reference	Date	Locality	Strat-gp	Lithology	Sample#	Meth	Phase	Age	Error	Comments-Interpretation
Pankhurst & Smellie	1983	Keller Peninsula	HF	Andesite dyke	P. 560.1	K-Ar	WR	41	1	
Pankhurst & Smellie	1983	Keller Peninsula	HF	Andesite dyke	P. 1452.2	K-Ar	WR	44	1	
Pankhurst & Smellie	1983	Keller Peninsula	HF	Andesite dyke	P. 1454.1	K-Ar	WR	42	1	
Birkenmajer et al.	1985	Point Hennequin	VGF	Andesite	A-141	K-Ar	WR	43.9	0.9	
Birkenmajer et al.	1985	Point Thomas	PTF	High Al-Basalt	A-200	K-Ar	WR	37.4	1.1	
Birkenmajer et al.	1985	Rakusa Pt	ABG-JHU	Andesite plug	A-201	K-Ar	WR	21	0.8	
Birkenmajer et al.	1985	PH-Basalt Point	ABG-JHU	Hyaloandesite plug	A-140	K-Ar	WR	28.3	1.7	
Birkenmajer et al.	1985	Jardine Peak	ABG-JHU	Basaltic andesite plug	A-250	K-Ar	WR	54.2	1.1	
Birkenmajer et al.	1986	Wegger Peak	WPG	Diorite	A-224	K-Ar	WR	43.5	4.8	
Birkenmajer et al.	1986	Wegger Peak	WPG	Quartz diorite	A-227	K-Ar	WR	43.7	9.5	
Birkenmajer et al.	1986	Admiralen Peak	CCG-APF	Basaltic andesite	A-244	K-Ar	WR	43.7	4.8	
Soliani & Kawashita	1986	Ullman Spur	USF	Andesite	Ant-13	K-Ar	WR	40.3	2	
Soliani & Kawashita	1986	Ullman Spur	USF	Andesite	Ant-15	K-Ar	WR	40.6	1.6	
Soliani & Kawashita	1986	Ullman Spur	DGF	Andesite	Ant-19	K-Ar	WR	48.8	4.6	
Soliani & Kawashita	1986	Keller Peninsula	DGF	Andesite	Ant-67	K-Ar	WR	53.5	1.4	
Soliani & Kawashita	1986	Keller Peninsula	VAF-BBM	Andesite	Ant-69	K-Ar	WR	38.8	4.2	
Soliani & Kawashita	1986	Keller Peninsula	VAF-BBM	Andesite	Ant-95	K-Ar	WR	57.3	3.9	
Soliani & Kawashita	1986	Keller Peninsula	KPF-MFM	Andesite	Ant-74	K-Ar	WR	37.3	1.5	
Soliani & Kawashita	1986	Keller Peninsula	MIG-KPF-PPM	Andesite	Ant-9	K-Ar	WR	4.63	1.4	

Table II.3. Continued.

Reference	Date	Locality	Strat-gp	Lithology	Sample#	Meth	Phase	Age	Error	Comments-Interpretation
Soliani & Kawashita	1986	Keller Peninsula	MIG-KPF-PPM	Andesite	Ant-76	K-Ar	WR	48.4	1.1	
Soliani & Kawashita	1986	Keller Peninsula	MIG-KPF-PPM	Andesite	Ant-77	K-Ar	WR	35.1	2.1	
Soliani & Kawashita	1986	Keller Peninsula	MIG-KPF-PPM	Andesite	Ant-93	K-Ar	WR	49.2	2.1	
Soliani & Kawashita	1986	Keller Peninsula	MIG-KPF-PPM	Andesite	Ant-96	K-Ar	WR	45.1	0.8	
Kawashita & Soliani	1988	Furmanczyk Pt	CCG-ZGF	Basaltic andesite	Ant-26C	Rb-Sr		60.4	5.3	Crystallisation age/homogenisation
Kawashita & Soliani	1988	Furmanczyk Pt	CCG-ZGF	Basaltic andesite	Ant-26G	Rb-Sr		60.4	5.3	Crystallisation age/homogenisation
Kawashita & Soliani	1988	Furmanczyk Pt	CCG-ZGF	Basaltic andesite	Ant-26I	Rb-Sr		60.4	5.3	Crystallisation age/homogenisation
Kawashita & Soliani	1988	Dufayel Island	CCG-ZGF	Basaltic andesite	Ant-32C	Rb-Sr		60.4	5.3	Crystallisation age/homogenisation
Kawashita & Soliani	1988	Pond Hill	CCG-ZGF	Basaltic andesite	Ant-89	Rb-Sr		60.4	5.3	Crystallisation age/homogenisation
Kawashita & Soliani	1988	Pond Hill	CCG-ZGF	Basaltic andesite	Ant-90B	Rb-Sr		60.4	5.3	Crystallisation age/homogenisation
Kawashita & Soliani	1988	Furmanczyk Pt	CCG-ZGF	Basaltic andesite	Ant-26C	K-Ar	WR	41.6	0.9	Complete Ar loss between 60-42Ma
Kawashita & Soliani	1988	Furmanczyk Pt	CCG-ZGF	Basaltic andesite	Ant-26G	K-Ar	WR	41.6	0.9	Complete Ar loss between 60-42Ma
Kawashita & Soliani	1988	Furmanczyk Pt	CCG-ZGF	Basaltic andesite	Ant-26I	K-Ar	WR	41.6	0.9	Complete Ar loss between 60-42Ma
Kawashita & Soliani	1988	Dufayel Island	CCG-ZGF	Basaltic andesite	Ant-32C	K-Ar	WR	41.6	0.9	Complete Ar loss between 60-42Ma
Kawashita & Soliani	1988	Pond Hill	CCG-ZGF	Basaltic andesite	Ant-89	K-Ar	WR	41.6	0.9	Complete Ar loss between 60-42Ma
Kawashita & Soliani	1988	Pond Hill	CCG-ZGF	Basaltic andesite	Ant-90B	K-Ar	WR	41.6	0.9	Complete Ar loss between 60-42Ma
Soliani & Bonhomme	1994	Furmanczyk Pt	CCG-ZGF	Basaltic andesite	Ant-26C	K-Ar	WR	42.4	1.2	Valid but with high K2O = some alteration
Soliani & Bonhomme	1994	Furmanczyk Pt	CCG-ZGF	Basaltic andesite	Ant-26G	K-Ar	WR	41.3	1.1	Valid but with high K2O = some alteration
Soliani & Bonhomme	1994	Furmanczyk Pt	CCG-ZGF	Basaltic andesite	Ant-26I	K-Ar	WR	41.7	1.2	Valid but with high K2O = some alteration
Soliani & Bonhomme	1994	Dufayel Island	CCG-ZGF	Andesite	Ant-32C	K-Ar	WR	44	1.6	Valid but with high K2O = some alteration
Soliani & Bonhomme	1994	Pond Hill	CCG-ZGF	Basaltic andesite	Ant-89	K-Ar	WR	46	8.8	Significant calcite = high analytical error
Soliani & Bonhomme	1994	Pond Hill	CCG-ZGF	Basaltic andesite	Ant-90b	K-Ar	WR	49.1	2.7	Significant calcite = high analytical error

Table II.3. Continued.

Reference	Date	Locality	Strat-gp	Lithology	Sample#	Meth	Phase	Age	Error	Comments-Interpretation
Dupre	1982	Potter Cove	TBH	Basaltic andesite porphyry	PC1-01	Ar-Ar	WR	46	1	Total gas age = 45.8Ma, Wtd apparent age = 46.7+/- 0.8Ma
Watts	1982	Potter Cove	EIG	Andesite		K-Ar	WR	49.1	0.9	Upper
Watts	1982	Potter Cove	EIG	Andesite		K-Ar	WR	57.9	0.8	Middle
Watts	1982	Potter Cove	EIG	Andesite		K-Ar	WR	49.7	1.7	Lower
Watts	1982	Three Brothers Hill	EIG	Basaltic plug		K-Ar	WR	50.6	0.7	
Watts	1982	Noel Hill	AIS	Granodiorite		K-Ar	WR	46	0.7	
Watts	1982	Noel Hill	AIS	Granodiorite		K-Ar	WR	50.2	0.6	
Pankhurst & Smellie	1983	Marian Cove	FF	Andesite	P. 1473.5	K-Ar	WR	46	1	
Pankhurst & Smellie	1983	Potter Peninsula	FF	Basalt	P. 232.1	K-Ar	WR	44	1	Ar loss
Pankhurst & Smellie	1983	Potter Peninsula	FF	Basaltic andesite dyke	P. 696.1	K-Ar	WR	45	1	Ar loss
Pankhurst & Smellie	1983	Potter Peninsula	FF	Basalt	P. 750.1	K-Ar	WR	42	1	Ar loss
Pankhurst & Smellie	1983	Potter Peninsula	FF	Basaltic andesite	P. 758.1	K-Ar	WR	47	1	Ar loss
Pankhurst & Smellie	1983	Potter Peninsula	FF	Andesite	P. 757.2	K-Ar	WR	48	1	Ar loss
Pankhurst & Smellie	1983	Three Brothers Hill	FF	Andesite plug	P. 685.4	K-Ar	WR	47	1	
Pankhurst & Smellie	1983	Noel Hill	FF	Granodiorite plug	P. 533.1	K-Ar	WR	48	1	
Pankhurst & Smellie	1983	Noel Hill	FF	Granodiorite (biotite)	P. 535.2/3	K-Ar	WR	46	1	
Tokarski et al.	1987	Barton Peninsula	?FF	Relative						Cretaceous or Palaeocene
Park	1989	Barton Peninsula	?FF	Andesite		K-Ar	WR	48.5	4	Possible resetting
Park	1989	Barton Peninsula	?FF	Basaltic andesite		K-Ar	WR	35.5	3.4	
Park	1989	Barton Peninsula	?FF	Lapilli tuff		K-Ar	WR	44.2	2.4	

Table II.4. Summary geochronological data for Barton and Potter Peninsulas.

Reference	Date	Locality	Strat-gp	Lithology	Sample#	Meth	Phase	Age	Error	Comments-Interpretation
Park	1989	Barton Peninsula	?FF	Granodiorite		K-Ar	WR	45.2	1.9	
Park	1989	Barton Peninsula	?FF	Granodiorite		K-Ar	WR	42.1	1.9	
Park	1989	Barton Peninsula	?FF	Quartz diorite		K-Ar	WR	45.2	2.4	

Table II.4. Continued.

Reference	Date	Locality	Strat-gp	Lithology	Sample#	Meth	Phase	Age	Error	Comments-Interpretation
Birkenmajer et al.	1988	Cape Vaureal	LBG-DRF	Andesite	A-203	K-Ar	WR	28	3.1	
Birkenmajer et al.	1988	Cape Vaureal	LBG-DRF	Andesite	A-220	K-Ar	WR	33.4	7	
Birkenmajer et al.	1988	Vaureal Peak	CRG-BPF	Andesite	A-209	K-Ar	WR	17.3	1.3	
Birkenmajer et al.	1988	Vaureal Peak	CRG-BPF	Andesite	A-218	K-Ar	WR			High CaCO3 - undatable
Birkenmajer et al.	1988	Cape Vaureal	Predates VPF	Andesite plug	A-219	K-Ar	WR	45.9	0.7	
Birkenmajer et al.	1988	Vaureal Peak	VPFT	Andesite block from tillite	A-213	K-Ar	WR	47	1.1	Poor minimum age constraint
Pankhurst & Smellie	1983	Lions Rump	HF	Andesite	P. 438.1	K-Ar	WR	42	1	
Birkenmajer et al.	1985	Dunikowski Ridge	DRF	Andesite	A-179	K-Ar	WR	25.7	1.3	
Birkenmajer et al.	1985	Martins Head	DRF	Andesite	A-221	K-Ar	WR	29.5	2.1	
Birkenmajer et al.	1985	Magda Nunatak	MPF	Basalt	A-667	K-Ar	WR	49.4	5	
Birkenmajer & Gazdzicki	1986	Polonez Cove	CSG	Aphanitic basalt dyke	A-166	K-Ar	WR	>21.8	0.6	
Birkenmajer & Gazdzicki	1986	Boy Pt-Dunikowski Ridge	CRG-BPF	Qtz-andesite	A-162	K-Ar	WR	>22.4	2/-0.4	
Birkenmajer & Gazdzicki	1986	Polonez Cove	CRG-MPF	Basalt	A-165	K-Ar	WR	74	1/-7	
Birkenmajer et al.	1986	Low Head	MPF	Ol-basalt plug	A-155	K-Ar	WR	14.4	1.4	

Table II.5. Summary geochronological data for the south east coast of King George Island.

Reference	Date	Locality	Strat-gp	Lithology	Sample#	Meth	Phase	Age	Error	Comments-Interpretation
Birkenmajer et al.	1986	Polonez Cove	CRG	Basaltic hyaloclastite	GP-1	K-Ar	WR	22.3	0.8	Described as in press - Ar loss, reheating - not true age
Birkenmajer et al.	1988	Cape Melville	CSG	Aphanitic basalt dyke	A-304	K-Ar	WR	23	1.4	Cuts Moby Dick Gp and older dykes - age too high by ~2Ma ?contamination
Birkenmajer et al.	1988	Cinder Spur	CSG	Aphanitic basalt dyke	A-180	K-Ar	WR	21.9	1.1	Cuts Dunikowski Ridge Fm
Birkenmajer et al.	1988	Harnassie Hill	CSG	Basalt dyke	A-210	K-Ar	WR	25.7	0.7	Cuts Harnassie Hill Fm
Birkenmajer et al.	1988	Harnassie Hill	CSG	Basalt dyke	A-211	K-Ar	WR	30.5	5.5	Cuts Harnassie Hill Fm
Birkenmajer et al.	1988	Dunikowski Ridge	LBG-MHF	Andesite	A-178	K-Ar	WR	27.4	1	Initial dating produced young ages of 20.4Ma+/-2.4 ?Reheating and argon loss
Birkenmajer et al.	1988	Dunikowski Ridge	LBG-DRF	Andesite	A-175	K-Ar	WR	30.8	2	
Birkenmajer et al.	1988	Low Head	CRG-PCF	Basalt frag from hyaloclastite	GP-44	K-Ar	WR			High CaCO3 - undatable
Birkenmajer et al.	1988	Mersey Spit (Turret Pt)	CRG-MPF	Basaltic andesite	A-297	K-Ar	WR	34.4	0.5	Field mapping shows that A-297 predates A-298
Birkenmajer et al.	1988	Mersey Spit (Turret Pt)	CRG-MPF	Andesite plug	A-298	K-Ar	WR	37.6	0.9	
Birkenmajer et al.	1988	Ternyck Needle	?CSG	Basalt plug	A-142	K-Ar	WR			High CaCO3 - undatable
Birkenmajer et al.	1988	Puchalski Peak	VPFT	Andesite dyke	AKT-10	K-Ar	WR	49	5.5	Attributed to dyke by Tokarski but could be from tillite

Table II.5. Continued.

Reference	Date	Locality	Strat-gp	Lithology	Sample#	Meth	Phase	Age	Error	Comments-Interpretation
Pankhurst & Smellie	1983	Esther Nunatak	HF	Andesite plug	G. 28.1	K-Ar	WR	32	1	
Hu et al.	1997	Davey Point		Basalt	A-635	Ar-Ar	ISO	52.4	1.1	Inhomogeneous K/Ar and ArE

Table II.6. Summary geochronological data for the north coast of King George Island.

Reference	Date	Locality	Strat-gp	Lithology	Sample#	Meth	Phase	Age	Error	Comments-Interpretation
Wang et al.	1993	Half-three Point	Fildes Fm	Tuffs & min separates	Gwp12	Rb-Sr	WR-MIN	71.33	0.3	Uncertain - too old?
Valencio et al	1979	Fildes Strait	Fildes Fm	Andesite, nr alteration	A23	K-Ar	WR	110	10.0	Too old - post-56 m'som-Sm et al 1984 also imprecise
Valencio et al	1979	E. Flat Top Point	Hypabyssal	Andesite plug, fresh	A24	K-Ar	WR	61	3.0	Emplacement?
Valencio et al	1979	Ardley Is	Fildes Fmn	Andesite plug, fresh	A6	K-Ar	WR	27	2.0	Too young Ar loss by sills?
Valencio et al	1979	E. Flat Top Point	Fildes Fmtn	Andesite plug, fresh	A11	K-Ar	WR	88	5.0	Too old - post-56 m'som-Sm et al 1984
Pankhurst & Smellie	1983	Suffield Point	Hypabyssal Fildes Fm	Andesite plug	P.611.1	K-Ar	WR	44	1.0	Emplacement?
Smellie et al.	1984	Horatio Stump	Hypabyssal Fildes Fm	Basalt plug	P.619.1	K-Ar	WR	51	1.0	Emplacement?
Watts	1982	Horatio Stump	Hypabyssal Fildes Fm	Basalt plug	5	K-Ar	WR	54.3	0.6	Emplacement?
Grikurov et al	1970	Horatio Stump	Hypabyssal	Andesite plug	134	K-Ar	WR	45		Too young? see Watts
Jwa et al.	1992	Fildes	Hypabyssal	Basalt	4	K-Ar	WR	53.2	2.5	Emplacement?
Jwa et al.	1992	Fildes	Hypabyssal	Basalt	5	K-Ar	WR	53.2	3.0	Emplacement?
Pankhurst & Smellie	1983	N. Fildes	Hypabyssal	Andesite plug	P.1149.1	K-Ar	WR	58	4.0	Emplacement? - concordant
Watts	1982	S. Fildes	Hypabyssal	Basalt dyke, altered	7	K-Ar	WR	79.2	2.6	Too old - post-56 m'som-Sm et al 1984
Pankhurst & Smellie	1983	S. Fildes	Fildes Fm	Basalt lava	P.629.1	K-Ar	WR	31	3.0	Too young Ar loss
Pankhurst & Smellie	1983	N. Fildes	Fildes Fm	Dacite lava	P.1182.1/2	K-Ar	WR	42	1.0	Too young Ar loss
Fensterseifer et al.	1988	Fildes	Fildes Fm	Basalt	Ant-B11	K-Ar	WR	42.9	1.3	Emplacement - agrees biostratigraphy
Pankhurst & Smellie	1983	N. Fildes	Fildes Fm	Basaltic-andesite	P.1125.1	K-Ar	WR	43	1.0	Too young Ar loss
Pankhurst & Smellie	1983	N. Fildes	Fildes Fm	Dacite lava	P.1183.2/7	K-Ar	WR	46	1.0	Too young Ar loss
Fensterseifer et al.	1988	Fildes	Fildes Fm	Basaltic-andesite	ANT-B11-D3	K-Ar	WR	46.6	1.4	Emplacement - agrees biostratigraphy
Pankhurst & Smellie	1983	N. Fildes	Fildes Fm	Basalt	P.1147.3	K-Ar	WR	48	1.0	Too young Ar loss
Pankhurst & Smellie	1983	N. Fildes	Fildes Fm	Basalt	P.1147.4	K-Ar	WR	48	1.0	Too young Ar loss
Pankhurst & Smellie	1983	N. Fildes	Fildes Fm	Basalt	P.1166.7	K-Ar	WR	52	1.0	Too young Ar loss
Jwa et al.	1992	Fildes	Fildes Fm	Basaltic-andesite	3	K-Ar	WR	56.2	2.7	Emplacement?

Table II.7. Summary geochronological data from Fildes Peninsula (compiled by R Willan, British Antarctic Survey).

Reference	Date	Locality	Strat-gp	Lithology	Sample#	Meth	Phase	Age	Error	Comments-Interpretation
Pankhurst & Smellie	1983	N. Fildes	Fildes Fm	Basalt	P.1162.5	K-Ar	WR	57	3.0	Emplacement? - concordant
Pankhurst & Smellie	1983	S. Fildes	Fildes Fm	Andesite	P.608.5a	K-Ar	WR	58	1.0	Emplacement? - concordant
Pankhurst & Smellie	1983	S. Fildes	Fildes Fm	Andesite	P.609.3	K-Ar	WR	58	2.0	Emplacement? - concordant
Pankhurst & Smellie	1983	S. Fildes	Fildes Fm	Andesite, altered	P.627.1	K-Ar	WR	58	1.0	Emplacement? - concordant
Pankhurst & Smellie	1983	S. Fildes	Fildes Fm	Andesite	P.604.1	K-Ar	WR	59	2.0	Emplacement? - concordant
Jwa et al.	1992	Fildes	Fildes Fm	Basaltic-andesite	1	K-Ar	WR	59.5	3.0	Emplacement?
Jwa et al.	1992	Fildes	Fildes Fm	Basaltic-andesite	2	K-Ar	WR	61.4	2.4	Emplacement?
Watts	1982	S. Fildes	Fildes Fm	Basalt lava	8	K-Ar	WR	64.4	0.8	Too old - post-56 m'som-Sm et al 1984
Grikurov et al	1970	Fildes	Fildes Fm	Basalt lava	20a	K-Ar	WR	83		Too old - post-56 m'som-Sm et al 1984
Watts	1982	N.C. Fildes	Fildes Fm	Basalt lava, altered	8	K-Ar	WR	106	1.2	Too old - post-56 m'som-Sm et al 1984
Soliani et al.	1988	N.C. Fildes	Hypabyssal	Andesite dyke	Ant-H-7-D2	K-Ar	WR	47.5	1.3	Emplacement?
Soliani et al.	1988	N.C. Fildes	Admiralty Bay Fm Hypabyssal Admiralty Bay Fm	Andesite plug	Ant-Q-11	K-Ar	WR	52.3	1.3	Emplacement
Soliani et al.	1988	N.C. Fildes	Fildes Fm	Basaltic-andesite	Ant-B-32A	K-Ar	WR	51.9	4.9	Uncertain- imprecise but emplacement agrees biostratigraphy
Soliani et al.	1988	N.C. Fildes	Fildes Fm	Basaltic-andesite	Ant-H-10A	K-Ar	WR	57.1	1.1	Emplacement - agrees biostratigraphy
Soliani et al.	1988	N.C. Fildes	Fildes Fm	Basalt	Ant-B-20	K-Ar	WR	57.7	1.2	Emplacement - agrees biostratigraphy
Soliani et al.	1988	N.C. Fildes	Fildes Fm	Andesite	Ant-H-7B	K-Ar	WR	58.5	1.4	Emplacement - agrees biostratigraphy
Hu et al	1995	Atherton Is	Hypabyssal	Basalt plug	A-642	K-Ar	WR	91.5	2.3	Too old - excess Ar (Hu 1995 ab in Korea mtg.)

Table II.7. Continued.

Sample/ Batch	Locality	Run No	Weight	Weight %K	*40Ar cm^3g^{-1}	Temp °C	$^{39}Ar_K$	$^{37}Ar_{Ca}$ {Vol. $x10^{-9}$ cm^3}	$^{38}Ar_{Cl}$	Ca/K	$^{40}Ar/^{39}Ar_K$	%Atm ^{40}Ar	Age Ma	Error Ma	$\%^{39}Ar_K$	Total gas age
P2789.1	VP	2496	0.07935g	0.06	1.2×10^{-7}	660	0.33	23.3	0.57	140	2.287	99.6	25.0	33.5	18.8	50.9 ± 7.3Ma
Plagioclase						749	0.30	35.2	0.02	232	6.120	85.8	59.8	7.1	17.2	
B1						797	0.18	14.5	0.00	163	6.505	57.9	63.2	14.9	10.1	
						880	0.35	29.7	0.01	168	4.547	64.7	45.6	6.9	20.1	
						950	0.17	11.9	0.01	144	6.146	75.4	60.0	8.1	9.4	
						1000	0.09	5.4	0.01	124	4.681	87.0	46.8	24.4	5.0	
						1060	0.09	4.2	0.01	99	6.238	80.3	60.8	18.9	4.9	
						1150	0.14	8.2	0.02	120	6.220	82.4	60.7	26.1	7.7	
						1240	0.12	7.8	0.02	128	7.167	85.3	69.1	21.3	6.9	
P2792.4	VP	2495	0.06861g	0.29	5.9×10^{-7}	540	0.13	0.9	0.40	14.1	2.266	99.8	24.9	109.4	1.8	50.7 ± 2.3Ma
Plagioclase						650	0.16	1.4	0.01	17.2	3.466	91.4	35.8	21.1	2.2	
B1						750	0.16	1.7	0.00	21.1	8.752	95.0	83.2	21.9	2.2	
						855	0.46	4.5	0.01	19.8	5.241	57.5	51.9	9.6	6.3	
						950	1.38	13.7	0.02	19.7	4.991	30.5	49.6	2.2	19.0	
						1025	1.09	10.9	0.02	19.8	5.229	36.8	51.7	1.9	14.9	
						1070	0.85	8.5	0.01	19.9	4.468	40.3	44.9	2.3	11.7	
						1127	0.83	8.2	0.01	19.8	4.726	43.6	47.2	3.1	11.3	
						1190	1.20	12.0	0.02	19.9	4.715	57.7	47.1	2.4	16.4	
						1290	1.03	10.9	0.02	20.9	6.695	60.6	64.9	3.6	14.2	
P2799-1A-D	VP	2493	0.03022g	0.04	4.0×10^{-7}	600	0.04	3.4	0.06	183	26.06	96.9	230	389	8.1	229 ± 48Ma
Plagioclase						661	0.02	5.6	0.00	472	17.37	97.6	158	673	5.2	
B1						750	0.04	8.6	0.00	489	5.96	97.7	58	101	7.6	

Table II.8. New $^{40}Ar/^{39}Ar$ step heating data. Batch 1(B1). J-Value = 0.00514 ± 0.5 %. Batch 2(B2) J-Value = 0.0112 ± 0.5 %. Errors are 1σ. $^{*40}Ar$ ≡ volume of Radiogenic ^{40}Ar, gas volumes corrected to STP. PH = Point Hennequin, VP = Vaureal Peak. WR = whole rock date, plagioclase = plagioclase separate date.

Sample	Locality	Run No	Weight	Weight %K	*40Ar cm^3g^{-1}	Temp °C	$^{39}Ar_K$	$^{37}Ar_{Ca}$	$^{38}Ar_{Cl}$ {Vol. $x10^{-9}$ cm^3}	Ca/K	$^{40}Ar/^{39}Ar_K$	%Atm ^{40}Ar	Age Ma	Error Ma	$\%^{39}Ar_K$	Total gas age
P2799-1A-D						853	0.07	17.2	0.00	473	14.69	70.4	135	33	15.8	
Plagioclase						940	0.05	7.3	0.00	303	24.62	74.9	218	42	10.5	
B1						1080	0.11	8.2	0.00	144	30.79	38.4	268	17	24.7	
						1150	0.06	6.0	0.00	204	39.54	48.4	337	46	12.8	
						1250	0.07	3.8	0.00	109	31.96	65.4	278	44	15.3	
P2809.4	PH	2498	0.06973g	0.24	4.7×10^{-7}	660	0.35	4.9	0.64	28.0	2.572	99.7	27.6	50.7	5.8	49.4 ± 3.3Ma
Plagioclase						710	0.21	3.5	0.01	33.9	6.785	94.3	65.7	13.0	3.4	
B1						780	0.22	3.8	0.00	34.3	6.440	55.3	62.6	10.9	3.7	
						848	0.44	6.9	0.01	31.3	5.161	44.1	51.1	7.0	7.3	
						910	1.28	20.3	0.02	31.6	4.886	8.8	48.6	3.5	21.3	
						958	0.85	14.5	0.01	34.1	4.496	32.3	45.1	3.6	14.1	
						1020	0.51	8.6	0.01	33.7	5.064	20.3	50.3	4.4	8.5	
						1100	0.84	14.7	0.01	35.0	5.072	20.8	50.3	2.5	13.9	
						1217	0.79	14.2	0.02	35.7	5.519	51.3	54.4	3.7	13.2	
						1300	0.54	9.5	0.01	35.2	4.963	74.5	49.3	6.5	8.9	
P2811.12	PH	2492	0.05252g	1.1	14.3×10^{-7}	560	2.5	1.7	0.94	1.4	0.929	98.4	12.6	1.3	11.3	31.5 ± 0.4Ma
WR						625	1.3	0.9	0.43	1.4	1.983	91.0	22.3	1.0	6.0	
B1						720	3.0	2.5	0.59	1.7	3.364	85.6	34.9	0.5	13.7	
						770	2.2	2.1	0.36	2.0	3.208	80.6	33.5	1.1	9.9	
						824	2.2	2.5	0.40	2.3	3.308	81.8	34.4	0.7	10.3	
						870	1.7	2.1	0.34	2.4	3.227	83.4	33.6	0.9	7.9	
						926	1.5	1.9	0.29	2.6	3.217	83.0	33.5	1.8	6.7	
						970	1.4	2.0	0.31	2.8	2.713	85.2	28.9	1.2	6.6	
						1023	2.6	3.3	0.59	2.5	3.132	84.0	32.8	0.9	11.8	
						1104	1.8	3.3	0.40	3.6	3.843	85.2	39.2	1.5	8.2	

Table II.8. Continued.

Sample	Locality	Run No	Weight	Weight %K	*40Ar cm^3g^{-1}	Temp °C	$^{39}Ar_K$	$^{37}Ar_{Ca}$	$^{38}Ar_{Cl}$	Ca/K	$^{40}Ar/^{39}Ar_K$	%Atm ^{40}Ar	Age Ma	Error Ma	$\%^{39}Ar_K$	Total gas age Ma
							{Vol. $x10^{-9}$ cm^3}									
P2811.12 WR						1250	1.7	6.8	0.36	8.0	4.099	88.2	41.5	1.1	7.7	
P2811.21	PH	2494	0.06622g	0.11	2.3×10^{-7}	705	0.40	34.0	0.36	172	4.973	98.7	49.4	8.1	14.7	52.2 ± 2.8Ma
Plagioclase						806	0.48	29.7	0.01	123	5.436	52.0	53.6	3.3	18.0	
B1						900	0.46	23.2	0.01	101	4.422	64.0	44.5	4.9	17.0	
						970	0.21	8.9	0.00	86	3.231	86.1	33.7	10.8	7.7	
						1035	0.19	6.5	0.01	69	4.811	55.8	48.0	13.3	6.9	
						1090	0.18	5.5	0.00	62	4.912	60.1	49.9	11.2	6.6	
						1160	0.28	9.0	0.01	64	3.643	82.3	37.4	6.8	10.5	
						1250	0.25	6.3	0.01	52	8.039	71.0	76.9	15.3	9.1	
						1290	0.26	5.0	0.01	39	8.391	58.5	80.1	8.3	9.5	
P2814.4B	PH	2497	0.07095g	0.20	3.9×10^{-7}	690	0.44	6.9	0.91	30.8	2.041	99.7	22.8	46.3	8.6	49.4 ± 4.2Ma
Plagioclase						760	0.20	3.6	0.01	36.4	6.504	80.3	63.2	10.6	3.8	
B1						820	0.34	6.2	0.01	35.8	3.275	64.7	34.1	6.4	6.7	
						896	0.75	13.4	0.01	35.7	4.575	29.5	45.8	2.6	14.5	
						1008	1.54	28.6	0.02	36.9	4.657	20.3	46.6	0.9	29.9	
						1063	0.30	5.5	0.01	35.9	5.002	47.1	49.7	14.5	5.9	
						1120	0.20	3.6	0.01	35.4	8.459	37.8	80.6	7.0	3.9	
						1205	0.49	8.8	0.01	35.6	5.649	72.7	55.5	5.3	9.6	
						1308	0.89	15.8	0.01	35.5	6.433	73.8	62.6	2.4	17.2	
P. 2799.1a-d	VP	2527	0.07105	0.1	0.5×10^{-7}	736	0.64	80.7	-	250	0.174	99.9	3.5	16.7	31.9	66 ± 13Ma
B2						787	0.10	19.0	-	371	4.013	96.7	79.3	70.5	5.1	
						851	0.16	35.9	-	444	3.760	94.2	74.4	36.8	8.0	
						900	0.29	74.5	-	509	0.622	97.8	12.5	24.6	14.5	
						950	0.17	39.4	-	459	3.822	93.5	75.6	26.9	8.5	

Table II.8. Continued.

Sample	Locality	Run No	Weight	Weight %K	*40Ar $cm^3 g^{-1}$	Temp °C	$^{39}Ar_K$	$^{37}Ar_{Ca}$	$^{38}Ar_{Cl}$	Ca/K	$^{40}Ar/^{39}Ar_K$	%Atm ^{40}Ar	Age Ma	Error Ma	$\%^{39}Ar_K$	Total gas age
							{Vol. $x10^{-9}$ cm^3}									
P. 2799.1a-d						1030	0.18	32.3	-	354	8.272	85.3	159.9	38.1	9.0	
						1080	0.09	11.4	-	248	6.185	93.8	120.8	138.3	4.5	
						1123	0.10	11.9	-	243	5.275	95.5	103.6	81.1	4.8	
						1180	0.11	12.3	-	214	0.657	99.4	13.2	73.8	5.7	
						1228	0.16	13.0	-	157	12.734	85.0	240.5	50.4	8.1	
P. 2807.6b	PH	2528	0.07419	0.22	3.6×10^{-7}	690	0.8	8.4	-	21.6	99.2	99.2	29.9	12.8	5.9	40.8 ± 1.6 Ma
B2						795	0.9	12.8	-	27.0	92.3	92.3	38.1	8.9	7.3	
						856	1.6	23.2	-	29.5	70.4	70.4	38.3	5.5	12.0	
						914	2.2	34.3	-	30.5	53.2	53.2	42.5	2.9	17.2	
						960	1.9	28.7	-	29.9	60.8	60.8	45.7	2.2	14.6	
						1010	1.1	16.1	-	29.3	67.2	67.2	41.9	4.4	8.4	
						1060	1.2	17.2	-	29.1	70.1	70.1	41.0	5.3	9.0	
						1110	1.7	25.0	-	29.2	73.3	73.3	44.2	3.0	13.1	
						1160	0.9	13.3	-	28.6	85.0	85.0	36.6	3.2	7.1	
						1220	0.7	9.9	-	28.1	85.8	85.8	38.3	5.8	5.4	
P. 2811.12	PH	2530	0.07392	0.26	4.1×10^{-7}	615	0.49	3.0	-	12.2	1.573	93.6	31.5	13.6	3.2	40.3 ± 1.5 Ma
30-60						750	0.79	9.0	-	22.8	1.710	97.8	34.2	8.1	5.2	
B2						842	1.62	22.8	-	28.0	2.088	76.0	41.7	3.0	10.7	
						895	2.21	32.4	-	29.2	1.788	65.2	35.8	2.5	14.6	
						955	1.90	27.6	-	28.9	1.907	58.7	38.1	2.6	12.5	
						1005	1.48	21.0	-	28.2	1.789	66.3	35.8	4.6	9.7	
						1055	1.85	26.0	-	27.9	1.881	65.5	37.6	2.5	12.2	
						1100	1.87	26.5	-	28.2	2.337	73.1	46.6	3.8	12.3	
						1150	1.62	23.4	-	28.8	2.218	87.8	44.3	5.4	10.6	

Table II.8. Continued.

Sample	Locality	Run No	Weight	Weight %K	*40Ar $cm^3 g^{-1}$	Temp °C	$^{39}Ar_K$	$^{37}Ar_{Ca}$	$^{38}Ar_{Cl}$	Ca/K	$^{40}Ar/^{39}Ar_K$	%Atm ^{40}Ar	Age Ma	Error Ma	$\%^{39}Ar_K$	Total gas age
							{Vol. x10^{-9} cm^3}									
P. 2811.12						1200	0.66	9.6	-	28.8	2.274	93.0	45.4	6.6	4.3	
30-60						1250	0.70	10.1	-	28.7	2.756	92.4	54.8	14.0	4.6	
P. 2811.12	PH	2532	0.07521	0.29	4.8×10^{-7}	726	1.20	10.3	-	17.1	1.886	96.7	37.7	4.5	6.9	42.0±1.1 Ma
60-90						825	1.29	16.4	-	25.3	2.092	79.8	41.8	3.3	7.5	
B2						866	2.29	32.5	-	28.2	2.005	61.2	40.1	2.5	13.3	
						920	2.93	41.6	-	28.3	2.048	51.5	40.9	2.5	17.0	
						975	2.02	28.2	-	27.7	1.926	59.3	38.5	2.1	11.7	
						1026	2.10	28.9	-	27.4	1.864	64.4	37.3	1.9	12.2	
						1075	1.91	25.9	-	27.0	2.338	63.4	46.6	3.5	11.1	
						1125	1.63	21.8	-	26.6	2.244	75.4	44.8	3.7	9.5	
						1175	1.17	15.7	-	26.7	2.498	84.7	49.8	6.1	6.8	
						1225	0.70	9.5	-	26.8	2.589	91.0	51.6	7.6	4.1	
P. 3031.LH	FH	2531	0.07463	-	-	-	-	-	-	-	-	-	-	-	-	-
P. 3031.4L	FH	2526	0.07053	0.09	1.8×10^{-7}	750	1.61	127.9	-	158	1.890	98.9	37.8	3.9	32.8	52 ± 4 Ma
B2						800	0.86	74.3	-	172	2.165	96.1	43.2	5.1	17.5	
						850	0.43	11.9	-	55	2.310	91.2	46.1	20.3	8.8	
						900	0.51	9.9	-	39	3.586	84.0	71.1	12.2	10.3	
						950	0.41	6.4	-	31	4.328	77.9	85.4	14.4	8.4	
						997	0.22	3.7	-	34	4.905	82.4	96.5	27.4	4.4	
						1050	0.23	6.2	-	55	1.033	96.7	20.8	27.6	4.6	
						1119	0.26	16.6	-	128	2.373	96.6	47.3	33.6	5.3	
						1170	0.22	13.6	-	126	4.217	95.6	83.3	22.3	4.4	
						1225	0.17	8.7	-	99	2.530	96.7	50.4	34.1	3.5	

Table II.8. Continued.

Appendix III Sedimentological data

III.1 Volcaniclastic grain size terminology

Grain Size ϕ	Grain Size (mm)	Pyroclastic fragments	Pyroclastic lithology	Tuffites (Mixed pyroclastic-epiclastic)	Epiclastic Volcanic and/or non-volcanic
		Coarse			
-8.0	256	Blocks and bombs	Agglomerate		Conglomerate, breccia
		Fine		Tuffaceous conglomerate, tuffaceous breccia	
-6.0	64				
		Lapilli	Lapillistone		
-1.0	2				
		Coarse		Tuffaceous sandstone	Sandstone
+4.0	1/16	Ash	(ash) Tuff		
		Fine		Tuffaceous siltstone Tuffaceous mudstone, shale	Siltstone Mudstone, Shale
		100%		75%	25%
		(increase) ← Pyroclasts			
		(increase) →		Volcanic and non-volcanic epiclasts (and minor amounts of biogenic, chemical sedimentary and authigenic constituents	

Table III.1. Grain size limits for pyroclastic fragments (after Fisher and Schmincke, 1984).

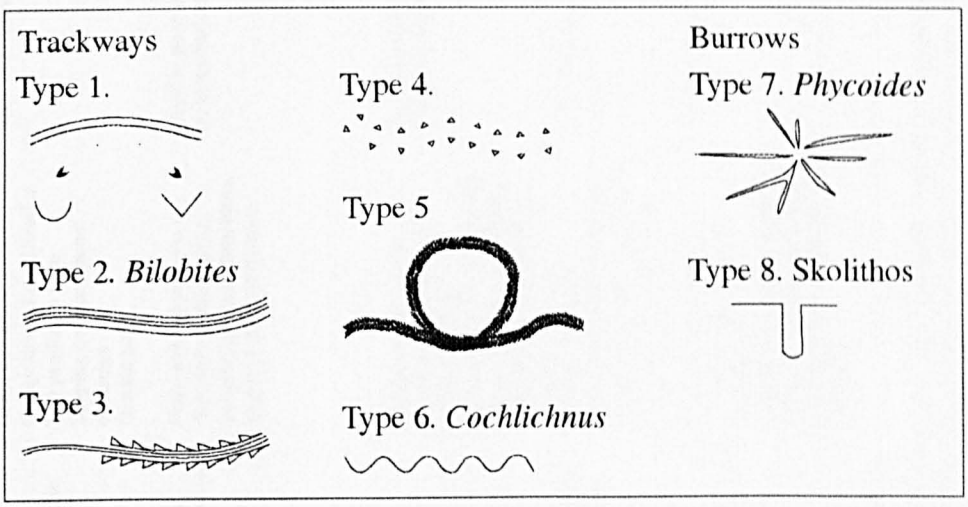

Figure III.1. Trace fossil types present in the Dragon Glacier flora, types defined in Table III.2.

Burrow	Description	Dimensions	Name	Interpretation
Type 1	Single, low sinuousity unlobed trail. U-shaped or V-shaped cross section.	W = 1.5 mm L= min 40 mm	?poorly preserved Diploichnites	Repichnial
Type 2	Low sinuousity, symmetrically bilobed trackway.	W = 2 mm L = min 70 mm	Bilobites or Diploichnites	Repichnial
Type 3	Low sinuousity furrowed trail with continuous triangular depressions arranged around the central furrow.	W = 8 mm L = 90 mm	?Ulmfolizia	Repichnial
Type 4	Alternate, roughly triangular imprints forming a low sinuousity trail.	W = 6 mm L = 65 mm	?Ulmfolizia	Grades into Type 4 Repichnial Grades into Type 3
Type 5	Bilobed track, with approximately orthogonal appendage grooves. The trace forms loops which cross cut earlier portions of the trackway.	L = min 220 mm Groove L = < 2 mm Loops < 70 mm diameter	?Siskemia	Paschichnial/ Repichnial
Type 6	Single furrow, highly sinuous trace with near perfect sinusoidal curve	L = min 120 mm w = 0.5 mm	Cochlichnus	Paschichnial
Type 7	Traces radiating from a central burrow	W = 22 mm.	Phycoides or Glockeria	Domichnia
Type 8	Simple cylindrical vertical burrows	W = 2.5 – 4 mm L = 10 - 20 mm	Skolithos	Domichnia

Table III.2. Trace fossils present in the Dragon Glacier flora.

Type of deposit	Overall geometry	Stratification	Sorting	Grading	Grain size	Other features
Pyroclastic fall	*Areal distribution* Fan shape or lobate Uniform thickness but Possible downwind thickness increase *Cross section* Wedge in transport direction Lensoid perpendicular to transport	Mantle bedding Grain size and Compositional stratification Top parallel to base Draping over or against obstacles Graded beds	Well-sorted Vary with distance	Normal and reverse often compositional	Ash to bombs Varies with distance from vent	Bomb sags Contacts may appear sharp if abrupt change in eruption conditions or gradational if deposition is slow
Subaqueous fallout	May be modified by water currents, regular to irregular fans, thicker toward source	Plane parallel beds Post depositional thickening, thinning and flow structures, load and slump structures	Good to poor dependent on bioturbation	Normal, from crystals and lithic- rich bases to shard-rich tops May be inverse graded if pumice is present		Commonly interbedded with terrigenous muds and silts Sharp basal contacts, upper contacts diffuse due to bioturbation Ancient layers often altered, to clays (montmorillonite) and zeolites
Pyroclastic flow	*Areal distribution* Topographically controlled Fan or lobate and valley fill *Cross Section* Valley profile shape	Flat top, base follows underlying surface, top parallel to base Structures in lee of obstacles Massive beds, graded beds, alignment and orientation bedding	Poorly sorted, possible coarse tail grading	Normal lithic grading and reverse pumice grading possible	Generally fine to coarse ash	May be welded
Pyroclastic surge	Blanket topography but generally more concentrated in topographic lows than air fall	Unidirectional flow structures, Stratification, anti-dunes, pinch and swell and chute and pool structures	Individual laminae well-sorted			Base Surge Bedding sags, convolute bedding, load casts and bedding sags, mudcracks, rills
Lahars	*Areal distribution* Topographically controlled Fan or lobate and valley fill *Cross Section* Valley profile shape	Flat top, base follows underlying surface, top parallel to base Structures in lee of obstacles Massive beds, graded beds, alignment and orientation bedding	Poorly sorted	Normal lithic grading and reverse pumice grading possible		Variable proportions of juvenile/ non-juvenile volcanic material Heterogeneous, lithics, boulders, carbonised organic material, fossil fumarole pipes

Table III.3. Features used to distinguish pyroclastic fall, flow and surge and lahar deposits (summarised from information in Fisher and Schmincke, 1984; Cas and Wright, 1987). NB All of the information summarised in this table is generalised and tends to vary according to the characteristics of individual eruptions, distance to source, composition etc.

Sample #	Area	Colour	Non-genetic grain size classification	Sorting/ support	Angularity	Textures	Composition		Alteration	Interpretation
P.933.2	E. Fossil Hill	Purple/ purple-brown	Siltstone to fine sandstone 0.1 – 0.4 mm 0.2 av. < 0.19 mm	Well sorted, clast supported	Angular – subangular	Laminated to massive Mottled.	PVC Crystals	< 15 % angular fragments ?glass shards < 50 % Plagioclase 5 – 10 % Clinopyroxene < 30 % Opaques		Reworked, clast supported crystal-rich siltstone
P.935.22	E. Fossil Hill	Purple/ purple-brown	Medium sandstone to granule conglomerate 0.38 - 2 mm av. 0.5 mm	Poorly sorted, - matrix supported	Subangular	Planar fabric defined by plant material.	Lithics Matrix Crystals	< 15 % Basic-intermediate < 60 % cryptocrystalline ash with microphenocryt plagioclase and opaques 10 % Plagioclase 5 – 10 % Clinopyroxene 10 % Opaques		Reworked, matrix supported crystal- and lithic-rich sandstone
G.458	E. Fossil Hill	Purple/ purple-brown	Fine sandstone to granule conglomerate 0.19 – 3 mm av. 1 mm	Poorly sorted matrix supported, 30 – 70 % matrix	Angular – subrounded	Bed parallel clast alignment Grading from lithics to crystals in some samples	As P.3031.2		Calcite infills cavities	Equivalent to P.3031.2
P.3031.2	W. Fossil Hill	Purple/ purple-brown	Granules to small pebble conglomerate 0.5 – 6 mm av. 1.5 mm	Poorly sorted, clast supported	Rounded-subangular	Massive or ?graded	PVC Lithics Crystals	< 30 % Scoria 15 % Basaltic andesite < 40 % Andesite < 2 % Clinopyroxene	Cavities < 15 % infilled with zeolite after smectite/chlorite	Reworked, clast-supported lithic breccia
P.3031.3	W. Fossil Hill	Grey/ dark brown	Very fine siltstone to mudstone < 0.19 mm	Very well sorted, matrix supported	Subangular	Massive to weakly laminated. Mottled ?bioturbated. Streaks of organic material in matrix.	Crystals	25 % Plagioclase 10 – 15 % Clinopyroxene 25 % Opaques	Mottling	Reworked, matrix supported crystal-rich siltstone
P.3031.4 Lower	W. Fossil Hill	Blue-grey	Granule conglomerate to small pebble conglomerate 0.2 – 9 mm av. 3 mm	Poor to moderate sorting, matrix to clast supported	Subangular to subrounded	Normally graded	PVC Crystals Matrix	< 40 % Scoria < 25 % Clinopyroxene < 25 % Plagioclase Possible orthopyroxene Locally < 50 %, comprising siltstone from P.3031.3	< 10 % Zeolite cavity fill, after smectite/chlorite Crystals are often heavily altered or weathered	Reworked, crystal and lithic breccia to conglomerate
P.3031.4 Upper	W. Fossil Hill	Blue-grey	Coarse sandstone to granule conglomerate 0.5 – 2 mm av. 1 mm	Slightly better sorting than P.3031.4L, matrix supported	Subangular to subrounded	Normally graded	As P.3031.4L except higher proportion of crystals to clasts ~ 60:40 Matrix < 40 %		< 5 % Zeolitised cavities, crystals often highly weathered/ altered	Reworked, crystal and lithic breecia to conglomerate

Table III.4. Thin section descriptions of plant-bearing lithologies discussed in this thesis. PVC – primary volcanic clasts

Sample #	Area	Colour	Non-genetic grain size classification	Sorting/ support	Angularity	Textures	Composition		Alteration	Interpretation
P.3031.5	W. Fossil Hill	Grey with green and orange staining	Coarse sandstone to small pebble conglomerate 0.5 – 6 mm av. 0.75 mm	Poorly sorted, matrix supported	Subangular	Massive, difficult to distinguish grain boundaries Streaks of organic material	PVC Lithics Matrix	5 – 10 % Scoria Andesite, basaltic-andesite, ?basalt 30 – 40 %, Crypto-crystalline ash with microcryst clino-pyroxene and plagioclase	Pervasively weathered/ altered with abundant iron staining Fractures infilled with iron oxide	Lithic rich sandstone to breccia. Reworked, ?possibly partially derived from underlying units,
P.3031.6	W. Fossil Hill	Purple – reddish black	Fine to coarse sandstone 0.19 – 0.75 mm av. 0.2 mm Rare granules to small pebbles < 5 mm	Poorly sorted to well sorted, matrix supported < 60 %	Subangular	Some bed parallel alignment of plagioclase long axis Normally graded, also fining from lithics at base to crystals at top	PVC Lithics Crystals Matrix	< 2 % ?Altered glass spherules 5 – 10 % Basaltic andesite < 25 % Plagioclase 20 % Clinopyroxene < 1 % ?Altered orthopyroxene < 60 % Opaque cryptocrystalline	Single infilled fracture with ?smectite	Reworked, crystal rich sandstone
P.212.7	Rocky Cove	Light brown/ green	Fine sandstone to granule conglomerate 0.19 – 4 mm av. 0.19 mm	Well sorted, ?clast supported	Angular – subangular,	Massive Rounded pumice grains	PVC Crystals	70 % Sideromelane 15 % Pumice 10 % Opaques 5 – 10 % Clinopyroxene 2 – 5 % Plagioclase	Smectite and ?zeolite infills vesicles of pumice	Lacustrine deposited shard-rich sandstone. Primary airfall tuff.
P.212.8	Rocky Cove	Green	Siltstone to fine sandstone < 0.19 mm Rare granules < 3 mm	Moderate, poorly sorted, matrix supported	Angular - subrounded	Laminated, truncated laminae Normally graded Organic material	Crystals Matrix	5 – 20 % Plagioclase 5 – 10 % Clinopyroxene 2 – 5 % Opaques < 95 % Cryptocrystalline matrix with microcryst plagioclase, clinopyroxene and opaques	Clinopyroxene generally smectised, minor smectite alteration of matrix	Reworked, matrix dominated crystal rich siltstone to fine sandstone
P.2145.2	Barton Peninsula	Purple/ grey	Siltstone to medium sandstone < 0.19 – 0.38 mm av. 0.19 mm	Moderate – well sorted, matrix to clast supported	Angular - subrounded	Laminated and cross laminated, laminae often truncated	Crystals Matrix	< 50 % Plagioclase < 20 % Opaques < 5 % Clinopyroxene < 30 % Cryptocrystalline ash matrix	Smectite alteration of groundmass, minor chlorite Some calcitisation of plagioclase Purple ?Mn-stain	Reworked, crystal rich siltstone to sandstone

Table III.4. Continued.

Sample #	Area	Colour	Non-genetic grain size classification	Sorting/ support	Angularity	Textures	Composition		Alteration	Interpretation
P.232.26	Potter Cove Compression	Purple	Medium sandstone to small pebble conglomerate 0.38 – 4.5 mm av. 0.5 mm	Poorly sorted, dominantly clast supported	Subangular to subrounded	Weakly laminated (1 - 4 mm thick), defined by alternations of purple siltstone and grey sandstone. Minor long axis alignment of clasts.	PVC Lithics Crystals	< 2 % Opaque scoria < 75 % Plagioclase dominated ?basaltic clasts < 15 – 20 % Plagioclase 2 – 5 % Clinopyroxene	< 15 % Heavily calcitised grains. Purple coloration due to iron oxide staining	Reworked, lithic-dominated sandstone to conglomerate
P.232.70i	Potter Cove Impression	Green	Fine sandstone 0.19 – 0.25 mm	Well sorted, clast supported	Angular to subrounded	Faintly laminated to massive. common organic material	Lithics Crystals	< 30 % Plagioclase dominated ?basaltic clasts < 2 – 10 % Opaques < 40 % Plagioclase < 2 % Clinopyroxene	< 25 % Smectite	Reworked, crystal-rich sandstone
G53	Dufayel Is.	Green	Fine to medium sandstone 0.19 – 0.38 mm av. 0.25 mm Rare granules < 2 mm	Generally well sorted, ?clast supported	Angular to subrounded	Bed parallel clast alignment	PVC Crystals	< 80 % Glass shards < 5 – 10 % Plagioclase < 2 % Clinopyroxene < 10 % Opaques < 1 % Quartz	Recrystallisation of matrix Abundant smectite/ chlorite alteration	Shard-rich sandstone. Primary airfall tuff.
G.47.2	Cytadela/ Platt Cliffs	Green	Fine sandstone to granule conglomerate 0.25 – 2 mm av. 0.5 mm	Poorly sorted. dominantly clast supported	Angular to subrounded	Massive Original porosity < 25 % Vesicular	PVC Crystals	< 80 % Glass shards 2 – 10 % Clinopyroxene 10 % Plagioclase < 2 % ?Orthopyroxene 2 % Opaques	Cavities are chloritised No calcitisation	Shard-rich sandstone. Primary airfall tuff.
G.50.12	Platt Cliffs	Green	Medium to very coarse sandstone 0.38 – 1.5 mm	Moderately sorted, clast supported	Angular to subrounded	Graded Original porosity Vesicular	PVC Crystals	< 85 % Glass shards 2 – 5 % Clinopyroxene 2 – 5 % Plagioclase < 5 % Opaques < 1 % ?Orthopyroxene	Grains commonly calcitised, with some entire replacement of plagioclase crystals	Shard-rich sandstone. Primary airfall tuff.
G.309.14	Cytadela/ Platt Cliffs	Green	Fine sand – coarse sand 0.19 – 1 mm av. 0.25 mm	Moderate to well sorted, matrix to clast supported	Angular to subrounded	Faint lamination Streaked organic material Original porosity Faint bedding Vesicular	PVC Crystals Matrix	< 70 % Glass shards 1 – 7 % Clinopyroxene < 20 % Plagioclase < 2 % ?Orthopyroxene 2 % Opaques Locally < 80 % cryptocrystalline ash	Heavy areas of smectisation 5 – 10 %	Shard- and crystal-rich sandstone. Slightly reworked ash fall tuff, with some concentration of plagioclase.

Table III.4. Continued.

Sample #	Area	Colour	Non-genetic grain size classification	Sorting/ support	Angularity	Textures	Composition		Alteration	Interpretation
P.236.21	Point Hennequin DGF-3	Grey-brown	Granules to small pebble conglomerate 0.5 – 9 mm av. 1 mm	Poorly sorted, matrix supported	Angular to subrounded	Massive	PVC Matrix	< 60 % Scoria < 20 % Glass shards < 10 – 20 % Plagioclase < 5 % Clinopyroxene < 1 % Opaques	Smectisation Scoria vesicles infilled with smectite and ?alkali feldspar	Primary, matrix supported scoria- and glass-rich breccia
P.2810	Point Hennequin DGF-5	Pink and grey	Siltstone to fine sandstone, rare medium sandstone < 0.19 mm to < 0.38 mm	Poor to well sorted	Subangular to subrounded	Bedded to laminated, laminae massive or normally graded. Organic material dispersed through matrix.	Crystals PVC Matrix	< 30 % Plagioclase < 10 % Clinopyroxene < 2 % glass shards < 60 % Microcryst plagioclase, clinopyroxene and opaques in cryptocrystalline ash material		Reworked, crystal-rich siltstone to sandstone
P.3007	Point Hennequin DGF-6	Light brown	Fine siltstone to fine sandstone 0.19 mm	Matrix supported Well sorted, variable matrix to clast supported	Angular	Diffusely laminated	PVC Crystals Matrix	< 60 % Glass shards (< 20 % vesicularity) < 1 % Opaques 10 – 25 % Plagioclase < 2 % Organic material < 40 % cryptocrystalline material	Recrystallisation, large patches of matrix with undulose extinction Iron oxides present in matrix, some smectite	Shard- and crystal-rich sandstone. Primary lacustrine deposited airfall tuff. Similar to P.1404.9.
P.1404.2b	Point Hennequin Smok-1	Pale green	Medium to coarse sandstone 0.5 – 0.75 mm av. 0.6 mm	Moderate to well sorted, clast supported	Angular to subangular	Massive Infilled cavities	PVC Crystals	50 – 70 % Sideromelane 5 – 10 % Plagioclase Possible single heavily altered orthopyroxene < 2 % Opaques	Calcite, smectite and ?chlorite infill of pore cavities	Primary, shard-rich sandstone
G.9.3	Point Hennequin DGF-6	Yellow brown	Siltstone to fine sandstone < 0.19 mm	Moderate to well sorted, matrix to clast supported	Angular to subrounded	Slight planar fabric and long axis alignment of clast. Streaks of organic material in matrix.	PVC Crystals Lithics	70 % Glass shards 10 % Plagioclase < 5 % Clinopyroxene 2 – 5 % Opaque grains < 40 % Basaltic andesite clasts comprising plagioclase, clinopyroxene and opaque grains		Primary – reworked ?lake deposited primary ash, shard- and lithic-rich sandstone

Table III.4. Continued.

Sample #	Area	Colour	Non-genetic grain size classification	Sorting/ support	Angularity	Textures	Composition		Alteration	Interpretation
P.1404.9	Point Hennequin DGF-5/6	Yellow brown	Fine – medium sand 0.19 – 0.25 mm av. 0.2 mm	Well – moderate sorting ?Clast supported	Angular Subangular	Cavities common 5 – 10 % Massive, matrix slightly recrystallised with large areas of undulose extinction	Uncertain because of matrix recrystallisation PVC Crystals	? < 40 % Glass shards slightly vesicular ?Altered clinopyroxene Plagioclase	Smecitite common throughout matrix	Shard-rich sandstone. Low degree of reworking ?lake deposited primary ash
P.2799.19	Vaureal Peak	Green	Fine to coarse sandstone 0.19 – 0.5 mm av. 0.25 mm	Poor to well sorted, clast to matrix supported	Rounded - subangular	Laminated to massive	PVC Lithics Crystals Matrix	< 1 % Scoria Single angular pumice fragment < 35 % Basic – intermediate volcanics < 11 % Plagioclase 6 – 7 % Opaques ?heavily altered Cpx < 50 % cryptocrystalline ash	Some smectisation of matrix. Some plagioclase and pyroxene highly degraded Fe-oxide staining	Reworked, matrix supported lithic-dominated sandstone.

Table III.4. Continued.

	Description	Interpretation
Unit 2 P.3030, P.3034, P.3036 - 3 m	Sections P.3031.2, P.933.2, P.935.22: Unit 2 is the most extensive unit at Fossil Hill. Basal contact erosive, upper contact not clearly exposed ?erosional. East end of Fossil Hill: Well laminated (0.1 – 6 mm thick) and bedded (9 – 24 mm), purple-brown mudstones and thin white siltstones. Thin interbeds (rarely < 0.75 m thick) of erosively based, poorly sorted, ±normally graded sandstones and breccias (clast size < 15 mm) are present with gradational upper contacts. Sandstone is clast supported with ≤25 % matrix and ≤ 75 % clasts and the matrix comprises white silt, rarely purple mudstone. Low angle cross sets suggest west to east transport. Dislocated slabs with lunate and elongate trough ripples (λ = < 200 mm, W = 6 cm, H = < 10 mm) are present at P.3030. A second set of troughs has an orthogonal orientation suggesting conditions of multidirectional flow. Flow structures include drag marks caused by plant stems (preserved in-situ) and rare flute casts. Bioturbation comprises common repichnial-type low sinuousity, bilobed horizontal traces simple unlobed traces (see also Yang and Shen, 1999). White siltstone balls (< 2 mm) commonly form in the underlying purple mudstones at P.3034 and P.3036. The contacts between the two sediment types are depositional, not erosive, suggesting sediment loading. Rare vertically-oriented, elliptical burrowing traces cross-cut the laminations. Western end of Fossil Hill: (e.g. P.3031) dominated by blue-grey to brownish purple, fine lithic and crystal-rich breccia to coarse sandstone beds, with minor fine grained siltstones. Iindividual beds laterally discontinuous. Rare sinuous bioturbation traces are present. Leaf and stem impressions, ±bird footprints, are commonly preserved in the mudstones and less frequently in coarse sandstones. Plant fossils are less abundant and less well preserved, than in Unit 3.	Eastern sections: The fine grain size and lamination suggest low energy lacustrine sedimentation. Alternations of fine mudstone and siltstone with soft sediment deformation are consistent with suspension fall out. Central sections: Ripples and flute casts observed at P.3031 are consistent with turbidity current deposition. Bird footprints imply extremely shallow conditions of sedimentation i.e. a mud flat or shallow water marginal environment. Western end: Sandstone and breccias with laterally discontinuous laminae and poor development of flow structures are interpreted as graded, stratified hyperconcentrated flow deposits. The transition from coarser grained sediments at the western end of the hill to thinner fine grained sediments in the east suggests a transition from proximal to distal deposition, which is also consistent with the W→E palaeocurrent indicators (cf Unit 1 flow direction). However the bird footprints imply shallow conditions and proximal shoreline conditions. A shallow-water, and therefore well-oxygenated, depositional environment would be able to rapidly degrade organic leaf material, explaining the low density of material preserved in this horizon.
Unit 1 - 4 – 5 m	No thin section. Basal boundary not exposed, upper boundary erosive. Divided into a massive lower section ~ 2 - 4 m and upper 2 m stratified section that are separated by an erosion surface. Unit thickness increases to the south. The unit comprises brownish purple breccia. Clasts size (10 – 150 mm av. 15 mm). Poorly sorted and matrix supported, becoming clast supported at the top. Matrix grades from fine sandstone to siltstone. Reverse grading of grey ?pumice clasts was observed to south of Fossil Hill, with coarse sand-grade sediments and carbonised wood being deposited at the same stratigraphic level. Lithic clasts are normally graded. To the north-west the material is diamictite with < 50 mm pebbles in a fine grained matrix (< 10 mm av. 1 mm). The matrix grades normally from granules to fine sand. Clasts comprise fine grained, plagioclase-rich, basic to intermediate volcanic clasts and fine grained vesicular grey pumice clasts. Clast imbrications in the southern outcrops yield an azimuth of 165°, suggesting a NNW→ SSE flow sense, but the unit shows an overall thickening to the south, suggesting that the material had a southern source. The middle section of Unit 1 is organic rich, sometimes shaley and Fe-stained. Fragments of vitreous compressed, carbonised wood (L = < 500 mm, Thickness = < 30 mm) are preserved in bed parallel orientation. Upper Unit 1 is angular to rounded, moderate to well sorted, clast supported (~ 5 % matrix), stratified and normal graded, sometimes reverse graded, arranged in metre scale fining-up packages. Clasts comprise basic-intermediate volcanic lithic clasts and juvenile volcanic material. Rare poorly developed flow structures, suggest current action with an ENE-WSW flow sense. Bed surfaces display long wavelength undulations, λ ~ 5 m that are suggestive of mantle bedding however abundant internal erosion surfaces argue for a flow related origin. To the south of Fossil Hill Lower Unit 1 is overlain and ?injects into lavas.	Lack of welding, the high proportion of silt/mud matrix and density stratification of carbonised wood suggests that Lower Unit 1 was deposited by a low temperature debris flow deposit ?lahar (Shen, 1994; Xue *et al.*, 1996). Poorly defined flow structures, horizontal and rare low angle stratification and internal scour surfaces in Upper Unit 2, are more consistent with normal dilute stream flow deposition or possibly lateral accretion surfaces (Smith, 1986, 1987; Smith and Lowe, 1991). Possibly represents the final stages of debris flow deposition. Injection of sediments into the plagiophyric based lavas suggests that the lavas were erupted prior to sediment lithification i.e. shortly after deposition. This would imply a proximal setting for Unit 1 (also suggested by the composite lapilli deposits described above).
Basal lava succession	Basic-intermediate lavas of the Lower sequence (Smellie et al., 1984) underlie the Fossil Hill sediments. The upper boundary is an erosional unconformity (Shen, 1994; Xue et al., 1996). Two bluish purple, friable outcrops comprising clast supported, normally graded and plagioclase rich composite lapilli (4 – 15 mm diameter), represent volcaniclastic sediments intermediate between the basal lavas and the sediments. The basal lavas have a blue amygdaloidal, plagiophyric, brecciated base, which contains rare, very fine-grained volcanic clasts and have an irregular outcrop pattern, hummocky bases and form isolated tongues or lenses, with an ENE-WSW orientation, suggesting a possible palaeoflow direction.	Composite lapilli are formed by cinder cones or maars during strombolian and phreatomagmatic activity (e.g. Fisher and Schmincke, 1984). They are proximal volcanic deposits. The composite lapilli may be related to the lavas on the basis of colour and abundant plagioclase.

Table III.5. Detailed sedimentary descriptions of the Great Wall Bay Submember at Fossil Hill.

	Description	Interpretation
Unit 6 - > 1 m	Section P.3031.6: Reddish purple, angular, poorly sorted, finely laminated siltstone with thin interbeds of moderate to well sorted pebble breccia. Matrix supported. Upper boundary erosional, thickness unconstrained. **No plant material was found in this unit, although Shen (1994) described leaf impressions of Nothofagus sp.**	Planar lamination and fine grain size suggests lacustrine deposition from suspension fallout. Coarse interbeds with an erosive base are interpreted as turbiditic sandstones. This unit is very similar to outcrops of Unit 2 at the west end of Fossil Hill.
Unit 5 - < 1.5 m	Section P.3031.5: Two outcrops of poorly exposed orange and green brown crystal and lithic rich sandstone and breccia that is grey on fresh surfaces. Matrix supported, moderate to poorly sorted and subangular. Basal and upper contacts not observed. **Plant material comprises poorly preserved carbonised angiosperm, gymnosperm and fern fragments.**	Uncertain origin. The grey coloration of the sediment is similar to that of Unit 3. The disjunct distribution of the two portions of the unit are suggestive of channelised deposition and could represent two incised fluvial units
Unit 4 - P.3031.4 - 2.5 m	Sections P.3031.4U/.4L: Indurated blue-grey, normally graded coarse crystalline and scoria-rich, basal breccia. Erosively based. Overlain by thin interbeds of laminated fossiliferous mudstones and coarse crystal and lithic sandstone (similar in appearance to Unit 2). The basal breccia wedges out laterally to the centre and north of Fossil Hill from a maximum thickness of 1.4 m at the western end (P.3031). To the north it forms a prominent bed < 0.47 m thick, divided into wedges of material ~ 5 m in length, that resemble low angle lateral accretion surfaces. Internally the wedges have a complex structure including planar laminations and small trough like features ?ripples. Some well preserved plant fossils are exposed in internal fine grained surfaces, including trifoliate leaves that suggest low energy deposition or a short transportation distances since they should easily disaggregate. **Plant fossils are abundant in the thin purple siltstone that caps the basal breccia at P.3030. The angle of preservation varies from bed parallel to orthogonal. Rarely the leaves are preserved as impressions in small mudstone intercalations within the coarser sandstone beds.**	The laterally discontinuous nature of the normally graded basal breccia is suggestive of hyperconcentrated flood flow deposition while the presence of fine grained siltstones, rare burrows, plane lamination and possible ripple casts is more consistent with waning floods and ephemeral lake deposits (Smith, 1987) or possible fluvial sequences. Repeated turbidite deposition could produce similar deposits, although the general fining up of the unit is suggestive of a single event under waning flow conditions. The upper part of the unit with fine sandstones/breccias and mudstones is also consistent with the waning portion of hyperconcentrated flood flow deposition or fine grained turbidites (Smith, 1987). The basal breccia unit thins to the east and north suggesting a west or south west source.
Unit 3 - P.3032 - < 0.5 m	Section P.3031.3: Laterally discontinuous bed, only present on the south side of the summit area. Dark grey to green very well sorted crystal rich mudstone to siltstone sometimes Fe-stained. Faintly laminated (0.1 – 6 mm), defined by streaks of carbonised material massive mudstone, which coarsens eastwards to fossiliferous siltstone at P.3032. Upper boundary erosional, basal contact not observed. Thins laterally towards the east, west and north. At P.3031, Unit 3 is an extremely fine grained grey-brown Occasional subrounded green ?pumice or juvenile volcanic clasts are present within the samples. **Abundant, well preserved carbonised plant compressions form leaf mats. Fossils comprise angiosperm and conifer leaves, stems, seeds, cone scales and rare moss. Some organic material is preserved. A single slab yields well rounded and sorted fragments of stem material ~1.5 cm in diameter suggesting moderate transport.**	The colour, grain size and style of plant preservation differs from the overlying and underlying units suggests a different sediment source or a change in redox conditions. In contrast to Shen (1994) the unit is interpreted as a wedge of material which thins out to the north, east and west. Probably as a result of erosion by the overlying Unit 4. Preservation of compressed organic material suggests low oxygen conditions. The resumption of sedimentation of a similar style to Unit 2 in the overlying Unit 4 supports a model of rapid deposition and burial of a large quantity of organic material perhaps during a single sedimentary event.

Table III.5. Continued.

Appendix IV Derivation of streamside index

IV.1 Streamside index

The streamside index used in this thesis to provide a simple qualitative measure of the taphonomic bias towards streamside vegetation in these floras. Higher values equate to a greater proportion of supposed streamside taxa. The index is derived in a similar fashion to the leaf size index (Wolfe and Upchurch, 1987).

Streamside index (SI) = 3 x %Stenophyll + 2 x %Compound + 0.5 x %Asymmetric bases

The different leaf types are weighted based on their inferred affinity for streamside settings, with asymmetric bases scoring lowest because they may or may not indicate a compound leaf species, a morphology associated with streamside settings. Stenophyll leaves are deemed to be most indicative of streamside vegetation and are therefore given the highest multiplier. It should be stressed that this is a very imprecise method and should not be used as a definitive guide. Rather it is a method for comparing the relative streamside signal from across a range of floras.

Appendix V Plant Morphotypes

V.1 Entire margined morphotypes

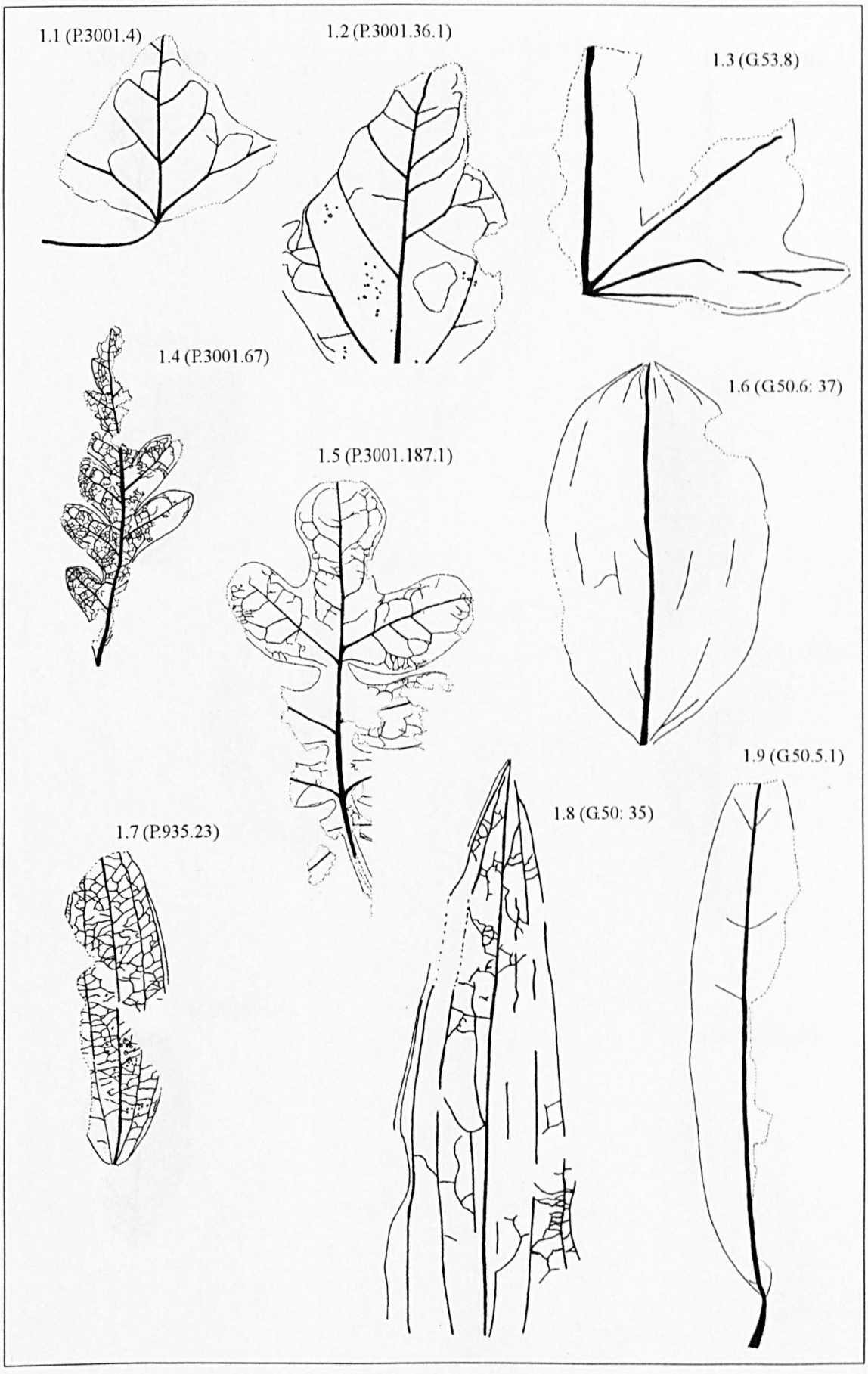

Figure V.1. Camera lucida drawings of entire margined morphotypes 1.1 - 1.9, showing major venation features. x1.

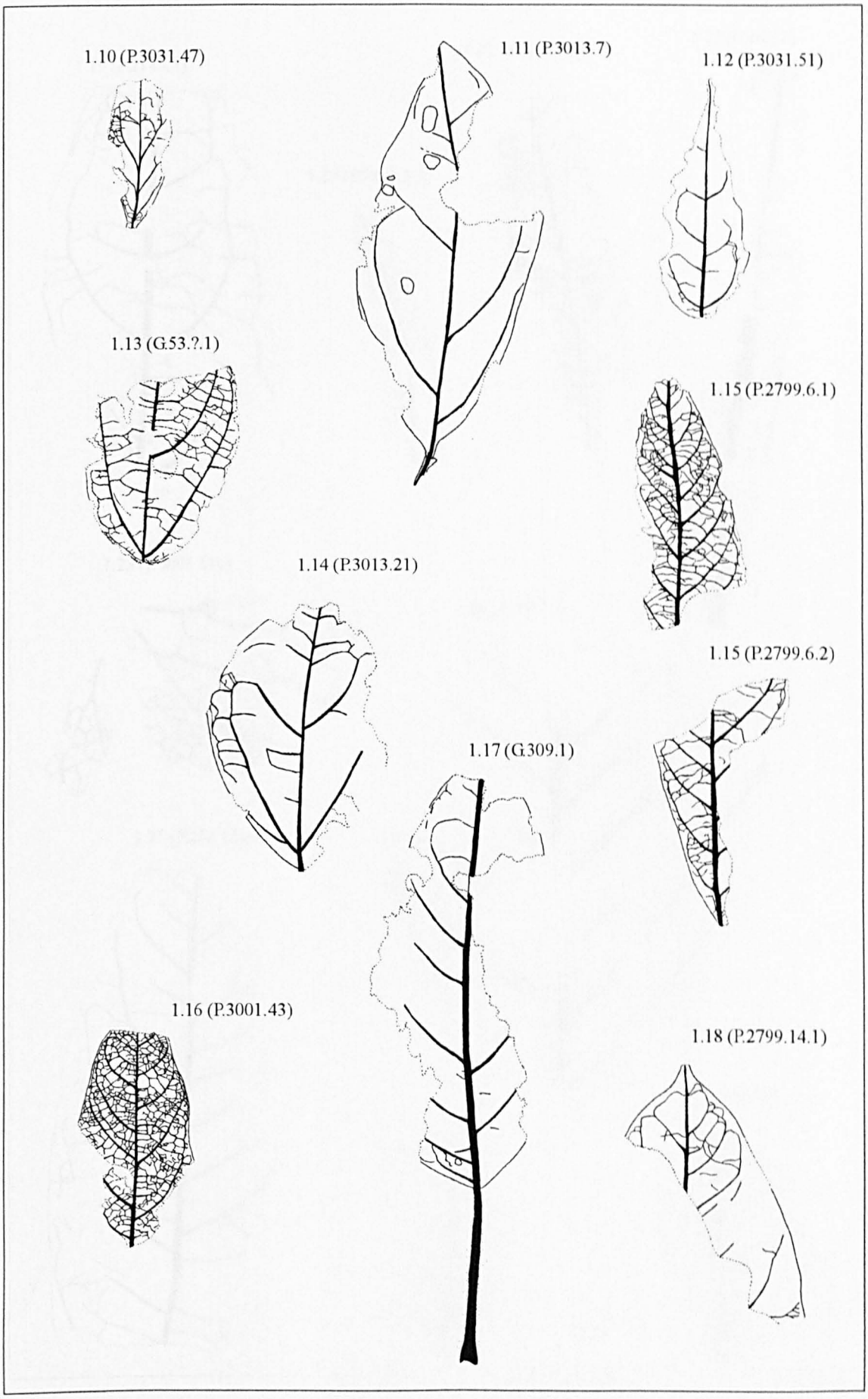

Figure V.2. Camera lucida drawings of entire margined morphotypes 1.10 - 1.18, showing main features of leaf architecture. x1.

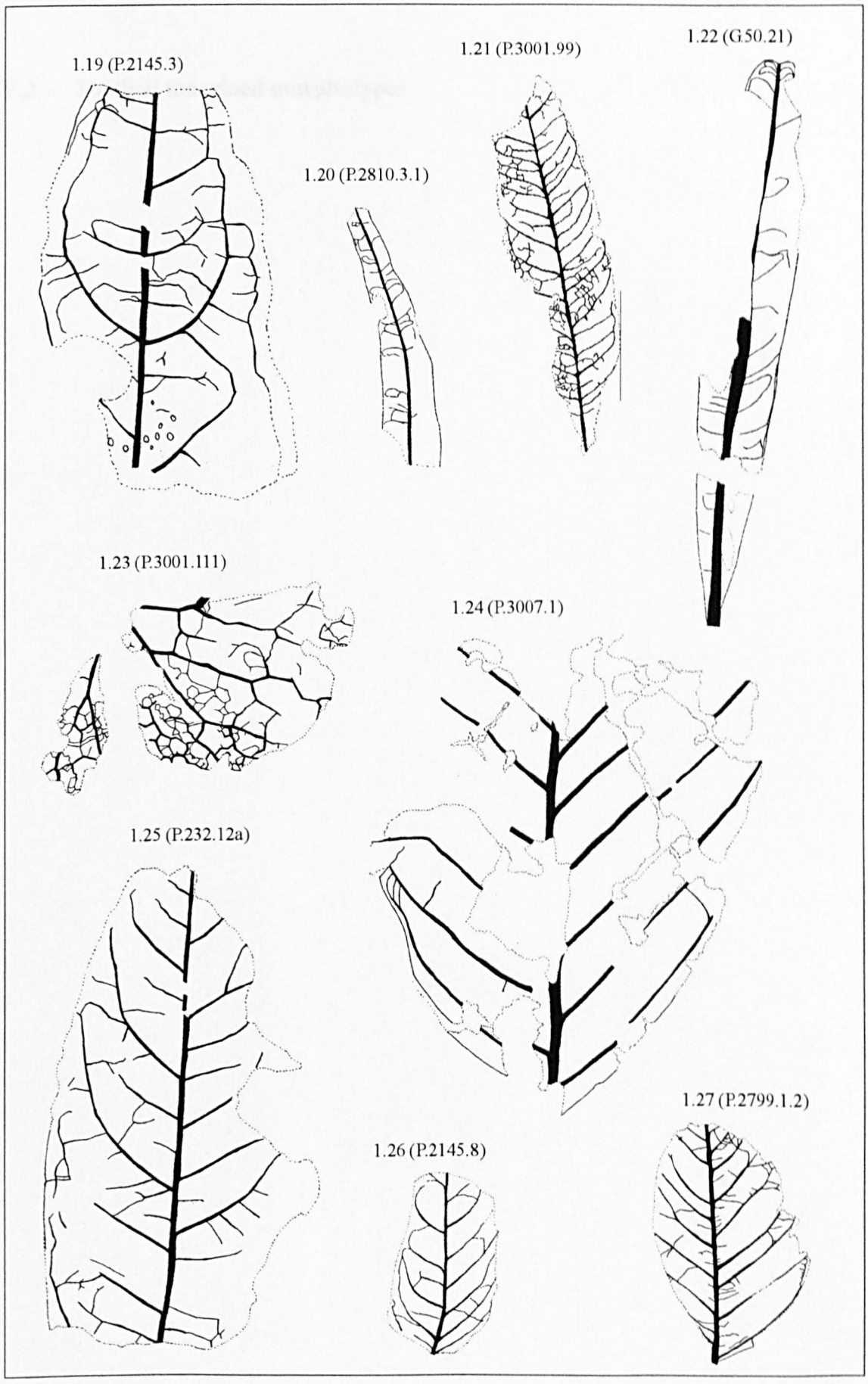

Figure V.3. Camera lucida drawings of entire margined morphotypes 1.19 - 1.27. x1.

V.2 Toothed margined morphotypes

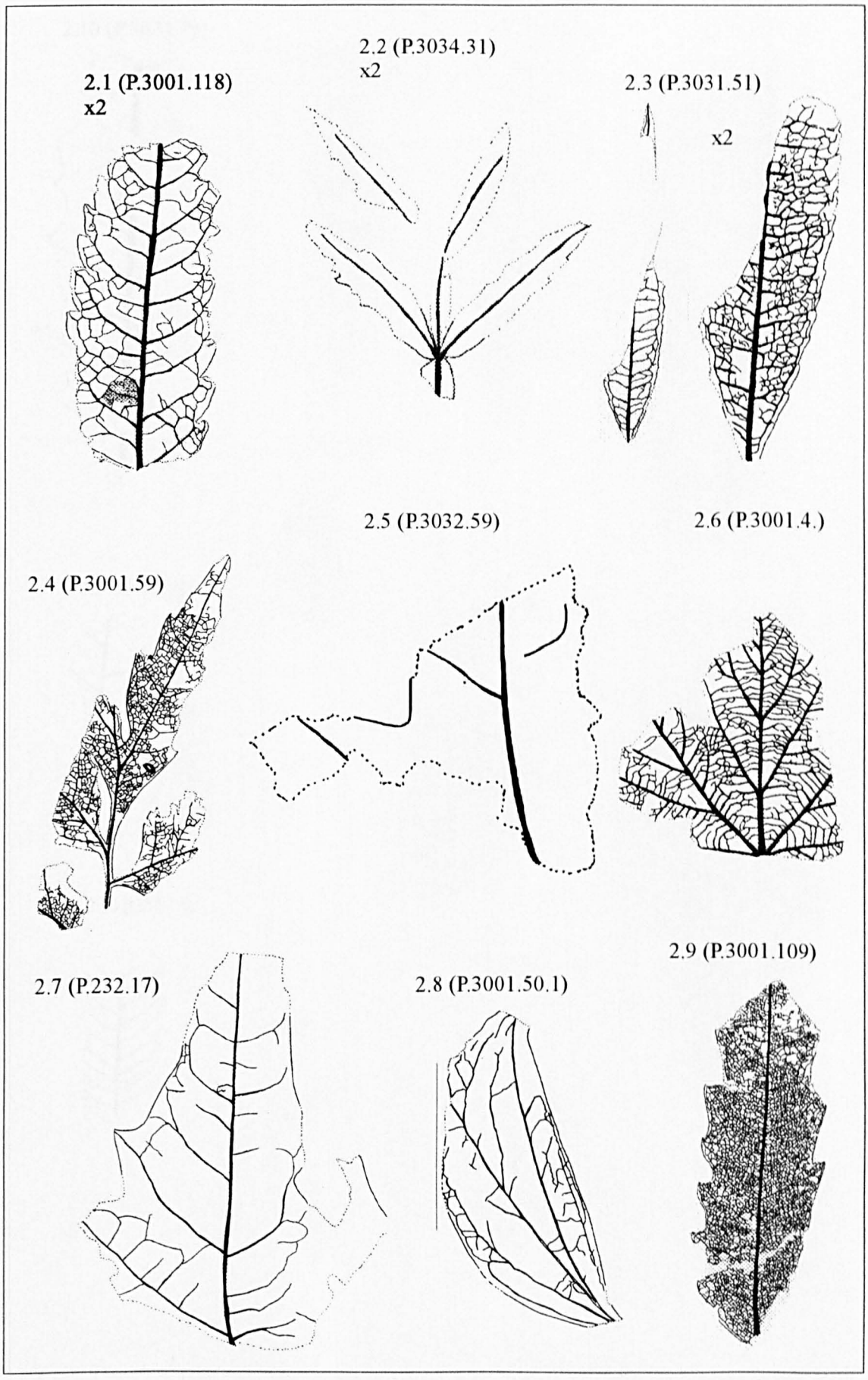

Figure V.4. Camera lucida drawings of toothed margined morphotypes 2.1 - 2.9. x1 unless otherwise stated

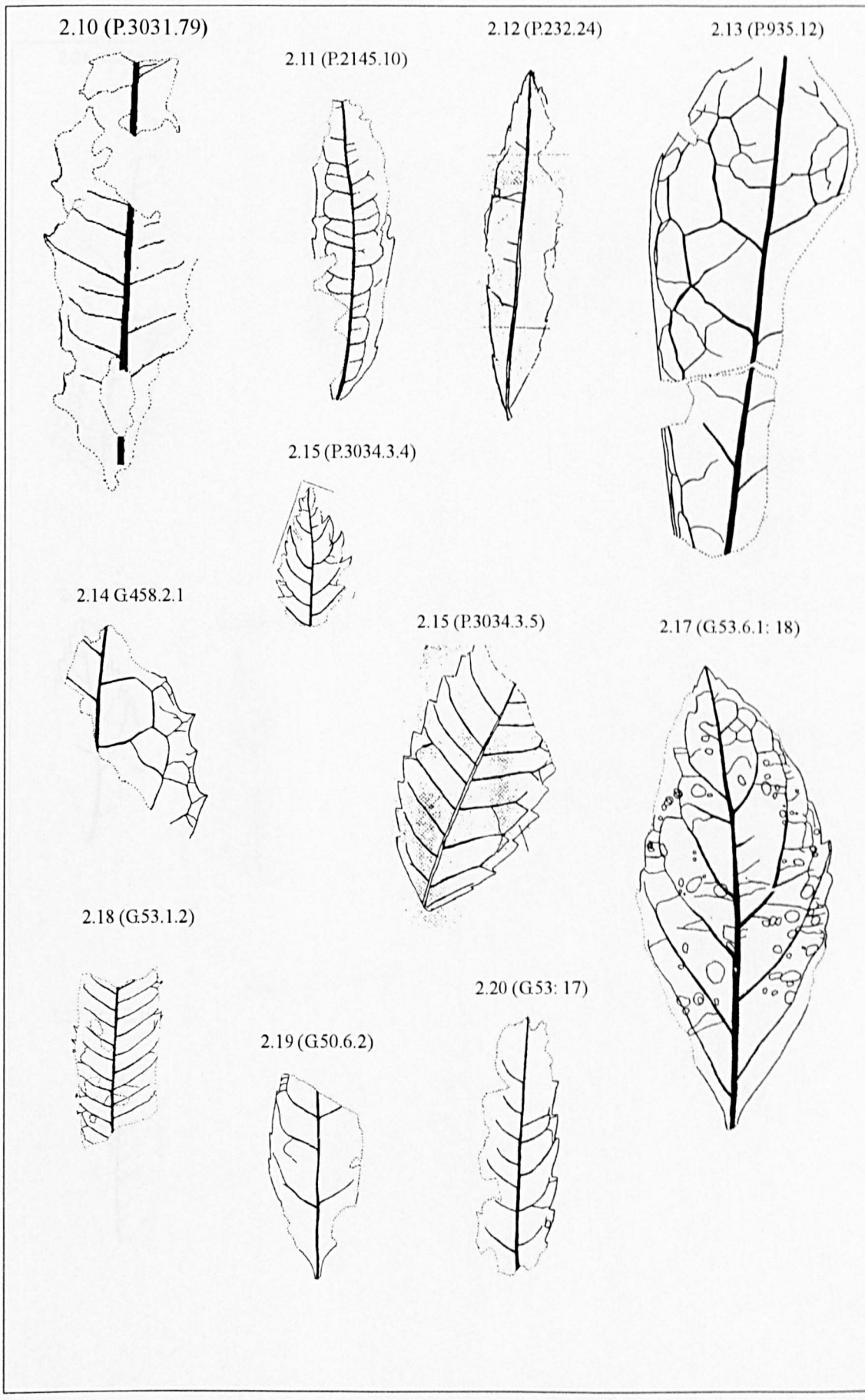

Figure V.5. Camera lucida drawings of toothed margined morphotypes 2.10 - 2.20. x1 unless otherwise stated.

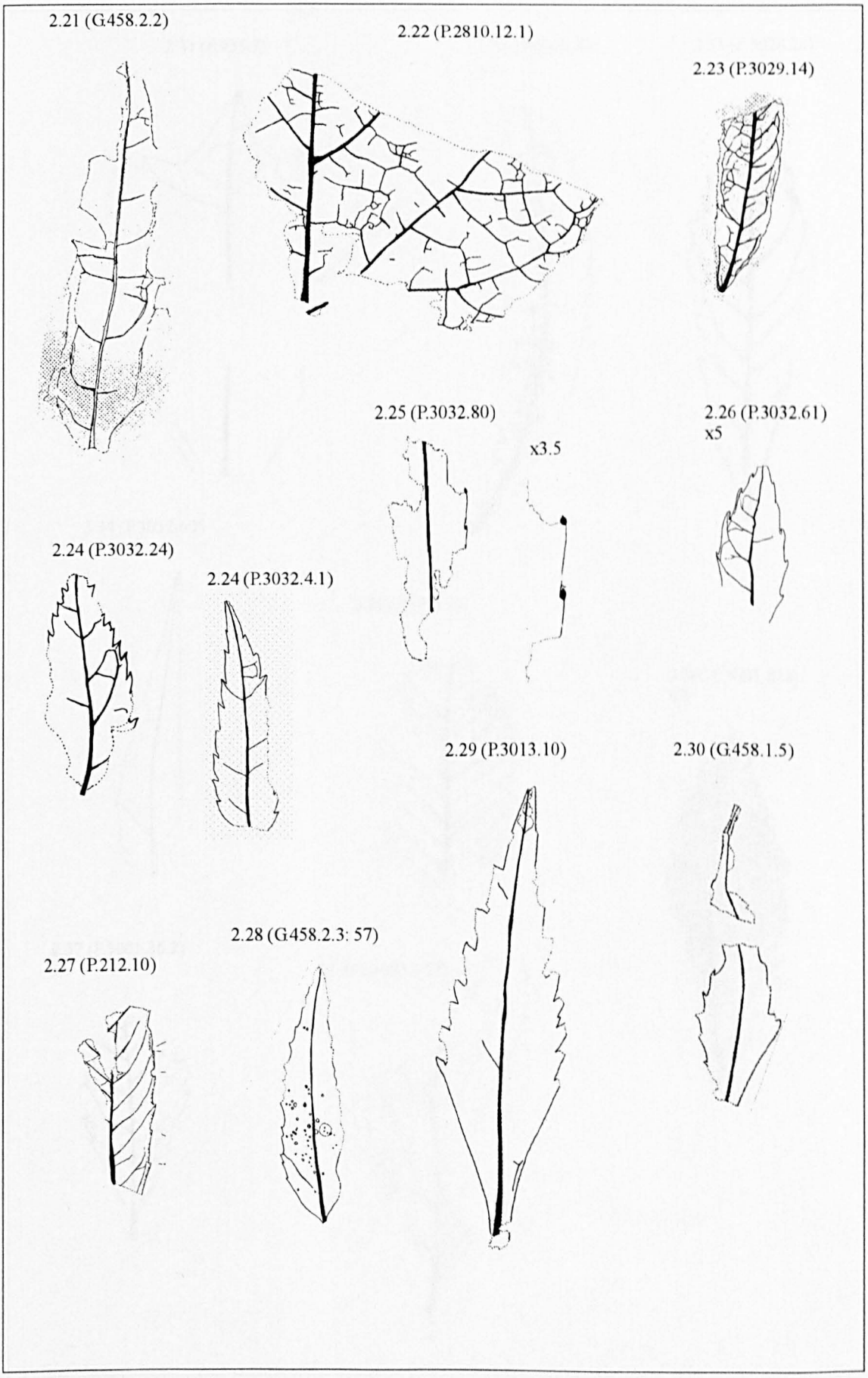

Figure V.6. Camera lucida drawings of toothed margined morphotypes 2.21 - 2.30. x1 unless otherwise stated.

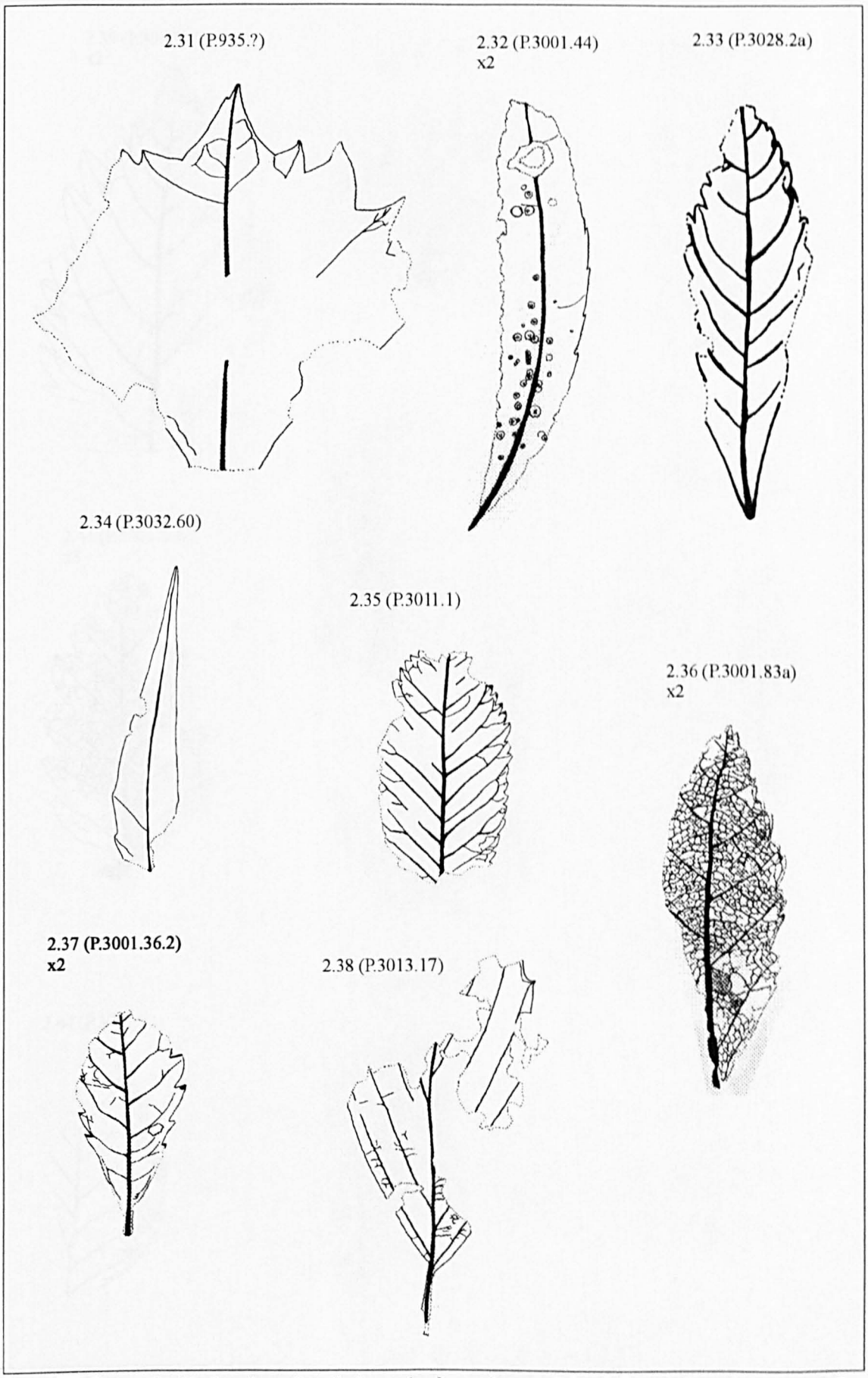

Figure V.7. Camera lucida drawings of toothed margined morphotypes 2.31 - 2.38. x1 unless otherwise stated.

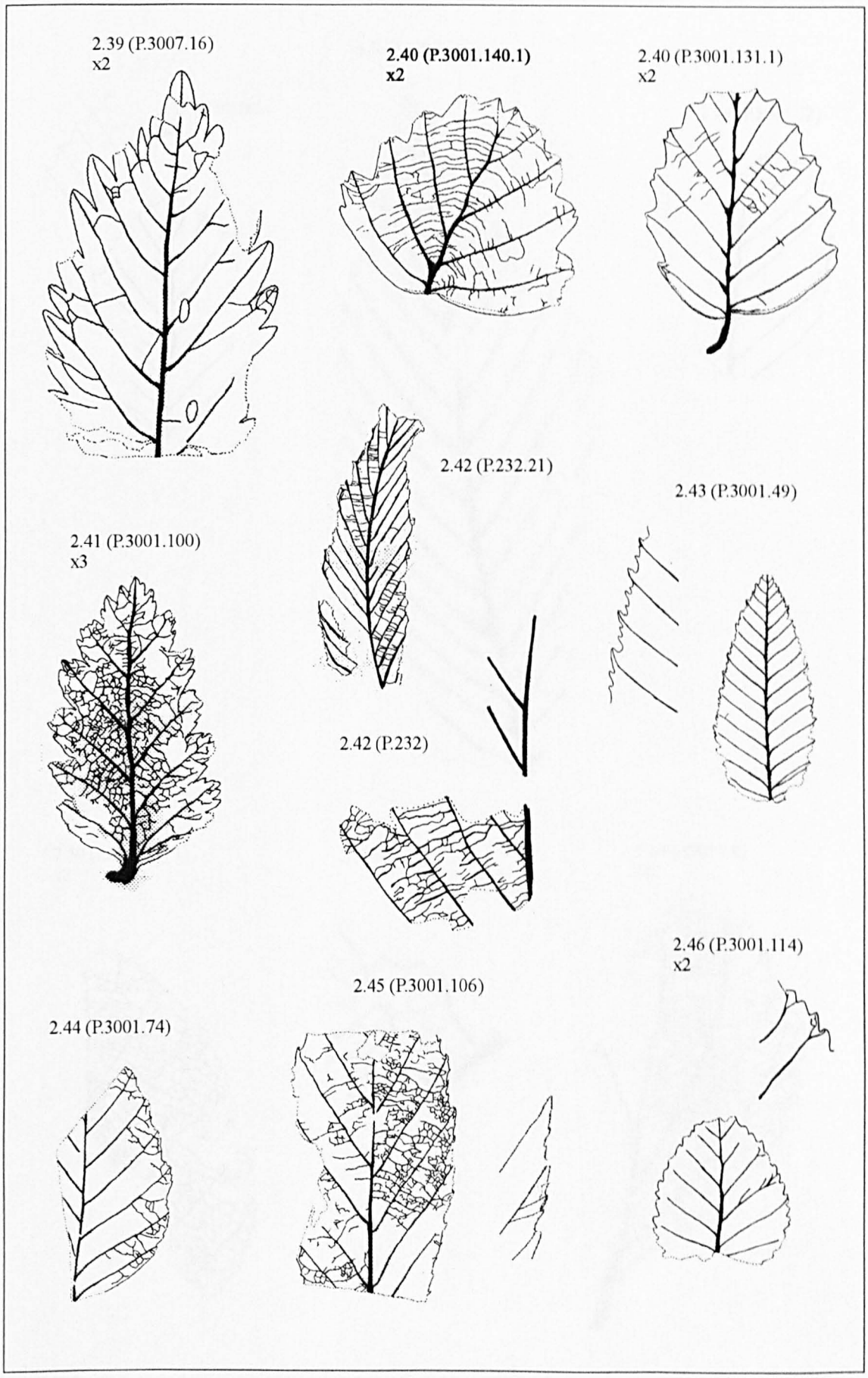

Figure V.8. Camera lucida drawings of toothed margined morphotypes 2.39 - 2.47. x1 unless otherwise stated.

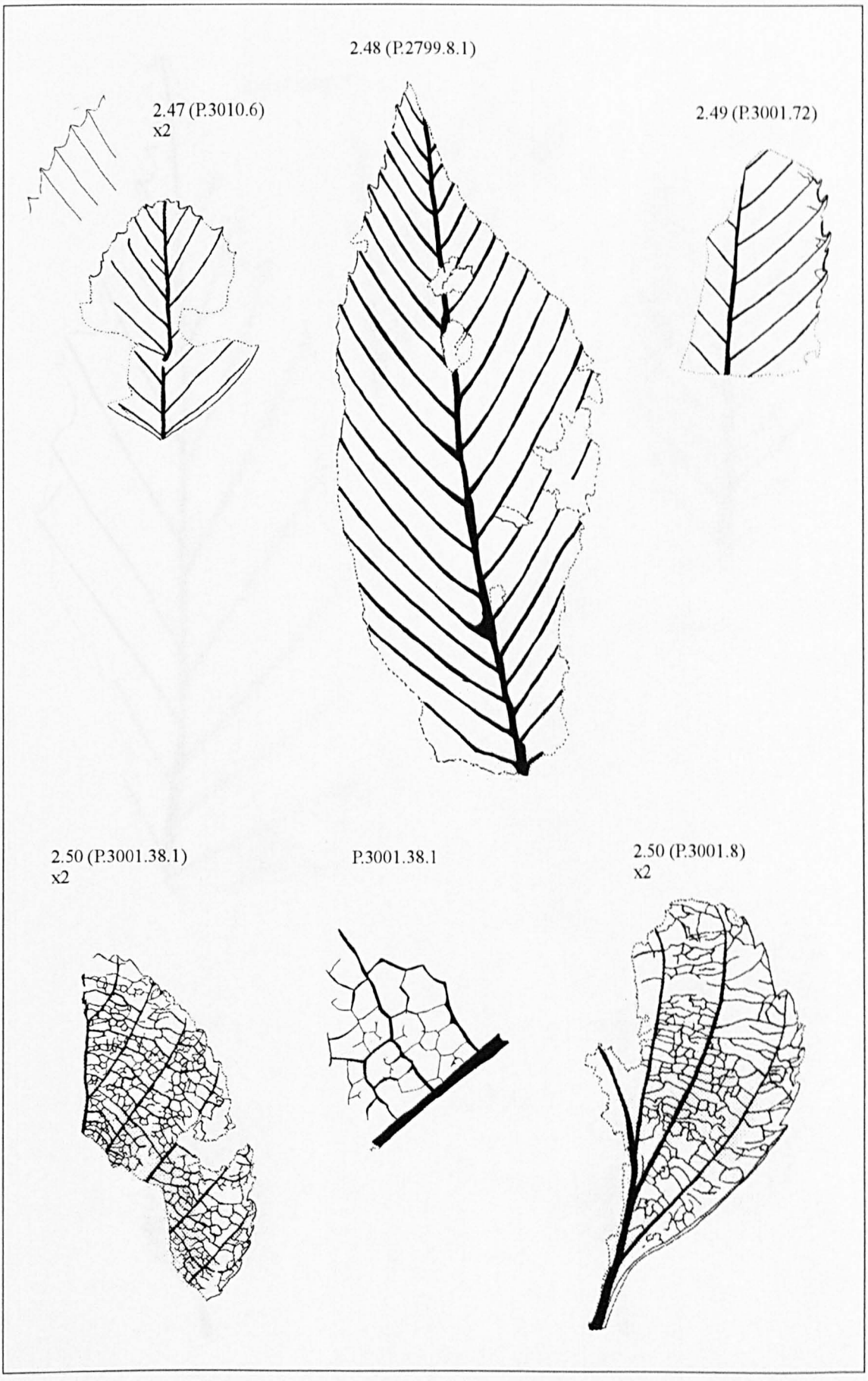

Figure V.9. Camera lucida drawings of toothed margined morphotypes 2.39 - 2.47. x1 unless otherwise stated.

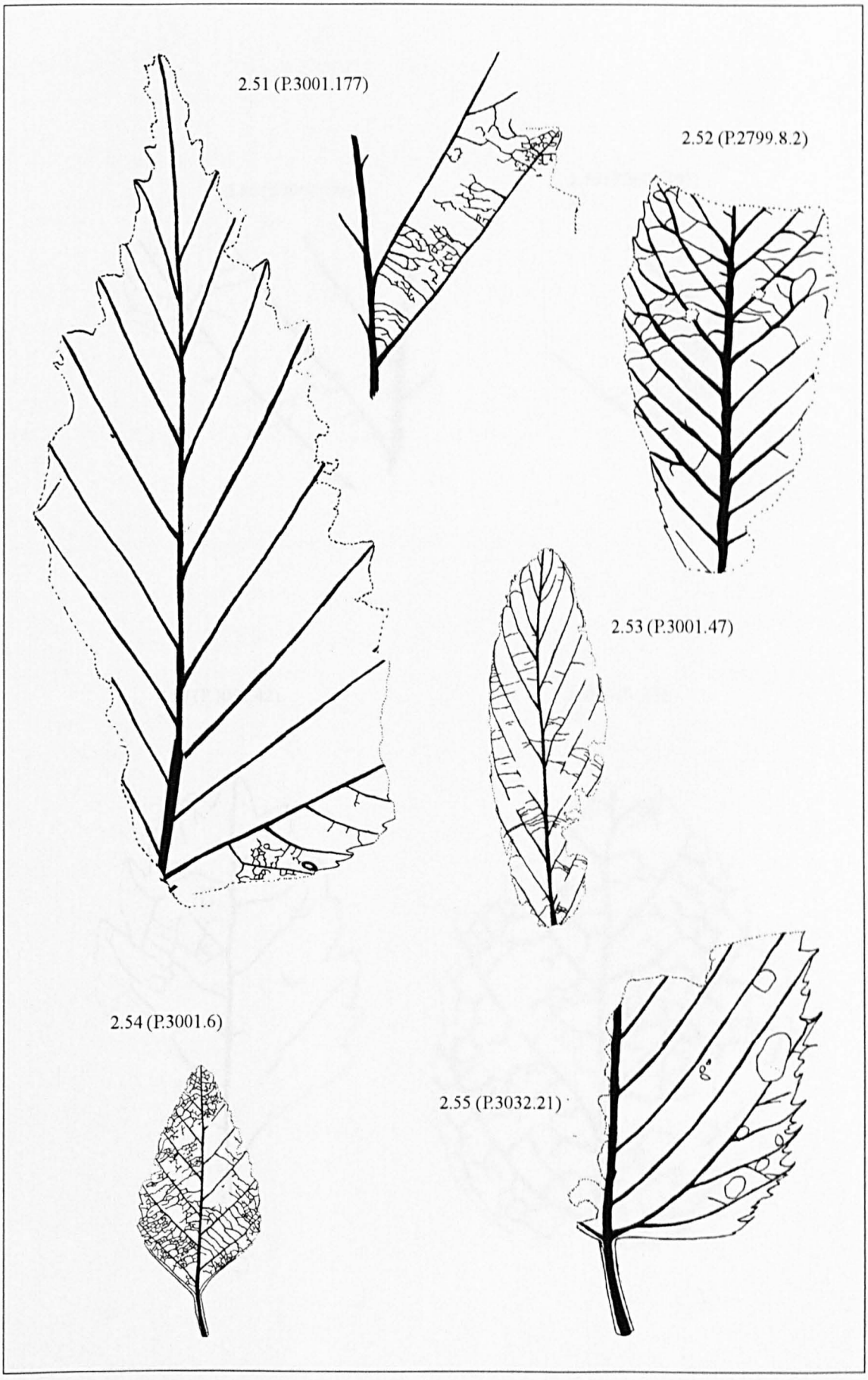

Figure V.10. Camera lucida drawings of toothed margined morphotypes 2.51 - 2.55. x1 unless otherwise stated.

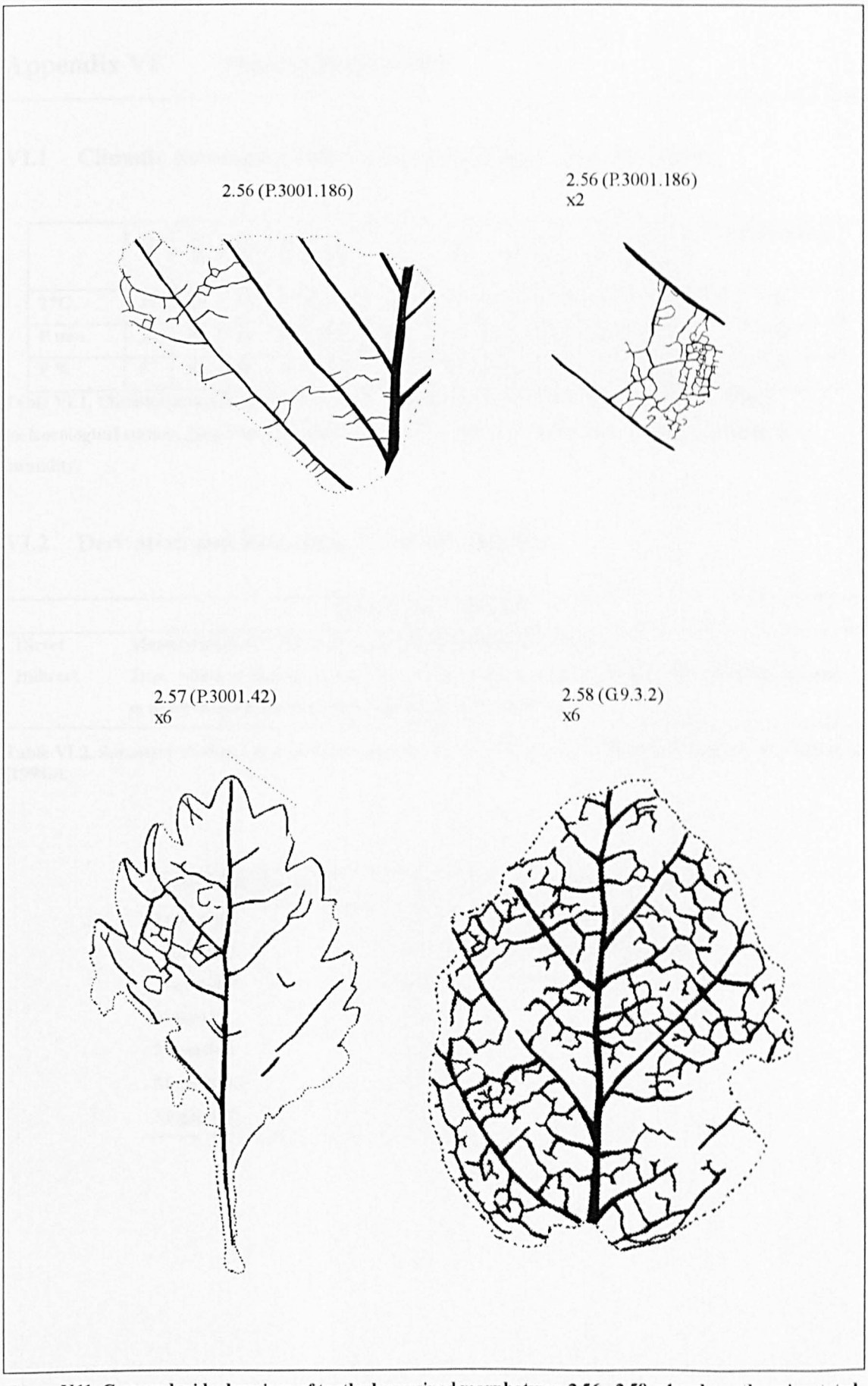

Figure V.11. Camera lucida drawings of toothed margined morphotypes 2.56 - 2.58. x1 unless otherwise stated.

Appendix VI Palaeoclimate data

VI.1 Climatic parameters inferred for *Thyrsopteris shenii* (Li, 1994)

	Jan	Feb	Mar	Apr	May	Jun	Jul	Aug	Sep	Oct	Nov	Dec	Annual Mean
T°C	19	19	17	17	16	14	13	12	13	13	15	17	16
P mm	20	30	41	86	150	162	147	112	73	48	41	25	935
F %	57	56	41	36	33	33	10	31	41	51	60	58	45

Table VI.1. Climatic paramaters for *Thyrsopteris elegans* derived from the Robinson Crusoe Island meteorological station, Juan Fernandez Islands (from Li, 1994). T = temperature, P = precipitation, F = humidity.

VI.2 Derivation and data tables for MAP estimates

	MlnA ($\Sigma a_i p_i$) estimation
Direct	Measurement or Cain and Castro (1959) estimate = 2/3 l x w
Indirect	$\Sigma a_i p_i$ where *ai* represents the seven means of the natural log areas of the size categories and p_i represents the proportions of species in each category

Table VI.2. Summary of direct and indirect methods used to calculate the MlnA/Σaipl parameter. Wilf et al. (1998b).

Webb (1959) size class	a_i
Leptophyll	2.12
Nanophyll	4.32
Microphyll	6.51
Notophyll	8.01
Mesophyll	9.11
Macrophyll	10.9
Megaphyll	13.1

Table VI.3. Summary of a_i values for each of the Webb (1959) categories (Wilf *et al.*, 1998b).

Morphotype	Dragon Glacier flora	Fossil Hill U2	Fossil Hill U3	Fossil Hill U4	Fossil Hill combined
1.1	Microphyll – Notophyll	Microphyll – Mesophyll		Microphyll - Mesophyll	Microphyll – Mesophyll
1.2	Notophyll				
1.4	Microphyll				
1.7		Microphyll		Microphyll	Microphyll
1.10				Microphyll	Microphyll
1.11	Microphyll			Microphyll	Microphyll
1.12				Microphyll	Microphyll
1.14	Notophyll				
1.16	Microphyll				
1.20	Microphyll				
1.21	Microphyll				
1.23	Mesophyll				
1.24	Microphyll -Mesophyll				
2.1	Nanophyll – Microphyll (leaflets)				
2.2		Nanophyll			Nanophyll
2.3		Microphyll		Microphyll	Microphyll
2.4	Microphyll (lobes)	Microphyll - notophyll	Microphyll	Microphyll - Notophyll	Microphyll – Notophyll
2.5			Mesophyll		Mesophyll
2.6	Notophyll				
2.8	Microphyll				
2.9	Microphyll				
2.10		Microphyll - Notophyll		Microphyll - Notophyll	Microphyll – Notophyll
2.13		Microphyll - Notophyll		Microphyll - Notophyll	Microphyll – Notophyll
2.14				Microphyll	Microphyll
2.15		Microphyll – Notophyll			Microphyll – Notophyll
2.21		Microphyll			Microphyll
2.22	Notophyll – Mesophyll				
2.24			Microphyll		Microphyll
2.25			Microphyll		Microphyll
2.28		Microphyll		Microphyll	Microphyll
2.29	Microphyll				
2.30				Microphyll	Microphyll
2.32	Microphyll				
2.30				Microphyll	Microphyll
2.31		Microphyll - Notophyll			Microphyll – Notophyll
2.34			Microphyll		Microphyll
2.36	Microphyll				
2.37	Microphyll				
2.38	Microphyll				
2.39	Microphyll				
2.40	Microphyll				
2.41	Leptophyll				
2.43	Microphyll				
2.44	Microphyll - Notophyll				
2.45	Microphyll - Notophyll				
2.46	Nanophyll – Microphyll				
2.49	Microphyll			Microphyll	Microphyll
2.50	Microphyll – Notophyll				
2.51	Microphyll – Mesophyll				
2.53	Microphyll				
2.54	Microphyll				
2.55			Microphyll - Mesophyll	Microphyll - Mesophyll	Microphyll - Mesophyll
2.56	Microphyll - Mesophyll				
Leptophyll	1				
Nanophyll	0	1	0	0	1
Microphyll	20	4	3	10	13
Notophyll	8	5	1	3	5
Mesophyll	5	1	2	2	3
%Leptophyll	2.94	0	0	0	0
%Nanophyll	0	9.09	0	0	4.55
%Microphyll	58.82	36.36	50	66.66	59.09
%Notophyll	23.53	45.45	16.67	20	22.73
%Mesophyll	14.71	9.09	33.33	13.33	13.64

Table VI.4. Size class data for leaf area analyses. Leaves with more than one size category are relegated to the larger size class.

VI.3 CLAMP scoresheet and percentage scores

Species/morphotypes	Margin Character States						
	Lobed	No Teeth	Tth Regular	Teeth Close	Teeth Round	Teeth Acute	Tth Compound
Morphotype 1.1	1	1	0	0	0	0	0
Morphotype 1.2	1	1	0	0	0	0	0
Morphotype 1.4	1	1	0	0	0	0	0
Morphotype 1.11	0	1	0	0	0	0	0
Morphotype 1.14	0	1	0	0	0	0	0
Morphotype 1.16	0	1	0	0	0	0	0
Morphotype 1.20	0	1	0	0	0	0	0
Morphotype 1.21	0	1	0	0	0	0	0
Morphotype 1.23	0	1	0	0	0	0	0
Morphotype 1.24	0	1	0	0	0	0	0
Morphotype 2.1	0	0	1	0	0	1	0
Morphotype 2.4	1	0	0.5	0	0	1	0.5
Morphotype 2.6	1	0					0
Morphotype 2.8	0	0		0	1	0	0
Morphotype 2.9	0	0	1	0	1	0	0
Morphotype 2.22	0	0	1	0	0	1	0
Morphotype 2.29	0	0	1	0	0	1	0
Morphotype 2.32	0	0	1	0	0	1	0
Morphotype 2.36	0	0	0	0	1	0	1
Morphotype 2.37	0	0	0.5	0	0	1	0
Morphotype 2.38	0	0		0	0	1	0
Morphotype 2.39	0	0	1	0	1	0	0
Morphotype 2.40	0	0	0.5	1	1	0	1
Morphotype 2.41	0	0	0.5	1	1	0	1
Morphotype 2.43	0	0	0.5	1	1	0	1
Morphotype 2.44	0	0	0.5	0	1	0	1
Morphotype 2.45	0	0	0.5	0	0	1	1
Morphotype 2.46	0	0	1	1	1	0	0.5
Morphotype 2.49	0	0	0.5	0	0	1	0
Morphotype 2.50	0	0	0.5	0	1	0	1
Morphotype 2.51	0	0	0.5	0	1	0	1
Morphotype 2.53	0	0		0	0	1	0
Morphotype 2.54	0	0		0	0.5	0.5	1
Morphotype 2.56	0	0	1	0	1	0	1

Table VI.5. Clamp scoresheet for the Dragon Glacier flora, downloaded from the CLAMP website (http://tabitha.open.ac.uk /spicer/CLAMP/Clampset1.html). Tth = teeth. Blank spaces = no data.

Size character states									
	Na	L1	L2	M1	M2	M3	Me1	Me2	Me3
Morphotype 1.1				0.25	0.25	0.25	0.25		
Morphotype 1.2						1			
Morphotype 1.4					1				
Morphotype 1.11				0.33	0.33	0.33			
Morphotype 1.14						1			
Morphotype 1.16					1				
Morphotype 1.20				0.5	0.5				
Morphotype 1.21					1				
Morphotype 1.23							1		
Morphotype 1.24					0.25	0.25	0.25	0.25	
Morphotype 2.1			0.33	0.33	0.33				
Morphotype 2.4					0.5	0.5			
Morphotype 2.6						1			
Morphotype 2.8						1			
Morphotype 2.9					1				
Morphotype 2.22					0.25	0.25	0.25	0.25	
Morphotype 2.29					0.5	0.5			
Morphotype 2.32				1					
Morphotype 2.36				1					
Morphotype 2.37				1					
Morphotype 2.38						1			
Morphotype 2.39					1				
Morphotype 2.40				1					
Morphotype 2.41				1					
Morphotype 2.43				0.33	0.33	0.33			
Morphotype 2.44					1				
Morphotype 2.45						0.5	0.5		
Morphotype 2.46				0.5	0.5				
Morphotype 2.49					1				
Morphotype 2.50				0.33	0.33	0.33			
Morphotype 2.51				0.25	0.25	0.25	0.25		
Morphotype 2.53					1				
Morphotype 2.54				1					
Morphotype 2.56						0.33	0.33	0.33	

Table VI.5. Continued. Na – nanophyll, L1/L2/L3 – Leptophyll 1/2/3, M1/2/3 – Microphyll 1/2/3, Me 1/2/3 – Mesophyll 1/2/3.

	Apex character states					Base character states	
	Apex Emarg.	Apex Round	Apex Acute	Apex Atten.	Base Cordate	Base Round	Base Acute
Morphotype 1.1	0		0.5	0.5	0.5	0.5	
Morphotype 1.2	0		1				1
Morphotype 1.4	0	1				1	
Morphotype 1.11	0	0.5	0.5			0.5	0.5
Morphotype 1.14	0	1				1	
Morphotype 1.16	0	1					
Morphotype 1.20	0		1				1
Morphotype 1.21	0	1				1	
Morphotype 1.23	0				1		
Morphotype 1.24	0	1				1	
Morphotype 2.1	0		1		0.5	0.5	
Morphotype 2.4	0	0.5	0.5				
Morphotype 2.6	0				1		
Morphotype 2.8	0	1					1
Morphotype 2.9	0	0.5	0.5				1
Morphotype 2.22	0		1			0.5	0.5
Morphotype 2.29	0		1				1
Morphotype 2.32	0						1
Morphotype 2.36	0		1				1
Morphotype 2.37	0						1
Morphotype 2.38	0						1
Morphotype 2.39	0	1					
Morphotype 2.40	0	1			1		
Morphotype 2.41	0	1				1	
Morphotype 2.43	0	1				1	
Morphotype 2.44	0					0.5	0.5
Morphotype 2.45	0						
Morphotype 2.46	0	1			1		
Morphotype 2.49	0						
Morphotype 2.50	0	0.5	0.5			0.5	0.5
Morphotype 2.51	0	0.5	0.5			0.5	
Morphotype 2.53	0	1				0.5	
Morphotype 2.54	0		1				1
Morphotype 2.56	0		1				1

Table VI.5. Continued. Emarg – Emarginate, Atten – Attenuated.

	Length to width character states					Shape character states		
	L:W<1:1	L:W 1-2:1	L:W 2-3:1	L:W 3-4:1	L:W>4:1	Obovate	Elliptic	Ovate
Morphotype 1.1	0.5	0.5						1
Morphotype 1.2		1						1
Morphotype 1.4			1				1	
Morphotype 1.11			1				1	
Morphotype 1.14	1						1	
Morphotype 1.16		1					1	
Morphotype 1.20					1		0.5	0.5
Morphotype 1.21					1		1	
Morphotype 1.23								1
Morphotype 1.24		0.5	0.5				1	
Morphotype 2.1		0.33	0.33	0.33			0.5	0.5
Morphotype 2.4								
Morphotype 2.6		1						1
Morphotype 2.8			1				1	
Morphotype 2.9				1			1	
Morphotype 2.22		0.5	0.5				0.5	0.5
Morphotype 2.29				1			0.5	0.5
Morphotype 2.32					1		1	
Morphotype 2.36			1				1	
Morphotype 2.37			1			1		
Morphotype 2.38		1				1		
Morphotype 2.39		1					1	
Morphotype 2.40	0.5	0.5						1
Morphotype 2.41		1						1
Morphotype 2.43			1					1
Morphotype 2.44		1						1
Morphotype 2.45		1					0.5	0.5
Morphotype 2.46		1						1
Morphotype 2.49		1						1
Morphotype 2.50		1				0.5		0.5
Morphotype 2.51		1						1
Morphotype 2.53				1			1	
Morphotype 2.54		0.5	0.5					1
Morphotype 2.56		1						1

Table VI.5. Continued.

	Margin character states						
	Lobed	No Teeth	Tth Regular	Teeth Close	Teeth Round	Teeth Acute	Tth Compound
Total Character State Score	5.0	10.0	13.0	4.0	12.5	10.5	11.0
No. Character States Present	5.0	33.0	33.0	33.0	33.0	33.0	33.0
Percentage Score	14.7	30.3	39.4	12.1	37.9	31.8	33.3

	Size character states								
	Na	Le I	Le II	Mil I	Mi II	Mi III	Me I	Me II	Me III
Total Character State Score	0.0	0.0	0.3	8.8	12.3	8.8	2.8	0.8	0.0
No. Character States Present	34.0	34.0	34.0	34.0	34.0	34.0	34.0	34.0	34.0
Percentage Score	0.0	0.0	1.0	25.9	36.2	25.9	8.3	2.4	0.0

	Apex character states				Base character states		
	Apex Emarg.	Apex Round	Apex Acute	Apex Atten.	Base Cordate	Base Round	Base Acute
Total Character State Score	0.0	14.5	11.0	0.5	5.0	10.0	13.0
No. Character States Present	26.0	26.0	26.0	26.0	29.0	29.0	29.0
Percentage Score	0.0	55.8	42.3	1.9	17.2	34.5	44.8

	Length to width character states					Shape character states		
	L:W<1:1	L:W 1-2:1	L:W 2-3:1	L:W 3-4:1	L:W>4:1	Obovate	Elliptic	Ovate
Total Character State Score	2.0	15.8	7.8	3.3	3.0	2.5	14.5	16.0
No. Character States Present	32.0	32.0	32.0	32.0	32.0	33.0	33.0	33.0
Percentage Score	6.3	49.5	24.5	10.4	9.4	7.6	43.9	48.5

Table VI.6. Percentage CLAMP scores for the Dragon Glacier flora based on 34 morphotypes.

	Lobed	No Teeth	Tth Regular	Teeth Close	Teeth Round	Teeth Acute	Tth Compound
Totals	5.0	10.0	18.0	4.0	13.0	11.0	12.0

	Nanophyll	Leptophyll I	Leptophyll II	Microphyll I	Microphyll II	Microphyll III	Mesophyll I	Mesophyll II	Mesophyll III
Totals	0.0	0.0	1.0	14.0	20.0	16.0	7.0	3.0	0.0

	Apex Emarg.	Apex Round	Apex Acute	Apex Atten.	Base Cordate	Base Round	Base Acute
Totals	0.0	17.0	14.0	1.0	6.0	14.0	15.0

	L:W<1:1	L:W 1-2:1	L:W 2-3:1	L:W 3-4:1	L:W>4:1	Obovate	Elliptic	Ovate
Totals	3.0	19.0	10.0	4.0	3.0	3.0	17.0	19.0

	Margin	Size	Apex	Base	L:W	Shape
Totals	33.0	34.0	26.0	29.0	32.0	33.0

Table VI.7. Working area – numbers of species and character states scored.